

Agronomy Research

Established in 2003 by the Faculty of Agronomy, Estonian Agricultural University

Aims and Scope:

Agronomy Research is a peer-reviewed international Journal intended for publication of broad-spectrum original articles, reviews and short communications on actual problems of modern biosystems engineering incl. crop and animal science, genetics, economics, farm- and production engineering, environmental aspects, agro-ecology, renewable energy and bioenergy etc. in the temperate regions of the world.

Copyright:

Copyright 2009 by Estonian University of Life Sciences, Latvia University of Life Sciences and Technologies, Vytautas Magnus University Agriculture Academy, Lithuanian Research Centre for Agriculture and Forestry. No part of this publication may be reproduced or transmitted in any form, or by any means, electronic or mechanical, incl. photocopying, electronic recording, or otherwise without the prior written permission from the Estonian University of Life Sciences, Latvia University of Life Sciences and Technologies, Vytautas Magnus University Agriculture Academy, Lithuanian Research Centre for Agriculture and Forestry.

***Agronomy Research* online:**

Agronomy Research is available online at: <http://agronomy.emu.ee/>

Acknowledgement to Referees:

The Editors of *Agronomy Research* would like to thank the many scientists who gave so generously of their time and expertise to referee papers submitted to the Journal.

Abstracted and indexed:

SCOPUS, EBSCO, CABI Full Paper and Thompson Scientific database: (Zoological Records, Biological Abstracts and Biosis Previews, AGRIS, ISPI, CAB Abstracts, AGRICOLA (NAL; USA), VINITI, INIST-PASCAL).

Subscription information:

Institute of Technology, EULS
St. Kreutzwaldi 56, 51014 Tartu, ESTONIA
E-mail: timo.kikas@emu.ee

Journal Policies:

Estonian University of Life Sciences, Latvia University of Life Sciences and Technologies, Vytautas Magnus University Agriculture Academy, Lithuanian Research Centre for Agriculture and Forestry, and Editors of *Agronomy Research* assume no responsibility for views, statements and opinions expressed by contributors. Any reference to a pesticide, fertiliser, cultivar or other commercial or proprietary product does not constitute a recommendation or an endorsement of its use by the author(s), their institution or any person connected with preparation, publication or distribution of this Journal.

ISSN 1406-894X

CONTENTS

- D. Baranenko, V. Bespalov, L. Nadtochii, I. Shestopalova, A. Chechetkina, A. Lepeshkin and V. Ilina**
Development of encapsulated extracts on the basis of meadowsweet (*Filipendula ulmaria*) in the composition of functional foods with oncoprotective properties1829
- V. Bulgakov, H. Kaletnik, I. Goncharuk, S. Ivanovs and M. Usenko**
Results of experimental investigations of a flexible active harrow with loosening teeth.....1839
- V. Bulgakov, H. Kaletnik, T. Goncharuk, A. Rucins, I. Dukulis and S. Pascuzzi**
Research of the movement of agricultural aggregates using the methods of the movement stability theory1846
- V. Chaloupková, T. Ivanova and V. Krepl**
Particle size and shape characterization of feedstock material for biofuel production.....1861
- L. Degola, V. Sterna, I. Jansons and S. Zute**
The nutrition value of soybeans grown in Latvia for pig feeding1874
- V. Dubrovskis, I. Plume and I. Straume**
Use of ethanol production and stillage processing residues for biogas production.....1881
- V. Gasiev, N. Khokhoeva and D. Mamiev**
Biological features of formation of perennial binary grass crops.....1891
- V. Hartová, J. Hart and M. Kotek**
Reliability of palms security under difficult conditions1898
- L. Hlisnikovský, P. Čermák, E. Kunzová and P. Barlóg**
The effect of application of potassium, magnesium and sulphur on wheat and barley grain yield and protein content1905
- M. Hruška**
Assessment of luggage compartment parameters based on the preferences of a heterogeneous driver group1918

- A. Kabutey, D. Herak, C. Mizera and P. Hrabec**
Theoretical analysis of force, pressure and energy distributions of bulk oil palm kernels along the screwline of a mechanical screw press FL 2001927
- A. Lenerts, D. Popluga and K. Naglis-Liepa**
Benchmarking the GHG emissions intensities of crop and livestock-derived agricultural commodities produced in Latvia1942
- J. McNamara, P. Griffin, J. Phelan, W.E. Field and J. Kinsella**
Farm health and safety adoption through engineering and behaviour change1953
- E. Mellelo, E.O. Samuilova, T.S. Denisov, D.M. Martynova and R.O. Olekhovich**
Influence of the bentonite-containing acrylic humectant composite on the soil microflora1960
- E. Merisalu, J. Leppälä, M. Jakob and R.H. Rautiainen**
Variation in Eurostat and national statistics of accidents in agriculture1969
- M.G. Morerira, G.A.S. Ferraz, B.D.S. Barbosa, E.M. Iwasaki, P.F.P Ferraz, F.A. Damasceno and G. Rossi**
Design and construction of a low-cost remotely piloted aircraft for precision agriculture applications1984
- A. Nemeikšis and V. Osadčuks**
Development of intelligent system of mobile robot movement planning in unknown dynamic environment by means of multi-agent system1993
- R. Nurzyńska-Wierdak, H. Łabuda, H. Buczkowska and A. Sałata**
Pericarp of colored-seeded common bean (*Phaseolus vulgaris* L.) varieties a potential source of polyphenolic compounds2005
- V.C. Oliveira, F.A. Damasceno, C.E.A. Oliveira, P.F.P. Ferraz, G.A.S. Ferraz and J.A.O. Saraz**
Compost-bedded pack barns in the state of Minas Gerais: architectural and technological characterization2016
- S. Palisoc, J. Leoncini and M. Natividad**
Trace level determination of cadmium and lead in coffee (*Coffea*) using gold nanoparticles modified graphene paste electrode2029

J. Rosend, R. Kuldjärv, G. Arju and I. Nisamedtinov Yeast performance characterisation in different cider fermentation matrices	2040
L.M.D. Santos, G.A.S. Ferraz, M.T. Andrade, L.S. Santana, B.D.S. Barbosa, D.T. Maciel and Giuseppe Rossi Analysis of flight parameters and georeferencing of images with different control points obtained by RPA.....	2054
I. Sivicka, A. Adamovics, S. Ivanovs and E. Osinska Some morphological and chemical characteristics of oregano (<i>Origanum vulgare</i> L.) in Latvia.....	2064
S. Stankowski, M. Bury, A. Jaroszewska, B. Michalska and M. Gibczyńska Effect of multi-component fertilizers on seeds yield, yield components and physiological parameters of winter oilseed rape (<i>Brassica napus</i> L.).....	2071
V. Strizhevskaya, M. Pavlenkova, S. Nemkova, N. Nosachyova, I. Simakova and E. Wolf Possibility and prospects of preservation of minor components in technology of fruit raw materials conservation.....	2082
L. Tyšer, M. Kolářová and T.T. Hoová Occurrence of archaeophytes in agrophytocoenoses – field survey in the Czech Republic.....	2089
A. Vagová, M. Hromasová, M. Linda and P. Vaculík Determining external friction angle of barley malt and malt crush.....	2106
L. Zihare, I. Muizniece and D. Blumberga A holistic vision of bioeconomy: the concept of transdisciplinarity nexus towards sustainable development	2115
O. Zinina, S. Merenkova, M. Rebezov, D. Tazeddinova, Z. Yessimbekov and V. Vietoris Optimization of cattle by-products amino acid composition formula	2127

Development of encapsulated extracts on the basis of meadowsweet (*Filipendula ulmaria*) in the composition of functional foods with oncoprotective properties

D. Baranenko^{1,*}, V. Bespalov^{1,2}, L. Nadtochii¹, I. Shestopalova¹,
A. Chechetkina¹, A. Lepeshkin¹ and V. Ilina¹

¹ITMO University, International research centre "Biotechnologies of the Third Millennium", Lomonosov street 9, RU191002 Saint-Petersburg, Russia

²N.N Petrov National Medical Research Center of Oncology, Laboratory of Cancer Chemoprevention and Oncopharmacology, Leningradskaya street 68, RU197758 St. Petersburg, Russia

*Correspondence: denis.baranenko@niuitmo.ru

Abstract. Meadowsweet (*Filipendula ulmaria*) is a quite common plant throughout the European countries, including Russia. Therapeutic and prophylactic properties of the meadowsweet are mainly associated with the action of biologically active substances (BAS), in particularly tannins, phenolic compounds, phenolcarboxylic acids, catechins, flavonoids, essential oils etc. The main substances with proven clinical effects are salicylates and flavonoids, what allows to consider meadowsweet as an anti-inflammatory, immunostimulating, antioxidant, hepatoprotective, nootropic, adaptogenic and antihypoxic agent.

The aim of this study was to analyze the content of BAS in water and 70% ethyl alcohol extract of *F. ulmaria* flowers from different regions of Russia and develop their encapsulated forms for further use as an ingredient for functional food products.

To increase the shelf life of meadowsweet extracts and create a stable form for their delivery to the human body with various food products, encapsulated forms of extracts in the form of micro- and nanosized capsules were developed. The method of encapsulation was carried out using a spray dryer. It was shown that encapsulated meadowsweet BAS can be added to a chicken pate without negative effect on the organoleptic properties of the finished product. The calculation of the cost of the meat product with the complex functional dry mixture showed a slight increase in the cost of the final product compared to the traditional analogue. This study shows that encapsulated meadowsweet BAS can be used for inclusion in various food products, to ensure the functional properties of food and optimize the population's rations.

Key words: meadowsweet (*Filipendula ulmaria*), flavonoids, encapsulated extracts, biologically active substances.

INTRODUCTION

Meadowsweet (*Filipendula ulmaria* L. Maxim.) is a perennial herbaceous plant of the family Rosaceae, growing in the wet meadows of Europe and Western Asia (Katanicet al., 2015; Shaldayeva et al., 2018). Over the years, various parts of the plant – aerial parts and roots were used in traditional medicine as a drug with

antibacterial, anti-inflammatory and other properties (Hasler et al., 1989; Vysochina et al., 2016; Shaldayeva et al., 2018). In previous studies extensive data on the antioxidant properties of the components of meadowsweet were obtained, which is associated with the chemical composition of the plant, in particular with the presence of a number of phenolic compounds: flavonoids, phenolic acids, tannins, salicylate aglycons and glycosides (Katanic et al., 2015; Vysochina et al., 2016; Shaldayeva et al., 2018). Meadowsweet extracts also have a pronounced antimicrobial effect, which is confirmed by a study against 11 human pathogens (Denev et al., 2014).

Biologically active substances (BAS) of meadowsweet are studied for preventive effect on cancer, vascular heart disease, atherosclerosis, hypertension, diabetes, neurodegenerative diseases, rheumatoid arthritis and aging (Bruneton, 1995; Schulz et al., 1998; Duke, 2001). Alcohol and water extracts of plants, including meadowsweet, as effective means in the prevention of cancer are reflected in the studies of Korsun et al., 2015 and Bespalov, et al., 2017; Bespalov, et al., 2018.

A variety of biologically active substances (BAS) of meadowsweet is of interest to the research of this plant in order to obtain new highly effective preparations of a wide action on its basis. There is also longtime growing interest in developing methods for preserving biologically active substances of plants (Popescu, 2000). Stabilization of the extracted forms of biologically active substances can be achieved by means of encapsulation (Dziedzic, 1988; Shahidi & Han, 1993). Currently technological methods of micro- and nanoencapsulation are widely used to ensure the transformation of BAS in a stable form (Zabodalova et al., 2014). Sensitive ingredients can retain their properties against the adverse reaction of the environment while preventing the loss of BAS by encapsulation. Modern technologies are also able to control the release of encapsulated ingredients. Different techniques are wide employed to microencapsulate food ingredients, the most often used technique in the food industry is spray-drying (Gibbs et al., 1999; Loksuan, 2007). Selection of encapsulating method and materials for the capsule shell are determining factors in the encapsulated biologically active substances development and directly influence the final product characteristics.

Up to the present time, no studies have been conducted on the encapsulation of meadowsweet biologically active substances for further use as a part of the formulations for functional food products. It is assumed that the encapsulated forms of meadowsweet with onco-protective properties will help providing the food product with the same effect.

Thus, the purpose of the study was to evaluate the content of flavonoids in extracts of the aerial part of *Filipendula ulmaria* L. Maxim. from different regions of the Russian Federation and to develop encapsulated forms of its biologically active substances for further use as a part of a complex dry mixture for functional food products.

MATERIALS AND METHODS

Aerial parts (flowers) of *Filipendula ulmaria* L. Maxim. were carefully selected in the phase of mass flowering of plants from nature populations in three regions of the Russian Federation: in the territory of the Leningrad and Yaroslavl regions and in the Republic of Bashkortostan in 2018. Currently, in these regions, *F. ulmaria* is being collected in commercial volumes, so they can be considered as its suppliers for possible industrial production. The plant samples of *Filipendula ulmaria* were confirmed and

deposited in the Herbarium at the Botanical Institute of the Russian Academy of Sciences, St. Petersburg. Flowers were subjected to convection drying to a moisture content of $8.1 \pm 0.5\%$.

Preparation of the meadowsweet extracts

Dried meadowsweet flowers were ground in a laboratory mill to the size of particles passing through a sieve with holes of 0.2 cm in diameter, then 1g of the crushed sample was placed in a conical flask with a capacity of 100 cm³, where 100 cm³ of ethyl alcohol with a volume fraction of 70% or 100 cm³ of distilled water was added.

Encapsulation of biologically active ingredients of meadowsweet

Production of encapsulated BAS of meadowsweet included some main stages: preparation of the extracts according to the scheme described above; mixing the extracts with a solution of maltodextrin; obtaining encapsulated BAS; drying of encapsulated biologically active substances and obtaining stable micro- and nanoscale capsules; packing and storage.

The prepared alcoholic extract of meadowsweet BAS was mixed with maltodextrin solution in a certain proportion 3:1, respectively, then the resulting solution was intensively mixed on a magnetic stirrer US-1550A (Ulab) at 1,000 rpm and kept for 30 minutes in a closed flask at room temperature. To achieve the smallest dispersion (with a nanoparticle size of not more than 500 nm), the prepared solution was subjected to mechanical treatment using the ultra-powerful ULTRATURREX dispersant at 30,000 rpm and the TwinPanda 600 high-pressure homogenizer at 60 MPa. The resulting dispersion was placed in a closed flask at a temperature of 4 ± 2 °C for at least 24 hours for stabilization. At the next step the dispersion was sent to the Eyela SD-1000 spray dryer (Japan), where the encapsulation process took place at input temperature of 150 ± 20 °C and output temperature of 50 ± 20 °C. The air flow rate was equal to 0.7–0.8 m³ h⁻¹, the fluid flow rate was 500–700 mL h⁻¹ and the inlet pressure was 8–10 atm. The obtained encapsulated meadowsweet BAS were removed from the receiving flask of the spray dryer and sent for further technological operations. The above presented modes and parameters are based on experimental data obtained in previous studies (Yoshiia et al., 2001; Ahmed et al., 2010; Choi et al., 2019) in modification to specific technological characteristics of the raw materials used.

Production of pate with the addition of a complex functional dry mixture

To ensure that encapsulated meadowsweet BAS can be used as a part of functional food products its was added to a complex functional dry mixture for emulsified meat products Optilad Plus from the manufacturer Nordena LLC (St. Petersburg, Russia). The original Optilad Plus dry mixture contains skim milk powder, mono- and diglycerides of fatty acids, wheat fiber, modified starch, salt. Encapsulated meadowsweet BAS were added in the amount of 4% to the dry mixture.

A chicken pate made according to the recipe developed by the authors was chosen as an example of a food product for encapsulated meadowsweet BAS introduction. The following broiler chicken raw materials were obtained from a local producer and used as ingredients: femur meat, mechanically deboned meat, raw fat and skin. Only browned onion was used as a flavor component in addition to the complex functional dry mixture, so it was easier to study encapsulated meadowsweet influence on the products

characteristics. Production of the pate was carried out by a standard hot technology with using a broth.

The total flavonoids content in extracts and encapsulated forms of meadowsweet

The total flavonoids content in extracts and encapsulated forms of meadowsweet was studied as follows: 1 cm³ of extract or water solution of capsules were placed in a 25 mL volumetric flask, where a 5 cm³ of an aluminum chloride solution was added with a mass fraction of 2% in ethyl alcohol, then the volume of the solution was adjusted to the mark by adding ethyl alcohol. The reference solution was prepared in the same way by mixing 1 cm³ solution of capsule with alcohol, but without introducing aluminum chloride with a mass fraction of 2% in ethanol. The resultant solution optical density was analyzed using Shimadzu UV-2600 spectrophotometer at a wavelength of 410 nm.

The calculation of the total content of flavonoids was carried out according to the calibration curve (Fig. 1). The calibration curve is a graph of the dependence of optical density on the concentration of rutin in solution. The above presented methods were previously used in the researches of other authors (Katanic et al., 2015; Bespalov et al., 2017).

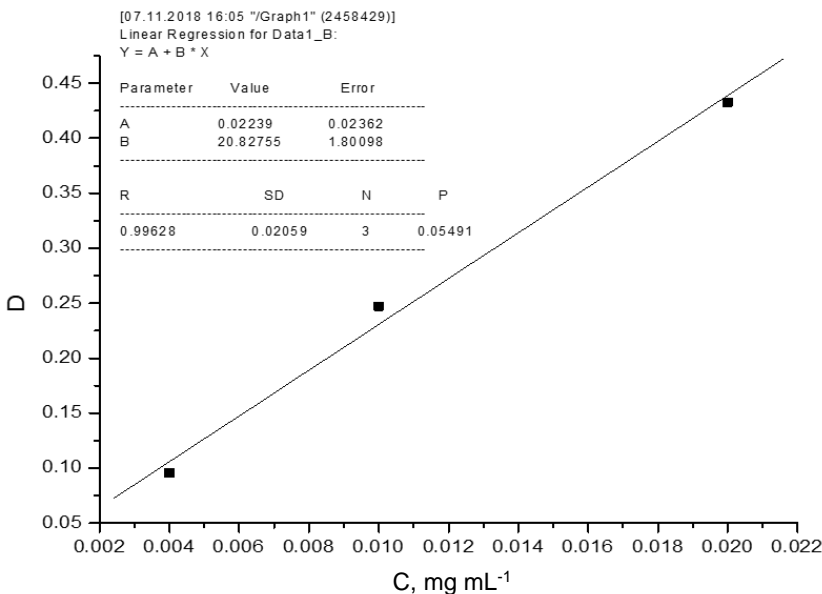


Figure 1. Calibration curve for determining the total flavonoid content.

Determination of the size of micro- and nanoparticles of meadowsweet BAS

Scanning electron microscope (SEM) of the Carl Zeiss brand Cross-Beam, model Neon40EsB was used to determine the size of developed micro- and nanocapsules of meadowsweet BAS.

Sensory evaluation of meat product (pate)

The organoleptic quality assessment of the developed functional meat product was carried out according to State Russian Standard 55334-2012 ‘Meat and meat containing pate. Technical conditions’.

Statistical analysis

The experiments were performed in triplicate, the data were processed by the methods of mathematical statistics with finding confidence intervals with a probability of 0.95.

RESULTS AND DISCUSSION

In this study, flavonoids isolated from the meadowsweet flowers from different regions of the Russian Federation were the objects of particular interest. The results of the study of the flavonoids quantitative content in water and alcoholic meadowsweet flowers extracts are shown in Table 1.

Table 1. The flavonoids content of meadowsweet flowers extracts from three regions of the Russia

Samples	Flavonoids (mean \pm confidence interval)					
	mg / 100 mL extract			mg / g dry substance meadowsweet		
	Leningrad Region	Yaroslavl Region	Bashkir Republic	Leningrad Region	Yaroslavl Region	Bashkir Republic
Water extract	403 \pm 32	309 \pm 33	287 \pm 36	80.6 \pm 2.9	61.8 \pm 1.8	56.4 \pm 1.9
Alcohol extract	529 \pm 34	390 \pm 50	360 \pm 40	105.8 \pm 3.1	78.8 \pm 2.5	69.3 \pm 2.2

Based on the Table 1 data, it can be concluded that the content of flavonoids in alcoholic extracts is higher than in water extracts of meadowsweet for all the samples studied. Moreover, the content of flavonoids in the studied samples of the meadowsweet extracts from the Leningrad region exceeds the studied indicator in other samples studied. The highest value of the content of flavonoids is observed in alcoholic extract of meadowsweet from the Leningrad region, which averaged 529 mg / 100 mL of extract or 105.8 mg / g of dry matter. The lowest content of flavonoids in the studied samples was found in the water extract of meadowsweet from the Bashkir Republic and the Yaroslavl Region and averaged 360 and 390 mg / 100 mL of extract or 69.3 and 78.8 mg / g of dry matter respectively. It should be noted that the content of flavonoids in the water extract of meadowsweet from the Leningrad region is comparable to the content of flavonoids in the alcohol extract of meadowsweet from the Yaroslavl region. This variation in the content of flavonoids in extracts of meadowsweet in various regions can be associated with regional climatic conditions of plants growth, for example, with the soil composition of the studied regions of Russia (Shamshev et al., 2003; Zhdanov et al., 2016; Vysochina et al., 2016; Shaldayeva et al., 2018).

Thus, the analysis of the chemical composition of meadowsweet extracts (water and alcohol extraction) showed high content of total flavonoids of meadowsweet from various regions of the Russian Federation. This data corresponds to the results of the other authors (Denev et al., 2014; Katanic et al., 2015; Bespalov et al., 2017).

The above-mentioned alcoholic and water extracts were taken as the basis for obtaining encapsulated meadowsweet BAS. Table 2 shows the results of the flavonoids content in them.

Table 2. Content of flavonoids in meadowsweet capsules

Samples	Content of total flavonoids, mg / g capsules (mean ± confidence interval)		
	Leningrad Region	Yaroslavl Region	Bashkir Republic
Capsules of water extract	37.1 ± 2.2	28.3 ± 1.9	21.5 ± 2.2
Capsules of alcohol extract	48.7 ± 1.9	35.2 ± 2.2	29.5 ± 2.8

The data presented in Table 2 confirmed the results of the previous study and showed the highest content of flavonoids in capsules produced on the basis of alcoholic extracts of meadowsweet from the Leningrad region, which averaged 48.7 mg / g capsules. The lowest content of flavonoids in the samples was found in capsules made on the basis of water extracts of meadowsweet from the Bashkir Republic, which averaged 21.5 mg / g capsules.

The loss of flavonoids from meadowsweet extracts during the encapsulation was 40–60%, depending on the raw materials and the extractant used, which is supposedly due to the substance’s oxidation during the process. The obtained results of the flavonoids content are correlated with the antioxidant activity of encapsulated preparations of meadowsweet and can exhibit various biological effects, including anticancer properties (Denev et al., 2014; Katanic et al., 2015; Bepalov et al., 2017).

The obtained results on the chemical composition of meadowsweet extracts are important because flavonoids have antioxidant activity and can exhibit various biological effects, including anti-carcinogenic properties (Oktyabrsky et al., 2009; Denev et al., 2014; Katanić et al., 2015; Bepalov et al., 2018). Pronounced antioxidant properties of meadowsweet extracts are shown on different models (Samardžić et al., 2018). In this study, extracts and encapsulated forms of meadowsweet contained concentrations of total flavonoids that suggest a possible oncoprotective effect.

Extractive BAS of meadowsweet were obtained in the form of micro- and nanosized capsules (Fig. 2) for the production of different functional foods.

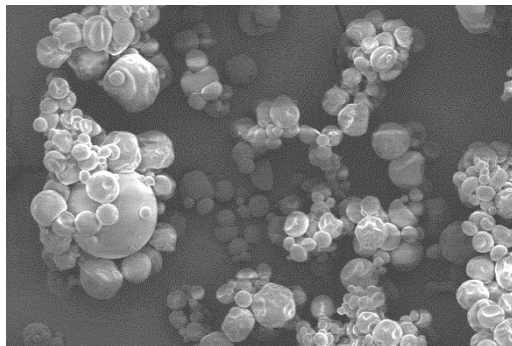


Figure 2. Micro- and nanosized capsules of meadowsweet BAS.

Evaluation of the structure of nano- and microcapsules of the meadowsweet BAS using a scanning electron microscope confirmed the particles sizes from 90 nm to 5 µm. The developed encapsulated form of meadowsweet extract for meat functional foods is presented in Fig. 3.

In this study, the possibility of producing a functional food product with the addition of the developed dry encapsulated meadowsweet BAS was considered on example of meat pate. Even though the physiological functionality of the developed encapsulated extracts is possible in the range from 1 to 4%, the decision was made to introduce the maximum dosage. Organoleptic evaluation of the pate with the addition of the encapsulated meadowsweet BAS in



Figure 3. Encapsulated form of meadowsweet extract for meat functional foods.

order to identify possible effects on the properties of the finished product was carried out. Table 3 shows the results of the organoleptic evaluation of the experimental pate and a control pate sample without adding the meadowsweet BAS.

Table 3. Organoleptic characteristics of the chicken pate

Descriptors	Control sample	Sample with the complex functional dry mixture
Appearance	pate with a clean, dry, evenly baked surface	the same
Consistency	easily smeared	the same
View on the cut	homogeneous, uniformly mixed mass of light beige	the same
Smell and taste	peculiar to this type of product, moderately salty and fatty with a creamy aftertaste, without foreign taste and smell, with a pronounced aroma	the same and a slight aroma of meadowsweet

Thus, the functional complex dry mixture as an ingredient in recipes of pate did not lead to a decrease in organoleptic characteristics and contributed to the enrichment with high content of meadowsweet BAS. Even though the encapsulated extracts have a yellow color, in the dosages used they did not have a strong coloring ability. Even with a physiologically high dosage of encapsulated extracts of 4%, their application did not change the color of the product as compared with the control sample without extracts. Perhaps this is due to the original beige color of the meat pate, in white milk and yogurt without fillers, the color could change more significantly.

To assess the industrial production of the developed product, an analysis of the cost of the meat product with the addition of the encapsulated meadowsweet BAS in comparison with the traditional pate (control sample) per a portion of the product (100 g of pate) was carried out. According to the results of a comprehensive calculation, it was established that the cost of a portion of the meat product with the addition of a complex functional dry mixture was 0.53 euros, which is 0.06 euros and 12.8% higher than the cost of a portion of traditional pate.

Improving the bioactive compound profile of food products is believed to elevate their cancer fighting properties (Vanamala, 2017). Fruit and vegetables are key components in the Mediterranean diet that provide health promoting effects, which mostly connected with flavonoids (Ortega, 2006). While it is not easy to increase fruit

and vegetable consumption in all vulnerable populations, developing functional food products and ingredients for their production can be one of innovative strategies to support increased consumption of bioactive compounds for cancer prevention. Flavonoids are often associated with the prevention of various forms of cancer with the help of food components (Terahara, 2015; Aghajanpour et al., 2017). Flavonoids are found in different types of common plant products such as citrus, parsley, broccoli, garlic, onion, blueberries, apples, tea, nuts, artichokes (Yao et al., 2004; Lattanzio et al., 2009). Thus, it is important to enrich the diet with flavonoids, including from more rare sources, such as red clover and meadowsweet (Kroyer, 2004; Vysochina et al., 2011). The found high content of flavonoids in the raw materials and encapsulated forms of extracts allow us to consider the developed ingredients as physiologically functional. The obtained results correspond with previous data on oncoprotective effect of plant flavonoids and extracts of this species (Lima et al., 2014; Ghasemi & Lorigooini, 2016; Bespalov et al., 2019). Thus, the developed encapsulated forms of meadowsweet extract are a promising ingredient for the creation of functional food products.

CONCLUSIONS

The phytochemical composition of alcoholic and water extracts of *Filipendula ulmaria* L. Maxim. from various regions of the Russian Federation showed that the flowers of the plant are rich in flavonoids. In addition, *F. ulmaria* exhibits antioxidant activity and anticancer properties according to present studies. This can be the basis for the assumption that the encapsulated extracted forms of meadowsweet can retain their properties in the composition of food. This study has shown that encapsulated extracts of meadowsweet can be incorporated into complex functional dry mixtures for food production with some loss in the content of flavonoids in the process of encapsulation. The experimental complex functional dry mixture is considered as an alternative to the existing one with some additional biological value. An assessment of the possibility of using the developed complex functional dry mixture in the composition of the meat product (pate), which proves the absence of any negative effect on the organoleptic properties of the finished product, was carried out. The calculation of the cost of the meat product with the complex functional dry mixture showed a slight increase in the cost of the final product compared to the traditional analogue. This study shows that encapsulated meadowsweet BAS can be used for inclusion in various food products, to ensure the functional properties of food and optimize the population's rations. However, the future studies are necessary on the content of meadowsweet BAS in food products during storage, as well as on their functional or health promoting properties in certain foods.

ACKNOWLEDGEMENTS. This research work was financially supported by the government of the Russian Federation, Grant RFMEFI58117X0020.

REFERENCES

- Aghajanpour, M., Nazer, M.R., Obeidavi, Z., Akbari, M., Ezati, P. & Kor, N.M. 2017. Functional foods and their role in cancer prevention and health promotion: a comprehensive review. *American journal of cancer research* 7(4), 740–769.

- Ahmed, M., Akter, M.S., Lee, J.-C. & Eun, J.-B. 2010. Encapsulation by spray drying of bioactive components, physicochemical and morphological properties from purple sweet potato. *LWT - Food Science and Technology* **43**(9), 1307–1312.
- Bespalov, V.G., Alexandrov, V.A., Vysochina, G.I., Kostikova, V.A. & Baranenko, D.A. 2017. The inhibiting activity of meadowsweet extract on neurocarcinogenesis induced transplacentally in rats by ethylnitrosourea. *Journal Neurooncol.* **131**, 459–467.
- Bespalov, V.G., Alexandrov, V.A., Semenov, A.L., Vysochina, G.I., Kostikova, V.A. & Baranenko, D.A. 2018. The inhibitory effect of (L.) Maxim. on colorectal carcinogenesis induced in rats by methylnitrosourea. *Journal of Ethnopharmacology* **227**, 1–7.
- Bespalov, V.G., Baranenko, D.A., Aleksandrov, V.A., Semenov, A.L., Kovan'ko, E.G. & Ivanov, S.D. 2019. Chemoprevention of Radiation-Induced Carcinogenesis Using Decoction of Meadowsweet (*Filipendula Ulmaria*) Flowers. *Pharmaceutical Chemistry Journal* **52**(10), 860–862.
- Bruneton, J. 1995. Pharmacognosy, Phytochemistry, Medicinal Plants. *Lavoisier Publishing*, **221**, 316–318.
- Choi, K.-O., Kim, D., Lim, J.D., Ko, S., Hong, G.-P. & Lee, S. 2019. Functional enhancement of ultrafine Angelica gigas powder by spray-drying microencapsulation. *LWT - Food Science and Technology* **101**, 161–166.
- Denev, P., Kratchanova, M., Ciz, M., Lojek, A., Vasicek, O., Blazheva, D., Nedelcheva, P., Vojtek, L. & Hyrs, P. 2014. Antioxidant, antimicrobial and neutrophil-modulating activities of herb extracts. *Biological activities of herbs* **61**(2), 359–367.
- Duke, J. 2001. *Handbook of Medicinal Herbs*. CRC Press, Boca Raton, FL, pp. 196–197.
- Dziejak, J.D. 1988. Microencapsulation and encapsulated ingredients. *Food Technology* **42**(4), 136–151.
- Ghasemi, S. & Lorigooini, Z. 2016. A review of significant molecular mechanisms of flavonoids in prevention of prostate cancer. *Journal of chemical and pharmaceutical sciences* **9**(4), 3388–3394.
- Gibbs, B.F., Kermasha, S., Alli, I. & Mulligan, N. 1999. Encapsulation in the food industry: A review. *International Journal of Food Science and Nutrition* **50**, 213–224.
- Hasler, A., Meier, B. & Sticher, O. 1989. HPLC analysis of 5 widespread flavonoid aglycones. *Planta Med.* **66**, 616–617.
- Katanić, J., Boroja, T., Stankovic, N., Mihailovic, V., Mladenovic, M., Kreft, S. & Vrvic, M.M. 2015. Bioactivity, stability and phenolic characterization of *Filipendula ulmaria* (L.) Maxim. *Food Funct.* **6**, 1164–1175.
- Korsun, V.F., Treskunov, K.A., Korsun, E.V. & Mizkonas, A. 2015. Medicinal plants in Oncology. *Guide to Clinical Phytotherapy* 431 pp. (in Russian).
- Kroyer, G.T. 2004. Red clover extract as antioxidant active and functional food ingredient. *Innovative Food Science & Emerging Technologies* **5**(1), 101–105.
- Lattanzio, V., Kroon, P.A., Linsalata, V. & Cardinali, A. 2009. Globe artichoke: a functional food and source of nutraceutical ingredients. *Journal of functional foods* **1**(2), 131–144.
- Lima, M.J., Sousa, D., Lima, R.T., Carvalho, A.M., Ferreira, I.C. & Vasconcelos, M.H. 2014. Flower extracts of *Filipendula ulmaria* (L.) Maxim inhibit the proliferation of the NCI-H460 tumour cell line. *Industrial Crops and Products* **59**, 149–153.
- Loksuwan, J. 2007. Characteristics of microencapsulated b-carotene formed by spray drying with modified tapioca starch, native tapioca starch and maltodextrin. *Food Hydrocolloids* **21**, 928–935.
- Oktyabrsky, O., Vysochina, G., Muzyka, N., Samoilo, Z., Kukushkina, T. & Smirnova, G., 2009. Assessment of anti-oxidant activity of plant extracts using microbial test systems. *J. Appl. Microbiol.* **106**, 1175–1183.

- Ortega, R.M. 2006. Importance of functional foods in the Mediterranean diet. *Public health nutrition* **9**(8A), 1136–1140.
- Samardžić, S., Arsenijević, J., Božić, D., Milenković, M., Tešević, V. & Maksimović, Z., 2018. Antioxidant, anti-inflammatory and gastroprotective activity of *Filipendula ulmaria* (L.) Maxim. and *Filipendula vulgaris* Moench. *J. Ethnopharmacol.* **213**, 132–137.
- Shahidi, F. & Han, X.Q. 1993. Encapsulation of food ingredients. *Critical Review of Food Science and Nutrition* **33**(6), 501–547.
- Shaldaeva, T.M., Vysochina, G.I. & Kostikova, V.A. 2018. Phenolic compounds and the antioxidant activity of certain species of the genus *Filipendula* Mill. (Rosaceae). *Vestnik VSU, Series: Chemistry. Biology. Pharmacy* **1**, 204–212 (in Russian).
- Shamshev, I., Selytskaya, O., Chermenskaya, T., Burov, V. & Roditakis, N. 2003. Behavioural responses of western flower thrips (*Frankliniella occidentalis* (pergande)) to extract from meadow-sweet (*Filipendula ulmaria* maxim.): Laboratory and field bioassays. *Archives of Phytopathology and Plant Protection* **36**, 111–118.
- Schulz, V., Hänsel, R. & Tyler, V.E. 1998. *Rational phytotherapy: a physicians' guide to herbal medicine*. Fully Rev. and Expanded, 4th ed. Springer, Berlin; New York, 304 pp.
- Terahara, N. 2015. Flavonoids in foods: a review. *Natural product communications* **10**(3), 521–528.
- Popescu, M.L., Istudor, V. & Parvu, C. 2000. Research on obtaining a preparation of external use with antimicrobial and anti-inflammatory activities. *Farmacia* **48**(3), 85–89.
- Vanamala, J. 2017. Food systems approach to cancer prevention. *Critical Reviews in Food Science and Nutrition* **57**(12), 2573–2588.
- Vysochina, G.I., Kostikova, V.A. & Vasfilova, E.S. 2016. Phenolic compounds of meadowsweet *Filipendula Ulmaria* (Rosaceae) and closely related taxa with different ecological confinement. *Flora of Asian Russia* **4**(24), 63–71 (in Russian).
- Vysochina, G.I., Kukushkina, T.A., Kotsupii, O.V., Zagurskaya, Y.V. & Bayandina, I.I. 2011. Flora of the forest-steppe zone of West Siberia as a source of biologically active compounds. *Contemporary Problems of Ecology* **4**(2), 202–211.
- Yao, L.H., Jiang, Y.M., Shi, J., Tomas-Barberan, F.A., Datta, N., Singanusong, R. & Chen, S.S. 2004. Flavonoids in food and their health benefits. *Plant foods for human nutrition* **59**(3), 113–122.
- Yoshiia, H., Soottitantawata, A., Liua, X.-D., Atarashia, T., Furutaa, T., Aishimab, S., Ohgawarab, M. & Linko, P. 2001. Flavor release from spray-dried maltodextrin/gum arabic or soy matrices as a function of storage relative humidity. *Innovative Food Science & Emerging Technologies* **2**, 55–61.
- Zabodalova, L., Ishchenko, T., Skvortcova, N., Baranenko, D. & Chernjavskij, V. 2014. Liposomal beta-carotene as a functional additive in dairy products. *Agronomy Research* **12**(3), 825–834.
- Zhdanov, V.A., Sobolev, I.S., Baranovskaya, N.V., Kolesnikova, E.A., Chernenkaya, E.V. & Yalaltdinova, A.R. 2016. Geochemical features of the elemental composition of meadowsweet (*Filipendula ulmaria* (L.) Maxim) in Kemerovo Oblast. *IOP Conference Series: Earth and Environmental Science* **43**(1), 012048.

Results of experimental investigations of a flexible active harrow with loosening teeth

V. Bulgakov¹, H. Kaletnik², I. Goncharuk², S. Ivanovs³ and M. Usenko⁴

¹National University of Life and Environmental Sciences of Ukraine, Heroiv Obrony 15, UA03041 Kyiv, Ukraine

²Vinnytsia National Agrarian University, Soniachna street 3, UA21008 Vinnytsia, Ukraine

³Latvia University of Life Sciences and Technologies, Liela street 2, LV-3001 Jelgava, Latvia

⁴Lutsk National Technical University, Lvivska street 75, UA43018 Lutsk, Volyn region, Ukraine

*Correspondence: semjons@apollo.lv

Abstract. Soil tillage processes significantly affect the growth of cultivated plants; therefore, improvement of various designs and combinations of ploughs is still an actual practical and scientific task. This paper presents investigations of the design of a soil tillage machine consisting of three plough bodies equipped from the lateral side with a module with a flexible active harrow driven by a support wheel. The technological process of tillage by this machine is carried out in such a way that the module of the flexible active harrow is installed at a certain depth of soil tillage. The purpose of this work is an experimental comparative investigation of the quality indicators of the work of a design of the soil tillage working body with a flexible active harrow having loosening teeth. In the process of comparative experimental investigations of the operation of ploughs with a standard flexible harrow and an experimental active harrow having loosening teeth, the soil lumpiness (characterising the quality of crumbling) and water permeability of the obtained soil structure were estimated. An experimental model of this working tool was tested under the production conditions, and it showed advantages of loosening and crumbling the soil compared to the conventional harrows. This can be explained by the fact that the harrow tines, freely mounted on the axes of its links, ensure their oscillatory movements when moving in two different planes, thereby creating conditions for more intense soil disintegration.

Key words: soil tillage, active harrow, harrow teeth, crushing, water resistance, structure.

INTRODUCTION

Despite the development of modern methods for killing weeds, mechanical tillage is the most important operation in the system of crop production (Valainis et al., 2014; Tamm et al., 2016; Milkevych et al., 2018). The first operation in the complex of cultivation operations of the agricultural crops are the main and the presowing tillage. Therefore the quality indicators of the performance of these operations determine also the quality indicators of further development of the plants.

Improvement of the technology and technical means of soil tillage applied to the soil and climatic features of regions is still an urgent task (Crittenden et al., 2015).

At present, in a number of regions, along with the combined machines for the main and the presowing tillage, ploughs with disc and with tine harrows are widely used (Alexandrjan, 1985; Bezdolny, 1996; Bulgakov et al., 2018). Such machines more intensely cultivate the soil under various working conditions. Also known are the designs of flexible harrows, which are more adapted to the field microrelief and have other advantages (Usenko et al., 2005; Adamchuk et al., 2016). Nevertheless, some authors note that combinations of ploughs with the known designs of flexible harrows still have a number of disadvantages due to the relatively low degree of crumbling on heavy soils, etc. oscillate because their teeth are not able to carry out constant oscillatory movements in the treated layer (Kanarev, 1983; Usenko et al., 2005; Segun, 2012). Therefore, a task was set to improve the design of harrows with an aim to improve the quality of treatment on heavy soils and to determine the comparative performance indicators.

The most important indicators that characterise the tillage quality of soil with harrows are the lumpiness and the water resistance of its structure (Dosphehov, 1985). In the structured soil packing of the particles is loose, capillary gaps predominate inside the lumps, and between the lumps there are large, non-capillary gaps; water is quickly distributed in the aggregates, the gaps between which are filled with air. In such a soil, water and air are simultaneously present in a sufficient quantity; it is rich in nutrients, available to the plants. The agronomically valuable lumpy-granular structure gives the soil a loose structure, which facilitates seed germination and spreading of the plant roots, as well as reduces the energy costs of mechanical tillage (Dosphehov, 1985; Kuht ae al., 2012; Valainis et al., 2014).

The purpose of this work is a comparative experimental investigation of the quality indicators of the operation of a new design of a tillage working tool with a flexible active harrow having loosening teeth.

MATERIALS AND METHODS

As a result of the preliminary investigations and design developments (Adamchuk et al., 2016), an experimental plough was made, equipped with a flexible active harrow having loosening teeth for minimal soil tillage (Fig. 1).

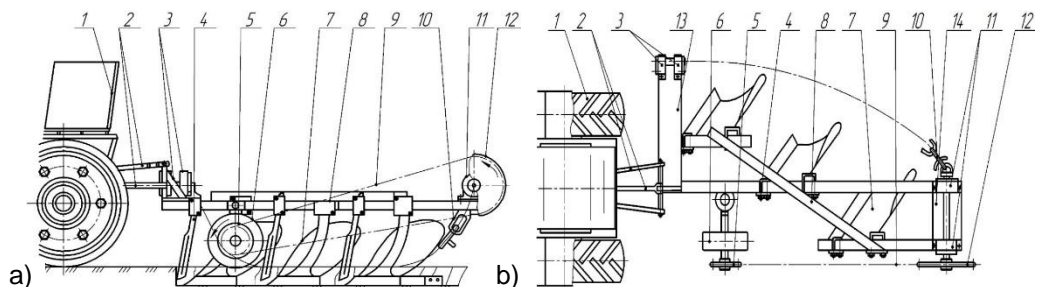


Figure 1. A plough, equipped with a flexible harrow driven by a support wheel (a – a side view; b – a top view): 1 – the aggregating tractor; 2 – the hitch mechanism of the tractor; 3 – the frontal support of the flexible harrow; 4 – the knives; 5 – the driving sprocket; 6 – the supporting wheel; 7 – the plough bodies; 8 – the main beam; 9 – the driving chain; 10 – a chain of the flexible harrow with the loosening teeth; 11 – the rear chain support; 12 – the driven sprocket; 13 – the frontal part of the frame; 14 – the rear part of the frame.

The design of a separate flexible harrow module with the loosening teeth is shown schematically in Fig. 2. It consists of links 1 of the chain, a pair of the basic working teeth 2, and a pair of additional teeth 3, both the basic pair of teeth and the additional pair being fixed to the sleeve 4 installed with the possibility of angular deviations and freely mounted on the axle 5, but the free ends of the axle 5 are connected by means of fastening elements 6 to the link 1 of the chain; the sleeve 4 is equipped with a fastening element 7 that is used depending on the type of the soil and its humidity.

The technological process of soil tillage by means of a flexible harrow, equipped with a three-body plough, is carried out as follows. The tractor 1 is aggregated with a plough having the plough bodies 7 installed at a predetermined depth of the basic tillage. The supporting wheel 6 moves along the untilled soil surface. The flexible harrow in the form of a chain with modules 10 moves on the side and behind the plough bodies 7 at a certain depth.

In addition, rotation from the support wheel 6 is transmitted to its modules with the loosening teeth (the torque is transmitted through the driving sprocket 5, the driven chain 9 and the driven sprocket 12 to the chain of the flexible harrow 10). Thus the chain of the flexible harrow 10 is forcibly continuously rotated, and, as a result, it crushes and loosens the solid soil masses remaining after the basic tillage by the plough bodies 7. The efficiency of the loosening teeth 2 and 3 (Fig. 2) is especially evident when working in heavy and excessively wet soils. Besides this, an additional pair of teeth 3 (Fig. 2) self-cleans the chain of the flexible harrow 10 from the adhered soil and plant residues. In case this plough is applied in light and dry soils, the additional pair of teeth 3 may not be used. In this case, the additional pair of teeth 3 is rigidly fixed inside the links of the chain 1 by means of the fastening elements 7.

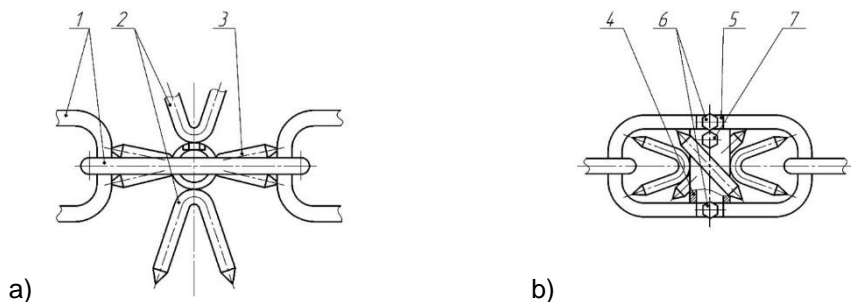


Figure 2. A flexible harrow module with the loosening teeth (a – a side view; b – a top view): 1 – links of the chain; 2 – the basic loosening teeth; 3 – the additional teeth; 4 – a rotary sleeve; 5 – the axle; 6 – fastening elements of the basic teeth; 7 – fastening elements of the additional teeth.

In the process of comparative experimental investigations of the operation of ploughs with a standard flexible harrow BP-3 and an experimental active harrow having loosening teeth, the soil lumpiness (characterising the quality of crumbling) and water permeability of the obtained soil structure were estimated (Bezdolny, 1995; Adamchuk et al., 2016). The research was conducted in the soil tillage zone by harrows in layers to the depth of up to 9–10 cm with the measurement of indicators on three backgrounds of the soil moisture (W): 18%, 22% and 25%.

The research was carried out using standard methods of the field experiments and processing of their results on the PC (Dospheov, 1985, Alexandrjan, 1985; Adamchuk

et al., 2016). Lumpiness or the percentage of the agronomically valuable fraction 0.25–10 mm characterises the crushing degree of the soil by the working bodies, and its condition for growing plants.

Water resistance of the lumps, not flooded out for 10 minutes, is taken as 100%. The stability of the aggregates against the destructive action of water (g , %) is determined by the formula:

$$g = \frac{(P_1K_1 + P_2K_2 + \dots + P_{10}K_{10})}{A} 100\% \quad (1)$$

where P_1, P_2, \dots, P_{10} – the number of aggregates disintegrated in the respective minute; K_1, K_2, \dots, K_{10} – correction factors for the respective minutes; A – total number of aggregates taken for analysis.

Within 10 minutes, with an interval of 1 min, completely disintegrated aggregates are counted. Since disintegration of the aggregates in water occurs at different time, then, to characterise the water resistance degree of the structure, the Kachinsky correction factor is introduced into the calculations, which is (%) for every minute: for the 1st, 5; 2nd – 15; 3rd – 25; 4th – 35; 5th – 45; 6th – 55; 7th – 65; 8th – 75; 9th – 85; 10th – 95.

RESULTS AND DISCUSSION

It has been established by our previous investigations and the data of other researchers that on the soils of the steppe zone of Ukraine the optimum percentage of the soil loosening quality on slopes with a steepness of up to 12° should be 45...50%, with the initial soil lumpiness before starting work (after tillage by the plough bodies) – 30...35% (Adamchuk et al., 2016).

The results of the experimental research of the soil crumbling quality using a plough with standard flexible harrows BP-3 and experimental active flexible harrows are respectively reflected in Fig. 3 and Fig. 4.

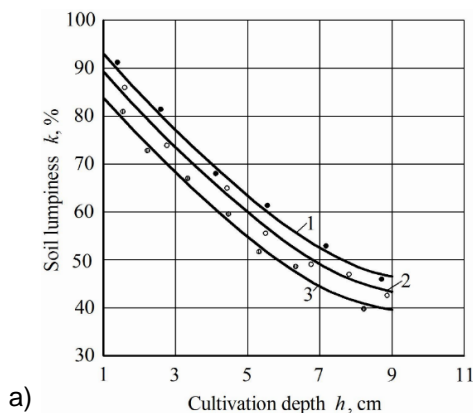


Figure 3. Dependence of the soil lumpiness k upon the depth of its tillage h at various soil humidities W while working with a standard flexible harrow: 1 – $W = 18\%$; 2 – $W = 22\%$; 3 – $W = 25\%$.

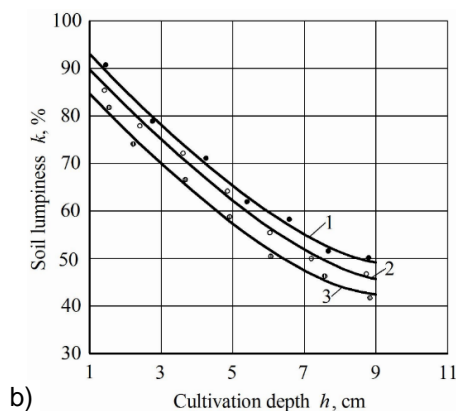


Figure 4. The value of the soil lumpiness k depending on the depth of its tillage h at different soil humidities W while working with an experimental flexible harrow: 1 – $W = 18\%$; 2 – $W = 22\%$; 3 – $W = 25\%$.

As it is evident from the graphs, when the depth of tillage is increased, the degree of crumbling of the soil decreases. Increased humidity also reduces the degree of crumbling of the soil. However, when using standard flexible harrows, the soil lumpiness within the required limits (40...45%) is ensured only at a depth of 4...6 cm. At other depths the value of the loosening quality differs from the required (optimal) agrotechnical requirements.

The value of indicators (Fig. 3) of statistical data processing for soil crushing in the experiments with standard flexible harrows was:

for $W = 18\%$: $\bar{k} = 64.4\%$, $\sigma = \pm 1.4\%$, $V = 2.17\%$,

for $W = 22\%$: $\bar{k} = 61.3\%$, $\sigma = \pm 1.7\%$, $V = 2.77\%$,

for $W = 25\%$: $\bar{k} = 60.2\%$, $\sigma = \pm 1.2\%$, $V = 2.00\%$.

Where \bar{k} – the average value of the indicator; σ – standard deviation; V – the coefficient of variation;

The value of indicators (Fig. 4) of statistical data processing for soil crushing in the experiments using a flexible harrow with the loosening teeth was:

for $W = 18\%$ – $\bar{k} = 69.2\%$, $\sigma = \pm 1.9\%$, $V = 2.75\%$,

for $W = 22\%$ – $\bar{k} = 67.5\%$, $\sigma = \pm 1.7\%$, $V = 2.52\%$,

for $W = 25\%$ – $\bar{k} = 63.7\%$, $\sigma = \pm 1.4\%$, $V = 2.2\%$.

As the curves of the graph show, the soil lumpiness within the required limits 40...45% – is ensured by an experimental harrow at the required tillage depth of 8...9 cm.

At other depths the quality of loosening changes (as the tillage depth increases, the quality of loosening decreases), and its values differ from the optimal ones.

The presence and degree of the erosion processes, especially on slopes, determines the water resistance of the soil structure. Compliance of this indicator with the agrotechnical rules allows avoiding or significant reduction of the negative effect of the water and wind erosion upon the soil.

For the conditions of the Ukrainian chernozem an important agronomic characteristic of the soil is the water resistance of its structure, i.e. the formation of solid, water non-eroded particles. Such a structure is formed as a result of the fastening of the mechanical elements by organomineral colloids that are irreversibly coagulated. Soils with a water-resistant structure have a water-air regime that is favourable for the development of plants, good mechanical properties, and so on. Soils that do not have a water-resistant structure quickly flood out, become impermeable to water and air, and, while drying, they crack into large blocks.

The graphs show the dependences of the water resistance of the soil structure tilled by a plough aggregate with a standard (Fig. 5) and an experimental active flexible harrow (Fig. 6).

The value of indicators (Fig. 5) of the statistical data processing for the water resistance of the obtained soil structure in the experiments using standard flexible harrows was:

for $W = 18\%$ – $\bar{g} = 20.4\%$, $\sigma = \pm 0.4\%$, $V = 1.96\%$,

for $W = 22\%$ – $\bar{g} = 20.1\%$, $\sigma = \pm 0.4\%$, $V = 1.99\%$,

for $W = 25\%$ – $\bar{g} = 19.8\%$, $\sigma = \pm 0.35\%$, $V = 1.78\%$.

Fig. 6 shows graphs of the water resistance of the soil structure tilled by a plough aggregate with an experimental flexible harrow.

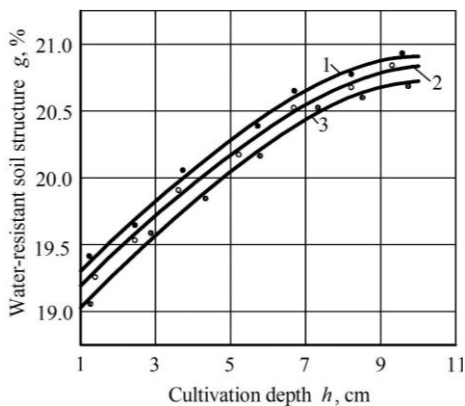


Figure 5. Dependence of the water resistance of the soil structure upon the tillage depth h at various soil moistures W when operating with a standard flexible harrow: 1 – $W = 18\%$; 2 – $W = 22\%$; 3 – $W = 25\%$.

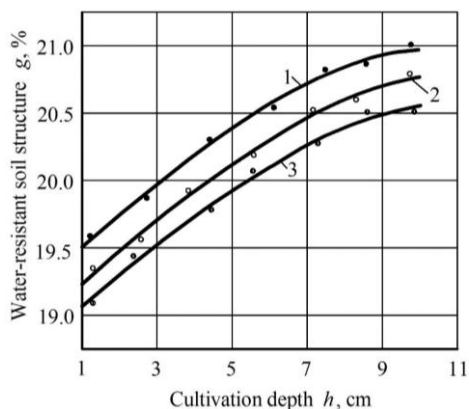


Figure 6. Dependence of the water resistance of the soil structure g upon the tillage depth h at various soil moistures W when working with the experimental active flexible harrow: 1 – $W = 18\%$; 2 – $W = 22\%$; 3 – $W = 25\%$.

The value of indicators (Fig. 6) of the statistical processing of data for the water resistance of the obtained soil structure in experiments using an experimental flexible harrow was:

- for $W = 18\%$ - $\bar{g} = 21.3\%$, $\sigma = \pm 1.1\%$, $V = 5.16\%$,
- for $W = 22\%$ - $\bar{g} = 20.7\%$, $\sigma = \pm 0.9\%$, $V = 4.35\%$,
- for $W = 25\%$ - $\bar{g} = 20.1\%$, $\sigma = \pm 0.8\%$, $V = 3.98\%$.

As the curves of the graph show, the water resistance of the soil structure within the required limits – 20...22% is provided by the experimental harrow working at the required depth of 9...10 cm. At other depths the value of this indicator changes (as the tillage depth increases, it increases), but its value somewhat differs from the required one by the agrotechnical rules. However, the experimental harrow provides an optimum value of the water resistance index of the soil structure in wider ranges than with the standard harrow.

CONCLUSIONS

The use of flexible active harrows on heavy soils in combination with a plough driven by the plough copying wheel, provides constant oscillating movements of the teeth in two planes, which intensively destroys large clumps and creates a more optimal soil structure. In contrast to the standard flexible harrow, the use of a flexible active harrow with the plough, 1.5 times (up to 9–10 cm) improves the soil layer with optimal lumpiness and a wider range of optimum soil water resistance.

REFERENCES

- Adamchuk, V., Bulgakov, V. & Kaletnik, H. 2016. *Small agricultural machines. Construction and theory*. Monograph. Agricultural Science, Kiev, 292 pp. (in Ukrainian).
- Alexandrjan, K. 1985. *Machines for mountain slopes and against soil water erosion*. Moscow, Nauka, 191 pp. (in Russian).
- Bezdolny, N. 1995. *Device for tillage*. A Patent RU 20445144.
- Bezdolny, N. 1996. *Agricultural aggregate*. A Patent RU 2046579.
- Bulgakov, V., Ivanovs, S., Bandura, V. & Ihnatiev, Y. 2018. Experimental investigation of harrow with spring teeth for cultivation of sugar beets. In: *Proceedings of International scientific conference Engineering for rural development* **17**, Jelgava, pp. 215.–220.
- Crittenden, S., Poot, N., Heinen, M., Van Balen, D. & Pulleman, M. 2015. Soil physical quality in contrasting tillage systems in organic and conventional farming. *Soil and Tillage Research* **154**, 136–144.
- Dospehov, B. 1985. *Methodology of field experiments*. Nauka, Moscow, 351 pp. (in Russian).
- Kanarev, F. 1983. *Rotary tillage machines*. Mashinostrojenie, Moscow, 144 pp. (in Russian).
- Kuht, J., Reintam, E., Edesi, L. & Nugis, E. 2012. Influence of subsoil compaction on soil physical properties and on growing conditions of barley. *Agronomy Research* **10**(2), 329–334.
- Milkevych, V., Munkholm, L., Chen, Y. & Nyord, T. 2018. Modelling approach for soil displacement in tillage using discrete element method. *Soil and Tillage Research* **183**, 60–71.
- Segun R. Bello. 2012. *Agricultural Machinery & Mechanization*. Sustainable Agriculture Group (SAG) Federal College of Agriculture, 480001, Ishiagu Nigeria, 448 pp.
- Tamm, K., Nugis, E., Edesi, L., Lauringson, E., Talgre, L., Viil, P., Plakk, T., Vosa, T., Vettik, R. & Penu, P. 2016. Impact of cultivation method on the soil properties in cereal production. *Agronomy Research* **14**(1), 280–289.
- Usenko, M., Ponikarchuk, A., Bozhidarnik, V., Mirchuk, V., Kuzhel, E. & Fesenko O.A. 2005. *Flexible rotary harrow module with tearing teeth*. Patent UA 74089.
- Valainis, O., Rucins, A. & Vilde, A. 2014. Technological operational assessment of one pass combined agricultural machinery for seedbed preparation and seeding. In: *Proceedings of International scientific conference Engineering for Rural Development* **13**, Jelgava, 37–43.

Research of the movement of agricultural aggregates using the methods of the movement stability theory

V. Bulgakov¹, H. Kaletnik², T. Goncharuk², A. Rucins^{3,*}, I. Dukulis³ and S. Pascuzzi⁴

¹National University of Life and Environmental Sciences of Ukraine, Heroyiv Oborony street 15, Kyiv UA 03041, Ukraine

²Vinnitsia National Agrarian University, Soniachna street 3, UA21008 Vinnitsia, Ukraine

³Latvia University of Life Sciences and Technologies, Liela street 2, Jelgava, LV-3001, Latvia

⁴University of Bari Aldo Moro, Via Amendola, 165/A, IT70125 Bari, Italy

*Correspondence: adolfs.rucins@llu.lv

Abstract. The theory of the movement stability is of crucial practical importance for mobile agricultural machines and machine aggregates, since it determines how qualitative and stable their performance is in a particular technological process. It is especially urgent To ensure stable movement for operation at high speeds of contemporary agricultural aggregates. The aim of this investigation is detailed examination of criteria for the stability assessment of a mechanical system used in agriculture, enabling their wide application in order to study the performance of the system in the case when it is affected by random forces that were not taken into account in the original model. The considered calculation methods and examples of their application make it possible to evaluate the performance of complex dynamic systems without numerical solution of complicated differential equations of the movement in the presence of external disturbances. The considered example of the stability determination of the movement of a trailed cultivator showed that this research method can be successfully used for practical purposes. Besides, a differential equation of disturbed movement has been composed for an actually symmetrical trailed agricultural machine with a particular mass, which moves at a constant forward speed under the impact of summary resistance force running along the symmetry axis of the cultivator and is applied at its centre of gravity. Reduced to normal Cauchy form, this equation was solved on the PC, which made it possible to determine immediately the conditions for stable movement of the trailed cultivator.

Key words: agricultural aggregates, movement stability, theoretical research.

INTRODUCTION

The movement stability is of great practical importance for the agricultural machinery, especially for agricultural aggregates (Schwabik, 1992; Bulgakov et al., 2017; 2018). It is widely applied in scientific research and in the calculations and design of automatic control systems, navigation instruments, airplanes, spacecraft, various kinds of engines (Matignon, 1996; Zaslavsky & Edelman, 2004).

The concept of stability in a broad sense is interpreted as the ability of an object to maintain its state, not submitting to earlier unforeseen external disturbances. This concept occupies one of the most important places in physics and technology. Depending on the nature of a specific process to be considered, there are also various implementations of this concept. This particularly concerns investigations of the movement stability of a number of mechanical systems for agricultural purposes for which observance of the stability conditions allows one to ensure high-quality execution of technological processes.

In the works by (Zhukovsky, 1948; Merkin et al., 1997), a number of general questions about the movement stability are considered. The foundations of the stability theory are outlined in the work by A.M. Lyapunov 'A General Problem of the Movement Stability', published in 1892 (Lyapunov, 1980; Momani & Hadid, 2004). Lyapunov presented a precise definition of the movement stability; he obtained a complete solution for the problem of stable movement; he proposed two methods for the investigation of the movement stability characterised by simplicity and efficiency.

From a physical point of view the equilibrium state is called stable if at sufficiently small initial deviations and velocities during the movement the system does not go beyond the limits of an arbitrarily small environment of the equilibrium state, while having arbitrarily small velocities. An elementary example is the physical pendulum. In the lower vertical position, it has stable equilibrium (after a series of vibrations it returns to its original rest position). In the upper vertical position the physical pendulum occupies an unstable equilibrium: with an arbitrarily small deviation it will move, moving towards a stable lower position.

In our time Lyapunov's methods are deepened; new application areas are emerging, in which general methods are being developed for studying the movement stability of individual broad classes of systems: automatic regulation systems, controlled systems, etc. (Matignon, 1996; Zaslavsky & Edelman, 2004).

The wide application of the theory of automatic control to modern agricultural machines and aggregates determines the creation of research methods ensuring the movement stability of the systems, which is one of the main tasks of this science. Yet, regardless of this, such investigations have not been developed to a sufficient degree in the field of soil tillage mechanics in which the mechanical systems of agricultural machines and machine aggregates should ensure high-quality execution of technological operations.

Consequently, a need arises to solve a very important scientific problem how to expand possibilities for an accurate analytical study of the movement stability of complex multi-mass mechanical systems, such as agricultural machines and aggregates since they are under constant impact of external disturbing influences. Therefore, in-depth consideration of the methods of studying the stability of movement, reduction of the basic assumptions of the classical theory of the movement stability to their specific application for the research of agricultural machines will help to improve further their dynamic, kinematic and design parameters.

Purpose of the research - to determine the criteria for the assessment of the movement stability of agricultural machines and aggregates which will be most efficient for the study of the plane-parallel movement of a trailed cultivator and the oscillations of a self-propelled tool frame in the longitudinal-vertical plane.

MATERIALS AND METHODS

The investigations have been carried out using methods of the theory of the movement stability, the theory of agricultural machines, as well as theoretical mechanics and higher mathematics (Halanay, 1966). There are used methods of the classical theory of the movement stability, based on the methods of constructing, solving and studying the systems of differential equations for the movement of agricultural machines and aggregates. Besides, there are considered differential equations of perturbed movement, and from them, by integrating in a closed form, the movement of the considered agricultural machine or aggregate is evaluated as stable or unstable. There are also used methods for estimating the movement stability without solving the systems of differential equations of the movement when finding the corresponding stability criteria. There are methods applied to linearise the differential equations of perturbed movement, as well a method of constructing special Lyapunov functions, which does not require solving these equations; in this case only the roots of the characteristic equations are investigated.

In order to achieve successful theoretical study of the movement stability of a concrete agricultural machine, it is necessary to consider and specify some general provisions for the stability of mechanical systems (Hale & Verduyn Lunel, 1993).

Sufficient conditions for the equilibrium stability of a system are reflected by the Lagrange – Dirichlet theorem (Malkin, 1996): ‘If in the equilibrium state the potential energy of a holonomic stationary system, being in the field of conservative forces, has an isolated minimum, then this equilibrium state is stable’.

For a conservative system, there is a law of mechanical energy conservation in force:

$$T_0 + \Pi_0 = T + \Pi \quad (1)$$

where T_0, Π_0, T, Π – the kinetic and potential energy in the state of equilibrium and at disturbance. Since always $T \geq 0$, then from expression (1) we have

$$T = T_0 + \Pi_0 - \Pi \geq 0 \quad (2)$$

From where

$$\Pi \leq T_0 + \Pi_0 \quad (3)$$

Inequalities (2) and (3) show that the movement of the system after its deviation from the equilibrium position occurs in the vicinity of the equilibrium position. Increase in the potential energy is limited by inequality (3) so much that it will be one of the values of the potential energy in the vicinity of the equilibrium position. Based on expression (2), we can assume that according to the indicated initial conditions the speeds of all points of the system are limited by the module: when T_0 and Π_0 decreasing to zero, T and Π also approach zero.

The Lagrange-Dirichlet theorem provides only sufficient conditions for the stability of the equilibrium state. The solution of the problem of the equilibrium instability of a conservative system is based on two well-known A.M. Lyapunov’s theorems (Lyapunov, 1980) on the equilibrium instability. The essence of the Lyapunov theorem on equilibrium instability is that instability takes place if:

1) the potential energy does not have a minimum that can be established by the terms of the second order in the layout of the potential energy in the Maclaurin series;

2) the potential energy has a maximum, and this can be established by the terms of the lowest order of smallness included in the Maclaurin series.

As it is known from the course of analytical mechanics, the expression of potential energy for a holonomic stationary system can be obtained in the quadratic form as a function of generalised coordinates:

$$\Pi = \frac{1}{2} \sum_{k=1}^N \sum_{j=1}^N C_{kj} q_k q_j \quad (4)$$

where C_{kj} – generalised stiffness coefficients (coefficients of the Maclaurin series); q_1, \dots, q_N – generalised coordinates of a mechanical system.

In expression (4) it is taken into account that the generalised coordinates and the potential energy in the equilibrium position are zero ($q_j = 0$; $\Pi(0) = 0$). In addition, the generalised forces in the equilibrium position are also equal to zero:

$$\left(\frac{\partial \Pi}{\partial q_1} \right)_0 = \left(\frac{\partial \Pi}{\partial q_2} \right)_0 = 0 \quad (5)$$

Since in the equilibrium position the potential energy is zero ($\Pi(0) = 0$), then it has a minimum in this position if $\Pi(\bar{q})$ is explicitly a positive function. The sign of a quadratic form is determined by Sylvester's theorem (Malkin, 1996).

For a positive-definite quadratic form it is necessary and sufficient that all the main diagonal minors of the matrix of a quadratic form be positive.

Let us write a matrix of coefficients of expression (4):

$$\begin{vmatrix} C_{11} & C_{12} & C_{13} & \dots & C_{1N} \\ C_{21} & C_{22} & C_{23} & \dots & C_{2N} \\ C_{31} & C_{32} & C_{33} & \dots & C_{3N} \\ \dots & \dots & \dots & \dots & \dots \\ C_{N1} & C_{N2} & C_{N3} & \dots & C_{NN} \end{vmatrix} \quad (6)$$

Let us create the main diagonal minors of the matrix (6):

$$\Delta_1 = C_{11}, \quad \Delta_2 = \begin{vmatrix} C_{11} & C_{12} \\ C_{21} & C_{22} \end{vmatrix}, \quad \Delta_3 = \begin{vmatrix} C_{11} & C_{12} & C_{13} \\ C_{21} & C_{22} & C_{23} \\ C_{31} & C_{32} & C_{33} \end{vmatrix}, \dots, \quad \Delta_N = \begin{vmatrix} C_{11} & \dots & C_{1N} \\ \dots & \dots & \dots \\ C_{N1} & \dots & C_{NN} \end{vmatrix}. \quad (7)$$

According to Sylvester's criterion the quadratic form is positive-definite, and hence there will be a minimum of potential energy in the equilibrium position if the main diagonal minors of the coefficient matrix are positive:

$$\Delta_1 > 0, \quad \Delta_2 > 0, \quad \dots, \quad \Delta_N > 0; \quad (8)$$

The movement stability of a mechanical system, for example, a car, an airplane, a projectile, etc., depends on the acting forces and the initial conditions of the movement (coordinates and velocities of the points of the system at the starting moment the movement). Knowing the forces and initial conditions, one can theoretically calculate how the mechanical system will move. A movement that agrees with the calculation is called undisturbed (Samoilenko & Perestyuk, 1995).

Due to certain inaccuracy in the measurement of the initial conditions their actual values, as a rule, differ from the calculated ones. Besides, the mechanical system during its movement may occur under random influences of various forces, which also equivalently change the initial conditions (Schwabik, 1984). Deviation of the initial

conditions arising because of a different reason, is called the initial disturbance, and the movement that the mechanical system performs in the presence of disturbances is called a disturbed movement. As a result of the above-mentioned, the following definition can be given: ‘If at sufficiently small initial disturbances any of the characteristics of the movement during the whole time differs little from the value that it should have during the undisturbed movement, then the movement of the system with respect to this characteristic is called stable’. The conditions under which the movement of a mechanical system is stable are called stability criteria. There are such kinds of stability: the stability of the equilibrium position and the stability of the movement.

Next let us consider the problem of the movement stability and give a definition for the stability of a mechanical system (Federson & Schwabik, 2006). Suppose that the motion of a mechanical system is described in the Cauchy form by a system of differential equations in the following way:

$$\frac{dy_k}{dt} = Y_k(t, y_1, y_2, \dots, y_n), \quad k=1, 2, \dots, n, \quad (9)$$

where y_k – some parameters that are connected with the movement, for example, coordinates, velocity projections, with the initial conditions at $t = 0$, equal to:

$$y_k(t_0) = y_{k0}, \quad k=1, 2, \dots, n. \quad (10)$$

Let a certain solution of system (9) corresponds to some fixed initial conditions (10):

$$y_k = f_k(t), \quad k=1, 2, \dots, n, \quad (11)$$

which describes a predetermined movement, but we may not know this movement because of the impossibility of integration.

Solution (11) that satisfies the initial conditions (10) and describes the predetermined movement is called an undisturbed movement of the mechanical system.

Further let us assign to the initial conditions y_{k0} some small increments $\delta_k, k = 1, 2, \dots, n$ behind the module, which are called the initial disturbances. Let the new partial solution of system (9) correspond to the new initial value $y_{k_1} = y_{k_0} + \delta_k$:

$$y_k = \varphi_k(t), \quad k=1, 2, \dots, n. \quad (12)$$

Solution (12) obtained taking into account the initial disturbances δ_k , and the respective movement of the system is called a disturbed movement.

Proceeding from solutions (11) and (12), we define their increments:

$$\delta_{y_k} = \varphi_k(t) - f_k(t) = u_k(t), \quad k=1, 2, \dots, n, \quad (13)$$

which are called variations of the movement parameters.

Let us consider the movement in coordinates u_1, u_2, \dots, u_n . In the stability theory space u_1, u_2, \dots, u_n is called the phase space, the coordinates - the phase coordinates, and their totality, which determines a certain state of the system, which is investigated - the phase of the system, the coordinates u_k are the phase coordinates, and their totality that determines a certain state of the investigated system is the phase of the system.

Any undisturbed movement is represented in the coordinate system u_1, u_2, \dots, u_n by a fixed point $M_0(0, \dots, 0)$ which coincides with the origin of the coordinates (all $u_k \equiv 0$). Point M_0 is called the equilibrium point of the system. The totality of values $u_1(t), \dots, u_n(t)$ at an arbitrary point of time t determines the respective phase state or

phase of the system. The geometric interpretation of the change in the phase coordinates determines the phase path L_k of the depicted point M_k in n -dimensional space u_k with the origin at point M_0 that corresponds to the origin of coordinates during the undisturbed movement. Proceeding from the above mentioned considerations, we denote the movement stability according to Lyapunov (Lyapunov, 1980).

If to an arbitrarily predetermined positive number ε , however small it may be, a second positive number $\delta = \delta(\varepsilon)$ can be put in correspondence, such that at any initial disturbances:

$$\delta_1 = u_1(t_0), \delta_2 = u_2(t_0), \dots, \delta_n = u_n(t_0), \tag{14}$$

which satisfy at inequalities $t = t_0$:

$$|u_1(t_0)| \leq \delta, |u_2(t_0)| \leq \delta, \dots, |u_n(t_0)| \leq \delta, \tag{15}$$

for all $t = t_0$ the following inequalities are fulfilled:

$$|u_1(t_0)| < \varepsilon, |u_2(t_0)| < \varepsilon, \dots, |u_n(t_0)| < \varepsilon, \tag{16}$$

this undisturbed movement is called stable.

In a flat phase subspace (u_1, u_2) this definition can be given a geometric interpretation (Fig. 1). The phase path L_1 of point M_1 belongs to steady movement.

A separate group of stable movements is formed from asymptotically stable movements which can be defined in this way. If the undisturbed movement of the system is stable and, in addition, any disturbed movement at sufficiently small initial disturbances tends to an undisturbed movement, i.e. if then such an undisturbed movement is called an asymptotically stable movement (path L_3 of point M_3 in Fig. 1).

$$\lim_{t \rightarrow \infty} \sum_{k=1}^n u_k^2(t) = 0, \tag{17}$$

In expression (17), the sum of squares of the phase coordinates u_k is taken as a measure of deviations of the disturbed movement from the undisturbed one. If the movement parameters of the system do not satisfy this definition, then such a movement is unstable (the phase path L_2 of point M_2 on (Fig. 1).

From the geometrical point of view conditions (17) are understood in the following way: at asymptotic stability the depicted point M of the phase path, without going beyond the boundaries of the radius sphere ε , must approach unlimited to the origin of coordinates 0 (line L_3 of point M_3 in Fig. 1). This means that the physical system, the movement of which is investigated, is trying to return to its original balanced state.

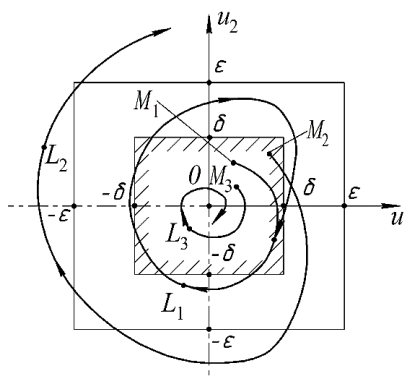


Figure 1. A scheme to the geometric interpretation of the movement stability of a mechanical system.

The peculiarities of determining the movement stability according to Lyapunov:

- disturbances are considered small;
- only initial conditions are subject to disturbances, i.e. at a certain point in time an instantaneous change in the movement parameters of the system takes place, after which its disturbed movement occurs under the action of the previous forces;
- the movement stability is studied in an infinite period of time.

In order to investigate the disturbed movement in accordance with its definition in the system of phase coordinates u_1, u_2, \dots, u_n , it is appropriate to reduce differential equations (9) to new variables $\delta y_k(t) = u_k(t)$, where $k = 1, \dots, n$. Substituting the parameters of the disturbed movement $\varphi_k = f_k + u_k$ into equation (9), we obtain a new system of equations:

$$\begin{aligned} \dot{u}_k &= Y_k(t, \varphi_1, \dots, \varphi_n) - Y_k(t, f_1, \dots, f_n) = \\ &= Y_k(t, f_1 + u_1, \dots, f_n + u_n) - Y_k(t, f_1, \dots, f_n) = \\ &= U_k(t, u_1, \dots, u_n), \quad k = 1, \dots, n, \end{aligned} \quad (18)$$

In the theory of the movement stability equations (18) are called the differential equations of the disturbed movement.

To each disturbed movement of the investigated object there corresponds a certain partial solution of system (18). It is known that zero values of phase coordinates $u_k(t)$ correspond to any undisturbed movement, i.e. a trivial solution $u_1 = u_2 = \dots = u_n = 0$ of system (18), which it must have. For this purpose it is necessary that functions $U_k(t, u_1, \dots, u_n)$ change into zero at $u_1 = u_2 = \dots = u_n = 0$.

Consequently, investigation of the stability of any undisturbed movement can be reduced to the stability research of a trivial solution of system (18). The physical sense of the system of equations (18) is that it determines the velocity vector of the depicted point M along the phase path L :

$$\bar{u}_M = \{u_1, u_2, \dots, u_n\} = \{U_1, U_2, \dots, U_n\}, \quad (19)$$

Equalities $U_k = U_k(t)$ may be considered as parametric equations of the motion of a point.

A system (18) in which the right-hand parts of equations depend on time $U_k = U_k(t)$ is called a non-stationary or non-autonomous one, like the physical system itself the movement of which is described by this system of equations. The corresponding movement of the physical system is unsteady.

However, in many cases, the right-hand parts of the equations of disturbed movement do not explicitly depend on time:

$$\dot{u}_k = U_k(u_1, \dots, u_n), \quad k = 1, 2, \dots, n. \quad (20)$$

System (20) is called stationary or autonomous, and its movement is steady. It is these systems that are discussed further.

Assuming that the right-hand parts of equations (20) are decomposed into a Taylor (Maclaurin) series by powers $u_k(t)$, we write:

$$\dot{u}_k = p_{k1}u_1 + p_{k2}u_2 + \dots + p_{kn}u_n + \overset{*}{U}_k(t, u_1, \dots, u_n), \quad k = 1, 2, \dots, n, \quad (21)$$

where coefficients $p_{ki} = p_{ki}(t) = \left(\frac{\partial U_k}{\partial u_j} \right)_0$ in a general case are functions of time t (for autonomous systems, steady); U_k – a totality of all the terms of decomposition of higher orders of smallness (starting from the second one) in relation to U_k .

Neglecting the higher order terms in equations (20), we obtain a linear homogeneous system for a steady movement.

$$\dot{u}_k = p_{k1}u_1 + p_{k2}u_2 + \dots + p_{kn}u_n, \quad k = 1, \dots, n. \quad (22)$$

RESULTS AND DISCUSSION

Theoretical investigation of disturbed movement of a symmetric trailed agricultural machine

Let us create a differential equation of a disturbed motion of the symmetric trailed agricultural machine (trailed cultivator) with mass m moving at a constant forward speed under the impact of the force of total resistance \bar{R} , which runs along the axis of symmetry and is applied to the centre of mass O . Force \bar{R} coincides with the direction of the traction force of the tractor applied at point $D(x_1, y_1)$ (Fig. 2). The moment of inertia of the cultivator l_0 relative to the centre of mass.

Because of the random lateral forces the total resistance \bar{R} of the cultivator has shifted. As a result of this, pair of forces have arisen under the impact of which the entire aggregate turns counterclockwise. The pair is partly compensated by a reactive pair $(\bar{F}, -\bar{F})$ which arises from the lateral resistance of the wheels and the working parts of the cultivator.

The cultivator is under the impact of the total disturbed moment:

$$M = R \cdot r - F \cdot l, \quad (23)$$

where r – deviation of force \bar{R} from the line of symmetry; L – the arm of the reactive pair $(\bar{F}, -\bar{F})$.

Confining to a small angle θ , which we take for the generalized coordinate, we will assume that:

$$F = R \cdot \tan \theta \approx R \cdot \theta, \quad (24)$$

Therefore, equation (23) will be as follows:

$$M = R(r - l \cdot \theta). \quad (25)$$

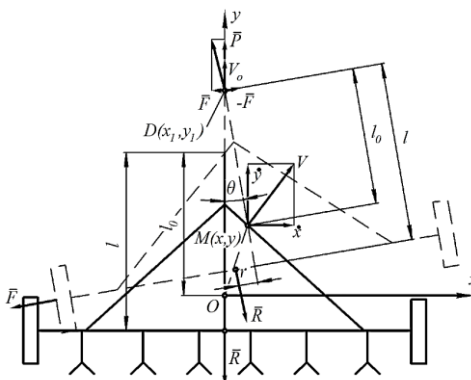


Figure 2. Plane-parallel movement of the trailed symmetric cultivator.

Let us write the equation of the link as distance which always remains preserved between the hitch point $D(x_1, y_1)$ and the centre of mass $M(x_1, y_1)$, L_0 is the distance between the indicated points:

$$(x_1 - x)^2 + (y_1 - y)^2 = l_0^2. \quad (26)$$

Since $x_1 = 0$, $y_1 = V_0 \cdot t + l$, equation (26) will change:

$$x^2 + (V_0 \cdot t + l_0 - y)^2 = l_0^2. \quad (27)$$

The Cartesian coordinates of the centre of mass, expressed in terms of the generalised coordinate θ , are equal to:

$$x = l_0 \cdot \sin \theta, \quad y = V_0 \cdot t + l_0(1 - \cos \theta). \quad (28)$$

Taking the time derivative from expression (28), we have:

$$\dot{x} = l_0 \cdot \dot{\theta} \cdot \cos \theta; \quad \dot{y} = V_0 + l_0 \cdot \dot{\theta} \cdot \sin \theta. \quad (29)$$

The machine is a system with one degree of freedom, so the Lagrange equation can be written as:

$$\frac{d}{dt} \left(\frac{\partial T}{\partial \dot{\theta}} \right) - \frac{\partial T}{\partial \theta} = Q_\theta, \quad (30)$$

where T – the kinetic energy; Q_θ – a generalised force; $\dot{\theta}$ – generalised speed.

Let us determine the kinetic energy of the machine:

$$T = \frac{1}{2} m \cdot V^2 + \frac{1}{2} I_0 \cdot \dot{\theta}^2 = \frac{1}{2} m (\dot{x}^2 + \dot{y}^2) + \frac{1}{2} I_0 \cdot \dot{\theta}^2. \quad (31)$$

By substituting expression (29) into (31), we have:

$$T = \frac{1}{2} m (l_0^2 \cdot \dot{\theta}^2 + V_0^2 + 2V_0 \cdot l_0 \cdot \dot{\theta} \cdot \sin \theta) + \frac{1}{2} I_0 \cdot \dot{\theta}^2. \quad (32)$$

We find the partial derivatives from expression (32). We have:

$$\frac{\partial T}{\partial \dot{\theta}} = (m \cdot l_0^2 + I_0) \dot{\theta} + m \cdot V_0 \cdot l_0 \cdot \sin \theta, \quad \frac{\partial T}{\partial \theta} = m \cdot V_0 \cdot l_0 \cdot \cos \theta \cdot \dot{\theta}. \quad (33)$$

In order to determine the generalised force Q_θ , we write the expression of the elementary work of the applied forces on the possible displacements of the points of the system:

$$\delta A = M \cdot \delta \theta = R (r - l \cdot \theta) \delta \theta, \quad (34)$$

hence:

$$Q_\theta = R (r - l \cdot \theta). \quad (35)$$

Substituting all the values that we found into expression (30), we have:

$$(m \cdot l_0^2 + I_0) \ddot{\theta} = R (r - l \cdot \theta), \quad (36)$$

or

$$\ddot{\theta} + \lambda^2 \cdot \theta = \lambda^2 \cdot k, \quad (37)$$

where $\lambda = \sqrt{\frac{R \cdot l}{m \cdot l_0^2 + I_0}}$; $k = \frac{r}{l}$.

It is equation (37) that is the differential equation for the disturbed movement of the trailed cultivator.

Let us reduce the differential equation (37) to the normal Cauchy form. We have:

$$\dot{x}_1 = x_2; \quad \dot{x}_2 = -\lambda^2 x_1 + \lambda^2 k. \quad (38)$$

Thus, a differential equation of the disturbed movement of a trailed symmetric cultivator has been compiled, which allows it to be used for further studies of the movement stability, as well as to determine its optimal design and kinematic parameters.

Investigation of the movement stability of the system

Let us further discuss methods for the investigation of the movement stability of the system. If the differential equation of the movement is integrated in a closed form, then the study of the stability movement occurs without complications. Yet such cases are practically very rare. As a rule, Lyapunov's predecessors used the linearisation method of the equations of the movement. Its essence is to replace equations (18) of the system to be investigated by a linear system (21). The solution of the problem was greatly simplified, especially for autonomous systems, the equation of the movement of which is integrated in a closed form, and with constant coefficients $p_{kj} = \alpha_{kj} = \text{const}$ it will look like:

$$\dot{u}_k = a_{k_1} u_1 + a_{k_2} u_2 + \dots + a_{k_n} u_n, \quad k = 1, \dots, n. \quad (39)$$

However, such a replacement means substitution of one task with another. Although the research of linearity, or as a first approximation, sometimes solves the problem correctly, in other cases, this method leads to incorrect conclusions. A question arises: What are the conditions for the credibility of the answer obtained on the basis of the study of the movement stability that will be in the first approximation?

For the first time the answer to this question was given by Lyapunov (Lyapunov, 1980). He received a complete solution of the problem for the steady-state and periodic movements, as well as for a wide range of unsteady movements. He also considered some of the main cases when one cannot confine to the first approximation.

Lyapunov divided all methods for studying motion on stability into two categories:

- the first method, which concerns systems the movement of which is described by nonlinear differential equations, is based on the study of linearised equations of disturbed movement or differential equations of the first approximation;
- the second (direct) method is connected with the construction of special Lyapunov functions, which have properties on the basis of which it can be concluded that the movement is stable without solving differential equations.

The study of the movement stability in the first approximation. Lyapunov's theorems. Let us consider a linearised system of the first approximation (39) in an expanded form, replacing $u_k = x_k$:

$$\begin{aligned} \dot{x}_1 &= \frac{dx_1}{dt} = a_{11}x_1 + a_{12}x_2 + \dots + a_{1n}x_n, \\ \dot{x}_2 &= \frac{dx_2}{dt} = a_{21}x_1 + a_{22}x_2 + \dots + a_{2n}x_n, \\ &\dots \dots \dots \dots \dots \dots \dots \dots \dots \dots \\ \dot{x}_n &= \frac{dx_n}{dt} = a_{n1}x_1 + a_{n2}x_2 + \dots + a_{nn}x_n. \end{aligned} \quad (40)$$

We remind that for the autonomous system, which is discussed here, all the coefficients of equations (40) α_k – are constant numbers. As it is known, a particular solution of linear systems is sought in the form:

$$x_1 = A_1 e^{\lambda t}, \quad x_2 = A_2 e^{\lambda t}, \quad \dots, \quad x_n = A_n e^{\lambda t}. \quad (41)$$

We substitute solution (41) into equation (40), and, after grouping the terms, we will have:

$$\begin{aligned} (a_{11} - \lambda)A_1 + a_{12}A_2 + \dots + a_{1n}A_n &= 0; \\ a_{21}A_1 + (a_{22} - \lambda)A_2 + \dots + a_{2n}A_n &= 0; \\ \dots \dots \dots \dots \dots \dots \dots \dots \dots & \dots \dots \dots \\ a_{n1}A_1 + a_{n2}A_2 + \dots + (a_{nn} - \lambda)A_n &= 0. \end{aligned} \quad (42)$$

In order the system of algebraic equations (42) had a solution, different from zero, it is necessary that its determinant be zero:

$$\begin{vmatrix} a_{11} - \lambda & a_{12} & \dots & a_{1n} \\ a_{21} & a_{22} - \lambda & \dots & a_{2n} \\ \dots & \dots & \dots & \dots \\ a_{n1} & a_{n2} & \dots & a_{nn} - \lambda \end{vmatrix} = 0 \quad (43)$$

The determiner (43), which is composed for the system (40), is called a characteristic. Expanding this determinant by the elements of the first line, we obtain an equation in relation to λ , which is called a characteristic and contains the unknown λ in the degree n , having roots $(\lambda_1, \lambda_2, \dots, \lambda_n)$.

We formulate the main conditions on the basis of the Lyapunov stability theorems in the first approximation:

1. If the valid parts of all roots of the characteristic equation are negative, then the undisturbed movement is asymptotically stable.
2. If among the roots of the characteristic equation there is at least one root, the valid part of which is positive, then the undisturbed movement is unstable.
3. If the valid parts of some roots of the characteristic equation are zero, and the valid parts of other roots are negative, then the undisturbed movement is stable, but not asymptotically stable.

The presented Lyapunov theorems on the movement stability in the first approximation completely solve the problem of the stability of movement. The assessment of the stability of the movement is also carried out applying the Hurwitz criterion. From the foregoing it is clear that, in order to make a conclusion about the movement stability it is of great importance to know what is the sign of the valid parts of the roots of the characteristic equation, that is, it is important to know the necessary and sufficient conditions under which the roots of the equation have negative valid parts. Such conditions must satisfy the Hurwitz criterion. Such conditions must satisfy the Hurwitz criterion.

Let us open determiner (43) by grouping the terms by powers λ :

$$a_0 \lambda^n + a_1 \lambda^{n-1} + \dots + a_{n-1} \lambda + a_n = 0. \quad (44)$$

In order to determine the movement stability using the equations of the first approximation, it is necessary to previously know when the valid parts of all the roots of the characteristic equation are negative, without solving the characteristic equation,

without calculating its roots. For this it is necessary to construct the Hurwitz matrix from the roots of the characteristic equation $\alpha_0, \alpha_1, \dots, \alpha_n$ (44):

$$\begin{vmatrix} a_1 & a_3 & a_5 & \dots & 0 \\ a_0 & a_2 & a_4 & \dots & 0 \\ 0 & a_1 & a_3 & \dots & 0 \\ \dots & \dots & \dots & \dots & \dots \\ 0 & 0 & 0 & \dots & a_n \end{vmatrix}. \quad (45)$$

We compose from the matrix (45) the main diagonal minors:

$$\Delta_1 = a_1; \Delta_2 = \begin{vmatrix} a_1 & a_3 \\ a_0 & a_2 \end{vmatrix}; \dots; \Delta_n = a_n \Delta_{n-1}. \quad (46)$$

In order all the roots of the characteristic equation (44) had negative valid parts, it is necessary and sufficient that all the main diagonal minors (46) were positive, that is:

$$\Delta_1 > 0; \Delta_2 > 0; \dots, \Delta_{n-1} > 0; \Delta_n > 0. \quad (47)$$

Let us discuss further the direct Lyapunov's method. Therefore, it is necessary to compile Lyapunov functions. This method is most suitable to examine the stability of the movement of autonomous systems. The direct or the second Lyapunov's method is characterised by the fact that in its application there is no need to integrate the differential equations of the disturbed movement. This method is connected with a search for some functions V of the disturbance variables t, x_1, x_2, \dots, x_N , where $x_j = y_j - f_j(t)$ – disturbance, y_j – a partial solution of the disturbed movement, $f_j(t)$ – a partial solution of the undisturbed programmed movement (basis). The method also involves the study of the properties of these functions, which are called Lyapunov functions, and the properties of their derivatives. Let us treat only a steady-state (stationary) movement (autonomous systems), for which $V = V(x_1, x_2, \dots, x_N)$ in the environment $|x_j| < h (j = 1, 2, \dots, N)$, where h is a sufficiently small positive number, considering these functions to be continuously differentiated, unambiguous, and such that they change into zero at the origin of the coordinates $x_{1o} = x_{2o} = \dots = x_{No} = 0$.

In the stability theory the direct method is considered the main one. It is a qualitative method since it does not need any solution of the equations of the movement but studies the properties of the 'test' functions, i.e. Lyapunov functions.

The simplest example of a 'test' function may be an expression of the potential energy of the system with which it is possible to establish stability or instability of equilibrium.

The derivative of the Lyapunov function is determined from the expression:

$$\frac{dV}{dt} = \sum_{j=1}^N \frac{\partial V}{\partial x_j} \frac{\partial x_j}{\partial t}. \quad (48)$$

In addition, the Lyapunov functions may have special properties. Function V is called a positively-defined function in the environment $|x_j| < h$ if at any point in this environment, except for the origin of coordinates (where function V is zero), the condition $V > 0$ is fulfilled. If $V < 0$, then function V is called a negatively-defined function. In these two cases, function V is called a sign-definite function. If in this environment $|x_j| < h$ function V acquires the value of only one sign ($V \geq 0$) or $V \leq 0$, but can change into zero not only at the origin of the coordinates, then it is called a sign-

fixed (positive or negative) function; if function V acquires both positive and negative values, then it is called an alternating function in this environment.

For example, function $V = x_1^2 - x_2^2$ at $N = 2$ is an alternating function, and function $V = x_1^2 + x_2^2$ is positively-definite, function $V = x_1^2$ is a sign-fixed function since it changes into zero on axis O_{x_2} , but beyond the boundaries of this axis it is positive.

So, if V it is a quadratic form, then definiteness of the sign can be established using the Sylvester criterion. If V is a form of an unpaired degree, then it is clear that it is a sign-alternating function. Consequently, Lyapunov functions are functions of variables x_1, x_2, \dots, x_N , each of which in a certain n -measurable region, containing the origin of space coordinates, is a sign-definite, a fixed or an alternating function, and in this region it has continuous first-order partial derivatives of the first order with respect to variables x_1, x_2, \dots, x_N , i.e. it has a full differential. The issue about the stability of undisturbed movement is solved on the basis of an investigation of the behaviour of function $V(x_1, x_2, \dots, x_N)$ and its derivatives in time. It should be taken in account that variables x_1, x_2, \dots, x_N are solutions of differential equations of the disturbed movement. The study of the behaviour of function V along the path of the system allows one to make a conclusion about the behaviour of the paths of a mechanical system being investigated, i.e. to solve the problem of the stability or instability of the movement.

Since the issue about the sign-definiteness of a quadratic form is solved quite simply (Sylvester's criterion (8)), when constructing Lyapunov functions, the sign-determined quadratic form is chosen as the basis, adding, if necessary, forms of higher orders. The resulting function will have the same sign-definiteness properties as the original quadratic form.

Theoretical investigation of the movement stability of a model of the self-propelled chassis

Let us investigate by the direct Lyapunov's method the movement stability of a model of the self-propelled chassis with mass m and the inertia moment in relation to the transverse axis that passes through its centre of mass $-mr^2$, where r is the inertia radius of the chassis body, C_p, C_z – the rigidity coefficients of the frontal and rear springs of the self-propelled chassis (Fig. 3).

We will discuss the longitudinal oscillations of the self-propelled chassis. In the process of oscillations its position is determined by two generalised coordinates: the vertical displacement of the centre of mass (point C) and the turning angle Θ of the frame. The kinetic energy of the self-propelled chassis is:

$$T = \frac{1}{2}m \cdot \dot{y}^2 + \frac{1}{2}I_c \cdot \dot{\theta}^2 = \frac{1}{2}m (\dot{y}^2 + r^2 \cdot \dot{\theta}^2) \quad (49)$$

The potential deformation energy of the chassis wheels:

$$\Pi = C_p (y + a \cdot \theta)^2 + C_z (y - b \cdot \theta)^2. \quad (50)$$

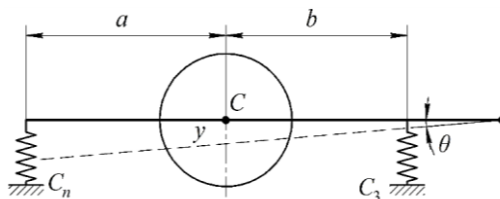


Figure 3. An equivalent scheme of the oscillation pattern of the self-propelled chassis.

Let us compile the movement equations of the self-propelled chassis using for this the initial equations in the Lagrange form of the II-nd kind:

$$\frac{d}{dt}\left(\frac{\partial T}{\partial \dot{y}}\right) - \frac{\partial T}{\partial y} = -\frac{\partial \Pi}{\partial y} \quad \frac{d}{dt}\left(\frac{\partial T}{\partial \dot{\theta}}\right) - \frac{\partial T}{\partial \theta} = -\frac{\partial \Pi}{\partial \theta}. \quad (51)$$

Substituting into equations (51) a derivative from T and Π , we obtain differential equations of the oscillatory movement of the self-propelled chassis:

$$\left. \begin{aligned} m\ddot{y} + 2C_p(y + a \cdot \theta) + 2C_z(y - b \cdot \theta) &= 0, \\ mr^2\ddot{\theta} + 2C_p(y + a \cdot \theta)a + 2C_z(y - b \cdot \theta)b &= 0. \end{aligned} \right\} \quad (52)$$

We transform differential equations (52) in the Cauchy normal form:

$$\left. \begin{aligned} \dot{x}_1 &= x_2, \\ \dot{x}_2 &= -\frac{1}{m}\left[2C_p(x_1 + a \cdot x_3) + 2C_z(x_1 - b \cdot x_3)\right], \\ \dot{x}_3 &= x_4, \\ \dot{x}_4 &= -\frac{1}{mr^2}\left(2C_p(x_1 + a \cdot x_3)a + 2C_z(x_1 - b \cdot x_3)b\right) \end{aligned} \right\} \quad (53)$$

These differential equations (53) are called the disturbed movement equations of the self-propelled chassis.

Let us select a Lyapunov function in the form of full mechanical energy:

$$V = T + \Pi = \frac{1}{2}m(\dot{y}^2 + r^2 \cdot \dot{\theta}^2) + C_p(y + a \cdot \theta)^2 + C_z(y - b \cdot \theta)^2 \quad (54)$$

We write the Lyapunov function in the new variables. We have:

$$V = \frac{1}{2}m(x_2^2 + r^2 \cdot x_4^2) + C_p(x_1 + a \cdot x_3)^2 + C_z(x_1 - b \cdot x_3)^2 \quad (55)$$

Let us take a full derivative of the Lyapunov function (55) with respect to time. We will have:

$$\frac{dV}{dt} = \frac{\partial V}{\partial x_1} \dot{x}_1 + \frac{\partial V}{\partial x_2} \dot{x}_2 + \frac{\partial V}{\partial x_3} \dot{x}_3 + \frac{\partial V}{\partial x_4} \dot{x}_4. \quad (56)$$

By virtue of the equations of disturbed movement we have $\frac{dV}{dt} = 0$. In this case the movement of the self-propelled chassis will be stable.

CONCLUSIONS

1. Since the stability of movement is one of the most important categories in the theoretical research of functioning of various mechanical systems, including the agricultural machines and equipment, finding methods for their efficient use is an important scientific task. Application of the basic assumptions of the classical theory of the movement stability in the analytical research of agricultural machines and aggregates is connected with considerable difficulties when integrating nonlinear differential equations in a closed form. However, it is possible to apply efficiently the criteria of the movement stability in order to evaluate how an agricultural machine will continue to move if it is accidentally subject to external forces that had not been taken into account in the model. The latter is equivalent to a change in the initial conditions on which the pattern of the movement of the agricultural machine or aggregate directly depends.

2. Presented scientific problem has been solved concerning the development of methods and their efficient application in the analytical research of agricultural aggregates, which provides an opportunity to consider the behaviour of a machine without using complex differential equations of the movement in the case of perturbations.

3. Application of various methods of the theory of the movement stability is considered in the research of the movement of a trailed cultivator and a self-propelled agricultural tool frame.

REFERENCES

- Bulgakov, V., Adamchuk, V., Arak, M., Petrychenko, I. & Olt, J. 2017. Theoretical research into the motion of combined fertilising and sowing tractor-implement unit. *Agronomy Research* **15**(4), 1498–1516. <https://doi.org/10.15159/AR.17.059>
- Bulgakov, V., Pascuzzi, S., Nadykto, V. & Ivanovs, S. 2018. A mathematical model of the plane-parallel movement of an asymmetric machine-and-tractor aggregate. *Agriculture* **8**(10), 151.
- Halanay, A. 1966. *Differential Equations: Stability, Oscillations, Time Lags*. Academic Press, New York, 528 pp.
- Hale, J. & Verduyn Lunel, S. 1993. Introduction to Functional Differential Equations, *Applied Mathematical Sciences* **99**, Springer-Verlag, New York.
- Federson, M. & Schwabik, S. 2006. Generalized ODEs approach to impulsive retarded differential equations, *Differential and Integral Equations* **19**, 1201–1234.
- Lyapunov, A. 1980. *The general problem of motion stability*. Gostekhizdat, Moscow, 472 pp. (in Russian).
- Malkin, I. 1996. *The theory of motion stability*. Nauka, Moscow, 532 pp. (in Russian).
- Matignon, D. 1996. Stability result on fractional differential equations with applications to control processing, In: *IMACS - SMC Proceeding*, Lille, France, 963–968.
- Merkin, D.R., Afagh, F.F. & Smirnov, A.L. 1997. *Introduction to the Theory of Stability (Texts in Applied Mathematics 24)*, ISBN-13: 978-0387947617, 320 pp.
- Momani, S. & Hadid, S.B. 2004. Lyapunov stability solutions of fractional integrodifferential equations. *Int. J. Math. Math. Sci.* **47**, 2503–2507.
- Samoilenko, A. & Perestyuk, N. 1995. Impulsive differential equations, *World Scientific Series on Nonlinear Science*. Vol. **14**. Singapore.
- Schwabik, S. 1992. Generalized Ordinary Differential Equations. *World Scientific, Series in Real Anal.* **5**.
- Schwabik, S. 1984. Variational stability for generalized ordinary differential equations. *Chasopis Pesht. Mat.* **109**(4), 389–420.
- Zaslavsky, G.M. & Edelman, M.A. 2004. Fractional kinetics: from pseudochaotic dynamics to Maxwell's demon. *Physica D* **193**, 128–147.
- Zhukovsky, N. 1948. *On the strength of movements*. Book 1, OGIZ, Moscow, 69–70. (in Russian)

Particle size and shape characterization of feedstock material for biofuel production

V. Chaloupková, T. Ivanova* and V. Krepl

Czech University of Life Sciences, Faculty of Tropical AgriSciences, Department of Sustainable Technologies, Kamýcká 129, CZ165 00 Prague, Czech Republic

*Correspondence: ivanova@ftz.czu.cz

Abstract. Particle size and shape are key factors influencing the properties of particulate and agglomerated materials, and having an impact on a quality as well as utilization of a final product. In case of plant biomass particle morphology is greatly irregular. Large errors at most determinations of biomass particle sizes are caused by simplification on a single parameter of size, assuming particle sphericity or circularity. Thus, the aim of a present research was to determine the particle size in a complex way. Pine sawdust as an experimental material and typical biofuel feedstock was ground by a hammer mill to a fraction size of 12 mm. The dimensional features of such ground sawdust particles were identified for all particles individually via photo-optical analysis, a method based on a digital image processing that is sensitive to irregular particles' shapes. The particles were described mainly by variables of length, max width, equivalent diameter, max and min feret diameter, sphericity, roundness, circularity together with length/width ratio and aspect ratio. Data were analysed by descriptive statistics, i.e. by arithmetic means, medians, minimum and maximum values, variance and standard deviation. The obtained results may contribute to a better knowledge of material properties needed for designing an optimal technology for the production of quality biofuels.

Key words: particle morphology, size variable, pine sawdust, photo-optical analysis.

INTRODUCTION

Understanding of particle morphological and rheological behaviour as well as measuring particle size and comprehension how it affects processes and final products can be critical to the success of many manufacturing businesses and industries (Shekunov et al., 2006; Guo et al. 2012; Vaezi et al., 2013; Agimelen et al., 2017; Cardona et al., 2018). In case of biomass it is significant in fields associated with the particle handling, transportation, mixing, dosing, flow-ability, densification, fluidization, gasification or combustion (Gil et al., 2014; Ahmad et al., 2016; Holmgren et al., 2017; Trubetskaya et al., 2017; Knoll et al., 2019).

Particle size and shape measurement has long tradition in soil and sediment sciences (Cox, 1927; Wadell, 1932; Krumbein, 1941; Koerner, 1970) and core of biomass morphology characterization originates from these disciplines. Classification of particular material based on dimensional properties has long been based upon sieve analysis where the material is separated by sieves of differently sized apertures into fractions of particle size distribution (Fernlund, 1998). This traditional approach

considers only one parameter: general particle diameter which is given by the aperture of a sieve (Igathinathane et al., 2009a). Often, particle morphology is simplified by a single parameter size, assuming sphericity or circularity (Lu et al., 2010; Ulusoy & Igathinathane, 2016). This assumption is convenient owing to numerous findings about behaviour properties of spherical particles (Walpole, 1972; Riguidel et al., 1994; Niazmand & Renksizbulut, 2003; Antonyuk et al., 2005). However presuming sphericity in case of biomass particle modelling is inadequate (Trubetskaya et al., 2017) and may result in large errors at most particle size estimations (Lu et al., 2010).

Due to high and varied proportion of cellulose, hemicellulose and lignin in biomass composition which is different for all plant species, the morphology of grinded/milled biomass is greatly non-uniform (Guo et al., 2012; Febbi et al., 2015). Biomass particles are in practise non-spherical and irregular (Dai et al., 2012). Since the particle size and shape are complex parameters (Fernlund, 1998), at least two parameters are necessary to describe particle size/shape (Trubetskaya et al., 2017). It can be represented by several variables, such as length, width, diameter, perimeter, surface area, volume and descriptors calculated from them, like sphericity, roundness and ratios of two object dimensions (Murphy, 1984; Vaezi et al., 2013; Bagheri et al., 2015; Zhao & Wang, 2016). There are several shapes qualitatively described by various studies, for instance flakes, rod-like and needle-like particle (Guo et al., 2012), or plate, slab, prism, cylinder, rod and sphere (Liliedahl & Sjøestroëm, 1998; Saastamoinen, 2006). Despite numerous studies on biomass particle morphology, there is no universal consensus on how to represent a biomass particle size and shape in some details, thus the combination of several descriptors is needed (Pons et al., 1999).

Computer vision-based methods are getting growing interest in various fields where greater precision, efficiency, quality and performance of observed objects are highly demanded (Davies, 2018). This approach can be used for two (2D) or three (3D) dimensional image analysis of particle morphology and particle size distribution (Zhao & Wang, 2016; Sunoj et al., 2018), where it is interesting alternative or even substitution for the traditional sieve analysis (Igathinathane et al., 2009a; Igathinathane et al., 2009b; Souza & Menegalli, 2011; Kumara et al., 2012; Gil et al., 2014; Febbi et al., 2015; Chaloupková et al., 2018). The image analysis is the technique being sensitive to the particle geometrical shape and considering more parameters than just sphericity which leads to more precise results (Dai et al., 2012; Ulusoy & Igathinathane, 2016).

More accurate data about material properties together with process variables may enhance efficiency of biomass energy conversion processes and may bring optimal products of higher quality with desired properties (Ndindeng et al., 2015). Thus, the aim of the present research was to determine the particle size and shape of pine sawdust in a complex way using a photo-optical analyser and 2D imaging.

MATERIALS AND METHODS

Pine sawdust (*Pinus* spp.) as a typical feedstock material for solid biofuel production (Deac et al., 2016) was selected as the experimental material in this study. The material originated from the Czech Republic was grinded into the fraction size of 12 mm by the hammer mill (model 9FQ - 40C, Pest Control Corporation, Ltd., Vlčnov, Czech Republic). Such prepared material was dried to the moisture content (w.b.) of

8.39% (determined according to EN ISO 18134-2, 2017) to decrease particle adhesion and agglomeration during the measurement.

A computerized photo-optical particle analyser Haver (model CPA 4-2, Haver & Boecker OHG, Oelde, Germany) was used to analyse particle properties. The automatic analyser worked under the particle measuring range 0.091–90 mm which was selected with respect to the material character. The analyser consisted of a feeding unit with the high of 6 mm being set for the regular and even particle layout on a vibration channel, a vibratory channel itself, an optical sensor in the form of CCD-line digital scan camera with the high-resolution (4,096 pixels line resolution) that scanned all free-falling particles of the studied sample against the background of a red LED lighting array module with a high recording frequency (up to 28,000 line scans per second) (Haver & Boecker, 2015). Amplitude of the vibrating feeder (feed rate) was automatically regulated by the analyzer as the particles were falling down. Minimum and maximum values of optical density were set as 0.5 and 2, respectively. Shape model was set as ‘*elongated*’ and volume model as ‘*elliptical segment*’. Control of the entire measurement process and data evaluation were performed from a portable computer equipped with a Gigabit Ethernet (GigE) interface as well as a RS 232 interface that was connected to the analyser. All passed particles were individually recorded, measured and their 2D profile parameters were processed via Haver CpaServ software (Haver & Boecker OHG, Oelde, Germany). The scanned particles were analysed in terms of variables stated and defined in the Table 1.

Obtained data were processed using MS Excel (version 2007, Microsoft, Redmond, WA, USA) and Statistica software (version 13.3, TIBCO Software Inc., Palo Alto, CA, USA) and summarized by descriptive statistics, i.e. measures of central tendencies (means), measures of variability and frequency distributions. Afterwards the obtained results were tabulated, graphically plotted and discussed.

Table 1. Variables measured by the photo-optical analyser


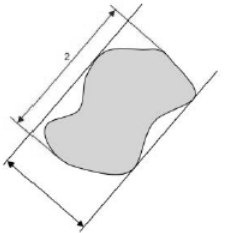

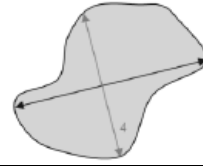
Variable and definition	Diagram
<p>Minimum feret diameter (X_{min}) Minimum distance of two tangents, which can be placed in parallel onto the outer particle contour (Haver & Boecker, 2014)</p>	
<p>Length (L) The length is determined perpendicularly to the minimum feret diameter and it corresponds to the long side of a rectangular shaped projection area; used for calculation of length/width ratio (R_{lw}) (Haver & Boecker, 2014)</p>	
<p>Maximum feret diameter (X_{max}) Maximum distance between two parallel tangents of the particle contour (Haver & Boecker, 2014)</p>	

Table 1 (continued)

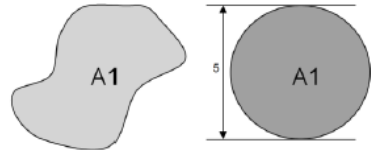
Maximum width (W_{max})
 Maximum extension of the particle projection area
 orthogonally to the maximum length
 (Haver & Boecker, 2014)



Equivalent diameter (X_a)

Diameter of a circle, the surface area of which corresponds to the projected area of the particle
 (Olson, 2011)

$$X_a = \sqrt{\frac{4 * A_1}{\pi}} \quad (1)$$



Projection area (A_1)

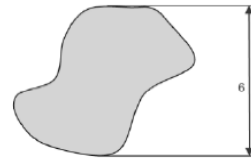
Sum of the areas of individual pixel (Olson, 2011)

$$A_1 = \sum a_p \quad (2)$$

where a_p is area of each individual pixel

Feret diameter* (X)

Distance between two parallel tangents of the particle
 contour, vertical to the direction of measurement
 (Haver & Boecker, 2014)



Martin-diameter* (X_m)

Length from the particle projection, it is the line that cuts
 the area in half, horizontally to the direction of
 measurement (Haver & Boecker, 2014)

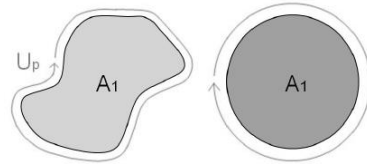


Circularity (C)

Degree of similarity of the particle projection area with a circle (Haver & Boecker, 2014)

$$C = \frac{U_p}{(2 * \sqrt{\pi * A_1})} \quad (3)$$

Where U_p is measured perimeter of particle and A_1
 measured projected area



Sphericity (ψ)

Degree of similarity of the particle with a sphere

$$\psi = \frac{\pi * d_v}{A_0} \quad (4)$$

where A_0 is the particle's calculated surface area and d_v is the diameter of an equal volume sphere
 (Wadell, 1932)

Roundness (R_d)

Degree of roundness the particle corners and edges (Wadell, 1932)

$$R_d = \frac{\frac{1}{n} \sum_{i=1}^n r_i}{r_{max}} \quad (5)$$

where r_i is the radius of the i-th corner curvature, n the number of corners, and r_{max} the radius of
 the maximum inscribed circle

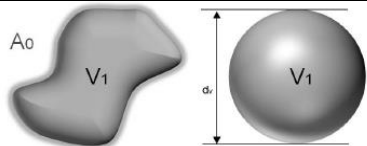


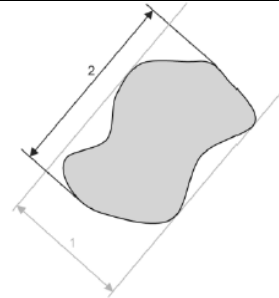
Table 1 (continued)

Length/width ratio (R_{lw})

The ratio of length to width was calculated from the ratio of length to the minimum feret diameter of the projection area (Haver & Boecker, 2014)

$$R_{lw} = \frac{L}{X_{min}} \quad (6)$$

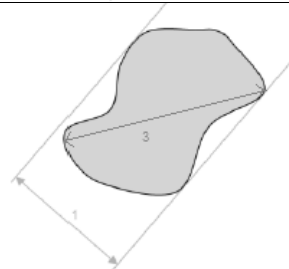
where L is length and X_{min} minimum feret diameter



Aspect ratio (A_r)

Ratio of maximum (X_{max}) to minimum (X_{min}) feret diameter (Agimelen et al., 2017)

$$A_r = \frac{X_{max}}{X_{min}} \quad (7)$$



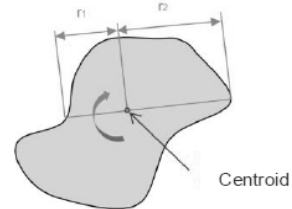
Symmetry (S_m)

For symmetry, the area centroid of the particle is determined.

Axes of symmetry run through the centroid. These axes are rotated in 1° increments. Here the ratio of radii is computed. The smallest result is denoted as the symmetry (Haver & Boecker, 2014)

$$S_m = \frac{r_1}{r_2} \quad (8)$$

where r_1 is the smallest radius and r_2 the largest radius

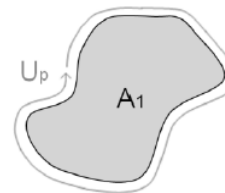


Perimeter (U_p)

Total length of the particle boundary (Olson, 2011)

$$U_p = \frac{\pi}{N} \sum_{\alpha} I_{\alpha} d_L \quad (9)$$

where I is number of intercepts, formed by series of parallel lines, with spacing dL , exploring N directions, from α to π



Notes: * position-dependent size; All diagrams adopted from Haver & Boecker (2014).

RESULTS AND DISCUSSION

In total 536,137 pine sawdust particles were analysed by the photo-optical image analyser to identify the particle morphology. This number brings precise statistical data, as Masuda & Gotoh (1999) determined that about 61,000 particles are required in order to get the mass median diameter within 5% error with 95% probability for a powder having a geometric standard deviation of 1.6.

Fig. 1 shows the 2D projections of selected pine sawdust particles recorded by the analyzer. As it can be seen, the material is composed of un-evenly shaped particles.

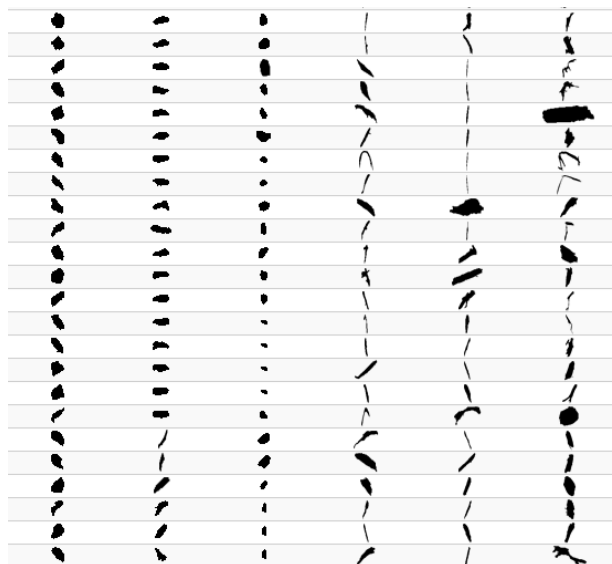


Figure 1. 2D projections of selected particles of pine sawdust.

Table 2 provides detailed descriptive statistics of the particles' measured variables, i.e. total number of analysed particles, their arithmetic mean, median, mode, frequency of mode, maximum and minimum values, lower and upper quartiles, together with variance, standard deviation and coefficient of variance, rounded to four decimal places.

Diameter of irregular particles is mostly evaluated by X , the distance between two furthest points of the particle is measured in a given direction (Igathinathane et al., 2009a; Dražić et al., 2016). In case of the studied material, mean value of X was 1.12 ± 0.88 mm. More useful information is given by X_{max} and X_{min} , since they calculate a diameter of the particle in all directions (Dražić et al., 2016). X_{max} is often associated to the 'length' of the particle (Pons et al., 1999). Length of the pine sawdust particles ranged from its maximum of 28.26 mm to its minimum of 0.16 mm (which was given by the measuring possibility of the analyser) and with arithmetic mean of 1.26 ± 0.94 mm. On the contrary, X_{min} is related to the particle 'breadth' (Pons et al., 1999). Mean, min and max values of X_{min} were 0.51 ± 0.33 mm, 0.09 mm and 10.04 mm, respectively. Feret diameter as an algorithm for particle dimension is often used to evaluate particle size distribution (Igathinathane et al., 2009a). X_{max} gives the value of the minimum sieve size through which the particle can pass through without any obstacle (Shanthi et al., 2014). On the Fig. 2 there is illustrated the histogram of X_{max} , where the particles are grouped into the fractions based on the sizes (holes' diameters) of standard sieves (EN ISO 17827-1, 2, 2016).

The observation indicates the increased presence of fine particles, since most of the material (~71%) has size of 1.0–2.0 mm. Even though the material was grinded into fraction size of 12 mm, only ~5% of the material has $X_{max} > 2.8$ mm. Presented result should be theoretically obtained by traditional oscillating analysis.

Table 2. Descriptive statistics of measured variables

Variable	Mean	Median	Mode	Mode Freq.	Min	Max	Lower Quart.	Upper Quart.	Var.	Std. Dev.	Coef. Var.
Min feret $X_{min}^{a)}$	0.5105	0.4550	0.0910	47,696	0.0910	10.0377	0.2730	0.6402	0.1078	0.3283	64.3059
Length $L^{a)}$	1.2292	1.0163	0.6083	21,668	0.0910	28.2639	0.6954	1.4877	0.8964	0.9468	77.0283
Max feret $X_{max}^{a)}$	1.2635	1.0596	0.1257	10,903	0.1257	28.2639	0.7188	1.5219	0.8859	0.9412	74.4932
Max width $W_{max}^{a)}$	0.4995	0.4569	0.1206	10,903	0.0869	8.7320	0.2826	0.6438	0.1016	0.3188	63.8187
Equiv.diam. $X_a^{a)}$	0.6591	0.6024	0.1003	10,903	0.1003	7.6619	0.4199	0.8222	0.1374	0.3707	56.2369
Feret $X^{a)}$	1.1179	0.8697	0.6083	40,002	0.0868	28.2639	0.6083	1.3064	0.7797	0.8830	78.9922
Martin diam. $X_m^{a)}$	0.5233	0.4550	0.3640	70,052	0.0910	12.1940	0.2730	0.6370	0.1569	0.3961	75.6862
Circularity $C^{d)}$	0.7280	0.7549	0.8860	10,903	0.1231	0.9732	0.6425	0.8367	0.0192	0.1385	19.0210
Sphericity $\psi^{d)}$	0.7008	0.7198	0.2964	10,903	0.2381	0.8735	0.6684	0.7579	0.0092	0.0957	13.6518
Roundness $R_d^{d)}$	0.3456	0.3429	0.6359	10,903	0.0064	0.8089	0.2330	0.4539	0.0219	0.1479	42.7937
Length/width $R_{lw}^{d)}$	3.0372	2.2223	1.0424	10,903	1.0128	90.6745	1.6299	3.3538	7.0271	2.6509	87.2802
Aspect ratio $A_r^{d)}$	2.9255	2.1544	1.3816	10,903	1.0687	55.0247	1.6328	3.2416	5.7653	2.4011	82.0755
Symmetry $S_m^{d)}$	0.6247	0.6393	1.0000	40,652	0.0000	1.0000	0.5181	0.7331	0.0423	0.2057	32.9203
Perimeter $U_p^{a)}$	3.0789	2.5701	0.3555	10,903	0.3555	78.2456	1.7621	3.7086	5.5166	2.3487	76.2843
Proj. Area $A_l^{b)}$	0.4491	0.2850	0.0079	10,903	0.0079	46.1066	0.1385	0.5309	0.4667	0.6832	152.1229
Surface area $A_{\theta}^{b)}$	2.0446	1.2985	0.0248	10,903	0.0248	226.9127	0.6343	2.4250	10.0162	3.1648	154.7911
Volume $V_l^{c)}$	0.2394	0.0825	0.0001	10,903	0.0001	127.0393	0.0277	0.2104	0.9265	0.9626	402.1449

Total count of observations: 536,137.

Notes: ^{a)} in [mm]; ^{b)} in [mm²]; ^{c)} in [mm³]; ^{d)} calculated as the ratio, i.e. without unit.

L , W_{max} , X_m and X_a define particle size in different manners (Pons et al., 1999). Mean value for L was 1.23 ± 0.95 mm, W_{max} 0.50 ± 0.32 mm, (X_m) 0.52 ± 0.40 mm and X_a 0.66 ± 0.37 mm. Mean X_m is smaller than X_a and both descriptors have smaller mean values than mean X ; this corresponds with experimental evidence of other studies (Yang, 2003).

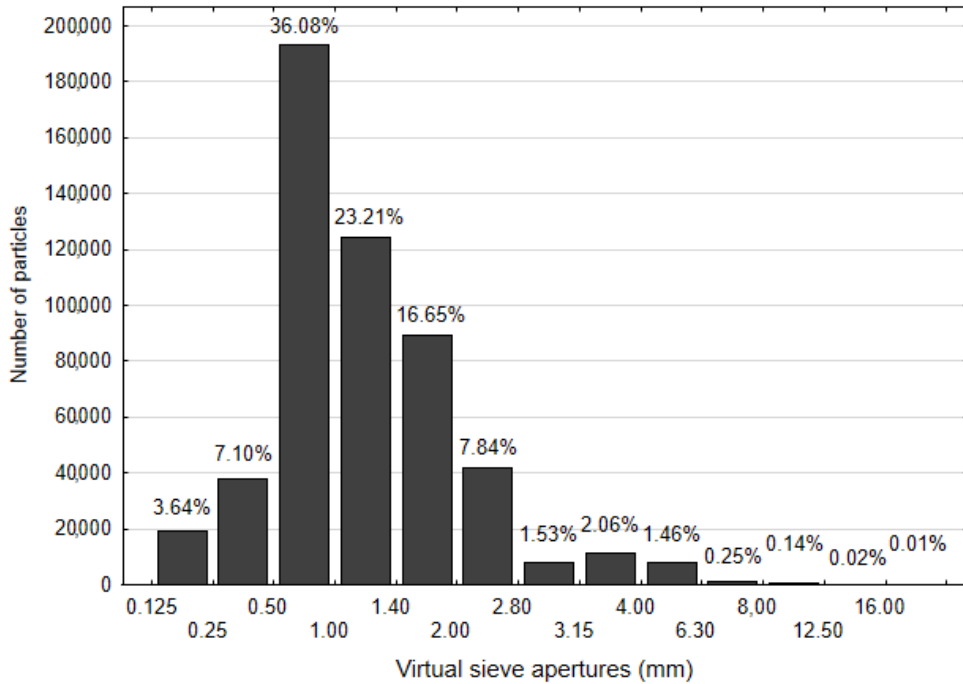


Figure 2. PSD of measured pine sawdust with max feret diameter (X_{max}) as measuring algorithm (in mm).

Shape of particles was defined by C , ψ and R_d , important parameters describing particle shape in several studies (Mora & Kwan, 2000; Cruz-Matías et al., 2019). They were measured in the range of 0.01–1. ψ describes a compactness of a particle in terms of the surface area (Zhao & Wang, 2016) and it is the most dependent on elongation (Olson, 2011; Cruz-Matías et al., 2019). R_d is a characteristic affected by a form, it is not a degree of ψ (ψ is a measure of a form) even though R_d is the best manifested by a perfect sphere. R_d is mainly dependent on the sharpness/roughness of angular convexities and concavities of a particle (Cruz-Matías et al., 2019). R_d of the corners is the opposite of the angularity of the corners and plays significant role in the abrasive and perforation features of the particles (Mora & Kwan, 2000). Wadell (1932) identified ψ and R_d as two independent aspects of a particle shape, however lately Zhao & Wang (2016) reported their dependency. In general, the particles that have larger ψ values also have larger values of A_r and mean R_d value (Zhao & Wang, 2016).

The sphericity index value of a perfect sphere is 1. In case of studied pine sawdust the ψ mean value was 0.70 ± 0.09 , thus the particles can be described as irregular (non-spherical) since their average ψ value is smaller than 0.8 (Zhao & Wang, 2016). Fig. 3 shows frequency distributions of ψ together with R_d . For an absolutely round and smooth object (i.e. sphere) the value of R_d is 1, for any other object the values is less than 1. According to the classification of Powers (1953), approx. 1% of particles, as it can be seen from the Fig. 3, is well rounded (range 0.70–1.0) and 18% rounded (range 0.49–0.70). The measured particles can be classified as subangular and subrounded since the average R_d is 0.35 ± 0.15 and majority (~53%) of the material belongs to the range of 0.25–0.35 (subangular) and 0.35–0.49 (subrounded). More or less 15% of particles can be called angular and ~14% very angular.

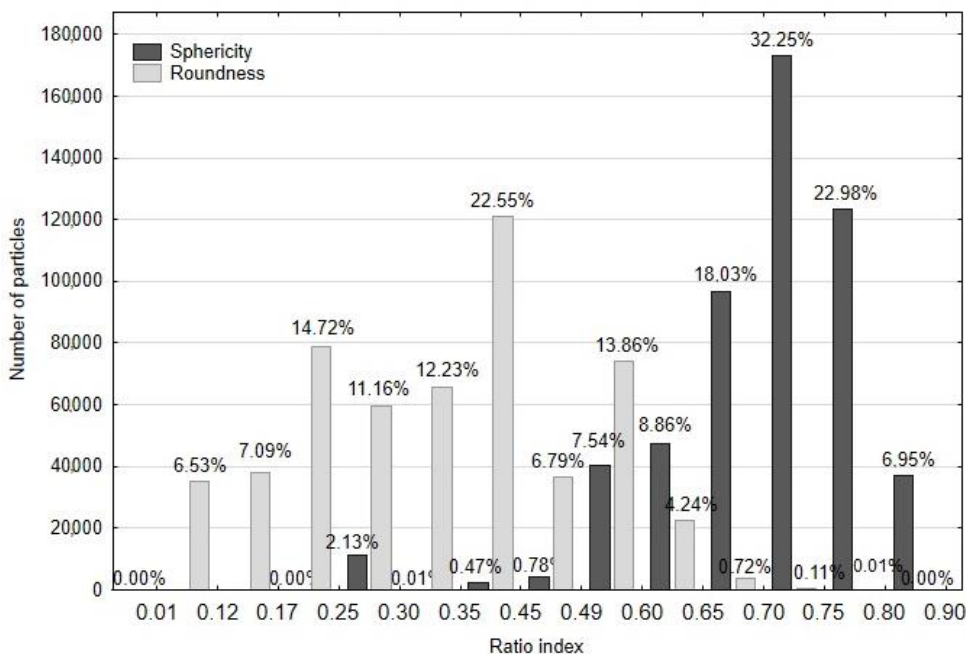


Figure 3. Histograms of sphericity (ψ) and roundness (R_d).

C is a measurement of both the particle form and roughness (Olson, 2011). It can also reach values ranging from 1, as it is in case of particle perfectly round and smooth circle, and up to 0, when conversely shape becomes more angular and rough (Olson, 2011). Average C value of analysed pine sawdust was 0.73 ± 0.14 , which means that the particles have slight surface irregularities.

Particle shape can be evaluated also in terms of S_m , ranging from 0 to 1. Perfectly symmetric objects (like sphere or cube) have S_m equal to 1. In case of measured pine sawdust particles mean S_m was 0.62 ± 0.21 , so the particles can be called moderately asymmetrical (Yang, 2003).

R_{lw} and A_r show the degree of particle elongation (Agimelen et al., 2017) based on two particle dimensions (Olson, 2011). The ratios can reach values in range of 1–10,000 (Haver & Boecker, 2014). Value 1 is for object with symmetric shape (e.g. sphere or

square) and 10,000 theoretically for very elongated and thin objects, however the ratios are suitable only for particles that are not very elongated and curved (ISO 9276-6, 2008), for example particles of needle-like and acicular shape (Olson, 2011), as it was in case of examined material. Since biomass particles are in practise non-spherical and irregular (Dai et al., 2012), their ratios normally belong to the range 2–15 (Lu et al., 2010). As it can be seen from the Table 2, the measured pine sawdust particles have average value of R_{lw} 3.04 ± 2.65 and A_r 2.93 ± 2.40 . Guo et al. (2012) reported similar result for R_{lw} (3.01) of pine milled into 300–425 μm . From the Table 3 it is clear that more than 90% of the material is in the range 1–6 which means that the particles are moderately elongated.

Table 3. Frequency of length/width ratio and aspect ratio values (1–15)

Interval (From – To)	Length/Width ratio R_{lw}			Aspect ratio A_r		
	Count	%	Cumulative %	Count	%	Cumulative %
1 \leq x < 1.5	97,935	18.3	18.3	92,320	17.2	17.2
1.5 \leq x < 2	132,528	24.7	43.0	136,130	25.4	42.6
2 \leq x < 2.5	82,803	15.4	58.4	94,986	17.7	60.3
2.5 \leq x < 3	59,140	11.0	69.5	53,578	10.0	70.3
3 \leq x < 3.5	34,249	6.4	75.8	42,795	8.0	78.3
3.5 \leq x < 4	29,928	5.6	81.4	28,373	5.3	83.6
4 \leq x < 4.5	18,756	3.5	84.9	15,526	2.9	86.5
4.5 \leq x < 5	15,499	2.9	87.8	15,971	3.0	89.5
5 \leq x < 5.5	10,211	1.9	89.7	8,824	1.6	91.1
5.5 \leq x < 6	10,017	1.9	91.6	9,581	1.8	92.9
6 \leq x < 8	21,525	4.1	95.6	18,703	3.4	96.4
8 \leq x < 10	9,992	1.9	97.5	8,629	1.7	98.0
10 \leq x < 15	9,818	1.8	99.3	5,151	1.0	99.5

Additional information about the particle morphology gave U_p , A_l , A_o and V_l . Mean values (together with maximum and minimum values) of these descriptors were U_p 3.08 ± 2.35 mm (0.36–78.25 mm), A_l 0.45 ± 0.68 mm² (0.01–46.11 mm²), A_o 2.04 ± 3.16 mm² (0.02–226.91 mm²) and V_l 0.24 ± 0.96 mm³ (0.00–127.04 mm³). Despite of the fact that surface area, volume and sphericity, representing 3D parameters (Zhao & Wang, 2016), were in this study calculated from 2D images, they offered valuable statistical data. 3D imaging could bring more precise results, however this would be associated with additional costs of equipment, longer analysing time and smaller amount of analysed particles bringing lower statistical confidence (Bagheri et al., 2015).

CONCLUSIONS

Particle size and shape are important factors that influence the final product's quality. A measurement of a single dimension may not be adequate to describe a typical non-spherical and irregular biomass particle with some extent of surface roughness. In this study particle size and shape of pine sawdust, the typical feedstock material for solid biofuel production, grinded to fraction size of 12 mm, was identified using the photo-optical analyzer based on digital image processing. The photo-optical particle analysis

provided far more detailed information about individual particle physical dimensions than conventional sieving approach, which only yields the cumulative mass curve and overall particle sizes given by the sieve size aperture. From the particle analysis, length, width, max feret, min feret, feret diameter, martin diameter and perimeter were obtained as well as sphericity, roundness, circularity, symmetry, volume, projection area, surface area, together with length/width and aspect ratio were calculated. Particles of pine sawdust can be described as irregular, slightly elongated with moderate degree of angularity, roughness and asymmetry. The real size of particles was much smaller than grinding size, and the fine particles were predominated. The obtained results may contribute to a better knowledge of material properties and facilitate the design of optimal technologies for biomass particle handling and production of quality biofuels with desired properties.

ACKNOWLEDGEMENTS. This research was supported by the Internal Grant Agency of the Faculty of Tropical AgriSciences (FTA), Czech University of Life Sciences (CULS), Prague [grant number 20185011 and 20195010]. Acknowledgement also goes to the Laboratory of biomass characterization CEDER-CIEMAT and specifically to Miguel Fernández Llorente, the head of the laboratory, for his assistance and valuable advice during the photo-optical analysis.

REFERENCES

- Agimelen, O.S., Mulholland, A.J. & Sefcik, J. 2017. Modelling of artefacts in estimations of particle size of needle-like particles from laser diffraction measurements. *Chemical Engineering Science* **158**, 445–452.
- Ahmad, A.A., Zawawi, N.A., Kasim, F.H., Inayat, A. & Khasri, A. 2016. Assessing the gasification performance of biomass: A review on biomass gasification process conditions, optimization and economic evaluation. *Renewable and Sustainable Energy Reviews* **53**, 1333–1347.
- Antonyuk, S., Jürgen, T., Heinrich, S. & Mörl, L. 2005. Breakage behaviour of spherical granulates by compression. *Chemical Engineering Science* **60**(14), 4031–4044.
- Bagheri, G.H., Bonadonna, C., Manzella, I. & Vonlanthen, P. 2015. On the characterization of size and shape of irregular particles. *Powder Technology* **270**, 141–153.
- Cardona, J., Ferreira, C., McGinty, J., Hamilton, A., Agimelen, O.S., Cleary, A., Atkinson, R., Michie, C., Marshall, S., Chen, Y.-C., Sefcik, J., Andonovic, I. & Tachtatzis, C. 2018. Image analysis framework with focus evaluation for in situ characterisation of particle size and shape attributes. *Chemical Engineering Science* **191**, 208–231.
- Cox, E.P.A. 1927. Method of Assigning Numerical and Percentage Values to the Degree of Roundness of Sand Grains. *Journal of Paleontology* **1**(3), 179–183.
- Cruz-Matías, I., Ayala, D., Hiller, D., Gutsch, S., Zacharias, M., Estradé, S. & Peiró, F. 2019. Sphericity and roundness computation for particles using the extreme vertices model. *Journal of Computational Science* **30**, 28–40.
- Dai, J., Cui, H. & Grace, J.R. 2012. Biomass feeding for thermochemical reactors. *Progress in Energy and Combustion Science* **38**(5), 716–736.
- Davies, E.R. 2018. Chapter 1 - Vision, the challenge. In Davies, E. R. (ed.): *Computer Vision (Fifth Edition)*. Academic Press, pp 1–15.
- Deac, T., Fechete-Tutunaru, L. & Gaspar, F. 2016. Environmental Impact of Sawdust Briquettes Use – Experimental Approach. *Energy Procedia* **85**, 178–183.
- Dražić, S., Sladoje, N. & Lindblad, J. 2016. Estimation of Feret’s diameter from pixel coverage representation of a shape. *Pattern Recognition Letters* **80**, 37–45.

- EN ISO 17827-1. 2016. Solid biofuels. Determination of particle size distribution for uncompressed fuels. Oscillating screen method using sieves with apertures of 3.15 mm and above. International Organization for Standardization, Geneva.
- EN ISO 17827-2. 2016. Solid biofuels. Determination of particle size distribution for uncompressed fuels. Oscillating screen method using sieves with apertures of 3.15 mm and below. International Organization for Standardization, Geneva.
- EN ISO 18134-2. 2017. Solid biofuels - Determination of moisture content - Oven dry method - Part 2: Total moisture - Simplified method. International Organization for Standardization, Geneva.
- EN ISO 9276-6. 2008. Representation of results of particle size analysis - Part 6: Descriptive and quantitative representation of particle shape and morphology. International Organization for Standardization, Geneva.
- Febbi, P., Menesatti, P., Costa, C., Pari, L. & Cecchini, M. 2015. Automated determination of poplar chip size distribution based on combined image and multivariate analyses. *Biomass and Bioenergy* **73**, 1–10.
- Fernlund, J.M.R. 1998. The effect of particle form on sieve analysis: a test by image analysis. *Engineering Geology* **50**, 111–124.
- Gil, M., Teruel, E. & Arauzo, I. 2014. Analysis of standard sieving method for milled biomass through image processing. Effects of particle shape and size for poplar and corn stover. *Fuel* **116**, 328–340.
- Guo, Q., Xueli, C. & Haifeng, L. 2012. Experimental research on shape and size distribution of biomass particle. *Fuel* **94**, 551–555.
- Haver & Boecker. 2014. Haver CpaServ Professional/Expert. Manual, Haver & Boecker, 85 pp.
- Haver & Boecker. 2015. Haver CPA 4-2, Haver CPA 4 Conveyor, operating instructions. Computer-supported photo-optical particle analysis. Manual, Haver & Boecker, 17 pp.
- Holmgren, P., Wagner, D.R., Strandberg, A., Molinder, R., Wiinikka, H., Umeki, K., Broström, M. 2017. Size, shape, and density changes of biomass particles during rapid devolatilization. *Fuel* **206**, 342–351.
- Igathinathane, C., Melin, S., Sokhansanj, S., Bi, X., Lim, C.J., Pordesimo, L.O. & Columbus, E.P. 2009a. Machine vision based particle size and size distribution determination of airborne dust particles of wood and bark pellets. *Powder Technology* **196**, 202–212.
- Igathinathane, C., Pordesimo, L.O., Columbus, E.P., Batchelor, W.D. & Sokhansanj, S. 2009b. Sieveless particle size distribution analysis of particulate materials through computer vision. *Computers and Electronics in Agriculture* **66**, 147–158.
- Knoll, M., Gerhardter, H., Prieler, R., Mühlböck, M., Tomazic, P. & Hochenauer, C. 2019. Particle classification and drag coefficients of irregularly-shaped combustion residues with various size and shape. *Powder Technology* **345**, 405–414.
- Koerner, R.M. 1970. Effect of particle characteristics on soil strength. *Journal of the Soil Mechanics and Foundations Division* **96**(4), 1221–1233.
- Krumbein, W.C. 1941. Measurement and geological significance of shape and roundness of sedimentary particles. *Journal of Sedimentation Research* **11**(2), 64–72.
- Kumara, G., Hayano, K. & Ogiwara, K. 2012. Image analysis techniques on evaluation of particle size distribution of gravel. *International Journal of GEOMATE* **3**(1), 290–297.
- Liliedahl, T. & Sjöström, K. 1998. Heat transfer controlled pyrolysis kinetics of a biomass slab, rod or sphere. *Biomass and Bioenergy* **15**(6), 503–509.
- Lu, H., Ip, E., Scott, J., Foster, P., Vickers, M. & Baxter, L.L. 2010. Effects of particle shape and size on devolatilization of biomass particle. *Fuel* **89**(5), 1156–1168.
- Masuda, H. & Gotoh, K. 1999. Study on the sample size required for the estimation of mean particle diameter. *Advanced Powder Technology* **10**(2), 159–173.

- Mora, C.F. & Kwan, A.K.H. 2000. Sphericity, shape factor, and convexity measurement of coarse aggregate for concrete using digital image processing. *Cement and Concrete Research* **30**(3), 351–358.
- Murphy, C.H. 1984. *Handbook of particle sampling and analysis methods*. Verlag Chemie International, 354 pp.
- Ndindeng, S.A., Mbassi, J.E.G., Mbacham, W.F., Manful, J., Graham-Acquaah, S., Moreira, J., Dossou, J. & Futakuchi, K. 2015. Quality optimization in briquettes made from rice milling by-products. *Energy for Sustainable Development* **29**, (Supplement C), 24–31.
- Niazmand, H. & Renksizbulut, M. 2003. Surface effects on transient three-dimensional flows around rotating spheres at moderate Reynolds numbers. *Computers and Fluids* **32**(10), 1405–1433.
- Olson, E. 2011. Particle shape factors and their use in image analysis – part 1: Theory. *Journal of GXP Compliance* **15**(3), 85–96.
- Pons, M.N., Vivier, H., Belaroui, K., Bernard-Michel, B., Cordier, F., Oulhana, D., Dodds, J.A. 1999. Particle morphology: from visualisation to measurement. *Powder Technology* **103**, 44–57.
- Powers, M.C. 1953. A new roundness scale for sedimentary particles. *Journal of Sedimentary Research* 117–119.
- Riguidel, F.-X., Jullien, R., Ristow, G.H., Hansen, A. & Bideau, D. 1994. Behaviour of a sphere on a rough inclined plane. *Journal de Physique I France* **4**, 261–272.
- Saastamoinen, J.J. 2006. Simplified model for calculation of devolatilization in fluidized beds. *Fuel* **85**(17), 2388–2395.
- Shanthi, C., Kingsley Porpatham, R. & Pappa, N. 2014. Image Analysis for Particle Size Distribution. *International Journal of Engineering and Technology* **6**, 5.
- Shekunov, B.Y., Chattopadhyay, P., Tong, H.H.Y. & Chow, A.H.L. 2006. Particle Size Analysis in Pharmaceuticals: Principles, Methods and Applications. *Pharmaceutical Research* **24**(2), 203–227.
- Souza, D.O.C. & Menegalli, F.C. 2011. Image analysis: Statistical study of particle size distribution and shape characterization. *Powder Technology* **214**(1), 57–63.
- Sunoj, S., Igathinathane, C. & Jenicka, S. 2018. Cashews whole and splits classification using a novel machine vision approach. *Postharvest Biology and Technology* **138**, 19–30.
- Trubetskaya, A., Beckmann, G., Wadenbäck, J., Holm, J.K., Velaga, S.P. & Weber, R. 2017. One way of representing the size and shape of biomass particles in combustion modeling. *Fuel* **206**, 675–683.
- Ulusoy, U. & Igathinathane, C. 2016. Particle size distribution modeling of milled coals by dynamic image analysis and mechanical sieving. *Fuel Processing Technology* **143**, 100–109.
- Vaezi, M., Pandey, V., Kumar, A. & Bhattacharyya, S. 2013. Lignocellulosic biomass particle shape and size distribution analysis using digital image processing for pipeline hydro-transportation. *Biosystems Engineering* **114**(2), 97–112.
- Wadell, H.A. 1932. Volume, Shape and Roundness of Rock Particles. *The Journal of Geology* **40**, 443–451.
- Walpole, L.J. 1972. The elastic behaviour of a suspension of spherical particles. *The Quarterly Journal of Mechanics and Applied Mathematics* **25**(2), 153–160.
- Yang, W.-C. 2003. Flow through fixed beds. In Yang, W.-C. (ed.): *Handbook of fluidization and fluid-particle systems*. Marcel Dekker, Inc: New York, pp. 29–53.
- Zhao, B. & Wang, J. 2016. 3D quantitative shape analysis on form, roundness, and compactness with μ CT. *Powder Technology* **291**, 262–275.

The nutrition value of soybeans grown in Latvia for pig feeding

L. Degola^{1,*}, V. Sterna², I. Jansons² and S. Zute²

¹Latvia University of Life Sciences and Technologies, Institute of Animal Sciences, Liela 2, LV3001 Jelgava, Latvia

²Institute of Agricultural Resources and Economics, “Dizzemes”, LV–3258 Dizstende, Libagi parish, Talsi County, Latvia

*Correspondence: lilija.degola@llu.lv

Abstract. Soybean products are excellent sources of protein for pigs because their amino acid profiles complement those of cereal grains. Soy protein is rich in the limiting amino acids lysine, threonine, and tryptophan that are present in relatively low concentrations in the most commonly fed cereal grains. Amino acids in soy protein are more digestible than amino acids in most other plants proteins, which results in less nitrogen being excreted in the manure from pigs fed diets containing soybean meal than if other protein sources are used. The phosphorus in soy products is bound to phytic acid, which has a low digestibility to pigs, but the digestibility of phosphorus in soy products may be increased to more than 60% if diets are supplemented with microbial phytase. There are no much results about nutrition value of soybean growing in Latvia. Therefore the aim of study was determined chemical composition of soybeans growing in Latvia and evaluates their potential in pig feeding.

Research object were soybeans growing in Latvia. In the studied samples content of protein, fat, ash, fibre, composition of amino acids were determined and metabolizable energy were calculated. Evaluated that protein content varied from 32.7 till 40.7%, fat content was from 18.4–21.4% and significantly differed ($p < 0.05$) among growing places, but the sum of essential amino acids in the soy beans determined 115–125 g kg⁻¹, and were not differed significantly by varieties. The content of lysine in protein were determined 5.1–5.5 g 100 g⁻¹. Concluded that soy bean growing in Latvia provides equilibrium high metabolizable energy for pigs – from 13.2 to 17.6 MJ kg⁻¹ and could be used in feed.

Key words: feed, amino acids, extruded soy bean.

INTRODUCTION

Soybeans are one of the most important protein sources in animal nutrition and are widely used in pig feeding. In the EU this crop is produced mainly in Italy (33%), Romania (18%), Croatia (14%), Austria, Hungary and France (all 9%) (EIP-AGRI report, 2014).

Several factors influence the chemical composition including concentration of amino acids present in soybeans, such as climatic changes, genetics, topography, and soil fertility (Wolf et al., 1982; Grieshop & Fahey, 2001; Grieshop et al., 2003; Carrera et al., 2011). Park & Hurburgh (2002) found that soybean meal samples from the European Union and United States had the greatest content of protein and the least amount of fiber compared with soybean meal from India, Brazil, Argentina, and China.

In the other research (Wang et al., 2011), the chemical analysis values showed that soybean meal from the United States had greater content of protein solubility and reduced concentration of crude fiber and ether extract compared with those from Brazil or India. Westgate et al. (2000) demonstrated that high environmental temperatures favor protein synthesis in the soybeans in detriment of oil production. Maximum oil accumulation in the soybeans occurs at 25–28 °C, according to experiments carried out by Piper & Boote (1999).

Soybeans are the gold standard of high quality protein for pigs because their amino acid profile complements the amino acid profiles of several cereal grains and have highest digestibility comparing with other proteins herbal origin (Stein et al., 2013). In particular, soybean protein is rich in lysine, threonine, and tryptophan. These are the most limiting amino acids in corn, wheat and barley. Despite the low levels of sulfur amino acids, soybean is the main source of lysine in swine diets (Goldflus, 2006), and could be complemented by barley or wheat in diet formulation. It is now well known that crude protein or the total amino acid amount from feedstuffs cannot be equally absorbed by the animal's digestive tract therefore it is necessary evaluate composition of amino acids and amount of essential amino acids. In the ideal protein concept, researchers recommend the precise amount of digestible amino acids. It is also important to evaluate the individual results of the limiting essential amino acids in soybean-based poultry and swine feeds, i.e., methionine, lysine, and threonine (Goldflus, 2006; Cervantes-Pahm & Stein 2010). Standardized ileal digestibility of amino acids (NRC, 2012) are: lysine is near 90%, methionine 90%, threonine 85% and tryptofane 90%, but in canola and sunflower meal amino acids digestibility are lower, 73–80%.

Productivity and rentability of livestock sector is strongly depending from availability and costs of feed, therefore in Latvia, same as in Baltic states and EU the role of local protein sources increasing. Some of farmers have started to grow soya beans to reduce imported feed and be safe about origin in last years but there are no much results about nutrition value of soybean growing in Latvia. Therefore the aim of study was determined chemical composition of soybean growing in Latvia and evaluate their potential in pig feeding.

MATERIALS AND METHODS

Experimental design. The research was conducted at the different places of Latvia – at Stende, Vilani and farms Rubuli, Jaunkalejini. Climatic conditions in 2018 determined untypically high temperature and low precipitation amount – sum of effective temperatures ($> +10$ °C) were calculate 2015 °C at Stende and 2019 °C at Vilani. It is necessary 350–500 mm precipitation for optimal soya development especially at germinating and leg formation period. In the mentioned period dripping 150 and 190 mm in Stende and Vilani, respectively.

The material consisted of soya varieties with early ripening ability (group 000) suitable for regions with lower (1,500–1,800 °C) sum of effective temperatures – ‘Abelina’, ‘Lajma’, ‘Laulema’, ‘Maja’, ‘Viola’, ‘Merlins’, ‘Mavka’, ‘Violetta’, ‘Madlena’, ‘Alexa’, ‘Tiguan’, ‘Paradis’, ‘Toultis’. The field treatments were laid out in a randomized complete block design (the plot size 10 m², four replicates) in Stende and Vilani, but in farms samples were taken from different places of 2 ha field. Mean samples from all (4) replications (0.5 kg) were taken for laboratory testing.

Chemical analyses

Protein content was determined as total nitrogen content by Kjeldahl method and using coefficient 6.25 for calculation (LVS NE ISO 5983-2:2009). Fat content was determined by Soxhlet method ISO 6492:1999.

Amino acids. Dried, defatted soya bean samples were hydrolysed with 6N HCl in sealed glass tubes at 110 °C for 23 h. Amino acids were detected using amino acids analyzer. The identity and quantitative analysis of the amino acids were assessed by comparison with the retention times and peak areas of the standard amino acid mixture. For statistical analysis purposes, essential amino acids (EAA) were considered the sum of arginine, phenylalanine, histidine, isoleucine, leucine, lysine, methionine, threonine, valine and tryptophan.

Ash were determined using ISO 5984: 2002/Cor1: 2005, calcium determined using LVS EN ISO 6869:2002, phosphorus using ISO 6491:1998, crude fibre determined using ISO 5498: 1981, ADF using LVS EN ISO 13906:2008, NDF using LVS EN ISO 16472:2006 methods. Metabolizable energy was calculated (Morgan et al., 1975). The obtained results were statistically processed using methods of descriptive statistics. Most data was reported as arithmetic means with the pooled SEM. Statistical significance was considered at probability $p < 0.05$.

RESULTS AND DISCUSSION

The results of chemical composition of soybeans grown in different regions of Latvia are assumed in Table 1.

Table 1. Chemical composition of soybeans grown in different fields

	n	Crudeprotein, %	Fat, %	Fibre, %	Ash, %	P, %	Ca, %
Stende C	22	32.7 ± 2.44	21.4 ± 1.45	11.8 ± 0.73	6.74 ± 0.28	0.58 ± 0.05	0.23 ± 0.02
Stende B	13	32.8 ± 2.90	20.9 ± 1.80	11.2 ± 0.73	6.70 ± 0.40	0.29 ± 0.05	0.29 ± 0.03
Rubuli C	4	40.7* ± 3.02	19.3 ± 2.04	11.5 ± 0.10	5.96 ± 0.08	0.49 ± 0.01	0.24 ± 0.02
Vilani C	14	35.7 ± 2.97	20.0 ± 1.21	11.5 ± 0.82	6.03 ± 0.50	0.42 ± 0.04	0.25 ± 0.02
Jaunkalejini	3	35.0 ± 1.70	18.4* ± 2.04	9.6 ± 1.10	6.14 ± 0.11	0.59 ± 0.03	0.21 ± 0.02

* $p < 0.05$.

The results assumed in Table 1. showed that protein content in soybean samples determined from 32.7 to 40.7% fat content from 18.4 to 21.4% and significantly differed ($p < 0.05$) among growing places. Metabolizable energy calculated for pigs varied from 13.2 to 17.6 MJ kg⁻¹ Preliminary results in Stende in 2015 showed similar composition of soya been seeds. Results showed that protein content in soy samples were determined from 35.9% to 40.9%, fat 16.6–19.3%, fibre 10.3–11.3% and ash 4.25–5.55% (Report, 2015). Must be concluded that as a result of weather conditions was higher content of ash (5.96–6.74%) and fiber (9.06–11.8%) in soya samples of year 2018 in comparison with results obtained in 2015 at Stende.

Pork producers often used unprocessed soy flour and data obtained from other investigations show that average crude protein in soy flour varied from 36–38% and fat content varied from 19 to 20% (Stein et al., 2013) similar results are obtained in Latvia in 2018.

The raw soybeans contains anti-nutrients, including phytic acid (from phytates), which binds and prevents mineral absorption, especially zinc, calcium, and magnesium (Humer et al., 2015).

The soybeans for pig feeding must be processed with aim avoid of anti-nutrients. Contents of secondary plant metabolites and α -galactosides may be reduced or eliminated by different processing methods, such as physical treatments (e.g. dehulling, soaking), heat treatments (e.g. extrusion, cooking) or biological methods (e.g. germination, enzyme supplementation). According to some studies (Stein & Bohlke, 2007) processing of soybeans and other grain legumes has been proven to efficiently improve starch and protein digestibility in pigs, which can be attributed, at least in part, to a reduction of secondary plant metabolites.

Composition of extruded fullfat soybean and low fat soybean samples prepared in this investigation showed in Table 2.

Table 2. Chemical composition of extruded soybeen samples

	Crude protein, %	Fat, %	Ash, %	Fibre, %	ADF, %	NDF, %	P, %	Ca, %
Full-fat soybean	37.02	21.13	6.78	5.46	9.84	10.23	0.49	0.38
Low fat soybean	43.36	6.71	7.81	5.75	8.07	12.00	0.56	0.39

Crude protein content in the extruded full fat soybean samples in this investigation were determined 37.02%, but in the extruded low fat soy samples 43.36%. The imported soybean meal in Latvia contains the 43.2% till 50.5% of crude protein (Latvian Feed tables, 2013) and depends on the country from which the feed is purchased. Results of other investigations showed the average crude protein on a dry matter basis, in soybean meal from China, the US, Brazil and Argentina was 50.2%, 49.4%, 51.1% and 48.8%, respectively. The chemical composition of the soybean meal sources was variable. The coefficient of variation of ether extract, crude fat, calcium and oligosaccharides was > 10% (Zhongchao et al., 2015).

Crude protein content is not the main indicator of quality of feed, more importantly is composition of amino acids. The analyzed levels of essential amino acids were not always directly related to the protein concentrations of the samples (Goldflus, 2006). Average daily mean air temperature and cumulative solar radiation during seed filling, precipitation minus potential evapotranspiration during the whole reproductive period, as well as combinations of these climatic variables, are significant explanatory variables for all amino acids. Each amino acid behaves differently according to environmental conditions, indicating compensatory effects among them (Carrera et al., 2011).

In the investigation determined composition of amino acids in soy samples obtained in Latvia in 2018 is showed in Table 3.

Amount of essential amino acids was determined 115–125 mg kg⁻¹. The ratio of essential amino acids to all was calculated 0.62–0.64 and it is higher than determined in faba beans and peas grown in Latvia.

The 10 essential amino acids that must be provided in pig diets are: lysine, threonine, tryptophan, methionine (and cystine), isoleucine, histidine, valine, arginine, and phenylalanine (and tyrosine). Most cereal grains are limiting in lysine, tryptophan, and threonine. Therefore, when evaluating feed ingredients, these amino acids, especially lysine, are most important in determining protein quality. Lysine the first

limiting amino acid in typical pig diets. Lysine is a substrate for generating body proteins, peptides, and non-peptide molecules, while excess lysine is catabolized as an energy source. Lysine can also affect the metabolism of other nutrients. Total amount of lysine in soya bean samples was determined 12.4–17.8 mg kg⁻¹.

Table 3. Composition of amino acids in soybean samples

Amino acids	Amount, mg kg ⁻¹	Average, mg kg ⁻¹	Amino acids	Amount, mg kg ⁻¹	Average, mg kg ⁻¹
Aspartic acid	22.1–33.2	28.01 ± 3.49	Valine	8.8–12.3	11.46 ± 1.54
Serine	9.6–14.9	12.19 ± 1.57	Methionine	2.7–3.9	3.29 ± 0.40
Glutamic acid	35.8–54.0	44.32 ± 5.73	Isoleucine	8.6–13.6	11.10 ± 1.52
Proline	9.71–15.7	12.19 ± 1.60	Leucine	15.2–22.5	19.1 ± 2.43
Glycine	8.6–12.6	10.44 ± 1.30	Tyrosine	6.1–11.0	8.71 ± 1.47
Alanine	9.1–12.6	10.52 ± 1.28	Phenylalanine	9.7–14.9	12.53 ± 1.73
Histidine	5.07–6.83	15.97 ± 0.70	Lysine	12.4–17.8	15.2 ± 1.77
Arginine	14.3–20.9	17.61 ± 2.10	Threonines	8.1–11.2	9.96 ± 1.17
Cysteine	2.9–4.0	3.63 ± 0.46	Tryptophane	2.8–3.6	3.3 ± 0.36

More often for feed quality characterization is calculated content of amino acid in protein, in this investigation content of lysine in proteine was 5.1–5.5%. Average content of lysine in soybean meal reported 6.0 g per 16g N (Hawhorne, 2006).

Soybeans importance as arginine source should not be disregarded, since arginine is a conditionally functional essential amino acid, amount of arginine in this investigation was determined 14.3–20.9 mg kg⁻¹

Formulators have already taken the opportunity to reduce CP content in European pig rations, going for a more concentrated formula through protein reduction and lysine incorporation. For example, between 2008 and 2013, the average lysine/CP percentage in piglet feeds went from 6.5 percent to 6.73 percent. Formulator’s responsiveness to those new practices varies between EU countries.

Comparison of extruded full-fat soybean and low-fat soybean with data of USDA database is showed in Fig. 1.

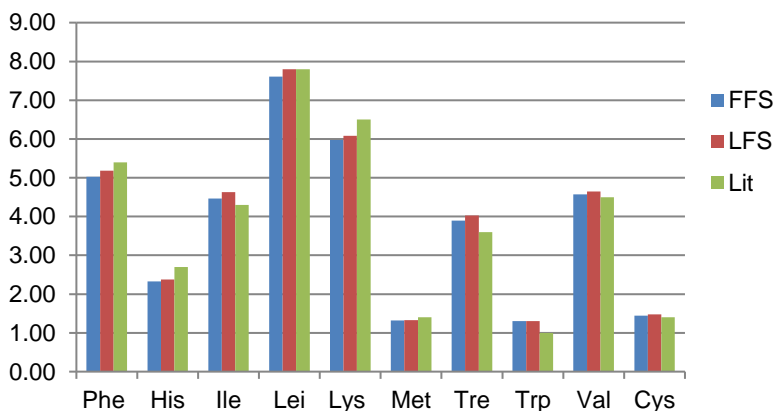


Figure 1. Content of essential amino acid in protein (g per 100 g), comparison of extruded full-fatsoybean (FFS) and low-fat soybean (LFS) grown in Latvia and data of USDA (Lit).

Content of essential amino acid in protein showed no significant difference in the extruded soybean grown and processed in Latvia compared to literature data. Content of isoleucine, threonine and tryptophan were determined higher than listed in database USDA. Moreover threonine and tryptophan along with methionine, cysteine and lysine are Critical Amino acids in pig feeding, Evaluation of first year data showed that in Latvia is possible to grow soybeans and produce an equivalent soybean meal according to the average values of the amino acid in the world.

CONCLUSIONS

Concluded that soy beans growing in Latvia provides equilibrium high metabolizable energy for pigs – from 13.2 to 17.6 MJ kg⁻¹ and could be used in feed. Protein content in soybean samples determined from 32.7 to 40.7% and significantly differed ($p < 0.05$) among growing places The ratio of essential amino acids to all was calculated 0.62–0.64 and it is higher than determined in faba beans and peas grown in Latvia. Content of lysine in protein was calculated 5.1–5.5% and it is high. Considering that these are one year results investigations must be continued.

ACKNOWLEDGEMENTS. Publication and dissemination of research results were carried out due to the support for EIP groups cooperation project ‘New technologies and economically viable solutions for the production of local feed for pig production: cultivation of non-genetically modified soybeans and new barley varieties in Latvia’ Nr. 18-00-A01612-000015.

REFERENCES

- Barbour, N., Westgate, M.E. & Orf, J.H. 1998. Response of soybean storage protein subunits to temperature. *In Agronomy Abstracts*, 121.
- Carrera, C.S., Reynoso, C.M., Funes, G.J., Martínez, M.J., Dardanelli, J. & Resnik, S.L. 2011. Amino acid composition of soybean seeds as affected by climatic variables *Pesq. agropec. bras.*, Brasilia, Vol. **46**(12), pp. 1579–1587.
- Cervantes-Pahm, S.K. & Stein, H.H. 2010. Ileal digestibility of amino acids in conventional, fermented, and enzyme-treated soybean meal and in soy protein isolate, fish meal, and casein fed to weanling pigs. *J. Animal Science* **88**, 2674–2683.
- EIP-AGRI Focus Group Protein Crops:final report 14 apr 2014
- Goldflus, F.I., Ceccantini, M.I.I. & Santos, W.I.I. 2006. Amino acid content of soybean samples collected in different Brazilian states – harvest 2003/2004. In *Brazilian Journal of Poultry Science* Print version ISSN 1516-635X On-line version ISSN 1806-9061 Rev. Bras. Cienc. Avic. Vol. **8**(2), <http://dx.doi.org/10.1590/S1516-635X2006000200006> [28.01.2019]
- Goldflus, F. 2004. The use of soybean protein sources in swine and poultry feeding. In: *7 World Soybean Research Conference; 6 International Soybean Processing and Utilization Conference, 3 Congresso Brasileiro de Soja*, Foz do Iguaçu, PR. Brasil. Londrina: SBS, pp. 882–891.
- Grieshop, C.M. & Fahey, G.C. Jr. 2001. Comparison of quality characteristics of soybean meals. *J. Agric. Food Chem.* **60**, 437–442.
- Grieshop, C.M., Kadzere, C.T., Clapper, G.M., Flickinger, E.A., Bauer, L.L., Frazier, R.L. & Fahey, G.C. Jr. 2003. Chemical and nutritional characteristics of United States soybeans and soybean meals. *J. Agric. Food Chem.* **51**, 7684–7691.
- Hawthorne, W. 2006. Pulses nutritional value and their role in the feed industry. Published by Pulse Australia Pty Ltd pp.22.
- Humer, E, Schwarz, C & Schedle, K. 2015. Phytate in pig and poultry nutrition. *Animal Physiology Animal Nutrition* **99**(4), 605–625.

- ISO 5498:1981. Agricultural food products. Determination of crude fibre content. ISO/TC34, ICS: 67.050, ed.1, 8 pp.
- ISO 5984: 2002/Cor.1:2005. Animal feeding stuffs. Determination of crude ash. ISO/TC34, Food products SC 10 ed.3, 10 pp.
- ISO 6491:1998. Animal feeding stuffs. Determination of phosphorus content. ISO/TC34/SC10, ICS: 65.120, ed.2, 7 pp.
- ISO 6492:1999. Animal feeding stuffs. Determination of fat content. ISO/TC34/SC10, ICS: 65.120, ed.1, 9 pp.
- LVS EN ISO 5983-2:2009. Animal feeding stuffs. Determination of nitrogen content and calculation of crude protein content. ISO 5983-2:2009, ISO/TC34/SC10, ICS: 65.120, ed. 2. part 2, 15 pp.
- LVS EN ISO 6869:2002. Animal feeding stuffs. Determination of calcium, magnesium and sodium. ISO 6869:2000, ISO/TC34/SC10, ed.1, 15 pp.
- LVS EN ISO 16472: 2006. Animal Feeding stuffs. Determination of amylase -treated neutral detergent fiber (NDF) content. ISO/TC34/SC10, ICS: 65.120, ed. 1, 16 pp.
- LVS EN ISO 13906: 2008. Animal Feeding stuffs. Determination of acid detergent fiber (ADF) and acid detergent lignin (ADL) contents. ISO 13906:2008. ISO/TC34/SC10, ICS: 65.120, ed. 1, 17 pp.
- Latvian Feed Tables. 2013. LLKC, Ozolnieki, Latvia, 36 pp.
http://new.llkc.lv/sites/default/files/baskik_p/pielikumi/lopbar.pdf
- Morgan, D.J., Cole, D.J.A. & Lewis, D. 1975. Energy value in pig nutrition. 1. The relationship between digestible energy, metabolizable energy and total digestible nutrient values of a range of feedstuffs. *J. Agric. Sci.* **84**, 717.
- NRC. National Research Council. 2012. Nutrient Requirements of Swine. 11th rev. ed. Natl. Acad. Press, Washington DC.
- Park, H.S. & Hurburgh, C.R. Jr. 2002. Improving the U.S. position in world soybean meal trade. MATRIC Working Paper 02-MWP 7. Accessed May 10, 2009
<http://www.card.iastate.edu/publications/DBS/PDFFiles/02mwp7.pdf>.
- Piper, E.L. & Boote, K.I. 1999. Temperature and cultivar effects on soybean seed oil and protein percentages. *Journal of the American Oil Chemists' Society* **76**, 1233–41.
- Report of Practical Applied Research Project from the Ministry of Agriculture 'Legumes - as an alternative to soybean in the production of protein-rich fodder: agrotechnical and economical substantiation for cultivation in Latvian conditions'. (Project manager Dr. agr. S. Zute, 2013–2015).
- Stein, H.H., Roth, J.A., Sotak, K.M. & Rojas, O.J. 2013. Nutritional Value of Soy Products Fed to Pigs. University of Illinois, Urbana-Champaign 'Swine Focus'. 01 August 2013.
- Stein, H.H. & Bohlke, R.A. 2007. The effects of thermal treatment of field peas (*Pisum sativum* L.) on nutrient and energy digestibility by growing pigs. *J. Anim. Sci.* **85**, pp. 1424–1431.
- United States Department of Agriculture Food Composition Databases <https://ndb.nal.usda.gov/ndb/>
- Wang, J.P., Hong, S.M., Yan, L., Cho, J.H., Lee, H.S. & Kim, I.H. 2011. The evaluation of soybean meals from 3 major soybean-producing countries on productive performance and feeding value of pig diets. *J. Anim. Sci.* **89**, 2768–2773. doi:10.2527/jas.2009-1800
- Westgate, M.E., Piper, E., Batchelor, W.D. & Hurburgh, C. Jr. 2000. Effects of cultural and environmental conditions during soybean growth on nutritive value of soy products. In: *Drackley JK. Soy in animal nutrition. Savoy: Federation of Animal Science Societies*, pp. 75–89.
- Wolf, R.B., Cavins, J.F., Kleiman, R. & Black, L.T. 1982. Effect of temperature on soybean seed constituents: oil, protein, moisture, fatty acids, and sugars. In *Journal of the American Oil Chemists' Society* **59**, pp. 230–32.
- Zhongchao, L., Xiaoxiao, W., Panpan, G., Ling, L., Xiangshu, P., Stein, H.H., Defa, L. & Changhua, L. 2015. Prediction of digestible and metabolisable energy in soybean meals produced from soybeans of different origins fed to growing pigs. *J. of Animal Nutrition* Vol. **69**(6), 473–486, <http://dx.doi.org/10.1080/1745039X.2015.1095461>

Use of ethanol production and stillage processing residues for biogas production

V. Dubrovskis*, I. Plume and I. Straume

Latvia University of Life Sciences and Technologies, Liela street 2, LV 3001 Jelgava, Latvia

*Correspondence: vilisd@inbox.lv

Abstract. In Latvia, ethanol is produced mainly from wheat grains. The production process involves the formation of the by-products of wheat bran, grains residues and stillage. By-products from production of alcohol distilling dregs (stillage) contain much organic matter therefore could be useful for the production of the biogas. The product with high protein content usable for feed can be produced from the stillage too. A liquid residue is formed during the production process. Purpose of study is the assessment of the methane volume obtainable from the stillage processing residue mixed with wheat brans and grains residues in anaerobic fermentation process and from wheat brans and grains residues mixed only with inoculum. Investigation was provided in 16 bioreactors operated in batch mode at 38 °C. Stillage processing residues mixed with the wheat brans and inoculum were filled into 4 bioreactors, mixed with grains residues were filled into 4 bioreactors and only inoculum was filled into two bioreactors for control. Wheat brans with inoculum were filled into 3 bioreactors. Into others 3 bioreactors were filled grains residues with inoculum. The yield of biogas from wheat brans was 1.151 L g⁻¹_{DOM} and methane 0.593 L g⁻¹_{DOM} after 30 days of anaerobic digestion. The yield of biogas from wheat brans with stillage processing residue was 1.098 L g⁻¹_{DOM} and methane 0.600 L g⁻¹_{DOM}. The yield of biogas from grains residues was 0.915 L g⁻¹_{DOM} and methane 0.451 L g⁻¹_{DOM}. The yield of biogas from grains residues with stillage processing residue was 1.01 L g⁻¹_{DOM} and methane 0.523 L g⁻¹_{DOM}. The study demonstrates that the investigated products are very good raw material for the production of methane. Stillage processing residue acted as a catalyst for the process.

Key words: methane; stillage, anaerobic digestion, wheat brans, grains residues, stillage processing residue.

INTRODUCTION

Most biogas plants built in Latvia are large and therefore require a lot of raw materials. Many of them do not have enough land to grow own raw materials and therefore raw materials are transported even from a long distance. The prices on raw materials increased significantly (Atanasiu, 2010). There has been fierce competition for arable land, and farmers who have been able to rent cheap land so far are particularly dissatisfied. Now, due to the development of biogas production, land prices have risen. Although there is a lot of unused or underutilized land in Latvia (Dubrovskis & Adamovics, 2012), competition is getting worse and owners of dairy farms, who do not have biogas plants, are putting pressure on the Ministry of Agriculture and the Ministry

of Economy to limit the use of arable land for biogas producers. At the same time, some food production facilities produce waste and it is difficult to dispose of such waste (Al Seadi et al., 2008). For example, a bioethanol plant stillage processing product still contains a lot of chemical oxygen demand (COD) and cannot be easily cleaned in biological treatment plants, because its pH is also low. One of solutions of this problem is its use for the biogas production, but effectiveness of anaerobic digestion process can be lowered due to too low dry matter content (Wilkie et al., 2000; Westerholm et al., 2012).

However, with rising energy prices bioethanol plants will need to optimize energy consumption in order to avoid a negative impact on the costs of ethanol production (Drosg et al., 2008).

Many researchers have been investigated the potential of biogas from the stillage (Stover et al., 1984; Wilkie et al., 2000; Schaefer, 2006; Kim et al., 2008; Schaefer & Sung 2008; Kaparaju et al., 2010; Ghorbani, 2011; Dubrovskis & Plume, 2017a). The study of the biochemical potential of methane (BMP) from the stillage gave methane yield $0.409.8 \text{ Nm}^3 \text{ CH}_4 \text{ kg}^{-1}_{\text{DOM}}$ from the raw grain and $0.467.6 \text{ Nm}^3 \text{ CH}_4 \text{ kg}^{-1}_{\text{DOM}}$ from greenery (Errata, 2015). Investigation conducted by the Swedish Boras University (Awosolu, 2008) identified and compared the theoretical methane potential for stillage produced from wheat $0.473 \text{ m}^3 \text{ kg}^{-1}_{\text{DOM}}$. For cellulose fibre it was $0.407 \text{ m}^3 \text{ kg}^{-1}_{\text{DOM}}$. Practically got methane $0.288 \text{ m}^3 \text{ kg}^{-1}_{\text{DOM}}$ from wheat stillage and $0.218 \text{ m}^3 \text{ kg}^{-1}_{\text{DOM}}$ from cellulose stillage. University of Vienna have been investigated (Drosg et al., 2013) found BMP for each stillage fraction. There are a lot of data on anaerobic fermentation of thin stillage. Methane BMP of thin stillage (TS = 7.5%) it was $500 \text{ Nm}^3 \text{ t}^{-1}_{\text{VS}}$ added. However, the amount of methane extracted from the stillage processing is a highly liquid product (1 to 1.5% dry matter), which is produced in the Iecava's bioethanol plant, was not found in the literature. In Latvia such the research has been carried out for the first time.

Biogas potential from the wheat bran has been investigated by several (Becker et al., 2007; Drosg, 2008; Wellinger et al., 2013) researchers. The substrate with and without pre-treatment gave daily methane yields of $0.430 \text{ m}^3 \text{ kg}^{-1}_{\text{DOM}}$ and $0.389 \text{ m}^3 \text{ kg}^{-1}_{\text{DOM}}$ respectively.

Researchers was investigated the potential of biogas and methane from different grains residues in the LULST Bioenergy Laboratory. Biomass were taken from a dryer where various grains were processed. In the first 2017 year study (Dubrovskis & Plume, 2017b) an average of $0.694 \pm 0.098 \text{ L g}^{-1}_{\text{DOM}}$ biogas and $0.383 \pm 0.08 \text{ L g}^{-1}_{\text{DOM}}$ methane were obtained. In another investigation (Dubrovskis et al., 2018) was yield of biogas from grains residues average $0.721 \pm 0.06 \text{ L g}^{-1}_{\text{DOM}}$ and methane $0.376 \pm 0.02 \text{ L g}^{-1}_{\text{DOM}}$. But preliminary investigation results (Dubrovskis & Plume, 2017b) were following: yield of biogas - $0.517 \pm 0.06 \text{ L g}^{-1}_{\text{DOM}}$ and methane $0.268 \pm 0.03 \text{ L g}^{-1}_{\text{DOM}}$. The great difference in results can be explained by the composition of the different grains residues and how many in there are whole grains.

The aim of this work is to find out the suitability of three different bioethanol waste products - stillage processing residue, wheat bran and grain residues for biogas production.

MATERIALS AND METHODS

The stillage contains not less than 17 different amino acids, the total content of which is 35.6% of the absolute dry matter. Carbohydrates account for an average of 13.5%, fat for 7–8% and mineral salts for 2.4%. One of the most valuable properties of the stillage is that the stillage contains the full spectrum of the B group vitamins, as well as vitamin B (folic acid), tocopherol, ergosterol, which are the regulators of animal metabolism. The dry matter of the stillage is also characterized by the presence of trace elements such as iron, zinc, manganese, copper, etc. rich content. After nutritional value, the stillage dry matter exceeds the standard compound feed and bran. Protein is produced from the stillage. Feed protein contains a large amount of raw protein that reaches and exceeds 37%, and is equivalent to sunflower cake protein after use efficiency and nutritional value. This amount of protein is determined by the course of yeast life processes during the fermentation of the alcoholic raw materials. Protein production from the stillage process produces a liquid residue. The stillage processing residue is shown in Fig. 1. This is the product that results from the residue in the protein product manufacturing process at the bioethanol plant.

Wheat bran is a product of grain milling residue. Grain casings consist mainly of fibre (cellulose, hemicellulose and lignin), minerals (potassium, calcium, magnesium, iron, etc.), group B vitamins, carotenoids and proteins. Grain germ contains fats of high-quality fatty acids (linoleic acid, linolenic acid, monounsaturated oleic acids). Grinding the grains, the casings and germ of high-quality nutrients are mechanically separated, bran still contains many valuable substances facilitating also anaerobic digestion process. Bran is an excellent product that mechanically cleans the digestive tract while providing the body with many high-quality substances. There are few simple sugars in bran, but they are very rich in protein and contains also soluble fibre. Fibres have a high absorption capacity, which absorbs 25 times more water than their volume.

Grain residues are very different depending on the type of grain have been treated to dryer. Also, the content of biogas and methane varies depending on the grain composition and content of the husks. The wheat and triticale grains residues of JP Iecava plant are shown in Fig. 3.

In the investigation, digestate, which was taken from the bioreactor of the Bioenergy Laboratory, operating with the cows manure in a continuous mode, was used. Wheat bran, grain residues and stillage processing residue (Figs 1, 2, 3) from JP Iecava's bioethanol plant were used as raw materials for anaerobic fermentation research.



Figure 1. Stillage processing residue.



Figure 2. Wheat bran.



Figure 3. Grain residues.

The methodology described below and similar with German VDI 4630 (VDI 4630, 2006) guideline and the German Methodenhandbuch Energetische Biomassennutzung (Thran, 2010) were used for the present study. The widely applied methods (Angelidaki et al., 2009) were used for the AD process investigation in 16 experimental bioreactors with volume of 0.75 litres. 2 bioreactors for control were filled with 400.0 ± 0.2 g inoculums and rest bioreactors were filled with mixtures of inoculums (400 g) and added biomass, according to experimental plan, see Table 1. Dry organic matter (DOM) content was determined by weighting of the initial biomass samples, drying in dry matter weights Shimazu at 105°C and then placed for ashing in oven ('Nabertherm' type) at 550°C . All the components were carefully mixed together and filled in bioreactors. All bioreactors were placed into heated thermostat SNOL in the same time before starting of anaerobic digestion. Gas released from each bioreactor was collected in storage bag positioned outside of the thermostat container. Gas volumes were measured using flow meter (Ritter drum-type gas meter). The composition of gases, including oxygen, carbon dioxide, methane, and hydrogen sulphide was measured help by gas analyser (model GA 2000). The substrate pH value was measured before and after finishing off the AD process, using a pH meter (model PP-50) with accessories. Scales (Kern, model KFB 16KO2) was used for weighting of the total weight of substrates before and after the AD process. Fermented cattle manure (from 120 L bioreactor working in continuous mode) was used as the inoculum. Batch mode AD process was ongoing at temperature $38 \pm 0.5^\circ\text{C}$. Biogas released was collected in gas bags for further measurements of gas volume and elemental composition. Biogas and methane volumes and gases composition were measured during AD process at regular time intervals. The AD process was provided until biogas emission ceases. Obtained experimental data were processed using appropriate statistical methods.

Three bioreactors (R2–R4) were filled with 400 g of inoculum (digestate) (weighing up to 0.2 g accuracy) and 10 g of wheat bran WB. The other two bioreactors (R5–R6) were filled with 400 g of inoculum (weighing up to 0.2 g) and 10 g of wheat bran and 100 g of stillage processing residues. The other two bioreactors (R7–R8) were filled with 400 g of inoculum and 5 g of wheat bran and 100 g of stillage processing residues. The R9–R11 bioreactor was filled with every 400 g of inoculum and 10 g of grain residues. Other two bioreactors (R12–R13) were filled with 400 g of inoculum and 10 g of grain residues and 100 g of stillage processing residues. Other two bioreactors (R14–R15) were filled with 400 g of inoculum and 5 g of grain residues and 100 g of stillage processing residues. In the bioreactor R1, R16 was filled with 400 g of inoculum - digestate (control sample) each. All data was recorded in the experiment log and on the computer. All bioreactors were connected to calibrated gas storage bags and taps, placed in an oven and set at a working temperature of $38 \pm 0.5^\circ\text{C}$. The amount and composition of the released gas was measured daily. Bioreactors were also shaken daily by mixing the substrate to wet and reduce the floating layer. The fermentation took place in a single filling (batch) mode and lasted until the biogas was released (25 days).

RESULTS AND DISCUSSION

The data on sample analysis and on amount of biogas and methane produced was estimated for all 16 bioreactors, and average results were calculated. The LUA

laboratory identified the main organic matter composition of the wheat bran sample: Protein 15.18%; Lipids 4.58%; Carbohydrates 16.83%.

The results of raw material analyses before anaerobic digestion are shown in Table 1.

Table 1. Results of analysis of raw materials

Raw material	pH	TS %	TS g	ASH %	DOM %	DOM g	Weight g
R1, R16 inoculum 400 g In	7.5	4.99	19.96	15.69	84.31	16.828	400
R2–R4 10 g WB		85.66	8.566	9.76	90.24	7.730	10
R2–R4 400 g In+10 g WB	7.5	6.96	28.526	13.91	86.09	24.558	410
R5–R6 10 g WB+400 g In+100 g SPR		5.89	30.026	13.47	86.53	25.982	510
R7–R8 5 g WB +100 g SPR+400 g In		5.10	25.743	14.09	85.91	22.117	505
R9–R11 10 g GR		88.35	8.835	13.39	86.61	7.652	10
R9–R11 10 g GR+400 g In		7.02	28.795	14.99	85.01	24.480	410
R12–R13 10 g GR+400 g In+100 g SPR		5.94	30.295	14.49	85.51	25.904	510
100 g SPR		1.50	1.50	5.10	94.90	1.424	100
R14–R15 5 g GR +400 g In+100 g SPR		5.12	25.878	14.68	85.32	22.078	505

Abbreviations: TS – total solids; ASH – ashes; DOM – dry organic matter; In – inoculums, 400 g In – 400 g inoculum; WB – wheat brans; GR – grains residues; SPR – stillage processing residues; 100 g SPR – 100 g stillage processing residues.

The results of biogas and methane from all raw materials are shown in Table 2 and in the figures. The table shows the results from the R2–R15 bioreactors, where the amount of gas obtained from the inoculum is already calculated.

Table 2. Biogas and methane yields

Raw material	Biogas, L	Biogas, L g ⁻¹ _{DOM}	Methane, aver. %	Methane L	Methane, L g ⁻¹ _{DOM}
R1 400 g In	0.3			0.09	
R16 400 g In	0.6			0.089	
R2WB10 g+ In 400 g	9.2	1.19	53.69	4.939	0.639
R3 WB 10g+ In 400 g	9.0	1.164	52.06	4.684	0.606
R4 WB10 g+ In 400 g	8.5	1.100	48.64	4.134	0.535
R2–R4	8.9	1.151	51.46	4.586	0.593
± st.dev.	± 0.36	± 0.046	± 2.58	± 0.411	± 0.053
R5 WB 10 g+ In 400 g+100 SPR	10.5	1.147	55.97	5.924	0.647
R6 WB 10 g+ In 400 g+100 SPR	9.6	1.049	52.72	5.065	0.553
R5–R6 WB	10.05	1.098	54.35	5.495	0.600
± st.dev.	± 0.64	± 0.069	± 2.30	± 0.607	± 0.066
R7 WB 5 g+ In 400 g+100 SPR	7.2	1.361	51.95	3.740	0.707
R8WB 5 g+ In 400 g+100 SPR	6.4	1.210	55.28	3.539	0.669
R7–R8	6.8	1.286	53.62	3.640	0.688
± st.dev.	± 0.57	± 0.107	± 2.35	± 0.142	± 0.027
R9 GR10 g+ In 400 g	7.7	1.006	47.22	3.633	0.475
R10 GR 10 g+ In 400 g	6.6	0.863	50.98	3.364	0.440
R11 GR 10 g+ In 400 g	6.7	0.876	50.11	3.363	0.439
R9–R11GR	7.0	0.915	49.44	3.453	0.451
± st.dev.	± 0.61	± 0.079	± 1.97	± 0.156	± 0.021

Table 2 (continued)

R12 10GR+ 100 SPR + In 400 g	6.8	0.749	55.27	3.757	0.414
R13 10GR +100 SPR + In 400 g	7.6	0.837	51.59	3.909	0.431
R12–R13	7.2	0.793	53.43	3.833	0.423
± st.dev.	± 0.57	± 0.062	± 2.60	± 0.107	± 0.012
R14 5GR +100 SPR + In 400 g	5.3	1.01	50.30	2.666	0.508
R15 5GR +100 SPR + In 400 g	5.3	1.01	53.28	2.824	0.538
R14–R15	5.3	1.01	51.79	2.745	0.523
± st.dev.	± 0.0	± 0.00	± 2.11	± 0.112	± 0.021

Abbreviation: L g⁻¹DOM – litres per 1 g dry organic matter added (added fresh organic matter into inoculum).

From the table data it was estimated that the inoculum (digestate) was still slightly digested. The digest of DOM cannot completely decompose because it contains many microorganism cells.

As shown in the table, methane was extracted more from bio-reactors, where 10 g of wheat brans and 100 g of stillage processing residue were filled. Also in bio-reactors, where 10 g of grain residues and 100 g of stillage processing residue, methane was formed more than in those bioreactors containing only 10 g of wheat bran or 10 g of grain residues. This shows that adding 100 g of the stillage processing residue is useful. Methane is derived from wheat bran more than from grain residues. Specific biogas and methane yields from bioreactors filled with wheat brans, grain residues and stillage processing residues shown in Fig. 4.

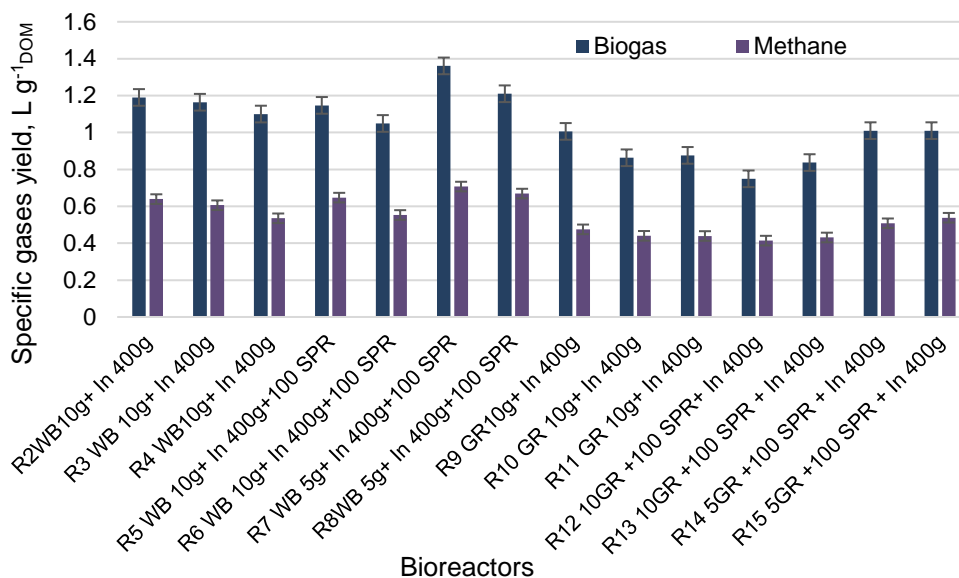


Figure 4. Specific biogas and methane yields from bioreactors filled with wheat brans, grain residues and stillage processing residues.

As seen from the figure, most methane is obtained from bioreactors, where 100 g of stillage processing residue was added to wheat bran and grain residues 5 g. From the bioreactors, where 10 g of wheat bran and the grain residues were filled, were obtained

less methane, because the optimum organic load was obviously exceeded and the AF process slightly inhibited.

Fig. 5 shows the average methane content of each bioreactor with wheat bran, grain residues and stillge processing residue.

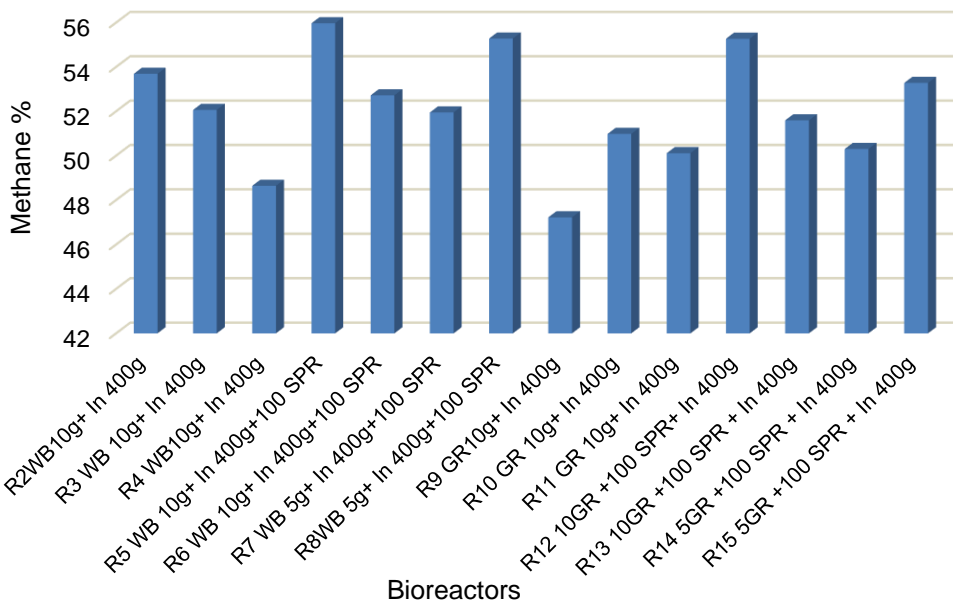


Figure 5. Average methane content of each bioreactor with wheat bran, grain residues and stillage processing residue.

To find out how fast methane production took place in the bioreactors of each raw materials group, the results were analyzed on average after 7, 14 and 25 days (Table 3).

Table 3. Average biogas and methane contents and yields after 7, 14 and 25 days

Bioreactor	Biogas, L			Methane, %			Methane, L			Methane, L g _{DOM} ⁻¹		
	7d	14d	25d	7d	14d	25d	7d	14d	25d	7d	14d	25d
R2–R4	6.033	8.33	8.9	74.1	47.37	51.46	2.944	4.374	4.586	0.381	0.566	0.593
R5–R6	4.95	8.4	10.1	74.95	60.65	54.34	2.369	4.709	5.495	0.259	0.514	0.600
R7–R8	5.6	6.2	6.8	72.25	46.55	53.62	3.205	3.57	3.64	0.606	0.675	0.688
R9–R11	4.2	6.17	7.0	67.23	54.87	49.44	1.876	3.071	4.455	0.245	0.402	0.451
R12–R13	4.45	6.15	7.2	73.55	47.3	53.38	2.607	3.646	3.833	0.287	0.402	0.423
R14–R15	4.35	4.95	5.3	66.1	49.55	51.78	2.322	2.642	2.745	0.442	0.504	0.523

The production of methane L g⁻¹_{DOM} from wheat bran and wheat bran with stillage processing residue after 7, 14 and 25 days is shown in Fig. 6. Methane produced very fast in bioreactors, with 5 g of WB and 100 g of stillage processing residues. Already in the first week, 88.05% of the total 25-day production of methane was produced. This proves that this proportion of wheat bran and stillage processing residues is very good and provides the correct AF process. The results obtained compared to the results of

other biomass are very good. Also, wheat bran and grain residues produce higher yields of methane as shown by other researchers and obtained from our previous research. This could be explained by the good quality of these biomass.

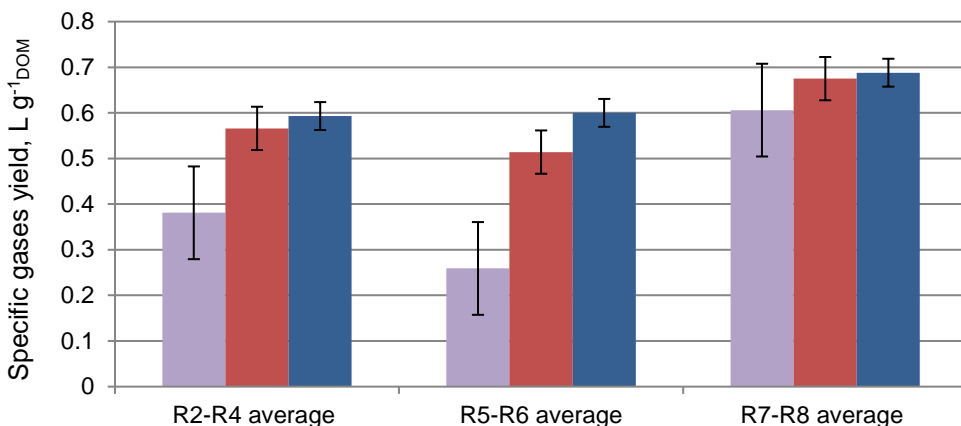


Figure 6. The production of methane L g⁻¹DOM from wheat bran and wheat bran with stillage processing residue after 7, 14 and 25 days.

Methane L g⁻¹DOM from grain residues and stillage processing residues is shown in Fig. 7. Extracting it to organic dry matter content exceeded not only the obtained from 10 g grain residues, but also from the 10 g grain residues and 100 g stillage processing residues. This can be explained by the inhibition of the AF process due to organic overload. Here, inhibition was greater than that of bioreactors with wheat bran.

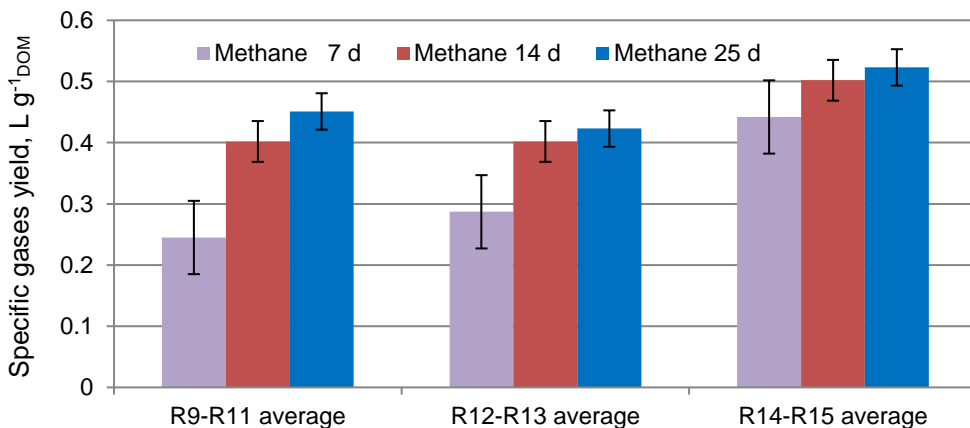


Figure 7. Methane L g⁻¹DOM from grain residues and stillage processing residues.

The results obtained from wheat bran, stillage processing residue and grain residues from natural mass are summarized in Table 4.

Table 4. The results obtained from wheat bran, stillage processing residue and grain residues from natural mass

Raw material	TS%	DOM%	Biogas L g ⁻¹ _{DOM}	Methane L g ⁻¹ _{DOM}	Vnm biogas m ³ t ⁻¹	Vnm methane m ³ t ⁻¹
WB	85.66	90.24	1.191	0.593	920.63	458.39
WB10+100SPR	9.15	90.94	1.098	0.600	91.36	49.93
WB5+100SPR	5.50	91.46	1.286	0.688	64.69	34.61
GR	88.35	86.61	0.915	0.451	700.15	345.10
GR10+100SPR	9.40	87.82	0.793	0.423	65.46	34.92
GR5+100SPR	5.64	88.71	1.010	0.523	50.53	26.17

Abbreviation: Vnm – volume obtained from natural mass.

CONCLUSIONS

1. Both wheat bran and grain residues produced a high yield of methane. Such raw materials can be well used in Latvian conditions.

2. When adding 100 g of stillage processing residue to wheat bran, methane yields increased, but only slightly when the optimum organic load was exceeded (10 g WB + 100 g SPR).

3. Adding 100 g of stillage processing residue to grain residues increased the yield of methane, but only did not when the optimum organic load was exceeded (10 g GR + 100 g SPR).

4. When 100 g of stillage processing residues were added to 5 g wheat bran, the methane yield increased by 16.02% compared to bioreactors with only wheat bran, although twice more. This proves the good effect of stillage processing residue.

5. When 5 g of grain residues was added to 100 g of stillage processing residues, the methane yield increased by 15.96% compared to bioreactors, containing 10 g of grain residues. It also proves the good effect of stillage processing residue.

6. In bioreactors, where the stillage processing residues were filled, the anaerobic fermentation process starts more rapidly and the organic matter decomposed more rapidly.

7. Comparison of raw materials by natural methane yields shows that wheat bran, which can yield 458.39 m³ t⁻¹, is the most valuable raw material. This is very good compared to other biomasses. A good raw material is also a grain residue that can produce 345 m³ t⁻¹ methane.

REFERENCES

- Al Seadi, T., Rutz, D., Prassl, H., Köttner, M., Finsterwalder, T., Volk, S. & Janssen, R. 2008. *Biogas handbook*. Published by University of Southern Denmark Esbjerg, Denmark, 127 pp.
- Angelidaki, I., Alves, M., Bolzonella, D., Borzacconi, L., Campos, J.L., Guwy, A.J. Kalyuzhnyi, S., Janicek, P., van Lier, J.B. 2009. Defining the biomethane potential: proposed protocol for batch assays. *Water Science & Technology*, WST **59**.5, pp. 1–8.
- Atanasiu, B. 2010. The Role of Bioenergy in the National Renewable Energy Action Plans: A First Identification of Issues and Uncertainties. Publication of the BIOMASS FUTURES project (IEE 08 653 SI2. 529 241) pp. 22.

- Awosolu, Mary. 2008. *Anaerobic digestion of ethanol distillery waste-stillage for biogas production. Msc. thesis*, University of Borås, 62 pp.
- Becker, K., Dowler, H. & Meckel, H. 2007. *Faustzahlen Biogas (Calculations of biogas)*, *Publisher Kuratorium für Technik und Bauwesen in der Landwirtschaft, Darmstadt*, 181 pp. (in German).
- Drosg, B. 2008. Comparing centralized and decentralized anaerobic digestion of stillage from a large scale bioethanol plant to animal feed production. *Water Science and Technology* **58**(7), 1483–1489.
- Drosg, B., Fuchs, W., Meixner, K., Waltenberger, R., Kirchmayr, R., Braun, R. & Bochmann, G. 2013. Anaerobic digestion of stillage fractions – estimation of the potential for energy recovery in bioethanol plants. *Water Science and Technology* **67**(3), 494–506.
- Dubrovskis, V. & Adamovics, A. 2012. *Bioenerģētikas horizonti (Horizons of Bioenergy)*, Jelgava, Latvia, 352 pp. (in Latvian).
- Dubrovskis, V. & Plume, I. 2017a. Methane production from stillage. *Proceedings of International conference Engineering for Rural Development*, Vol **16** pp. 431–436.
- Dubrovskis, V. & Plume, I. 2017b. Enzymatic and catalytic enhancement of methane production from corn silage and grain residues. *Proceedings of 16. Conference Engineering for Rural Development* Vol. **16**, pp. 443–448.
- Dubrovskis, V., Plume, I. & Straume, I. 2018. Co-fermentation of carrots, grain residues and potato chips. *Proceedings of 16 conference ERDEV*, Vol. **17**, pp. 1833–1837.
- Errata, A. 2015. Anaerobic digestion of thermal pretreated Brewers' spent grains. Volume **34**(6), 1832. Article first published online: 12 November 2015.
- Ghorbani, M. 2011. Effect of inoculum/substrate ratio on mesophilic anaerobic digestion of bioethanol plant whole stillage in batch mode. *Process Biochemistry* **46**(8), 1682–1687.
- Kaparaju, P., Serrano, M. & Angeldaki, I. 2010. Optimization of biogas production from wheat straw stillage in UASB reactor. *Applied Energy* **87**, 3779–3783.
- Kim, Y., Mosier, N.S., Hendrickson, R., Ezeji, T. & Blaschek, A. 2008. Composition of corn dry-grind ethanol by-products: DDGS, wet cake and thin stillage. *Bioresource Technology* **99**, 5165–5176.
- Schaefer, S.H. & Sung, S. 2008. Retooling the ethanol industry: Thermophilic anaerobic digestion of thin stillage for methane production and pollution. *Water Environ. Res.* **80**(2), 101–108.
- Schaefer, S.H. 2006. Re-tooling the ethanol industry: Thermophilic anaerobic digestion of thin stillage for methane production. *Master's thesis – Civil Engineering Department*, Iowa State University, Ames Iowa, U.S.A. Retrospective Theses and Dissertations. 17762, 70 pp.
- Stover, E.L., Gomathinayagam, G. & Gonzalez, R. 1984. Use of methane from anaerobic treatment of stillage for fuel alcohol production. *Proceedings of the 39th Industrial Waste Conference*, Purdue University, West Lafayette, Indiana. Boston: Butterworth, pp. 57–63.
- Thran, D. 2010. *Methodenhandbuch Energetische Biomassenutzung, (Methods Manual Energetic use of biomass)*, Leipzig, 93 pp. (in German).
- VDI 4630 2006. *Vergärung organischer Stoffe Substrat charakterisierung, Probenahme, Stoffdatenerhebung, Gärversuche. Vereindeutscher Ingenieure, (Fermentation of organic substances Substrate characterization, sampling, substance data collection, fermentation tests. German engineers)* Düsseldorf, 48 pp. (in German).
- Wellinger, A., Murphy, J. & Baxter, D. 2013. *The biogas handbook*. Woodhead Publishing, 512 pp.
- Westerholm, M., Hansson, M. & Schnürer, A. 2012. Improved biogas production from whole stillage by co-digestion with cattle manure. Swedish Institute of Agricultural and Environmental Engineering, Science Direct. *Bioresour Technol.* **Jun**(114), pp. 314–319.
- Wilkie, A.C., Riedesel, K.J. & Owens, J.M. 2000. Stillage characterization and anaerobic treatment of ethanol stillage from conventional and cellulosic feedstocks. *Biomass and Bioenergy* **19**, 63–102.

Biological features of formation of perennial binary grass crops

V. Gasiev*, N. Khokhoeva and D. Mamiev

Vladikavkaz scientific center of the Russian Academy of Sciences,
22 Markus street, RU362027 Vladikavkaz, Republic of North Ossetia-Alania, Russia

*Correspondence: gasiev77@mail.ru

Abstract. The paper deals with the impact of binary mixtures of perennial grasses on the productivity and quality of forage crops that differ in their species composition. The studies have shown that mixed crops exceeded single-species crops in all indicators of forage crops productivity. In total over five years binary crops of *Poterium polygamum* exceeded single-species ones in all productivity indicators. The plants safety by the end of vegetation was also slightly lower than in single-species crops, which can be explained by greater competition for light, moisture and nutrients. So the safety of *Medicago sativa* L. was 81.8%, *Onobrychis* – 83.6%, *Galéga orientális* L – 89.7%, *Poterium polygamum* – 74.6%, which is lower than that of legumes in single-species crops. In all years of herbage use, the binary crops exceeded single-species ones. On average, for 5 years of research, the yield of *Poterium polygamum* was 25.5 t ha⁻¹, *Medicago sativa* L. – 22.5 t ha⁻¹, *Onobrychis* – 23.7 t ha⁻¹. Among legumes, the maximum yield had *Galéga orientális* L agrocecnosis – 26.1 t ha⁻¹. Mixed crops of burnet with leguminous grasses were characterized for yielding the vegetative mass on average 28.5–30.9 t ha⁻¹. Maximum values of binary *Poterium polygamum* crops characterized crops with the leguminous plant component of goat's rue in all years of research. Mixed crops also showed maximum values of dry matter per unit area and amounted respectively 33.52–36.74 t ha⁻¹. The same pattern continued in the yield of fodder units, digestible protein and metabolic energy, their maximum was obtained at the variant *Poterium polygamum*+ *Galéga orientális* L.

Key words: sowing, mixed, grasses, productivity, yield.

INTRODUCTION

An important reserve for increasing the efficiency of feed production in the North Caucasus is perennial grasses, which are the main component of forage crop rotations and an important link of the green conveyor. Perennial grasses are used as hay, silage and green feed (Lewandowski et al., 2003; Navickas et al., 2003; Bekuzarova et al., 2018; Obraztsov et al., 2018). Feeds that contain such crops are rich in essential for growth and development proteins, carbohydrates, vitamins and minerals. As a green feed and raw materials for silage is also used aftergrowth of perennial grasses. Most of these crops are excellent honey plants (Jolayemi et al., 1995; Lafolie et al., 1999; Mengistu et al., 2000; Wilman, 2004).

Perennial grasses are highly competitive, so they are often used for weeds control. They also significantly increase soil fertility, and representatives of the legume family due to symbiosis with nodule bacteria absorb air nitrogen, enriching the soil (Sapoukhina et al., 2010; Epie et al., 2015; Kuznetsov et al., 2018).

The perennial grasses layer through the ability to the soil structuring and drainage prevents water and wind erosion (Williams et al., 2001; Jordan et al., 2003; Bransby et al., 2010; Cui et al., 2014; Stahn et al., 2017).

Mixed crops development in the agricultural production is the most important among the effective ways to manage quantitative and qualitative indicators of plant products, and their further functioning in agroecosystems (Lemaczyk et al., 2002; Obraztsov et al., 2011).

Ignoring the principles of biological diversity in agrophytocenoses, manifested in the transition to monoculture, is a classic example of reducing the heterogeneity in agroecosystems. Therefore, agricultural production should be developed through the refuse of monoculture and transition to multicultural farming. In this regard, mixed crops are an important reserve for the alternative way of intensifying the crop production field (Catt et al., 1998).

Creation of simple and complex agrophytocenoses that ultimately characterize their productivity, in general, depends on a number of factors: correct selection of different species, number and ratio of components, habitat conditions.

To achieve these goals, it is necessary to expand the crops of herbs such as alfalfa, sainfoin, goat and blackthorn, which are most in demand in our agro-climatic zone. The study of the biological characteristics of these crops will further develop the basic elements of the technology of their cultivation in relation to the conditions of the foothills of the RSO-Alania.

Therefore, studying productivity and quality of forage crops in agrophytocenoses differing in their species composition is relevant (Carpenter-Boggs et al., 2003; Das et al., 2016).

The research aim was to study methods of creating highly productive binary mixtures of burnet and leguminous grasses, which provide high-quality feed of North Ossetia–Alania.

Scientific novelty. Productivity of binary burnet and leguminous grasses crops, fodder value, their role in enriching soil with organic matter was firstly determined in the environmental conditions of the foothill zone of North Ossetia–Alania.

MATERIALS AND METHODS

Field studies were conducted in the experimental field of the North Caucasus research institute of mountain and foothill agriculture. The soil of the experimental plot is leached middle thick middle loamy chernozem with 5.8% humus, easily hydrolyzed nitrogen – 80 mg kg⁻¹, available phosphorus – 118 mg kg⁻¹, exchangeable potassium – 120 mg kg⁻¹, pH_{salt} – 5.8–6.

During the years of research (2011–2015) meteorological conditions were different. In 2011–2013, an average of 502 mm of precipitation fell during the growing season, which is lower than the long-term norm by 47 millimeters. In the smaller side deviations from the norm were observed during the growing season for all months except September and August. The most favorable weather conditions were in 2014–2015.

During the growing season, 518 mm of precipitation fell, which is 31 mm below the long-term norm, but their distribution by months was the most optimal. The air temperature during the growing season in 2014 was 14.4 °C, which is 0.2 °C above the long-term norm.

Consequently, the meteorological conditions over the years of research were generally favorable for the cultivation of herbs.

The research objects were binary mixtures of *Poterium polygamum* and grasses: the Slava *Poterium polygamum* variety, the Osetinskaja *Medicago sativa* L., the Severo-Cavcazkij dvoukosnij *Onobrychis* variety, the Bimbolat *Galéga orientális* L. variety.

The seeding rate in mono crops was 4 million seeds/ha. In mixed crops the ratio of components was 1:1.

The soil preparation to sowing was conventional for seed swards of perennial grasses in the North Caucasus. After harvesting grasses preceding cropprimary tillage was fulfilled to the depth of 10–12 cm, then in two weeks the soil was plowed using jointer shares to the depth of 25–30 cm. In spring, as far as the soil was ready, we performed early tandem disk harrowing, secondary tillage, soil packing before sowing, coverless wide-row (45 cm) sowing to the depth of 1.0 cm at the seeding rate of 12.0 kg ha⁻¹, and soil packing after sowing. Registration plot area was 10 sq. m., randomized experiments were carried out in fourfold replication. The agricultural equipment complied with the standard for grasses cultivation in this zone.

Organization of field experiments, observations, biometric measurements, laboratory analyses was performed in accordance with the generally accepted guidelines.

The sowing density was determined on three standard of one linear meter, located diagonally plots. Seeds and field germination rate was determined considering the sown and germinated seeds. The dry matter accumulation was determined by the phases of plant growth and development.

Protein (total Kjeldahl nitrogen – 6.25) GOST 51417-99, fat – by method of fat-free residue extracted in Soxhlet apparatus, cellulose – by Henneberg-Stohmann method, ash – by ashing in a muffle furnace were determined in plant samples. Number of root and crop residues calculation was done by N.Z. Stankov method of the soil frame excavation. Yield of digestible protein feed units – by the calculation method based on the data of plants chemical analysis due to Tomme M.F. digestibility coefficient. Metabolic energy concentration in dry matter of forage crops was calculated basing on the percentage of crude fiber (CF) and crude protein (CP) in dry matter of feed according to the formula: ME MJ ha⁻¹ DM = 13.4 - 0.14 CF % . + 0.03 CP % . Yield calculation was done by the method of test sites from six points of the plot, followed by its evaluation in 100% purity and normal amount of moisture.

RESULTS AND DISCUSSION

One of the main productivity indicators of perennial grasses is plants stand density. Its importance especially increases in mixed crops, in which plants compete for light and moisture.

In our studies, field germination ranged from 64.8–69.1% in single-species legume crops (Table 1).

The lowest indicators were in burnet crops – 62.6%. In mixed burnet-based crops, the germination indicators of alfalfa, sainfoin and goat’s rue were lower than in single-species crops and ranged from 62.2; 64.3; 63.7%.

The plants safety by the end of vegetation was also slightly lower than in single-species crops, which can be explained by greater competition for light, moisture and nutrients. So the safety of *Medicago sativa L.* was 81.8%, *Onobrychis* – 83.6%, *Galéga orientális L.* – 89.7%, *Poterium polygamum* – 74.6%, which is lower than that of legumes in single-species crops. The same trend continued in the mixed crops: leguminous grasses exceeded burnet in plants safety per unit area.

Analyzing Table 2, it might be concluded that in single-species crops, compared to binary ones, the percentage of overwintered plants was slightly lower and ranged from 79.1–83.4% in the leguminous plant component of the first year of use, and in the *Poterium polygamum* – 80.2%. In this indicator mixed crops of the first year of use that contained *Poterium polygamum* and leguminous grasses ranged between 84.5–86.3%. With the increase in herbage age and years of agrocenosis use, the percentage of overwintered plants has slightly decreased both in *Poterium polygamum* single and binary crops.

Table 1. Field germination and safety of single-species and mixed crops of perennial grasses (2011–2015)

Variant	Field germination, %	Plants safety, %
<i>Poterium polygamum</i>	62.6	74.6
<i>Medicago sativa L.</i>	64.8	84.8
<i>Onobrychis</i>	66.3	83.6
<i>Galéga orientális L.</i>	69.1	89.7
<i>Poterium polygamum</i> +	62.2	60.3
<i>Medicago sativa L.</i>	47.6	70.2
<i>Poterium polygamum</i> +	64.3	59.5
<i>Onobrychis</i>	57.4	63.9
<i>Poterium polygamum</i> +	63.7	56.7
<i>Galéga orientális L.</i>	59.2	74.2

*Correspondence: e-mail: gasiev77@mail.ru

Table 2. Overwintering of single-species and binary crops, %

Variant	1 year of overwintering 2011	2 year of overwintering 2012	3 year of overwintering 2013	4 year of overwintering 2014	5 year of overwintering 2015
<i>Poterium polygamum</i>	80.2	87.4	94.1	96.3	95.2
<i>Medicago sativa L.</i>	79.1	86.9	95.7	97.1	96.0
<i>Onobrychis</i>	81.2	88.0	96.2	97.6	96.3
<i>Galéga orientális L.</i>	83.4	90.2	96.8	97.4	97.0
<i>Poterium polygamum</i> +	86.3	92.7	97.7	98.3	97.4
<i>Medicago sativa L.</i>					
<i>Poterium polygamum</i> +	84.5	91.4	95.9	97.8	95.9
<i>Onobrychis</i>					
<i>Poterium polygamum</i> +	85.6	92.0	96.7	98.0	96.5
<i>Galéga orientális L.</i>					

The yield of green mass increased with the increase in age of both single-species and mixed crops. In all the years of herbage use, binary exceeded single species, on average over 5 years of research *Poterium polygamum* yield was 25.5 t ha⁻¹,

Medicago sativa L. – 22.5 t ha⁻¹, *Onobrychis* – 23.7 t ha⁻¹. Among legumes, the maximum yield had *Galéga orientális L.* agrocenosis – 26.1 t ha⁻¹. Mixed crops of *Poterium polygamum* with leguminous grasses were characterized for yielding the vegetative mass on average 28.5–30.9 t ha⁻¹. Maximum values of binary *Poterium polygamum* crops characterized crops with *Galéga orientális L.* in all years of research (Table 3).

Table 3. Green mass yield of single-species and binary perennial grasses agrocenoses, t ha⁻¹

Variant	1 year of overwinterin g 2011	2 year of overwinterin g 2012	3 year of overwinterin g 2013	4 year of overwinterin g 2014	5 year of overwinterin g 2015	Average
<i>Poterium polygamum</i>	16.7	24.5	28.3	29.2	28.9	25.5
<i>Medicago sativa L.</i>	14.3	21.3	24.7	26.4	25.7	22.5
<i>Onobrychis</i>	15.8	23.0	26.2	27.0	26.4	23.7
<i>Galéga orientális L.</i>	17.0	26.2	29.6	29.2	28.3	26.1
<i>Poterium polygamum</i> + <i>Medicago sativa L.</i>	21.4	28.7	32.4	34.7	33.4	30.1
<i>Poterium polygamum</i> + <i>Onobrychis</i>	20.9	26.9	31.5	32.8	30.6	28.5
<i>Poterium polygamum</i> + <i>Galéga orientális L.</i>	21.8	29.8	33.7	35.0	34.1	30.9
LSD ₀₅	0.26	0.37	0.42	0.44	0.42	-

Analyzing Table 4, it might be concluded that maximum values for the dry matter yield in single-species crops has *Galéga orientális L.* agrocenosis – 26.73 t ha⁻¹, the for remaining legumes in total over 5 years, dry matter yield was: *Medicago sativa L.* – 23.61 t ha⁻¹, *Onobrychis* – 24.32 t ha⁻¹. Mixed crops showed the highest values of dry matter per unit area and amounted to 33.52–36.74 t ha⁻¹ respectively. The same pattern continued in the yield of fodder units, digestible protein and metabolic energy, their maximum was obtained at the variant *Poterium polygamum*+ *Galéga orientális L.*

Table 4. Productivity of perennial grasses in total over 5 years (2011–2015)

Variant	Dry matter, t ha ⁻¹	Feed units, t ha ⁻¹	Digestible protein, t ha ⁻¹	ME, GJ
<i>Poterium polygamum</i>	25.79 ± 0.38	13.24 ± 0.63	3.07 ± 0.54	209.14 ± 0.85
<i>Medicago sativa L.</i>	23.61 ± 0.21	10.92 ± 0.56	2.93 ± 0.61	199.36 ± 0.56
<i>Onobrychis</i>	24.32 ± 0.33	12.10 ± 0.61	2.55 ± 0.38	204.11 ± 0.63
<i>Galéga orientális L.</i>	26.73 ± 0.45	13.87 ± 0.68	2.74 ± 0.47	223.40 ± 0.66
<i>Poterium polygamum</i> + <i>Medicago sativa L.</i>	34.38 ± 0.41	18.42 ± 0.49	3.81 ± 0.55	311.42 ± 0.61
<i>Poterium polygamum</i> + <i>Onobrychis</i>	33.52 ± 0.51	17.94 ± 0.54	3.47 ± 0.59	294.37 ± 0.72
<i>Poterium polygamum</i> + <i>Galéga orientális L.</i>	36.74 ± 0.37	19.28 ± 0.23	3.92 ± 0.44	314.28 ± 0.61

CONCLUSION

On the basis of the above, it can be stated the fact that perennial leguminous grasses in mixed crops with *Poterium polygamum* are the most highly productive in relation to their single-species crops.

The most productive option in terms of dry matter content was *Poterium polygamum*+ *Galéga orientális* L. (36.74 t ha⁻¹). This option is superior to others and the content of digestible protein and feed units.

ACKNOWLEDGEMENTS. The work was prepared with the support of the Ministry of Education and Science of the Russian Federation.

REFERENCES

- Bekuzarova, S.A., Gasiev, V.I., Lushchenko, G.V. 2018. Phytocenotic paradigm in the selection of legumes in the North Caucasus. *Forage Production* **8**, 24–29.
- Bransby, D.I., van Santen, E., Allen, D.J., Gutterson, N., Ikonen, G., Richard, E., Rooney, W. 2010. Engineering advantages, challenges and status of grass energy crops. *Biotechnology in Agriculture and Forestry* **66**, 125–154.
- Carpenter-Boggs, L., Stahl, P.D., Lindstrom, M.J., Schumacher, T.E. 2003. Soil microbial properties under permanent grass, conventional tillage, and no-till management in South Dakota. *Soil & Tillage Research* **71**(1), 15–23.
- Catt, J.A., Howse, K.R., Christian, D.G., Lane, P.W., Harris, G.L., Goss, M.J. 1998. Strategies to decrease nitrate leaching in the brimstone farm experiment, oxfordshire, UK, 1988–1993: The effects of winter cover crops and unfertilised grass leys. *Plant and Soil* **203**(1), 57–69.
- Cui, G.W., Li, H.Y., Sun, T., Xi, L.Q., Wang, Z. 2014. An Experimental study of variety screening, sequential cropping, compaction and mixed cropping techniques for the cultivation of annual forage crops in agro-pastoral area of Tibet, China. *International Journal of Agriculture and Biology* **16**(1), 97–103.
- Das, A., Lal, R., Somireddy, U., Verma, S., Rimal, B.K., Bonin, C. 2016. Changes in soil quality and carbon storage under biofuel crops in Central OHIO. *Soil Research* **54**(4), 371–382.
- Epie, K.E., Stoddard, F.L., Cass, S. 2015. Earthworm communities under boreal grass and legume bioenergy crops in pure stands and mixtures. *Pedobiologia* **58**(1), 49–54.
- Jolayemi, J.K., Olaomi, J.O. 1995. A mathematical programming procedure for selecting crops for mixed-cropping schemes. *Ecological Modelling* **79**(1–3), 1–9.
- Jordan, C., Shi, Z., Bailey, J.S., Higgins, A.J. 2003. Sampling strategies for mapping 'within-field' variability in the dry matter yield and mineral nutrient status of forage grass crops in cool temperate climes. *Precision Agriculture* **4**(1), 69–86.
- Kuznetsov, I.Y., Akhiyarov, B.G., Asylbaev, I.G., Davletov, F.A., Sergeev, V.S., Abdulvaleyev, R.R., Valitov, A.V., Mukhametshin, A.M., Ayupov, D.S., Yagafarov, R.G. 2018. The Effect of sudan grass on the mixed sowing chemical composition of annual forage Crops. *Journal of Engineering and Applied Sciences* **13**(S8), 6558–6564.
- Lafolie, F., Bruckler, L., Ozier-Lafontaine, H., Tournebize, R., Mollier, A. 1999. Modeling Soil-root water transport and competition for single and mixed Crops. *Plant and Soil* **210**(1), 127–143.

- Lemanczyk, G., Sadowski, C.K. 2002. Fungal communities and health status of roots of winter wheat cultivated after oats and oats mixed with other crops. *BioControl* **47**(3), 349–361.
- Lewandowski, I., Jonathan, M.O., Scurlock, J. & et al. 2003. The development and current status of perennial rhizomatous grasses as energy crops in the US and Europe. *Biomass and Bioenergy* **25**, 335–361.
- Mengistu, L.W., Mueller-Warrant, G.W., Barker, R.E. 2000. Genetic diversity of POA *Annua* in western oregon grass seed crops. *Theoretical and Applied Genetics TAG* **101**(1–2), 70–79.
- Navickas, K., Župerka, V. & Janušauskas, R. 2003. Utilisation of perennial grasses for biogas generation. Agricultural Engineering, Research papers. *Raudondvaris* **35**(4), pp. 109–116.
- Obraztsov, V., Shchedrina, D., Kadyrov, S. 2018. Festulolium seed production dependence on Fertilizer application system. *Agronomy Research* **16**(3), 846–853.
- Obraztsov, V., Shchedrina, D., Kadyrov, S., Bekuzarova, S., Dmitrieva, O., Kondratov, V. 2011. *Method for Pre-Harvesting Treatment of Festulolium Seed Crops*. Patent No 2420050 of Russian Federation, Bullet in **16**, 4pp. (in Russian).
- Sapoukhina, N., Tyutyunov, Y., Sache, I., Arditi, R. 2010. Spatially mixed crops to control the stratified dispersal of airborne fungal diseases. *Ecological Modelling* **221**(23), 2793–2800.
- Stahn, P., Salzmann, T., Miegel, K., Busch, S., Eichler-Löbermann, B. 2017. Combining global sensitivity analysis and multiobjective optimisation to estimate soil hydraulic properties and representations of various sole and mixed crops for the agro-hydrological swap model. *Environmental Earth Sciences* **76**(10), 367 pp.
- Williams, P.H., Rowarth, J.S., Tregurtha, R.J. 2001. Uptake and residual value of ¹⁵N-labelled fertilizer applied to first and second year grass seed crops in new zealand. *Journal of Agricultural Science* **137**(1), 17–25.
- Wilman, D. 2004. Some changes in grass crops during periods of uninterrupted growth. *Journal of Agricultural Science* **142**(2), 129–140.

Reliability of palms security under difficult conditions

V. Hartová¹, J. Hart² and M. Kotek¹

¹Czech University of Life Sciences Prague, Faculty of Engineering, Department of Vehicles and Ground Transport, Kamýcká 129, CZ16500 Prague, Czech Republic

²Czech University of Life Sciences Prague, Faculty of Engineering, Department of Technological Equipment of Buildings, Kamýcká 129, CZ16500 Prague, Czech Republic
Correspondence: nidlova@tf.czu.cz

Abstract. Reliability of biometric identification systems is a much discussed topic and nowadays security of premises is very important. The work is focused on palms security research and reliability of the system under adverse conditions, the aim of the measurement was to determine the reliability of readers under adverse conditions that may occur in an industrial environment. Difficult conditions include dirty surface of hand by water, dust, oil and writing accessories. First, a sample measurement was carried out, where the hands of the subjects were washed and thoroughly dried. This measurement was used to compare with measurements under adverse conditions. The results show that the more viscous the fluid the lower the reliability and also dusty hands caused considerably distorted results. The reliability of biometric systems still needs to be improved, as it often happens that the real values do not match the parameters that are declared by the manufacturers. Certain conditions must be met for the proper functioning of palms security, so that identifying persons are allowed access to the protected areas and have not been repeatedly denied.

Key words: palms security, reliability, biometrics, difficult conditions.

INTRODUCTION

Nowadays, more and more emphasis is placed on the safety and security of buildings and personal documents. There are many I&Has systems (Intrusion and Hold-up Alarm System) that deal with this problem, and these also include biometric identification systems. Fingerprint systems are the most widely used, which are used not only as access systems but also as attendance systems (Rak et al., 2012). These systems have been tested by a number of scientists and it was concluded that their reliability is sufficient for common modes of use, in particular as an increase in security of access to a building (Lee, 2012). At the same time, it is also pointed out that their reliability is limited by the environment and the difficult conditions under which these readers evaluate (Athalea et al., 2015). Other most frequently used devices include biometric readers using facial scans for identification. This method has been, and still is, problematic in terms of the length of identifying a person, as well as reliability, where the surrounding circumstances play a major role, as well as the covering of identification points of the face - hair, beard, etc (Abudarham et al., 2019).

The issue addressed in this paper is based on a scan of the bloodstream of the hand. This system is used not only to authorize a user to enter a protected area, but also as a payment confirmation or as a control element for working on a laptop or computer. At present, all of the documents are being worked with and are stored in electronic form. Communication between people is also getting limited to electronic form, and it is therefore necessary to address the problem of protecting these documents and communication. Today, passwords and codes are used for these purposes, but these are very unstable from a security perspective and their security is very low. Therefore, biometric methods have begun to be introduced into this issue, and the question is to what extent they are reliable. In recent years, the biometric method palms security has started to develop, which is quite reliable under standard conditions (Wang et al., 2008; Zhou & Kumar, 2011). It is used not only for building entrances but also as a card payment password. These are still touch devices that have their pitfalls under difficult conditions. Laptops and computers are used in all industries and environments, so their reliability under difficult conditions needed to be determined. As the reader is integrated into the notebook, there is a presumption that it will be exposed to difficult conditions as the notebook is nowadays used for both office work and industry where it is possible to meet very dusty environments and people who want to authorize they may have very dirty hands. It is important to solve the problem of whether the device using the bloodstream scan of the hand is reliable and can be used even in difficult conditions of normal operation.

MATERIALS AND METHODS

The research was carried out in the laboratory and buildings of the Faculty of Engineering of the Czech University of Life Sciences Prague. Measurements were carried out in two environments. The first environment was a standard office. The ambient average office conditions were: temperature 23 °C, air humidity 49% and light intensity 313 lx. The second environment was an outdoor tent located in the school field, and here the average values of the environment were as follows: temperature -1 °C, air humidity 42% and light intensity 7,224 lx. A set of 30 measurements were carried out for each user under individual difficult and standard conditions, from which a standard sample was created on each device in both measuring environments. There were a total of 50 users, 25 of whom were women aged 22–64 and 25 men aged 21–73.

The measuring device used was an external reader for scanning the bloodstream: Fujitsu Accessory PalmSecure ID Match Security Access Protection, see Fig. 1, which was connected via a USB interface to a Dell Inspiron notebook, into which the appropriate evaluation software was uploaded. The other device was a Fujitsu Lifebook U757 with an integrated hand bloodstream scanner.



Figure 1. Fujitsu Accessory PalmSecure ID Match Security Access Protection.

It was firstly necessary to determined suitable difficult conditions. The conditions were determined according to the environment in which a laptop can be used. The following difficult conditions were determined: wet hands, undercooled, smeared, soiled and contaminated with oil. Prior to each measurement of each difficult condition, it was necessary to measure each person's standard template, which was measured on clean and warm hands. This benchmark was used to evaluate the reliability level. The measurements were made with each user first performing a set of standard measurements, with difficult conditions then gradually being fulfilled and other sets of measurements were carried out. After measuring each difficult condition, the hands were washed, and an hour break was set in order to normalize the condition of the skin.

The first set of measurements that were carried out in the office space was more reliable than the set of measurements outdoors at -1 °C. This increased error rate is attributed to the fact that the biometric identification system did not operate well at a temperature below 0 °C. The measured values from the two devices were very similar and it was therefore not necessary to process them separately; however, an average value was created from these values. This solution was also relevant because both the reader in the laptop and the external reader work on the same technology principle and with the same recognition software.

The following formula (1) was used to calculate reliability:

$$FRR = \frac{N_{FR}}{N_{EIA}} \cdot 100(\%) \quad (1)$$

FRR – False Rejection Rate; *N_{FR}* – Number of False Rejection; *N_{EIA}* – Number of Enrolle Identification Attempts.

During the measurements, it was first necessary to set a time limit after which it would be assumed that the person was denied by the biometric identification device. This time period was 2.4 seconds.

RESULTS AND DISCUSSION

In Figs 2 and 3, it can be seen that this period depends not only on the ambient temperature, but also on the state of the hands, i.e. on the relevant difficult conditions. Fig. 2 shows the time limit being exceeded in the office space, and Fig. 3 in outdoor areas. It is evident from both graphs that the highest time exceeded was for hands soiled with dirt of clay, as the contamination layer prevented the reader from functioning correctly. On average, the value of the time overlap was 66%. The results were better for hands soiled with oil, where the overlap was 54% on average, as this was due to the reflection of the oil and thus the read surface of the hand was devalued, and the reader could no longer be as accurate as for the standard measurement. For hands dirty with hot silicone, the reliability changed in climatic environments. In outdoor areas the readers showed a lower time overlap than in the indoor areas due to the high ambient temperature difference and the difficult conditions tested. On the other hand, in the case of undercooled hands, the values of the time overlap in the outdoor areas were lower; it can be said that they were zero compared to the interior spaces, which was again caused by the ambient temperature and the biometric features examined.

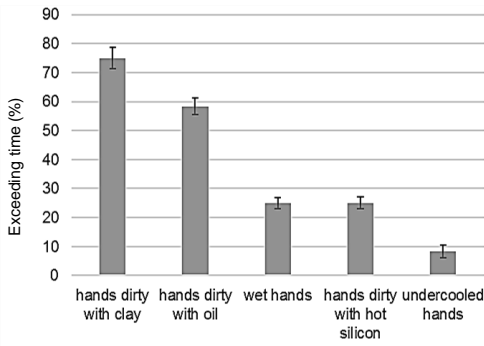


Figure 2. Time limit being exceeded in the office space.

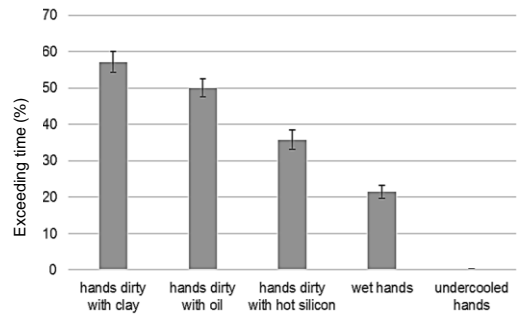


Figure 3. Time limit being exceeded in the outdoor areas.

Another monitored value was the time difference compared to the measured values under normal conditions (benchmark). The average of the measured values in the office space was 1.2 s and the average value of the benchmark was 1.4 seconds for the external areas. The graphs in Figs 4 and 5 show that in the inside areas, the biggest difference compared to the benchmark of 0.9 seconds under difficult conditions was for hands dirty with clay, followed by hands dirty with oil with a difference of 0.7 seconds. The situation was similar in the outdoor areas where, in addition to the two aforementioned difficult conditions, hands dirty with hot silicone with a difference of 0.5 seconds from the benchmark also played a role. As summarized in Table 1 statistically significant differences were achieved in all cases except undercooled hands in the outdoor areas.

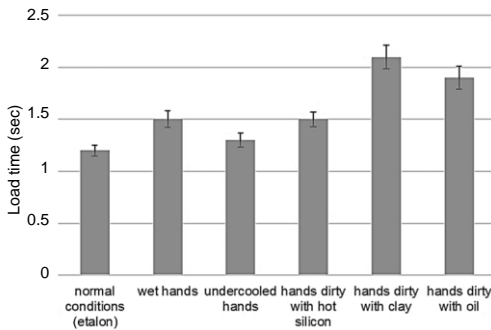


Figure 4. Load time difference compared to the benchmark in the office space.

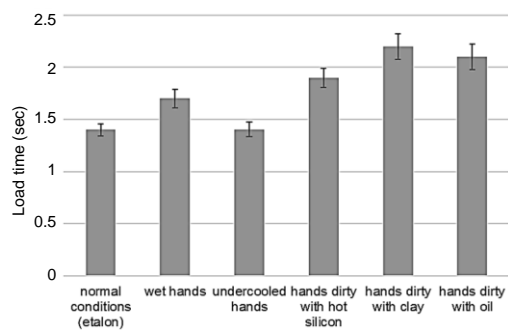


Figure 5. Load time difference compared to the benchmark in the outdoor areas.

Table 1. T-test statistical analysis of load time

T criteria	Wet hands	Undercooled hands	Hands dirty with hot silicon	Hands dirty with clay	Hands dirty with oil
T (indoor)	146	60	161	302	242
T (outdoor)	129	1.66	42	256	219
$t_{0,05}(1,499)$	1.96	1.96	1.96	1.96	1.96

For the final assessment of the reliability of biometric systems identifying the bloodstream of the hand based on a scan, a formula (1) used to calculate invalid user rejection was used. The time limit for determining when a user could not log in to the system was set to 2.4 seconds. The graph in Fig. 6 shows the percentage of reliability, i.e. the percentage of invalid user rejection in both indoor and outdoor conditions. The least reliable proved to be hands dirty with clay with nearly 30%, followed by hands with oil, where reliability was reduced by about 26%. Other difficult conditions were much better, i.e. by up to 10% reduced reliability. As is summarized in Table 2 all values reached significant statistical difference compared to normal condition.

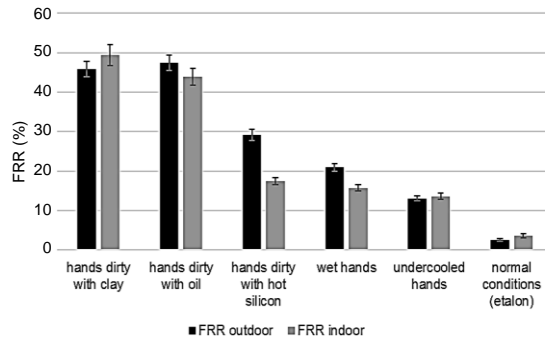


Figure 6. Percentage of invalid user rejection in both areas.

Table 2. T-test statistical analysis of FRR parameter

T criteria	Wet hands	Undercooled hands	Hands dirty with hot silicon	Hands dirty with clay	Hands dirty with oil
T (indoor)	678	712	643	546	486
T (outdoor)	831	896	709	715	576
<i>t_{0,05(1,499)}</i>	1.96	1.96	1.96	1.96	1.96

The research of biometric systems recognizing users on the basis of the bloodstream of the hand was also addressed by the authors of the publication (Athalea et al., 2015). In their research, they came to the conclusion that the system they were examining identified users with 92% reliability under normal conditions. Also, in (Lee, 2012) the reliability of this identification method is shown, and the reliability values range from 94% to 98%. According to the used method, this research was also performed under standard conditions and in the beginnings of this technology. We have also reached these values under standard conditions and it is clear from the results that readers no longer have an acceptable level of error in difficult conditions. Authors (Thakuria et al., 2017) in their article A Comparative Study of Vein Pattern Recognition for Biometric Authentication discuss the overall use of this biometric technology to identify people. In article Development and evaluation of the authentication systems by using phase-only correlation palm print identification methods by authors (Ucan et al., 2017) is investigate palm prints used in biometric authentication and matching systems. The aim was to match two images of one hand of the person taken from the different perspectives and damaged because of the action. The image took from the palm print reader was softened through the Gauss filter. In addition to the reliability of the device itself, it is very important that this device is protected against external attacks, and the authors (Bhilare & Kanhangad, 2018) of the article Securing palm-vein sensors against presentation attacks using image noise residuals deal with it. Their method is based on analysis of

noise residual computed from the acquired image. The palm-vein image acquired by the sensor was denoised through median filtering, a well-known nonlinear technique for noise reduction. Subsequently, a noise residual image was obtained by subtracting the denoised image from the acquired image. The local texture features extracted from the noise residual image were then used to detect the presentation attack by means of a trained binary support vector machine classifier. They have performed evaluations on a publicly available palm-vein dataset consisting of 4,000 bona fide and fake images collected from 50 subjects in two different sessions. Their approach consistently achieves a perfect average classification error rate of 0.0%.

Palms print identification is a relatively new method of identification, and so there are very few scientific studies on the subject.

CONCLUSIONS

Research on biometric identification systems is still a current topic. Emphasis on security is on the rise and it is necessary to continually improve these systems. Based on the results of the measurements, it is evident that identification based on the bloodstream scanning in the relevant systems is sufficient under normal conditions, as reliability in outdoor areas is reduced by 1.52% and in internal area by 2.12%, which is very acceptable for users. The question, however, was how these systems work in difficult conditions that can occur during normal operation. Reliability under difficult conditions dropped between 29.64% and 7.84%. The lowest reliability was found in hands with clay. The best difficult condition was undercooled hands. In addition to difficult conditions, the environment has also had an impact on identification. Under such difficult conditions, it would be preferable to use a biometric identification device that identifies on the basis of a face scan or a fingerprint where skin care is better. However, in subsequent research, it would be suitable to focus on the improvement of systems for biometric identification of persons under difficult conditions, as there is a relatively large gap and important work is not limited to office activities in the interior, but it is also necessary to have high quality and secure access under non-standard conditions and in exteriors.

ACKNOWLEDGEMENTS. It is a project supported by the CULS IGA TF 2017: 31150/1312/3121 - The Consumption of Transport Energy in Rural Households - Perspectives of Electromobility.

REFERENCES

- Abudarham, N., Shkiller, L. & Yovel, G. 2019. Critical features for face recognition. *Cognition* **182**, 73–83.
- Athalea, S., Patilb, D., Deshpandec, P. & Dandawated, Y. 2015. Hardware Implementation of Palm Vein Biometric Modality for Access Control in Multilayered Security System, *Procedia Computer Science* **58**, pp 492–498.
- Bhilare, S. & Kanhangad, V. 2018, Securing palm-vein sensors against presentation attacks using image noise residuals. *Journal of electronic imaging* **27**, 126–134.
- Lee, J.-Ch. 2012. A novel biometric system based on palm vein image. *Pattern Recognition Letters* **33**, pp 1520–1528.

- Morales, A., Kumar, A. & Ferrerc, M. 2016. Interdigital palm region for biometric identification. *Computer Vision and Image Understanding* **142**, pp 125–133.
- Rak, R., Matyáš, V. & Říha, Z. 2012. Biometrics and identity of man in forensic and commercial applications. Praha: Grada Publishing, a.s., pp. 281–285 (in Czech).
- Thakuria, H., Dutta, A., Sarkar, A., Ghosal, A., Saha, R., Pramanik, S., Mitra, S., Mukherjee, C., Thakur, U.N. & Mukherjee, D. 2017, A Comparative Study of Vein Pattern Recognition for Biometric Authentication. In: *2017 8TH IEEE Annual information technology, electronics and mobile communication conference, IEMCON*, Vancouver, Canada, pp. 689–694.
- Ucan, O.N., Bayat, O. & Coskun, M.B. 2017. Development and evaluation of the authentication systems by using phase-only correlation palm print identificaton methods. In: *2017 International conference on engineering and technology, ICET*. Antalya, Turkey, pp. 1–4.
- Wang, J.G., Yau, W.Y., Suwandy, A. & Sung, E. 2008. Person recognition by fusing palmprint and palm vein images based on ‘Laplacianpalm’, *Pattern Recognition* **41**, pp 1514–1527.
- Zhou, Y. & Kumar, A. 2011. Human Identification using Palm-Vein Images, *IEEE Transactions on Information Forensics and Security* **6**, pp. 1259–1274.

The effect of application of potassium, magnesium and sulphur on wheat and barley grain yield and protein content

L. Hlisnikovský^{1,*}, P. Čermák¹, E. Kunzová¹ and P. Barłóg²

¹Department of nutrition management, Crop Research Institute, Drnovská 507, CZ16101 Prague 6, Ruzyně, Czech Republic

²Department of Agricultural Chemistry and Environmental Biogeochemistry, Poznan University of Life Sciences, Wojska Polskiego 71F, PL60-625 Poznan, Poland

*Correspondence: l.hlisnik@vurv.cz

Abstract. The objective of our experiment was to study the effect of mineral fertilizers, rich mainly in the K, Mg and S content, and compare their effect on grain yield and protein content of winter wheat and winter barley with fertilizer treatments without these elements. The analyzed fertilizer treatments were 1) Control, 2) mineral nitrogen treatment (N), 3) mineral nitrogen with phosphorus (NP), 4) NP with potassium, magnesium, and sulphur (NP+KMgS), and 5) NP with magnesium, sulphur and minor part of manganese (4%) and zinc (1%) (NP+MgSMnZn). The experiment was established in Lukavec experimental station (the Czech Republic) in 2013 and lasted until 2017. The crop rotation consisted of four arable crops: winter wheat, winter barley, rapeseed, and potatoes, but only winter wheat and winter barley are analyzed in this paper (grain yields and crude protein content).

In comparison with the Control, the application of mineral fertilizers significantly increased grain yield and protein content of both kinds of cereal. Comparing mineral fertilizers, no significant differences were recorded between N, NP, NP+KMgS and NP+MgSMnZn treatments, showing that nitrogen was the most limiting factor affecting yield and protein content, and initial concentrations of K and Mg were suitable and capable to cover cereal's demands. However, application of fertilizers has increased the K and Mg soil content and thus prevents the soil from the element's deficiency, which does not have to be recognized in the early stages by visual observation of arable plants. The effect of the year was also significant as two out of four seasons were characterized by high temperatures and drought.

Key words: crude protein content, grain yield, *Hordeum vulgare* L., magnesium, mineral fertilizers, potassium, sulphur, *Triticum aestivum* L.

INTRODUCTION

Nitrogen is the key nutrient significantly influencing the affectivity of water utilization by plants as well as accumulation and shoot-root partitioning of photo-assimilates. Therefore, the nitrogen supply must be considered as a prime factor of crop production (Gonzalez-Dugo et al., 2010). However, it is well recognized that productivity of nitrogen fertilizers is related not only to its doses or chemical form but also to adequate relationships between nitrogen and other nutrients (Fageria, 2001). Phosphorus, potassium, and magnesium are, together with sulphur and calcium, the most important

and principal plant macronutrients, directly influencing nitrogen uptake and utilization, and in this way the agriculture production.

The potassium is the most concentrated ion in the plant water tissue. The role of potassium is connected with physiological processes affecting the growth, development, and protein metabolism of arable plants, although it's not an integral part of any cellular organelle or structural part of the plant. According to Pettigrew (2008) the potassium is in plant involved in photosynthesis, assimilate transportation, enzyme activation and water management. Together with zinc, potassium plays a vital role in salt stress tolerance. It significantly minimize the NaCl-induced oxidative stress, enhance the photosynthetic pigment, counteract the adverse effect of salinity, enhance activity of antioxidant enzymes and increase root, shoot and spike length in wheat cultivars (Jan et al., 2017), while its deficiency significantly reduces the plant stature (Ebelhar & Varsa, 2000) and the number or the size of the leaves (Jordan-Meille & Pellerin, 2004). This reduction is then connected with decreased production of photosynthetic assimilates. The average consumption of potassium fertilizers has decreased significantly in the Czech Republic since the Velvet revolution in 1989, which is connected with the transition from socialism to capitalism, and is now approximately 13 kg ha⁻¹ of arable land. The current average concentration of the potassium in the arable land of the Czech Republic is 253 mg kg⁻¹ (2012–2017), 7.5% of arable land needs intensive fertilization and 28% of the land needs moderate fertilization (Smatanová & Sušil, 2018).

Magnesium is an essential element connected with activation of cellular enzymes, especially enzymes activating phosphorylation. Magnesium also plays a significant role in the signal transduction in the plant (Yu et al., 2011). The most crucial function of magnesium is in the formation of chlorophyll and thus plays an important role in the absorption of light energy required for photosynthesis. Acute magnesium deficiency can be recognized as chlorosis. Magnesium participating as the central atom of chlorophyll represents approximately one-fifth of all its plant content and is strongly bound to the chlorophyll. Thus, the chlorosis is a final demonstration of acute deficiency and low yields can be expected (Gransee & Führs, 2013). Deficiency of magnesium can occur because of low Mg contents in the source rocks forming the soil, because of losses from the soil by mobilization and leaching and because of inadequate agricultural practices (Gransee & Führs, 2013). The average concentration of magnesium in the Czech Republic is 194 mg kg⁻¹ and the ratio of arable land with very low concentration is 15%, while high and very high concentrations were recorded on 17% of arable land (Smatanová & Sušil, 2018).

The sulphur is another essential element important for plant growth and structure elements. It is the main component of cysteine, methionine and several co-enzymes. The total sulphur uptake by winter wheat is usually 15–25 kg ha⁻¹ under non-deficient situations (Zhao et al., 1999). Conventional fertilizer treatment with sulphur can increase the nitrogen content in the wheat organs and kernels, prolamin and total protein content in the kernels. On the other hand, the same treatment can also decrease the 1,000 grain kernels weight (Yang et al., 2007). Sulphur fertilization is also important for barley, as it positively modifies the hordein composition, increase malt extract and decrease malt hardness (Prystupa et al., 2018). The official statistical database of the Czech Republic does not analyze the consumption of fertilizers containing magnesium and sulphur. The deficiency of sulphur for arable crops was not considered as a problem during the second half of the 20th century as the energy industry supplied more than a sufficient amount of

sulphur to the atmosphere and environment. The problem with sulphur as a limiting factor for crop production has been recognised when mechanisms of the cleaner production started to be implemented to the power plants in Europe. Another shortage of sulphur to the environment is connected with the replacement of ammonium sulphate with mineral fertilizers not containing sulphur. According to Ceccoti & Messick (1994) the share of ammonium sulphate dropped from 7.2% in 1973 to 3% in 1991. A significant decrease in the plant available sulphur was recorded in the last twenty years in the Czech Republic. The mean concentration of the sulphur in arable soil is approximately 15 mg kg⁻¹ (51.1% of the arable land), which is evaluated as a low content. A suitable concentration of sulphur can be found only on 8.8% of the arable land (Smatanová & Sušil, 2018).

Concerning the roles of potassium, magnesium and sulphur in plants and the concentrations of these elements in the soil, we decided to analyze the effect of the application of fertilizers containing potassium, magnesium and sulphur to the most important cereals in the Czech Republic, wheat and barley, and analyze how these fertilizers affect their grain yield and protein content.

MATERIALS AND METHODS

Site description

The field trial was established in Lukavec experimental station (49°33.83347', E 14°59.38932', 625 m a.s.l.). The mean annual precipitation was 600 mm and the mean annual temperature was 7.0 °C in the spring of 2013, when the experiment was established. The type and kind of soil are sandy-loamy Cambisol. Basic chemical parameters of the soil at the beginning of the experiment show Table 1. The weather conditions (temperature and precipitation) of each season are presented in Fig. 1.

Table 1. Soil chemical properties in 2013. Soil reaction pH was measured in CaCl₂ solution and concentrations of plant available P, K, Ca, and Mg in soil samples were extracted by Mehlich III reagent and determined by ICP-OES

Soil depth	pH	P (mg kg ⁻¹)	K	Mg	Ca
0–15 cm					
Mean value	5.7	132	123	146	1,662
Assessment	slightly acid	high	suitable	suitable	suitable
15–30 cm					
Mean value	5.8	148	131	147	1,751
Assessment	slightly acid	high	suitable	suitable	suitable

Experimental design

The experiment consists of four fields, the area of one field is 1,568 m². Seven fertilizer treatments were evaluated in the experiment, but only five treatments are evaluated in this paper. The size of the experimental plot of one fertilizer treatment was 56 m² (7 x 8 m), including buffer strips to prevent the edge effect. The harvesting area for the purpose of the experiment was 24 m² (4 x 6 m) in the plot's central area. The crop

rotation consisted of potato (var. Ditta), winter wheat (var. Mulan), rapeseed (var. Sharpa) and winter barley (var. Nero). The experiment was established in 2013 and each crop was grown for four consecutive seasons. The fertilizer treatments (with four replications on each field) were: 1) unfertilized Control, 2) mineral nitrogen – N, 3) mineral nitrogen with phosphorus – NP, 4) mineral NP with the addition of magnesium and sulphur (NP+KornKali) – NP+KMgS, and 5) mineral NP in combination with magnesium, sulphur and micronutrients (NP+Kieserite and EPSO Combipop) – NP+MgSMnZn.

The mineral nitrogen was applied as ammonium nitrate, phosphorus as diammonium phosphate, potassium as KornKali (40% K₂O, 6% MgO, 4% Na₂O and 12.5% SO₃). The Kieserite consists of 27% MgO and 55% of SO₃. The EPSO Combipop consists of 13% MgO, 34% SO₃, 4% of Mn and 1% of Zn.

The dose of nitrogen was 150 kg ha⁻¹ for winter wheat and 100 kg ha⁻¹ for winter barley. Phosphorus was applied at a dose of 50 kg ha⁻¹ (P₂O₅) and potassium at a dose of 80 kg ha⁻¹ (K₂O). Magnesium was applied at a dose of 12 kg ha⁻¹ in the NP+KMgS treatment and 26 kg ha⁻¹ in the NP+MgSMnZn treatment. The foliar application of EPSO Combipop (NP+MgSMnZn treatment) was done in three dressings (3 x 15 kg ha⁻¹) at the BBCH stages 15, 30 and 49. The cereal's straw was removed from the field after the harvest. The doses of applied mineral fertilizers and scheme of fertilizer application dressings are shown in Table 2 and 3.

Table 2. Doses of mineral nutrients (kg ha⁻¹) applied to the winter wheat and winter barley in the analyzed fertilizer treatments

Fertilizer treatment	N (kg ha ⁻¹)	P ₂ O ₅ (kg ha ⁻¹)	K ₂ O (kg ha ⁻¹)	MgO (kg ha ⁻¹)	SO ₃ (kg ha ⁻¹)	Mn (kg ha ⁻¹)	Zn (kg ha ⁻¹)
Control	0	0	0	0	0	0	0
N	150 (100*)	0	0	0	0	0	0
NP	150 (100*)	50	0	0	0	0	0
NP+KMgS	150 (100*)	50	80	12	25	0	0
NP +MgSMnZn	150 (100*)	50	0	20 + 5.9	41 + 15.3	1.8	0.45

* – winter barley.

Table 3. Scheme of dressings of mineral fertilizers applied to the winter wheat and winter barley

Nutrients	Basal	1 st dressing	2 nd dressing	3 rd dressing
N (ammonium nitrate)	15 kg N from DAP	The beginning of tillering (BBCH 21)-50%*	The phase of stem elongation (BBCH 30)-30%*	The phase of ear emergence (BBCH 51)-20%*
P ₂ O ₅ (DAP)	Before sowing			
K ₂ O (KornKali)	Before sowing			
MgO (Kieserite)		Together with the first N app.		
MgO (EPSO Combipop 3 x 15 kg ha ⁻¹)		Autumn (BBCH 15)	The phase of stem elongation (BBCH 30)	The phase of early ear emergence (BBCH 49)

* – ratio of the applied nitrogen.

Analytical methods

The soil's value of pH was determined in the CaCl₂ solution, soil's available nutrients were determined according to the Mehlich III method, followed by ICP-OES analysis. Winter wheat and barley crude protein content was analyzed according to the Kjeldahl method (ČSN EN ISO 20483).

Data analysis

All statistical analyses were performed using STATISTICA 13.3 software (www.StatSoft.com). The effect of treatment, year and treatment*year was analyzed by one-way and factorial ANOVA. After obtaining significant ANOVA (MANOVA) results, the Tukey HSD post hoc test was applied to determine significant differences among individual treatments and years.

RESULTS AND DISCUSSION

Soil analysis

The value of pH and the concentration of P, K, Ca and Mg (mg kg⁻¹) in the soil at the end of the experiment (2017) show Table 4. The table shows two pH values and elements concentrations as the soil analyses were performed on each field following the harvest of winter wheat (WW) and winter barley (WB). The concentration of P decreased at the end of the experiment in all treatments. Concentrations of K and Mg slightly increased during the time, which could be a partial contribution of mineral fertilizers containing these elements. The concentration of Ca fluctuated over the fertilizer treatments. Unfortunately, the results of the concentration of S in the soil at the end of the experiment are not available.

Table 4. Soil chemical properties in 2017 (0–15 cm) after completing the field experiment

Fertilizer treatment	pH		P (mg kg ⁻¹)		K		Mg		Ca	
	WW*	WB**	WW	WB	WW	WB	WW	WB	WW	WB
Control	6.5	5.9	131	96	182	198	1,958	1,685	180	177
N	6.4	6.0	108	92	141	161	1,896	1,616	165	165
NP	6.1	6.0	129	111	188	175	1,726	1,577	151	165
NP+KMgS	6.0	5.8	106	119	213	191	1,642	1,373	151	147
NP+MgSMnZn	5.7	5.8	95	121	198	253	1,339	1,562	147	163

* – winter wheat; ** – winter barley.

Grain yield

The winter wheat GIY was significantly affected by fertilizer treatment ($p < 0.001$), conditions of the year ($p < 0.001$) and by treatment*year interaction ($p < 0.001$). According to MANOVA results, the fertilizer treatment was the major factor influencing GIY by 67%. Weather conditions of each year influenced GIY by 30% and treatment*year interaction by 3%. The lowest GIY were recorded in the Control (3.59 t ha⁻¹), while the highest in the NP (7.31 t ha⁻¹). Comparing the years, the lowest GIY were recorded in 2016 (5.82 t ha⁻¹), while the highest in 2017 (7.48 t ha⁻¹) (Table 5).

Table 5. Winter wheat grain yield (t ha⁻¹) as affected by fertilizer treatments and years (2014–2017)

Fertilizer treatments	GIY (t ha ⁻¹)				Mean treatments
	2014	2015	2016	2017	2014–2017
Control	2.87 ± 0.13 ^{Aa}	4.81 ± 0.11 ^{Ab}	3.16 ± 0.31 ^{Aa}	3.54 ± 0.16 ^{Aa}	3.59 ± 0.21 ^A
N	7.59 ± 0.21 ^{Ba}	7.15 ± 0.28 ^{Ba}	5.89 ± 0.16 ^{Bb}	7.79 ± 0.23 ^{Ba}	7.10 ± 0.22 ^B
NP	7.95 ± 0.27 ^{Bb}	6.90 ± 0.12 ^{Ba}	6.16 ± 0.17 ^{Ba}	8.21 ± 0.15 ^{Bb}	7.31 ± 0.23 ^B
NP+KMgS	7.54 ± 0.14 ^{Bbc}	6.64 ± 0.16 ^{Bab}	6.26 ± 0.34 ^{Ba}	8.03 ± 0.36 ^{Bc}	7.12 ± 0.22 ^B
NP+MgSMnZn	7.61 ± 0.10 ^{Bb}	6.82 ± 0.07 ^{Ba}	6.36 ± 0.18 ^{Ba}	8.24 ± 0.28 ^{Bb}	7.26 ± 0.20 ^B
Mean years	7.03 ± 0.33 ^c	6.59 ± 0.16 ^b	5.82 ± 0.23 ^a	7.48 ± 0.32 ^d	

Means with the standard errors of the mean (SEM) followed by the same letter (^A vertically, ^a horizontally) were not significantly different at 0.05 probability level.

The winter barley GIY was significantly affected by fertilizer treatment ($p < 0.001$), conditions of the year ($p < 0.001$) and by treatment*year interaction ($p < 0.01$). Winter barley GIY was mainly affected by weather conditions (56%), followed by fertilizer treatment (42%) and slightly by treatment*year interaction (2%). The lowest winter barley GIY was recorded in the Control (2.35 t ha⁻¹), while the highest in the NP+KMgS treatment (5.27 t ha⁻¹). Comparing the years, the lowest GIY were recorded in 2015 (3.69 t ha⁻¹), while the highest in 2017 (5.66 t ha⁻¹) (Table 6).

Table 6. Winter barley grain yield (t ha⁻¹) as affected by fertilizer treatments and years (2014–2017)

Fertilizer treatment	GIY (t ha ⁻¹)				Mean treatments
	2014	2015	2016	2017	2014–2017
Control	2.10 ± 0.16 ^{Aa}	2.10 ± 0.07 ^{Aa}	2.68 ± 0.10 ^{Ab}	2.53 ± 0.09 ^{Aab}	2.35 ± 0.08 ^A
N	4.05 ± 0.06 ^{Ba}	3.83 ± 0.56 ^{Ba}	5.50 ± 0.18 ^{Bb}	5.80 ± 0.16 ^{Bb}	4.79 ± 0.26 ^B
NP	4.43 ± 0.10 ^{B^{Ca}}	3.55 ± 0.33 ^{Ba}	5.50 ± 0.35 ^{Bbc}	5.83 ± 0.30 ^{Bc}	4.83 ± 0.27 ^B
NP+KMgS	4.88 ± 0.17 ^{Ca^b}	4.25 ± 0.32 ^{Ba}	5.83 ± 0.31 ^{Bbc}	6.13 ± 0.13 ^{Bc}	5.27 ± 0.22 ^B
NP+MgSMnZn	4.48 ± 0.14 ^{BC^a}	3.75 ± 0.10 ^{Ba}	5.88 ± 0.19 ^{Bb}	6.20 ± 0.28 ^{Bb}	5.08 ± 0.27 ^B
Mean years	4.16 ± 0.18 ^a	3.69 ± 0.17 ^a	5.18 ± 0.22 ^b	5.66 ± 0.26 ^b	

Means with the standard errors of the mean (SEM) followed by the same letter (^A vertically, ^a horizontally) were not significantly different at 0.05 probability level.

Crude protein content

The winter wheat CPC was significantly affected by fertilizer treatment ($p < 0.001$), conditions of the year ($p < 0.001$) and slightly by treatment*year interaction ($p < 0.05$). Unlike the GIY, the CPC was mainly affected by conditions of the year (72%), then by fertilizer treatment (27%) and finally by treatment*year interaction (1%). The lowest CPC was recorded in the Control (7.97%), the highest in NP treatment (11.68%). Comparing the years, the lowest CPC was recorded in 2014 (9.45%), while the highest in 2015 (12.66%) (Table 7).

Table 7. Winter wheat crude protein content (%) as affected by fertilizer treatments and years (2014–2017)

Fertilizer treatment	CPC (%)				Mean treatments 2014–2017
	2014	2015	2016	2017	
Control	7.38 ± 0.23 ^{Aa}	8.54 ± 0.15 ^{Aa}	7.48 ± 0.30 ^{Aa}	8.47 ± 0.44 ^{Aa}	7.97 ± 0.19 ^A
N	10.42 ± 1.04 ^{Bab}	13.30 ± 0.34 ^{Bc}	9.92 ± 0.17 ^{Ba}	12.95 ± 0.55 ^{Bbc}	11.65 ± 0.48 ^B
NP	10.40 ± 0.58 ^{Ba}	13.24 ± 0.42 ^{Bb}	9.88 ± 0.35 ^{Ba}	13.22 ± 0.09 ^{Bb}	11.68 ± 0.44 ^B
NP+KMgS	9.44 ± 0.31 ^{ABa}	13.50 ± 0.43 ^{Bb}	10.51 ± 0.31 ^{Ba}	12.22 ± 0.21 ^{Bb}	11.42 ± 0.43 ^B
NP+MgSMnZn	9.59 ± 0.22 ^{ABa}	13.19 ± 0.36 ^{Bb}	9.44 ± 0.35 ^{Ba}	12.39 ± 0.51 ^{Bb}	11.15 ± 0.46 ^B
Mean years	9.45 ± 0.24 ^a	12.66 ± 0.34 ^c	9.63 ± 0.20 ^a	12.07 ± 0.32 ^b	

Means with the standard errors of the mean (SEM) followed by the same letter (^A vertically, ^a horizontally) were not significantly different at 0.05 probability level.

The winter barley CPC was significantly affected by fertilizer treatment ($p < 0.001$) and weather conditions ($p < 0.001$). The effect of treatment*year interaction was not statistically significant ($p = 0.06$). The major factor influencing winter barley CPC was the year (75%), followed by fertilizer treatment (23%). The lowest CPC was recorded in the Control (8.64%), while the highest in the N treatment (10.17%). Comparing the years, the lowest CPC was recorded in 2016 (9.10%), while the highest in 2017 (10.76%) (Table 8).

Table 8. Winter barley crude protein content (%) as affected by fertilizer treatments and years (2014–2017)

Fertilizer treatment	CPC (%)				Mean treatments 2014–2017
	2014	2015	2016	2017	
Control	9.04 ± 0.25 ^{Aa}	8.28 ± 0.18 ^{Aa}	8.21 ± 0.28 ^{Aa}	9.03 ± 0.29 ^{Aa}	8.64 ± 0.15 ^A
N	10.11 ± 0.13 ^{Ba}	9.57 ± 0.17 ^{Ba}	9.71 ± 0.15 ^{Ba}	11.30 ± 0.16 ^{Bb}	10.17 ± 0.19 ^B
NP	9.77 ± 0.31 ^{ABa}	9.40 ± 0.18 ^{Ba}	9.58 ± 0.19 ^{Ba}	11.14 ± 0.20 ^{Bb}	9.97 ± 0.20 ^B
NP+KMgS	9.51 ± 0.24 ^{ABa}	9.52 ± 0.31 ^{Ba}	8.93 ± 0.20 ^{ABa}	10.58 ± 0.23 ^{Bb}	9.64 ± 0.19 ^B
NP+MgSMnZn	10.26 ± 0.14 ^{Bbc}	9.72 ± 0.27 ^{Bab}	9.20 ± 0.13 ^{Ba}	10.99 ± 0.24 ^{Bc}	10.08 ± 0.19 ^B
Mean years	9.82 ± 0.11 ^b	9.41 ± 0.12 ^{ab}	9.10 ± 0.11 ^a	10.76 ± 0.16 ^c	

Means with the standard errors of the mean (SEM) followed by the same letter (^A vertically, ^a horizontally) were not significantly different at 0.05 probability level.

Weather conditions

The basic characteristic of weather conditions are shown in Fig. 1, a, b, c, d. Generally, the 2014/2015 and 2015/2016 seasons can be characterised as standard or normal seasons typical for the experimental site. In other words, no extreme conditions have occurred and grain yields and CPC were appropriate to the production area, also showing general unsuitability of the area for growing wheat selected for production of leavened bakery products, even with the application of mineral fertilizers at ordinary doses. On the other hand, the 2014/2015 and 2016/2017 seasons were a little bit unusual (Fig. 2, a). The 2014/2015 winter started as very warm, with average precipitation. The field was covered by snow only during the January and spring started quite early (at the beginning of March). The whole growing season is characterised by very low precipitation with no rainfalls from June till August and also by very high temperatures

(36 tropical days altogether). This lack of precipitation significantly and positively affected the winter wheat CPC with average content 12.66%. Interestingly, the GIY of winter wheat was not negatively affected, showing good accessibility of nitrogen during the grain filling period. The protein content is mostly affected by external factors (Johnson et al., 1985) and is inversely proportional to precipitation during the growing season (López-Bellido et al., 1998). According to Rharrabti et al. (2003) and Hlisenikovsky et al. (2015) the dry seasons provide wheat grains with high protein content. On the other hand, a low CPC shall be expected during the seasons with abundant precipitation (Flagela et al., 2010; Gürsoy et al., 2010). The 2016/2017 season was characterised by dry autumn (September, October and November 2016) and winter wheat and barley have a problem to emerge. The start of 2017 was extremely cold with temperatures below -10 °C during the nights, but with snow cover during the whole month. The spring was very cold and with an abundance of precipitation, while summer was very hot and dry, affecting the CPC similarly to the season 2014/2015. As extreme conditions will occur often in the near future in Europe (Grillakis, 2019) the application of mineral fertilizers will be more important factor in securing soil's fertility and sustainable production.

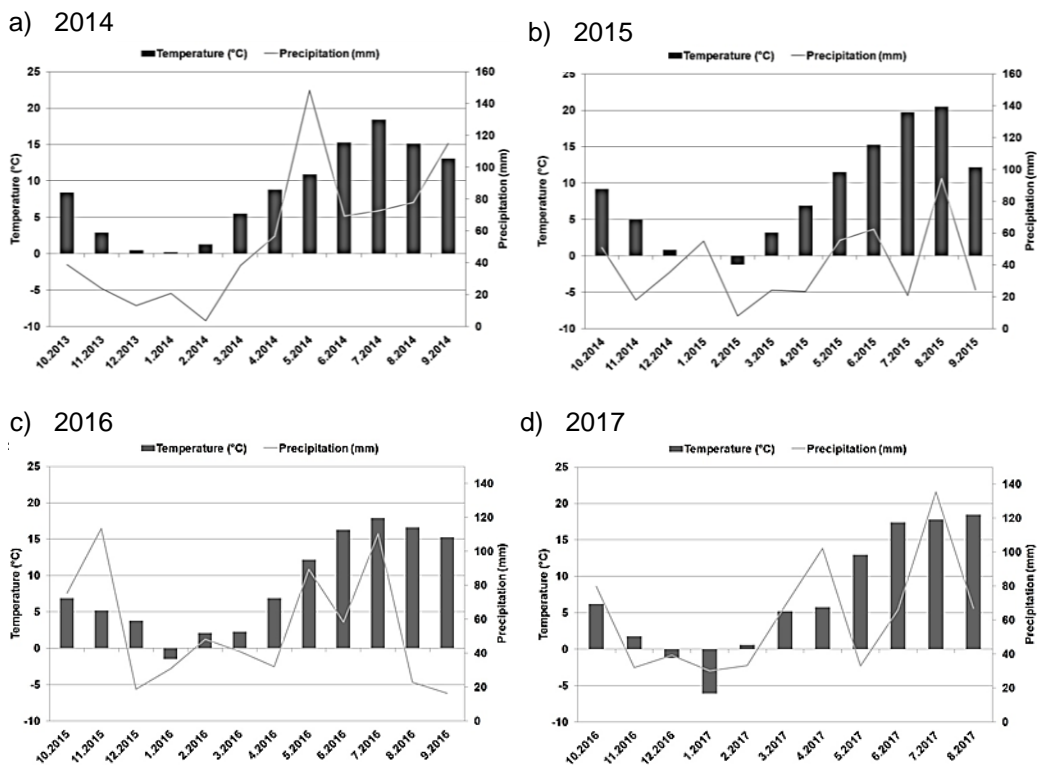


Figure 1. The average temperature (°C) and precipitation (mm) on the experimental site in a) 2014, b) 2015, c) 2016, and d) 2017 seasons.

Fertilizer treatments

According to the results, fertilizer treatment significantly influenced all analyzed parameters in both kinds of cereals, but the main message of this paper is that application of mineral fertilizers containing K, Mg and S (KornKali – NP+KMgS treatment and Kieserit together with EPSO Combipot – NP+MgSMnZn treatment) provided over the whole time of the experiment GIY and CPC comparable with fertilizer treatments without these elements (N and NP treatments) (Tables 5, 6, 7, 8 and Fig. 2, b).

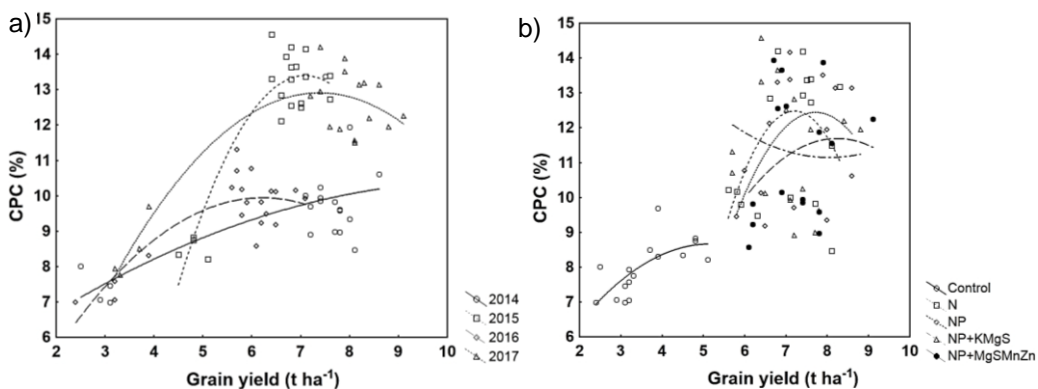


Figure 2. The effect of the a) years and b) fertilizer treatments on grain yield (t ha⁻¹) and CPC (%).

Nitrogen is the most important element for cereals, directly affecting chlorophyll content in leaves (Blandino et al., 2009) and key processes connected with solar-energy capture, moderating transformation and distribution of assimilates, thus influencing grain yields (Hejcman & Kunzová, 2010; Kunzová & Hejcman, 2010; Morell et al., 2011; Hejcman et al., 2012; Chen et al., 2018; Maresma et al., 2019) and protein content (Gooding et al., 2007; Hlisenikovský et al., 2015). It seems that nitrogen was the major contributor to the statistical differences recorded between the Control treatment and the rest of the analyzed fertilizer treatments in our experiment. According to Liebig's law of the minimum the growth and production of plants is not primarily dictated by total amount of the available nutrients, but by the important nutrient which is available in the smallest concentration. As the soil's concentrations of all important nutrients at the experimental site were evaluated as suitable (Table 1), the response of winter wheat and winter barley on fertilizers with K, Mg and S was neutral (without any positive effect in comparison with N and NP treatments).

Application of K increased the soil's concentration of this element (Table 4), which could be taken as a beneficial contribution of KornKali fertilizer. In comparison with the Control the grain yield and CPC were also significantly higher and winter barley grain yields were highest in the treatment with K. Though, no significant differences were recorded in comparison with N and NP treatments. This shows that both kinds of cereal were mainly limited by nitrogen availability and initial concentrations of K in the soil were sufficient for the production of high grain yields. Similar results were published by Hejcman & Kunzová (2010).

According to Grzebisz (2013) the positive reaction of cereals to magnesium fertilizers depends on many factors, such the initial concentration of the nutrient in the soil and the growth stage of cereals at the time of application. According to Matłosz (1992) the positive reaction of winter rye on the addition of magnesium was recorded only on soils with a low concentration of magnesium. Concerning the stage of growth, the best response of cereals on magnesium fertilization was connected with the application at the stage of heading (BBCH 51). The low level of Mg in the soil can have several reasons, as mentioned earlier. The non-visible deficiency is characterized by the decreased root system, directly influencing the performance of the plant and its yield and quality. The visible deficiency is expressed by chlorosis, particularly on older leaves, which has been not recorded on the experimental site. The chlorosis was not even recorded in the long-term fertilizer experiment established in 1955, located in the very same area (Hejzman & Kunzová 2010), where the concentration of Mg in the soil was 98 mg kg^{-1} (low) in the Control treatment after fifty years. And this is crucial for understanding the results we obtained. It can be supported that the positive reaction of cereals on Mg fertilization can be expected on soils with a low level of Mg (exchangeable or in the fixed pool). On the other hand, soils with sufficient concentration of Mg, whether it is based on the soil's origin rocks, or on the agronomical measures and practices, provide an adequate supply of this element and its added application don't have to directly affect, or improve, grain yield and grain quality. The regular application of Mg fertilizers maintains, or even increases, its soil concentration (Table 4) and thus prevent and protect the arable soil from the long-term depletion, which doesn't have to be recognized in the early stages. This was proved by the two-year pot experiment of Lošák et al. (2018), where the concentration of Mg and S linearly increased with the application rate of fertilizers. Our results are not as explicit as conditions in the field are more complex and non-space-limited in comparison with bounded pots, but the pattern can be recognized.

Application of sulphur was also not connected with any positive reaction from winter wheat and barley. Same results were published by Reneau Jr. et al. (1986), who suggested that atmospheric accretions of sulphur from nearby industry supplied a sufficient amount of sulphur during the season. Recently, however, industrial emissions have been significantly reduced and the crop yield depends more on the content of plant available form of sulphur in the soil than deposition from the atmosphere (Scherer, 2009). Salvagiotti & Miralles (2008) and Salvagiotti et al. (2009) documented that sulphur fertilization can positively influence nitrogen use efficiency with increasing doses of applied nitrogen, showing synergism between these two elements. That means that the effect of sulphur is without effect at low nitrogen rates and reveals the synergism with increasing nitrogen rates. That synergism was previously recorded by Reneau Jr. (1986). As we applied only one dose of nitrogen we cannot confirm such synergism. On the other hand, we also cannot confirm the positive effect of the addition of sulphur on grain yield and grain quality even when sulphur was applied together with high doses of nitrogen. This was kind of expected as cereals are crops not so dependent on sulphur in comparison with other arable crops, such as rapeseed or garlic. Probably the soil contained a sufficient amount of sulphur to nutrient requirements of both kinds of cereal.

In our study, we also applied manganese and zinc, together with magnesium and sulphur. Both elements are essential micronutrients involved in a wide variety of physiological processes (Barker & Eaton, 2015; Eaton, 2015). Foliar application of

manganese can increase grain yield and protein content in winter wheat grain (Barlog & Grzebisz, 2008). However, the effect of its application depended on experimental sites, course of weather during growth seasons, growth stage, variety and soil pH. In general, manganese deficiency occurs on soils with pH above 6–6.5. In our study, the soil pH was below this value. Therefore, the plants were probably well supplied with this element. Peck et al. (2008) reported that foliar zinc application can also increase protein content and improve the protein composition in the wheat grain. The positive yield-forming effect of zinc, however, is manifested particularly under conditions of alkaline soils (Cakmak, 2008).

CONCLUSIONS

According to our results nitrogen was the limiting factor in the experiment and additional application of mineral fertilizers, containing K, Mg, S, and microelements, was not connected with a direct effect on grain yield and crude protein content of winter wheat and winter barley, as the initial content in the soil was suitable. However, application of these elements beneficially affected their soil's concentration (not analyzed in the case of S in our experiment, but proved by another papers), which is important as 26.3%, 7.5%, 15% and 50% of the arable land in the Czech Republic need intensive fertilization with P, K, Mg, and S, respectively. The regular application of these fertilizers can prevent the one-way deprivation of the soil, which doesn't have to be recognizable in the early stages.

ACKNOWLEDGEMENTS. The writing of the paper was supported by the Ministry of Agriculture of the Czech Republic by project MZE-RO0419 and by financial support of K+S KALI GmbH.

REFERENCES

- Barker, A.V. & Eaton, T.E. 2015. Zinc. In: Handbook of Plant Nutrition. Ed. Barker, A.V. & Pilbeam, D.J., CRS Press, Boca Raton, London, New York, pp. 537–486.
- Barlóg, P. & Grzebisz, W. 2008. Winter wheat yielding response to manganese foliar application and fungicide canopy protection. *Fertilizers and Fertilization* **32**, 18–31.
- Blandino, M. & Reyneri, A. 2009. Effect of fungicide and foliar fertilizer application to winter wheat at anthesis on flag leaf senescence, grain yield, flour bread-making quality and DON contamination. *Eur. J. Agron.* **30**, 275–282.
- Cakmak, I. 2008. Enrichment of cereal grains with zinc: Agronomic or genetic biofortification? *Plant Soil* **302**, 1–17.
- Ceccoti, S.P. & Messick, D.L. 1994. Increasing plant nutrient sulphur use in the European fertilizer industry. *Agro. Food Ind. Hi Tec.* **5**, 9–14.
- Chen, H., Deng, A., Zhang, W., Li, W., Qiao, Y., Yang, T., Zheng, Ch., Cao, Ch. & Chen, F. 2018. Long-term inorganic plus organic fertilization increases yield and yield stability of winter wheat. *The Crop Journal* **6**, 589–599.
- Eaton, T.E. 2015. Manganese. In: Handbook of Plant Nutrition. Ed. Barker, A.V. & Pilbeam, D.J., CRS Press, Boca Raton, London, New York, pp. 427–486.
- Ebelhar, S.A. & Varsa, E.C. 2000. Tillage and potassium placement effects on potassium utilization by corn and soybean. *Commun. Soil Sci. Plan.* **31**, 2367–2377.
- Fageria, V.D. 2001. Nutrient interactions in crop plants. *J. Plant Nutr.* **2498**, 1269–1290.

- Flagella, Z., Giuliani, M.M., Giuzio, L., Volpi, Ch. & Masci, S. 2010. Influence of water deficit on durum wheat storage protein composition and technological quality. *Eur. J. Agron.* **33**, 197–207.
- Gonzalez-Dugo, V., Durand, J.L. & Gastal, F. 2010. Water deficit and nitrogen nutrition of crops. A review. *Agron. Sustain. Dev.* **30**, 529–544.
- Gooding, M.J., Gregory, P.J., Ford, K.E. & Ruske, R.E. 2007. Recovery of nitrogen from different sources following applications to winter wheat at and after anthesis. *Field Crop Res.* **100**, 143–154.
- Granse, A. & Führs, H. 2013. Magnesium mobility in soils as a challenge for soil and plant analysis, magnesium fertilization and root uptake under adverse growth conditions. *Plant Soil* **368**, 5–21.
- Grillakis, M.G. 2019. Increase in severe and extreme soil moisture droughts for Europe under climate change. *Sci. Total Environ.* **660**, 1245–1255.
- Grzebisz, W. 2013. Crop response to magnesium fertilization as affected by nitrogen supply. *Plant Soil* **368**, 23–39.
- Gürsoy, S., Sessiz, A. & Malhi, S.S. 2010. Short-term effects of tillage and residue management following cotton on grain yield and quality of wheat. *Field Crop Res.* **119**, 260–268.
- Grzebisz, W. 2013. Crop response to magnesium fertilization as affected by nitrogen supply. *Plant Soil* **368**, 23–39.
- Hejzman, M., Kunzová, E. & Šrek, P. 2012. Sustainability of winter wheat production over 50 years of crop rotation and N, P and K fertilizer application on illimerized luvisol in the Czech Republic. *Field Crop Res.* **139**, 30–38.
- Hejzman, M. & Kunzová, E. 2010. Sustainability of winter wheat production on sandy-loamy Cambisol in the Czech Republic: Results from a long-term fertilizer and crop rotation experiment. *Field Crop Res.* **115**, 191–199.
- Hlisnikovský, L., Kunzová, E., Hejzman, M. & Dvořáček, V. 2015. Effect of fertilizer application, soil type, and year on yield and technological parameters of winter wheat (*Triticum aestivum*) in the Czech Republic. *Arch. Acker. Pfl. Boden.* **61**, 33–55.
- Jan, A.U., Hadi, F., Midrarullah, Nawaz, M.A. & Rahman, K. 2017. Potassium and zinc increase tolerance to salt stress in wheat (*Triticum aestivum* L.). *Plant Physiol. Bioch.* **116**, 139–149.
- Johnson, V.A., Mattern, P.J., Peterson, C.J. & Kuhr, S.L. 1985. Improvement of wheat protein by traditional breeding and genetic techniques. *Cereal Chem.* **62**, 350–355.
- Jordan-Meille, L. & Pellerin, S. 2004. Leaf area establishment of maize (*Zea Mays* L.) field crop under potassium deficiency. *Plant Soil* **265**, 75–92.
- Kunzová, E. & Hejzman, M. 2010. Yield development of winter wheat over 50 years of nitrogen, phosphorus and potassium application on greyic Phaeozem in the Czech Republic. *Eur. J. Agron.* **33**, 166–174.
- López-Bellido, L., Fuentes, M., Castillo, J.E. & López-Garrido, F.J. 1998. Effects of tillage, crop rotation and nitrogen fertilization on wheat-grain quality grown under rainfed Mediterranean conditions. *Field Crop Res.* **57**, 265–276.
- Lošák, T., Elbl, J., Kintl, A., Čermák, P., Mühlbachová, G., Neugschwandtner, R.W., Torma, S. & Hlušek, J. 2018. Soil agrochemical changes after kieserite application into chernozem and its effect on yields of barley biomass. *Agriculture (Poľnohospodárstvo)* **64**, 183–188.
- Maresma, Á., Martínez-Casasnovas, J.A., Santiveri, F. & Lloveras, J. 2019. Nitrogen management in double-annual cropping system (barley-maize) under irrigated Mediterranean environments. *Eur. J. Agron.* **103**, 98–107.
- Matłoz, C. 1992. Effect of cereals fertilization with magnesium conducted in different stages of growth on yields of grain and straw and some grain quality parameters. PhD thesis. Poznań University of Life Sciences, Poznań, 47 pp. (in Polish). In: Grzebisz W. (2013): Crop response to magnesium fertilization as affected by nitrogen supply. *Plant Soil* **368**, 23–39.

- Morell, F.J., Lampurlanés, J., Álvato-Fuentes, J. & Cantero-Martínez, C. 2011. Yield and water use efficiency of barley in a semiarid Mediterranean agroecosystem: Long-term effects of tillage and N fertilization. *Soil Till Res.* **117**, 76–84.
- Peck, A.W., McDonald, G.K. & Graham, R.D. 2008. Zinc nutrition influences the protein composition of flour in bread wheat (*Triticum aestivum* L.). *J. Cereal Sci.* **47**, 266–274.
- Pettigrew, W.T. 2008. Potassium influences on yield and quality production for maize, wheat, soybean and cotton. *Physiol. Plantarum* **133**, 670–681.
- Prystupa, P., Peton, A., Pagano, E. & Gutierrez Boem, F.H. 2018. Sulphur fertilization of barley crops improves malt extract and fermentability. *J. Cereal Sci.* **85**, 228–235.
- Reneau Jr., R.B., Brann, D.E. & Donohue, S.J. 1986. Effect of sulphur on winter wheat grown in the coastal plain of Virginia. *Commun. Soil Sci. Plan.* **17**, 149–158.
- Rharrabti, Y., Royo, C., Villegas, D., Aparicio, N. & García del Moral, L.F. 2003. Durum wheat quality in Mediterranean environments I. Quality expression under different zones, latitudes and water regimes across Spain. *Field Crop Res.* **80**, 123–131.
- Salvagiotti, F. & Miralles, D.J. 2008. Radiation interception, biomass production and grain yield as affected by the interaction of nitrogen and sulfur fertilization in wheat. *Eur. J. Agron.* **28**, 282–290.
- Salvagiotti, F., Castellarín, J.M., Miralles, D.J. & Pedrol, H.M. 2009. Sulfur fertilization improves nitrogen use efficiency in wheat by increasing nitrogen uptake. *Field Crop Res.* **113**, 170–177.
- Scherer, H.W. 2009. Sulfur in soils. *J. Plant Nutr. Soil Sc.* **172**, 326–335.
- Smatanová, M. & Sušil, A. 2018. The results of agro-chemical testing of arable soils between 2012–2017. Central Institute for Supervising and Testing in Agriculture (in Czech).
- Yang, G., Zhao, G., Liu, L. & Yang, Y. 2007. Sulphur effect on protein components and grain yield of wheat. *Chinese Journal of Soil Science* **38**, 89–92.
- Yu, L., Xu, L., Xu, M., Wan, B., Yu, L. & Huang, Q. 2011. Role of Mg²⁺ ions in protein kinase phosphorylation: insights from molecular dynamics simulations of ATP-kinase complexes. *Mol. Simulat.* **37**, 1143–1150.
- Zhao, F.J., Hawkesford, M.J. & McGrath, S.P. 1999. Sulphur assimilation and effects on yield and quality of wheat. *J. Cereal Sci.* **30**, 1–17.

Assessment of luggage compartment parameters based on the preferences of a heterogeneous driver group

M. Hruška

Czech University of Life Sciences, Faculty of Engineering, Department of Technological Equipment of Building, Kamýcká 129, CZ165 21 Praha 6, Czech Republic

*Correspondence: jabko@tf.czu.cz

Abstract. This work deals with the assessment of driver preferences in the area of passenger car luggage compartments. The data collected is compared to that of real vehicles from the full range of passenger cars available on the European market. The data used for the research described in this work was obtained using a questionnaire survey on a large heterogeneous group of drivers in the Czech Republic. All of the research participants had three categories of vehicles available during testing - for better imagination and the possibility of personal comparison of parameters. The collected data was subsequently subjected to statistical evaluation, where mainly statistically significant dependencies in the preferences of individual drivers were sought out given their personal and anthropometric parameters. On the basis of the statistical evaluation of the obtained data, a difference was found in the preferences of the types and dimensions of the individual luggage compartments for the individual respondents depending on the selected parameters. The results of this work can be used in the process of designing luggage compartments of passenger cars, in particular with regard to the specific needs of drivers. The results of the work could thus contribute to improving the safety in handling cargo in the luggage compartments of vehicles and to improving health protection.

Key words: driver, luggage space, vehicle, gender, age.

INTRODUCTION

Nowadays, passenger car ergonomics are considered to be an increasingly important part of the car design process (Wang et al., 2007). An optimally ergonomically designed luggage compartment is of the same importance as, for example, the driver's workplace and plays a large role both in terms of the safety of the person who uses the luggage compartment, and in terms of the complete vehicle crew (Reed, 1998). The luggage compartment of a modern passenger car is the part of the car that is used practically constantly during the use of a passenger car, not only by the driver but also by other persons using the vehicle (Bhise, 2012). However, the person who decides on the parameters of a newly purchased car intended for personal use is usually the person who will most often use and drive it. Therefore, when determining the luggage compartment motivation and preference, it is necessary to use a test group as a reference, in particular drivers. The basic dimensions of the luggage compartments of modern passenger cars are generally determined primarily according to the type of vehicle, its determination and its basic external dimensions. Nevertheless, during design processes,

the dimensions of the luggage compartments can be influenced to a certain extent to achieve optimization in order to increase the utility value and optimize the ergonomic parameters of the luggage compartment. The degree of optimization and adaptation of the luggage compartment to the driver's requirements can thus directly influence not only the vehicle's utility value, but also the driver's feelings and overall comfort, and thus also the safety of the vehicle (Matoušek, 1998; Reed, 1998; Hruška 2016). For example, this concerns the driver's motivation process to make better use of the luggage compartment to store cargo, instead of placing cargo in other areas of the vehicle's cabin where it could pose a potential safety risk (Tilley, 2002; Vágnerová, 2007).

The volume of the luggage compartment in liters (dm³) is now commonly used as a reference value for comparing luggage cars. However, this value is inadequate in terms of practical use in ergonomics because it does not take into account the basic geometric arrangement of the luggage compartment. With respect to the operator's health, in particular the length (sometimes also referred to as depth) of the luggage compartment is a key value when handling cargo. For optimal handling of cargo in the entire luggage compartment area, it is necessary to combine two basic movements, which are very complicated in terms of human biomechanics because several muscle groups are involved in them at once (Haug et al., 2004). The basic movement is the (forward bend) anteflexion of the thoracic and lumbar spine, and the secondary movement is the stretching of one or both arms forward, depending on the weight and shape of the load (Véle, 1995; Havlíčková, 1999). The load rate of muscle groups is determined by several factors, and if we ignore the shape and weight of the load, the main factor is the geometric shape of the luggage compartment and the anthropometric data of the driver.

The primary goal of this work is to find out if there is any dependency between the measured parameters of drivers and their preferences in the luggage compartment area. The secondary goal of this work was to find out what luggage compartment dimensions the drivers of the selected test group prefer and whether there is any dependency between the preferred luggage compartment dimensions and the parameters of a specific driver.

MATERIALS AND METHODS

Participants

For the purposes of measurement, 140 participants (72 women and 68 men) from the Czech Republic were obtained, all of whom are in the university environment – students or teachers of technical or economic orientation. The age of the participants ranged from 19 to 67 years (the average age was 34 years). It was unambiguously required and verified that all of the participants were to have a driver's license enabling them to drive passenger cars. All of the participants were also in good health and had no restrictions on the musculoskeletal system.

Table 1. Number of persons tested and their primary parameters in relation to measurement

	Number	Age (number in age group)			Partner relationship	
		18–25	25–35	35+	single	In a relationship
Men	68	18	29	21	19	49
Women	72	6	22	44	14	58
Total	140	24	51	65	33	107

In addition to their age and gender, each tested subject also specified their marital status (single or in a relationship) and stated which car they most commonly used at the time of measurement. The most commonly used vehicle was then assigned to one of the pre-selected categories, as shown in Table 2. Body height was also measured for each subject when wearing normal walking shoes. All of the testing was done anonymously and according to the principles for work with personal data.

Table 2. Number of tested persons and their secondary parameters in relation to measurement

	Number	Height (number)			Vehicle that they primarily drive		
		Up to 172	172–180	over 180	small	medium	large
Men	68	3	22	43	13	35	19
Women	72	45	26	1	25	34	13
Total	140	48	48	44	38	69	32

*Note: Small hatchbacks and mini-cars were classified in the **small** vehicle category. Medium limousines and a small SUVs were included in the vehicle group designated as **medium**. Limousines, large sedans and large SUVs were included in the **large** vehicle group.*

Test environment

Testing was conducted under laboratory conditions with uniform illumination and a working temperature of 20 °C. The tested individuals were provided with the comparative vehicles specified in Table 3. The luggage compartment dimensions of the comparative vehicles specified in Table 2 were taken from the official sources of the manufacturers and subsequently additionally checked using a laser rangefinder prior to testing. Each person tested also had a manual measuring meter in the metric system, so that everyone could check the dimensions of each luggage compartment. Roughly 20 percent of the tested persons did not trust some of the specified luggage compartment dimensions, and therefore took advantage of the opportunity to measure specific dimensions. At the time of measurement, all of the vehicles had open luggage compartments with doors in maximum position and the luggage compartments were empty and without any additional adjustments.

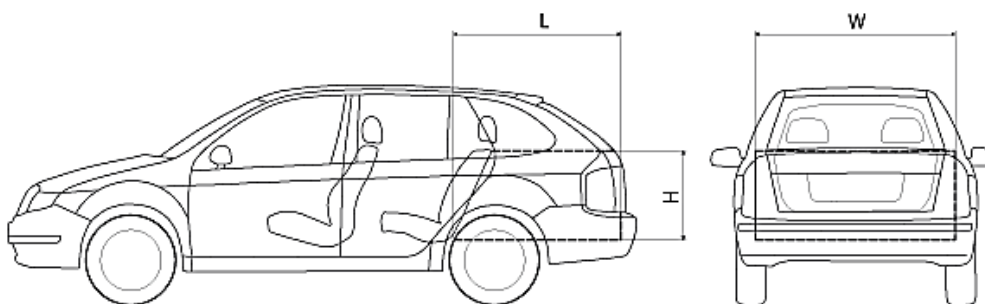


Figure 1. Position ranges of seat and steering wheel in the test vehicles.

Data Collection Procedures

Each person tested had a trained assistant available who recorded their responses. First, each tested subject carefully inspected, and possibly measured all of the comparative vehicles and then answered the questions asked. After asking the question,

the test person’s assistant always asked if he or she understood the question and whether he or she needed to add or explain something. If the person tested was not sure about a question, the assistant always explained the question so that the baseline information level of all of the tested persons was adequately balanced. There was no time limit set for answering the questions, and therefore each tested subject had enough time to think about their answers.

Table 3. Basic dimensions of luggage compartments of comparative vehicles

Type of vehicle	Length (L) (cm)	Height (H) (cm)	Width (W) (cm)	Volume (dm ³)
Škoda Fabia Combi 2018	96	60	95	530
Škoda Octavia Combi 2016	105	63	101	610
Škoda Superb Combi 2015	114	65	101	660
Škoda Yeti 2013	80	72	103	405 ¹⁾
Škoda Kodiaq 2016	116	74	100	650 ¹⁾
Ford Mondeo Combi 2013	118	42	114	554

Note: The length, height and width dimensions were verified as part of testing on specific test models. The luggage compartment volume values were measured according to standard VDA V210-2 and were taken from the official databases of the manufacturers. 1) The lowest luggage compartment volume value is used.

The test subjects were asked a total of 10 questions divided into three basic groups. The first group consisted of questions identifying the drivers’ preferences in terms of the luggage compartment when buying a new vehicle. The second group of questions concerned how the luggage compartment was used. The last group of questions examined what luggage compartment parameters would be considered optimal by the tested drivers (Table 4).

Table 4. Questions and response variants used in clinical data collection

Question	Wording of question	Answer 1	Answer 2	Answer 3
A	What do you prefer for the LC ¹⁾ ...	Length	Width	-
B	What bottom limit for the LC do you prefer ¹⁾ ...	Even	Raised	-
C	What criterion is the LC ¹⁾ for you when choosing a new vehicle...	Primary	Secondary	-
D	I usually place luggage on...	The floor	The seat	In the LC ¹⁾
E	I put cargo in the LC ¹⁾ ...	Freely	I use organizers-	
F	Load limit of the LC ¹⁾ when handling cargo...	I use it	I do not use it	I’m afraid to encumber it
Ranges of values				
G	In my opinion, I can encumber the load limit with a weight of about	10–25–50–75–100 kg – more		
H	In your opinion, what is the optimum width of the LC?	Up to 105 cm	105–115 cm	Over 115 cm
I	In your opinion, what is the optimum length of the LC?	Up to 100 cm	100–120 cm	Over 120 cm
J	In your opinion, what is the optimum height of the LC?	Up to 60 cm	60–70 cm	Over 70 cm

1) LC – luggage compartment.

After the measurements were completed, all of the data was digitized and evaluated using PivotTables and Pearson’s chi-squared test. In order to facilitate statistical evaluation of the measured values, some quantitative results were divided equally into three groups.

RESULTS AND DISCUSSION

The results obtained during the measurements were statistically processed and evaluated using PivotTables and Pearson’s chi-squared test at a significance level of 0.05. Furthermore, the adjusted residuals method was used for further refinement and better interpretation of the found dependencies. The tables below show only those results that were found to be dependent. There were no dependencies found for questions that are labelled B, D, and G in Table 4, and therefore these results are not shown, and they are no longer worked with.

In Table 5, which shows the results related to question A, a dependency was manifested between the width to length preference of the luggage compartment and the type of partnership relationship that the respondent is in. Using the adjusted residuals method, it can be stated that respondents who are in a relationship prefer a significantly longer length (depth) of the luggage compartment compared to width. For respondents who are not in a relationship, the width or length preference was nowhere near as strong, and in this respect, respondents from this group do not make significant differences.

Table 5. Dependence of preferred luggage compartment dimensions (question A) on driver parameters as specified in Tables 1 and 2.

Driver parameter	X ²	Critical value	Cramer V	Dependence
Gender	0.003	3.84	0.005	None
Partnership	8.29	3.84	0.24	Medium dependence
Primarily driven vehicle	5.05	5.99	0.19	None
Body height	0.64	5.99	0.06	None
Driver age	0.72	5.99	0.07	None

In Table 6, where the statistical results related to question C are shown, dependencies were observed for virtually all of the assessed parameters, with the exception of the parameter that takes into account the type of vehicle most frequently driven by the respondent. Using the adjusted residual method, the results can be interpreted as meaning that for women, the luggage compartment is a more important criterion that plays a role in the decision-making process when buying a new vehicle than for men. For men, this criterion tends to be considered secondary.

Table 6. Dependence of the luggage compartment as a criterion on the selection of a new vehicle (question C) on driver parameters as specified in Tables 1 and 2

Driver parameter	X ²	Critical value	Cramer V	Dependence
Gender	8.36	3.84	0.24	Medium dependence
Partnership	10.89	3.84	0.27	Strong dependence
Primarily driven vehicle	0.95	5.99	0.08	None
Body height	12.71	5.99	0.30	Strong dependence
Driver age	13.41	5.99	0.31	Strong dependence

Furthermore, it can be stated that for respondents who are in a relationship, the luggage compartment is a significantly more important decision parameter than for respondents who are not in a relationship. This parameter is also very significant for smaller respondents and for older respondents. Conversely, younger respondents mostly consider this a secondary parameter.

In Table 7, where the results relating to question E are presented, only a single, strong statistical dependency emerged between the way in which the respondent arranges cargo in the luggage compartment and the respondent's gender. Using the adjusted residual method, it can be stated that men more often deposit cargo in a luggage compartment in a disorderly manner, whilst women much more often use a variety of organizers for attaching cargo. Dependencies on other parameters were not manifested in this case.

Table 7. Dependence of organizing a load in the luggage compartment (question E) on driver parameters as specified in Tables 1 and 2.

Driver parameter	X ²	Critical value	Cramer V	Dependence
Gender	12.07	3.84	0.29	Strong dependence
Partnership	2.19	3.84	0.12	None
Primarily driven vehicle	0.95	5.99	0.08	None
Body height	3.01	5.99	0.14	None
Driver age	4.64	5.99	0.18	None

In Table 8, where the results relating to question F are presented, dependencies were manifested between the use of the lower load limit of the luggage compartment and the gender and age of the respondent. Using the adjusted residuals method, it can be stated that men use the load limit more than women. Furthermore, it can also be claimed that younger respondents are very often afraid to use the load limit for fear of damaging the vehicle. This finding can be considered surprising and can only be explained by a lower level of general technical knowledge and awareness of the structure of a passenger car in the younger population of respondents.

Table 8. Dependence of the load limit of a luggage compartment (question F) on driver parameters as specified in Tables 1 and 2.

Driver parameter	X ²	Critical value	Cramer V	Dependence
Gender	11.23	5.99	0.29	Strong dependence
Partnership	3.49	5.99	0.16	None
Primarily driven vehicle	7.52	9.48	0.17	None
Body height	7.91	9.48	0.14	None
Driver age	15.33	9.48	0.24	Medium dependence

In Table 9, where the results relating to question H are presented, only a weak statistical dependence was manifested among the preferred optimal luggage compartment width and the type of vehicle that the respondent most often drives. Using the adjusted residuals method, it can be stated that respondents who are currently driving in small cars prefer a small luggage compartment width. These findings could be interpreted as a coincidence of the compliance of preferences of drivers who have chosen a small vehicle, are satisfied with it, and hence do not wish for a wider luggage

compartment. Other dependencies could not be proven. Overall, however, all of the respondents cited the optimum luggage compartment width size of an average of 5–10 cm wider than the average width of luggage compartments of models commonly available on the European market (Table 3).

Table 9. Dependence of the preferred width of the luggage compartment (question H) on driver parameters as specified in Tables 1 and 2.

Driver parameter	X ²	Critical value	Cramer V	Dependence
Gender	1.08	5.99	0.08	None
Partnership	4.04	5.99	0.17	None
Primarily driven vehicle	9.97	9.48	0.19	Weak dependence
Body height	2.08	9.48	0.08	None
Driver age	1.47.	9.48	0.07	None

In Table 10, where the results relating to question I are presented, dependencies were manifested in the preferred optimum length (depth) of the luggage compartment and the type of respondents' relationship, as well as the type of vehicle the respondent most often drives. Using the adjusted residuals methods, it can be stated that single respondents are much more satisfied with short luggage space, while respondents in a relationship prefer medium and longer luggage compartments. Furthermore, it can be claimed that the luggage compartment length preference of the respondents accurately reproduces the type of vehicle that the respondents are used to driving. Respondents who use large vehicles prefer a long luggage compartment, while respondents with small cars prefer a shorter luggage compartment. This can be interpreted in a similar way to Question H, where there is a clear correlation between respondent preferences and the vehicle types they use.

Table 10. Dependence of the preferred length of the luggage compartment (question I) on driver parameters as specified in Tables 1 and 2.

Driver parameter	X ²	Critical value	Cramer V	Dependence
Gender	1.29	5.99	0.09	None
Partnership	8.33	5.99	0.24	Medium dependence
Primarily driven vehicle	14.34	9.48	0.22	Medium dependence
Body height	5.36	9.48	0.13	None
Driver age	7.45	9.48	0.16	None

Table 11. Dependence of the preferred height of the luggage compartment (question J) on driver parameters as specified in Tables 1 and 2.

Driver parameter	X ²	Critical value	Cramer V	Dependence
Gender	8.50	5.99	0.24	Medium dependence
Partnership	2.52	5.99	0.13	None
Primarily driven vehicle	10.86	9.48	0.19	Weak dependence
Body height	9.60	9.48	0.19	Weak dependence
Driver age	7.84	9.48	0.16	None

In Table 11, where the statistical results relating to question J are presented, dependencies were manifested in the preferences of the height of the luggage compartment on the gender of the respondent, the type of vehicle that the respondent

most often drives and the height of the respondent. Using the adjusted residuals method, the results can be interpreted in such a way that women prefer a higher luggage compartment, while men prefer a lower height. Even with this question, it can be stated that drivers who drive small vehicles also prefer a lower luggage compartment. For drivers of other types of vehicles, the dependencies are not as obvious. Furthermore, it can be stated that respondents of medium height most often prefer low luggage compartments, whilst shorter respondents prefer high luggage compartments. Here, above all, we can see the strong influence of the factor of the tested women, who are naturally smaller, and who prefer high luggage compartments, as described above. Both of these findings correlate well with each other.

CONCLUSIONS

In this work we managed to obtain a large number of valuable primary data from a relatively homogeneous group of respondents, which may be statistically interesting in terms of possible comparisons with other statistics obtained from respondents with different parameters, such as different education, nationality, cultural habits, etc. By dividing the data using PivotTables and using the adjusted residuals method, it was found that statistically significant dependencies can be found between the preferences of the interviewed drivers with regard to the luggage compartments of passenger cars and their anthropometric and sociological parameters.

Based on the above results, it can be stated that the existence of a dependency between anthropometric and sociological parameters of the tested subjects and parameters related to the working area of the luggage compartments of passenger cars was proven. It should be noted, however, that the number of found dependencies is relatively small and manifests itself especially where the dependence on gender or the possible existence of a respondent's partnership relationship is evaluated. Parameters such as age or body height of respondents do not play almost any, or only a minimal role in the sought out dependencies. These parameters play an exceptional role only in some sought out dependencies, such as the significance of the luggage compartment in the decision-making process during the purchase of a new passenger car.

The ascertained results could be used in passenger car development processes and the subsequent optimization of their luggage compartments to better suit users' needs. For example, according to their preferences, all of the respondents would appreciate wider luggage compartments, regardless of the particular category of passenger car. It can also be stated that for a statistically significant group of respondents, the luggage compartment and its processing and parameters are an important factor in the decision-making process when buying a new passenger car. This criterion is particularly important for women and for respondents who are in a relationship. Another interesting result was the assessment of the dependency of organizing cargo in the luggage compartment on the gender of the respondent, where it was clearly demonstrated that women are more responsible in this respect and, in significantly more cases, they use different types of organizers to arrange and secure cargo in the luggage compartment of a passenger car.

The results presented in this work could serve as a basis for further research to further refine the above findings. The data and hypotheses presented in this paper could serve as ancillary factors in the car design process with regard to potential customer target groups.

The development of passenger cars always moving forward, and the parameters of vehicles and their luggage compartments are constantly evolving and changing to better meet the demands of vehicle users. It can be claimed that the results described in this work can further improve the understanding of luggage compartment optimization of a passenger car, in particular with regard to the requirements of drivers, customers or, in general, passenger car users.

No references are given for the above conclusions because no comparable studies are currently available.

REFERENCES

- Bhise, V. 2012. *Ergonomics in the automotive design process*, Taylor & Francis Group, 309 pp. ISBN 978-1-4398-4210-2
- Haug, E., Choi, H.Y. & Beaugonin, M. 2004. Handbook of Numerical Analysis, Volume XII: Computational Models for the Human Body — Human Models for Crash and Impact Simulation. Elsevier. 297–361, [https://doi.org/10.1016/S1570-8659\(03\)12004-2](https://doi.org/10.1016/S1570-8659(03)12004-2)
- Havlíčková, L. 1999. *Physical load physiology I. General part*. Praha: Karolinum, 205 pp. ISBN 9788071848752
- Hruška, M. & Jindra, P., 2016, *Ability to handle unfamiliar systems in passenger cars according to driver skills*. *Agronomy Research* **14**(5), 1601–1608.
- Matoušek, O. 1998. *Workplace & Health: Ergonomic layout and workplace equipment*. Praha: Státní zdravotní ústav, 23 pp.
- Reed, M.P. 1998. *Statistical and Biomechanical Prediction of Automobile Driving*. Ph.D. Dissertation. University of Michigan. USA, 234 pp. <http://hdl.handle.net/2027.42/131082>
- Tilley, A R. 2002. *The measure of man and woman: human factors in design*. Rev. ed. New York: Wiley, 98 pp. ISBN 04-710-9955-4.
- Vágnerová, M. 2007. *Psychology*, Karolinum, 358 pp. ISBN 978-80-246-0841-9
- Véle, F. 1995. *Kinesiology of postural system*, Praha, Karolinum, 85 pp. ISBN 80-7184-100-5
- Wang, M.J.J., Wu, W.Y., Lin, K.C., Yang, S.N. & Lu, J.M. 2007. Automated anthropometric data collection from three-dimensional digital human models. *International Journal of Advanced Manufacturing Technology* **32**, 109–115. <https://doi.org/10.1007/s00170-005-0307-3>

Theoretical analysis of force, pressure and energy distributions of bulk oil palm kernels along the screwline of a mechanical screw press FL 200

A. Kabutey^{1,*}, D. Herak¹, C. Mizera¹ and P. Hrabec²

¹Czech University of Life Sciences Prague, Department of Mechanical Engineering, Faculty of Mechanical Engineering, Kamycka 129, CZ165 00 Prague, Czech Republic

²Czech University of Life Sciences Prague, Department of Material Sciences and Manufacturing Technology, Kamycka 129, CZ165 21 Prague, Czech Republic

*Correspondence: kabutey@tf.czu.cz

Abstract. The present study is a follow-up of the previously published study on the mathematical description of loading curves and deformation energy of bulk oil palm kernels under compression loading, aimed at determining theoretically the amounts of force, pressure and energy along the screw lamella positions SL_p of the screw press FL 200 by applying the tangent curve mathematical model and the screwline geometry parameters (screw shaft diameter, screw inner and outer diameters, screw pitch diameter and the screw thickness). The fitting curve value F_v of the tangent mathematical model was further examined at $F_v = 2$ and $F_v = 3$ by identifying the force, deformation, stress and compression coefficients at varying vessel diameters D_v and initial pressing heights H_t of the bulk oil palm kernels. Based on the results of the stepwise regression analysis, the amounts of the theoretical deformation energy T_{DE} in linear pressing as well as the theoretical force F_r , pressure P_r and energy SL_E of the screw press FL 200 were statistically significant (P -value < 0.05) or (F -value $>$ significance F) in relation to the predictors (H_t , D_v , F_v and SL_p). The coefficient of determination (R^2) values between 61 and 86% were observed for the determined regression models indicating that the responses T_{DE} , F_r , P_r and SL_E can accurately be predicted by the corresponding predictors. The normal probability plots of the responses approximately showed a normal distribution.

Key words: experimental data, mathematical model, screw geometry parameters, compression loading, responses and predictors.

INTRODUCTION

Advanced oil extraction techniques such as microwave-assisted extraction, ultrasound-assisted extraction and pressurized liquid extraction are alternative oil extraction techniques to replace the conventional oil extraction methods namely solvent (hexane) extraction and mechanical pressing. These new extraction techniques provide several advantages over the traditional processes including shorter extraction time, reduced energy, greener solvents, less solvent use, full automation, greater reliability and environmentally friendly (Dutta et al., 2015; Castejon et al., 2018; Pandey & Shrivastava

2018). In spite of the advantages underlined, the application of these modern techniques in developing countries is very limited due to the high cost and operational skills.

The mechanical pressing (screw press or expeller) is more popular in developing countries due to the several advantages including simple equipment and sturdy in construction, easy maintenance, semi-skilled operator, easy adaption to processing other oilseeds, continuous oil process and chemical free protein of by-product (seedcake) (Kartika et al., 2010; Singh & Bargale 2000; Pradhan et al., 2011; Karaj & Muller 2011; Mridula et al., 2015; Liu et al., 2016; Uitterhaegen & Evon, 2017). Several efforts have been considered to improving the performance of mechanical screw press or expellers through modifications in press design and optimization of process variables as well as physical, thermal and chemical pretreatments. These efforts have helped to increase oil recovery levels from 50% to 80% for various oilseeds (Singh & Bargale 2000; Deli et al., 2011; Karaj & Muller 2011; Pradhan et al., 2011). In achieving higher oil extraction efficiency of the mechanical screw pressing, continuous research is still needed to understand the whole process. Theoretical analysis of the screw press configuration and design parameters (screw pitch diameter, pitch angle, screw thickness and screw shaft inner and outer diameters) in terms of pressure requirement is one of the research approaches (Herak et al., 2010; Sayin et al., 2015; Shankali et al., 2017; Pradhan et al., 2017; Bogaert et al., 2018). This, however, requires an in-depth knowledge of the linear compression process (Gupta & Das, 2007; Lysiak, 2007; Herak et al., 2013; Divisova et al., 2014; Demirel et al., 2017).

In the linear compression process, the deformation of the bulk oilseeds at varying initial pressing heights and vessel diameters in relation to the compression force and speed is examined. Based on the experimental dependency between the force and deformation curves of the bulk oilseeds/kernels, the tangent curve mathematical model can be used to describe the linear compression process (Herak et al., 2013; Sigalingging et al., 2014, 2015). The model can also be applied to the non-linear process (mechanical screw press FL 200) to theoretically analyze the pressure and energy requirements (Herak et al., 2010; Kabutey et al., 2016). The mechanical screw press FL 200 with 44 lamellas along the screwline can be divided into seven pressing positions, and for each pressing position, the mechanical behaviour (the dependency between the force and deformation curve) of the bulk oilseeds/kernels can be described where the theoretical force, pressure and energy can be determined. At the moment, the screw press FL 200 has not been used to process or recover the kernel oil which is semi-solid at room temperature compared to other vegetable oils that can easily be processed using the screw press FL 200. It is based on this background that the present study is essential to understand theoretically the mechanical behaviour of the bulk kernels along the screwline of screw press FL 200.

The present study, however, is a continuation of the previous study (Kabutey et al., 2018) aimed at analyzing the theoretical deformation energy of the bulk kernels based on the fitting curve values of the tangent mathematical model, determining the stress and compression coefficients of the tangent mathematical model and determining the theoretical amounts of force, pressure and energy along the screwline or screw lamella positions of screw press FL 200.

MATERIALS AND METHOD

Sample and compression test

Bulk oil palm kernels of moisture content of 9% w.b. were used for the compression test. The pressing vessels of diameters D_v , 60, 80 and 100 mm with a plunger together with the universal compression-testing machine (ZDM 50, Czech Republic) were used to recover the kernel oil from the bulk kernels at initial pressing heights H_t 40, 60 and 80 under a maximum load of 200 kN and a speed of 5 mm min⁻¹ (Fig. 1) (Kabutey et al., 2018).

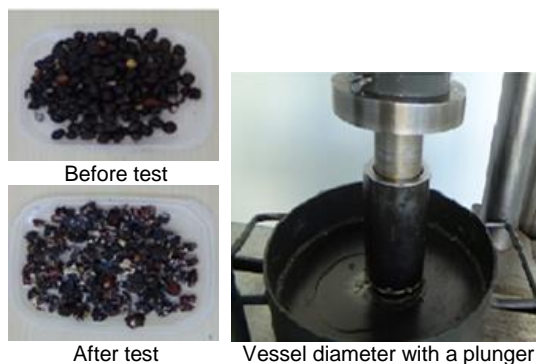


Figure 1. Compression test of bulk oil palm kernels for recovering the kernel oil.

Parameters obtained/calculated from the compression test

The deformation of the bulk kernels as well as the dependency between the force and deformation curves at varying D_v and H_t were obtained from the compression test. The percentage kernel oil and deformation energy T_{DE} were calculated as indicated in our previous publication (Kabutey et al., 2018).

Theoretical description of experimental curves

The theoretical description of the force and deformation curves of the bulk kernels was also described based on the tangent curve mathematical model (Herak et al., 2013; Sigalingging et al., 2014, 2015; Kabutey et al., 2018) by determining the force A (kN) and deformation B (mm⁻¹) coefficients at varying D_v and H_t of the bulk oil palm kernels (Kabutey et al., 2018). Here, the tangent curve model fitting value F_v was examined only at $F_v = 1$ (-). The present study, however, further evaluated $F_v = 2$ and $F_v = 3$ respectively to accurately compare the theoretical amounts of T_{DE} in linear pressing as well as the amounts of force F_r , pressure P_r and energy SL_E along the screwline of screw press FL 200.

Determination of the theoretical amounts of F_r , P_r and SL_E

The average stress and compression coefficients of the tangent curve mathematical model (Herak et al., 2013; Kabutey et al., 2016) were calculated. These coefficients and the expression of the cross-sectional area of the screwline were used to determine the theoretical amounts of F_r , P_r and SL_E distributions along the screwline of the screw press FL 200 with 44 lamellas divided into seven positions (0–7) (Fig. 2) (Kabutey et al., 2010; 2016).

The screwline parameters (screw shaft diameter, screw inner and outer diameters, screw pitch diameter and the screw thickness) designed for processing jatropha seeds were considered for the bulk oil palm kernels. Here, the amounts of the theoretical volume, initial pressing height, deformation and compression ratio of the bulk kernels along the screwline of the screw press FL 200 were similar to jatropha bulk seeds (Kabutey et al., 2016). However, at $F_v = 1$ for $D_v = 60, 80$ and 100 (mm); the compression

ratio in the tangent curve model (Herak et al., 2013; Sigalingging et al., 2014, 2015; Kabutey et al., 2018) was divided by the pressing factor coefficients of 1.637, 2.14 and 2.89 (-). At $F_v = 2$ the pressing factor coefficients were 1.59, 1.88 and 2.42 while at $F_v = 3$ the values of 1.508, 1.825 and 1.254 were considered. It is worth indicating that the pressing factor coefficients were guessed to correspond to the maximum force of 200 kN at a speed of 5 mm min^{-1} applied to the bulk oil palm kernels during the compression test.

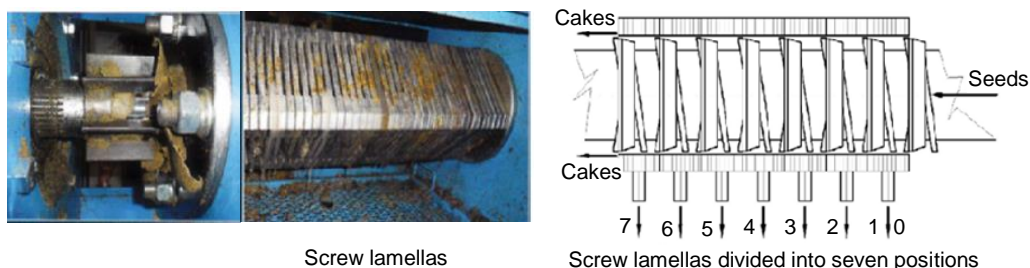


Figure 2. Screw press FL 200 geometry (Farmet, 2015; Kabutey et al., 2016).

Statistical analysis

The experimental and theoretical data obtained were analysed using the MathCad 14, IBM SPSS Statistics 25 and Statistica 13 by employing the general linear model and stepwise regression techniques.

RESULTS AND DISCUSSION

In the previously published study (Kabutey et al., 2018), the tangent curve model fitting value $F_v = 1$ (-) was examined where the theoretical dependency between the force and deformation curves as well as deformation energy of the bulk oil palm kernels at varying vessel diameters $D_v = 60, 80$ and 100 mm and initial pressing heights $H_t = 40, 60$ and 80 mm were described. The present study, however, further examined $F_v = 2$ and $F_v = 3$ as indicated in Tables 1 to 3 respectively. The theoretical force A and deformation B coefficients at F_v values were statistically significant ($P \text{ values} > 0.05$) or values of $F\text{-critical} > F\text{-ratio}$ according to the Mathcad 14 program. From the results obtained, it was observed that the $D_v = 100 \text{ mm}$ at $H_t = 80 \text{ mm}$, the trigonometric function (\sin) instead of a (\tan) function of the tangent curve model (Herak et al., 2013; Sigalingging et al., 2014, 2015) best described the experimental data. In view of the above, the results $H_t = 80 \text{ mm}$ were not included in any further calculations due to the change of the trigonometric function. The average coefficients of force A (kN), deformation B (mm^{-1}), stress C (N mm^{-1}) and compression G (-) at varying H_t for each D_v are shown in Table 4. These coefficients showed both decreasing and increasing trends in relation to F_v values for all D_v . The results were statistically significant based on the linear regression analysis with a coefficient of determination values (R^2) between 40 to 77%. The average coefficients of C (N mm^{-1}) and G (-) were determined based on the expressions given by Herak et al., 2013; Sigalingging et al., 2014, 2015.

Table 1. Theoretical description of the experimental force-deformation curve for $D_v = 60$ mm

H_t (mm)	A (kN)	B (mm^{-1})	F_v (-)	F-ratio (-)	F-critical (-)	P -value (-)	R^2 (-)
40	19.88	0.058	1	0.024	3.853	0.876	0.997
40	16.68	0.058	1	0.015	3.863	0.903	0.999
60	13.87	0.039	1	$2.067 \cdot 10^{-3}$	3.848	0.989	0.999
60	16.19	0.039	1	$6.149 \cdot 10^{-3}$	3.848	0.938	1
80	14.27	0.03	1	$8.813 \cdot 10^{-5}$	3.862	0.993	0.999
80	13.3	0.03	1	$1.363 \cdot 10^{-5}$	3.862	0.997	0.999
40	11.98	0.052	2	0.01	3.853	0.919	0.999
40	9.519	0.052	2	0.069	3.863	0.792	0.997
60	6.496	0.036	2	0.18	3.848	0.671	0.993
60	9.393	0.036	2	0.131	3.848	0.717	0.996
80	9.318	0.027	2	0.242	3.862	0.623	0.989
80	6.856	0.028	2	0.236	3.862	0.627	0.991
40	12.47	0.047	3	0.039	3.853	0.844	0.998
40	9.158	0.047	3	0.156	3.863	0.693	0.994
60	5.027	0.033	3	0.295	3.848	0.587	0.988
60	9.313	0.032	3	0.229	3.848	0.632	0.993
80	10.81	0.024	3	0.425	3.862	0.515	0.982
80	5.821	0.025	3	0.424	3.862	0.515	0.986

F-ratio < F-critical or P -value > 0.05 is significant (Mathsoft 2014); D_v is the vessel diameter (mm); H_t is the initial pressing height of the bulk palm kernels (mm); A is the force coefficient of mechanical behaviour (kN); B is the deformation coefficient of mechanical behaviour (mm^{-1}); F_v is the fitting curve value (-); F-ratio is the value of the F test, F-critical is the value that compares a pair of models, R^2 is the coefficient of determination (-).

Table 2. Theoretical description of the experimental force-deformation curve for $D_v = 80$ mm

H_t (mm)	A (kN)	B (mm^{-1})	F_v (-)	F-ratio (-)	F-critical (-)	P -value (-)	R^2 (-)
40	24.84	0.061	1	$2.21 \cdot 10^{-3}$	3.848	0.963	1
40	27.51	0.064	1	$2.251 \cdot 10^{-3}$	3.848	0.962	0.999
60	25.7	0.041	1	$2.618 \cdot 10^{-3}$	3.847	0.959	1
60	23.56	0.041	1	$1.513 \cdot 10^{-3}$	3.848	0.969	0.999
80	23.69	0.032	1	$1.879 \cdot 10^{-4}$	3.847	0.989	0.999
80	23.39	0.032	1	$1.031 \cdot 10^{-4}$	3.847	0.992	0.999
40	19.45	0.053	2	0.154	3.848	0.694	0.996
40	25.82	0.054	2	0.207	3.848	0.649	0.995
60	21.9	0.036	2	0.146	3.847	0.703	0.996
60	19.97	0.035	2	0.231	3.848	0.631	0.992
80	22.38	0.027	2	0.192	3.847	0.661	0.993
80	19.94	0.028	2	0.171	3.847	0.68	0.993
40	27.92	0.046	3	0.23	3.848	0.631	0.993
40	48.62	0.045	3	0.297	3.848	0.586	0.992
60	35.16	0.03	3	0.244	3.847	0.622	0.992
60	32.74	0.03	3	0.345	3.848	0.557	0.987
80	43.48	0.022	3	0.31	3.847	0.578	0.988
80	32.55	0.023	3	0.285	3.847	0.593	0.988

Table 3. Theoretical description of the experimental force-deformation curve for $D_v = 100$ mm

H_t (mm)	A (kN)	B (mm ⁻¹)	F_v (-)	F-ratio (-)	F-critical (-)	P-value (-)	R ² (-)
40	39.67	0.059	1	0.053	3.848	0.818	0.999
40	39.3	0.057	1	$3.539 \cdot 10^{-3}$	3.848	0.953	1
60	40.04	0.04	1	0.016	3.848	0.9	0.999
60	38.11	0.041	1	0.024	3.848	0.876	0.999
80	44.47	0.032	1	$2.866 \cdot 10^{-3}$	3.848	0.957	0.999
80	43.81	0.033	1	0.034	3.848	0.855	0.999
40	65.49	0.044	2	0.1	3.848	0.752	0.997
40	53.63	0.045	2	0.207	3.848	0.65	0.997
60	74.85	0.03	2	0.145	3.848	0.704	0.995
60	63.7	0.031	2	0.124	3.848	0.725	0.995
80	106.5	0.022	2	0.186	3.848	0.666	0.995
80	116.2	0.022	2	0.108	3.848	0.743	0.996
40	413.8	0.028	3	0.165	3.848	0.684	0.994
40	197.6	0.033	3	0.297	3.848	0.586	0.995
60	846.1	0.016	3	0.236	3.848	0.628	0.99
60	442.5	0.019	3	0.211	3.848	0.646	0.991
*80	13,940	$5.488 \cdot 10^{-3}$	3	0.299	3.848	0.584	0.99
*80	14,060	$5.668 \cdot 10^{-3}$	3	$3.247 \cdot 10^{-3}$	3.848	0.955	0.992

* Trigonometric function (*sin*) instead of a (*tan*) function of the tangent models best described the experimental data.

Table 4. Cumulative amounts of the tangent curve model coefficients at $H_t = 40, 60$ and 80 mm

D_v (mm)	F_v (-)	A (kN)	B (mm ⁻¹)	C (N mm ⁻²)	G (-)
60	1	15.70 ± 1.53	0.04 ± 0.00	4.36 ± 0.43	2.35 ± 0.00
80		24.78 ± 1.20	0.05 ± 0.00	3.87 ± 0.19	2.51 ± 0.03
100		40.90 ± 0.70	0.04 ± 0.00	4.09 ± 0.07	2.45 ± 0.05
60	2	30.98 ± 4.88	0.05 ± 0.00	4.16 ± 0.68	2.00 ± 0.02
80		32.72 ± 3.77	0.03 ± 0.00	4.14 ± 0.53	2.04 ± 0.03
100		46.87 ± 3.44	0.03 ± 0.00	5.56 ± 0.48	2.05 ± 0.04
60	3	8.77 ± 2.97	0.03 ± 0.00	2.44 ± 0.82	1.93 ± 0.03
80		36.75 ± 8.03	0.03 ± 0.00	5.74 ± 1.25	1.81 ± 0.03
100		475.00 ± 219.13	0.02 ± 0.00	47.50 ± 21.91	1.14 ± 0.13

Table 5. Cumulative amounts of T_{DE} at $H_t = 40, 60$ and 80 mm

D_v (mm)	F_v (-)	T_{DE} (J)
60		990.74 ± 41.77
80	1	818.39 ± 53.29
100		709.40 ± 108.73
60		1,245.48 ± 34.48
80	2	1,041.10 ± 39.85
100		947.05 ± 42.69
60		1,579.50 ± 20.03
80	3	1,445.43 ± 47.09
100		1,148.56 ± 41.44

The cumulative values of the theoretical deformation energy T_{DE} (J) of bulk oil palm kernels based on the tangent curve model (Herak et al., 2013; Kabutey et al., 2018; Sigalingging et al., 2014, 2015) and the regression analysis are given in Tables 5 to 8.

Table 6. Regression statistics of the dependent variable: T_{DE}

Model parameters	R	R Square	Adjusted R Square	Standard error of the estimate
H_t, F_v, D_v	0.960 ^a	0.922	0.917	114.57

^a Predictors: (Constant): Height H_t , vessel diameter D_v , tangent curve model fitting value F_v .

Table 7. Anova analysis of the dependent variable: T_{DE}

Model parameters	Sum of squares	Degree of freedom	Mean square	F	Significance F
Regression	7,399,540.422	3	2,466,513.474	187.914	0.000 ^a
Residual	630,036.842	48	13,125.768		
Total	8,029,577.264	51			

Table 8. Regression coefficients of the dependent variable: T_{DE}

Model parameters	Unstandardized coefficients		Standardized coefficients <i>Beta</i>	t-value	P-value
	<i>B</i>	<i>Standard error</i>			
Constant	-785.227	112.174		-7.000	0.000
H_t	16.432	0.987	0.675	16.640	0.000
D_v	15.064	0.987	0.619	15.255	0.000
F_v	-142.997	19.749	-0.294	-7.241	0.000

The linear regression model expressing the response T_{DE} of bulk oil palm kernels in linear pressing at a maximum force of 200 kN and a speed of 5 mm min⁻¹ is described in Eq. 1 as follows:

$$T_{DE}(J) = -785.227 + 16.432 \cdot H_t + 15.064 \cdot D_v - 142.997 \cdot F_v \quad (1)$$

Eq. 1 is significant based on the fact that the significance F value of the Anova results was less than the 5% significance level or the F value was much greater than the significance F. The coefficient of determination was 0.922, that is, 92.2% of the variation in the theoretical deformation energy is explained by the predictors (H_t , D_v and F_v). The normal probability plot of the response T_{DE} is shown in Fig. 3. The data points followed the normal distribution assumption with no strong deviations.

The theoretical amounts of the force F_r , pressure P_r and energy SL_E of bulk oil palm kernels along the screw lamella positions SL_p of screw press FL 200 are indicated in Tables 9 to 11 and graphically described in Figs 4 to 6. These amounts were determined based on the tangent curve model (Herak et al., 2013; Kabutey et al., 2018; Sigalingging et al., 2014, 2015), screwline geometry information (screw shaft diameter, screw inner and outer diameters, screw pitch diameter and the screw thickness) and other mathematical equations as described in our previous publication on jatropha bulk oilseeds (Kabutey et al., 2016). The cumulative amounts of F_r , P_r and SL_E are also given in Tables 12 to 14 respectively.

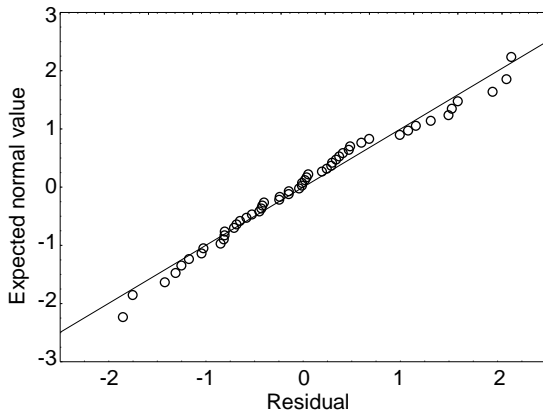
**Figure 3.** Normal probability plot of the regression standardized residual of the dependent variable: $T_{DE}(J)$.

Table 9. Calculated parameters at the screw lamellas positions for $F_v = 1$

SL_p (-)	D_v (mm)	F_r (kN)	P_r (MPa)	SL_E (J)
0	60	0	0	0
1	60	10.32	2.129	102.963
2	60	24.01	7.681	179.566
3	60	25.43	8.575	180.461
4	60	28.47	10.878	180.025
5	60	30.23	12.388	178.631
6	60	35.55	17.852	170.587
7	60	46.58	34.581	145.322
0	80	0	0	0
1	80	12.75	2.629	99.442
2	80	26.11	8.321	163.667
3	80	27.17	9.161	163.534
4	80	29.46	11.257	161.022
5	80	30.71	12.585	158.59
6	80	34.18	17.162	148.187
7	80	40.13	29.794	121.116
0	100	0	0	0
1	100	14.63	3.018	86.216
2	100	27.19	8.666	135.621
3	100	28.04	9.456	134.973
4	100	29.82	11.396	131.756
5	100	30.76	12.605	129.153
6	100	33.22	16.679	119.109
7	100	37.02	27.468	95.216

F_v : fitting curve value; SL_p : screw lamellas positions; D_v : vessel diameter; P_r : force; F_r : pressure; SL_E : energy at screw lamellas positions.

Table 11. Calculated parameters at the screw lamellas positions for $F_v = 3$

SL_p (-)	D_v (mm)	F_r (kN)	P_r (MPa)	SL_E (J)
0	60	0	0	0
1	60	1.634	0.337	8.548
2	60	16.11	5.134	58.853
3	60	18.4	6.204	63.732
4	60	24.2	9.247	73.99
5	60	27.9	11.435	79.351
6	60	40.5	20.334	92.5
7	60	72.14	53.561	106.147
0	80	0	0	0
1	80	2.822	0.582	12.701
2	80	20.2	6.439	71.036
3	80	22.38	7.546	75.414
4	80	27.48	10.501	83.773
5	80	30.49	12.494	87.647

Table 10. Calculated parameters at the screw lamellas positions for $F_v = 2$

SL_p (-)	D_v (mm)	F_r (kN)	P_r (MPa)	SL_E (J)
0	60	0	0	0
1	60	4.682	0.966	31.655
2	60	21.09	6.721	105.076
3	60	23	7.755	109.149
4	60	27.48	10.499	116.335
5	60	30.13	12.348	119.351
6	60	38.32	19.24	123.924
7	60	55.46	41.178	118.872
0	80	0	0	0
1	80	5.866	1.21	34.231
2	80	23.09	7.358	105.201
3	80	24.85	8.378	108.479
4	80	28.82	11.015	113.747
5	80	31.09	12.741	115.632
6	80	37.69	18.927	116.962
7	80	50.02	37.137	107.03
0	100	0	0	0
1	100	7.106	1.465	32.928
2	100	24.53	7.817	93.79
3	100	26.09	8.797	96.07
4	100	29.5	11.274	99.287
5	100	31.38	12.86	100.136
6	100	36.59	18.375	99.094
7	100	45.46	33.747	87.395

Table 12. Cumulative amounts of F_r (kN) at SL_p

D_v (mm)	$F_v = 1$ (-)	$F_v = 2$ (-)	$F_v = 3$ (-)
60	200.59	200.16	200.88
80	200.51	201.43	200.80
100	200.68	200.66	200.28

F_r : force; SL_p : screw lamella positions (-); D_v : vessel diameter (mm); F_v : fitting curve value (-).

Table 13. Cumulative amounts of P_r (MPa) at SL_p

D_v (mm)	$F_v = 1$ (-)	$F_v = 2$ (-)	$F_v = 3$ (-)
60	94.084	98.707	106.252
80	90.909	96.766	100.371
100	89.288	94.335	96.33

P_r : pressure.

Table 11 (continued)

6	80	39.62	19.893	95.197
7	80	57.81	42.916	96.175
0	100	0	0	0
1	100	4.269	0.88	16.224
2	100	23.11	7.366	75.5
3	100	25.01	8.432	78.933
4	100	29.2	11.157	84.841
5	100	31.52	12.917	87.198
6	100	38.03	19.095	90.238
7	100	49.14	36.483	84.25

Table 14 Cumulative amounts of SL_E (J) at SL_p

D_v (mm)	$F_v = 1$ (-)	$F_v = 2$ (-)	$F_v = 3$ (-)
60	1,137.555	724.362	483.121
80	1,015.558	701.282	521.943
100	832.044	608.7	517.184

SL_E : energy at screw lamellas positions.

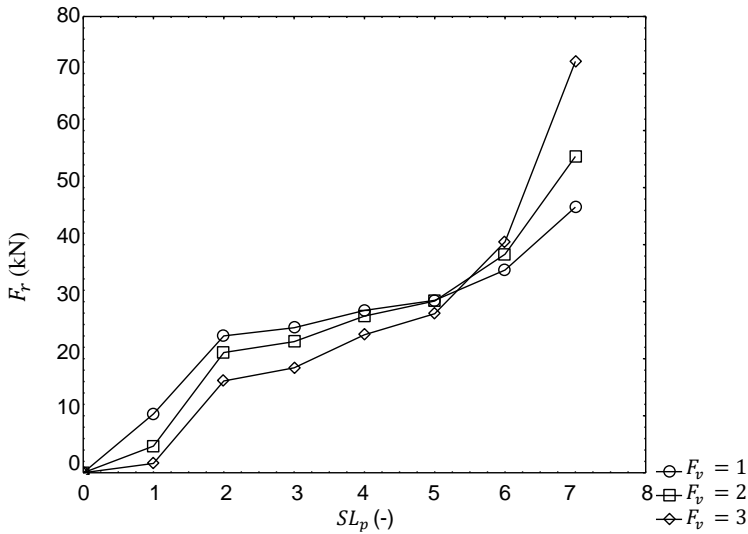


Figure 4. Relationship between F_r and SL_p in relation to F_v for $D_v = 60$ mm.

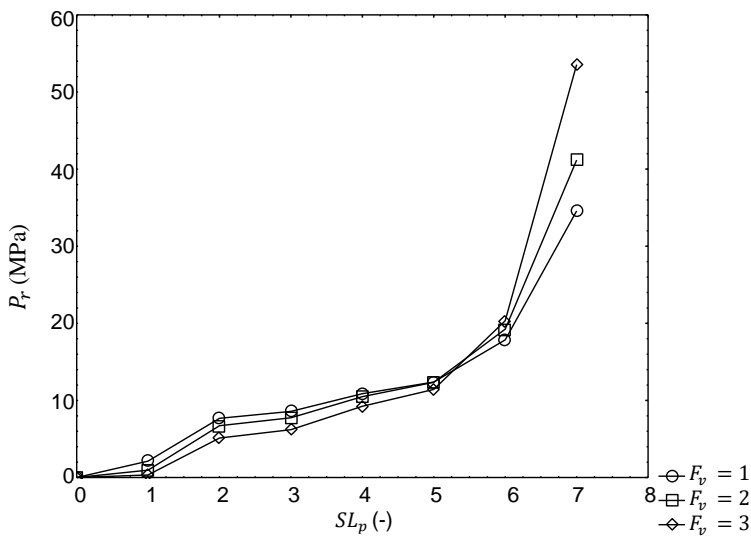


Figure 5. Relationship between P_r and SL_p in relation to F_v for $D_v = 60$ mm.

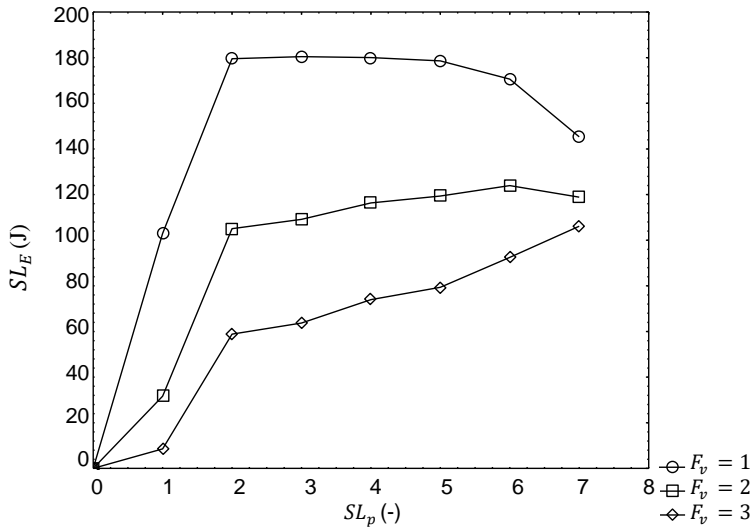


Figure 6. Relationship between SL_E and SL_p in relation to F_v for $D_v = 60$ mm.

The results of the regression analysis employing the stepwise method for the responses or dependent variables (F_r , P_r and SL_E) and the predictors or independent variables (SL_p , D_v and F_v) are given in Tables 15 to 23 respectively. The response F_r turned out to be predicted only by the SL_p as shown in Tables 15 to 17.

Table 15. Regression statistics of the dependent variable: F_r (kN)

Model parameter	R	R Square	Adjusted R Square	Standard error of the estimate
SL_p	0.931 ^a	0.867	0.865	5.735

^a Predictor: (Constant); SL_p : screw lamella positions (-).

Table 16. Anova analysis of the dependent variable: F_r (kN)

Model parameters	Sum of squares	Degree of freedom	Mean square	F	Significance F
Regression	15,015.391	1	15,015.391	456.582	0.000 ^a
Residual	2,302.057	70	32.887		
Total	17,317.448	71			

Table 17. Regression coefficients of the dependent variable: F_r (kN)

Model parameters	Unstandardized coefficients		Standardized coefficients	t-value	P-value
	B	Standard error	Beta		
Constant	3.024	1.234		2.451	0.017
SL_p	6.303	0.295	0.931	21.368	0.000

The regression equation of the response F_r is given in Eq. 2 as follows:

$$F_r(kN) = 3.024 + 6.303 \cdot SL_p \quad (2)$$

Eq. 2 is significant based on the fact that the significance F value of the Anova results was less than the 5% significance level or the F value was much greater than the significance F. The coefficient of determination was 0.867, that is, 86.7% of the variation in the response F_r is explained by the predictor SL_p . The response P_r also correlated with the SL_p as shown in Tables 18 to 20.

Table 18. Regression statistics of the dependent variable: P_r (MPa)

Model parameter	R	R Square	Adjusted R Square	Standard error of the estimate
SL_p	0.875 ^b	0.765	0.762	5.609

^b Predictor: (Constant), SL_p : screw lamella positions (-).

Table 19. Anova analysis of the dependent variable: P_r (MPa)

Model parameters	Sum of squares	Degree of freedom	Mean square	F	Significance F
Regression	7,173.121	1	7,173.121	228.028	0.000 ^a
Residual	2,202.003	70	31.457		
Total	9,375.124	71			

Table 20. Regression coefficients of the dependent variable: P_r (MPa)

Model parameters	Unstandardized coefficients		Standardized coefficients	t-value	P-value
	B	Standard error	Beta		
Constant	-3.204	1.207		-2.655	0.010
SL_p	4.356	0.288	0.875	15.101	0.000

The regression equation of the response P_r is given in Eq. 3 as follows:

$$P_r(MPa) = -3.204 + 4.356 \cdot SL_p \quad (3)$$

Eq. 3 is significant based on the fact that the significance F value of the Anova results was less than the 5% significance level or the F value was much greater than the significance F. The coefficient of determination was 0.875, that is, 87.5% of the variation in the response P_r was explained by the predictor SL_p . The response SL_E also correlated with predictors SL_p and F_v as shown in Tables 21 to 23.

Table 21. Regression statistics of the dependent variable: SL_E (J)

Model parameters	R	R Square	Adjusted R Square	Standard error of the estimate
SL_p, F_v	0.776 ^c	0.602	0.591	32.786

^c Predictors: (Constant), screw lamella positions, SL_p ; fitting curve value, F_v .

Table 22. Anova analysis of the dependent variable: SL_E (J)

Model parameters	Sum of squares	Degree of freedom	Mean square	F	Significance F
Regression	112,336.987	2	56,168.494	52.253	0.000 ^a
Residual	74,169.713	69	1,074.923		
Total	186,506.701	71			

Table 23. Regression coefficients of the dependent variable: SL_E (J)

Model parameters	Unstandardized coefficients		Standardized coefficients <i>Beta</i>	t-value	P-value
	<i>B</i>	<i>Standard error</i>			
Constant	104.954	11.804		8.891	0.000 ^c
SL_p	13.388	1.686	0.603	7.939	0.000 ^c
F_v	-30.477	4.732	-0.489	-6.440	0.000 ^c

The regression equation of the response SL_E is given in Eq. 4 as follows:

$$SL_E(J) = 104.954 + 13.388 \cdot SL_p - 30.477 \cdot F_v \quad (4)$$

Eq. 4 is significant based on the fact that significance F value of the Anova results was less than the 5% significance level or the F value was much greater than the significance F. The coefficient of determination was 0.602, that is, 60.2% of the variation in the response SL_E was explained by the predictors SL_p and F_v . The normal probability plots of the responses F_r , P_r and SL_E are shown in Figs 7 to 9. Approximately, the data points showed a normal distribution.

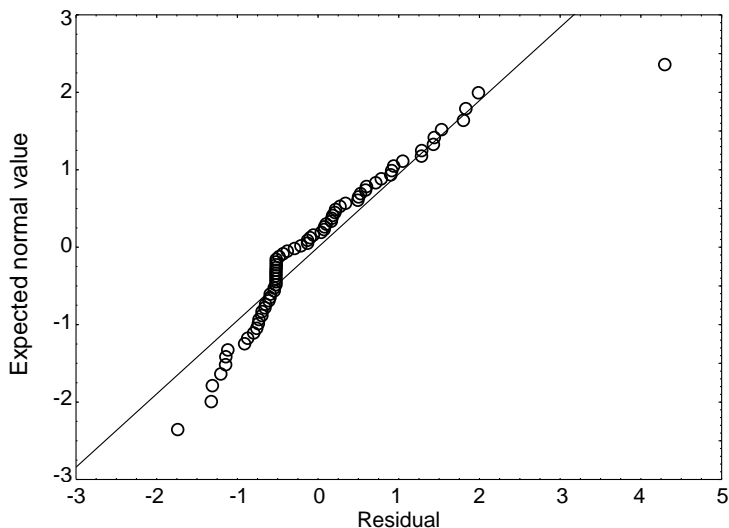


Figure 7. Normal probability plot of the regression standardized residual of the dependent variable: F_r (kN).

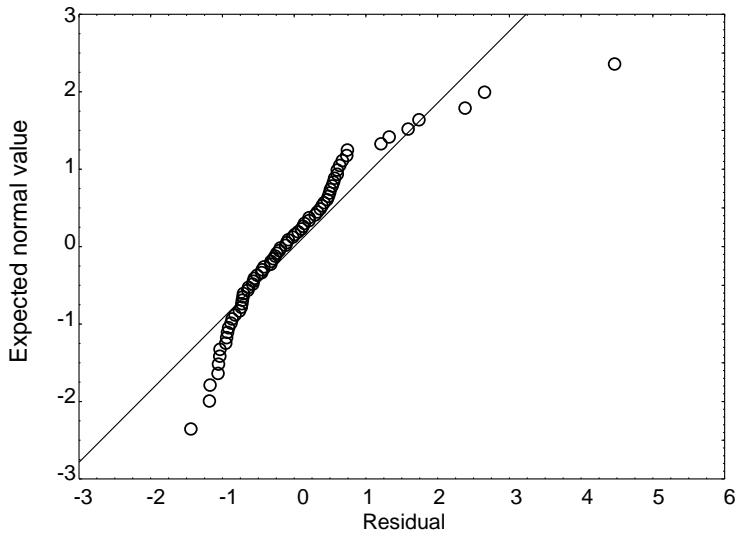


Figure 8. Normal probability plot of the regression standardized residual of the dependent variable: P_r (MPa).

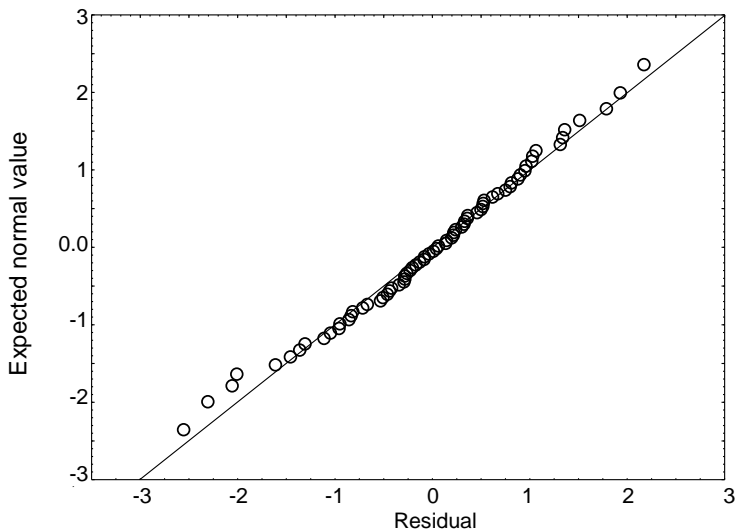


Figure 9. Normal probability plot of the regression standardized residual of the dependent variable: SL_E (J).

CONCLUSIONS

The average force, deformation, stress and compression coefficients were determined for describing bulk oil palm kernels at varying initial pressing heights, vessel diameters and fitting values of the tangent curve mathematical model. A linear regression model was described for the theoretical deformation energy of bulk oil palm kernels under compression loading based on the initial pressing heights of bulk kernels, vessel diameters and fitting values of the tangent curve models. Linear regression models were

also described for the theoretical force, pressure and energy of the bulk kernels along the screwline of the mechanical screw press FL 200 based on the screw lamella positions and fitting values of the tangent curve models. From the industrial/design point of view, the screw press FL 200 can be used to process a wide range of oilseeds such as jatropha seeds, rapeseeds, sunflower seeds and others by both cold-pressing and extrusion pressing. There is limited information in the literature about the cold-pressing and extrusion pressing of bulk oil palm kernels. Therefore, the present study results provide the background information for using the screw press FL 200 and Farnet Duo for processing bulk oil palm kernels as well as optimizing the process in terms of maximum kernel oil recovery and minimum energy input.

ACKNOWLEDGEMENTS. The research was financially supported by the project ‘supporting the development of international mobility of research staff at CULS Prague’ registration number: CZ.02.2.69/0.0/0.0/16_027/0008366.

REFERENCES

- Bargale, P.C., Wulfsohn, D., Irudayaraj, J., Ford, R.J. & Sosulski, F.W. 2000. Prediction of Oil Expression by Uniaxial Compression using Time-varying Oilseeds Properties. *Journal of Agricultural Engineering Research* **77**(2), 171–181.
- Bogaert, L., Mathieu, H., Mhemdi, H. & Vorobiev, E. 2018. Characterization of oilseeds mechanical expression in an instrumented pilot screw press. *Industrial Crops and Products* **121**, 106–113.
- Castejon, N., Luna, P. & Senorans, F.J. 2018. Alternative oil extraction methods from *Echium plantagineum* L, seeds using advanced techniques and green solvents. *Food Chemistry* **244**, 75–82.
- Deli, S., Farah Masturah, M., Tajul Aris, Y. & Wan Nadiah, W.A. 2011. The effects of physical parameters of the screw press oil expeller on oil yield from *Nigella sativa* L. seeds. *Journal International Food Research* **18**(4), 1367–1373.
- Demirel, C., Kabutey, A., Herak, D. & Gurdil, G.A.K. 2017. Numerical estimation of deformation energy of selected bulk oilseeds in compression loading, IOP Conference, Series: *Material Science Engineering* **237**(1), 1–5.
- Divisova, M., Herak, D., Kabutey, A., Sleger, V., Sigalingging, R. & Svatonova, T. 2014. Deformation curve characteristics of rapeseeds and sunflower seeds under compression loading. *Scientia Agriculturae Bohemica* **45**, 180–186.
- Dutta, R., Sarkar, U. & Mukherjee, A. 2015. Process optimization for the extraction of oil from *Crotalaria juncea* using three phase partitioning. *Industrial Crops and Products* **71**, 89–96.
- Farnet, 2015. Oil and Feed Tech, Jirinkova 276, Czech Republic
- Gupta, R.K. & Das, S.K., 2000. Fracture resistance of sunflower seed and kernel to compressive loading. *Food Engineering* **46**, 1–8.
- Herák, D., Kabutey, A., Divišová, M. & Simanjuntak, S. 2013. Mathematical model of mechanical behaviour of *Jatropha curcas* L, seeds under compression loading. *Biosystems Engineering* **114**(3), 279–288.
- Herak, D., Sedlacek, A. & Kabutey, A. 2010. Determination of the complete geometry of the worm extruder screwline for compressive pressing of the oil bearing crops. *Conference Proceeding, 4th International Conference TAE*, pp. 207–210.
- IBM Corp., Released 2017. IBM SPSS Statistics for Windows, Version 25.0. Armonk, NY: IBM Corp.

- Kabutey, A., Herak, D., Hanus, J., Choteborsky, R., Dajbych, O., Sigalingging, R. & Akangbe, O.L. 2016. Prediction of pressure and energy requirement of *Jatropha curcas* L. bulk seeds under non-linear pressing. *Conference Proceeding, 4th International Conference TAE*, pp. 262–269.
- Kabutey, A., Herak, D., Mizera, C. & Hrabě, P. 2018. Mathematical description of loading curves and deformation energy of bulk oil palm kernels. *Agronomy Research* **16**(4), 1686–1697.
- Karaj, S. & Muller, J. 2011. Optimizing mechanical oil extraction of *Jatropha curcas* L. seeds with respect to press capacity, oil recovery and energy efficiency. *Industrial Crops Products* **34**, 1010–16.
- Kartika, I.A., Pontalier, P.Y. & Rigal, L. 2010. Twin-screw extruder for oil processing of sunflower seeds: Thermo-mechanical pressing and solvent extraction in a single step. *Industrial Crops Products* **32**, 297–304.
- Liu, J., Gasmalla, M.A.A., Li, P. & Yang, R. 2016. Enzyme-assisted extraction processing from oilseeds: Principle, processing and application. *Innovative Food Science & Emerging Technologies* **35**, 184–193.
- Lysiak, G. 2007. Fracture toughness of pea: Weibull analysis. *International Journal of Food Engineering* **83**, 436–443.
- Mathsoft. 2014. Parametric Technology Corporation, Needham, MA02494, USA.
- Mridula, D., Barnwal, P. & Singh, K.K. 2015. Screw pressing performance of whole and dehulled flaxseed and some physico-chemical characteristics of flaxseed oil. *Journal of Food Science Technology* **52**, 1498–1506.
- Pandey, R. & Shrivastava, S.L. 2018. Comparative evaluation of rice bran oil obtained with two-step microwave assisted extraction and conventional solvent extraction. *Journal of Food Engineering* **218**, 106–114.
- Pradhan, R.C., Mishra, S., Naik, S.N., Bhatnagar, N. & Vijay, V.K. 2011. Oil expression from *Jatropha* seeds using a screw press expeller. *Biosystems Engineering* **109**, 158–166.
- Sayin, R., Martinez-Marcos, L., Osorio, J.G., Cruise, P., Jones, I., Halbert, G.W., Lamprou, D.A. & Litster, J.D. 2015. Investigation of an 11 mm diameter twin screw granulator: Screw element performance and in-line monitoring via image analysis. *International Journal of Pharmacy* **496**, 24–32.
- Shankali, U.P., Sen, M., Li, J., Litster, J.D. & Wassgren, C.R. 2017. Granule breakage in twin screw granulation: Effect of material properties and screw element geometry. *Powder Technology* **315**, 290–299.
- Sigalingging, R., Herák, D., Kabutey, A., Čestmír, M. & Divišová, M. 2014. Tangent curve function description of mechanical behaviour of bulk oilseeds: A review, *Scientia Agriculturae Bohemicae* **45**(4), 259–264.
- Sigalingging, R., Herák, D., Kabutey, A., Dajbych, O., Hrabě, P. & Mizera, C. 2015. Application of a tangent curve mathematical model for analysis of the mechanical behaviour of sunflower bulk seeds. *International Agrophysics* **29**(4), 517–524.
- Singh, J. & Bargale, P.C. 2000. Development of a small capacity double stage compression screw press for oil expression. *Journal of Food Engineering* **43**, 75–82.
- Statsoft, 2013. Inc, Tulsa, OK74104, USA.
- Uitterhaegen, E. & Evon, P. 2017. Twin-screw extrusion technology for vegetable oil extraction: A review. *Journal of Food Engineering* **212**, 190–200.

Benchmarking the GHG emissions intensities of crop and livestock–derived agricultural commodities produced in Latvia

A. Lenerts*, D. Popluga and K. Naglis-Liepa

Latvia University of Life Sciences and Technologies, Faculty of Economics and Social Development, Institute of Economics and Regional Development, Svetes street 18, LV-3001, Jelgava, Latvia

*Correspondence: arnis.lenerts@llu.lv

Abstract. With the production of grain and livestock–derived agricultural commodities increasing, the agricultural sector has become one of the main sources of greenhouse gas emissions (GHG) in Latvia. In 2016, the agricultural sector contributed to 23.6% of the total GHG emissions originated in Latvia (266.4 kt CO₂eq), and therefore the mitigation of the emissions is important. Considering the new indicative target, Latvia must reduce its GHG emissions in the non-ETS sectors by 2030 (Regulation 2018/842) so that the emissions do not exceed the 2005 level. The research aims to estimate the emissions intensities (EI) of grain and livestock-derived commodities produced in Latvia and benchmark the EI against those for other countries. The GHG EI were analysed per kilogram of product (kg CO₂eq kg⁻¹) and per hectare currently in use agricultural land (kg CO₂eq ha⁻¹). The main part of the GHG emissions of crop production originated from fertilizer application (direct N₂O emissions) and soil liming (direct CO₂ emissions). The main part of the GHG emissions of livestock–derived production originated from livestock enteric fermentation (direct CH₄ emissions) and from manure management systems (direct CH₄ and N₂O emissions). The EI per hectare of industrial crops and grain were 550.5 and 438.4 kg CO₂eq ha⁻¹, respectively. The yield and fertilizer application had a strong impact on the EI per kilogram of product. Pulses had a lower EI (0.003 kg CO₂eq kg⁻¹), while industrial crops (0.17 kg CO₂eq kg⁻¹) and grain (0.09 kg CO₂eq kg⁻¹) had the highest EI. A comparison of the GHG EI of crop and livestock–derived agricultural commodities per kilogram of product between Latvia and other EU Member States showed: Latvia had the lowest grain EI (0.09 kg CO₂eq kg⁻¹), but one of the highest cattle meat EI (25.18 kg CO₂eq kg⁻¹) and milk EI (0.64 kg CO₂eq kg⁻¹).

Key words: GHG, emissions intensity, commodities, benchmarking.

INTRODUCTION

In 2016, agricultural GHG emissions made up 23.6% of the total GHG emissions originated in Latvia (NIR, 2018), and the emissions are viewed as an important factor affecting the sustainability of agriculture (Lenerts et al., 2017). An increase in the emissions makes a negative impact on the value of natural capital. The accumulated information on agricultural GHG emissions is a basis for decision-making regarding how to mitigate the negative environmental impact. At the same time, agriculture has to meet the growing demand for food under available resource constraints (FAO, 2017). A priority for the nearest future for agriculture is to find a solution to how to produce more

food without decreasing the value of natural capital. One of the solutions is to estimate and account for the environmental impact of agricultural holdings (Lenerts et al., 2017). This implies establishing an economic system that considers a decrease in the value of natural capital to be external costs related to GHG emissions produced by economic activity. One of the indicators for estimating an impact at the micro-level is agricultural GHG emissions intensity (EI). In the EU, research on GHG EI focuses on both livestock production (Leip et al., 2010) and grain production (Carlson et al., 2017). Such a metric/indicator could contribute to adapting the management system to a low emission cycle, which could be an opportunity for economic growth as well as sustainability in the future. Based on this metric, it is possible to assess an economic process on agricultural holdings and identify whether the economic growth pattern of the agricultural holdings is extensive or intensive. The economic growth pattern makes a significant effect on the EI of agriculture (Bonesmo et al., 2013 and Bonesmo et al., 2012).

The research **aim** is to assess the emissions intensity of agriculture in Latvia and benchmark it against those in other EU Member States. To achieve the aim, the following specific **research tasks** were set: to examine a methodology for calculating and assessing agricultural GHG emissions intensity; to perform an assessment of the GHG emissions intensity of agriculture in Latvia; to benchmark the agricultural GHG emissions metrics among the EU Member States.

The research used the Central Statistical Bureau of Latvia (CSB), Eurostat and FAO databases. To process the data, the following economic **research methods** were employed: data grouping for statistical indicator calculation; time series, correlation and regression analysis.

MATERIALS AND METHODS

GHG emissions from agriculture are quantified by using the IPCC guidelines and methodology (IPCC 2018). The calculated indicators show the intensity of economic activity in a particular territory (country), yet they do not reveal emissions intensity for the production process as well as products produced. The characteristics and distribution of GHG emission sources and categories are presented in Table 1.

Table 1. Distribution of agricultural GHG emissions accounted for by group of sources and by category

Characteristics of groups of GHG emission sources	GHG emission category
Change in carbon (C) stocks (GHG emissions produced or C absorbed) in agricultural land for the entire utilised agricultural area	CO ₂
Natural soil emissions for the entire utilised agricultural area	N ₂ O
Emissions from soil liming for the entire utilised agricultural area	CO ₂
Emissions from fertiliser application for the entire utilised agricultural area	N ₂ O
Emissions from organics soils for the utilised agricultural area	N ₂ O
Emissions from livestock enteric fermentation	CH ₄
Emissions from manure management systems	CH ₄ ; N ₂ O

For the purpose of simple comparison and interpretation of data, emission inventory reports use a calculated CO₂ equivalent (eq) value, depending on the potential of anthropogenic greenhouse gases for making impacts on climate change (CH₄; N₂O and CO₂). Were used 25 CH₄ and 298 for N₂O global warming potential values to determine the effect of CH₄ and N₂O on climate change. Generalised emission factor values are used based on the IPCC Tier 1 methodology. The groups of emission sources determined in reality pertain to various technological processes and production systems, yet the mentioned methodology does not allow detailing the processes and systems and calculating an accurate emission factor for a particular country. The Tier 2 methodology employs emission factors for individual countries that have been proved by research investigations. Calculations are constrained by the extent of detail provided for technological processes and systems. The Tier 3 methodology allows for an individual approach to GHG emission calculations by each country. The current GHG emission inventory data are considerably constrained (MacLeod., 2018) because: agricultural GHG emissions are determined for individual processes instead of integrated ones; GHG emission calculations do not take into account the factors of technological processes and production systems (crop rotation, soil tillage etc.); the calculations determine total emissions instead of EI (per some unit of measure).

The data might be misleading, as changes in emissions could occur owing to changes in agricultural activity as a whole rather than changes in EI. That is why it is necessary to complement quantitative agricultural GHG emission indicators by EI metrics. The recommended EI metrics are summarised in Table 2.

Table 2. Agricultural GHG emission intensity indicators

Emissions intensity metric	Attributable to	Description
kg CO ₂ eq/country/territory	Country, territory	It is used in current national GHG emission inventories; does not show the amounts of GHG emissions produced by various industries and production efficiency
kg CO ₂ eq/kg product ⁻¹	Food produced	It allows analysing the emissions intensity of the same product produced in various territories and production systems. It is not possible to compare products of different energy values.
kg CO ₂ eq/kg CP kg DM ⁻¹	Value of crude protein (CP)	It allows comparing emissions intensity of products measured per unit of weight, nutritional value and energy value.
kg CO ₂ eq/MJ kg DM ⁻¹	Energy value produced (MJ)	
kg CO ₂ eq/EUR ⁻¹	Economic value of production	It allows assessing economic growth. It is difficult to interpret the role of the metric in practice. Changes in emissions intensity might be related to changes in: 1) production efficiency; 2) increase in value; 3) both.

Emissions intensity indicates the production efficiency of agricultural commodities, which depends on the accumulated disposable energy and nutrients of the commodities. Agricultural commodities that should be produced might be identified depending on needs and future market demand, thereby contributing to a low GHG-emissions-intensity production system (Audsley & Wilkinson, 2014). GHG emissions

from the production of key agricultural commodities and the accumulated disposable energy and nutrients are presented in Table 3.

Table 3. Yield, composition and GHG emissions of key crops

Production indicator	Average yield, t ha ⁻¹	Dry matter (DM) content g kg ⁻¹	Metabolisable energy (ME) MJ kg DM ⁻¹	Crude protein (CP) content g kg DM ⁻¹	GHG emissions, kg CO ₂ eq per unit of measure:		
					kg ⁻¹	GJ ME ⁻¹	kg CP ⁻¹
Winter wheat for food	7.7	860	13.6	130	0.51	0.044	4.56
Winter wheat for feed	8.1	860	13.6	116	0.46	0.039	4.61
Barley	5.7	860	13.2	116	0.38	0.033	3.81
Winter rapeseed	3.2	930	23.1	212	1.05	0.049	5.33
Sugar beet	63	220	13.2	68	0.04	0.015	2.87
Potato	48	200	13.3	93	0.1	0.038	5.38
Field beans	3.4	860	13.3	298	0.03	0.056	1.99
Maize (green forage)	11.2	280	11	101	0.3	0.027	2.97

The research results (Audsley & Wilkinson, 2014) revealed that the most emissions-intensive crops were potato – if measured per unit of accumulated crude protein content – and field beans – if measured per unit of accumulated energy. In the context of GHG emission change/reduction, a prudent and purposely-shaped cropping pattern and technologies and production systems used become increasingly important.

Crop and livestock production requires a certain amount of production resources. Upon starting agricultural business, an agricultural holding can decide what to produce and how to do it by employing all the disposable resources. The production process could be expressed as a function of the factors of production.

$$P=f(x_1, x_2, x_3, \dots, x_n) \tag{1}$$

where P – output; $x_1, x_2, x_3, \dots, x_n$ – GHG-intensive factors of production used.

The function shows how and how fast resources are turned into a final product and how many units of (for example) nitrogen (N) fertiliser or soil liming material have to be applied to acquire the crop yield planned. A linear increase in use of the factors of production logically increases the amount of GHG emissions and decreases the use efficiency of resources. Research studies have proved that GHG emission intensity decreases if production inputs are accurately accounted for and compared with output. An increase in the area sown with emission-intensive crops inevitably increases the total amount of emissions produced. According to the research studies examined, EI is lower if papilionaceous crops are included in crop rotation (Brock et al., 2012; Gan et al., 2014 and Alhajj Ali et al., 2015) and the crop rotation is observed (Kustermann et al., 2013). EI increases if growing monocrops (Barber et al., 2011; Roos et al., 2011; Ma et al., 2013; Wojcik-Gront & Bloch-Michalik, 2016). The research studies examined indicate the need to determine GHG emission factors tailored to the conditions in Latvia. It is recommended employing the Tier 2 methodology where appropriate and enhancing the Tier 3 methodology, as a dispersion analysis of emission factor values (552–8,360 kg CO₂eq ha⁻¹) allows concluding that the emission factors are significantly affected by the technologies and production systems used by each agricultural holding.

Fig. 1 shows GHG emissions intensity values (kg CO₂eq ha⁻¹) for various soil tillage technologies and different kinds of crop rotation.

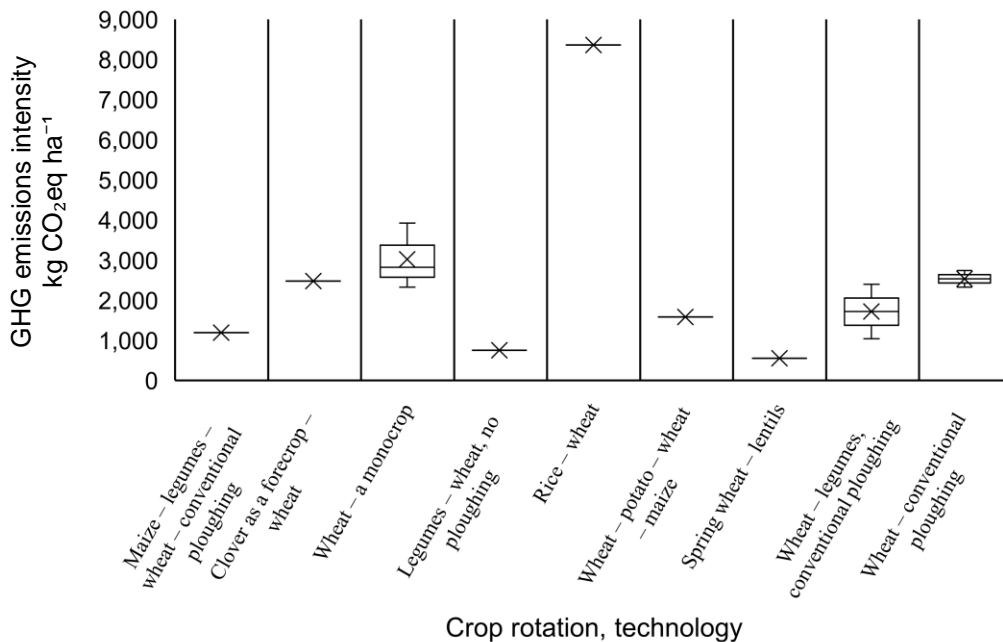


Figure 1. GHG emissions intensity values for wheat production (kg CO₂eq ha⁻¹) by kind of agricultural practice.

In Latvia, GHG emissions intensities can vary across regions and agricultural holdings. The production of one tonne of wheat results in GHG emissions of up to 500 kg CO₂eq. An increase in N fertiliser application efficiency and N₂O emissions is directly affected by the type of soil, meteorological conditions and soil quality characteristics. Depending on the type of soil, the performance of an amelioration system and soil temperature, for example, N₂O emissions from N fertilisers applied vary in the range from 0.84% for loamy soils to 4.67% for wet clay soils (Brentrup & Pallière, 2008).

Two approaches are employed to calculate GHG EI values (MacLeod et al., 2016). Depending on the purpose, emissions are categorised:

- direct GHG emissions from agricultural production;
- direct and indirect emissions from agricultural production (Life Cycle Analysis, LCA).

The research determines direct GHG emissions from agricultural production for the purpose of calculation of GHG EI.

RESULTS AND DISCUSSION

In 2016 in Latvia, the key sources of agricultural GHG emissions were as follows: nitrous oxide (N₂O) emissions from agricultural soils, accounting for most (59.5%) of

the total emissions, and methane (CH₄) emissions from livestock enteric fermentation, which was the second largest emission source, comprising 32.3% of the total. Methane CH₄ and nitrous oxide (N₂O) emissions from manure management comprised 7.1%, while CO₂ emissions from soil liming and urea application totally made up 1.1% of the total agricultural emissions in 2016 (NIR 2018).

In 2015, 1,884.8 thou. ha of land was utilised in Latvia. Of this area, 1,229.8 thou. ha was arable land. The key crops grown in arable land were as follows: grains 672,4 thou. ha; industrial crops 91 thou. ha; maize for silage and green forage 25,5 thou. ha; potato 24,8 thou. ha; legumes 31,6 thou. ha and open field vegetables 8,1 thou. ha. In 2015 compared with 2005, the utilised agricultural area rose by 8.7%. However, the arable land area increased by 12.6%.

An analysis of EI values measured per unit of agricultural area revealed that industrial crops had the highest EI value (550.4714 kg CO₂eq ha⁻¹). Grains demonstrated a 20% lower emissions intensity (438.43 kg CO₂eq ha⁻¹), whereas legumes had the lowest EI value (9.3 kg CO₂eq ha⁻¹).

GHG emissions intensity values measured per unit of output (kg CO₂eq product kg⁻¹) are presented in Fig. 2.

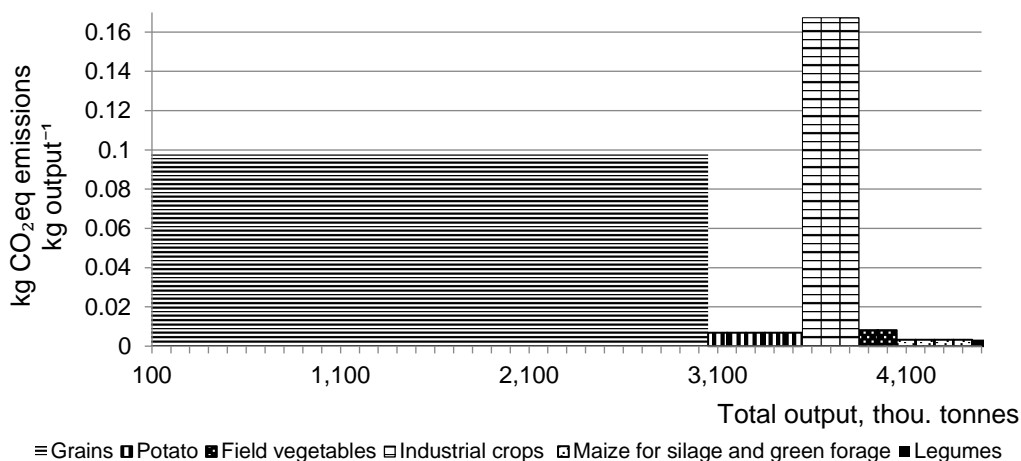


Figure 2. Total crop output (thou. t.) and the EI (kg CO₂eq product kg⁻¹) of N fertiliser applied to agricultural soils for selected crops in Latvia in 2015.

The calculations revealed that industrial crops had the highest per-unit emissions intensity (0.17 kg CO₂eq product kg⁻¹). In grain production, the GHG emission intensity was 58% lower, reaching 0.09 kg CO₂eq production kg⁻¹.

CSB and FAO data were employed to calculate changes in GHG EI in Latvia in the period 2005–2015. In the period of analysis, grain yields rose by 60%, while the GHG EI of grains rose by 12% (0.09 kg CO₂eq grain kg⁻¹). Milk yields per cow rose by 35%, whereas the GHG EI of milk production decreased by 25%. A negative trend was demonstrated by beef production, as the beef output decreased by 18%, while the GHG EI of beef production increased even by 35%. Latvia had the second highest proportion of agricultural GHG emissions in the total emissions among the non-ETS sectors across

EU Member States. In the period 2005–2015 in Latvia, agricultural output rose by 69%, and the GHG EI of it (kg CO₂eq UAA ha⁻¹) rose by 13%.

Changes in GHG EI values are summarised in Table 4.

Table 4. Output of grain, milk and beef and the GHG EI of grain, milk and beef production (kg CO₂eq product kg⁻¹) in Latvia in the period 2005–2015

Year	Grain		Milk		Beef	
	Yield, t. ha ⁻¹	EI, kg CO ₂ eq grain kg ⁻¹	Milk yield per cow, kg year ⁻¹	EI, kg CO ₂ eq milk kg ⁻¹	Beef per animal, kg year ⁻¹	EI, kg CO ₂ eq beef kg ⁻¹
2005	2.8	0.08	4,364	0.89	52.99	16.46
2006	2.26	0.09	4,492	0.88	54.91	17.6
2007	2.94	0.08	4,636	0.84	57.14	15.57
2008	3.1	0.08	4,822	0.83	56.32	18.53
2009	3.08	0.09	4,892	0.79	54.23	18.67
2010	2.65	0.09	4,998	0.77	48.54	21.03
2011	2.68	0.09	5,064	0.75	47.24	21.76
2012	3.7	0.08	5,250	0.72	44.02	22.76
2013	3.34	0.09	5,508	0.69	41.13	24.92
2014	3.4	0.08	5,812	0.65	41.94	24.89
2015	4.49	0.09	5,905	0.64	44.87	25.18
Change from 2005 base year, %	+60	+12	+35	-25	-18	+35

An increase in agricultural output considerably increases agricultural GHG emissions. The results for all the EU Member States are presented in Fig. 3.

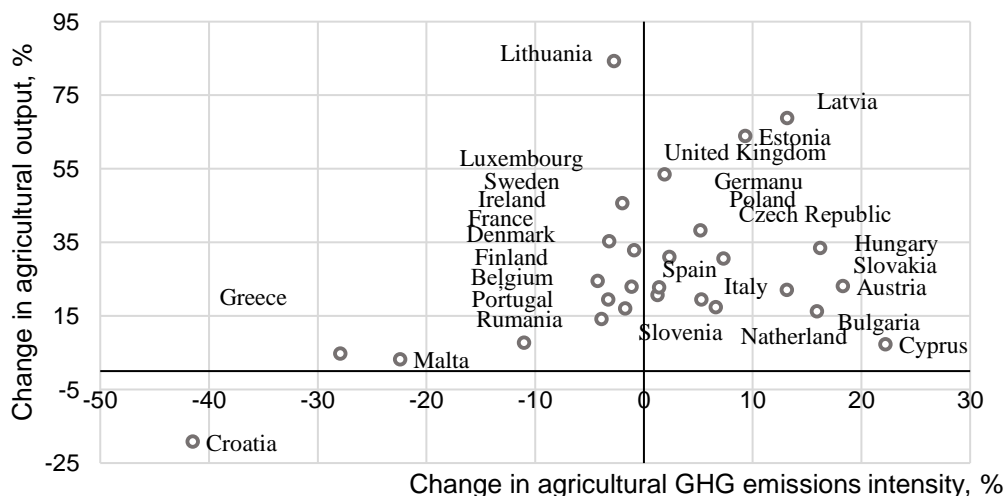


Figure 3. Changes in agricultural output and GHG emissions intensity (CO₂eq ha⁻¹), % in EU Member States in the period 2005–2015.

A positive correlation between GHG emissions and agricultural output for the period 2005–2015 was observed in the countries that increased their arable land areas and areas under grains. The amounts of N₂O emissions considerably increased in

Bulgaria, Latvia and Estonia. A group of the Member States, Lithuania in particular, have proved that they could considerably increase their agricultural output (+84%) while also lowering the GHG EI (-2% CO₂eq ha⁻¹). An increase in the output of grain in Latvia is likely to lead to a higher EI, thereby creating a serious challenge for farmers.

The benchmarking analysis of agricultural GHG EI for the EU Member States reveals the different levels of agricultural intensification. The overall GHG EI of beef production for the EU Member States are presented in Fig. 4.

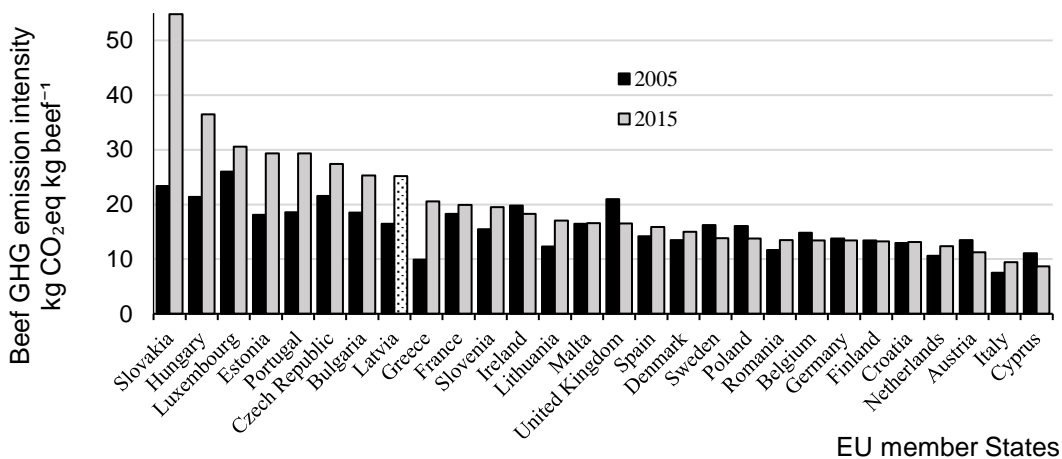


Figure 4. Beef GHG emission intensity (kg CO₂eq kg beef⁻¹) in the EU Member States in the period 2005–2015.

Among the typical agricultural commodities produced in Latvia, beef production had the highest GHG EI, exceeding the EU average by 27% (19.77 kg CO₂eq kg beef⁻¹).

The GHG emissions intensities of grain production for the period 2005 – 2015 are presented in Fig. 5.

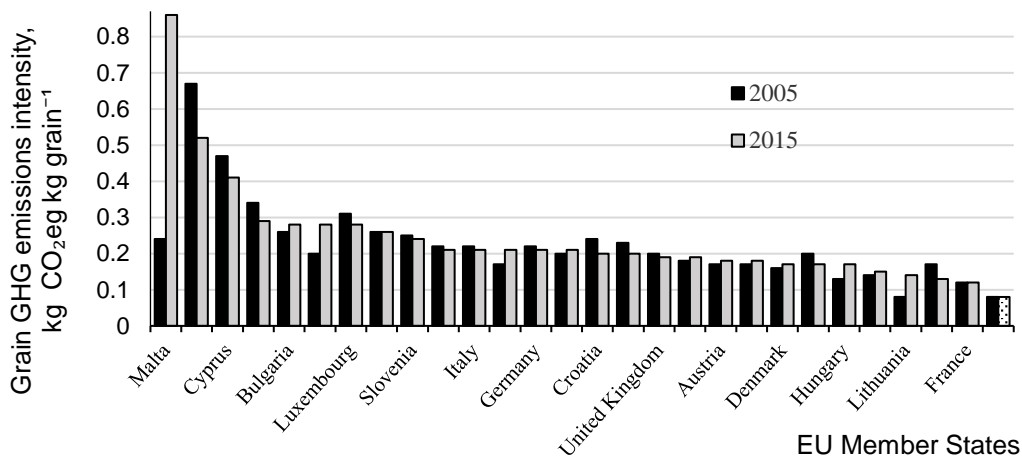


Figure 5. Grain GHG emissions intensity (kg CO₂eq kg grain⁻¹) in the EU Member States in the period 2005–2015.

The average GHG EI of grain production in the EU was 0.24 kg CO₂eq kg grain⁻¹, which was three-fold higher than in Latvia. This indicates that an increase in the output of grain was achieved by extensively increasing the area under grains and applying relatively low fertiliser rates. Using agricultural land with low quality characteristics for grain production, the GHG emissions intensity might increase in the future, as it requires applying higher fertiliser rates to increase crop yields. The differences in the GHG emissions intensity of grain production among the EU Member States affect differences in soil quality characteristics and climatic factors, which were not examined because of the limitations of the research.

The GHG emissions intensities of milk production are presented in Fig. 6.

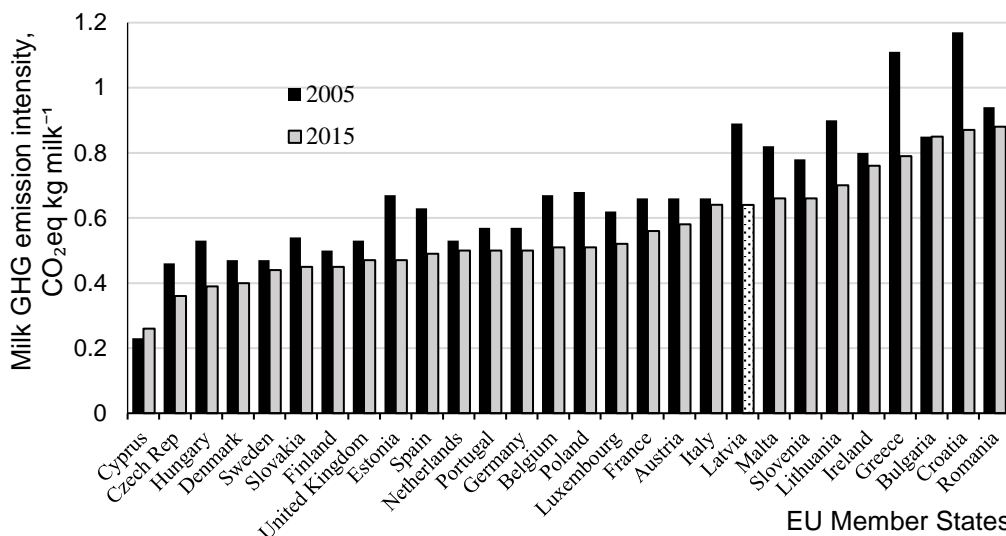


Figure 6. Milk GHG emission intensities (kg CO₂eq kg milk⁻¹) in the EU Member States in the period 2005–2015.

In the period of analysis, Latvia demonstrated the largest decrease in the GHG emission intensity of milk production at 28%, thereby approaching the EU average (0.54 kg CO₂eq kg milk⁻¹). The GHG emission intensity of milk production was strongly associated with dairy cow productivity. A strong positive correlation could be found between dairy cow productivity and GHG emission intensity among the EU Member States.

CONCLUSIONS

The quantitative (kg CO₂eq/kg product⁻¹) and value (kg CO₂eq/EUR⁻¹) metrics better explain production efficiency of agricultural commodities and more objectively indicate agricultural GHG EI.

A positive correlation between GHG EI (CO₂eq ha⁻¹), and agricultural output for the period 2005–2015 was observed in the countries that increased their arable land areas and areas under cereals. The amounts of N₂O emissions considerably increased in Bulgaria, Latvia and Estonia.

Study found Lithuania considerably increased its agricultural output (+84%) while also lowering the GHG EI (-2%) with changes in arable crops structure.

Calculated among the typical agricultural commodities produced in Latvia, beef production had the highest GHG EI, exceeding the EU average by 27% (19.77 kg CO₂eq kg beef⁻¹). Results show we need to improve production efficiency.

Growing cereals in Latvia may be more intense as the average GHG EI of grain production in the EU was 0.24 kg CO₂eq kg grain⁻¹, which was three-fold higher than in Latvia.

Improving production efficiency Latvia demonstrated the largest decrease in the GHG EI of milk production at 28%, thereby approaching the EU average (0.54 kg CO₂eq kg milk⁻¹).

REFERENCES

- Alhaji Ali, S., Tedone, L., Verdini, L. & De Mastro, G. 2017. Effect of different crop management systems on rainfed durum wheat greenhouse gas emissions and carbon footprint under Mediterranean conditions. *Journal of Cleaner Production* **140**, 608–621.
- Audsley, E. & Wilkinson, M. 2014. What is the potential for reducing national greenhouse gas emissions from crop and livestock production systems? *Journal of Cleaner production* **73**, 263–268.
- Barber, A., Pellow, G. & Barber, M. 2011. Carbon footprint of New Zealand arable production – wheat, maize silage, maize grain and ryegrass and forestry. *MAF technical paper* No: **97** AgriLINK New Zealand Ltd.
- Bonesmo, H., Beauchemin, K.A., Harstad, O.M. & Skjelvag, A.O. 2013. Greenhouse gas emission intensities of grass silage based dairy and beef production: A systems analysis of Norwegian farms. *Livestock science* **152**(Issues 2–3), 239–252. 37.
- Bonesmo, H., Skjelvag, A.O., Janzen, H., Klakegg, O. & Tveito, O.E. 2012. Greenhouse gas emission intensities and economic efficiency in crop production: a systems analysis of 95 farms. *Agricultural Systems* **110**, 142–151.
- Brentrup, F. & Pallière, C. 2008. GHG Emissions and Energy Efficiency in European Nitrogen Fertiliser Production and Use. *International Fertiliser Society: Proceedings 639*, York, UK.
- Brock, P., Madden, P., Schwenke, G. & Herridge, D. 2012. Greenhouse gas emissions profile for 1 tons of wheat produced in Central Zone (East) New South Wales: a life cycle assessment approach. *Crop Pasture Science* **63**(4), 319–329.
- Carlson, K.M., Gerber, J.S., Mueller, N.D., Herrero, M., MacDonald, G.K., Brauman, K.A., Havlik, P., O’Connell, C.S., Johnson, J.A., Saatchi, S. & West, P.C. 2017. Greenhouse gas emissions intensity of global croplands. *Nature Climate Change* **7**, 63–68.
- FAO 2017. The future of food and agriculture – Trends and challenges. Rome. Available: <http://www.fao.org/3/a-i6583e.pdf>. Accessed 1.12.2018.
- Gan, Y., Liang, C., Chai, Q., Lemke, R. L., Campbell, C. A. & Zenthner, R.P. 2014. Improving farming practices reduces the carbon footprint of spring wheat production. *Nature Communications*, Volume **5**.
- IPCC 2018. 2006 IPCC Guidelines for National Greenhouse Gas Inventories. *Prepared by the National Greenhouse Gas Inventories Programme*. Accessed 7.12.2018.
- Kustermann, B., Munch, J.C. & Hulsbergen, K.J. 2013. Effects of soil tillage and fertilization on resource efficiency and greenhouse gas emissions in a long-term field experiment in Southern Germany. *European Journal Agronomy* **49**, 61–73.

- Leip, A., Weiss, F., Wassenaar, T., Perez, I., Fellmann, T., Loudjani, P., Tubiello, F., Grandgirard, D., Monni, S. & Biala, K. 2010. Evaluation of the livestock sector's contribution to the EU greenhouse gas emissions (GGELS) – final report. *European Commission, JRC*.
- Lenerts, A., Popluga, D., Schulte, R.P.O. & Pilvere, I. 2017. Sustainability assessment of agricultural production: case study of Latvian crop sector. In: *Engineering for Rural Development: Proceedings of the 16th International Scientific Conference*. Jelgava: LLU, pp. 1312–1320. ISSN 1691-5976 33.
- Ma, Y.C., Kong, X.W., Yang, B., Zhang, X.L., Yan, X.Y., Yang, J.C. & Xiong, Z.Q. 2013. Net global warming potential and greenhouse gas intensity of annual rice – wheat rotations with integrated soil – crop system management. *Agronomy, Ecosystem and Environment* **164**, 209–219.
- MacLeod, M., Sykes, A., Leinonen, I., Eory, V., Creamer, E. & Govan, S. 2018. Developing a model to quantify the greenhouse gas emission intensity of Scottish agricultural commodities. *Summary Report*, ClimateXChange, Scotland.
- NIR 2018. Latvia's National Inventory report. Latvian Environment Geology and Meteorology Centre. Accessed 7.12.2018.
- Roos, E., Sundberg, C. & Hansson, P.A. 2011. Uncertainties in the carbon footprint of refined wheat products: a case study on Swedish pasta. *International Journal of Life Cycle Assessment* **16**, 338–350.
- Wojcik-Gront, E. & Bloch-Michalik, M. 2016. Assessment of greenhouse gas emission from life cycle of basic cereals production in Poland. *Zemdirbyste Agriculture* **103**(3), 259–266.

Farm health and safety adoption through engineering and behaviour change

J. McNamara^{1,2,*}, P. Griffin³, J. Phelan², W.E. Field⁴ and J. Kinsella²

¹Teagasc- Agriculture and Food Development Authority, E32YW08 Kildalton, Co. Kilkenny, Ireland

²School of Agriculture and Food Science, University College Dublin, D04 V1W8 Dublin 4, Ireland

³Health and Safety Authority, Metropolitan Building, D01 K0Y8 Dublin 1, Ireland

⁴Purdue University, Agricultural & Biological Engineering Department, IN 47907-2093 West Lafayette, Indiana, U.S.A.

*Correspondence: john.g.mcnamara@teagasc.ie

Abstract. The agriculture sector is one of the most hazardous occupations worldwide. The EU farming population is predominantly self-employed, who are largely outside the scope of EU occupational safety and health (OSH) legislation. Utilising effective communications approaches to transmit clear messages is a possible way of motivating farmer OSH adoption. The Public Health Model (PHM) of accident causation conceptualises an accident as occurring due to multiple interacting physical and human factors while the Social-Ecologic Framework enhances the PHM by defining various levels of the social environment which are influential on persons' OSH actions. A knowledge gap exists in how farmers conceptualise accident causation. The aim of this study is to report findings of a Score Card exercise conducted among Irish farmers ($n = 1,151$) to reveal knowledge on farmers' conceptualisation of accident causation where farmers ranked in order of importance up to five causes of farm accidents. First ranked items related to 'machinery/ vehicles', 'organisational' and 'livestock' as accident causation factors (92%). Overall rankings for up to five ranked causes identified six causes: 'machinery/ vehicles', 'organisational', 'livestock', 'slurry related', 'trips, falls, buildings-related' and 'electrical' (96.5%). The study data indicated that farmers' perceptions of accident causes were inaccurate when compared with objective fatal farm accident data. The study concluded that communicating accurate and contemporary OSH messages to farmers has potential to assist with farm accident prevention. Based on the multiple and interacting risk factors arising in agriculture it is suggested that more elaborate study of farm accident prevention is warranted.

Key words: agriculture, accident, osh, causation, communications, hazard.

INTRODUCTION

Agriculture is one of the most hazardous occupational sectors worldwide (ILO, 2011). Worldwide 170 thousand fatal accidents to agricultural workers occur annually while in the EU up to 170 thousand injury-causing accidents occur in the agricultural sector annually (Merisalu, 2018). The EU farming population is predominantly self-employed with 94% having family workers only and just 3% of farms having solely

non-family workers (Eurostat, 2014). Worldwide, individual farms are both dispersed in the countryside and operate in discrete units and use a wide range and variety of resources including: farm infrastructure and buildings, machinery and equipment; livestock; and products such as chemicals and pesticides, all of which present hazards (Field & Thoromolen, 2006).

As regulatory compliance is difficult to implement among a largely self-employed work sector such as agriculture (Gunningham, 2002), and in-any-event the EU Framework Directive for Occupational Safety and Health (OSH) (EC/89/391) does not cover self-employed workers, utilising effective communications approaches to transmit clear OSH messages is a possible way of motivating OSH improvements in the agriculture sector. Furthermore, the majority of farmers have been found to be positive to farm OSH as an issue (McNamara & Reidy, 1997; Knowles, 2002).

This paper, firstly, provides a brief review of contemporary accident causation theory and then provides the findings of a study of opinions of a large sample of Irish farmers on accident causation. The paper then considers the findings in relation to communication of accident causes to farmers.

Regarding Accident Causation Theory an accident is defined as an event which leads to bodily injury and the Public Health Model (PHM) of accident causation conceptualises an accident as occurring due to multiple interacting physical and human factors (Runyan, 2003). In this model a transfer of energy is the vector which causes injury and where a time dimension leads to all factors occurring in the same time and place (Fig. 1). Regarding accident prevention models, the conceptual work of Haddon (1980) indicates that accidents are prevented by applying multi-faceted approaches including both physical and organisational measures (Runyan, 2003). This author proposed that the social-ecologic framework as described by Bronfenbrenner (1979), enhances the PHM model of accident prevention as it defines various levels of the social environment in concentric nested roles of intrapersonal and interpersonal factors as well as institutional and cultural elements which are influential on persons related to accident prevention.

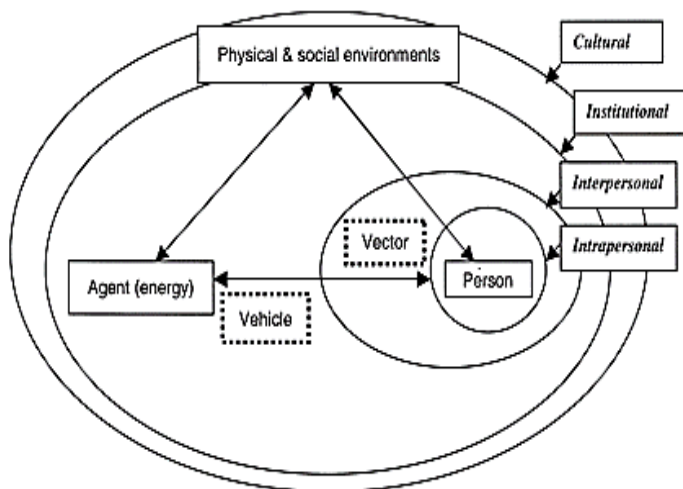


Figure 1. Integration of the Public Health Model and Social-ecologic Framework. Source: Runyan (2003).

A further injury prevention framework proposed by Gielen & Sleet (2003), suggests that a combination of behavioural, work environmental *and* policy approaches are required to gain injury prevention (Fig. 2).

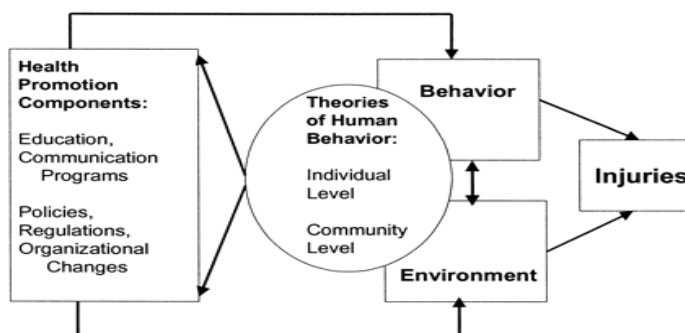


Figure 2. Framework for Promotion of Injury Prevention: Source: Gielen & Sleet, 2003.

Legal preventative approaches emphasise a hierarchical approach which gives preference to physical hazard elimination firstly and then organisational approaches such as work procedures, operator training and personal protective equipment (NIOSH, 2019). This approach is based on the premise that physical controls are collective and remove or reduce hazards while organisational approaches require individual human implementation and accordingly are less reliable and less effective.

The aim of this study is firstly to describe the findings of a Score Card exercise conducted among Irish farmers aimed at revealing knowledge on farmers’ conceptualisation of accident causation where farmers ranked in order of importance up to five causes of farm accidents. The findings of the study are then considered in relation to scientific literature on accident causation and prevention.

MATERIALS AND METHODS

In Ireland, the enactment of the Safety, Health and Welfare at Work Act 2005 provided a new approach to improving the safety, health and welfare record among farmers in Ireland. This legislation permits the vast majority of farms, where three or less persons are employed, to complete and implement a Risk Assessment Document (RAD) prepared under a statutory Code of Practice (COP) as an alternative to preparing a written Safety Statement (SS) required by previous 1989 legislation. Following the enactment of the 2005 Act, the Irish Health and Safety Authority (H.S.A.) and Teagasc, the Irish Agriculture and Food Development Authority, commenced a Prevention Initiative (PI) to develop the statutory COP and RAD. The PI also researched the utility of extension approaches on a pilot basis, including document circulation and provision of training and follow-up advice provision to assist farmers to comply with the statutory requirements. Research on implementation of the PI has been published (McNamara et al., 2017). To implement the PI a pilot RAD was produced which included an analysis of fatal farm accidents for the decade up to year 2005. Subsequently a statutory COP and RAD were published in 2006 and these were revised and updated in 2016 and are available on the H.S.A website (H.S.A., 2019).

As part of the Prevention Initiative (PI) half-day training (circa 3.5 hours) on RAD completion and implementation by farmers was provided at circa 40 courses. At the commencement of these training courses the participants were asked to individually rank their opinion of the causes of farm accidents on a Ranking Card (Fig. 3). The objective of the exercise was two-fold: firstly to provide a means to facilitate discussion among participants on farm accident causation early during the training and secondly to provide a possible source of data on farmers' perceptions of farm accident causation before the influence of RAD training occurred as this data had the potential to reveal information on farmers' understanding of farm accident causation. This paper reports on the findings of the second objective and data is provided in Table 1.

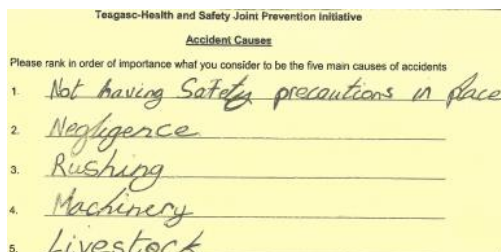


Figure 3. Sample of completed Ranking Card.

Table 1. Ranking of Causes of Farm Accidents in Order of Importance

Ranking Order	1 st		2 nd		3 rd		4 th		5 th		Total	
Accident Causes	Score	%	Score	Score	Score	Score	Score	Score	Score	Score	Score	%
Machinery/vehicles	3,165	55	1,091	485	262	80	5,083	31.6				
Organisational	1,554	27	819	582	337	138	3,430	21.3				
Livestock	576	10	1,364	679	262	80	2,964	18.4				
Slurry related	230	4	773	614	200	305	2,122	13.2				
Trips, Falls, Buildings related	115	2	227	420	281	124	1,167	7.2				
Electrical	58	1	136	194	262	116	766	4.8				
Children	12	1	23	97	56	15	203	1.3				
Chemicals	0	0	46	65	0	6	117	0.7				
Other	0	0	45	97	56	44	242	1.5				
Total	5,710	100	-	-	-	-	16,094	100				

In total, 1,151 completed Ranking Cards were returned by farmer participants in training. In total, 5,029 accident causes were identified on ranking cards, with 1,151, 1,137, 1,077, 937 and 727 causes listed from 1st to 5th ranking. As accidents may have multiple causes the term ‘cause’ is used subjectively in this paper reflecting farmers rankings. To analyse the data, 1st ranked accident causes were allocated a weighting of 5, and sequentially each rank was allocated a lower weighting with 5th ranked allocated a weighting of 1. Thus the Score for each ranking and the Total were calculated for each cause by multiplying the number of reported causes by the weighting. The percentage of the total score for 1st and Total causes was then calculated. Farmer responses to the ‘Score Card’ exercise limit the extent of data analysis in this study and only data that was unambiguous is presented.

RESULTS AND DISCUSSION

The results for the farm accident ranking exercise provided in Table 1 indicate that 92% of 1st Ranked scores related to ‘machinery/ vehicles’ (55%), ‘organisational’ (27%) and ‘livestock’ (10%). In contrast, among Total scores, six scores contributed to over ninety per cent (96.5%) of the total with ‘slurry related’, ‘trips, falls, buildings related’ and ‘electrical’ being the additional ‘causes’. First ranked scores are taken to indicate what is most prominent in farmers minds related to accident causation while the total score provides a more broadly-based ranking with more causes included. Notably, ‘children’ as associated with farm accident occurrence was lowly ranked at 1% of 1st ranked causes while the issue of ‘older’ farmers having a farm accident received no ranking whatsoever.

Within the ‘machinery/vehicles’ category, accidents associated with ‘Power Take Off (PTO) / power shafts’ accounted for 56% of first ranked and 46.9% of all ranked accident causes. Within the ‘organisational’ category, ‘carelessness/ rushing’ accounted for 84.1% of first ranked and 65.5% of all ranked causes. For livestock, ‘bull-related’ causes accounted for 41.6% of first ranked and 46% of all causes in this category.

The findings of this research indicate that participants attributed farm accidents to a number of physical causes and work organization issues. This attribution is in broad accord with general theory on accident causation which indicates that accidents have multiple causes (Haddon, 1980; Laflamme, 1990). However, the data presented in Table 1 indicates that participants’ perceptions of accident causation were not in line with the actual causes of fatal farm accidents as compiled for the pilot RAD. This is in accord with the findings of other studies on farm accident causes (Sandall & Reeve, 2000; Knowles, 2002; Murphy, 2003; Durey & Lower, 2004; Australian Safety and Compensation Council, 2006). For instance, data from the pilot RAD indicated that 32% of fatal farm accidents in the ‘vehicle and machinery category’ were entanglements in PTO/ power drives while Score Card entries attributed almost 47% of accidents to this cause. Furthermore, the pilot RAD indicated that 20% and 38% of accidents respectively were associated with children and older farmers (over 65 years old), while in the score card ranking exercise, children were stated as associated with accidents in 1% of 1st rankings of accident causes and older farmers were not ranked.

The data from this research supports the assertions in the literature (Sandman et al., 1987; Conroy, 1994; Wilde, 1994; Hodne et al., 1999) which suggest that accurate communication of objective accident risk to a target population is an imperative requirement to promote accident reduction.

Further, review of fatal farm accident trends in the RAD documents published in 2006 and 2016 indicates that farm accident causation may change over time. For instance, comparison of fatal accidents in the RAD documents in 2006 and 2016 in respect of machinery PTO entanglement as a percentage of all machinery, declined from 32% to 11%; while for livestock fatalities, cow attacks increased from 16% to 50% of the total related to these causes (H.S.A., 2006; H.S.A., 2016). Thus, on-going injury surveillance is warranted to inform communication strategies related to farm accidents.

As accident causation theory indicates that most accidents have multifactoral causes with both physical and organisational factors, more elaborate study of farm accident causation and prevention is warranted. Holden (2009), for instance, considered that changes in safety are likely to be achieved ‘through changes that address not only

people but also the many system components with which people interact'. Kim et al. (2018) further proposed that in designing programmes for farmers related to OSH prevention items should reflect use of a range of safety systems. Analytical approaches such as Fault Tree Analysis may be applied to farm accidents to gain both a broader and deeper understanding of farm accident causation (Kingman & Field, 2005). Further, Rogers (2003) noted that the discipline of Extension has the potential to make progress with a range of farm management issues, including OSH, over time using diffusion adoption approaches.

CONCLUSIONS

Overall this paper indicates that farmer perception of accident causation was broadly based. However, their perceptions of accident causation were inaccurate when compared with objective fatal farm accident data. Thus the study suggests that communicating accurate and contemporary OSH messages to farmers based on objective data is likely to be a crucial requirement to make progress with accident prevention in agriculture.

ACKNOWLEDGEMENTS. Farmer participation in this study is acknowledged. Ms Vivienne Burke and Ms Leanne Tobin are acknowledged for processing the study data.

REFERENCES

- Australian Safety and Compensation Council. 2006. The Cost of work-related injury and illness for Australian employers, workers and the community: 2005–06, ASCC, Canberra.
- Bronfenbrenner, U. 1979. *The ecology of human development: Experiments by nature and design*. Harvard University Press, Cambridge, MA, USA, 330 pp.
- Conroy, R.M. 1994. Culture, health beliefs and attitudes in a rural Irish community. *Anthropology Ireland* **4**(1), 22–32.
- Durey, A. & Lower, T. 2004. The culture of safety on Australian farms. *Rural Society* **14**(1), 57–69.
- Eurostat. 2014. Statistical books-agriculture, forestry and fishery. Farm Structure Survey data for 2010, 198 pp.
- Field, W.E. & Tormoehlen, R.L. 2006. Education and Training as Intervention Strategies. In: *Agricultural Medicine - A Practical Guide*, Ed. Lessenger J.E., Springer Publishing, pp. 42–52.
- Gielen, A. & Sleet, D. 2003. Application of behavior-change theories and methods to injury prevention. *Epidemiologic Reviews* **25**, 65–76.
- Gunningham, N. 2002. *Regulating Farm Safety: Towards an Optimal Policy Mix*. National Research Centre for OHS Regulation, Working Paper No.2, Australia, 15 pp.
- Haddon, W.Jr. 1980. The Basic Strategies for preventing damage from hazards of all kinds. *Hazard Prevention* **16**, 8–11.
- Health & Safety Authority (HSA). 2006. *Code of Practice/ Risk Assessment Document for Preventing Injury and Occupational Ill in Agriculture*. Health and Safety Authority publication, Dublin, Ireland, 124 pp.

- Health and Safety Authority (HSA) 2019. Code of Practice/ Risk Assessment Document for Preventing Injury and Occupational Ill in Agriculture. Health and Safety Authority publication, Dublin, Ireland, 106 pp. (Updated 2016 version). Available at: https://www.hsa.ie/eng/Your_Industry/Agriculture_Forestry/Overview/Agriculture_Code_of_Practice/
- Hodne, C.J., Thu, K., Donham, K.J., Watson, D. & Roy, N. 1999. Development of the Farm Safety and Health Beliefs Scale. *Journal of Agricultural Safety and Health* **8**(2), 225–239.
- Holden, R.J. 2009. People or systems? To blame is human. The fix is to engineer. *Professional Safety* **54**(12), 34–41.
- International Labour Organization (ILO). 2011. *Safety and health in agriculture: Code of Practice*. International Labour Office. Geneva, Switzerland, 380 pp.
- Kim, H., Räsänen, K., Chae, K. & Lee, K. 2018. Analysis of checklists for agricultural safety management. *Annals of agricultural and environmental medicine* **25**(3), 494–499.
- Kingman, D.M. & Field, W.E. 2005. Using Fault Tree Analysis to Identify Contributing Factors to Engulfment in Flowing Grain in On-Farm Grain Bins. *Journal of Agricultural Safety and Health* **11**(4), 395–405.
- Knowles, D. 2002. *Risk perception leading to risk taking behaviour amongst farmers in England and Wales*. Contract Research Report 404/2002 prepared by Dr David Knowles, ADAS Consulting Ltd for the Health and Safety Executive, United Kingdom. 158 pp.
- Laflamme, L. 1990. A Better Understanding of Occupational Accident Genesis to Improve Safety in the Work Place. *Journal of Occupational Accidents* **12**, 155–65.
- McNamara, J., Griffin, P., Kinsella, J. & Phelan, J. 2017. Health and Safety adoption resulting from use of a Risk Assessment Document on Irish Farms. *Journal of Agromedicine* **22**(4), 384–394.
- McNamara, J. & Reidy, K. 1997. *A Survey of Farm Safety and Health on Irish Farms*. Published by Teagasc and Health and Safety Authority, Dublin, Ireland, 61 pp. Available at: https://www.researchgate.net/profile/John_Mcnamara3/
- Merisalu, E. 2018. Strengths and weaknesses of existing EU data collection mechanisms for Farm In: *Proc. Joint NMAOHS & EU COST Action CA16123-Sacurima Conference, Hurdal, Norway, Date 11.09.2018*
- Murphy, D.J. 2003. *Safety and Health for Production Agriculture*. American Society of Agricultural Engineers. St Joseph, MI, USA, 253 pp.
- NIOSH-National Institute of Occupational Safety and Health (USA). 2019. Hierarchy of Controls. Available at: <https://www.cdc.gov/NIOSH/>
- Rogers, E.M. 2003. *Diffusion of Innovations (5th Edition)*. Free Press. New York, USA, 543 pp.
- Sandall, J. & Reeve, I. 2000. *New Ways of Promoting Farm Health and Safety: through analysing farmers' perception of risk*. Rural Industries Research & Development Corporation. 00/138 Canberra, Australia.
- Sandman, P.M., Sachsman, D.B., Greenberg, M.P., Gochfeld, M. & Dunwoody, S. 1987. *Environment Risk and the Press*. Transaction Books, New Jersey, U.S.A, 164 pp.
- Runyan, C.W. 2003. Back to the Future – Revisiting Haddon's Conceptualisation of Injury Epidemiology and Prevention. *Epidemiologic Review* **25**, 60–64.
- Wilde, G.J.S. 1994. *Target risk: dealing with the danger of death, disease and damage in everyday decisions*. Toronto: PDE Publications. Toronto, Canada, 204 pp. ISBN 0-9699124-0-4

Influence of the bentonite-containing acrylic humectant composite on the soil microflora

E. Mellelo, E.O. Samuilova, T.S. Denisov, D.M. Martynova and
R.O. Olekhnovich*

International Research Center BioEngineering, ITMO University, Kronverkskiy Prospekt, 49,
RU197101 St. Petersburg, Russia

*Correspondence: r.o.olekhnovich@mail.ru

Abstract. Acrylic derivative-based superabsorbents are widely used currently in agriculture as the soil conditioners, plant growth regulators, etc. Their usage has a positive effect on the growth and survival of the plants cultivated in the arid regions. However, the effects of hydrophilic acrylic polymers on the soil microbiocenosis still remain unknown. The influence of the moisture-absorbing acrylic acid-based hydrogels with different proportions of bentonite filler was studied on the soil microbiota. N,N-methylenbisacrylamide was used as a crosslinking agent. Acrylic hydrogels were synthesized by radical polymerization in an aqueous medium at a synthesis temperature of 45 °C during 4 hours. The application of hydrogel of the certain concentrations (1.0, 1.5, and 2.5% wt) into the soil did not cause significant changes in the total abundance of heterotrophic bacteria and the length of the fungal mycelium. The CO₂ emission rates did not change after and during the application of the hydrogel, which indicated the same level of carbon mineralization in the soil with presence of acrylic bentonite-containing hydrogels. The nitrogen fixation rate decreased on the first day after hydrogel application; after 14 days, it was close to the control values. We assume the activity of nitrogen-fixing bacteria has though turned to the normal level.

Key words: acrylic hydrogels, bentonite, soil microflora.

INTRODUCTION

Nowadays, crosslinked hydrophilic acrylic polymers called superabsorbents (SAPs) or hydrogels, which absorb well and retain large amounts of water, are widely used in various fields of agriculture (Magalhaes et al., 2012; Amira & Qados, 2015; Olekhnovich et al., 2015a; Olekhnovich et al., 2015b). Production of water-holding polymer composites for agriculture, ornamental and home gardening is one of the areas of their promising use (Uspenskaya, 1998; Ekebafe et al., 2011).

The use of moisture-absorbing agents based on acrylic derivatives is well-known to have a positive effect on the growth and survival of plants in the soils of arid regions (Hayat & Ali, 2004; Abd El-Rehim, 2006).

However, the effects of hydrophilic acrylic polymers on the soil microbiocenoses are still not entirely clear. For example, hydrogel based on polyacrylamide (PAA) stimulated the growth of *Pseudomonas* bacteria to a small extent (Gula & Huang, 1981;

Gula et al., 1994), which the authors attributed primarily to the additional intake of ammonium nitrogen on the medium during the hydrolysis of the amide groups of the polymer. Later, it has been found that soil microorganisms characterized by amidase activity can utilize PAA as the only source of nitrogen for them (Kay-Shoemake et al., 1998b). Some authors believe that this may be due to the fact that polyacrylamide gradually turns into long-chain polyacrylate, which later decomposes under the influence of physical and / or biological factors (Kay-Shoemake et al., 1998a, 1998b, 2000).

The direct effect of SAPs' content on the soil microflora, i.e. dependence of the number of heterotrophic bacteria on the amount of acrylamide-based hydrogel introduced into the soil, was also studied. Finally, the number of cultivated heterotrophic bacteria increased in the soils treated with PAA and sown with potatoes (1), which was not observed for treated soils with acrylic hydrogel, but sown with beans (2). In the first case, the soils were characterized by significantly higher concentrations of NO_3^- and NH_4^+ than the untreated soils, whereas in the soils that were sown with beans, such a difference was not observed. In addition, PAA-based hydrogel does not adversely affect the viability of soil bacteria in model experiments with pure cultures (Maksimova et al., 2010).

However, the data on the dynamics of heterotrophic bacteria abundance, the length of the mycelium, as well as carbon dioxide emissions from the soil, nitrogen fixation and denitrification, are very scarce. That is why our study targets on the extremely important issue of the effect of acrylic hydrogels on the soil microbial communities.

MATERIALS AND METHODS

Soil sampling and soil parameters. The sampling was carried out in the Chekhovskii District of the Moscow Oblast (Russia), 500 meters from the Simferopol Highway, in the field. The soil was acidic sod-podzolic, medium-grained. Samples were taken from a square plot of 1 ha on a grid with a side of 50 meters from a depth of 5–15 cm in the form of a monolithic cube of 3,000 cm³ volume. The soil samples were mixed together to obtain a combined sample of a total weight of 21 kg, the sub-samples from this one were then used for the study. Samples of the soil were not subjected to additional processing.

Hydrogel synthesis. The hydrogels (HG) based on sodium acrylate and moisture-absorbing bentonite-containing composites based on HG (the mass fraction of bentonite was 0.5% wt and 1.0% wt) have been tested. HG was synthesized by radical polymerization in an aqueous medium at a synthesis temperature of 45 °C for 4 hours. N,N-methylenebisacrylamide was used as a crosslinking agent. Ammonium persulfate-tetraethylethylenediamine was used as the initiating system.

Experimental scheme. The experiment was carried out in the 2-L glass vials, each contained 1 kg of soil. The vials were exposed in the laboratory for 14 days at natural air humidity (80%), illumination cycle of 12/12 L/D, and air temperature range of 25–27 °C. Moisture-absorbing materials were introduced into the soil with thorough mixing. Then the soil was moistened up to 60% of the field capacity.

Assessing bacteria abundance and mycelium length. The aqueous soil suspension in the ratio of 1:9 (10 g of soil per 90 g of water) was treated in an ultrasonic bath for 3 min. After this pre-treatment, the soil suspension was transferred to a 100 mL measuring cylinder for 2 min. The 2 mL of suspension from the middle part (at 50-mL mark) were

diluted by 18 mL of water. From this mixture, 0.01 mL of the secondary suspension was applied to a glass slide by micropipette. The sampled was evenly distributed on an area of $\varnothing 4 \text{ cm}^2$ and air-dried in a drying chamber at a temperature of $27 \text{ }^\circ\text{C}$ for 5 hours. Then the slide was heated lightly on the flame of a gas burner. The slide was then dyed with acridine orange (bacteria, 4 min) or calcofluor-white, CFW (fungal mycelium, 15 min). Direct microscopy of soil suspension under a fluorescent microscope Axioscop 2 plus (Zeiss, Germany), oil immersion objectives of $40\times$ and $100\times$ magnification, have been performed to count the total bacteria abundance and the mycelium length in the samples according to standard methods (Rodríguez-Urra et al., 2009; Sandle, 2016). In total, 30 slides were prepared with a total number of fields of view equal to 300 in order to fit the significance level of 0.05 and a relative error of 10%.

The number of bacteria per 1 gram of cells was calculated by the formula:

$$M = \frac{4 \cdot K \cdot N}{p} \cdot 10^{10} \quad (1)$$

where K is the average number of cells in the field of view, N is the dilution rate, p is the area of the field of view.

Measuring of nitrogen fixation and denitrification rates. A 5-g sample of soil was cleaned to remove all the foreign inclusions and placed in a 15-mL vials each. The 6 mL of an aqueous solution of glucose (2.5 mg of glucose per 1 g of soil) and potassium nitrate (0.3 mg of potassium nitrate per 1 g of soil) have been added in each vial. The vials were closed with a rubber stopper and washed with argon for 30 s. Then, 1.5 mL of acetylene was injected in each vial. The vials were shaken for 60 s and incubated upside down for 24 hours at $28 \text{ }^\circ\text{C}$. After incubation, 1 mL of the gas mixture was taken with a syringe from each vial. The nitrogen fixation and denitrification rates were determined on a gas chromatograph with a flame ionization detector ‘Kristall-2000’ (Russia).

Measuring of carbon dioxide emission. The 5 g of the root-free soil were sifted through a 1-mm sieve and placed in a 15-mL vials each. The standard aqueous solution of glucose (2% from the mass of absolutely dry soil) was added, the soil was then moistened with sterile water to a moisture content of 80% of the full water capacity. The soil was then stirred until homogeneous. The vials were closed with a cotton stopper and incubated for 24 hours at $28 \text{ }^\circ\text{C}$. Then the vials were re-closed with a rubber stopper, 0.5 mL of acetylene was injected into the vials. After 1-hour incubation, 1 mL of the gas mixture was taken with a syringe from each vial.

The chamber static method was used to determine the rate of CO_2 emissions. An insulator (height 20 cm, diameter 15 cm) was cut into the soil to a depth of 10 cm. A gas sample was taken from the top of the insulator with a syringe immediately after installation, at 10 and 20 minutes of exposure. Samples were transferred to pre-vacuumed 15-mL vials. The emission of carbon dioxide was determined on a chromatograph ‘Khromatograf 3700/4’ (Russia) equipped with a thermal conductivity detector. The obtained concentrations of carbon dioxide in the samples are used to determine the rate of carbon dioxide emission:

$$F = D' \frac{(C_{10} - C_0)}{1 - e^{-\frac{-D'\tau}{H}}} \quad (2)$$

where $D' = -H \cdot \ln \ln \left(\frac{(C_{10} - C_0)}{(C_{20} - C_{10})} \right)$, τ is 10-min period, C_0 , C_{10} , C_{20} are the carbon dioxide concentration at the beginning of experiment, in 10 and 20 minutes after, respectively, H is the height of the isolation layer above the soil surface.

Statistics. In all the experiments and measurements, the number of replications varied from 3 to 30 in regard to the method applied. One-way ANOVA has been used in order to test the effect of HG introduction to the bacteria abundance, mycelium length, carbon dioxide emission, and nitrogen fixation and denitrification rates. The level of significance was set as $p < 0.05$.

RESULTS AND DISCUSSION

Visually, the soil enriched with the polymer moisture sorbent (pure hydrogel and hydrogel + bentonite with a concentration of 0.5% wt and 1.0% wt) became well-structured and had a clearly pronounced grain structure (grains of 3–5-mm diameter), which can be considered as close to the agronomically valuable granular structure. The soil enriched with pure bentonite of the same concentrations without a hydrogel and the control soil (no additives) did not have such a clearly defined structure (Fig. 1).

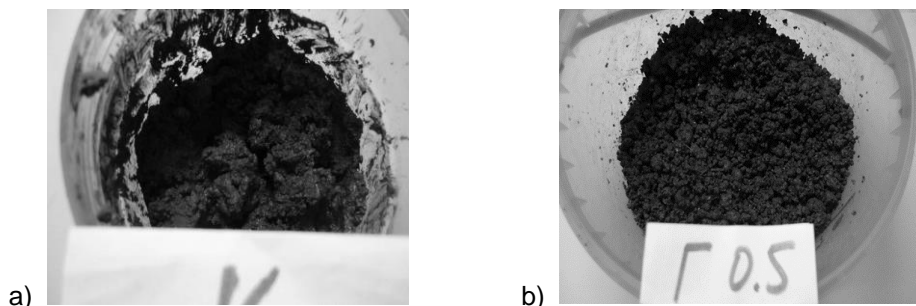


Figure 1. Appearance of the moistened soil: a – control sample; b – hydrogel-applied soil (0.5% wt).

The total bacteria abundance in the studied treatments ranged from 7.05 to 10.52 billion cells per 1 g of soil, which corresponded to the values usually recorded in the cultivated soils of the forest zone (Mamai et al., 2013). The bacteria abundance during the first day was higher in the control and in the treatments containing bentonite with a mass fraction of the filler of 0.5% wt and 1.0% wt (Fig. 2).

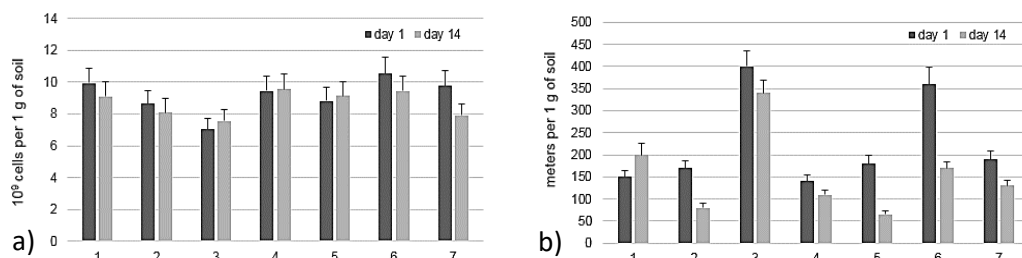


Figure 2. Total bacteria abundance (a) and the total length of mycelium (b) in the soil, $M \pm m$, 24 hours and 14 days after the experiment has been started: 1 – control; 2 – hydrogel 0.5% wt; 3 – hydrogel 1.0% wt; 4 – hydrogel + bentonite 0.5% wt; 5 – hydrogel + bentonite 1.0% wt; 6 – bentonite 0.5% wt; 7 – bentonite 1.0% wt.

During the first day, the bacteria abundance compared to control sample has reduced by 30% and less in the soil enriched with HG (1.0% wt) without bentonite. Opposite to our data, an increase in bacteria numbers has been observed earlier in the soils conditioned with superabsorbent polymers (Achtenhagen & Kreuzig, 2011). However, it was later reported that the efficiency of applying the lower rate of hydrogels is better for soil conditioning without adverse effects on plant growth and the beneficial microorganisms of the soil (El-Saied et al., 2016). In addition, a significant increase in the amount of soil bacteria at 1.8 g dm⁻³ superabsorbent dose and no significant influence on actinomycetes and fungi (irrespective of the dose used) has been found (Mikiciuk et al., 2015). Hence, we argue that the effect of SAPs can be adverse and depends, probably, on the certain concentration of agents.

The bacterial cells in the treatments with hydrogel (treatment no. 3, Fig. 2, a) and a hydrogel + bentonite (no. 5, Fig. 2, a) were both single (green glow) and formed the free cell clusters (yellow glow) and the cell clusters in the hydrogel ‘capsules’ (yellow-green dots in red encirclement) (Fig. 3, a), none of the listed was found in the control (Fig. 3, b).

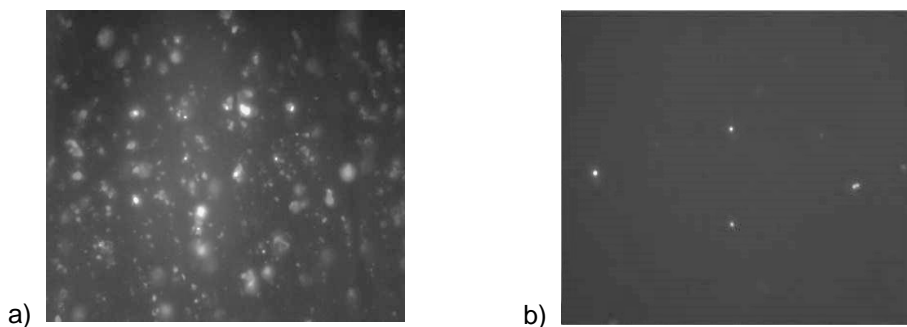


Figure 3. Bacteria in the soil samples after 24 hours the experiment has been started: a – soil with a hydrogel 1.0% wt applied; b – control sample (soil without modifiers). Individual cells give a green glow; clumps of cells, yellow glow; clusters of cells covered with a layer of hydrogel, red glow; 1,000×magnification.

The length of the mycelium varied from 65 to 400 m per 1 g of soil, which corresponds to the values commonly observed in the cultivated soils of the forest zone (Mamai et al., 2013). The application of a hydrogel of various concentrations (treatments nos. 2, 3), as well as a hydrogel + bentonite (no. 5), and pure bentonite of various concentrations (nos. 6, 7) led to an increase in the mycelium length compared to the control in 1.5–2.5 times even within the first 24 hours after the application of soil modifiers (Fig. 2, b).

However, on the 14th day of the experiment, the opposite pattern has been observed (Fig. 2b). Particularly, the application of pure bentonite (treatments nos. 6, 7) and bentonite-containing mixtures (nos. 4, 5) into the soil reduced the length of the mycelium by 1.5–2.0 times in the end of the experiment. In the soil where a pure hydrogel 1% wt has been applied, the length of the mycelium increased by 1.5 times compared with the control. This indicates that the mixtures used did not affect negatively the development of the filamentous fungi in the soil.

Thus, the application of HG, as well as a mixture of HG + bentonite, did not cause a significant reduction in the bacteria abundance both on the first day and after the two weeks of exposition, although a slight decrease in their numbers was recorded in the treatment with 1% wt HG.

The parameters of carbon and nitrogen transformation have been measured on the same dates of the experiment in order to obtain more information about the activity of the soil microflora in the treatments (Fig. 4).

The CO₂ emission rates ('soil respiration') varied from 57 (control) to 96 μg CO₂ g⁻¹ day⁻¹ (Fig. 4, a), which corresponds to the values usually recorded in the soils of the forest zone (Mamai et al., 2013). At the same time, the application of HG and a mixture of HG + bentonite (treatments nos. 2–5) increased the CO₂ emission rates by 1.5–2.0 times. The application of pure bentonite of various concentrations into the soil had practically no effect on the carbon dioxide emission rate (Fig. 4, a).

In the two weeks after the experiment has started, carbon dioxide emission rate ranged from 26 μg CO₂ g⁻¹ day⁻¹ (bentonite 0.5% wt) to 41 μg CO₂ g⁻¹ day⁻¹ (HG + bentonite 1% wt), which corresponded to the range usually recorded in the soils of the forest zone (Mamai et al., 2013). After the two weeks, the application of both HG and bentonite did not have a significant effect on the intensity of CO₂ emission, except for the treatment no. 5 (HG + bentonite 1% wt), where the carbon dioxide emission rate was an average by 10–30% higher comparing with the control and other treatments (Fig. 4, a).

Recently, a positive effect of hydrogels on the nitrate fixation by microflora has been reported (El Saied et al., 2016). Particularly, application of the hydrogels positively affects bio-chemical properties of the soil, including slightly decreasing soil pH, increasing cation exchange capacity of the soil indicating improvement in activating chemical reactions in the soil, increasing organic matter, organic carbon, and total nitrogen percent in the soil. A narrower C/N ratio of treated soils is linked to the increase in organic nitrogen surpassed that in organic carbon (El Saied et al., 2016). Authors

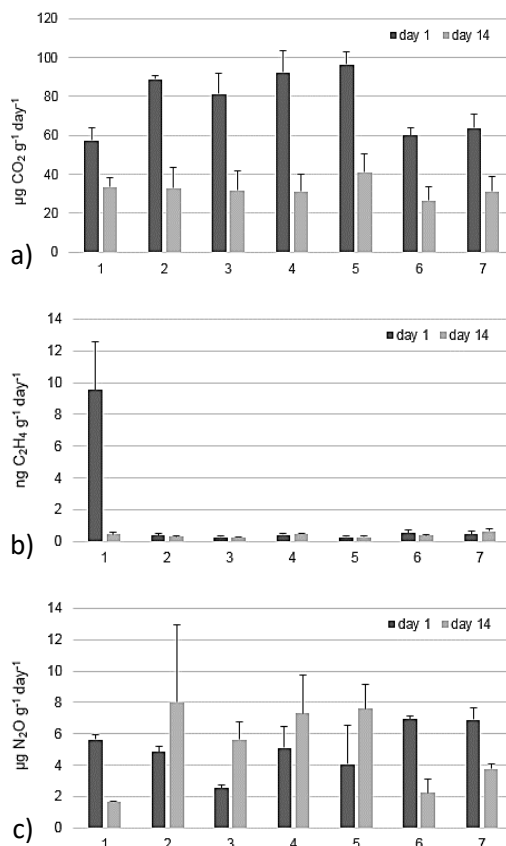


Figure 4. Rates of CO₂ emission (a), nitrogen fixation (b), and denitrification (c) in the soil with composite applied, $M \pm m$, 24 hours and 14 days after the experiment has been started: 1 – control; 2 – hydrogel 0.5% wt; 3 – hydrogel 1.0% wt; 4 – hydrogel + bentonite 0.5% wt; 5 – hydrogel + bentonite 1.0% wt; 6 – bentonite 0.5% wt; 7 – bentonite 1.0% wt.

conclude on the mineralization of nitrogen compounds and hence the possibility to save and provide available forms of N to growing plants, increasing available N, P and K in treated soil, and improving biological activity of the soil expressed as total count of bacteria and counts of *Azotobacter* sp., phosphate dissolving bacteria, fungi and actinomycetes in the soil as well as the activity of both dehydrogenase and phosphatase.

In our study, absolute nitrogen fixation rate was highest in the control sample ($9.56 \text{ ng C}_2\text{H}_4 \text{ g}^{-1} \text{ day}^{-1}$), it decreased significantly in all the other treatments; in addition, the decrease was highest in the samples where HG was applied in 1% wt concentration (Fig. 4, b: treatments nos. 3 and 5). This may indicate the oppressed state of bacteria in these treatments, since the process of nitrogen fixation in soils is carried out only by bacteria (Mamai et al., 2013). This result can also be considered as a negative consequence of both HG and bentonite application within the studied period of 14 days. However, this fact requires additional verification and the final conclusion can be made only after the measuring of the nitrogen fixation rates for a longer period.

After two weeks of the experiment, the absolute nitrogen-fixing activity was highest in the three treatments, somehow distinct by the fertilizer parameters: pure bentonite (treatment no. 7), HG + bentonite 0.5% wt (no. 4), and control (Fig. 4b). In the treatments HG and HG + bentonite, the activity of nitrogen fixation was significantly reduced, and this decrease was highest in the treatments HG + bentonite 1 wt% (nos. 3 and 5). However, the decrease was not as significant as on the first day of the experiment, which indicates minimizing of the negative effect of HG on bacteria after two weeks of the experiment.

The denitrification activity in the studied samples varied from 2.52 to $6.93 \mu\text{g N}_2\text{O g}^{-1} \text{ day}^{-1}$, it was lower in the treatment, where the HG concentration was 1% wt (Fig. 4, c). The application of bentonite slightly increased the denitrification activity compared to the control. The decrease of the denitrification activity in the HG-containing treatments should be considered as a positive effect, since an increase in denitrification activity indicates the removal of nitrogen from the soil (Ishii et al., 2011).

After two weeks of the experiment, the denitrification activity varied from $1.67 \mu\text{g N}_2\text{O g}^{-1} \text{ day}^{-1}$ (control) to $8.03 \mu\text{g N}_2\text{O g}^{-1} \text{ day}^{-1}$ (HG 0.5% wt). Although no specific analyses were performed to determine the abundance of particular groups of microorganisms (i.e. nitrate-assimilating and nitrogen-fixing bacteria), an increase in denitrification activity when introducing HG and a mixture of HG + bentonite indicates the development of nitrate-assimilating bacteria and fungi in the soil, which have amidase activity, i.e. capable of cleaving the amide group from the PAA polymer chain and transforming it into N_2O (Kay-Shoemaker et al., 1998b). The application of bentonite somewhat reduced the denitrification activity.

Hence, on the 14th day of the experiment, no significant decrease in CO_2 emissions has been observed in the HG-treatments, the activity of nitrogen fixation has increased in the HG-treatments and was close to that in the control, and denitrification activity in HG and HG + bentonite treatments has increased (Fig. 4). We argue this can indicate the development of bacteria and fungi characterized by amidase activity, however, a targeted research is necessary to prove or decline this.

CONCLUSIONS

The application of hydrogel into the soil at the tested concentrations did not cause significant changes in the total abundance of native bacteria and the length of the mycelium. The CO₂ emission rates did not change significantly, which indicates the absence of any hydrogel effect on the processes of carbon transformation in the soil. The denitrification rate has increased by 14 days after the hydrogel application, this can be considered as a certain negative impact on the processes of nitrogen transformation in the soil (removal of nitrogen from the soil). The activity of nitrogen fixation during the application of hydrogel decreased on the first day after application, but by 14th day, it has restored to the 'normal' values (close to the control); this evidences on the restoration of the activity of nitrogen-fixing bacteria and thus the normal functioning of the soil microbial complex.

REFERENCES

- Abd El-Rehim, H.A. 2006. Characterization and possible agricultural application of polyacrylamide/sodium alginate crosslinked hydrogels prepared by ionizing radiation. *Appl. Polymer Sci.* **10**(1), 3572–3580.
- Amira, M.S. & Qados, A. 2015. Effects of Super Absorbent Polymer and *Azotobacter vinelandii* on Growth and Survival of *Ficus benjamina* L. Seedlings under Drought Stress Conditions. *International Research Journal of Agricultural Science and Soil Science* **5**(2), 45–57.
- Achtenhagen, J. & Kreuzig, R. 2011. Laboratory tests on the impact of superabsorbent polymers on transformation and sorption of xenobiotics in soil taking 14C-imazalil as an example. *Science of the Total Environment* **409**(24), 5454–5458.
- Ekebafé, L.O., Ogbeifun, D.E. & Okieimen, F.E. 2011. Polymer Applications in Agriculture. *Biokemistri* **23**, 81–89.
- El-Saied, H., El-Hady, O.A., Basta, A.H., El-Dewiny, C.Y. & Abo-Sedera, S.A. 2016. Biochemical properties of sandy calcareous soil treated with rice straw-based hydrogels. *Journal of the Saudi Society of Agricultural Sciences* **15**(2), 188–194.
- Gruła, M. & Huang, M. 1981. Interactions of polyacrilamides with certain soil pseudomonas. *Dev. Ind. Microbiol.* **22**, 451–457.
- Gruła, M., Huang, M. & Sewell, G. 1994. Interaction of certain polyacrilamides with soil bacteria. *Soil Sci.* **158**(4), 291–300.
- Hayat, R. & Ali, S. 2004. Water absorption by synthetic polymer (Aquasorb) and its effect on soil properties and tomato yield. *Int. J. Agri. Biol.* **6**(6), 998–1002.
- Ishii, S., Ikeda, S., Minamisawa, K. & Senoo, K. 2011. Nitrogen Cycling in Rice Paddy Environments: Past Achievements and Future Challenges. *Microbes and environments* **26**, 282–292.
- Kay-Shoemake, J.L., Watwood, M.E., Lentz, R.D. & Sojka, R.E. 1998a. Polyacrylamide as an organic nitrogen source for soil microorganisms with potential effects on inorganic soil nitrogen in agricultural soil. *Soil Biol. Biochem.* **30**(8/9), 1045–1052.
- Kay-Shoemake, J.L., Watwood, M.E., Sojka, R.E. & Lentz, R.D. 1998b. Polyacrylamide as a substrate for microbial amidase in culture and soil. *Soil Biol. Biochem.* **30**(13), 1647–1654.
- Kay-Shoemake, J.L., Watwood, M.E., Sojka, R.E. & Lentz, R.D. 2000. Soil amidase activity in polyacrilamide-treated soils and potential activity toward common amide-containing pesticides. *Biol. Fertil. Soils* **31**, 183–186.
- Magalhaes, A.S.G., Almeida, M.P.A.N., Bezerra, M.N., Ricardo, N.M.P.S. & Feitosa, J.P.A. 2012. Application of FTIR in the determination of acrylate content in poly(sodium acrylate-co-acrylamide) superabsorbent hydrogels. *Co Quimica Nova* **35**(7), 1464–1467.

- Maksimova, Yu.G., Maksimov, A.Yu., Demakov, V.A. & Budnikov, V.I. 2010. Effect of polyacrylamide hydrogels on soil microflora. *Vestnik Permskogo Universiteta. Ser. Biologija* **1**(1), 45–49 (in Russian).
- Mamai, A.V., Stepanov, A.L. & Fedorets, N.G. 2013. Microbial transformation of nitrogen compounds in the soils of middle taiga. *Moscow Univ. Soil Sci. Bull.* **68**(4), 174–179.
- Mikiciuk, G., Mikiciuk, M. & Hawrot-Paw, M. 2015. Influence of superabsorbent polymers on the chemical composition of strawberry (*Fragaria* × *ananassa* Duch.) and biological activity in the soil. *Folia Hort.* **27**(1), 63–69.
- Olekhovich, R.O., Volkova, K.V., Uspenskii, A.A., Slobodov, A.A. & Uspenskaya, M.V. 2015a. Synthesis of poly(Acrylic acid)-co-acrylamide/bentonite polymer nanocomposite as an absorbent for removal of heavy metal ions from water. *International Multidisciplinary Scientific GeoConference Surveying Geology and Mining Ecology Management, SGEM* **2**(5), 477–484.
- Olekhovich, R.O., Glazacheva, E.N., Uspenskii, A.B., Slobodov, A.A., Uspenskaia, M.V. 2015b. Investigation of hydrogel on the base the phosphorus-containing acrylic copolymer for use in agriculture. *International Multidisciplinary Scientific GeoConference Surveying Geology and Mining Ecology Management, SGEM*, **2**(3), 207–214.
- Rodríguez-Urra, A.B., Jimenez, C., Dueñas, M. & Ugalde, U. 2009. Bicarbonate gradients modulate growth and colony morphology in *Aspergillus nidulans*. *FEMS Microbiology Letters* **300**, 216–221. doi:10.1111/j.1574-6968.2009.01780.x
- Sandle, T. 2016. Microbiology laboratory techniques. *Pharmaceutical Microbiology*, Woodhead Publishing, 63–80.
- Uspenskaya, M.V. 1998. Swelling of hydrogels formed by copolymers of acrylic and 3-chloro-1,3-butadiene-2-phosphinic acids. *Russian Journal of Applied Chemistry* **71**(3), 521–523 (in Russian).

Variation in Eurostat and national statistics of accidents in agriculture

E. Merisalu^{1,*}, J. Leppälä², M. Jakob³ and R.H. Rautiainen^{2,4}

¹Estonian University of Life Sciences, Fr.R. Kreutzwaldi 56/1, EE51006 Tartu, Estonia

²Natural Resources Institute Finland (Luke), Latokartanonkaari 9, FI-00790 Helsinki

³Leibniz Institute for Agricultural Engineering and Bioeconomy, Max-Eyth-Allee 100, DE14469 Potsdam, Germany

⁴University of Nebraska Medical Center, Omaha, Nebraska, US68198-4388, USA

*Correspondence: eda.merisalu@emu.ee

Abstract. Agriculture is known as a hazardous industry worldwide, although there are great challenges in enumerating the size of the workforce and numbers of accidents at work. The aim of the study was to characterize variation in agricultural accident statistics in European countries and opportunities to improve collection and reporting of accident data in agriculture on the national and European levels. This study explored the incidence of fatal (FA) and non-fatal work accidents (NFA) in agriculture (excluding forestry and fishing) in selected European countries, using Eurostat and national sources in 2013. Eurostat reported highest NFA rates (per 100,000 workers) in Finland (5331) and lowest in Greece (5). The highest FA rate was reported in Malta (51), while zero fatalities were reported in Estonia, Greece, Luxembourg, Slovenia, Sweden and Iceland. Eurostat and national statistics differed in many cases. Some variations were observed in European and national statistics. Germany reported 89 fatalities (rate 2.3/100,000) in Eurostat and 160 (rate 16.3/100,000) in national sources. Poland, with a similar land area and five times more farms and workers as Germany, reported only 4 fatalities in agriculture in Eurostat. The Estonian Labour Inspectorate (2013) registered 785 NFAs per 100,000 agricultural workers, while the rate in Eurostat was more than twice as high (1914/100,000). Finland and Sweden with similar agricultural structures had a ten-fold difference in NFA rates in Eurostat; Finland 5,331 and Sweden 554 per 100,000 workers. These examples illustrate the large variation in agricultural accident statistics due to: a) farm structure, b) use of reference populations, c) under-reporting, d) different inclusion/exclusion criteria and e) interpretation by users. Some inconsistencies are structural due to lacking social insurance schemes for farmers, family labour and undocumented workers. Some inconsistencies could be addressed by better implementation of ESAW harmonizing rules. Alternative methods, such as standardized surveys, could be considered to augment Eurostat statistics.

Key words: agriculture, farm, worker, accident, injury, quality, statistics.

INTRODUCTION

Agriculture is one of the most hazardous industries worldwide, along with construction and mining (ILO, 2015). While it is difficult to obtain recent estimates for occupational injuries, illnesses and exposures in agriculture, numerous studies and

reports have documented the hazardous nature of the agriculture industry (Rautiainen & Reynolds, 2002; European Communities, 2004; Donham & Thelin, 2016). ILO (2004) estimated that 335,000 fatal work accidents occurred worldwide in a year, and over 50% (170,000) of them involved agricultural workers. About 1,300 NFAs and 4.2 FAs were registered per 100,000 farm workers on average each year between 2008 and 2013 in European countries. The highest FA rates in agriculture, forestry and fishing were registered for Malta (46), Austria (31) and Ireland (23), and the lowest for Poland (1.8) and Finland (2.5) (Thomson, 2016). In many cases, similar neighbouring countries have showed over ten-fold differences in agricultural accident rates. There is great variation in published rates between countries, which raises questions about the accuracy of the reporting of accidents in agriculture.

Collection and reporting of agricultural injury and illness data is challenging worldwide, particularly for self-employed farmers. For instance, in the United States, national surveys of NFAs in agriculture have suffered from measurement errors, untimeliness and insufficient data quality (Patel et al., 2017). However, reliable, timely statistics are necessary for understanding the financial and social burden of accidents at work, as well as for designing preventive efforts and monitoring if progress is being made (COWI, 2013).

Improvements in data collection and quality of statistics are important objectives in the European Commission strategic framework on health and safety at work 2014–2020 (European Commission, 2019). Improving statistics of work-related accidents, injuries, illnesses and exposures in agriculture is also a major goal of the current ‘Safety Culture and Risk Management in Agriculture’ COST Action (SACURIMA, 2019).

This study was conducted as part of the SACURIMA COST Action, and it aimed to characterize variation and inconsistencies in agricultural accident statistics in selected European countries and opportunities to improve collection and reporting of accident data in national and Eurostat statistics.

MATERIALS AND METHODS

Data sources and content

The European Union collects data on accidents at work using a harmonized ‘European Statistics on Accidents at Work (ESAW)’ methodology, first published in 1990 (ESAW, 2008). ESAW uses the NACE Rev. 2 system for the ‘Statistical Classification of Economic Activities in the European Community’, managed by Eurostat (NACE Rev 2, 2008). Eurostat publishes data on FA and NFA by economic sector using the NACE methodology. Sector A includes agriculture, forestry and fishing and A.1 includes agriculture alone, consisting of crop production, animal production, support activities and hunting. A.1 data for agriculture are reported in 39 sub-categories at three levels.

Agriculture, forestry and fishing is one of the nine themes in the Eurostat database (available at: <https://ec.europa.eu/eurostat/data/database>). Detailed information for agriculture is available on farm structure, economics, production, types of farms, environmental measures and labour. Accidents at work are reported in Eurostat database under ‘Cross cutting topics > Quality of employment > Safety and ethics of employment > Safety at work’ in several tables with options to define specific search criteria by geography, NACE sector, sex, year and unit (number, incidence rate).

EU member states have a legal requirement to send data described in ESAW to Eurostat by the end of June each year. New countries have been added to Eurostat during 1995–2012 including Croatia, Iceland, Norway, Switzerland, Montenegro and Serbia (ESAW, 2008; Eurostat, 2019). Eurostat publishes work accident statistics at the national and European aggregate levels to enable comparisons between countries, regions and economic sectors.

One important definition in ‘ESAW 3.6. Statistical population’ states that ‘Member States are required to report on ‘employees’. Reporting on other employment types (self-employed, family members, students and others) is voluntary.’ Agriculture in most countries is based on small family farms, and therefore the majority of agricultural workers are likely to fall under ‘voluntary’ reporting in ESAW.

An accident at work is defined in ESAW as ‘a discrete occurrence in the course of work, which leads to physical or mental harm’, augmented with additional inclusion and exclusion criteria. The data include fatal accidents and non-fatal accidents involving 4 or more calendar days of absence from work. If the accident does not lead to the death of the victim it is called a ‘non-fatal’ (or ‘serious’) accident. A fatal accident at work is defined as an accident which leads to the death of a victim within one year of the accident (ESAW, 2008).

National sources for ESAW include national accident insurance systems, private insurance carriers for accidents at work and other relevant national authorities (incl. labour inspectorates). As an exception, the accident statistics for the Netherlands are based on survey data.

The accident data are presented as numbers, percentages, incidence rates and standardised incidence rates for non-fatal and fatal accidents at work, either for EU aggregates, countries or certain breakdowns by dimensions such as age, sex etc.

- Numbers correspond to a simple count of all non-fatal and fatal accidents for the entirety or certain breakdowns of the data;
- Percentages represent shares of breakdowns;
- The incidence rate of non-fatal or fatal accidents at work is the number of non-fatal or fatal accidents per 100,000 persons in employment;
- The standardized incidence rates of non-fatal or fatal accidents at work aim to eliminate differences in the structures of countries' economies.

National sources of information vary by country; some have national social security and accident insurance (workers’ compensation) systems that cover practically all workers in the agriculture sector, also self-employed farmers. Some countries rely on a mix of insurance-based data and self-reporting, and some use surveys to augment other data sources. The national sources cited in this article were found on the internet, publications of national authorities, agricultural journals and scientific articles, or by requests to national experts in the field. The statistics of farm structure and accidents are presented for all Eurostat member countries. National data to validate Eurostat information are presented for selected countries participating in the SACURIMA COST Action.

Methods of data analysis

This study presents descriptive statistics on holdings (farms), labour and fatal and non-fatal accidents in agriculture in EU countries. The data were extracted from Eurostat and augmented with national data sources. The study focused on NACE category A.1 –

agriculture, excluding forestry and fishing. The year 2013 was the most recent year available for some data, and therefore, all statistics are presented for the year 2013.

Descriptive statistics on holdings (farms, n) include the count of holdings, utilized agricultural area (area used for farming, ha), total area and standard output (€); each presented by country as total and average per farm. The share (%) of utilized agricultural area out of total area was calculated for each country to illustrate the proportion of agricultural vs. non-agricultural (incl. forest production) economic activity. These indicators describe the general size of the national agriculture sector, as well as the geographic and economic size of an average agricultural holding in each member country. The data were extracted from Eurostat table [ef_kvftaa].

The labour force is described using the number of persons in employment and the Annual Work Units (AWU), which combines full-time and part-time workers converting the amount of labour into full-time equivalent numbers. The amount of family labour is described as persons and AWU, and the amount of total labour, including family and non-family labour, is described as 'Regular labour force', similarly in persons and AWU. The share (%) of the family labour out of total regular labour force (in AWU) was calculated for each country. The data were extracted from Eurostat table [ef_olfftecs]. Annual work unit (AWU) is defined as full-time equivalent employment corresponding to the number of full-time equivalent jobs, i.e. as total hours worked divided by the average annual number of hours worked in full-time jobs within the economic territory (Eurostat, DG AGRI, 2019). AWU corresponds to the work performed by one person who is occupied on an agricultural holding on a full-time basis. If the national provisions do not indicate the number of hours, then 1,800 hours are taken to be the minimum annual working hours: equivalent to 225 working days of eight hours each. As the volume of agricultural labour is being calculated on the basis of full-time equivalent jobs, no one person can therefore represent more than one AWU. This constraint holds even if it is known that someone is working on agricultural activities for more than the number of hours defining full-time in the Member State concerned (Eurostat, 2018).

The incidence of non-fatal and fatal accidents was described using annual numbers and rates of fatal and non-fatal accidents (injuries) that occurred in 2013. Incidence rates for both fatal and non-fatal accidents are expressed in Eurostat as accidents per 100,000 workers in employment. Accident data were extracted from Eurostat tables [hsw_n2_01] and [hsw_n2_02]. The term 'accident' was used in this paper as it is still used in Eurostat and many European countries to describe an 'injury' or 'acute injury event'. These terms are commonly preferred in the injury prevention field.

The following calculations were performed for each country; 1) to quantify the size of the reference population used in the accident rate calculations and 2) to compare the reference population to the published regular labour force. If the reference population ratio deviates considerably from 1.0, there is a concern about how the incidence rate was calculated, as published in Eurostat.

1: $\text{Number of accidents} * 100,000 / \text{incidence rate} = \text{Reference population};$

2: $\text{Reference population} / \text{Regular labour force (AWU)} = \text{Reference population ratio}.$

Finally, national data sources were explored to validate the accuracy of Eurostat fatal and non-fatal accident reporting by comparing Eurostat numbers and rates to those found in national sources. These comparisons were performed primarily for Germany, Finland, Estonia and the neighbouring countries (incl. Ireland, Norway, Sweden) where

the authors have access and familiarity with national sources in local languages. In addition to national reports, normally published in the language of the member state, personal contacts with health and insurance authorities etc. were utilized to find out national information about non-fatal and fatal accidents for the selected year, 2013.

RESULTS

Number and size of agricultural holdings

According to Eurostat, EU (28) countries had approximately 10.8 million farms in 2013. Family farm is the most common farm type in Europe; approximately 90% of farms (10.1 million) are family farms, utilizing about half of the farmland in Europe.

Table 1 shows the numbers of holdings, utilized agricultural area, total area and standard output, in total and per farm, for the EU 28 and each Eurostat member country. The average size of utilized agricultural land (area used for farming) was 16 hectares (ha) per farm, and the total area (including forest and other land) was 20 ha per farm. The share of utilized agricultural land out of total was 82% on average, ranging from 19% in Norway to 97% in Belgium. In addition to Norway, the share of arable land out of total land was less than 50% also in Finland, Sweden and Austria where most farms involve significant forest production. Most Eastern and Southern European countries have large numbers of very small (micro) farm holdings specialized in horticulture. For example, Poland had 1.4 million farms and 14.4 million hectares of arable land accounting to 10.1 ha of arable land per farm. The ‘Farm Structure Survey’ shows a general trend of decreasing farm numbers and increasing arable land areas per farm in EU countries (Eurostat, 2013). Besides farm sizes, there is also great variability in the Standard Output by country and by farm on average. The countries with the largest farm output were France, Germany and Italy, and the smallest were Malta, Luxembourg and Cyprus. The largest standard outputs by farm were found in the Netherlands, Belgium and Denmark, and the smallest in Romania, Malta and Lithuania.

Table 1. Holdings, area and output in agriculture, Eurostat 2013

Country	Total number of holdings	Utilized agricultural area, ha		Total area, ha		Standard output	
		Total	Holding, avg.	Total	Holding, avg.	Total (million Euros)	Holding, avg. (Euros)
EU (28)	10,838,290	174,613,900	16	213,749,800	20	331,105	30,550
Austria	140,430	2,726,890	19	5,815,840	41	5,671	40,383
Belgium	37,760	1,307,900	35	1,350,200	36	8,407	222,643
Bulgaria	254,410	4,650,940	18	5,608,980	22	3,336	13,113
Croatia	157,440	1,571,200	10	1,728,100	11	2,029	12,887
Cyprus	35,380	109,330	3	123,810	3	495	13,991
Czech Rep	26,250	3,491,470	133	5,076,430	193	4,447	169,410
Denmark	38,280	2,619,340	68	2,920,610	76	9,580	250,261
Estonia	19,190	957,510	50	1,229,420	64	676	35,227
Finland	54,400	2,282,400	42	5,786,690	106	3,398	62,463
France	472,210	27,739,430	59	29,264,400	62	56,914	120,527
Germany	285,030	16,699,580	59	18,305,150	64	46,252	162,271

Table 1 (continued)

Greece	709,500	4,856,780	7	5,062,500	7	8,103	11,421
Hungary	491,330	4,656,520	9	7,048,760	14	5,578	11,353
Ireland	139,600	4,959,450	36	5,277,990	38	5,013	35,910
Italy	1,010,330	12,098,890	12	15,933,790	16	43,794	43,346
Latvia	81,800	1,877,720	23	3,058,780	37	990	12,103
Lithuania	171,800	2,861,250	17	3,125,370	18	1,919	11,170
Luxembourg	2,080	131,040	63	137,790	66	314	150,962
Malta	9,360	10,880	1	11,980	1	97	10,363
Netherlands	67,480	1,847,570	27	2,008,870	30	20,498	303,764
^a Norway	43,270	996,270	23	5,372,090	124	3,410	78,807
Poland	1,429,010	14,409,870	10	16,487,480	12	21,797	15,253
Portugal	264,420	3,641,590	14	4,625,700	17	4,509	17,052
Romania	3,629,660	13,055,850	4	14,661,380	4	11,990	3,303
Slovakia	23,570	1,901,610	81	3,067,090	130	1,812	76,877
Slovenia	72,380	485,760	7	902,160	12	1,009	13,940
Spain	965,000	23,300,220	24	30,042,210	31	35,979	37,284
Sweden	67,150	3,035,920	45	6,424,370	96	4,679	69,680
United Kingdom	183,040	17,326,990	95	18,663,950	102	21,819	119,203

^a - non-EU country.

The size of the farms, intensity of production, geography, climate and growing conditions are closely tied to the structure of the workforce, nature of work and injury and illness hazards.

Labour force in agriculture

Eurostat reports labour force numbers by person, Annual Work Unit (AWU) and type of employment. Following are the AWU numbers for EU (28) countries by category: Family labour force (7,271,360), Regular non-family labour force (1,460,240), Total regular labour force (8,731,620), Non-family labour force working on non-regular basis (774,770) and Labour force directly employed by the holding (9,506,410), all expressed in Annual Work Units (Table 2). The workforce numbers counted in persons are more than twice as large as the numbers in AWU, indicating that a large proportion of the workforce in agriculture works on a part-time basis. As an example, the count of persons in EU (28) family labour force (20,199,360) was 2.8 times larger than the AWU count of family labour force (7,271,360). A nearly as large difference (2.5 times) was found in total regular labour force. The largest numbers of family labour were found in Romania, Poland and Italy and the smallest in Luxembourg, Malta and Estonia. Family labour's share of the total regular labour force was 75% in EU (28) countries combined, ranging from 27% in Czech Republic to 97% in Slovenia.

The size of the labour force, counted as persons and AWU, as well as the share of family labour out of total labour in AWU are shown in Table 2.

Table 2. Labour force in Agriculture, Eurostat 2013

Country	Labour force, persons		Labour force, Annual Work Units (AWU)		
	Family	Regular labour force	Family	Regular labour force	Family's share of total (%)
EU (28)	20,199,360	22,205,300	7,271,360	8,731,620	75
Austria	308,670	337,580	92,920	107,740	86
Belgium	59,290	74,830	40,220	52,010	77
Bulgaria	499,690	557,670	245,090	298,380	82
Croatia	374,910	388,370	163,140	173,250	94
Cyprus	73,090	77,390	11,510	15,240	76
Czech Rep	49,420	132,130	27,070	101,070	27
Denmark	53,630	79,580	28,020	51,090	55
Estonia	30,900	44,220	10,240	21,550	48
Finland	101,030	120,020	42,480	52,990	80
France	491,050	907,080	296,680	640,480	46
Germany	529,290	706,260	322,920	466,830	69
Greece	1,213,420	1,238,490	395,300	412,450	96
Hungary	962,570	1,059,940	314,710	400,020	79
Ireland	252,270	269,510	150,480	160,610	94
Italy	1,992,690	2,139,060	617,150	696,240	89
Latvia	153,610	173,920	67,810	81,770	83
Lithuania	264,070	297,950	114,850	142,450	81
Luxembourg	3,790	4,950	2,410	3,380	71
Malta	14,310	14,870	3,960	4,380	90
Netherlands	133,320	193,140	88,730	131,750	67
ⁿ Norway	106,940	124,900	33,930	40,860	83
Poland	3,480,250	3,558,710	1,799,160	1,866,450	96
Portugal	565,830	626,390	250,060	298,550	84
Romania	6,488,130	6,577,930	1,386,370	1,451,870	95
Slovakia	39,090	80,020	13,960	49,030	28
Slovenia	198,000	200,630	77,290	79,470	97
Spain	1,437,190	1,782,690	485,960	661,050	74
Sweden	108,740	130,710	40,620	55,670	73
United Kingdom	321,110	431,260	182,250	255,850	71

ⁿ non-EU country.

Number and rate of fatal and non-fatal accidents

In 2013, Eurostat reported 366 FA and 135,260 NFA in EU (28) countries for the NACE A.1 Agriculture sector (without forestry and fishing). Table 3 shows the counts and rates of FA and NFA in EU (28) and Eurostat member countries. The corresponding rates were 4.14 for fatal and 1,528 for NFA per 100,000 workers. Italy, Germany and Austria had the highest fatality counts while Estonia, Greece, Luxembourg, Slovenia, Sweden and Iceland reported zero fatalities. Very low rates (below 1/100,000) were reported for Poland, Switzerland and Germany. The highest fatality rates were reported in Malta, Austria and Norway. Germany, Italy and Spain had the highest numbers of NFA, accounting for about 79% of all accidents in EU countries. The remaining 21% were spread between 25 EU member countries. The highest rates of NFA were reported in Finland, Italy and Spain, and the lowest in Greece, Poland and Bulgaria.

Table 3. Number and rate of fatal and non-fatal accidents, Eurostat 2013

Country	Fatal accidents		Non-fatal accidents		Reference population**	
	Number	Rate*	Number	Rate*	Reference population**	Ratio***
EU (28)	366	4.14	135,260	1528	8,849,256	1.01
Austria	49	26.14	3,968	2117	187,426	1.74
Belgium	1	5.12	315	1612	19,538	0.38
Bulgaria	2	3.19	34	54	62,650	0.21
Croatia	2	3.07	314	483	65,070	0.38
Cyprus	1	9.52	18	171	10,504	0.69
Czech Rep	16	13.74	2,558	2196	116,480	1.15
Denmark	8	12.72	995	1583	62,872	1.23
Estonia	0	0	338	1914	17,658	0.82
Finland	4	5.27	4,048	5331	75,939	1.43
France	1	8.67	403	3494	11,534	0.02
Germany	76	2.33	60,693	1858	3,265,979	7.00
Greece	0	0	25	5	457,038	1.11
Hungary	6	3.53	487	287	169,846	0.42
Iceland	0	0	16	408	3,919	-
Ireland	12	12	1849	1848	100,035	0.62
Italy	81	10.94	26,819	3621	740,752	1.06
Latvia	3	23.8	35	278	12,606	0.15
Lithuania	4	4.19	96	101	95,484	0.67
Luxembourg	0	0	123	2170	5,668	1.68
Malta	1	51.26	7	359	1,951	0.45
Netherlands	3	1.85	3,169	1892	167,478	1.27
ⁿ Norway	8	19.2	135	324	41,629	1.02
Poland	4	0.24	831	49	1,699,734	0.91
Portugal	11	2.59	2,773	654	424,162	1.42
Romania	12	13.22	49	54	90,774	0.06
Slovakia	7	13.25	481	910	52,848	1.08
Slovenia	0	0	65	121	53,870	0.68
Spain	24	4.38	19,319	3524	548,158	0.83
Sweden	0	0	370	554	66,744	1.20
Switzerland	1	0.71	1,316	934	140,848	-
United Kingdom	38	14.59	5,078	1949	260,520	1.02

* Rate (accidents / 100,000 persons in employment) (ESAW, 2019); ** Reference population = Number of accidents * 100,000 / incidence rate; *** Ratio = Reference population / reported Regular labour force; ⁿ non-EU country.

There are large differences in work accident counts and rates between countries with similar agricultural structures, such as number of workers, average farm size, utilized agricultural area or farming activities and even reported output coming from nature of production. For example, Germany and Poland have similar sizes of arable land. The numbers of farms and workers in Poland are about five times larger compared to Germany. Yet, the NFA rate in Germany was 1,858; nearly 40 times higher than the rate in Poland (49). While Germany reported 76 fatalities in agriculture, Poland reported 4 and France reported only one. The Nordic countries have relatively similar numbers of farms, farm sizes and production, yet the NFA rates were 324 for Norway, 554 for Sweden and 5,331 for Finland; about ten-fold difference between Finland and the two

neighbouring countries. Ireland at one extreme has a reported output of € 1,000/utilized ha – whereas the Netherlands is the other end of the scale at over € 11,000. My guess is that this reflects the nature of the production, for example a lot of unirrigated grass-fed grazing - versus a significant amount of intense horticulture and barn-raised animals.

The rate of work accidents is generally higher among male workers. Females had a higher rate in four countries, nearly four times higher rate in Estonia, and somewhat higher rates in Denmark, Ireland and Sweden.

There is large fluctuation in annual accident counts and rates in some countries. For instance, the NFA count for Finland showed large fluctuation by year; the NFA counts were 4,350, 586 and 4,048 for the years 2011, 2012 and 2013, respectively (Eurostat table [hsw_n2_01]). The FA rate for Germany was 13.84 in 2008, but then abruptly dropped to a level fluctuating between 1.64 and 3.36 during 2009–2016 (Eurostat table [hsw_n2_02]).

A back-calculation of the reference populations as described in Methods was performed to detect errors or unusually large deviations, potentially due to recording or calculation errors or weighting used in rate calculations. Germany's reported fatality rate in Eurostat was 2.33/100,000 workers in 2013. However, the reference population would need to be 3,265,979 to have the published 2.33/100,000 fatality rate and 76 fatalities. The actual Eurostat regular labour force count (AWU) was reported as 466,830 in 2013. The fatality rate for Germany would be 16.3/100,000 when calculated with the regular labour force number as denominator – a seven-fold difference compared to the Eurostat published rate. Large deviations were found in other countries as well. France only reported one fatality in agriculture, but the rate was reported as 8.67/100,000. With this rate, the reference population would be 11,534, while the actual reported regular labour force was 907,080 in 2013 – nearly 80-fold difference.

The counts and rates of fatal and non-fatal accidents and the back-calculated reference populations and ratios are presented in Table 3.

National and Eurostat statistics

Eurostat and national FA and NFA counts and rates were compared for selected countries. Germany reported 160 fatalities in national statistics and 89 in Eurostat; these numbers are for the NACE A (agriculture, forestry and fishing combined).

A Spanish survey of Arana et al. (2010) found, that only 62% of the fatal accidents were recorded by the Labour and Social Affairs Spanish Ministry (Ministerio de Trabajo y Asuntos Sociales, MTAS) in the years 2004–2008. Reasons for this difference were not investigated.

The Estonian Labour Inspectorate (LI) reported 785 non-fatal accidents per 100,000 agricultural workers while Eurostat reported 1914. The Estonian Statistics Agency (ESA) combines cases from LI and the Estonian Working Life Survey (ELFS) (Enn, 2018).

Finland's NFA counts for 2011, 2012 and 2013 were: 4,350, 586 and 4048, respectively. It is likely that 2012 count excludes self-employed farmers, insured by the Farmers Social Insurance Institution (Mela) as Mela (2019) reported 4,567 agricultural accidents in 2012 (including those that may not exceed 3 days of absence from work).

The Agricultural Social Insurance Fund (KRUS) in Poland registered 15,803 accidents resulting in health detriment or death among farmers in 2013 while Eurostat shows 813 NFAs and 4 FAs, which in only about 5% of the total reported by the national insurance fund (KRUS, 2016).

DISCUSSION

There are great challenges in collecting and reporting information on occupational injuries and illness. The challenges are worldwide; statistics are often incomplete due to under-reporting of injury and illness incidents, and incomplete coverage of workers, particularly those in the informal economy (Thomson, 2016; COWI, 2013; Karttunen & Rautiainen, 2013b; ILO, 2012). The majority of the workforce in agriculture consists of self-employed family labour that may not be covered by social insurance schemes with ability to report occupational injury and illness cases. ILO (2015) has estimated that agriculture employs 1.3 billion workers worldwide; half of the world's workforce; and that agriculture is one of the three most hazardous industries globally, along with construction and mining. In the United States, fatal accidents are quite well known (CFOI, 2019), but there is no national system to collect NFA information for farmers, as surveys conducted by national agencies have been discontinued (Patel et al., 2017). In Canada, Provinces have different data collection systems, and information on agricultural injuries and fatalities is collected periodically through volunteer efforts (CAIRS, 2019). In Europe, there is great variability in farm structure, working populations and accident data collection systems, including insurance, administrative and survey sources (ESAW, 2008; Eurostat 2019). There are no uniform data collection and reporting systems, making it possible to compare data between continents and countries with reasonable accuracy.

The current study focused on the variability and accuracy of agricultural accident (injury) and fatality statistics in Europe using Eurostat and national sources. The results show large variation in fatal and non-fatal accident rates in Eurostat statistics between countries. The Eurostat accident counts and rates can also vary widely in one country from year to year, and there are large differences in accident counts and rates between Eurostat and national sources for a given year.

The reasons for the variability are complex. Without in-depth investigation of national data collection and reporting systems, it is not possible to identify reasons for inconsistencies comprehensively. However, the current study identified some sources of variation, based on limited examination of Eurostat and national statistics. The identified sources of variation are discussed in the following.

a) Differences in farm structure

Structural changes in agriculture, decreasing farm numbers and increasing farm sizes influence the economic and social well-being of the farming population, including the risk of FA and NFA (Leppälä, 2016). The numbers and sizes of holdings differ widely between Eurostat countries. These differences affect working conditions and the risk of accidents. Based on systematic reviews, greater farm area, income and number of workers on the operation; being owner/operator (vs. hired worker); being full-time farmer; living on (vs. off) the farm and raising livestock are among risk factors for agricultural injuries. Other factors, such as challenging social conditions, stress,

depression, sleep deprivation and regular medication use also increase the risk of injury. There is conflicting evidence for other factors, such as off-farm work, marital status, work experience, age, smoking and alcohol use (Jadhav et al., 2015, Jadhav et al., 2016). Greater forest area also increases the risk of injury among farmers (Karttunen & Rautiainen, 2013a).

Some of the variation in accident counts and rates between Eurostat member states could be explained by farm structure. Given the known risk factors, countries with large farms based on full-time family labour and significant livestock and forestry production should have similar high accident rates. However, Eurostat fatality counts and rates from three large advanced agricultural nations show clear inconsistencies: France (1 fatality, rate: 8.67/100,000), Germany (76 fatalities, rate: 2.33/100,000) and United Kingdom (38 fatalities, rate: 14.59/100,000). The differences in Eurostat accident rates can be more than ten-fold between similar countries in some cases. The effect of identified risk factors is much smaller, typically about two-fold increase in accident risk. Therefore, farm structure may explain some, but not nearly all of the variation in accident rates.

b) Selection of reference populations

Eurostat accident rates are based on 'persons in employment'. ESAW (2008) defines the statistical population as follows: 'Member States are required to report on 'employees'. The other employment types (self-employed, family members, students and others) are voluntary.' This definition is problematic for agriculture. The average share of family labour out of total labour in Eurostat countries was 75%. Therefore, reporting of accidents is voluntary for the vast majority; $\frac{3}{4}$ of the workforce in agriculture.

Eurostat agricultural statistics provide labour force numbers by person and by Annual Work Unit (AWU) in the following categories: 1) Family labour force, 2) Regular non-family labour force, 3) Total regular labour force, 4) Non-family labour force working on non-regular basis and 5) Labour force directly employed by the holding. It is likely that for most countries, the FA and NFA counts exclude family labour. It is also possible that the reference population for rate calculations includes family labour, given the complexity how agricultural labour is counted, in persons and AWU.

We examined the published Eurostat FA and NFA rates, and back calculated the size of the reference population from the counts and rates for each Eurostat country. On the EU (28) level, our calculated reference population was 8,849,256; almost the same as the Regular labour force (in AWU), 8,731,620. Examination of the ratio: calculated reference population / Regular labour force (AWU) revealed that while the ratio was 1.01 for the EU (28), it varied widely from 0.02 (France) to 7.00 (Germany). This variation demonstrates that there are inconsistencies in the selection of reference populations for accident rate calculations. It is likely that in many countries, accidents are reported only for regular non-family labour, but rate calculations use Total regular labour force, Labour directly employed by the holding, or another version of the total labour force, resulting in significant under estimation of the accident rates in agriculture.

c) Under-reporting of work accidents

ESAW (2008) mandatory accident reporting to Eurostat is based on European Commission Regulations. The national ESAW sources include accident insurance of the national social security system, private insurance for accidents at work or other relevant national authorities (labour inspection etc.) or surveys.

Only few countries have statutory accident insurance schemes for self-employed farmers. Without incentive, such as insurance benefits, farmers are unlikely to report their injuries, even if reporting is mandatory. In some cases, there may even be real or perceived penalties for reporting accidents. Lack of accident insurance coverage for family labour results in systematic underreporting of agricultural accidents. For example, Pinzke & Lundqvist (2011) found that as many as 90% of agricultural work accidents remained unreported in Sweden. This finding is in accordance with Eurostat NFA data: the rate was 554/100,000 in Sweden and 5,331/100,000 in Finland; a ten-fold difference although these neighbouring countries have quite similar geography and farm structures. The source of the difference is likely that Finland has a mandatory accident insurance scheme for practically all farmers and hired workers, and under reporting is not a major issue (Karttunen & Rautiainen, 2013b). Similar mandatory accident insurance does not exist in Sweden.

The ESAW definition of reportable accident, '4 or more calendar days of absence from work', is difficult to apply for family labour in agriculture. In most countries, there is no accident insurance that provides compensation for 'absence from work' for self-employed farmers. In case of an accident to a farmer, such 'absence from work' period remains undefined. Further, farmers regulate their own working hours, and they are likely to work in limited capacity in health situations where they would be 'absent from work', if working for an employer in another sector. This ESAW definition is likely to result in under-reporting of accidents to family labour in Eurostat statistics.

Migrant workers often work without permanent job contracts and their employment and work accident numbers are likely under-reported. Migrant workers (globally about 244 million people) often work in unsafe conditions, which leads to poor health, injuries and deaths at work. Their employers often evade responsibility to report and pay compensation for work injuries for the workers without permanent contracts (Sousa et al., 2010; Ronda-Perez et al., 2012; Moyce & Schenker, 2018).

d) Inclusion/exclusion criteria and weighting in national and ESAW reporting

Eurostat and national statistics may have different inclusion and exclusion criteria. As an example, Germany reported 160 fatalities in national statistics and much lower number (89) in Eurostat for agriculture, forestry and fishing combined. Request of information to the national authority revealed some reasons for the difference in national and Eurostat statistics. For instance, persons over 70 and under 18 years of age are included in national statistics but excluded from Eurostat.

The Estonian Labour Inspectorate (LI) reported a lower number (785) of non-fatal accidents per 100,000 agricultural workers than Eurostat (1914). The Estonian Statistics Agency (ESA) combines cases from LI and the ELFS (Enn, 2018). Estonia is one of 10 out of 31 countries that applies weights for non-fatal accidents. Data are weighted through three dimensions: calculation of design weights, non-response correction and calibration of non-response corrected weights. The weighting shows how many objects from the population the respondent represents. Due to the stratification the design weight depends on the inclusion probability. The design weight of the household is inversely proportional to the inclusion probability and it depends on the size of the stratum in the population and the number of units selected into the sample from the stratum (ELFS, 2013).

Inconsistencies can occur even if a country has good data. Some data may not be reported to Eurostat because reporting is 'voluntary' for family labour according to

ESAW. Finland's NFA counts for consecutive years showed large differences, likely due to including or excluding self-employed farmers in different years.

Variation in national and Eurostat figures could result from inclusion or exclusion of commuting accidents, transportation accidents and accidents to seasonal and undocumented workers. These sources were not investigated in the current study.

One systematic problem has been that some Eastern European countries have not reported information about agricultural accidents in Eurostat at all in some years. For our selected year 2013, the data were complete for EU (28) countries while it is likely that under-reporting occurs for most countries.

e) interpretation by users

One common error in interpretation of accident statistics involves mixing the accident counts and reference populations when constructing accident rates. Users may present accident counts and rates for 'agriculture' while in fact, the counts and rates are calculated for agriculture, forestry and fishing combined. In other cases, users may construct accident rates for 'agriculture' by using the (bigger) number of accidents for the agriculture, forestry and fishing, sector, but using only agricultural population numbers as denominator. Given the complexity in retrieving Eurostat numbers and rates, and the added complexity from differing national data, it is very challenging for researchers and educators to obtain reliable and correct data.

CONCLUSIONS

The European Statistics on Accidents at Work (ESAW) methodology was developed first in 1990, and it aims to harmonize work accident data collection in Europe. Agriculture sector, defined in the Statistical Classification of Economic Activities in the European Community (NACE) is included, but it is not possible to get an accurate picture of the work accident situation from Eurostat statistics, and hence these statistics are not helpful for making policy decisions to address hazards and risks in agriculture. This study identified great variation in reported fatal and non-fatal accident counts and rates in Eurostat and national sources. Sources of variation include differences in a) farm structure, b) use of reference populations c) under-reporting, d) inclusion/exclusion criteria and e) interpretation of data by users. Some inconsistencies are structural due to lacking social insurance schemes for farmers and family labour. Some could be addressed by better implementation of ESAW harmonizing rules, including clarification of including/excluding self-employed farmers, who form the majority of the agricultural workforce in most countries. Better regulation of work contracts in agriculture could prevent under-reporting of work accidents among migrant workers. Alternative methods, such as standardized surveys, could be considered to augment Eurostat statistics.

ACKNOWLEDGEMENTS. This study was conducted as part of the COST Action 16123, Safety Culture and risk Management in Agriculture (SACURIMA). The authors are members of the SACURIMA COST Action. The authors thank other SACURIMA members listed in <https://www.sacurima.eu/> as well as officials who helped collect national data for the present paper. The work effort of Risto Rautiainen was supported by The Central States Center for Agricultural Safety and Health, University of Nebraska Medical Center (CDC/NIOSH Award U54OH010162).

REFERENCES

- Arana, I., Mangado, J., Arnal, P., Arazuri, S., Alfaro, J.R. & Jarén, C. 2010. Evaluation of risk factors in fatal accidents in agriculture. *Span. J. Agric. Res.* **8**(3), 592–598.
- CAIRS. 2019. Canadian Agricultural Injury Reporting. Available at: <https://www.cair-sbac.ca/> Accessed March 12, 2019.
- CFOI. 2019. Census of Fatal Occupational Injuries. Bureau of Labor Statistics. Available at: <https://www.bls.gov/iif/oshcfoi1.htm> Accessed March 16, 2019.
- COWI. 2013. DG Employment, Social Affairs and Inclusion. Evaluation of the European Strategy on Safety and Health at Work 2007–2012. Final Report. Available at: <https://ec.europa.eu/social/main.jsp?langId=en&catId=151> Accessed March 16, 2019
- Donham, K.J. & Thelin, A. (ed.). 2016. *Agricultural Medicine: Rural occupational and environmental health, safety and prevention, 2nd edition*. Wiley-Blackwell, 600 pp.
- ELFS. 2013. Estonian Labour Force Survey 1995–2012. Methodology. Tallinn. <https://www.stat.ee/dokumendid/72595> Accessed July 19, 2019.
- Enn, A. 2018. Prevalence and dynamics of work accidents in Estonian agriculture. MSc Thesis. Tartu, 102 pp. https://dspace.emu.ee/xmlui/bitstream/handle/10492/4357/Anni_Enn_MA2018.pdf?sequence=1&isAllowed=y Accessed February 16, 2019.
- ESAW. 2008. Accidents at work. Available at: https://ec.europa.eu/eurostat/cache/metadata/en/hsw_acc_work_esms.htm Accessed February 17, 2019.
- European Commission. 2019. EU Occupational Safety and Health (OSH) Strategic Framework 2014–2020. Available at: <https://ec.europa.eu/social/main.jsp?langId=en&catId=151> Accessed February 17, 2019.
- European communities. 2004. Work and health in the EU. A Statistical portrait. Data 1994–2002. (117 pages) Available at: <https://ec.europa.eu/eurostat/documents/3217494/5657469/KS-57-04-807-EN.PDF/d1c5fda3-290d-4265-8a96-1059628d2729> Accessed December 9, 2018.
- Eurostat. 2019. Your key to European statistics. Available at: <https://ec.europa.eu/eurostat/data/database> Accessed February 17, 2019.
- Eurostat, DG AGRI. 2019. Agricultural factor income per annual work unit (AWU). Available at: https://ec.europa.eu/eurostat/web/products-datasets/-/sdg_02_20 Accessed July 18, 2019.
- Eurostat. 2018. Glossary: Annual work unit (AWU). https://ec.europa.eu/eurostat/statistics-explained/index.php/Glossary:Annual_work_unit_%28AWU%29 Accessed July 19, 2019.
- Eurostat. 2013. Farm Structure Survey, 2013. Available at: https://ec.europa.eu/eurostat/statistics-explained/index.php?title=Farm_structure_survey_2013_-_main_results Accessed March 21, 2019.
- ILO. 2004. Towards a fair deal for migrant workers in the global economy. Available at: <http://www.ilo.org/wcmsp5/groups/public/---dgreports/---dcomm/documents/meetingdocument/kd00096.pdf> Accessed July 18, 2019.
- ILO. 2012. Improvement of national reporting, data collection and analysis of occupational accidents and diseases. Available at: https://www.ilo.org/safework/info/publications/WCMS_207414/lang--en/index.htm Accessed March 16, 2019.
- ILO. 2015. Agriculture: A hazardous work. Available at: <https://www.ilo.org/safework/areasofwork/hazardous-work/lang--en/index.htm> Accessed March 16, 2019.
- Jadhav, R., Achutan, C., Haynatzki, G., Rajaram, S. & Rautiainen, R. 2015. Risk Factors for Agricultural Injury: A Systematic Review and Meta-analysis. *J. Agromedicine* **20**(4), 434–49. doi: 10.1080/1059924X.2015.1075450

- Jadhav, R., Lander, L., Achutan, C., Haynatzki, G., Rajaram, S., Patel, K. & Rautiainen, R. 2016. Review and Meta-analysis of Emerging Risk Factors for Agricultural Injury. *J. Agromedicine* **21**(3), 1–14. <http://dx.doi.org/10.1080/1059924X.2016.1179611>
- Karttunen, J.P. & Rautiainen, R.H. 2013a. Occupational injury and disease incidence and risk factors in Finnish agriculture based on 5-year insurance records. *J. Agromedicine* **18**(1), 50–64. PubMed PMID: 23301890. doi: 10.5603/IMH.2016.0031
- Karttunen, J.P. & Rautiainen, R.H. 2013b. Distribution and characteristics of occupational injuries and diseases among farmers: a retrospective analysis of workers' compensation claims. *Am. J. Ind. Med.* **56**(8), 856–869. <https://doi.org/10.1002/ajim.22194>
- KRUS. 2016. Agricultural Social Insurance Fund (KRUS). Basic information. Warsaw, 52 pp.
- Leppälä, J. 2016. Systematic risk management on farms. Doctoral Dissertation. Department of Industrial Engineering and Management. Aalto University publication series 17/2016. *Aalto-yliopiston teknillinen korkeakoulu*. Espoo, 152 pp.
- Mela. 2019. Farmers Social Insurance Institute in Finland. MATA-compensation statistics. Available at: <https://www.mela.fi/>.
- Moyce, S.C. & Schenker, M. 2018. Migrant workers and their occupational health and safety. *Annu. Rev. Public Health* **39**, 351–365. doi: 10.1146/annurev-publhealth-040617-013714
- NACE Rev. 2. 2008. Statistical classification of economic activities in the European Community. Available at: <https://ec.europa.eu/eurostat/documents/3859598/5902521/KS-RA-07-015-EN.PDF/dd5443f5-b886-40e4-920d-9df03590ff91?version=1.0>. Accessed March 10, 2019.
- Patel, K., Watanabe-Galloway, S., Kofin, R., Haynatzki, G. & Rautiainen, R. 2017. Non-fatal agricultural injury surveillance in the United States: A review of national-level survey-based systems. *Am. J. Ind. Med.* **60**, 599–620. <https://doi.org/10.1002/ajim.22720>
- Pinzke, S. & Lundqvist, P. 2011. Occupational injuries in agriculture and forestry 2004. Swedish University of Agricultural Sciences. LTJ-report 2011:44. Alnarp, Sweden (in Swedish).
- Rautiainen, R.H. & Reynolds, S.J. 2002. Mortality and morbidity in agriculture in the United States. *J. Agric. Saf. Health* **8**(3), 259–76. doi: 10.13031/2013.9054
- Ronda Pérez, E., Benavides, F.G., Levecque, K., Love, J.G., Felt, E. & Van Rossem, R. 2012. Differences in working conditions and employment arrangements among migrant and non-migrant workers in Europe. *Ethnicity & Health* **17**(6), 563–77. doi: 10.1080/13557858.2012.730606.
- SACURIMA. 2019. Safety Culture and Risk Management in Agriculture. COST Action 16123. Available at: <https://www.cost.eu/actions/CA16123/#tabs|Name:overview> <https://www.sacurima.eu/> Accessed February 17, 2019.
- Sousa, E., Agudelo-Suarez, A., Benavides, F.G., Schenker, M., García, A.M., Schenker, M., García, A.M., Joan Benach, J., Delclos, C., López-Jacob, M.J., Ruiz-Frutos, C., Ronda-Pérez, E. & Porthé, V. 2010. Immigration, work and health in Spain: the influence of legal status and employment contract on reported health indicators. *Int. J. Public Health* **55**(5), 443–51. doi: 10.1007/s00038-010-0141-8
- Thomson, K. 2016. Health and Safety in EU Agriculture. Presentation paper for the 160th EAAE Seminar 'Rural Jobs and the CAP'. Warsaw, 14 pp. Available at: https://ageconsearch.umn.edu/record/249792/files/H_S%20Paper%20Thomson%20FinalS%20submitted.pdf Accessed March 10, 2019.

Design and construction of a low-cost remotely piloted aircraft for precision agriculture applications

M.G. Morerira¹, G.A.S. Ferraz^{1,*}, B.D.S. Barbosa¹, E.M. Iwasaki, P.F.P Ferraz¹,
F.A. Damasceno² and G. Rossi³

¹Federal University of Lavras, Department of Agricultural Engineering, University Campus, BR37.200-000, Lavras, Brazil

²Federal University of Lavras, Department of Engineering, University Campus, BR37.200-000, Lavras, Brazil

³University of Florence, Department of Agriculture, Food, Environment and Forestry (DAGRI), Via San Bonaventura, 13, IT50145 Florence, Italy

*Correspondence: gabriel.ferraz@ufla.br

Abstract. This study aimed to construct a low cost RPA capable of recording georeferenced images. For the construction of the prototype of a quadcopter type RPA, only essential materials were used to allow stable flight. A maximum total weight of 2 kg was stipulated, including frame weight, electronic components, motors and cameras. The aircraft was programmed using a low-cost microcontroller widely used in prototyping and automation research. An electronic circuit board is designed to facilitate the connection of the microcontroller with the other components of the design. Specific software was used for flight control. The prototype was built successfully, being able to lift stable and controllable flight. However, we still need to acquire equipment and programming components capable of enabling autonomous images and flights. The final cost of the RPA was on average \$ 427.00 on average 50% lower than the values found in the Brazilian ARP market (\$ 772.81 to \$ 1,288.00)

Key words: arduino, prototype, drone, UAV.

INTRODUCTION

An unmanned aerial vehicle (UAV) is defined as an aircraft without a human pilot aboard (Nonami et al., 2010). The National Civil Aviation Agency (Agência Nacional de Aviação Civil – ANAC) of Brazil classifies a UAV as a function of its operation, defining it as a remotely piloted aircraft (RPA) when controlled by a ground operator (Decea, 2017). This low-cost RPA is able to perform photogrammetric work with digital cameras attached to its frame, and the flight mode may alternate between manual, semi-manual, and automatic (Nex & Remondinho, 2013).

Early in their development, UAVs were primarily used for military purposes, such as the surveillance, reconnaissance and mapping of enemy areas. Currently, UAVs are widely used in several areas such as agriculture, silviculture, archaeology, environment, emergency and ground traffic monitoring services (Nex & Remondinho, 2013). These various applications of UAVs are presently considered a low-cost option for

photogrammetric work (Nex & Remondinho, 2013). In addition to remote sensing (RS) work, UAVs have a high potential for terrain mapping, generating digital elevation models (DEM) to assess flood risk areas (Covaney & Roberts, 2017).

Due to the increasing number of technological innovations and to greater applicability of RPA in the civil sector, measures are being adopted to regulate the use of this equipment. No international regulation on the use and operation of RPA is available yet. Several countries have adopted different regulations, thus making it difficult to list the specific objectives of each policy (Nex & Remondinho, 2013).

In recent years, the demand for RPA has increased thanks to technological advances and cost reduction and to the size of the sensors and the benefits they provide, especially low-cost RPA (Segales et al., 2016). These RPA could be operated by farmers themselves to diagnose crop characteristics, such as water stress, and then they can adjust their water management practices as needed (Romero-Trigueros et al., 2016). Hence, UAV technology may bridge the knowledge gap between leaf and canopy, improving the spatiotemporal resolution of data on the vegetative state (Gago et al., 2015).

When using RPA for data collection in agriculture, RS has advantages over satellite and manned aircraft imagery due to the frequency of the image capture and processing, thus meeting the requirements for the rapid monitoring, evaluation and mapping of natural resources on a user-defined spatiotemporal scale (Feng et al., 2015). In addition, the flight height is lower, which can result in images with a higher resolution. This is necessary for managing small crop fields (Huang et al., 2013).

According to Ibrahim et al. (2017), images acquired by RPA have been rather efficiently used in irrigated areas. Furthermore, according to these authors, red, green, and blue (RGB) cameras can be used to identify crop failures and thus plan irrigation. Conversely, the use of near-infrared (NIR) cameras enables farmers to identify irrigation performance factors, such as leaks in the water supply system.

Based on the above, the need for building a low-cost RPA prototype as a tool for precision agriculture applications was identified.

MATERIALS AND METHODS

The first step of this study was to research components available on the market, checking their specifications and performing calculations to decide whether the components were suitable for the project. Initially, we intended to purchase only essential equipment to build an RPA able to maintain a stable and controlled flight. At first, this aircraft would not be able to perform autonomous flights due to the lack of a global positioning system (GPS). The objective will be to develop an aircraft stable enough to record images at the lowest possible cost, thereby establishing the groundwork for developing a more complex and robust system. A maximum total weight of 2 kg, including the weight of the frame, electronic components, motors, and camera, was calculated. This calculated weight made it possible to define which engines should be used to support the aircraft. To support the engines and other components of the RPA, the frame chosen was the generic model F450. This frame is one of the most commonly used in the hobbyist market for recreational drone construction. Weighing approximately 282 grams, with a wingspan of 450 mm, this frame is made of high-strength nylon. The frame also has a printed circuit board (PCB) power distribution board for the engines

and landing gear, in flexible plastic. Despite its recreational use, this frame is strong and easily found on the market and is thus a good choice as a development platform.

Turnigy brushless direct current (BLDC) engines were chosen because they can be easily purchased in the Brazilian market. Accordingly, the 1100KV 2836-8 engine was selected. This engine is capable of generating a maximum propulsive efficiency of 1,130 g, according to the manufacturer, providing the RPA with a theoretical propulsive efficiency of 4.5 kg. In practice, part of the propulsion should be reserved to maintain aircraft manoeuvrability. The designed RPA will hover at 50% engine power considering a linear power thrust function, thus reserving 50% of the engine power for ascent and wind resistance manoeuvres. Importantly, the relationship between the thrust generated by the engine-propeller set and the power applied is not linear. However, this consideration suffices for the initial engine choice of the aircraft.

The next step was to choose the battery, Li-Po 4S (14 V), with 5,000 mAh. Despite an approximate weight of 500 g, which accounts for 25% of the total aircraft weight, according to calculations made using the eCalc web tool, the weight-to-load-capacity ratio is appropriate for an acceptable flight time in agricultural applications. The minimum estimated flight time is 10 minutes, when the engines work at full power. BLDC engines require an electronic speed controller (ESC) for coil switching. Four 30 A ESCs (one for each engine), compatible with a 4S battery, were purchased. The propellers selected to build the RPA were plastic ABS propellers sized 10 x 4.5 inches, according to the engine manufacturer's instructions.

The Arduino Nano, an open-source electronic prototyping platform based on the Atmel microcontroller, was chosen as the flight controller and programmed using the manufacturer's open-source integrated development environment (IDE).

An MPU6050, an inertial measurement unit (IMU) capable of communicating through the I2C protocol, was chosen because this unit has 3 accelerometer sensors, along the three Cartesian axes, which are capable of providing acceleration measurements at a resolution ranging from 160 m s^{-2} to 20 m s^{-2} . The unit also has 3 gyro sensors, also along the three Cartesian axes. The resolution of the angular velocity measurement in the MPU6050 is approximately 200° s^{-1} . The direction of the vehicle can be determined using both data to feed a complementary filter.

A TGY-i6 is a 6-channel telemetry 2.4 GHz transmitter. The information transmitted by the TGY-i6 radio control (RC) is converted by the pulse-width modulation (PWM) receiver, and the signal peaks at 5 V, with a standardised pulse width time ranging from 1,000 to 2,000 μs .

An electronic circuit board was designed (Fig. 1) to facilitate the connection between the Arduino and the other components of the project. A voltage divider circuit was used to send a signal proportional to the battery charge to the controller, to allow decision-making when the battery is running low. The controller communicates with the radio receiver and with the ESCs through Arduino I/O digital pins 4 to 11, using 4 pins to receive information from 4 receiver channels and 4 to control the ESCs. The ESC control cable has 3 pins, voltage at the common collector (VCC), ground (GND) and signal pins. Only the Signal and GND pins are used in the connection, and the VCC pin is not necessary. The Wire library of the Arduino IDE implements I2C communication. For this communication, the arduino serial data line (SDA) and serial clock line (SCL) pins are used, which correspond to A4 and A5 in the nano model. The circuit diagram of Fig. 1 shows the circuits used in this project in detail.

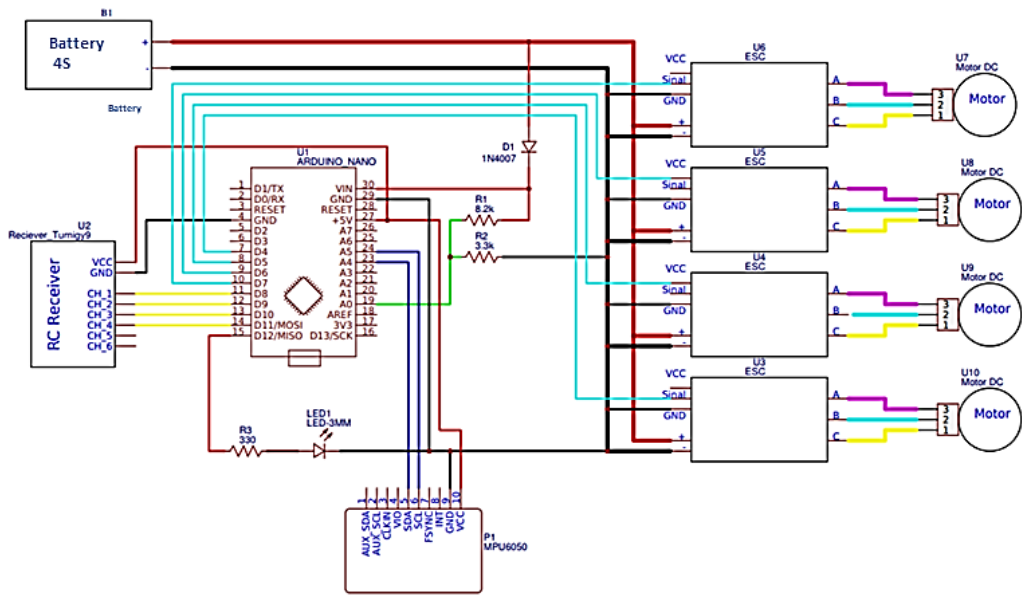


Figure 1. Electronic circuit diagram.

The flight control programme of the RPA was based on YMFC-AL software, created by J. Brokking, which consists of a simple Arduino flight controller, capable of maintaining flight stability from a single IMU. This programme is divided into 3 separate modules due to limited controller memory. Those modules should be manually uploaded to the Arduino memory to set up, test, and fly the aircraft. The configuration programme is used to assess whether all components essential to the RPA are correctly assembled and to calibrate the limits of the radio control signal. To use the radio control, the Arduino Nano is connected to a computer through a USB cable. The propellers of the aircraft should be removed and the battery turned off to avoid inadvertently turning the engines on. In the computer, using the Arduino IDE, the configuration programme of the aircraft should be opened and uploaded to the Arduino. Then, when opening the IDE serial monitor, messages are displayed on the computer screen requesting specific user commands. Those messages ask the user to perform some specific actions using the radio control buttons to identify which channels are being used, the signal amplitude of each channel and the central point. All data are stored in the non-volatile memory (electrically erasable programmable read-only memory – EEPROM) when running the programme. Subsequently, the programme asks the user to rotate the RPA to identify the direction in which the MPU6050 was installed. All configurations saved are used by the other programmes and are not erased when a new code is uploaded to Arduino.

The second programme is used to test the radio communication, the balance of the propellers and the kinetic sensor. To use the sensor, the Arduino should be connected to the computer again and the programme uploaded with the IDE. In the serial monitor, the user can send a letter to the Arduino, requesting one of the aforementioned tests. The radio communication test is activated by sending the letter ‘r’ in the serial monitor. The current position of the controls and the function activated (acceleration, pitching, rolling, yawing) are shown in the monitor. Then, moving the radio controls should change the

values shown on the computer screen. The kinetic sensor test is activated by sending the letter 'a'. The computer screen shows the current orbital inclination of the RPA in degrees. The values of the orbital inclination displayed when the aircraft is levelled should be recorded because they will be subsequently used to calibrate the sensor. The propellers are balanced based on the vibration caused by the rotating propellers. Vibration impairs the stability of the aircraft during flight and therefore should be minimised. To use the aircraft, the propellers should be installed in the aircraft, the remote control turned on and the acceleration control set to the lowest level. With the battery connected to the RPA, a specific engine can be turned on by sending a number from 1 to 4 in the serial monitor. To increase the engine rotation, the RC accelerator should be used. The serial monitor displays the vibration perceived by the IMU. Adhesive tapes were placed to adjust the weight of each side of the propeller to reduce the vibration detected by the sensor. The first two programmes were run with the RPA connected to a computer, and the last programme was used to fly the aircraft. This programme was uploaded by connecting the Arduino to the computer and transferring the programme through the IDE, removing the connection cable after transferring the programme. The programme is run as soon as the battery connector is plugged in. The programme cyclically runs a proportional–integral–derivative (PID) controller for each axis of the aircraft, totalling three PID controllers. The controller of each axis is responsible for controlling the angle of the aircraft along that axis.

The programme consists of three steps that should be cyclically run and a fourth step that is sporadically run. When starting the programme, a configuration sequence runs only once. This sequence assesses whether the configuration programme was run correctly and calibrates the IMU. Data sent by the radio control sets the target aircraft orbital inclination and engine acceleration. Whenever the controller detects a change in the state of communication with the RC, an interrupt is generated, and the desired operation points of the RPA are updated. This operation is the sporadic step that occurs only when the user changes a command in the RC. The first step of the flight algorithm is to collect orbital inclination data and to compare them with the desired point. Then, those differences are used in three PID control algorithms, one for each Cartesian axis. Finally, the result from those operations is interpolated and sent as a control signal to turn the four engines on. The algorithm also includes sequences that limit the amplitude of the signals generated, settings to compensate for battery power loss, and locks in case any faults are detected. To analyse the results of this newly built RPA, a test flight was performed, visually comparing its flight stability with that of a commercial RPA.

RESULTS AND DISCUSSION

The final weight of this newly built RPA was 1.4 kg, at a total cost of \$ 412.66. The costs of the individual components are outlined in Table 1.

A GPS module and a telemetry radio are necessary for automatic flight. A GPS 6M sensor is capable of providing global positioning data to the RPA. The telemetry radio enables communication between the ground control station and the RPA. Both components are available on the Brazilian market. The GPS NEO-6M sensor costs approximately \$ 25.76, and a telemetry radio transmitter-receiver kit costs approximately \$ 38.64. The gimbal should be purchased according to the weight of the camera. A generic 2-axis gimbal for RPA is commercially available for approximately \$ 77.28.

The total price of the RPA prototype is \$412.66. RPAs with similar capabilities, such as the DJI Spark, Mavic and Phantom IV (DJI, Shenzhen, China) models in the Brazilian market range from \$ 772.81 to \$ 1,288.00. This difference of price of more than 50% between the prototype and the models available in the market, reintroduces the potential of the equipment under construction in this study. Other items that allow automatic flight modes can be installed in the drone, keeping the price below \$ 500.00.

The project of low cost drone was organized in several stages during one and a half year of development. Most of the time was taken during the research, design, programming and testing.

After arrival of all components, the complete assembly of the low cost RPA took 12 full hours including soldering of custom PCB divided in three workdays.

Table 1. Costs of the pieces for assembling the RPA

Parts	Amount	Value (\$)	Total (\$)
Engine1,100 KV	4	21.08	84.32
ESC 30 ^a	4	12.15	48.60
Battery 4S	1	66.00	66.00
Frame F450	1	24.03	24.03
Battery charger	1	21.35	21.35
Arduino nano	1	5.54	5.54
Radio control and receiver	1	108.29	108.29
MPU6050	1	3.43	3.43
Board PCB	1	2.64	2.64
Freight	-	32.34	32.34
Other expenses*	-	15.85	15.85
Total	-	-	412.66

* Expenses related to screws and fittings, wires, insulation tape, battery, weld and others.



Figure 2. Low-cost RPA prototype.

The calculated flight time was 13 minutes. A test performed with motors continuously connected to 50% of power showed that the prototype has an average autonomy of 14 minutes of flight. During the aircraft setup process, an orbital tilt of 2 degrees on the pitch axis was detected in the IMU. This slope has been corrected by changing a section of the flight code reserved for that purpose. During the RPA flight test, the aircraft took off successfully, showing that the engines chosen for this project

were of adequate size. By keeping the rolling, throwing and yaw controls in the center position, the aircraft remained level, thus proving that a stability control algorithm with a single PID axis controller can be used.

When moving the controls, the RPA responded to the commands, moving in the desired direction. In the current state, the algorithm run in the flight controller is only responsible for keeping the aircraft level. The pilot should constantly adjust the accelerator to keep the aircraft hovering at a specific altitude and should also compensate for the wind. This aspect of the flight mode makes piloting difficult for beginners, which is undesirable for the purpose of the aircraft.

During the code compilation, we observed that the flight control programme takes up 12104 bytes of memory, corresponding to 40% of the programme memory available in the Arduino Nano. The global variables take up 516 bytes, corresponding to 25% of the available dynamic memory. To avoid future expansion problems, a more powerful controller must be purchased. A promising controller is the Raspberry Pi, a small, inexpensive Unix-based computer (Torres et al., 2016). According to the manufacturer, the simplest version has a single-core 1 GHz processor and 512 MB of RAM.

An altitude hold algorithm should be implemented to avoid the need for adjusting the pilot acceleration. For this purpose, some type of sensor should be used to measure the aircraft altitude. A barometer can be installed to perform this function of measuring the aircraft altitude (Silva, 2013).

The RPA must also hold on the other horizontal axes, known as position hold. For this purpose, the RPA must know its global positioning somehow. Hold algorithms require higher sensor accuracy. Inertial models show a lot of noise, which causes drifting over time (Alexa, Nikolakopoulos & Tzes, 2012). This characteristic prevents its use in defining the local position of the aircraft. To avoid this effect, according to Kim et al. (2003), a GPS must be used to correct this deviation. Sensor fusion techniques can be used to integrate GPS, IMU and barometer data.

Lastly, a telemetry device will be necessary to allow communication between a ground control station and the aircraft. From this station, complex commands may be sent to the RPA, such as the trajectory, altitude and camera operation data. After implementing these changes, already predicted in the project, the aircraft will be able to perform image acquisition tasks for PA applications (Jorge & Inamasu, 2014).

These additional implementations will presumably make it possible to build an aircraft ready for flight at a final cost of \$ 679.00. This value is 60% lower than that found on the market for an aircraft capable of performing similar functions. Abade et al. (2016) built a UAV prototype for agricultural monitoring purposes at a final cost of \$ 1,242.00

The RPA is presently an optimal base to build a more complex and robust system and makes it possible to easily understand the dynamics involved in the control process, albeit without recording images. For such a purpose, a camera gimbal, a GPS module and a barometer must be installed. The installation of these additional components will overload the Arduino controller. The replacement of this controller by a more powerful one capable of performing operations faster and preferably in parallel should be studied. By introducing these modifications, the RPA may be used to map crops.

CONCLUSION

A low-cost RPA prototype capable of stably lifting off and hovering with potential for future agricultural monitoring applications was built. The final cost of the RPA was \$ 412.66. Because it is modular, various other functions can be implemented, and the RPA has a robust base for such purposes.

ACKNOWLEDGEMENTS. The authors thank, the Foundation for Research of the State of Minas Gerais (FAPEMIG), the National Council for Scientific and Technological Development (CNPq), the Coordination for the Improvement of Higher Education Personnel (CAPES), the Federal University of Lavras (UFLA) and University of Firenze (UniFI).

REFERENCES

- Abade, A., de Campos, M.D., Porto, L.F., de Farias Coelho, Y., de Moura Sousa, Y. & Nespolo, J.P. 2016. The Optimized Construction of a Drone for Applications in Agriculture and Precision Livestock. *Proceedings of the Regional Computer Science School of the Brazilian Computer Society (SBC) - Regional of Mato Grosso* **7**, pp. 1–10 (in Portuguese).
- Alexis, K., Nikolakopoulos, G. & Tzes, A. 2012. Model predictive quadrotor control: attitude, altitude and position experimental studies. *IET Control Theory & Applications* **6**(1), 1812–1827.
- Coveney, S. & Roberts, K. 2017. Lightweight UAV digital elevation models and orthoimagery for environmental applications: data accuracy evaluation and potential for river flood risk modelling. *International journal of remote sensing* **38**(8–10), 3159–3180.
- Department of Airspace Control (DECEA). Portaria DECEA nº 415/DGCEA, 9.11.2015. Available in: <<http://publicacoes.decea.gov.br/?i=publicacao&id=4262>>. Accessed in: 2.10.2017
- DJI Store. Available in: <<https://store.dji.com/>>. Accessed in: 04.17. 2018.
- ECalc. The most reliable electric Motor Calculator on the web. Available in: <<https://ecalculator.com/>>. Accessed in: 04.05 2017.
- Feng, Q., Liu, J. & Gong, J. 2015. UAV remote sensing for urban vegetation mapping using random forest and texture analysis. *Remote sensing* **7**(1), 1074–1094.
- Gago, J., Douthe, C., Coopman, R.E., Gallego, P.P., Ribas-carbo, M., Flexas, J., Escalona, J. & Medrano, H. 2015. UAVs challenge to assess water stress for sustainable agriculture. *Agricultural Water Management* **153**, 9–19. doi: <https://doi.org/10.1016/j.agwat.2015.01.020>
- Huang, Y., Thomson, S.J., Hoffmann, W.C., Lan, Y., & Fritz, B.K. 2013. Development and prospect of unmanned aerial vehicle technologies for agricultural production management. *Int. J. Agric. & Biol. Eng.* **6**(3), 1–10. doi:10.3965/j.ijabe.20130603.001
- Ibrahim, J.T., Waskitho, N.T., Wahono, W. & Ma'mun, S.R. 2017. Survey of irrigation area using micro unmanned aerial vehicle (micro-uav) in gumbasa irrigation area. *Agricultural Socio-Economics Journal* **17**(1), 1–5.
- Jorge, L.A de C. & Inamasu, R.Y. 2014. Use of unmanned aerial vehicle (UAV) in precision agriculture. In Bernardi, A.D.C., Naime, J.D.M., Resende, A.D., Inamasu, R.Y., Bassoi, L. *Precision Agriculture: Results of a New Look*. Embrapa Instrumentation-Tecnical book (INFOTECA-E), Brasilia, pp. 109–134 (in Portuguese).
- Kim, J.H. & Sukkarieh, S., Wishart, S. 2016. Real-Time Navigation, Guidance, and Control of a UAV Using Low-Cost Sensors. In: Yuta, S., Asama, H., Prassler, E., Tsubouchi, T., Thrun, S. (eds) *Field and Service Robotics. Springer Tracts in Advanced Robotics*, Springer, Berlin, Heidelberg, pp. 299–309

- Nex, F. & Remondino, F. 2014. UAV for 3D mapping applications: a review. *Applied Geomatics* **6**(1), 1–15. doi: <https://doi.org/10.1007/s12518-013-0120-x>
- Nonami, K., Kendoul, F., Suzuki, S., Wang, W. & Nakazawa, D. 2010. Autonomous Flying Robots. *Unmanned Aerial Vehicles and Micro Aerial Vehicles*. Springer. Tokyo New York, 328 pp.
- Romero-Trigueros, C., Nortes, P.A., Alarcón, J.J., Hunink, J.E., Parra, M., Contreras, S., ... & Nicolás, E. 2017. Effects of saline reclaimed waters and deficit irrigation on Citrus physiology assessed by UAV remote sensing. *Agricultural Water Management* **183**, 60–69.
- Segales, A., Gregor, R., Rodas, J., Gregor, D. & Toledo, S. 2016. Implementation of a low cost UAV for photogrammetry measurement applications. In *Unmanned Aircraft Systems (ICUAS)*, Arlington, VA. pp. 926–932.
- Silva, Leonam Peçly da. 2013. Design and construction of a remotely piloted quadricopter and its attitude control and determination system. Instituto Federal Fluminense, Campos dos Goytacazes, 107 pp.
- Torres, A.B.B., Rocha, A.R. & DE Souza, J.N. 2016. Performance analysis of mqtt brokers in low cost system. In: *Proceedings of the XXXVI Congress of the Brazilian Computer Society. Brazilian Society of Computation*. Porto Alegre, Brazil (in Portuguese).

Development of intelligent system of mobile robot movement planning in unknown dynamic environment by means of multi-agent system

A. Nemeikšis and V. Osadčuks

Latvia University of Life Sciences and Technologies, Faculty of Engineering,
5 J. Cakstes blvd., Jelgava LV-3001, Latvia

*Correspondence: nemeiksis.andrius@llu.lv; vitalijs.osadcuks@llu.lv

Abstract. Through the ages the world has conceived the projects which are aimed at creating diverse models of robots that would be beneficial for exploration of different dangerous surfaces where human participation is excluded. Therefore, the main task of the study of this article is to develop the researches, the object of which is mobile robot movement in unfamiliar environment, based on multi agent apparatus system and neural networks. The aim of the research is to develop methods for creating intellectual systems for planning mobile robot movement in unfamiliar environment applying the methods of multi agent apparatus and neural networks ensuring the robot executes the planned and adjusted on the way safe trajectory in an environment with unknown obstacles. Accordingly, the entire study of the article is based on a two-stage process. The first stage involves determination of distance between the robot and the obstacles in its operating area as well as classification of the possible location of obstacles, based on the information received from distance sensors, using the model of multilayer neural networks. During the second stage bypassing obstacles, wall tracking, movement-to-destination as well as speed management agents are developed. As the result of the study, a method was suggested for creating neural network model for classification of environment into agents and their consistent switching, which, according to the classification table compiled, involves all the possible locations of obstacles occurring on the robot's movement trajectory and allows reducing the number of unfamiliar environment situations that are necessary to identify.

Key words: multi-agent system, unknown environment, neural network, dynamic obstacles, planned track.

INTRODUCTION

For neural network training, scientists have been determining various robot's target positions provided movement strategies the neural network was taught under conditions of certain environment could be easily adjusted in a new dynamic environment. In the event of moving obstacles in the robot's operation zone, robot could avoid collision only when the speed of moving obstacles allowed the robot to stop and respond in a timely manner. The probability of the moving robot colliding into obstacles increased also because ultrasound distance sensors could not recognise their sharp edges. For this reason, during their experiments, scientists positioned obstacles with polished edges in

the robot's operation area at the same time recognising the necessity to improve the structure of sensors (Panigrahi & Sahoo, 2014; Ko et al., 2017).

The neural network model was directly used for trajectory formation. The space for neural network states was defined by the robot configuration space, and each neuron was described by a respective movement equation. This model allowed implementing real-time multi-target planning of robot's movement, including planning under the conditions of unpredictable changes in the environment. This process is based on variable activity of the neural network reflecting the instability of the environment. Determining the direction of robot's safe movement did not require optimising energy, advance information on dynamic environment, nor training. The complexity of the calculations had a linear dependence on the size of the neural network, where each neuron had only a local lateral relationship with neighbouring neurons (Cardenas et al., 2013; Kagan et al., 2016; Luo, 2017).

Thus, the study performed in this article is aimed at developing this area of robotics and analysing the development of an intelligent system for planning mobile robot movement in an unknown dynamic environment using multi-agent system with neural networks in more detail, which could be defined as the subject of the study. The article studies the intelligent system the essence of which lays in the combination of the possibilities offered by fuzzy system and neural networks, and the robot in question has the main structure composed of four fuzzy blocks intended for different agents. The study in the article is limited, on one side, to the analysis of a neural network as a component of an intelligent planning system used for simulating the developed classification of the positions of unknown obstacles in the robot's operation area and for switching the agents of obstacle circumvention, wall tracking, and movement towards the target, and, on the other side, analyses the method of developing an intelligent system which is based on a two-stage robot and its environment information processing system. Also, the study assesses the advantages of the combined neural networks and multi-agent method, and the accuracy of its application in an unknown dynamic environment.

MATERIALS AND METHODS

The intelligent system for planning mobile robot movement in an unknown dynamic environment using a multi-agent system is based on processing the information concerning the robot and the surrounding unknown dynamic environment with a help of two-stage process. The structure of this system is presented in Fig. 1.

During the first stage of planning, the distance (d_{st}) between the robot and the obstacles located in its operating area as well as the safe distance (d_{safe}) are established; also, the possible position of obstacles is classified based on the information from ultrasound and infra-red distance sensors with their model being in a form of a multi-layer neural network trained using the method of error back propagation in autonomous mode).

During the second stage, obstacle-bypass, wall-tracking, movement-to-destination and speed control agents are developed using fuzzy blocks.

The intelligent system for planning mobile robot movement (Fig. 1) is composed of five agents. Beside the four agents, i.e. obstacle-bypass, wall-tracking, movement-to-destination and speed control, one more – safety agent – is used to ensure the mobile robot does not collide into obstacles while moving. Safety agent gives the STOP

command and stops the robot when an obstacle occurs on the robot's movement trajectory in the so-called 'safety zone' ($d_{safe} = 0.10$ m). Safety agent has the highest degree of priority.

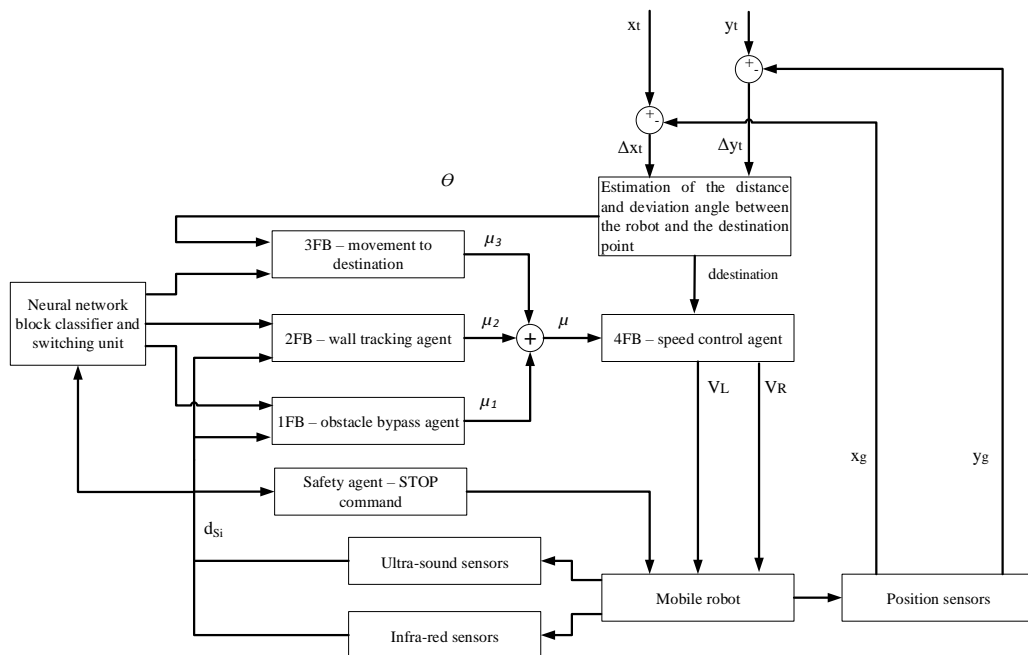


Figure 1. Intelligent system for planning mobile robot movement in an unknown dynamic environment using multi-agent system.

Development of a neural network for classification and switching of environment situations

Development of a neural network intended for simulating classification and switching of the situations related with the mobile robot movement starts from defining the situations. Classification of different situations involves systemization through each iteration of the position of unknown obstacles in the operating area and corresponding robot movement directions. Agent switching depend on the ultra-sound sensor signals.

To solve this task, operation zone of distance sensors (ultra-sound and infra-red sensors) is divided into 3 zones, as presented in the Fig. 2:

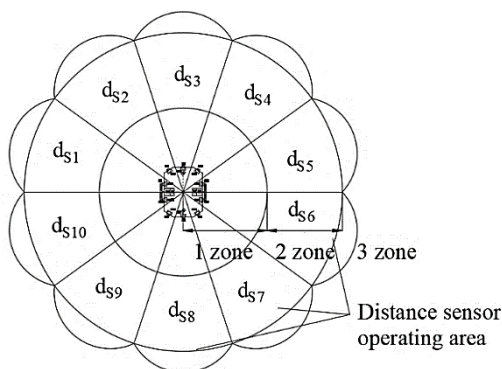


Figure 2. Three zones of distance sensors (ultra-sound and infra-red sensors) operation area.

Zone 1 – safe zone defined by the safe distance d_{safe} (0.3 m). The safe zone does not play any role in the process of neural network classification.

Zone 2 – active detection zone restricted by 0.3 to 4 m with respect to ultra-sound sensors, and 0.3 to 0.7 m with respect to infra-red sensors.

Zone 3 – distant zone, where the distance to the obstacle is more than 4 m or 0.7 m.

Information from sensors represents one of the three situations marked by numbers 0, 1, 2, which mean:

‘0’ – no obstacles, i.e. they are in zone 3, and does not get into zone of distance sensor operation area;

‘1’ – detects any obstacle inside the zone 2;

‘2’ – irrelevant, which means there are no obstacles or they are located in zone 3.

Figs 3, 4 and 5 presents classification of the possible obstacle position in the movement-to-destination, wall-tracking and obstacle-bypass agents respectively.

Circles located on the left, in the front of, and on the right to the mobile robot mark the obstacles. Individual circles can mark both individual obstacles and a group of obstacles.

The movement-to-destination agent is activated when no obstacle is detected by the sensors US2-IR2, US3-IR3, US4-IR4 or US7-IR7, US8-IR8, US9-IR9, and no obstacle is at the same time detected by the sensors located on the same side (US1-IR1, US10-IR10 or US5-IR5, US6-IT6) (Fig. 3).

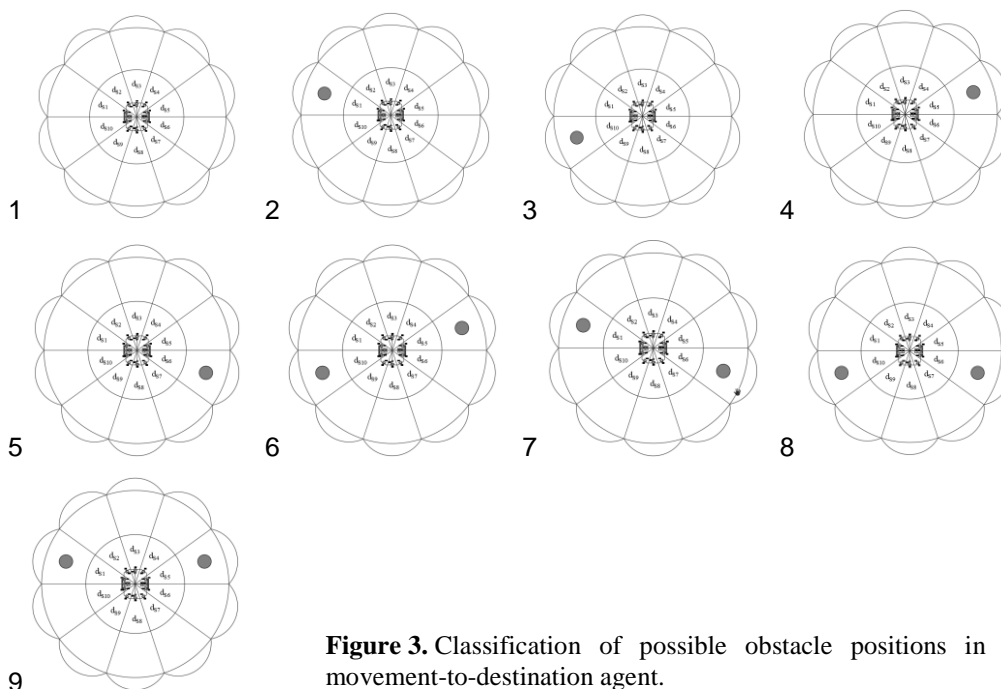


Figure 3. Classification of possible obstacle positions in the movement-to-destination agent.

The wall-tracking agent is activated when no obstacle is detected by the sensors US2-IR2, US3-IR3, US4-IR4 or US7-IR7, US8-IR8, US9-IR9, but obstacles are detected by the sensors located on the same side (US1-IR1, US10-IR10 or US5-IR5, US6-IT6).

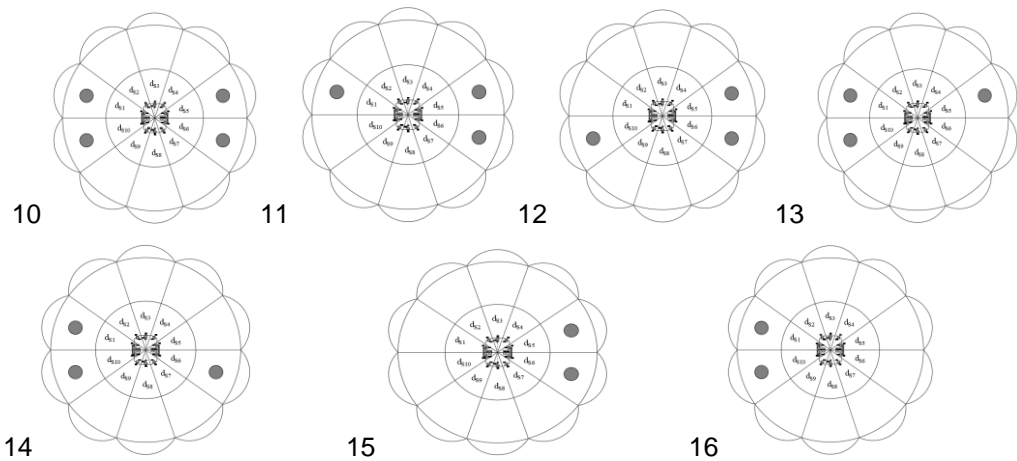


Figure 4. Classification of possible obstacle positions in the wall-tracking agent.

Obstacle-bypass agent is set up when one of the sensors US2-IR2, US3-IR3, US4-IR4 or US7-IR7, US8-IR8, US9-IR9 detects an obstacle.

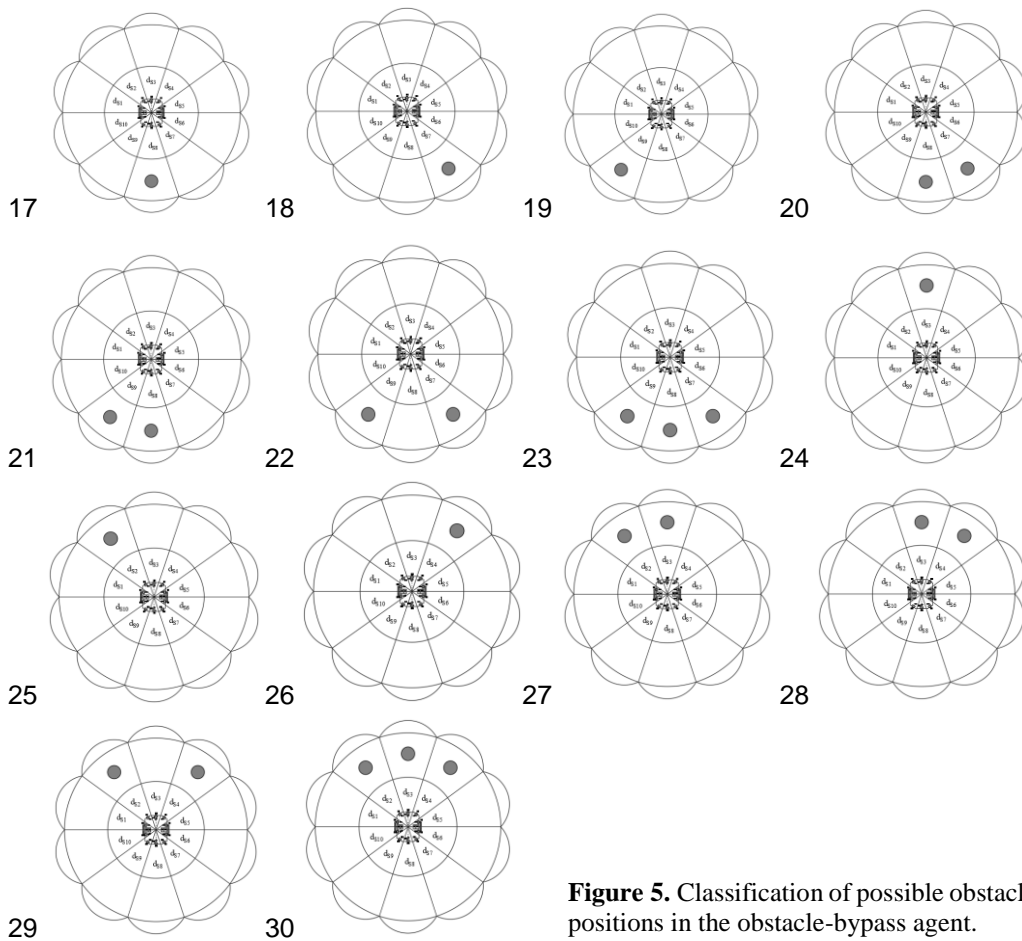


Figure 5. Classification of possible obstacle positions in the obstacle-bypass agent.

The classification of the positions of unknown dynamic obstacles for mobile robot presented in the present article covers 30 possible variants of situations. The detailed classification table contains 30 positions describing possible mobile robot movement in the operation zone and the situations of the related decisions made during each iteration during the planning process.

The detailed classification table model outputs are agents which are marked by numbers: 1 – obstacle-bypass, 2 – wall tracking, 3 – movement to destination.

Table 1. Classification of obstacles and agents

Type	d _{S10}	d _{S1}	d _{S2}	d _{S3}	d _{S4}	d _{S5}	d _{S6}	d _{S7}	d _{S8}	d _{S9}	Agent
1	0	0	0	0	0	0	0	0	0	0	Movement to destination
2	0	1	0	0	0	0	0	0	0	0	Movement to destination
3	1	0	0	0	0	0	0	0	0	0	Movement to destination
4	0	0	0	0	0	1	0	0	0	0	Movement to destination
5	0	0	0	0	0	0	1	0	0	0	Movement to destination
6	1	0	0	0	0	1	0	0	0	0	Movement to destination
7	0	1	0	0	0	0	1	0	0	0	Movement to destination
8	1	0	0	0	0	0	1	0	0	0	Movement to destination
9	0	1	0	0	0	1	0	0	0	0	Movement to destination
10	1	1	0	0	0	1	1	0	0	0	Wall tracking
11	2	1	0	0	0	1	1	0	0	0	Wall tracking
12	1	2	0	0	0	1	1	0	0	0	Wall tracking
13	1	1	0	0	0	1	2	0	0	0	Wall tracking
14	1	1	0	0	0	2	1	0	0	0	Wall tracking
15	2	2	0	0	0	1	1	0	0	0	Wall tracking
16	1	1	0	0	0	2	2	0	0	0	Wall tracking
17	0	0	0	0	0	0	0	2	1	2	Obstacle bypass
18	0	0	0	0	0	0	0	1	2	2	Obstacle bypass
19	0	0	0	0	0	0	0	2	2	1	Obstacle bypass
20	0	0	0	0	0	0	0	1	1	2	Obstacle bypass
21	0	0	0	0	0	0	0	2	1	1	Obstacle bypass
22	0	0	0	0	0	0	0	1	2	1	Obstacle bypass
23	0	0	0	0	0	0	0	1	1	1	Obstacle bypass
24	2	2	2	1	2	2	2	2	2	2	Obstacle bypass
25	2	2	1	2	2	2	2	2	2	2	Obstacle bypass
26	2	2	2	2	1	2	2	2	2	2	Obstacle bypass
27	2	2	1	1	2	2	2	2	2	2	Obstacle bypass
28	2	2	2	1	1	2	2	2	2	2	Obstacle bypass
29	2	2	1	2	1	2	2	2	2	2	Obstacle bypass
30	2	2	1	1	1	2	2	2	2	2	Obstacle bypass

The neural network consists of two hidden layers and one output layer. The first hidden layer covers 10 neurons, while the second covers 6, and the output layer contains 3 neurons. The proposed structure of neural network is trained using the method of error back-propagation, and the calculations for the error back-propagation method to train the neural network are expressed by the following equations:

Output layer (1):

$$\delta_k(i) = (y_{dk}(i) - O_k(i)) \cdot f'(net_k) \quad (1)$$

$$f'(net_k) = 1$$

Neural network output layer uses linear activation function (Khnessi et al., 2018; Wang et al., 2018) (2; 3):

$$\delta_k(i) = (\delta_{dk}(i) - O_k(i)) \quad (2)$$

$$w_{kh}(i) = \eta \cdot \delta_k(i) \cdot O_h(i) \quad (3)$$

The second hidden layer (4):

$$\delta_k(i) = (1 - O_h^2(i)) \sum_k \delta_k(i) \cdot w_{kh}(i) \quad (4)$$

$$w_{kh}(i) = \eta \cdot \delta_h(i) \cdot O_j(i)$$

The first hidden layer (5):

$$\delta_j(i) = (1 - O_j^2(i)) \sum_h \delta_h(i) \cdot w_{hj}(i) \quad (5)$$

$$w_{jm}(i) = \eta \cdot \delta_j(i) \cdot O_m(i)$$

New weight matrix value (6; 7; 8):

$$w_{kh}(i + 1) = w_{kh}(i) + \Delta w_{kh}(i) + \alpha \cdot \Delta w_{kh}(i - 1) \quad (6)$$

$$w_{hj}(i + 1) = w_{hj}(i) + \Delta w_{hj}(i) + \alpha \cdot \Delta w_{hj}(i - 1) \quad (7)$$

$$w_{jm}(i + 1) = w_{jm}(i) + \Delta w_{jm}(i) + \alpha \cdot \Delta w_{jm}(i - 1) \quad (8)$$

During the first iteration (i = 1) (9; 10; 11):

$$\Delta w_{kh}(i - 1) = 0 \quad (9)$$

$$\Delta w_{hj}(i - 1) = 0 \quad (10)$$

$$\Delta w_{jm}(i - 1) = 0 \quad (11)$$

where $\delta_k(i)$ – is the error propagated in the k^{th} neuron of the output layer; $y_{dk}(i)$ – normalized desired neural network output; $\Delta w_{kh}(i)$ – updated matrix values of the weights between the output and the second hidden layer; η – training speed coefficient; α – inertia coefficient; $\Delta w_{kh}(i - 1)$ – previous weight matrix value update; $\Delta w_{kh}(i + 1)$ and $\Delta w_{kh}(i)$ – new and current values of the weight matrix; $y_h(i)$ – propagated error in the second hidden layer; $\Delta w_{hj}(i)$ – updated matrix values of the weights between the second hidden and the first hidden layers; $\Delta w_{hj}(i - 1)$ – previous weight matrix value update; $\Delta w_{hj}(i + 1)$ and $\Delta w_{hj}(i)$ – new and current values of the weight matrix; $\delta_j(i)$ – propagated error in the second hidden layer; $\Delta w_{jm}(i)$ – updated matrix values of the weights between the second hidden and the first hidden layers; $\Delta w_{jm}(i - 1)$ – previous weight matrix value update; $\Delta w_{jm}(i + 1)$ and $\Delta w_{jm}(i)$ – new and current values of the weight matrix (Zhao & Wang, 2018; Dewi et al., 2017; Omrane et al., 2017).

The model of classification and agent behaviour determination model on the basis of neural network involve three stages. During the first stage, mobile robot movement is replaced by codes according to the classification variants: 0, 1, 2. An encoding unit was developed to implement this process.

During the second stage, the encoded parameters get into the multilayer perceptron of the multilayer network. Finally, during the third stage, the outputs of neural network are the variables 1, 2 and 3, which mark the respectively obstacle-bypass, wall-tracking, and movement-to-destination agents. These are used in the process of dynamic switching of agent fuzzy blocks.

RESULTS AND DISCUSSION

Based on the information from the distance sensors (ultra-sound and infra-red sensors), neural network classifies the operating area located in a complex environment based on three specific situations by three respective agents: obstacle-bypass, wall-tracking, and movement-to-destination. Taking into account the current situation of the environment, neural network switches and activates one specific agent. Later, using the fuzzy blocks 1FB, 2FB and 3FB (to determine the mobile robot rotation angle μ_1, μ_2, μ_3 in the respective obstacle- bypass, wall-tracking and movement-to-destination agents) and 4FB (to control the $V_{average} = 0.2343 \text{ m s}^{-1}$ speed), the neural-fuzzy system performs the task with the selected agent. Thus, during the process of planning mobile robot movement, agents are being constantly switched to other agents, and the movement trajectory is a combination of movement sub-trajectories in agents.

Simulation of an intelligent system for planning mobile robot movement in an unknown dynamic environment using multi-agent system involves four pilot testings.

During the first testing, mobile robot moves from the starting point A ($x_1 = 2 \text{ m}$; $y_1 = 1 \text{ m}$) to the destination point B ($x_2 = 6 \text{ m}$; $y_2 = 4 \text{ m}$) Fig. 6.

Dynamic obstacle moves past the robot and affect its movement towards the destination (Fig. 6). After 464 iterations of the program (the set time is 11.95 s) the mobile robot reached the destination without colliding with a dynamic obstacle.

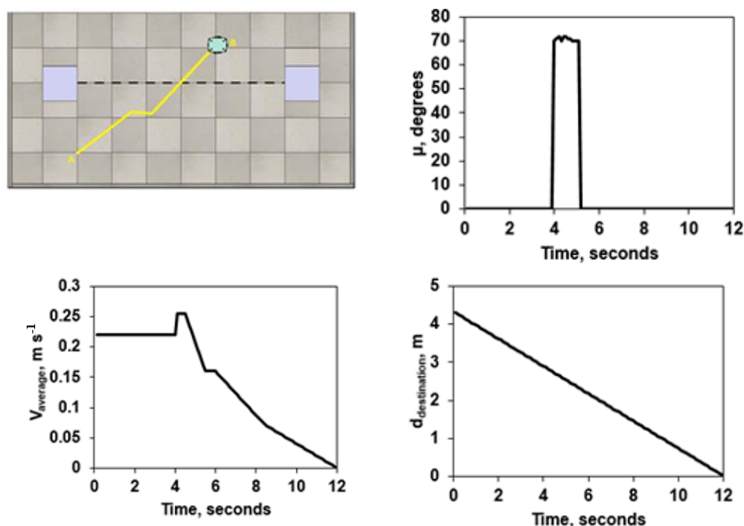


Figure 6. Results of the testing of the intelligent system for planning mobile robot movement in an unknown dynamic environment.

Variations of the mobile robot parameters – rotation angle μ , mobile robot average velocity $V_{average}$, distance between the robot and the destination point $d_{destination}$ – are presented by diagrams in the Fig. 6. At first, robot moves forward towards the destination and the angle μ remain the same (equal to 0) until the distance sensors US2-IR2, US3-IR3, US4-IR4 or US7-IR7, US8-IR8, US9-IR9 detects a dynamic obstacle. Value μ changes rapidly and substantially with the help of 1FB, which is dedicated to bypass the moving obstacle. Later, the value of μ decreases to zero and remains unchanged.

When using the fuzzy block 1FB, the average velocity $V_{average}$ of the mobile robot remains stable, and reduces to zero after circumventing the obstacle. The distance between the robot and the destination point $d_{destination}$ also is approaching zero.

During the second testing, mobile robot was moving in the operating area with the obstacle being the surface of a wall, from the starting point A($x_1 = 6$ m; $y_1 = 4$ m) to the destination point B ($x_2 = 3$ m; $y_2 = 0.5$). After 1,389 iterations of the program (over 33.79 s) the mobile robot reached the destination point. Mobile robot movement trajectory and variations of the mobile robot parameters – rotation angle μ_3 , mobile robot average velocity $V_{average}$, distance between the robot and the destination point $d_{destination}$ – during the second testing are presented in the Fig. 7.

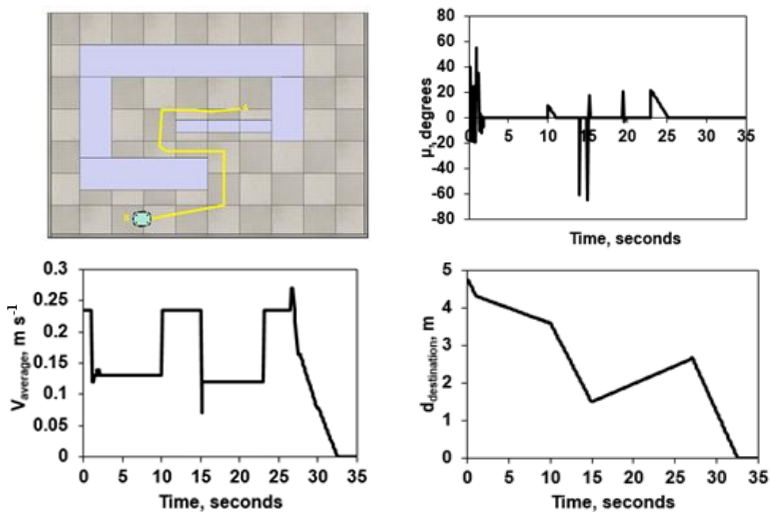


Figure 7. Results of the second testing of the intelligent system for planning mobile robot movement in an unknown environment.

During the third testing, mobile robot was moving from the starting point A($x_1 = 5$ m; $y_1 = 4$ m) to the destination point B ($x_2 = 2$ m; $y_2 = 0.5$ m). After 1,574 iterations of the program (the set time is 38.31 s) the robot reached the destination without colliding with a dynamic obstacle. Variations of the robot trajectory and the mobile robot parameters – rotation angle μ , mobile robot average velocity $V_{average}$, distance between the robot and the destination point $d_{destination}$ – based on the results of the third testing are presented in the Fig. 8.

During the fourth testing, mobile robot was moving from the starting point A($x_1 = 5$ m; $y_1 = 4$ m) to the destination point B ($x_2 = 2$ m; $y_2 = 0.5$ m). In the operating area, there were a wall and one dynamic obstacle, which affected the robot's moving

trajectory. After 1482 iterations of the program (the set time is 36.29 s) the mobile robot reached the destination without colliding with a dynamic obstacle. Variations of the robot trajectory and the mobile robot parameters – rotation angle μ , mobile robot average velocity $V_{average}$, distance between the robot and the destination point $d_{destination}$ – based on the results of the fourth testing are presented in the Fig. 9.

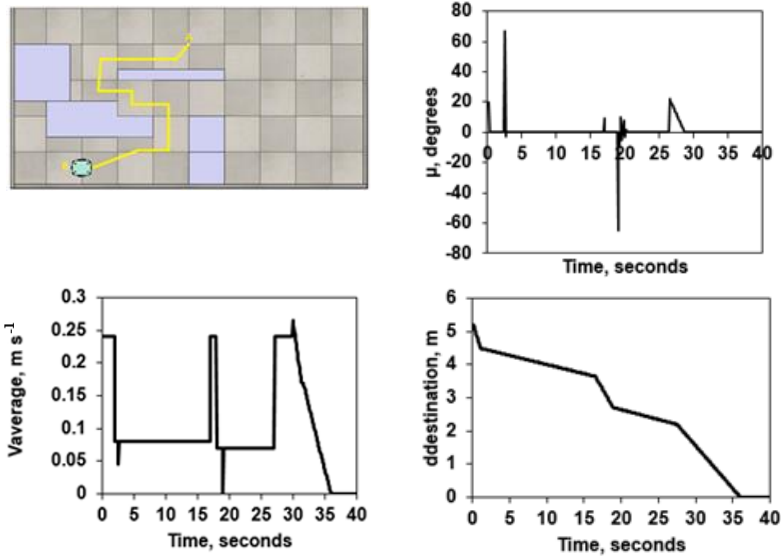


Figure 8. Results of the third testing of the intelligent system for planning mobile robot movement in an unknown environment.

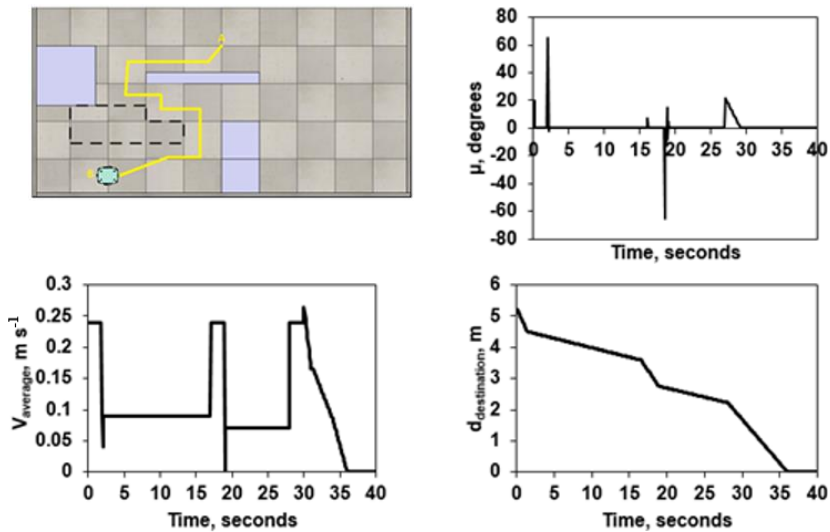


Figure 9. Results of the fourth testing of the intelligent system for planning mobile robot movement in an unknown environment.

CONCLUSIONS

Based on the simulation performed in this article and the analysis of the obtained results, the following conclusions can be made:

Moving in an unknown environment mobile robot performs three tasks: circumvent obstacles, tracks wall, and moves towards the destination point. Therefore, a combination of four fuzzy blocks dedicated to different agents was offered as a method of developing an intelligent system for planning the real-time mobile robot movement in an unknown dynamic environment. The first three blocks, according to the behaviour of each agent, perform the preliminary estimation of the robot's rotation angle in the direction of the surrounding obstacles. The fourth block deals with the problem of how to prevent collision of the robot with unknown dynamic obstacles located in the operating area. The computer simulation shows that the mobile robot managed to reach the destination point in all the situations.

A neural network, as a component of the intelligent planning system, was used for simulation of the developed classification of unknown obstacles in the robot's operating area and switching the obstacle-bypass, wall-tracking, and movement-to-destination agents.

The presented method of developing the intelligent system for planning robot movement in an unknown dynamic environment is based on the two-stage process of processing the information about the robot and its environment in order to plan a safe trajectory. The first stage involves determination of the distance between the robot and the obstacles located in its operating area, and classification of the possible positions of obstacles based on the information from the distance sensors using the model of multi-layer neural network. During the second stage, obstacle-circumvention, wall-tracking, movement-to-destination and speed control agents are developed. Based on the results obtained during the first stage, the value of the mobile robot rotation angle μ is determined. Mobile robot rotation angle and the distance between the robot and the destination point are the inputs of the fourth fuzzy block. Outputs – controlled gear signals, which enable the robot to avoid collisions with unknown obstacles and reach the destination point.

This method applied to mobile robots allows the following:

- simplify the analysis of the dynamic environment, dividing the environment into a few simple and specific situations;
- take into account each specific situation in the operation area and position of the obstacles around the robot during every iteration;
 - reduce the number of the fuzzy planning system input parameters;
 - successfully avoid collision of the robot with the unknown obstacles and reach the destination point with high accuracy.

REFERENCES

Cardenas, A.M., Rázuri, J.G., Sundgren, D. & Rahmani, R. 2013. Autonomous Motion of Mobile Robot Using Fuzzy-Neural Networks. In: *2013 12th Mexican International Conference on Artificial Intelligence*. Mexico City, Mexico, pp. 80–84.

- Dewi, T., Risma, P., Oktarina, Y. & Roseno, M.T. 2017. Neural network controller design for a mobile robot navigation; A case study. In: *2017 4th International Conference on Electrical Engineering, Computer Science and Informatics (EECSI)*, Yogyakarta, Indonesia, pp. 1–5.
- Kagan, E., Rybalov, A. & Ziv, H. 2016. Uninorm-based neural network and its application for control of mobile robots. In: *2016 IEEE International Conference on the Science of Electrical Engineering (ICSEE)*. Eilat, Israel, pp. 1–5.
- Khnissi, K., Seddik, C. & Seddik, H. 2018. Smart Navigation of Mobile Robot Using Neural Network Controller. In: *2018 International Conference on Smart Communications in Network Technologies (SaCoNeT)*. El Oued, Algeria, pp. 205–210.
- Ko, B.S., Choi, H.J., Hong, C., Kim, J., Kwon, O.C. & Yoo, C.D. 2017. Neural network-based autonomous navigation for a homecare mobile robot. In: *2017 IEEE International Conference on Big Data and Smart Computing (BigComp)*, Jeju, South Korea, pp. 403–406.
- Luo, C. 2017. Neural-network-based fuzzy logic tracking control of mobile robots. In: *2017 13th IEEE Conference on Automation Science and Engineering (CASE)*. Xi'an, China, pp. 1318–1319.
- Omrane, H., Masmoudi, M.S. & Masmoudi, M. 2017. Intelligent mobile robot navigation. In: *2017 International Conference on Smart, Monitored and Controlled Cities (SM2C)*, Sfax, Tunisia 2017, pp. 27–31.
- Panigrahi, P.K. & Sahoo, S. 2014. Navigation of autonomous mobile robot using different activation functions of wavelet neural network. In: *International Conference for Convergence for Technology-2014*. Pune, India, pp. 1–6.
- Wang, H., Duan, J., Wang, M., Zhao, J. & Dong, Z. 2018. Research on Robot Path Planning Based on Fuzzy Neural Network Algorithm. In: *2018 IEEE 3rd Advanced Information Technology, Electronic and Automation Control Conference (IAEAC)*. Chongqing, China, pp. 1800–1803.
- Zhao, T. & Wang, Y. 2018. A Neural Network Based Mobile Robot Autonomous Tracking System. In: *SoutheastCon 2018*. St. Petersburg, FL, USA, pp. 1–2.

Pericarp of colored-seeded common bean (*Phaseolus vulgaris* L.) varieties a potential source of polyphenolic compounds

R. Nurzyńska-Wierdak, H. Łabuda, H. Buczkowska* and A. Sałata

University of Life Sciences in Lublin, Faculty of Horticulture and Landscape Architecture, Department of Vegetable Crops and Medicinal Plants, Akademicka 15, PL20-950 Lublin, Poland

*Correspondence: halina.buczkowska@up.lublin.pl

Abstract. Bioactive substances produced by plants are defined as secondary metabolites causing different pharmacological effects in human organism. Various plant raw materials, some known as vegetables or spices, are their source. Pericarp of white-seeded common bean varieties is a pharmacopoeial product traditionally used as an antidiabetic agent. The object of this study was to evaluate the biological value of pericarp of colored beans (cultivars: ‘Małopolanka’, ‘Nida’, ‘Rawela’, ‘Tip Top’, and ‘Nigeria’) compared to the reference white-seeded cultivar (‘Laponia’). Bean pericarp was characterized by a high level of polyphenolic compounds and antioxidant activity. Its phenolic acid content (expressed as caffeic acid equivalents) was at a similar level, at least 0.1 mg g⁻¹ (0.01%). The highest amount of flavonoids was accumulated by the cultivars with dark blue and black seeds, respectively 0.138 and 0.139 mg g⁻¹ DW, as well as by the white-seeded cultivar (0.132 mg g⁻¹ DW). The highest antioxidant activity (AA) was found for bean extracts of the cultivars ‘Laponia’ and ‘Małopolanka’, respectively 12.35 and 12.10%. Phenolic acid content was significantly positively correlated with AA of the bean extracts tested. This study indicates that pericarp of the colored-seeded bean cultivars is characterized by high biological value and can be used as a source of polyphenolic compounds.

Key words: *Phaseoli pericarpium*, phenolic acids, flavonoids, tannins, DPPH.

INTRODUCTION

Leguminous plants are a good source of starch, dietary fiber, protein, and minerals as well as of bioactive substances. Legumes that are most frequently consumed in the world include bean (*Phaseolus vulgaris*), chickpea (*Cicer arietinum*), lentil (*Lentis esculenta*), pea (*Pisum sativum*), faba bean (*Vicia faba*), peanut (*Arachys hipogea*), and soybean (*Glycine max*) (Sánchez-Chino et al., 2015; Bitocchi et al., 2017). The common bean (*Phaseolus vulgaris* L.), which is also known for its health-promoting effects, is a widely used component of many traditional diets (Madhujith et al., 2004; Sánchez-Chino et al., 2015). Evangelho et al. (2016) report that protein hydrolysates extracted from black beans can be used in specialized diets as valuable protein components with high antioxidant activity and high digestibility. Numerous studies have shown that common bean polyphenols have various effects on human health, exhibiting antimutagenic, antimicrobial, antidiabetic, and anti-inflammatory activities (Yang et al., 2018). The common bean is a very diverse species in terms of its morphological and biochemical

characteristics (Stoilova et al., 2005; Bozoglu & Sozen, 2011). Bean populations with different seed form, weight and color also show a varying level of polyphenols: anthocyanins, phenolic acids, and flavonoids (Zhao et al., 2014; García-Díaz et al., 2018; Armendáriz-Fernández et al., 2019). The color of bean flowers and seeds is associated with the presence of polyphenolic compounds, mainly flavonoids such as flavonic glycosides, anthocyanins, and condensed tannins, but the presence of anthocyanins has only been found in black and blue-violet beans (Reynoso-Camacho et al., 2006). The seed coat color not only defines and characterizes a specific bean variety, but also provides protection against seed pathogens (Armendáriz-Fernández et al., 2019). Scientific research links the antioxidant activity of beans to the presence of polyphenols (Akond et al., 2011; Hanis et al., 2017; Silva et al., 2018; Armendáriz-Fernández et al., 2019). Beninger et al. (2003) demonstrated that anthocyanins, glycosides, quercetins, and proanthocyanidins present in the seed coat of common bean exhibit significant antioxidant activity. These authors suggest that the antioxidant activity of the studied extracts can be due to the presence of condensed tannins. Akond et al. (2011) proved that bean genotypes rich in anthocyanins and other polyphenols show strong antioxidant activity, while the content of the above-mentioned compounds is generally higher in dark-seeded varieties than in light-seeded ones. The studies by Madhujith et al. (2004) and Oomah et al. (2010) indicated that beans, particularly those with colored seed coats, exhibit strong antioxidant activity, which is contributed by tannins and other phenolic compounds, formerly classified as non-nutritional factors. Likewise, Dzomba et al. (2013) evaluated that dark-seeded varieties are characterized by stronger antioxidant activity than light-seeded ones. When studying the antioxidant and antiproliferative activity of polyphenolic extracts derived from seeds of old endemic bean (*Phaseolus vulgaris*) varieties grown in southern Italy, Ombra et al. (2016) demonstrated that colored (spotted, red, and black) varieties are more active than non-pigmented ones.

Common bean pericarp (*Phaseoli pericarpium*) is a pharmacopoeial product with a high level of active substances (Łabuda et al., 2017), which is traditionally used as an antidiabetic agent (Helmstädter, 2010). A bean pod extract shows hypoglycemic and hypolipidemic activity, and also prevents fatty acid changes during diabetes (Pari & Venkateswaran, 2004). Berbecaru-Iovan et al. (2016) revealed that administration of ethanol extract of bean pericarp to rats with diabetes resulted in reduced blood glucose and cholesterol. Application of this extract had a significant antioxidant effect at reduced lipid peroxidation, which suggests its protective role probably associated with the presence of polyphenols. Bean extracts are nowadays perceived as promising agents in treatment of metabolic diseases: obesity and diabetes (Carai et al., 2009; Wu et al., 2010; Carai et al., 2011). Their potential importance as protective and preserving agents is also emphasized. *Parkia speciosa* Hassk., a tropical perennial plant of the Fabaceae family called bitter bean, is an edible and medicinal plant known in south Asia; its pods with beans have antioxidant activity, while pericarp extracts are reported to be antioxidant and hypotensive agents (Ko et al., 2014). Compared to an antibiotic, extracts from *Parkia speciosa* pods exhibit strong antioxidant activity and also noticeable antimicrobial activity against foodborne disease-causing bacteria (Gram-positive and Gram-negative ones) as well as against food spoilage causing bacteria (Wonghirundecha et al., 2014). The results obtained by Ko et al. (2014) indicate that gallic acid, catechin, ellagic acid, and quercetin can be the main polyphenolic constituents contributing to the strong antioxidant activity of empty *P. speciose* pods. Taking into account the valuable and

wide biological activity of bean pericarp extracts, a study was undertaken to determine the biological value of *Phaseoli pericarpium* herbal raw material originating from colored flowered and seeded varieties of common bean (*Phaseolus vulgaris* L.) compared to a typical pharmacopoeial variety with white flowers and seeds used as a reference variety in this experiment.

MATERIALS AND METHODS

Plant material and experimental design

The experimental material was bean pericarp (*Phaseoli pericarpium*) of six common bean (*Phaseolus vulgaris* L.) cultivars varying in seed color (Table 1). Five colored-seeded cultivars: 'Małopolanka', 'Nida', 'Rawela', 'Tip Top', and 'Nigeria', and a white-seeded cultivar, 'Laponia', were used in this study. All the bean cultivars tested are dwarf cultivars, domestically bred and used for dry beans. Seed material came from the following seed breeding and production companies: Krakowska Hodowla i Nasiennictwo Ogrodnicze POLAN sp. z o.o.–'Małopolanka', Plant Breeding and Acclimatization Institute in Radzików–'Nida', PlantiCo Hodowla i Nasiennictwo Ogrodnicze Gołębiew sp. z o.o.–'Rawela' and 'Tip Top', PlantiCo Hodowla i Nasiennictwo Ogrodnicze Zielonki sp. z o.o.–'Laponia'. Bean pericarp came from field experiments carried out over the period 2014–2015 at an experimental farm of the University of Life Sciences in Lublin (south-eastern Poland; 51°23'N, 22°56'E). No mineral fertilization or plant protection products were used in bean cultivation. Bean ripening occurred in the first half of August; harvest was done once at the stage of 75% of pods fully ripe. Bean plants were cut by hand and dried in a well-ventilated and darkened storage shed for a period of 3 weeks. After the bean plants were dried completely, pods were stripped by hand, they were additionally dried for a short time (7 days) in openwork crates, marketable pods, well-grown, without any symptoms of infection by pathogenic agents, and uninjured, were separated, and beans were removed from them by hand. Bean pericarp of all the cultivars was characterized by uniform color without spots and injuries as well as by a specific bean scent; was twisted, slightly tapered at the ends of the strands, up to 20 cm long. The outer surface of the pericarp was matt, crème yellow, and the inner whitish covered with a shiny skin and met the requirements of Polish Pharmacopoeia XI (2017). The material was stored in paper bags containing 500 g of pericarp material from each cultivar in a dry room at a temperature of 15–18 °C, in the absence of light and moisture as well as without foreign odors. Randomly selected pericarp samples, 30 pieces from each cultivar, were used to determine pericarp weight and color. The pericarp color (30 pieces of each variety) was assessed by a team of 5 people previously trained in this field. The color was determined taking into account various shades of crème yellow on a scale of 1–4, where 1 was the bright color (bright crème) and 4 the darkest (sandy). 1,000 seed weight was determined for large marketable beans (at a seed moisture content of 13%) based on a weight of 100 randomly selected seeds in 4 replicates (average of 4 replicates was multiplied by 10 and a weight of 1,000 seeds per g was obtained). Dry matter content in bean pericarp was determined by the oven-dry method at 105 °C. The seed and pericarp characteristics of the studied bean cultivars based on the two-year results are shown in Table 1.

Table 1. Morphological characteristic of the seed and pericarp of common bean cultivars

Cultivar	Seed color	Weight of 1,000 seeds, g	Weight (g) of pericarp mean \pm SD	Pericarp color	Dry matter content of pericarp % mean \pm SD
Małopolanka	dark chestnut	405 ^a \pm 65	0.54 ^a \pm 0.08	bright crème	91.26c \pm 0.15
Nida	orange-brown	456 ^a \pm 74	0.46 ^a \pm 0.09	bright crème	91.73c \pm 0.11
Rawela	dark red	595 ^b \pm 91	0.69 ^b \pm 0.14	yellow/ crème	91.24c \pm 0.22
Tip Top	navy blue with beige spots	270 ^c \pm 72	0.54 ^a \pm 0.07	bright crème	91.67c \pm 0.10
Nigeria	black	773 ^d \pm 136	1.00 ^c \pm 0.19	sandy	90.65b \pm 0.32
Laponia (control)	white	554 ^b \pm 105	0.79 ^b \pm 0.10	yellow/ crème	90.10a \pm 0.24

SD standard deviation; The same letters mean no significant differences.

Chemical analysis

All of the chemicals used in this study were purchased from Sigma-Aldrich Chemical Co. (France) and/or Merck Company (Germany). A Hitachi U-2900 spectrophotometer was used for absorbance measurements. All the chemical determinations were carried out in triplicate.

Total phenolic acids estimation

Total phenolic acids estimation was carried out according to Arnov method [Polish Pharmacopoeia VI, 2002]. 20 mL of methanol were added to 2.0 g of homogenized raw material placed in a round-bottomed flask and the mixture was heated at reflux for 30 min at 70 °C in a water bath. The hydrolysate was filtered through hard filter paper into a 100-mL Erlenmeyer flask. The filtered medium was returned to the round-bottomed flask with 20 mL of methanol and heated at reflux for 30 min. This process was repeated 3 times. The combined filtrates were taken to a tube with 1 mL of blueberry extract, 1 mL of 0.5 N hydrochloric acid, 1 mL of Arnov's reagent, and 1 mL of 1 N sodium hydroxide, and filled up to 10 mL with distilled water. The absorbance was measured at 490 nm. The total phenolic acid content was expressed as caffeic acid equivalent (CAE).

Total flavonoid estimation

Total flavonoid were estimated according to the spectrophotometric method according to Christ and Müller [Polish Pharmacopoeia IX, 2011], expressed as quercetin equivalent (QE). After 45 minutes the absorbance at 425 nm was measured. The concentration of total flavonoid content in the test samples was calculated from the calibration plot ($Y = 0.0159x + 0.0048$, $R^2 = 0.999$) and expressed as mg quercetin equivalent (QE)/g of dried plant material.

Total condensed tannin contents

The tannins were determined by Folin-Ciocalteu method. About 0.1 mL of the sample extract was added to a volumetric flask (10 mL) containing 7.5 mL of distilled water and 0.5 mL of Folin-Ciocalteu reagent, 1 mL of 35% Na_2CO_3 solution and dilute to 10 mL with distilled water. The mixture was shaken well and kept at room temperature for 30 min. A set of reference standard solutions of gallic acid (20, 40, 60, 80 and 100 $\mu\text{g mL}^{-1}$) were prepared in the same manner as described earlier. Absorbance for test and standard solutions were measured against the blank at 725 nm with an UV/Visible

spectrophotometer. The tannin content was expressed in terms of % of GAE of extract [Polish Pharmacopoeia IX, 2011].

Anti-oxidation activity (AA)

AA (%) was evaluated on a base of the ability to neutralize the DPPH radicals by means of spectrophotometry according to Chen & Ho (1997): to do this, water extracts were prepared from raw material, extracts were then evaporated till dry and lyophilized. Analyses were performed for 20 µg mL⁻¹ concentration. The absorbance measurements were made at λ = 517 nm after 30 minutes wavelength using spectrophotometer UVIKON 932 (Canberra Packard). The percent inhibition of DPPH radical was calculated as: DPPH inhibition (%) = [(Abs₀ - Abs₃₀)/Abs₀] × 100%, where: Abs₀ is the absorbance of the control and Abs₃₀ is the absorbance of the sample after 30 min.

Statistical analysis

The obtained study results for the period 2014–2015, both as regards the morphological characteristics of bean pericarp and the laboratory tests, were at a similar level and therefore the 2-year means are presented. The results were statistically analyzed by one-way analysis of variance and Tukey's t-test at a significance level of 5%. The correlation analysis between variables was done. Correlation coefficients were determined at significance level of 0.05. Calculations were performed using Statistica 13.1 software.

RESULTS

Polyphenolic compounds

Bean pericarp (*Phaseoli Pericarpium*), originating from the common bean cultivars of different seed color and seed size (as determined by thousand seed weight), was characterized by significant variations in weight (Table 1). The bean pericarp color at the physiological maturity stage slightly varied depending on the genetic characteristics of the specific cultivar, from light crème through yellow crème to sandy color. Pericarp of the black-seeded cultivar was characterized by the darkest color

(sandy). The percentage of dry matter in pericarp of the white-seeded cultivar 'Laponia' was 90.1%, being significantly lower than in the cultivars with darker beans. The phenolic acid content (expressed as caffeic acid equivalents) in bean pericarp of the studied cultivars was at a similar level (Table 2), standing at least at 0.1 mg g⁻¹ (0.01%) and thus meeting the pharmacopoeial requirements (Polish Pharmacopoeia IX, 2017). According to the statistical analysis there was no significant difference between bean varieties in the content of total phenols (Table 2).

Table 2. Total phenolic acid content expressed as caffeic acid equivalents in the dry mater of the pericarp of common bean cultivars

Cultivar	Phenolic acid (CAE) mg g ⁻¹			
	Value ± SD	Min.	Max.	V (%)
Małopolanka	0.18 ^a ± 0.01	0.16	0.20	6.0
Nida	0.17 ^a ± 0.02	0.15	0.19	9.5
Rawela	0.17 ^a ± 0.02	0.15	0.19	11.2
Tip Top	0.17 ^a ± 0.04	0.12	0.21	25.1
Nigeria	0.16 ^a ± 0.03	0.12	0.19	21.5
Laponia	0.18 ^a ± 0.02	0.16	0.21	10.0
(control)				
Mean ±SD	0.15 ± 0.02			

SD standard deviation; V – variability coefficient; The same letters mean no significant differences.

The dark blue- and black-seeded cultivars ('Tip Top' and 'Nigeria') accumulated most flavonoids, respectively 0.138 and 0.139 mg g⁻¹ DW, as well as the control cultivar (0.132 mg g⁻¹ DW) (Table 3). There was a significant statistical difference between cultivars in the flavonoid content, where Tip Top, Nigeria and Lapland had the highest concentration of these bioactive compounds, while the cultivars Małopolanka, Nida and Rawela had lower concentrations without significant statistical difference between them. The bean cultivars studied did not differ significantly in terms of pericarp tannin content (Table 4), which was from 2.51% DW in the cultivar 'Tip Top' (dark blue seeds) to 2.99% DW in cv. 'Rawela' (dark red seeds).

Antioxidant activity (AA)

The study demonstrated that AA of the bean pericarp extracts, as measured by DPPH method, significantly varied depending on the cultivar (Table 5). The highest AA was found for the bean extracts from the cultivars 'Laponia' (white seeds) and 'Małopolanka' (dark chestnut seeds), respectively 12.35 and 12.10%. AA of the investigated bean extracts was determined to be a trait characterized by low variation.

The analysis of the correlation coefficients of the studied parameters provided interesting information (Table 6). Phenolic acid content was found to be significantly positively correlated ($r = 0.51$) with AA of the extracts tested. At the same time, the contents of phenolic acids and tannins were significantly positively correlated ($r = 0.68$), whereas a negative correlation ($r = -0.60$) was revealed between the contents of tannins and flavonoids as well as between the contents of flavonoids and phenolic acids ($r = -0.55$).

Table 3. Flavonoid content (expressed as quercetin equivalents) in the dry mater of the pericarp of common bean cultivars

Cultivar	Flavonoid (QE) mg g ⁻¹		
	Value ±SD	Min.	Max. V (%)
Małopolanka	0.127 ^a ± 0.013	0.114	0.140 10.4
Nida	0.101 ^a ± 0.006	0.092	0.107 6.4
Rawela	0.111 ^a ± 0.010	0.099	0.122 9.2
Tip Top	0.138 ^b ± 0.030	0.109	0.167 21.9
Nigeria	0.139 ^b ± 0.036	0.105	0.172 25.7
Laponia	0.132 ^b ± 0.027	0.106	0.159 20.5
(control)			
Mean ±SD	0.14 ± 0.03		

SD standard deviation; V – variability coefficient; The same letters mean no significant differences.

Table 4. Tannin content (%) in the dry mater of the pericarp of common bean cultivars

Cultivar	Tanins (% DM)		
	Value ±SD	Min.	Max. V (%)
Małopolanka	2.76 ^a ± 0.30	2.37	3.22 11.1
Nida	2.57 ^a ± 0.30	1.99	2.86 11.8
Rawela	2.99 ^a ± 0.31	2.49	3.34 10.5
Tip Top	2.51 ^a ± 0.74	1.64	3.24 29.7
Nigeria	2.68 ^a ± 0.72	1.57	3.28 26.8
Laponia	2.85 ^a ± 0.16	2.61	3.01 5.7
(control)			
Mean ±SD	2.51 ± 0.49		

SD standard deviation; V – variability coefficient; The same letters mean no significant differences.

Table 5. Antioxidant activity (AA) of the pericarp extracts determined by DPPH of common bean cultivars

Cultivar	Value ±SD	Min.	Max. V (%)
Małopolanka	12.10 ^{a,b} ± 1.11	11.02	13.26 9.55
Nida	9.82 ^{a,b,c} ± 1.12	8.74	10.98 11.43
Rawela	8.15 ^c ± 1.13	7.07	9.30 13.77
Tip Top	9.06 ^{b,c} ± 1.12	7.98	10.22 12.39
Nigeria	8.76 ^c ± 1.10	7.67	9.92 12.81
Laponia	12.35 ^a ± 1.18	11.02	13.26 9.54
(control)			
Mean ±SD	10.04 ± 1.93		

SD standard deviation; V – variability coefficient; The same letters mean no significant differences.

Table 6. Pearson correlation coefficients between the active substances content and antioxidant activity (AA) for common bean dried pericarp extracts

Variable	Tanins	Flavonoids	Phenolic acids	AA
Tanins	1.00	-0.60*	0.68*	0.22
Flavonoids	-0.60*	1.00	-0.55*	0.17
Phenolic acids	0.68*	-0.55*	1.00	0.51*
AA	0.22	0.17	0.51*	1.00

* significant correlation.

DISCUSSION

The pharmacopoeial standards define bean raw material as dried common bean pericarp of exclusively white-flowered varieties (Polish Pharmacopoeia IX, 2017). The results presented in this paper indicate that colored flower and seed varieties are also potentially important material for phytotherapeutic use. Pericarp of the bean cultivars studied was characterized by a high level of bioactive compounds and antioxidant activity (AA), both in the group of colored-seeded cultivars and in the white-seeded cultivar. Despite their high morphological variation, the investigated cultivars were not strongly differentiated in the level of the analyzed polyphenolic components in pericarp as well as in the antioxidant activity of their respective extracts. This is in agreement with the hypothesis of Bitocchi et al. (2017) who suggest that the adaptation of European common bean varieties to long days, their cold tolerance as well as resistance to pests and diseases were of key importance, and this probably led to a reduction in their initial diversity. Polyphenols participate in defensive responses during infection, excessive sun exposure, injuries, and heavy metal stress, and one of their most important characteristics is their antioxidant activity, which is strictly related to the chemical structure (Kulbat, 2016). A similar level of polyphenols and little varying AA of European common bean varieties seem to be an effect of their adaptation to different and even less favorable growth and development conditions.

Phenolic acid content has a decisive influence on the suitability of bean pericarp as pharmacopoeial raw material (Ramírez-Jiménez et al., 2015). Hanis et al. (2017) showed that colored bean cultivars are characterized by higher total phenolic content and antioxidant capacity compared to the other ones. Likewise, García-Díaz et al. (2018) proved the level of polyphenols and AA to be higher in extracts from bean cultivars with a dark-pigmented seed coat compared to those obtained from white-seeded cultivars. Troszyńska & Ciska (2002) demonstrated that the total free phenolic acids, released from soluble esters and glycosides, were higher for the colored seed coat in beans than for the white one. In the present study, the content of phenolic acids in bean pericarp of the colored cultivars was statistically equal to the content of these constituents in the reference white-seeded cultivar. It was also shown that it is phenolic acids that have a major contribution to AA of bean extracts. Furthermore, there is a possibility of synergism of the action of phenolic acids and tannins in creating the antioxidant potential of beans because the contents of the above-mentioned polyphenolic components (known for their antioxidant action) were significantly correlated with each other. Phenols perform diverse and important functions in the plant. Phenylpropanoid metabolism and the amount of phenolic compounds increase under the influence of various environmental factors and stress conditions (Michalak, 2006). Seed polyphenolic

compounds are usually stored in the seed coat due to their antipathogenic activity (Dinelli et al., 2006). The seed coat in beans is characterized by a higher concentration of phenolic compounds than cotyledons. Condensed tannins and flavonoids mainly occur in the seed coat, whereas cotyledons are rich in cinnamic acid derivatives (Ranilla et al., 2007). Therefore, bean pericarp and seed coat remain a valuable source of polyphenolic compounds, known for their antioxidant action. In the present study, AA of the bean pericarp extracts was highest for the white- and dark chestnut-seeded cultivars. This can be due to the qualitative differences of the polyphenolic complex related to genetic variation. Ombra et al. (2016) found a clear correlation between the level of polyphenols and free radical absorption properties, and they also observed certain variation that can be attributed to the qualitative differences of the polyphenol mixture. Zhao et al. (2014) showed a significant positive correlation of phenolic substances and total antioxidant activity to DPPH scavenging activity for seed extracts from legume plants. Hanis et al. (2017) also revealed a positive and significant correlation between AA and total phenolic content, which was higher for dark colored legumes than for light colored ones. Ombra et al. (2016) suggest that flavonoids and anthocyanins are responsible for the antioxidant and antiproliferative effects of bean extracts, though extracts from dark beans showed lower values with respect to AA, despite their higher anthocyanin content, than extracts from speckled beans, which indicates that mainly flavonoids are responsible for their biological activity (Ombra et al., 2016). It should be mentioned that a certain divergence in the study results can arise from the methodological differences. Anti-inflammatory activity of the bean seed coat depends on phenolic content and antioxidant activity, which is significantly affected by the cultivar and extraction solvent (Oomah et al., 2010).

White beans are usually considered to have a low level of tannins (Diaz et al., 2010). Colored bean varieties, which are characterized by uniform or non-uniform color of the seed coat, accumulate larger amounts of pigments. Diaz et al. (2010) showed the content of condensed tannins and anthocyanins to vary and they found some relationship between the level of these components and seed color. In the opinion of these authors, the primary seed color determines the majority of the biochemical characteristics of the seed coat, whereas the secondary seed color, which is limited to small sectors such as strips or spots on the seed coat, is of lesser importance. The study results presented in this paper confirm this hypothesis in some way with respect to the pericarp, but not to the seed coat. The cultivars with the darkest primary seed color ('Tip Top' and 'Nigeria') analyzed in this study accumulated in their pericarp more flavonoids than the cultivars with a lighter primary color (except for the control cultivar), regardless of the secondary color. On the other hand, the equal level of tannins in the bean extracts analyzed suggests that these compounds are accumulated in the bean pericarp predominantly for defensive purposes. Troszyńska & Ciska (2002) showed the presence of condensed tannins in the colored seed coat of pea, but they did not find them to be present in the white coat. Moreover, these authors inform that pea tannins can be considered to be thermostable natural antioxidants, effective in food systems. Similarly, Amarowicz et al. (2008) inform that tannin extracts from common bean seeds exhibit potentially useful antibacterial activity.

CONCLUSIONS

The analysis of the chemical composition and antioxidant activity of the extracts from common bean pericarp proves that (i) pericarp of the colored bean cultivars is characterized by high biological value and can be used as a potential source of polyphenolic compounds; (ii) pericarp of the bean cultivars with colored and white seeds does not differ significantly in the level of phenolic acids and tannins as well as flavonoids in the case of the cultivars with the darkest seeds ('Tip Top' and 'Nigeria'); (iii) the cultivars with dark chestnut /orange-brown seeds ('Małopolanka' and 'Nida') are distinguished by high antioxidant activity (AA), which is equal to the action strength of the reference extracts obtained from the white-seeded cultivar ('Laponia') that meets the pharmacopoeial criteria; (iiii) phenolic acids are the group of components that are mainly responsible for AA of the bean pericarp extracts. The results presented in this paper indicate that it is justified to continue further detailed research in this area.

ACKNOWLEDGEMENTS. The research was financed by the Ministry of Science and Higher Education as a part of the statutory activity of the Department of Vegetable Crops and Medicinal Plants, University of Life Sciences in Lublin. We acknowledge Dr. Rafał Papliński from the Laboratory of Quality of Vegetables and Medicinal Plants - Department of Vegetable Crops and Medicinal Plants - University of Life Sciences in Lublin for his help in carrying out the chemical and statistical analysis.

REFERENCES

- Akond, G.M., Khandaker, L., Berthold, J., Gates, L., Peters, K., Delong, H. & Hossain, K. 2011. Anthocyanin, total polyphenols and antioxidant activity of common bean. *American Journal of Food Technology* **6**(5), 385–394.
- Amarowicz, R., Dykes, G.A. & Pegg, R.B. 2008. Antibacterial activity of tannin constituents from *Phaseolus vulgaris*, *Fagopyrum esculentum*, *Corylus avellana* and *Juglans nigra*. *Fitoterapia* **79**, 217–219.
- Armendáriz-Fernández, K.V., Herrera-Hernández, I.M., Muñoz-Márquez, E. & Sánchez, E. 2019. Characterization of Bioactive Compounds, Mineral Content, and Antioxidant Activity in Bean Varieties Grown with Traditional Methods in Oaxaca, Mexico. *Antioxidants* **8**, 26. doi:10.3390/antiox8010026
- Beninger, C.W. & Hosfield, G.L. 2003. Antioxidant Activity of Extracts, Condensed Tannin Fractions, and Pure Flavonoids from *Phaseolus vulgaris* L. Seed Coat Color Genotypes. *Journal of Agricultural Food Chemistry* **51**, 7879–7883.
- Berbecaru-Iovan, A., Andrei, A.M., Nicolae, A.C., Stănculescu, C.E., Berbecaru-Iovan, S., Mogosanu, G.D. & Pisoschi, C.G. 2016. Research concerning metabolic and antioxidant effects of the ethanolic extract from *Syringae vulgaris flos* f. *alba* in streptozotocin-induced diabetic rats. *Farmacia* **64**(5), 722–727.
- Bitocchi, E., Rau, D., Bellucci, E., Rodriguez, M., Murgia, M.L., Gioia, T., Santo, D., Nanni, L., Attene, G. & Papa, R. 2017. Beans (*Phaseolus* spp.) as a Model for Understanding Crop Evolution. *Frontiers in Plant Science* **8**(722). doi: 10.3389/fpls.2017.00722
- Bozoglu, H. & Sozen, O. 2011. A sample for biodiversity in Turkey: Common bean (*Phaseolus vulgaris* L.) landraces from Artvin. *African Journal of Biotechnology* **10**(63), 13789–13796.

- Carai, M.A.M., Fantini, M., Loi, B., Colombo, G., Riva, A. & Morazzoni, P. 2009. Potential efficacy of preparations derived from *Phaseolus vulgaris* in the control of appetite, energy intake, and carbohydrate metabolism. *Diabetes, Metabolic Syndrome and Obesity: Targets and Therapy* **2**, 145–153.
- Carai, M.A.M., Fantini, M., Loi, B., Colombo, G., Gessa, G.L., Riva, A., Bombardelli, E. & Morazzoni, P. 2011. Multiple cycles of repeated treatments with a *Phaseolus vulgaris* dry extract reduce food intake and body weight in obese rats. *British Journal of Nutrition* **106**, 762–768.
- Chen, J.H. & Ho, C.T. 1997. Antioxidant Activities of Caffeic Acid and Its Related Hydroxycinnamic Acid Compounds. *Journal of Agricultural Food Chemistry* **45**, 2374–2378.
- Diaz, A.M., Caldas, G.V. & Blair, M.W. 2010. Concentrations of condensed tannins and anthocyanins in common bean seed coats. *Food Research International* **43**, 595–601.
- Dinelli, G., Bonetti, A., Minelli, M., Marotti, I., Catizone, P. & Mazzanti, A. 2006. Content of flavonols in Italian bean (*Phaseolus vulgaris* L.) ecotypes. *Food Chemistry* **99**(1), 105–114.
- Dzomba, P., Togarepi, E. & Mupa, M. 2013. Anthocyanin content and antioxidant activities of common bean species (*Phaseolus vulgaris* L.) grown in Mashonaland Central, Zimbabwe. *African Journal of Agricultural Research* **8**(25), 3330–3333.
- Evangelho, J.A., Berrios, J.J., Pinto, V.Z., Antunes, M.D., Vanier, N.L. & Zavareze, E.R. 2016. Antioxidant activity of black bean (*Phaseolus vulgaris* L.) protein hydrolysates. *Food Science and Technology, Campinas* **36**(Suppl. 1), 23–27.
- García-Díaz, Y.D., Aquino-Bolaños, E.N., Chávez-Servia, J.L., Vera-Guzmán, A.M. & Carrillo-Rodríguez, J.C. 2018. Bioactive compounds and antioxidant activity in the common bean are influenced by cropping season and genotype. *Chilean Journal of Agriculture Research* **78**(2), 255–265.
- Helmstädter, A. 2010. Beans and Diabetes – *Phaseolus vulgaris* Preparations as Antihyperglycemic Agents. *Journal of Medicinal Food* **13**(2), 1–4.
- Hanis, M.Y., Hasnah, H. & Dang, T.N. 2017. Total phenolic content and antioxidant capacity of beans: organic vs inorganic. *International Food Research Journal* **24**(2), 510–517.
- Ko, H.J., Ang, L.H. & Ng, L.T. 2014. Antioxidant activities and polyphenolic constituents of bitter bean *Parkia speciosa*. *International Journal of Food Properties* **17**, 1977–1986.
- Kulbat, K. 2016. The role of phenolic compounds in plant resistance. *Biotechnol and Food Science* **80**(2), 97–108.
- Łabuda, H., Buczkowska, H., Papliński, R. & Najda, A. 2017. Secondary metabolites of *Phaseoli pericarpium*. *Acta Scientiarum Polonorum, Hortorum Cultus* **16**(6), 187–200.
- Madhujith, T., Nacz, M. & Shahidi, F. 2004. Antioxidant activity of common beans (*Phaseolus vulgaris* L.). *Journal of Food Lipids* **11**, 220–233.
- Michalak, A. 2006. Phenolic Compounds and Their Antioxidant Activity in Plants Growing under Heavy Metal Stress. *Polish Journal of Environmental Studies* **15**(4), 523–530.
- Ombra, M.N., d’Acerno, A., Nazzaro, F., Riccardi, R., Spigno, P., Zaccardelli, M., Pane, C., Maione, M. & Fratianni, F. 2016. Phenolic Composition and Antioxidant and Antiproliferative Activities of the Extracts of Twelve Common Bean (*Phaseolus vulgaris* L.) Endemic Ecotypes of Southern Italy before and after Cooking. *Oxidative Medicine and Cellular Longevity*, Article ID 1398298. <http://dx.doi.org/10.1155/2016/1398298>
- Oomah, B.D., Corbe, A. & Balasubramanian, P. 2010. Antioxidant and anti-inflammatory activities of bean (*Phaseolus vulgaris* L.) hulls. *Journal of Agriculture and Food Chemistry* **58**, 8225–8230.
- Pari, L. & Venkateswaran, S. 2004. Protective role of *Phaseolus vulgaris* on changes in the fatty acid composition in experimental diabetes. *Journal of Medicinal Food* **7**(2). <https://doi.org/10.1089/1096620041224120>

- Polish Pharmacopoeia VI. (2002). Warszawa. (in Polish).
- Polish Pharmacopoeia IX. (2011). Warszawa. (in Polish).
- Polish Pharmacopoeia XI. (2017). Warszawa. (in Polish).
- Ramírez-Jiménez, A.K., Reynoso-Camacho, R., Tejero, M.E., León-Galván, F. & Loarca-Piña, G. 2015. Potential role of bioactive compounds of *Phaseolus vulgaris* L. on lipid-lowering mechanisms. *Food Research International* **76**, 92–104.
- Ranilla, G.G., Genovese, M.I. & Lajolo, F.M. 2007. Polyphenols and Antioxidant Capacity of Seed Coat and Cotyledon from Brazilian and Peruvian Bean Cultivars (*Phaseolus vulgaris* L.). *Journal of Agriculture and Food Chemistry* **55**, 90–98.
- Reynoso-Camacho, R., Ramos-Gomez, M. & Loarca-Pina, G. 2006. Bioactive components in common beans (*Phaseolus vulgaris* L.). *Advances in Agricultural and Food Biotechnology*, ISBN: 81-7736-269-0. Editors: Ramón Gerardo Guevara-González and Irineo Torres-Pacheco, pp. 217–236.
- Sánchez-Chino, X., Jiménez-Martínez, C., Davila-Ortiz, G., Álvarez-González, I. & Madrigal-Bujaidar, E. 2015. Nutrient and Nonnutrient Components of Legumes, and Its Chemopreventive Activity: A Review. *Nutrition and Cancer* **67**(3), 401–410.
- Silva, M.O., Brigide, P., Viva de Toledo, N.M. & Canniatti-Brazaca, S.G. 2018. Phenolic compounds and antioxidant activity of two bean cultivars (*Phaseolus vulgaris* L.) submitted to cooking. *Brazilian Journal of Food Technology* **21**, 016072.
- Stoilova, T., Pereira, G., Sousa, M.M.T. & Carnide, V. 2005. Diversity in common bean landraces (*Phaseolus vulgaris* L.) from Bulgaria and Portugal. *Journal of Central European Agriculture* **6**(4), 443–448.
- Troszyńska, A. & Ciska, E. 2002. Phenolic Compounds of Seed Coats of White and Coloured Varieties of Pea (*Pisum sativum* L.) and Their Total Antioxidant Activity. *Czech Journal of Food Sciences* **20**, 15–22.
- Wonghirundecha, S., Benjakul, S. & Sumpavapol, P. 2014. Total phenolic content, antioxidant and antimicrobial activities of stink bean (*Parkia speciosa* Hassk.) pod extracts. *Songklanakarin Journal of Science and Technology* **36**(3), 301–308.
- Wu, X., Xu, X., Shen, J., Perricone, M.V. & Preuss, H.G. 2010. Enhanced Weight Loss From a Dietary Supplement Containing Standardized *Phaseolus vulgaris* Extract in Overweight Men and Women. *The Journal of Applied Research* **10**(2), 73–79.
- Zhao, Y., Du, S., Wang, H. & Cai, M. 2014. In vitro antioxidant activity of extracts from common legumes. *Food Chemistry* **152**, 462–466.
- Yang, Q.Q., Gan, R.Y., Ge, Y.Y., Zhang, D. & Corke, H. 2018. Polyphenols in Common Beans (*Phaseolus vulgaris* L.): Chemistry, Analysis, and Factors Affecting Composition. *Comprehensive Reviews in Food Science and Food Safety* **17**, 1518–1539.

Compost-bedded pack barns in the state of Minas Gerais: architectural and technological characterization

V.C. Oliveira¹, F.A. Damasceno^{1,*}, C.E.A. Oliveira¹, P.F.P. Ferraz¹,
G.A.S. Ferraz¹ and J.A.O. Saraz²

¹Federal University of Lavras, Engineering Department, BR37200-000, Lavras - Minas Gerais, Brazil

²Univeridad Nacional de Colombia, Agrarians Faculty, Department of Agricultural and Food Engineering, Carrera 65 # 59A - 110, CO050001 Medellin, Colombia

*Correspondence: flavio.damasceno@ufla.br

Abstract. Compost bedding pack (CBP) barns have been receiving increased attention as an alternative housing system for dairy cattle. Thus, a systematic investigation of the primary management practices of dairy cattle in CBP barns in the state of Minas Gerais (Brazil) has proven to be of environmental and economic relevance. The aim of this research was to summarize the compost bed data, barn dimension data and to determine the major interactive factors in the success of bed composting from qualitative and quantitative methods. Data for this study was collected from 16 CBP barns, distributed throughout the southern state of Minas Gerais (Brazil) between March 2017 and July 2018. These data were used to describe the building layouts and dimensions, to identify barn management practices, and to characterize the compost bedding material concerning moisture content. The majority of these barns had feed alleys and driveways; overshot ridges with frequent orientation from NE to SW; bedding process and aeration using mechanical tillage. The average bedding moisture content was found to be $36.9 \pm 5.2\%$ (w.b.). Based on the information found, it is possible to evaluate that there is still no defined construction pattern, with a high variation of size and technologies employed.

Key words: dairy cattle, animal facility, management.

INTRODUCTION

Milk production occupies a prominent position in Brazilian agribusiness. When considering milk production in Brazil by region, the state of Minas Gerais was responsible for the largest production volume in 2018, with 9.0 billion liters per year, corresponding to 27% of the total produced in Brazil (Embrapa, 2018).

However, to maintain this growth in production and productivity, dairy farmers need to invest in new technologies and improve their production systems to make their results even more satisfying. For this they need to overcome many challenges, among them, the improvement of the physical structure, thermal environment, and management, which are factors directly related to animal welfare and, consequently, to production (Costa & Silva, 2014).

The Compost bedding pack barn (CBP) has emerged as a viable alternative to conventional milk production structures. The CBP is an alternative loose housing system for dairy cows (Eckelkamp et al., 2014), which allows the animals more freedom of movement and comfort, enabling them to lie down in a more natural manner (Barberg, 2007a). In the CBP, the resting area is covered by a collective bed composed of organic material (Ofner-Schröck et al., 2015).

According to Damasceno (2012), the CBP system provides greater longevity, a dry and safe environment, comfort and well-being to the animal, an increase in production, a reduction of production costs, as well as a correct way of handling organic waste.

The CBP system has gained supporters around the world, who recognize the efficiency of CBP concerning productivity and animal comfort, this success has caused other countries to adopt it to improve their milk activity. The facilities followed U.S. standards, with the same constructive characteristics, management techniques, and system; although changes have been made to these initial system standards, a specific standard in the design and management of the facilities has not been found.

The aim of this research was to summarize the compost bed data, barn dimension data and to determine the major interactive factors in the success of bed composting from qualitative and quantitative methods.

MATERIALS AND METHODS

Characterization of the animal facility

The data for this study were collected in different CBP barns, distributed throughout the State of Minas Gerais between April 2017 to September 2018. Cooperatives and dairy farmers assisted in locating the farms that used the CBP system. A survey was carried out in 14 city of the state of Minas Gerais (Tiros, Sete Lagoas, Lagoa da Prata, Candeias, Perdões, Coqueiral, Santana da Vargem, Ingai, Varginha, Três Corações, Madre de Deus de Minas, Ressaquinha, and Cláudio) for a total of 20 CBP barns examined (Fig. 1).

During each visit, a questionnaire was applied to the producer and employees to evaluate the financial management practices and management system. The questionnaire was applied to gather data regarding the facility's design, implantation and production costs, herd characteristics, degree of producer's satisfaction and all management practices, including degree of success when implanting the system, bed and animal management, among others. After completing the questionnaire, the team went to the facility to collect variables related to architectural characteristics, thermal and acoustic environment, bed characteristics (temperature, humidity, pH and penetration resistance), animal handling, lactation, productivity, locomotion score, hygiene score, and body condition score, among others.



Figure 1. Cities in the State of Minas Gerais where CBP barns were visited.

Determination of architectural, technological and environmental variables

The following information was collected for the architectural characterization of each of the CBP barns: ridge orientation, dimensions (length and width), structural characteristics (number of posts and material, wall and sidewall height), waterers (type of material, dimensions), feed alley (floor type, length, width and scraping frequency), roof (type and color of tile, roof pitch, eave height, eave overhangs, roof type, etc.). All data were measured with a tape measure and a laser (Bosch, Mod. GLM60, accuracy ± 1.5 mm). The constructed area and resting area of the CBP barns available per animal and the linear meter of waterers and feeder per animal were calculated.

For the technological characterization, the following data were collected: fans (type, quantity, power, and dimension), lighting (type of lamps, quantity, and power), tractor (power and model), implements (type and model) and waste treatment system (lagoon or biodigester).

Instrumentation and data collection

The parameters evaluated for the environmental characterization of the CBP barns were measured inside each animal facility. For this, a grid was drawn on the bed area with nine collection points, according to the methodology used by Damasceno (2012). All data collections were carried out between 12:00 to 16:00 hours.

The environmental variables were measured near the geometric center of the animals (1.5 m height). A portable Digital Thermo-Hygro-Decibel meter-Luxmeter was used to measure air temperature (tbs), relative humidity (RH) and noise level (Instrutherm®, model THDL-400, with an accuracy of $\pm 3.5\%$). The air velocity was measured using a hot wire anemometer (Instrutherm®, model TAFR-190, with an accuracy of ± 0.1 m s⁻¹).

Bed temperature and resistance to penetration were measured, and samples were collected to determine the humidity and pH of the bedding. The bed temperature was measured using an infrared thermometer (Incoterm®, model ST-500, measuring range -30 to 260 °C and resolution of 0.1 °C) for the surface temperature and a digital rod thermometer (Tp101, measuring range -50 to 300 °C and resolution of ± 0.1 °C) to measure at a depth of 0.2 m.

A Penetrometer (PenetroLOG PLG1020 and 3.1 kPa resolution) was previously calibrated for use with bed materials in CBP barns. The penetrometer was introduced into the bed (maximum insertion velocity of 50 mm s⁻¹) at each of the nine previously established points, where the sensor measured the penetration resistance of the bed every 1.0 cm, in the bands of 0–5 cm, 5–10 cm, 10–15 cm, and 15–20 cm and recorded the information in the memory. This data was downloaded to the computer and manipulated using the Microsoft Excel®. Bedding samples at different depths were collected to determine the moisture of the bed and to perform corrections of the penetrometer readings.

The samples to determine humidity and pH were taken with the help of an articulated trough with cable, then placed in plastic bags and stored in an airtight container with a lid.

The bedding moisture analysis was carried out following the methodology adopted by Damasceno (2012); For this 10 g of sample was placed in a ceramic container and introduced in an oven at a temperature of 105 °C for 24 hours. After this period, the dry samples were weighed, and the bed moisture was calculated.

Another part of the collected samples was used to determine the pH. The analyses were carried out in the laboratory in the same week of collection, in order to guarantee the reliability of the samples. The pH analysis in the laboratory followed the methodology described by Zhao et al. (2012), where 10 g of sample was collected and diluted in 25 mL of distilled water. The solution (sample and distilled water) was stirred for 3.0 minutes and allowed to stand for half an hour. After this period, the solution was placed in contact with the electrode of a bench pH meter (measuring range 0 to 14, resolution ± 0.01 and accuracy ± 0.02), after waiting for a few moments for the solution to stabilize, the pH value was recorded.

Characterization of the herd

The evaluation of the herd was made through the collection of information about the number of animals, average daily production and animal health (locomotion score, hygiene score, and body condition score). For these variables, two previously prepared evaluators visually assessed the animals and determined the values for each of the scores and then calculated the means of the two evaluations. For facilities with up to 50 animals, the entire herd was evaluated, and for installations with more than 50 animals, at least 50% of the herd was evaluated.

The evaluation of the body condition score was performed according to the methodology proposed by Machado et al. (2008), and was given through visual assessment of the animal's body situation using a scale with values ranging from 1 to 5, and graded every 0.25 points; The extreme numbers 1 and 5 of the scale represent an excessively lean animal and an obese one, respectively. The anatomical parts analyzed in the evaluation were ribs, transverse processes of the lumbar vertebrae, tips of the ilium and ischium, and tail head. At these specific points the disposition of adipose tissue and muscle mass over the bones was visually assessed.

The locomotion score was evaluated using the methodology presented by Sprecher et al. (1997) and was assessed through the observation of the animals on a flat surface while they were walking and standing. A scale with values from 1 to 5 was used, and graded every 0.25 points, numbers 1 and 5, the extremes of the scale, represent normal locomotion and severe lameness, respectively.

The hygiene score evaluation was performed according to the methodology proposed by Cook et al. (2007). For the evaluation, some anatomical parts of the animal such as the leg, udder, flank and upper leg were observed. A scale of 1 to 4 was used, graded every 0.5 points. Number 1: corresponds to the absence of dirt in the evaluated regions; number 2: regions with small dirt spots; number 3: regions with the presence of some dirt plates adhered to the fur; and number 4: regions with dirt plates preventing the visualization of the fur.

Statistical analysis

All the information collected in the field was recorded in spreadsheets and later inserted and manipulated with Microsoft Excel®. For the characterization of the animal facilities that use the CBP system descriptive statistics were used to evaluate the data obtained, thus, the means, standard deviations, minimum and maximum were calculated. Based on the results, frequency histograms were created and the data presented in bar graphs for better visualization.

RESULTS AND DISCUSSION

All CBP barns assessed in the present study were already involved with dairy production, and in the majority of the cases evaluated, the animals were raised in an extensive and semi-extensive system.

The majority of dairy farmers stated that the main factor that motivated them to adopt the CBP system was the need to increase milk production and to reduce the mastitis infection rates in the herd. Approximately 75% of the installations were designed and built, without adaptations, the rest were adapted according to the infrastructure previously in place.

All farmers considered themselves very satisfied with the results achieved, reporting improved herd health and increased productivity. Only 30% of the facilities did not have computers installed on the farm, and in those cases, the farmers were getting updates from magazines, scientific articles, technical assistance and contact with other professionals in the dairy business.

Architectural characterization

The most common roof orientation was Northwest-Southeast (52.9%), with only 29.5% of the facilities being in the East-West direction. According to Damasceno (2012), for the southern hemisphere, the East-West orientation is the most appropriate because it reduces the heating in the largest walls and direct solar exposure during the hottest periods of the day. Radavelli (2018) observed that at least 50% of the CBP barns were in the recommended orientation.

The average dimensions found at the facilities were 73.3 m (length) and 20.6 m (width). Most of the CBP barns analyzed had lengths and widths between 50 and 100 m (Fig. 2, a) and 16 and 22 m (Fig. 2, b), respectively. The average length of the facilities assessed in this study was significantly higher than those observed by Radavelli (2018) and Damasceno (2012). Most of them had an area between 45 and 1,215 m² (53.0%), as can be seen in Fig. 2, c.

The mean of the resting area dimensions found at the CBP barns was 64.1 ± 27.1 m (length) and 17.7 ± 4.1 m (width), and the average resting area dimension was $1,134.1 \pm 537.6$ m², with an average value greater than 750.0 ± 551.1 m².

The dairy farms had an average herd size of 130 ± 68 animals, ranging from 32 to 325 animals, respectively. The average stock density was 10.4 m² per animal. Most of the CBP barns (41.2%) had a stock density between 9.9 and 12.9 m² per animal (Fig. 2, d), which is higher than the values observed by Janni et al. (2007) and Black et al. (2014) in the U.S. states of Minnesota (7.4 m² per animal) and Kentucky (9.0 m² per animal), respectively. However, the mean value is lower than the one found by Radavelli (2018) in the West of the Brazilian state of Santa Catarina (15.2 m² per animal).

The majority of CBP barns (52.9%) have a sidewall opening between 3.0 and 4.5 m (Fig. 2, e). The sidewall openings and eaves provide protection against sun, rain, and strong winds while helping to maintain adequate ventilation and animal comfort (Damasceno, 2012).

For the support pillars, the most used material found was metal, present in 53% of the evaluated facilities. The mean eave height was 4.7 ± 0.4 m, with 47.0% of the CBP barns (Fig. 2, f) having a dimension higher than the 4.5 m recommended by Graves &

Brugger (1994). The average eave height is close to the ones found by Radavelli (2018) and Damasceno (2012), 4.3 ± 0.8 m and 4.2 ± 0.5 m, respectively.

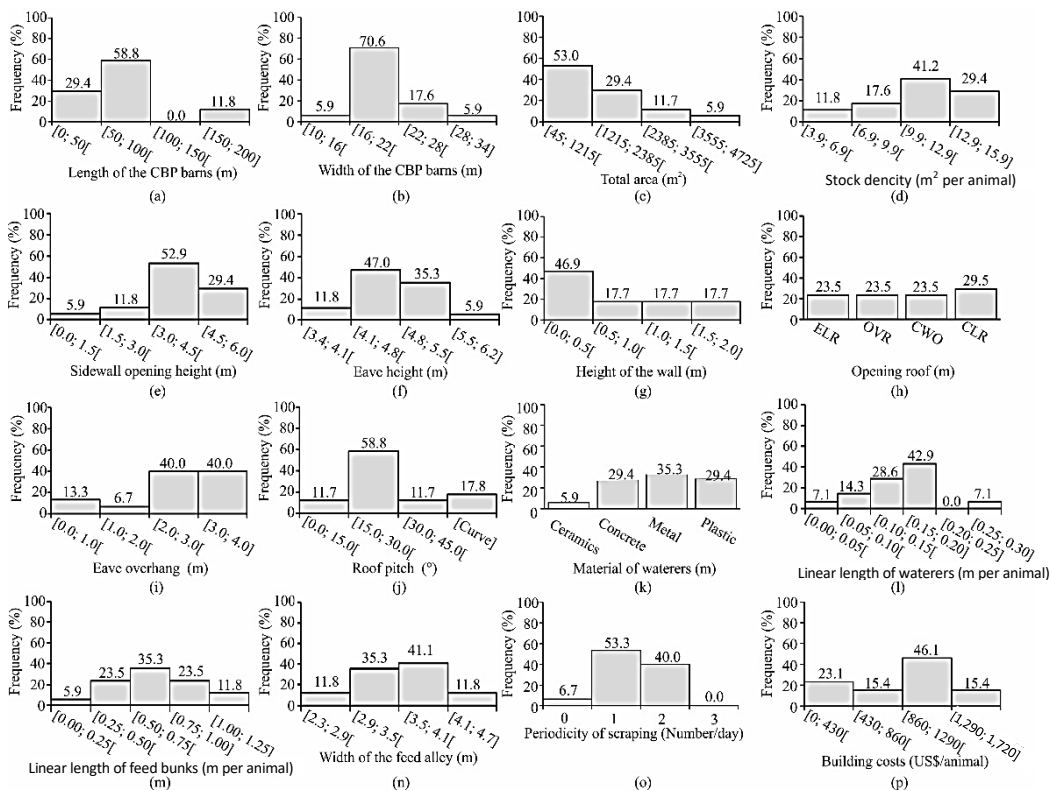


Figure 2. Frequency distribution of: a) Length of the CBP barns; b) Width of the CBP barns; c) Total area of CBP barns; d) Stock density; e) Sidewall opening height; f) Eave height; g) Wall height; h) Roof opening; i) Eave overhang; j) Roof pitch; k) Material of waterers; l) Linear length of the waterers; m) Linear length of feedbunks; n) Width of the feed alley; o) Periodicity of scraping; and p) Building costs.

*ELR – elevated ridge; OVR – overshoot ridge; CWO – curved without opening; and CLR – closed ridge.

In the majority of the CBP facilities assessed walls with heights up to 0.5 m were more frequent (46.9%) (Fig. 2, g). If the height of the wall which is intended to contain bedding material is too high it can cause air circulation problems on the bed; if it is too low, it may limit bed replacements, making it impossible to use the bed for more extended periods due to lower volumetric capacity (Damasceno, 2012).

The most common type of roof opening found was the one with the closed ridge - CLR (29.5%), the other three types found (elevated ridge - ELR; overshoot ridge - OVR; curved without opening - CWO) had the same frequency (23.5%).

The most common widths for the eave overhang (Fig. 2, i) were between 2.0 to 3.0 m (40%), and 3.0 to 4.0 m (40%). In CBP barns from the state of Kentucky (U.S.), the eave overhang was higher than 1.0 m (Damasceno, 2012). The eave overhang should be big enough to minimize the entry of sunlight and rain through the open sidewall, according to Gay (2009), it should be at least 1/3 of the sidewall height.

A higher frequency (58.8%) was observed for roof pitch between 15 to 30° (Fig. 2, j). The roof pitch and the type of roof opening are constructive characteristics that influence the natural ventilation of the animal facility, contributing to the ventilation of moisture, odors, and gases (MWPS-7, 2000).

According to Damasceno (2012), water intake is a critical factor in milk production and the reproductive performance of dairy cattle, since it regulates dry matter intake, so it is essential to ensure adequate access of the animal to the waterers. In the CBP barns evaluated it was observed that the most common material used for the waterers was metal (35.3%), followed by plastic, concrete (29.4%), and finally ceramic (5.9%) (Fig. 2, k).

It was also observed that there were five waterers per CBP barn. Tavares & Benedetti (2011) recommend that at least 0.10 m of linear length of waterers per animal should be available. When observing the CBP barns evaluated (Fig. 2, l), it was concluded that 78.6% were following the recommendations, a fact that contradicts the reality observed by Damasceno (2012) in the U.S. state of Kentucky, where only 19% of the CBP barns met the recommendations.

On average the feedbunks space per animal was 0.67 ± 0.2 m, and that 35.3% of the CBP barns (Fig. 2, m) followed the recommendation of 0.75 m or more feederbunk space available per animal (Arachchige et al., 2014). Access to food is another factor that may limit milk production because if there is not enough space for the animals in the feed alley, there will be greater competition among cows, which could damage the adequate food intake of some animals (Damasceno, 2012).

All feed alleys of the CBP barns were covered with concrete, and the mean dimensions was 66.2 ± 25.7 m (length) and 3.3 ± 0.7 m (width), the frequency distribution of the dimensions of the feed alley (Fig. 2, n) was greater between 3.5 and 4.1 m (41.1%). The width values of the feed alley were close to the ones found by Radavelli (2018) and Damasceno (2012), 3.4 ± 1.8 m and 4.1 ± 0.7 m, respectively.

A daily frequency of feed alley scraping was observed in 53.3% of the CBP barns evaluated (Fig. 2, o). In the research conducted by Radavelli (2018), the daily frequency was part of 40.9% of the evaluated animal facilities. The most common ways of performing the scraping were mechanized (66.7%) and manual (26.6%).

The total building costs ranged from 15,150 to 515,000 US\$, with an average cost per animal of $\text{US\$ } 877.1 \pm 387.1$. The significant difference in values may be associated with the type of design and structures used. The cost of building per animal was between 860.0 to 1,290.0 US\$ (Fig. 2, p).

Technological Characterization

In all the cases observed, every milk farm had at least one agricultural tractor. The average power of tractors was 67.0 hp, ranging from 54.0 to 75.0 hp (Fig. 3, a). When evaluating CBP facilities in the West part of the State of Santa Catarina, Radavelli (2018) mentions that the average horsepower of tractors was 76.0 ± 12.5 hp. The difference in power can be associated with the type of work performed by the tractors in the facilities and also to the different types of implements used in the bed stirring, as this is one of the activities that demand the most power of a tractor.

According to the frequency distribution of the bed tillage equipment (Fig. 3, b), there was no greater predominance of a specific implement with the Rotary Tiller with Cultivator (RC) having the highest occurrences (27.8%). Radavelli (2018) mentions that 93.3% of the CBP barns evaluated, used a cultivator.

In most of the CBP barns assessed (88.8%), the pack material was stirred twice a day (Fig. 3, c). Bewley et al. (2012), the process was performed at least twice a day. The pack temperature is affected by compost management, more specifically by the machinery used for stirring (Janni et al., 2007). This predominance was also observed by Radavelli (2018) in 53.3%.

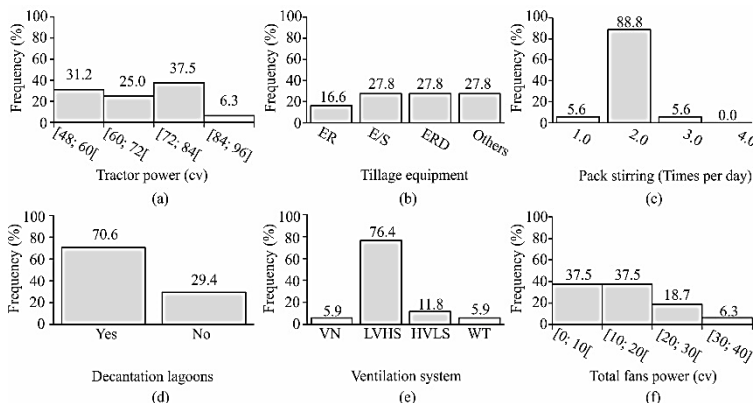


Figure 3. Frequency distribution of: a) Tractor power; b) Tillage equipment used to stir the bed pack; c) Pack stirring; d) Decantation lagoons; e) Ventilation system and f) Fans total power.

*ER – Rototiller; E/S – Cultivator; ERD – Rotary Tiller and Cultivator; Other – Equipment that uses more than one implement; VN – Natural ventilation; LVHS – low volume and high speed; HVLS – high volume and low speed; and WT – acclimatized wind tunnel.

In 70.6% of the CBP barns evaluated (Fig. 3, d), the animals' waste was stored in a decantation lagoon. According to Arceivala (1981), the decantation lagoon process consists in the retention of raw effluents, for a period, which must be sufficient for the organic matter to be stabilized by natural processes.

In most cases (94.1%), the ventilation system used by the CBP barns was mechanical (Fig. 3, e). The mechanical ventilation system used in 76.4% of cases was performed by low-volume high-speed fans (LVHS) and in 11.8 of the cases by high-volume low-speed fans (HVLS). According to Damasceno (2012), LVHS fans were used in 48.0% of CBP barns in Kentucky (U.S.). The average power of the fans was 13.4 ± 6.6 hp (Fig. 3, f), with a minimum and maximum value of 6.0 and 30.0 hp, respectively. These values differ considerably from the results presented by Damasceno (2012) of 5.8 ± 3.1 hp.

Environmental characterization

The mean value of the air temperature (t_{db}) at the surface and 1.5 m height from the bed was 26.9 ± 2.4 °C and 26.7 ± 2.3 °C, respectively (Fig. 4, a and 4, b). The highest thermal amplitude was observed at 1.5 m height from the bed (11.7 °C). The average t_{db} of the CBP barns is generally below the thermo-neutral zone (26 to 28 °C).

The average relative humidity at 0.05 m and 1.50 m height was $48.3 \pm 9.3\%$ and $46.4 \pm 9.7\%$, respectively (Fig. 4, c and 4, d). The average humidity of the CBP barns was below the recommended upper limit (70%); however, a large percentage of the installations had an air humidity lower than the lower limit (60%), a condition that is not ideal for maintaining animal welfare.

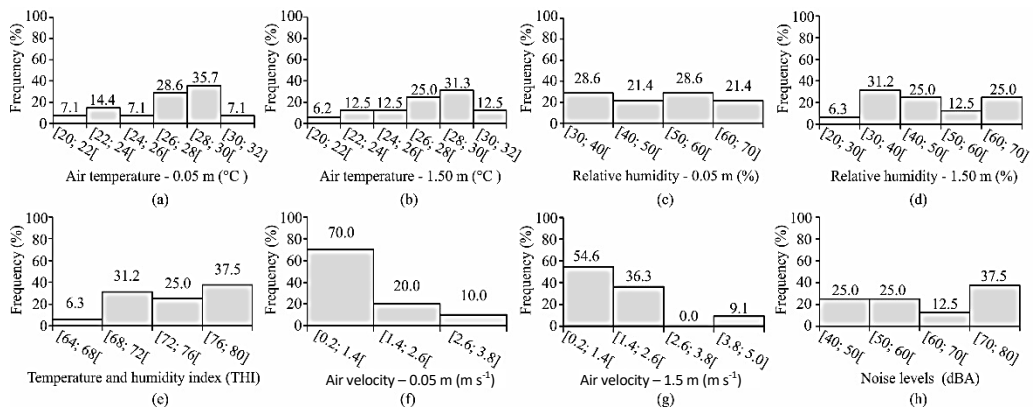


Figure 4. Frequency distribution of: a) Air temperature at 0.05 m; b) Air temperature at 1.50 m; c) Relative humidity at 0.05 m; d) Relative humidity at 1.50 m; e) Temperature and humidity index (THI); f) Air velocity at 0.05 m; g) Air velocity at 1.50 m; and g) Noise levels.

The THI is higher than the value allowed for adequate thermal comfort of the animals, only in 6.3% of the cases evaluated the THI was less than 68 (Fig. 4, e); The average THI for all CBP barns was 73.6 ± 3.0 . These conditions were also verified by Radavelli (2018) who found an average THI of 77.5.

The average air velocity at 0.05 and 1.50 m height was 1.3 ± 0.7 and 1.7 ± 0.8 m s⁻¹, respectively. Most of the air velocity values were between 0.2 and 1.4 m s⁻¹ (Fig. 4, f and 4, g). These values are statistically within the recommended range, that is between 1.4 to 2.2 m s⁻¹ (Bewley et al., 2012). According to Black et al. (2013), the air velocity close to the surface of the bed should be around 1.8 m s⁻¹.

The most predominant noise levels range was 70 to 80 dBA for 37.5% of CBP barns evaluated (Fig. 4, h). In the barns assessed in this study, higher noise intensities (62.7 ± 9.9 dBA) were produced by the LVHS fans. Dairy cows can adapt to different types and levels of sound pressure; However, stress animals should not be exposed to sudden or high sound pressures; otherwise, this may cause sound stress, which could lead to productivity losses and consequently to economic damages for the producer.

Characterization of the bedding material

The most commonly employed bedding material among the CBP barns evaluated in this study was sawdust (52.9%). The reason for this, according to the dairy farmers, is easy access and cost of the material. However, the growing demand for this product has driven up the price pushing farmers to look for new materials. The prevalence of sawdust use for bedding composition (70.0%) was also observed by Radavelli (2018).

According to Black et al. (2013), the bedding surface temperature tends to have values closer to air temperature. This tendency was verified in this study since the average bed surface temperature at the premises was 22.0 ± 3.6 °C and the average air temperature close to the bed was 26.7 ± 2.3 °C. The frequency distribution of the bed surface temperature (Fig. 5, a) shows that the predominant temperature range was between 20 to 23 °C.

The average bedding temperature at 0.20 m depth was 35.9 ± 3.9 °C, similar to that found by Black et al. (2013) in the U.S. state of Kentucky (36.1 ± 11.0 °C). Most of the bedding temperatures found were between 35 and 40 °C. The bedding temperature at the 0.20 m is below the recommendation in 75% of the CBP barns analyzed (Fig. 5, b). In order to ensure that the bedding is at the proper temperature for the composting process of the material to occur between 0.15 and 0.30 m depth, the temperature should be between 43 and 65 °C (Janni et al., 2007; Bewley et al., 2013).

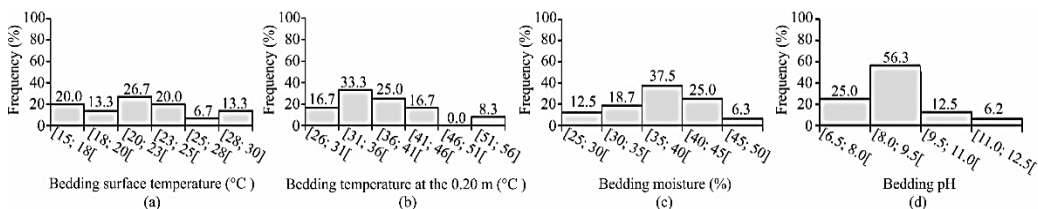


Figure 5. Frequency distribution of: a) Bedding surface temperature; b) Bedding surface temperature at 0.20 m; c) Bedding moisture; and d) Bedding pH.

The average bedding moisture was $36.9 \pm 5.2\%$, lower than the one found by Damasceno (2012), which was $59.0 \pm 9.0\%$. The mean value of the bedding moisture (37.5) of the CBP barns evaluated was between 35 and 40% (Fig. 5, c).

The mean pH value was 9.0 ± 0.8 , where the highest and lowest values were 20 cm depth, 11.4 and 7.3, respectively. In most of the bedding materials evaluated, the pH value was between 8.0 and 9.5 (Fig. 5, d). The mean value was close to the one determined by Janni et al. (2007), Radavelli (2018), and Fávero et al. (2015).

The penetration resistance values determined for each bedding layer are shown in Table 1. Table 1 shows an increase in the penetration resistance of the bedding as layer becomes deeper (113.4 to 1079.2 kPa). The deeper bedding layers carry a greater load, from the weight of the upper layers, remaining naturally more compacted.

This fact is evidenced by the increase in the mean values of penetration resistance, as the bedding layer get deeper.

Table 1. Penetration resistance values for the different bedding layers

Layer (mm)	Average (kPa)	SD (kPa)	Maximum (kPa)	Minimum (kPa)
0–50	113.4	87.5	414.6	21.9
50–100	529.4	252.3	1,408.7	94.5
100–150	850.1	331.1	1,704.9	186.1
150–200	1,079.2	348.9	1,698.2	319.6

Evaluation of locomotion score, hygiene score, and body condition score

The predominant breed was $\frac{3}{4}$ Holsteins and $\frac{1}{4}$ Gyr (35.7%). The average milk production of the herds was 28.4 ± 2.4 kg animal⁻¹ day⁻¹ (Fig. 6, a), which is higher than the production found by Radavelli (2018) in CBP barns in the south of Brazil, 22.4 ± 3.8 kg animal⁻¹ day⁻¹. This difference can be attributed to better food management, herd genetics and animal welfare of the facilities.

The mean locomotion score of the herd was 1.83 ± 0.25 . The most frequent range was 1.5 to 2.0 (41.7%), in general, the cows had a good locomotion score, and the incidence of lameness is not common (Fig. 6, b).

The mean hygiene score of the herd was 1.56 ± 0.39 (Fig. 6, c). The frequency distribution of hygiene score showed that dairy cows generally had an excellent hygiene score, which is evident when comparing it to the results obtained by Barberg et al. (2007) and Shane et al. (2010), where the mean scores were 2.6 and 3.1, respectively.

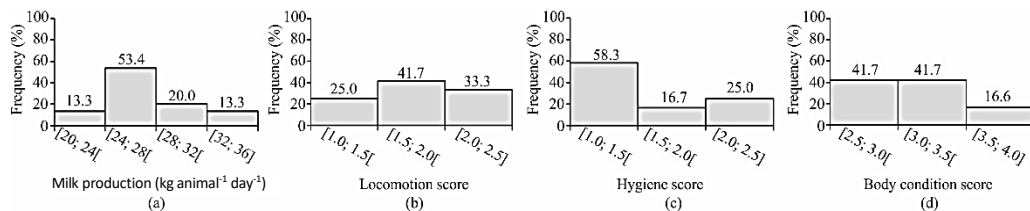


Figure 6. Frequency distribution of: a) Milk production; b) Locomotion score; c) Hygiene score; and d) Body condition score.

The average body condition score of the milking herd was 3.15 ± 0.24 (Fig. 6, d). The body condition score of the animals was satisfactory, and the variations presented are acceptable due to the performance of the evaluation in animals that were at different productive levels and lactation stages.

CONCLUSIONS

In general, dairy farmers were satisfied with the results obtained by the compost dairy barn (CBP), they observed a significant increase in milk production and improvement of herd hygiene and comfort.

The CBP barns architectural characteristics showed great variability in designs, dimensions, and materials used for the creation of the system. Some of these characteristics were not in accordance with the values recommended in the literature, a fact that can cause severe difficulties in the handling and operation of the system.

Cow stocking density on the composted pack is a crucial element of barn management. The average frequency of cow stocking density found in this study was 10.4 m² per animal

In general, the bedding was stirred twice a day using a rotary tiller with a cultivator. The LVHS fans are predominant among CBP barns with a high air velocity and noise levels.

The supply of bedding material is one of the biggest concerns for many farmers. Sawdust (52.9%) is being used more frequently, but there was a tendency to increase the use of coffee husk, due to the availability, cost, and accessibility of the material in the assessed regions. The bedding surface temperature was similar to air temperature, 22.0 ± 3.6 °C. The average bedding temperature at 0.20 m depth was 35.9 ± 3.9 °C. The importance of the bedding moisture content is reflected in the bedding temperature. In this study, the bedding moisture was $36.9 \pm 5.2\%$. The moisture content range for minimum aerobic microorganism heat production is 40–60%.

In general, the dairy cows showed a good locomotion score, hygiene score, and body condition score.

ACKNOWLEDGEMENTS. We would like to thank the following groups for their help with this study: The Federal University of Lavras for this great opportunity; the Brazilian State Government Agency, FAPEMIG; the National Counsel of Technological and Scientific Development (CNPq - Brazil); and the Federal agency, CAPES, for their financial support.

REFERENCES

- Arachchige, A.H., Fisher, A.D., Wales, W.J., Auldist, M.J., Hannah, M.C. & Jongman, E.C. 2014. Space allowance and barriers influence cow competition for mixed rations fed on a feed-pad between bouts of grazing. *Journal of dairy science* **97**, 3578–3588.
- Arceivala, S.J. 1981. Wastewater treatment and disposal; engineering and ecology in pollution control: M. Dekker, 862 pp.
- Barberg, A.E., Endres, M.I., Salfer, J.A. & Reneau, J.K. 2007. Performance and welfare of dairy cows in an alternative housing system in Minnesota. *Journal of Dairy Science* **90**, 1575–1583.
- Bewley, J.M., Taraba, J.L., Day, G.B., Black, R.A. & Damasceno, F.A. 2012. Compost bedded pack barn design features and management considerations. Cooperative Extension Publ. ID-206, Cooperative Extension Service, University of Kentucky College of Agriculture, Lexington KY.
- Bewley, J.M., Taraba, J.L., Mcfarland, D., Garrett, P., Graves, R., Holmes, B. & Wright, P. 2013. Guidelines for managing compost bedded-pack barns. The dairy practices council, 19 pp.
- Black, R.A., Taraba, J.L., Day, G.B., Damasceno, F.A. & Bewley, J.M. 2013. Compost bedded pack dairy barn management, performance, and producer satisfaction. *Journal of Dairy Science* **96**, 8060–8074.
- Black, R.A., Taraba, J.L., Day, G.B., Damasceno, F.A., Newman, M.C., Akers, K.A., Wood, C.L., Mcquerry, K.J. & Bewley, J.M. 2014. The relationship between compost bedded pack performance, management, and bacterial counts. *Journal of Dairy Science* **97**, 2669–2679.
- Cook, N.B., Mentink, R.L., Bennet, T.B. & Burgi, K. 2007. The Effect of Heat Stress and Lameness on Time Budgets of Lactating Dairy Cows. *J Dairy Sci.* **90**, 1674–1682.
- Costa, M.J. & Silva, L.C. 2014. *Good practices in handling: Dairy calves* (Boas práticas no manejo: Bezerros leiteiros). 1. ed. (2. rev.) Jaboticabal: FUNEP. 51 pp. (in Portuguese).
- Damasceno, F.A. 2012. Compost bedded pack barns system and computational simulation of airflow through naturally ventilated reduced model. *Thesis*, Universidade Federal de Viçosa, Brazil, 404 pp.
- Eckelkamp, E.A. Gravatte, C.N., Coombs, C.O. & Bewley, J.M. 2014. Case study: characterization of lying behavior in dairy cows transitioning from a freestall barn with pasture access to a compost bedded pack barn without pasture access. *The Professional Animal Scientist* **30**, 109–113.
- Embrapa. 2018. Milk yearbook 2018: Indicators, trends and opportunities for people living in the dairy sector. Available in: <https://www.embrapa.br/busca-de-noticias/-/noticia/36560390/anoario-do-leite-2018-e-lancado-na-agroleite>. Acesso em 19 nov. 2018.
- Fávero, S., Portilho, F.V., Oliveira, A.C., Langoni, H. & Pantoja, J.C. 2015. Factors associated with mastitis epidemiologic indexes, animal hygiene, and bulk milk bacterial concentrations in dairy herds housed on compost bedding. *Livestock Science* **181**, 220–230.
- Gay, S.W. 2009. Bedded-pack Dairy Barns. Virginia Cooperative Extension, 442–124.
- Graves, R.E. & Brugger, M.F. 1994. Naturally ventilated freestall barns. Expansion Strategies for Dairy Farms: Facilities and Financial Planning. New York: NRAES77, 409–417.

- Janni, K.A., Endres, M.I., Reneau, J.K. & Schoper, W.W. 2007. Compost dairy barn layout and management recommendations. *Applied engineering in agriculture* **23**, 97–102.
- Machado, R., Corrêa, R.F., Barbosa, R.T. & Bergamaschi, M.A. 2008. Body condition score and its application in the reproductive management of ruminants. Embrapa Pecuária Sudeste-Circular Técnica (INFOTECA-E), 16 pp. (in Portuguese).
- MWPS-7. 2000. *Dairy Freestall Housing and Equipment*, 7th ed. Ames, Iowa: MidWest Plan Service, 232 pp.
- Ofner-Schröck, E., Zähner, M., Huber, G., Guldemann, K., Guggenberger, T. & Gasteiner, J. 2015. Compost barns for dairy cows aspects of animal welfare. *Journal of Animal Science* **5**, 124–131.
- Radavelli, W.M. 2018. *Characterization of the compost barn system in Brazilian subtropical regions*. Dissertation (Master in Animal Science) - University of Santa Catarina, Chapecó, Brazil, 89 pp. (in Portuguese, English abstr.)
- Shane, E.M., Endres, M.I. & Janni, K.A. 2010. Alternative bedding materials for compost bedded pack barns in Minnesota: a descriptive study. *Applied Engineering in Agriculture* **26**, 465–473.
- Sprecher, D.J., Hostetler, D.E. & Kaneene, J.B. 1997. A lameness scoring system that uses posture and gait to predict dairy cattle reproductive performance. *Theriogenology* **47**, 1179–1167.
- Tavares, J.E.; Benedetti, E. 2011. Water: use of drinking fountains and their influence on pasture cattle production. *FAZU em Revista* **8**, 152–157 (in Portuguese, English abstr.).
- Zhao, S., Liu, X. & Duo, L. 2012. Physical and Chemical Characterization of Municipal Solid Waste Compost in Different Particle Size Fractions. *Polish Journal of Environmental Studies* **21**, 509–515.

Trace level determination of cadmium and lead in coffee (*Coffea*) using gold nanoparticles modified graphene paste electrode

S. Palisoc^{1,2}, J. Leoncini¹ and M. Natividad^{1,2,*}

¹De La Salle University, Condensed Matter Research Laboratory, Physics Department, 2401 Taft Avenue, PH922 Manila, Philippines

²De La Salle University, Condensed Matter Research Unit, CENSER, 2401 Taft Avenue, PH922 Manila, Philippines

*Correspondence: michelle.natividad@dlsu.edu.ph

Abstract. Gold nanoparticles (AuNP) modified graphene paste electrodes (GPE) were fabricated using graphene powder, gold nanoparticles, and mineral oil. The fabricated electrodes were used as working electrode in anodic stripping voltammetry (ASV) for the determination of trace concentrations of cadmium (Cd^{2+}) and lead (Pb^{2+}). The modified GPE was characterized using scanning electron microscopy and cyclic voltammetry. Optimization of the electrode's AuNP content and the ASV parameters was performed. It was determined that the GPE modified with 0.5 mg AuNP obtained the highest anodic current peaks for both Cd^{2+} and Pb^{2+} . The calibration curves obtained using the said electrode showed a linear relationship between heavy metal concentration and peak current and the detection limits were found to be 256 ppb for lead and 267 ppb cadmium. The modified electrode was successful in determining traces of Cd^{2+} and Pb^{2+} in coffee samples. The presence of the heavy metals in the samples were verified using atomic absorption spectroscopy.

Key words: gold nanoparticles, graphene, heavy metals, coffee, voltammetry.

INTRODUCTION

Heavy metals when accumulated in soils and plants pose great risks to human health through direct ingestion or the food chain (soil-plant-human or soil-plant-animal-human) (Wuana & Okieimen, 2011). Any kind of heavy metal is considered to be a contaminant if found where it is unusual or if it has detrimental effects on humans and on the environment. Some metals such iron, cobalt, copper, manganese, molybdenum, and zinc, in trace amounts, are required by the human body (Soetan et al., 2010). They are part of the ‘minerals’ the ‘glow’ portion of the food pyramid. Consumed in large amounts, however, they are dangerously toxic and cause serious damage to human health. Heavy metals such as lead, cadmium, mercury, and arsenic have no beneficial effect on the human body. These metals, when accumulated in the human body over time, cause serious damage to the liver and kidneys or even the nervous system (Singh et al., 2011). Furthermore, these metals displace the significant nutritional minerals from their original place and cause to hinder its biological functions (Jaishankar et al., 2014).

Coffee plantations are now adversely affected by environmental pollutants emanating from mining sites near them. Even if the mines are considerably far from the plantations, their effluents are transported by the river systems passing through them. These river systems are the sources of irrigation of the plantations. Through absorption by the root, heavy metals are accumulated in plants (Dalcorsio et al., 2013). These metals are transported via the xylem and distributed to the above-ground sink tissues. However, the absorption and distribution of heavy metals in plants vary depending on the property of the species. A study was conducted to investigate the effects of cadmium (Cd), zinc (Zn) and nickel (Ni) on adult coffee plants (Tezotto et al., 2012). The result showed that after three months, the heavy metals penetrated the soil within the first 50 cm depth. This is the region where the concentration of the coffee plant roots is found. The leaf is not obviously affected but the Zn level in branches are very high. In the same study, it was found that coffee plants are highly tolerant to the metals and high doses of metals transport only little amount to the beans that are what humans are consuming.

Due to the possible adverse effects of heavy metals on human health through consumption of contaminated food and beverages, it is necessary to determine their heavy metal content. One of the methods used for heavy metal detection is anodic stripping voltammetry (ASV) which is a cost-effective method as opposed to spectroscopic methods. In ASV, the choice of the working electrode material is crucial for the success of the detection process. In recent years, modified carbon paste electrodes (MCPE) have been used as the working electrode in voltammetry due to its simplicity, versatility, low cost and easy construction (Almeida & Giannetti, 2002; Vytras et al., 2009; Afkhami et al., 2013; Zaidi, 2013; Kalambat & Srivastava, 2015; Chen et al., 2016; Saleh et al., 2018). Carbon-based nanomaterials such as graphene have been used in the construction of MCPEs due to their excellent conductivity which makes them ideal for sensor applications (Parvin, 2011; Gutierrez et al., 2014; Palisoc et al., 2018a, b). They possess unique physical and chemical properties such as their large surface area, high mechanical strength, and excellent thermal & electrical conductivity (Palisoc et al., 2016; Palisoc et al., 2019). Gold nanoparticles (AuNPs) are used as electrode modifier due to its good conductivity and large surface area. These nanoparticles show excellent sensitivity and selectivity in detecting trace heavy metals (Palisoc et al., 2017a, 2017b).

In this study, a novel gold nanoparticle modified graphene paste electrode (AuNP/GPE) was fabricated, optimized, and used to detect heavy metals in coffee (*Coffea*) via anodic stripping voltammetry.

MATERIALS AND METHODS

Glassware and equipment

A BOSCHE SAE200 electronic balance (BOSCH-Wagesysteme GmbH, Hungingen, Germany) was used in measuring the amounts of graphene and AuNPs. All glassware was cleaned using a BANDELIN SONOREX ultrasonic bath (BANDELIN electronic GmbH & Co. KG, Berlin, Germany). A BST8 potentiostat/galvanostat was used in the cyclic voltammetry and anodic stripping voltammetry analyses. A JEOL 5300 scanning electron microscope was used to characterize the morphology of the fabricated electrodes.

Chemicals, reagents, and real samples

Graphene nanopowder (multilayer graphene; average flake thickness: 60 nm) was purchased from Graphene Supermarket (Calverton, NY, USA). Gold nanopowder (< 100 nm particle size), sodium chloride, lead chloride, cadmium chloride, copper chloride, mineral oil, and nitric acid were purchased from Sigma, Aldrich (Sigma-Aldrich Pte Ltd, Singapore). Organic Arabica coffee beans, coffee leaves, stems and soil in which the coffee was grown were used for real sample analysis.

Fabrication of bare and AuNP-modified GPEs

The graphene paste mixture was prepared by mixing 0.80 μL of mineral oil, 0.21 g of graphene powder and varying amounts of AuNP for 30 min using agate mortar and pestle. The resulting mixture was packed in a Teflon syringe with a diameter of 6mm. The tip of the electrode was polished with wet filter paper and a copper wire was attached to it with silver paste for the ohmic contact.

Mineral Oil and AuNP amount optimization

The amount of AuNP was varied and the amount that yields the highest anodic current peak was determined. The amount of AuNP are the following: 0.1 mg, 0.2 mg, 0.3 mg, 0.4 mg, 0.5 mg, 1 mg, 1.5 mg, and 2.0 mg. The amount of graphene and mineral oil were held constant at 0.21 g and 0.80 μL , respectively. The optimized electrode was used to simultaneously detect trace amounts of cadmium and lead.

Cyclic voltammetry and Anodic stripping voltammetry

Cyclic voltammetry (CV) and ASV measurements were done using a BST8 potentiostat/galvanostat. The working electrode, which is the fabricated AuNP/GPE, was placed together with the silver/silver chloride reference electrode and platinum counter electrode in the voltammetric cell. Sodium chloride of mass 0.5844 g was dissolved in 100 mL of deionized water to make the electrolyte solution.

Real Sample Analysis

Chopped coffee leaves and stalks, and ground coffee beans were dried in a furnace. One gram of each sample was weighed and carbonized on a hot plate and then transferred to the furnace with a temperature of 500 $^{\circ}\text{C}$ to dry ash the sample. The ashes were dissolved in nitric acid and placed back on the hot plate for the acid to evaporate. The sample was then transferred to an electrolyte solution for ASV and atomic absorption spectroscopy (AAS) analyses to simultaneously detect Pb^{2+} and Cd^{2+} .

Atomic Absorption Spectrometry

The presence of cadmium and lead in the real samples was verified by flame atomic absorption spectroscopy (AAS) using a Shimadzu (Japan) AA-6300 atomic absorption spectrophotometer. Standard solutions of lead and cadmium were used to obtain the calibration curve. Three trials were done in the AAS analysis of the real samples.

RESULTS AND DISCUSSION

Optimization of electrode modifier

The determination of the best-modified electrode was done by varying the amounts of AuNP while the graphene powder (0.21 g) and mineral oil (0.80 μL) were held constant. Eight electrodes were prepared with different amounts of AuNP from 0.1 mg to 2.0 mg. The resulting electrodes were then used to detect 10 ppm each of Cd^{2+} and Pb^{2+} . The bar graph in Fig. 1 shows that 0.5 mg AuNP attained the highest peak current for both Cd^{2+} and Pb^{2+} . Therefore, this was considered as the optimum AuNP content in this study.

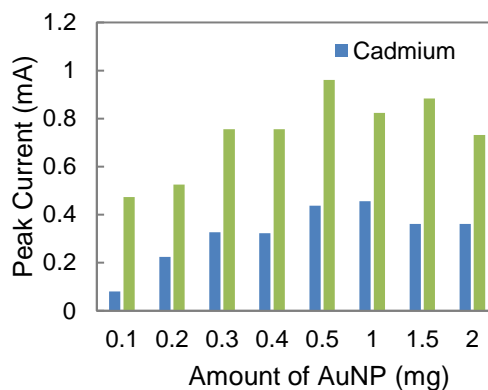


Figure 1. Comparison of peak currents of Cd^{2+} and Pb^{2+} using AuNP/GPE with varying AuNP content.

Characterization of the fabricated electrodes

Cyclic voltammetry was used to characterize the electrochemical response of the fabricated electrodes. Fig. 2 shows the cyclic voltammograms of the bare GPE for 10 scans. The graph shows that the bare electrode is conducting but there are no peaks. In Fig. 3, the cyclic voltammograms obtained from the AuNP-modified GPE show that an anodic peak is present but it is not reversible. This indicates that the AuNP modified GPE is more conductive as compared to the bare GPE.

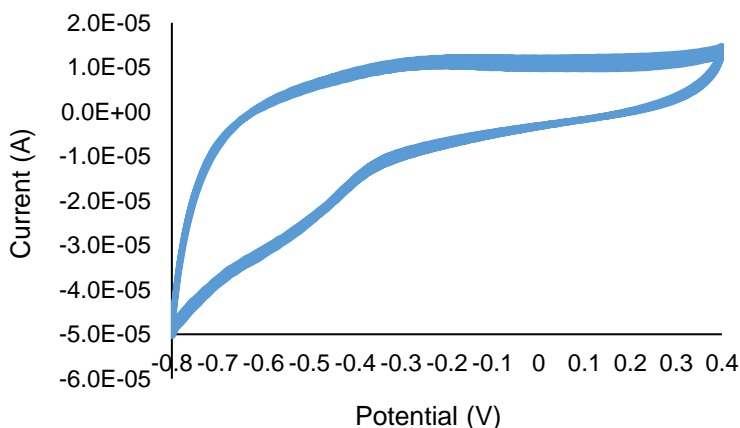


Figure 2. Cyclic voltammograms of the bare GPE for 10 scans.

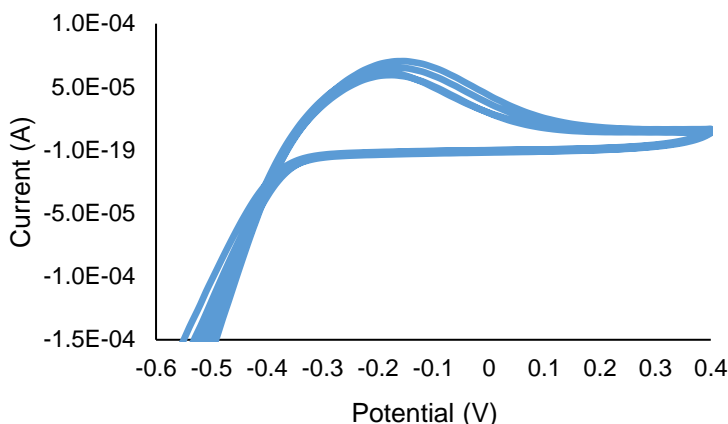


Figure 3. Cyclic voltammograms of the AuNP-modified GPE for 10 scans.

Fig. 4 shows the SEM image of the bare GPE at 20,000x magnification. The flakes reveal the presence of graphene in the electrode. Fig. 5 shows the SEM image of the AuNP-modified GPE. The granular microstructures represent the gold nanoparticles that adhered to the graphene surfaces. The gold nanoparticles can be seen as white cloudy spherical shaped particles based on the SEM image.

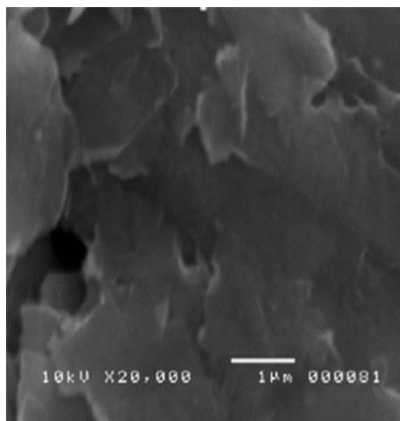


Figure 4. SEM image of bare GPE.

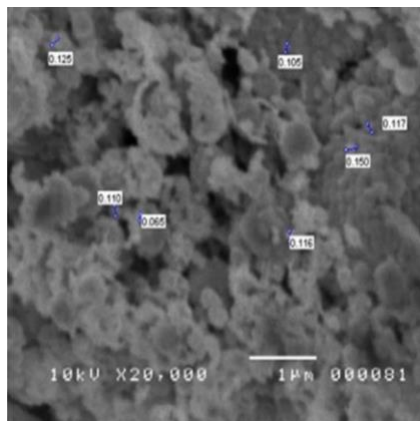


Figure 5. SEM image of AuNP-GPE.

Optimization of ASV Parameters

To obtain the highest peak current for the optimized electrode, different ASV parameters such as accumulation time, accumulation potential, deposition time, deposition potential and scan rate were optimized. The optimization of ASV parameters used the best-modified electrode to detect 10 ppm each of Cd^{2+} and Pb^{2+} in the electrolyte solution. Results were obtained by observing the relationship between the parameters and the peak current.

Accumulation Time

The accumulation time was set from 30 seconds to 180 seconds with increments of 30 seconds. A time with less than 30 s increment e.g. 15 s would be inefficient whereas a time increment greater than 30 e.g. 60 s would result in bigger gaps of data points and may affect the smoothness of the voltammogram. Fig. 6 shows that 60 s as the optimum accumulation time.

Deposition Time

To determine the optimum deposition time, the accumulation potential was set to -0.80V and accumulation time to 60s and were held constant. The deposition time was varied from 30s to 150s with 30s interval. From Fig. 7, it can be observed that the peak current is highest at 90s.

Deposition Potential

The deposition potential was varied from -0.8V to 1.0V. It can be seen from the bar graph in Fig. 8 that the optimum deposition potential is 0.8V for Cd and -0.85V for Pb.

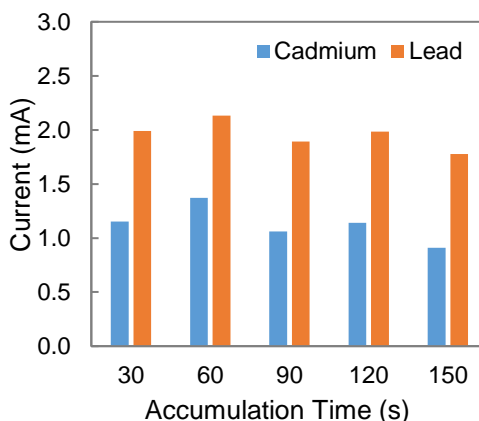


Figure 6. Optimization of accumulation time.

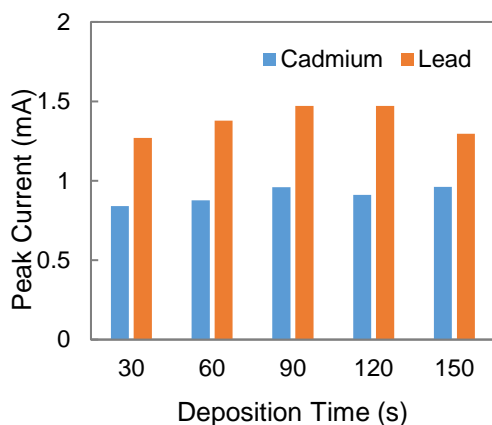


Figure 7. Optimization of deposition time.

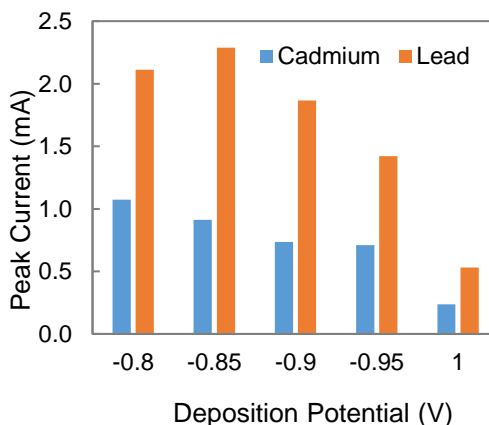


Figure 8. Bar graphs of optimization of deposition potential.

Calibration Curve

The calibration curves of the best electrode were obtained by varying the concentration of cadmium and lead from 750 ppb to 1,000 ppb. Figs 9 to 11 show the voltammograms and the obtained calibration curves for Cd^{2+} and Pb^{2+} . It can be seen from the figure that the peak current increased as the heavy metal concentration

increased which means that more heavy metals accumulate on the surface of the electrode. The Pearson correlation coefficient (R^2) for both heavy metals are close to 1 indicating that there is a strong linear relationship between the peak current and heavy metal concentration.

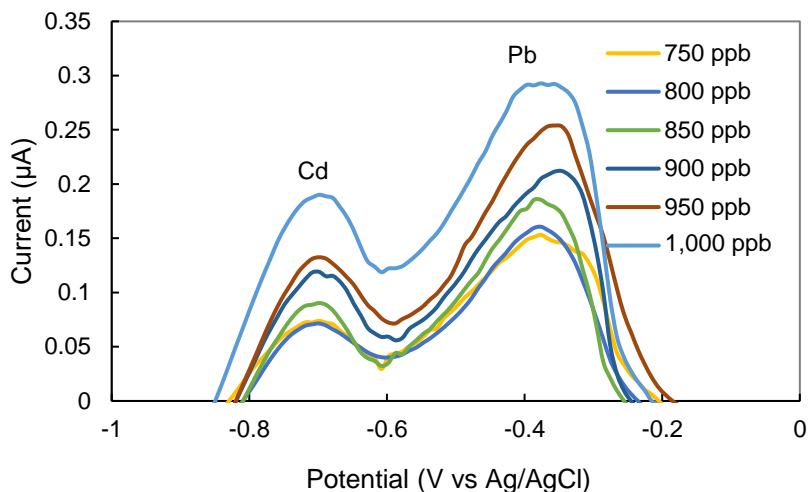


Figure 9. Anodic stripping voltammograms for various concentrations of Pb and Cd.

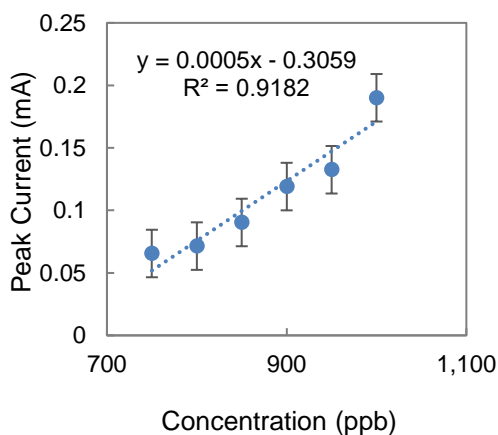


Figure 10. Calibration curve for cadmium.

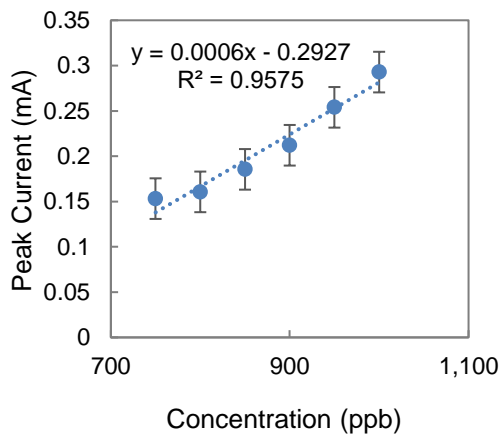


Figure 11. Calibration curve for lead.

Figures of Merit

The limit of detection (LOD) of the fabricated AuNP-GPE was found to be 267 ppb for cadmium and 256 ppb for lead while the limit of quantitation (LOQ) is 810 ppb for cadmium and 776 ppb for lead. The performance comparison of the fabricated electrode with previous works Table 1.

Table 1. Performance comparison of the fabricated electrode with other works

Electrode	Modifier	LOD	Method	Reference
ITO	[Ru(NH ₃) ₆] ³⁺ /Nafion	Pb & Cd – 500 ppb	ASV	Palisoc et al., 2015
GCE	AuNP/[Ru(NH ₃) ₆] ³⁺ /Nafion	Pb – 45 ppb Cd – 200 ppb	ASV	Palisoc et al., 2017a
GCE	Chitosan/carbon nanotubes	Pb – 600 ppb Cd – 800 ppb	SWASV	Wu et al., 2017
CPE	AgNP	Pb – 111 ppb Cd – 183 ppb	ASV	Palisoc et al., 2018b
GPE	AuNP	Pb – 256 ppb Cd – 267 ppb	ASV	this work

ITO – Indium Tin Oxide; GCE – Glassy Carbon Electrode; CPE – Carbon Paste Electrode.

Real Sample Analysis

A total of twenty (20) samples from five (5) different farms were obtained. The selection of the samples was composed of soil, stalks, leaves, and beans (raw). Each sample underwent dry ashing and acid digestion and was subjected to ASV and AAS analyses. The ASV results of the 20 samples are summarized in Table 2. The corresponding bar graph is shown in Fig. 12. It can be seen from Table 2 and Fig. 12 that Cd²⁺ was detected in all the samples while Pb²⁺ was not detected in some samples. The concentration of Pb²⁺ in said samples was probably below the detection limit of the electrode. Table 3 and the corresponding bar graph in Fig. 13 show the results obtained from AAS. It can be observed that Cd²⁺ was present in all the samples verifying the ASV result. Lead was also not detected in some samples. The discrepancies in the ASV and AAS results can be attributed to the different LOD and sensitivities of the two methods.

Table 2. Results of Real Sample Analysis via ASV

	Farm 1	Farm 2	Farm 3	Farm 4	Farm 5
Soil					
Cd (in ppb)	1978.33	1953.33	630	686.67	1,400
Pb (in ppb)	ND	ND	607.43	ND	910
Stalk					
Cd (in ppb)	970	711.67	785	815.83	1,400
Pb (in ppb)	ND	633.71	741.43	ND	910
Leaves					
Cd (in ppb)	711.67	715	800	785	719.83
Pb (in ppb)	ND	690	ND	738.57	ND
Beans					
Cd (in ppb)	677	691.66	810	708.33	675.83
Pb (in ppb)	ND	ND	ND	ND	ND

ND – not detected.



Figure 12. Comparison of Cd and Pb concentrations in the real samples measured using ASV.

Table 3. Results from Real Sample Analysis via AAS

	Farm 1	Farm 2	Farm 3	Farm 4	Farm 5
Soil					
Cd (in ppb)	142	111.67	111.83	107	113.33
Pb (in ppb)	792.5	337.5	1975	292.5	350
Stalk					
Cd (in ppb)	108.67	105.5	105.83	109.33	107.5
Pb (in ppb)	100	6.25	ND	227.5	55
Leaves					
Cd (in ppb)	110	116.33	110.33	113.67	110.67
Pb (in ppb)	82.5	147.5	47.5	92.5	17.5
Beans					
Cd (in ppb)	115.83	105.5	152.83	104.83	107.83
Pb (in ppb)	35	2.5	35	ND	17.5

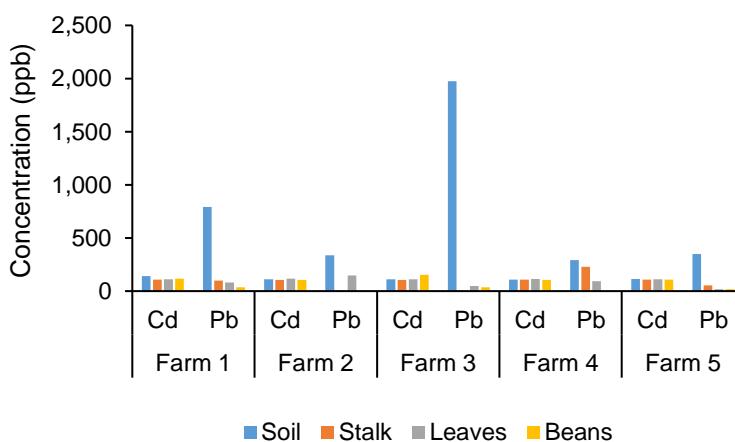


Figure 13. Comparison of Cd and Pb concentrations in the real samples measured using ASV.

The maximum level of heavy metal intake according to the World Health Organization is 10 ppb for lead and 3 ppb for cadmium (WHO, 2008). Based on the results from both AAS and ASV, it can be concluded that most of the samples are toxic. It is probable that the metals that were detected in the samples came from the mine tailings from the mining operations that have accumulated through the soil and nearby waters.

CONCLUSIONS

Gold nanoparticles modified graphene paste electrodes were fabricated and were used for the simultaneous detection of lead and cadmium via anodic stripping voltammetry. The amount of gold nanoparticles was varied while the amounts of graphene and mineral oil were kept constant. The AuNP content that obtained the highest peak current for both Cd^{2+} and Pb^{2+} was the 0.5 mg. Thus, this was chosen as the best-modified electrode. Anodic stripping voltammetry parameters were optimized to improve the performance of the best modified electrode. Under optimum conditions, the calibration curves obtained for both Cd^{2+} and Pb^{2+} showed a linear relationship between the peak current and heavy metal concentration and the limit of detection is 256 ppb for lead and 267 ppb cadmium. The AuNP-GPE was successful in detecting trace metals in coffee and soil samples. The presence of Cd^{2+} and Pb^{2+} in the real samples was verified by AAS analysis.

REFERENCES

- Afkhami, A., Soltani-Felehgari, F. & Madrakian, T. 2013. Gold nanoparticles modified carbon paste electrode as an efficient electrochemical sensor for rapid and sensitive determination of cefixime in urine and pharmaceutical samples. *Electrochimica Acta* **103**, 125–133.
- Almeida, C.M.V.B. & Giannetti, B.F. 2002. A new and practical carbon paste electrode for insoluble and ground samples. *Electrochemistry Communications* **4**, 985–988.
- Chen, G., Hao, X., Li, B.L. & Li, N.B. 2016. Anodic stripping voltammetric measurement of trace cadmium at antimony film modified sodium montmorillonite doped carbon paste electrode. *Sensors and Actuators B: Chemical* **237**, 570–574.
- Dalcorso, G., Manara, A. & Furini, A. 2013. An overview of heavy metal challenge in plants: from roots to shoots. *Metallomics* **5**, 1117–1132.
- Gutierrez, F., Comba, F., Gasnier, A., Gutierrez, A., Galicia, L., Parrado, C, Rubianes, M. & Rivas, G. 2014. Graphene Paste Electrode: Analytical Applications for the Quantification of Dopamine, Phenolic Compounds and Ethanol. *Electroanalysis* **26**, 1–9.
- Jaishankar, M., Tseten, T., Anbalagan, N., Mathew, B. & Beeregowda, K. 2014. Toxicity, mechanism and health effects of some heavy metals. *Interdisciplinary Toxicology* **7**, 60–72.
- Kalambat, P., Biradar, M., Karna, S. & Srivastava, A. 2015. Adsorptive stripping differential pulse voltammetry determination of rivastigimine at graphene nanosheet-gold nanoparticle/carbon paste electrode. *Journal of Electroanalytical Chemistry* **757**, 150–158.
- Palisoc, S., Bentulan, J.M. & Natividad, M. 2019. Determination of trace heavy metals in canned food using Graphene/AuNPs/[$\text{Ru}(\text{NH}_3)_6$] $^{3+}$ /Nafion modified glassy carbon electrodes. *Journal of Food Measurement and Characterization* **13**, 169–176.
- Palisoc, S., Estioko, L.C. & Natividad, M. 2018a. Voltammetric determination of lead and cadmium in vegetables by graphene paste electrode modified with activated carbon from coconut husk. *Materials Research Express* **5**, 1–10.

- Palisoc, S., Lee, E., Natividad, M. & Racines, L. 2018b. Silver Nanoparticle Modified Graphene Paste Electrode for the Electrochemical Detection of Lead, Cadmium and Copper. *International Journal of Electrochemical Science* **13**, 8854–8866.
- Palisoc, S., Causing, A.M. & Natividad, M. 2017a. Gold nanoparticle/hexaammineruthenium/Nafion® modified glassy carbon electrodes for trace heavy metal detection in commercial hair dyes. *Analytical Methods* **9**, 4240–4246.
- Palisoc, S., Valeza, N. & Natividad, M. 2017b. Fabrication of an effective gold nanoparticle/graphene/Nafion® modified glassy carbon electrode for high sensitive detection of trace Cd²⁺, Pb²⁺ and Cu²⁺ in tobacco and tobacco products. *International Journal of Electrochemical Science* **12**, 3859–3872.
- Palisoc, S., Natividad, M., Calde, D.M. & Rosopa, E.R. 2016. Trace Determination of Lead and Cadmium using Graphene/[Ru(NH₃)₆]³⁺/Nafion Modified Glassy Carbon Electrodes. *Journal of New Materials for Electrochemical Systems* **19**, 223–228.
- Palisoc, S., Natividad, M., Martinez, N., Ramos, R. & Kaw, K. 2015. Fabrication and electrochemical study of [Ru(NH₃)₆]³⁺/Nafion modified electrodes for the determination of trace amounts of Pb²⁺, Cd²⁺, and Zn²⁺ via anodic stripping voltammetry. *e-Polymers* **16**, 117–123.
- Parvin, M.H. 2011. Graphene paste electrode for detection of chlorpromazine. *Electrochemistry Communications* **13**, 366–369.
- Saleh, T., AlAqad, K. & Rahim, A. 2018. Electrochemical sensor for the determination of ketoconazole based on gold nanoparticles modified carbon paste electrode. *Journal of Molecular Liquids* **256**, 39–48.
- Singh, R., Gautam, N., Mishra, A. & Gupta, R. 2011. Heavy metals and living systems: An overview. *Indian Journal of Pharmacology* **43**, 246–253.
- Soetan, K., Olaiya, C. & Oyewole, O. 2010. The importance of mineral elements for humans, domestic animals and plants: A review. *African Journal of Food Science* **4**, 200–222.
- Tezotto, T., Favarin, J.L., Azevedo, R.A., Alleoni, L.R.F. & Mazzafera, P. 2012. Coffee is highly tolerant to cadmium, nickel and zinc: Plant and soil nutritional status, metal distribution and bean yield. *Field Crops Research* **125**, 25–34.
- Vytras, K., Svancara, I. & Metalika, R. 2009. Carbon paste electrodes in electroanalytical chemistry. *Journal of the Serbian Chemical Society* **74**, 1021–1033.
- WHO. 2008. *Guidelines for drinking-water quality*. 3rd edition incorporating 1st and 2nd addenda. Vol. **1**. Recommendations. Geneva, World Health Organization, pp. 392–394.
- Wu, K., Lo, H., Wang, J., Yu, S. & Yan, B. 2017. Electrochemical detection of heavy metal pollutant using crosslinked chitosan/carbon nanotubes thin film electrodes. *Materials Express* **7**, 15–24.
- Wuana, R. & Okieimen, F. 2011. Heavy Metals in Contaminated Soils: A Review of Sources, Chemistry, Risks and Best Available Strategies for Remediation. *ISRN Ecology* **2011**, 1–20.
- Zaidi, S.A. 2013. Graphene: A comprehensive review on its utilization in carbon paste electrodes for improved sensor performance. *International Journal of Electrochemical Science* **8**, 11337–11355.

Yeast performance characterisation in different cider fermentation matrices

J. Rosend^{1,3}, R. Kuldjärv^{1,3}, G. Arju^{2,3} and I. Nisamedtinov^{1,4}

¹Tallinn University of Technology, School of Science, Department of Chemistry and Biotechnology, Division of Food Technology, Ehitajate tee 5, EE12616 Tallinn, Estonia

²Tallinn University of Technology, School of Science, Department of Chemistry and Biotechnology, Division of Chemistry, Ehitajate tee 5, EE12616 Tallinn, Estonia

³Center of Food and Fermentation Technologies, Akadeemia tee 15A, EE12618 Tallinn, Estonia

⁴Lallemand Inc., 1620 Rue Préfontaine, Montréal, QC H1W 2N8 Canada

*Correspondence: julia@tftak.eu

Abstract. Nitrogen content management before fermentation is often used in cider production to avoid sluggish fermentations. In addition to enhanced fermentation rates, the proper nitrogen content in the apple must may have an impact on the flavour characteristics of cider. This research aimed to assess yeast performance in two different commercially available musts with similar non-limiting yeast available nitrogen (YAN) content. In addition to fermentation kinetics, volatile ester production by yeast, and sensory properties of the final product were evaluated. The results showed that the fermentation rate and consumption of sugar and nitrogen sources by yeast did not vary between the two different musts. Yeasts consumed more malic acid in the environment of higher initial malic acid content. The content of volatile esters and sensory properties of the final products varied significantly. The occurrence of intense sulfur off-flavour was noted in one of the products.

Key words: cider, fermentation rate, gas chromatography, sensory analysis.

INTRODUCTION

Cider is a beverage made from apples through alcoholic fermentation, although in North-America, the term ‘cider’ generally refers to cloudy unpasteurized apple juice, and the term ‘hard cider’ – to a fermented product (Downing, 1995). The alcohol content of cider usually varies between 1.2 to 8.5% by volume (Lea & Piggott, 2003). However, the official alcohol limits are country-specific and defined by local laws. Notably, there are no definitive sensory characteristics for cider since the parameters like that colour, odour, sweetness, and bitterness vary significantly between the apple varieties and regions (Santos et al., 2016). Therefore, in order to obtain a cider with high quality, it is crucial to understand key parameters that contribute to the formation of desirable sensory characteristics during cider fermentation.

The main factors that influence the sensory quality of fermented beverages are the quality of must, the fermentation conditions, and yeast culture (Belda et al., 2017; Laaksonen et al., 2017). One of the primary parameters for successful fermentation is the proper yeast assimilable nitrogen (YAN) content of the must (Swiegers et al., 2008; Seguinot et al., 2018). In apple must, YAN is primarily composed of free amino acids (the so-called free amino nitrogen, FAN) and ammonium ions (Santos et al. 2016; Bourdeau et al., 2018). The contribution of amino acids to YAN can vary across different apple cultivars (Bourdeau et al., 2018).

Even though the average YAN content in apple juice is 120 mg L^{-1} , it can be as low as 30 mg L^{-1} (Drilleau, 1990; Cruz et al., 2002). The lack of initial nitrogen is strongly associated with slow fermentation or incomplete sugar utilisation, i.e. stuck fermentation (Alberti et al., 2014; Boudreau et al., 2018). Nitrogen can be a limiting nutrient in peptide/protein synthesis, sugar transport system, and fermentative activity during the initial stages of alcoholic fermentation (Santos et al., 2016). Initial nitrogen is also essential in terms of aroma generation during fermentation (Carrau et al., 2008; Barbosa et al., 2009; Seguinot et al., 2018) with amino acids acting as metabolic precursors for the biosynthesis of different volatile compounds, e.g. esters (Santos et al., 2016). The lack of nitrogen is often associated with hydrogen sulphide (H_2S) production, although the exact mechanisms of how YAN deficiency influences H_2S formation by yeast are still not clearly defined (Ugliano et al., 2007; Ugliano et al., 2010; Ugliano et al., 2011; Barbosa et al., 2012). Therefore, the management of H_2S in fermented beverages through nitrogen supplementation requires knowledge of both initial YAN and yeast H_2S production characteristics (Ugliano et al., 2011; Barbosa et al., 2012).

Nowadays, the selection of different yeasts (strains of *Saccharomyces cerevisiae* as well as non-*Saccharomyces* yeast species) for fermented beverages production is very diverse. Therefore, the information about yeast performance shared by yeast starter culture manufacturers is of great value for cider producers for choosing the right strain. Today, most yeast manufacturers provide information on the recommended fermentation conditions (e.g. temperature range and optimum temperature, alcohol tolerance), yeast nutrition requirements, expected fermentation duration, and possible sensory properties of the final product. With growing cider production and the increasing number of craft cider producers on the market (The European Cider and Fruit Wine Association, 2018) there is a need for product differentiation in order to gain a competitive advantage while maintaining stable quality. Thus, the proper selection of yeasts along with nutrition management of the fermentation process to ensure sufficient fermentation rate, complex aroma development and avoid off-aroma related defects (e.g., H_2S formation) is becoming more critical.

This study aims to explore and compare the performance of five different commercially available wine yeast strains in fermentation of different apple musts. The free amino nitrogen (FAN) content was brought to a similar level in the used apple musts to observe yeast behaviour in different matrices where free amino nitrogen is not a limiting factor. Yeast performance was observed in terms of fermentation efficiency, consumption of nutrients, production of ethyl and acetate esters, and overall sensory properties of the final product, including H_2S .

MATERIALS AND METHODS

Cider fermentation

This study made use of two different apple musts: M1 (Aspall, Suffolk, United Kingdom; Brix 12.8%, pH 3.28, titratable acidity 6.7 g L⁻¹ in malic acid equivalents, initial FAN 69.48 ± 2.00 mg L⁻¹) and M2 (Döhler, Darmstadt, Germany; Brix 11.7%, pH 3.18, titratable acidity 3.8 g L⁻¹ in malic acid equivalents, initial FAN 51.21 ± 1.84 mg L⁻¹). Free amino nitrogen content in both matrixes was brought to a similar content of 80 ± 2 mg L⁻¹ by using organic yeast nutrient (Fermaid K; Lallemand Inc.). The musts (400 mL) were distributed into sterile 500 mL fermentation bottles.

Each bottle was inoculated with a chosen rehydrated yeast starter culture, according to the manufacturer's (Lallemand, Inc.) instructions. The starter cultures used in this study were as follows: Y1 (*Torulaspora delbrueckii*), Y2 (*Saccharomyces cerevisiae*; white wine yeast selected through directed breeding), Y3 (*Saccharomyces cerevisiae* var. *bayanus*; red and white wine yeast for demanding conditions), Y4 (*Saccharomyces cerevisiae* var. *bayanus*; sparkling wine yeast), and Y5 (*Saccharomyces cerevisiae*; red, rosé, and white wine yeast selected through evolutionary adaptation).

Inoculated bottles (5 × 10⁶ CFU mL⁻¹) were sealed using screw caps with septums pierced with syringe needles (19G × 1 ½, 1.1 × 40 mm; Terumo Medical Corporation) and coupled with microfilters to vent carbon dioxide. Fermentations were carried out at 18 ± 1 °C by following carbon dioxide production by weighing of the fermentation bottles once per day on a daily basis. Fermentations were considered completed when the mass loss due to carbon dioxide dissipation could not be observed anymore (approx. 336 hours). Samples were withdrawn every second day for subsequent analysis. For each experiment, two parallel fermentations were performed.

Sugar and malic acid content

Sugars and malic acid content during the fermentation was analysed using high-performance liquid chromatograph (Alliance HPLC) equipped with BioRad HPX87H column, RI and UV detectors. Prior to analysis, the samples were diluted 1:10 with MilliQ water and filtered (Whatman Spartan 13; Dassel, Germany). 0.005 M H₂SO₄ solution was used as mobile phase with a flow rate of 0.6 mL min⁻¹. Standard solutions of fructose, glucose, sucrose, and malate were used for calibration curves.

FAN content

The FAN content at different stages of fermentation was assessed using DNFB (dinitrofluorobenzene) method which is based on the reaction of amino groups of free amino acids with 2,4-dinitrofluorobenzene. The reaction derivatives were subsequently measured by spectrophotometry at 420 nm. Standard solutions of glycine with known nitrogen content were used to obtain calibration curve. Results were expressed as mg L⁻¹ in glycine equivalents. Three analytical replicates were used for each sample.

GC-TOF-MS analysis of volatile esters

Headspace – solid phase microextraction (HS-SPME) was used for the extraction of volatile compounds. For that, 50 µL of each sample was diluted with 950 µL of distilled water; 2-chloro-6-methylphenol (100 µg L⁻¹) was used as an internal standard for quantitation purposes. Vials were pre-incubated at 45 °C for 5 minutes. An SPME

fiber (30/50 μm DVB/Car/PDMS Stableflex, length 2 cm; Supelco, Bellefonte, PA, USA) was used to extract the volatile compounds from the headspace for 20 minutes.

GCT Premier 6890N gas chromatograph system (Agilent Technologies, Santa Clara, CA, USA) equipped with TOF mass spectrometer (Waters, Milford, MA, USA) and a DB5-MS column (30 m length \times 0.25 mm i.d. \times 1.0 μm film thickness; J&W Scientific, Folsom, CA, USA) was used with helium as a carrier gas at a flow rate of 1.0 mL min⁻¹. The oven was programmed to ramp up from 40 °C at a rate of 7.5 °C min⁻¹ to a final temperature of 280 °C with an additional holding time of three minutes (total run time 35 min). Mass spectra were obtained at an ionization energy of 70 eV and a scan speed of 10 scans s⁻¹, with a mass scan range of 35 to 350 Da. Two analytical replicates were used for each sample.

A presence of selected ethyl (medium-chain fatty acid ethyl esters) and acetate esters was monitored across the samples. These two groups of esters are synthesized through different pathways and play a primary role in the perception of desired fruity attributes in fermented beverages (Saerens et al., 2010). A complete list of the compounds of interest and their odour descriptions is provided in Table 1. Accurate identification of the compounds was achieved using respective analytical standards. The concentrations were expressed in $\mu\text{g L}^{-1}$ of internal standard equivalents.

Sensory analysis

Descriptive analysis was used in the study to assess the sensory properties of the cider samples. A local sensory panel of 8 highly trained assessors with previous experience in working with cider samples carried out the analysis. There was no pre-session to familiarize assessors with the samples. The working linear scale was established at 0–15, and relative intensities were used. A complete list of assessed attributes and their definitions is provided in Table 2. Additional commentary (e.g., the presence of off-flavours) was encouraged if necessary. Samples were assessed independently by each assessor. Prior to the assessment, all samples were adjusted for sweetness to balance out the sour taste since the secondary malolactic fermentation was not carried out. For that, 3% of diluted sucrose was added. All samples were encoded with a randomized three-digit numerical key.

Table 1. A list of selected volatile esters and their odour descriptions

Ester	CAS	Odour description*
Ethyl acetate	141-78-6	Ethereal, fruity, green
Isobutyl acetate	110-19-0	Fruity, ethereal, banana
Isoamyl acetate	123-92-2	Fruity, banana
Butyl acetate	123-86-4	Ethereal, fruity, banana
Hexyl acetate	142-92-7	Fruity, green apple, banana
Ethyl butanoate	105-54-4	Fruity, pineapple, cognac
Ethyl hexanoate	123-66-0	Fruity, pineapple, waxy, green
Ethyl octanoate	106-32-1	Fruity, wine, apricot, banana
Ethyl decanoate	110-38-3	Waxy, fruity, apple, grape
Ethyl dodecanoate	106-33-2	Waxy, floral, soapy

*According to www.thegoodscentcompany.com

Table 2. A complete list of sensory attributes and their definitions

Attribute	Description
Odour	
Overall intensity	Overall strength of the perceived odour
Fruity	Strength of all fruity odours (excluding apple)
Cooked apple	Strength of odours characteristic to cooked apples
Apple-like	Strength of odours characteristic to fresh apples
Sweet	Strength of all sweet odours
Sour	Strength of all sour odours
Taste	
Fruity	Strength of overall sensation characteristic to fruits (excluding apples)
Cooked apple	Strength of overall sensation characteristic to cooked apples
Apple-like	Strength of overall sensation characteristic to fresh apples
Sweet	Strength of overall sweet sensation
Sour	Strength of overall sour sensation
Bitter	Strength of overall bitter sensation
Astringency	Strength of overall drying sensation

Data processing

The results of chemical analysis were averaged across biological and analytical replicates. The analysis of variance was performed using ANOVA (R software 3.4.0; Boston, MA, USA), and $p < 0.05$ was considered statistically significant. The results of sensory analysis were statistically evaluated by principal component analysis (PCA) using OriginPro software (OriginLab; Northampton, MA, USA). Prior to the application of PCA, the results were autoscaled.

RESULTS AND DISCUSSION

Fermentation kinetics with different yeasts (Fig. 1a, 2b) did not seem to be dependent on the apple must. Each yeast strain showed similar performance (i.e., fermentation duration, maximum speed of carbon dioxide production) in both matrices. Various authors have previously linked fermentation activity to the nitrogen content of the must (Santos et al., 2016; Boudreau et al., 2017; Lemos Junior et al., 2017; Seguinot et al., 2018). In this study, the nitrogen content of both musts was adjusted to the same value (80 ppm). Thus, the same nitrogen content might be the reason behind the absence of visible differences in fermentation rates between the studied musts M1 and M2.

The composition of initial fermentable sugars in the musts and residual sugars in the samples after the fermentation is summed up in Table 3. Up to 60% of initial sugar content in both apple musts consisted of fructose. The main difference in residual sugar consumption between the musts fermented with different yeasts was due to the different ability of the studied yeasts to consume fructose. For example, residual fructose concentrations in fermentations with *T. delbrueckii* (Y1) were up to 7 times higher than with the other studied strains. In general, sugar consumption patterns for the same strains were quite similar in the two studied musts, and small differences in residual amounts could instead be attributed to the initial Brix%.

Comparing fermentation kinetics and fructose consumption (Fig. 1a, 2b, Table 3) it becomes evident that yeasts with more fructophilic characteristics conduct a more intense fermentation. Thus, intrinsic differences in yeast fructose uptake could be utilised in cider production for process optimisation.

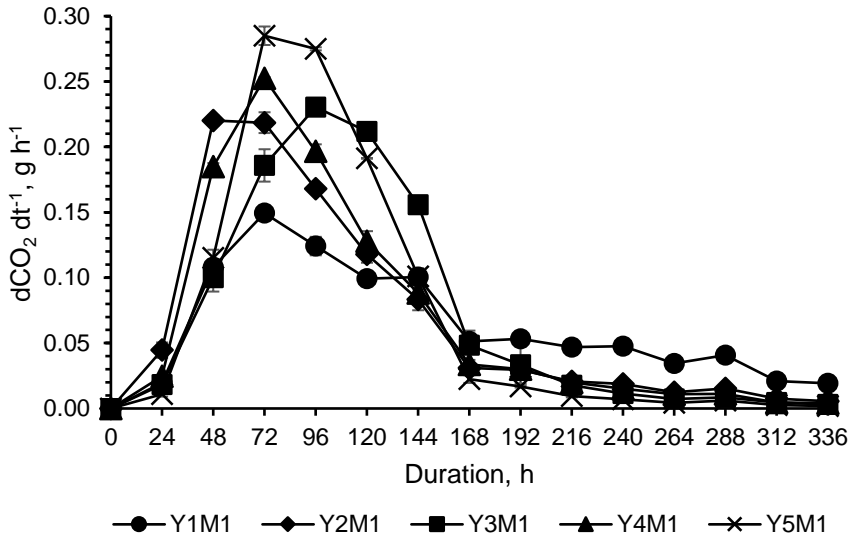


Figure 1a. Fermentation kinetics with different yeasts (Y1-5) in must M1.

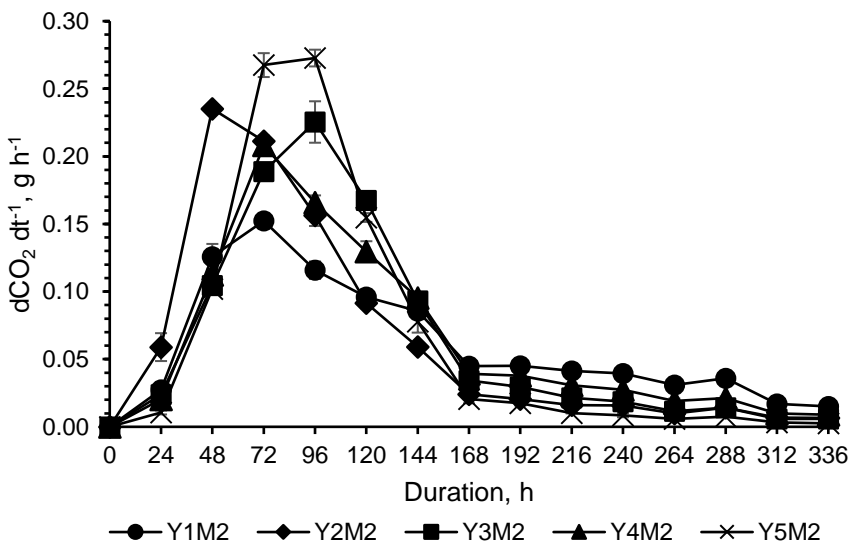


Figure 1b. Fermentation kinetics with different yeasts (Y1-5) in must M2.

Table 3. Composition of initial sugars in the musts (M) and residual sugars at the end of fermentation with different yeasts (YM) and musts ($p < 0.05$)

Amount, g L ⁻¹	Glucose	Fructose	Sucrose	TOTAL
M1	25.61 ± 2.18	74.93 ± 2.88	20.35 ± 3.02	120.89 ± 8.08
M2	26.83 ± 3.65	70.69 ± 2.93	16.33 ± 3.94	113.85 ± 10.52
Y1M1	0.67 ± 0.03	8.85 ± 0.94	1.15 ± 0.31	10.67 ± 0.96
Y1M2	1.12 ± 0.33	8.74 ± 0.86	1.27 ± 0.39	11.13 ± 0.79
Y2M1	0.45 ± 0.02	1.81 ± 0.18	0.60 ± 0.06	2.86 ± 0.58
Y2M2	1.29 ± 0.20	3.12 ± 0.29	1.19 ± 0.23	5.60 ± 0.93
Y3M1	0.24 ± 0.05	1.22 ± 0.17	0.53 ± 0.08	1.99 ± 0.12
Y3M2	1.31 ± 0.19	2.17 ± 0.40	1.27 ± 0.27	4.75 ± 0.98
Y4M1	0.22 ± 0.04	2.07 ± 0.18	0.57 ± 0.15	2.86 ± 0.22
Y4M2	1.20 ± 0.25	3.72 ± 0.49	1.15 ± 0.14	6.07 ± 0.81
Y5M1	0.23 ± 0.02	1.11 ± 0.10	0.60 ± 0.03	1.94 ± 0.19
Y5M2	1.36 ± 0.12	1.16 ± 0.17	1.70 ± 0.18	4.22 ± 0.50

A decrease in malic acid concentration was observed to some extent as a result of the fermentation process regardless of the must used (Fig. 2). The consumption of malic acid by yeasts was significantly higher in the must M1 where the initial concentration was approximately two times bigger than in the must M2 ($5.02 \pm 0.09 \text{ g L}^{-1}$ vs $3.03 \pm 0.13 \text{ g L}^{-1}$). The most drastic decrease of almost 44% in the malic acid concentration was observed in the case of *S. cerevisiae* var. *bayanus* (Y3) in M1 must. It has been previously reported that up to 50% of extracellular malic acid can be metabolised by *Saccharomyces* sp. yeasts during alcoholic fermentation of wine (Barnett & Kornberg, 1960; Delfini & Formica, 2001). The effect of more significant consumption of malic acid at its higher concentration by yeast could potentially be attributed to otherwise low affinity to malic acid of yeast malic enzyme (Mae1p) responsible for its decarboxylation to pyruvate (Volschenk et al., 2003). The K_m of Mae1p enzyme for malic acid is reported to be 50 mM (Boles et al., 1998) or approximately 6.7 g L^{-1} which is close to the initial concentration in M1.

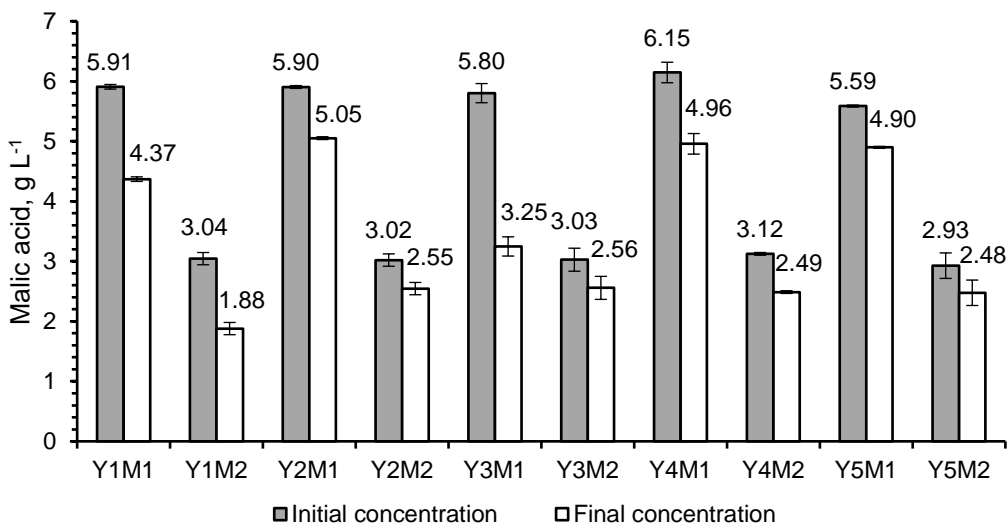


Figure 2. Malic acid consumption by different yeasts (Y1-5) in the two apple musts (M1 and M2) used in the study ($p < 0.05$).

The assimilation of free amino nitrogen (FAN) by the yeast strains used in this study is shown in Fig. 3a, 3b. Notably, complete depletion of FAN was not observed with any of the yeasts regardless of the fermentation matrix. The intense FAN consumption occurred in case of all strains within 2–4 days. The residual concentration of FAN at the end of fermentation was similar regardless of the yeast and must used although differences occurred in the FAN consumption rates. Notably, the consumption rates of FAN by yeasts used in this study did not always correlate with their fermentation activity. However, there might be a potential difference between yeasts with regards to their preference for specific amino acids for synthesis of volatile compounds (Lambrechts & Pretorius, 2000; Santos et al., 2015; Belda et al., 2017; Gobert et al., 2017; Fairbairn et al., 2017).

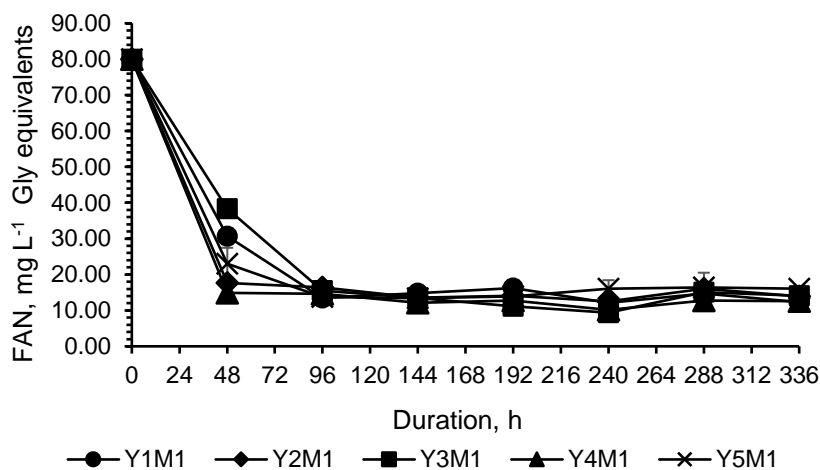


Figure 3a. Free amino nitrogen consumption by yeasts (Y1-5) during cider fermentation in the must M1.

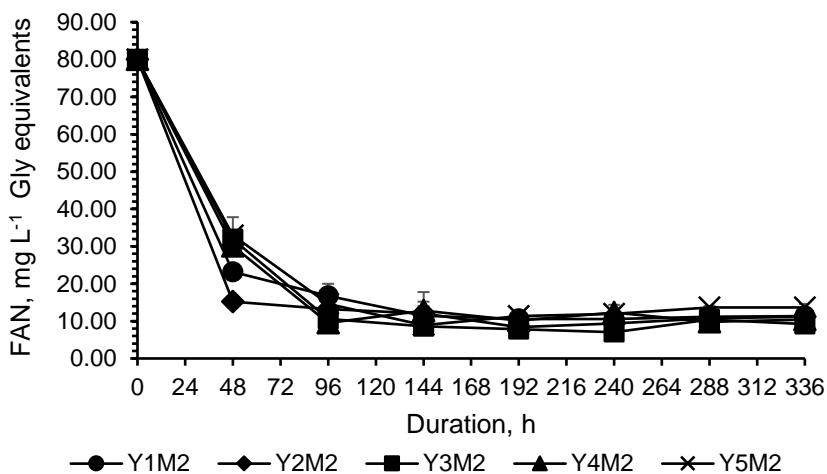


Figure 3b. Free amino nitrogen consumption by yeasts (Y1-5) during cider fermentation in the must M2.

In total, the concentration of 10 ethyl and acetate esters was monitored in the cider samples produced with five different yeasts and two musts (Table 4). Isobutyl acetate, butyl acetate, and ethyl dodecanoate were not detected in any of the analysed samples. *T. delbrueckii* (Y1) showed the lowest production of esters except isoamyl acetate. Others have previously noted significant production isoamyl acetate in *T. delbrueckii/S. cerevisiae* mixed inoculation during winemaking trials (Herraiz et al., 1990; Zhang et al., 2018). In addition to *T. delbrueckii*, *S. cerevisiae* var. *bayanus* (Y4) also produced considerably more (up to 3.5 times) isoamyl acetate in comparison to the others. The formation of three esters – ethyl acetate, isoamyl acetate, hexyl acetate depended on the matrix used. Both ethyl acetate and isoamyl acetate were produced in considerably (up to 7 and 2 times, respectively) higher concentrations by most strains in the must M2. Hexyl acetate, on the other hand, had higher relative concentrations in the samples made with the must M1. All three aforementioned esters are yeast metabolites produced during fermentation process. Ethyl acetate is formed in anaerobic glucose metabolism from acetyl-CoA with glutamate, methionine and cysteine precursors in its synthesis pathway (Nordström, 1962). Isoamyl acetate can either be created from amino acids (leucine, valine) or de novo synthesised from isoamyl alcohol (Eden, et al., 1996; Plata et al., 2003). Hexyl acetate originates from C6 alcohols and aldehydes (e.g., hexanol, 2-hexenol, 2-hexenal) (Dennis et al., 2012). Thus, in terms of volatile composition development of the final product, other intrinsic properties of the fermentation matrix than the YAN content should also be taken into account. The amount of ethyl esters depended on the particular yeast-must combination. For example, Y2 (*S. cerevisiae*) and Y4 (*S. cerevisiae* var. *bayanus*) favoured the production of ethyl decanoate in M1; Y3 (*S. cerevisiae* var. *bayanus*) and Y5 (*S. cerevisiae*)– in M2.

Table 4. Relative concentration (in $\mu\text{g L}^{-1}$ of IS equivalent) of selected esters at the end of fermentation with different yeasts (Y1-5) and apple musts (M1 and M2) ($p < 0.05$)

	Y1M1	Y2M1	Y3M1	Y4M1	Y5M1
Ethyl acetate	93.33 ± 18.86	95.00 ± 16.50	53.33 ± 0.00	456.67 ± 4.71	350.00 ± 4.71
Isobutyl acetate	n.d.	n.d.	n.d.	n.d.	n.d.
Isoamyl acetate	3,970.00 ± 381.84	2,646.67 ± 405.41	2,160.00 ± 341.50	4,933.33 ± 150.85	1,640.00 ± 18.86
Butyl acetate	n.d.	n.d.	n.d.	n.d.	n.d.
Hexyl acetate	n.d.	213.33 ± 37.71	156.67 ± 4.71	120.00 ± 18.86	580.00 ± 107.50
Ethyl butanoate	115.56 ± 15.40	248.89 ± 30.79	253.33 ± 18.86	222.22 ± 30.79	120.00 ± 18.86
Ethyl hexanoate	253.33 ± 56.57	1,484.44 ± 253.45	1,564.44 ± 320.37	1,366.67 ± 250.51	2,862.22 ± 348.03
Ethyl octanoate	24.44 ± 3.85	1,733.33 ± 188.56	1,960.00 ± 320.56	1,066.67 ± 149.27	6,680.00 ± 358.27
Ethyl decanoate	n.d.	66.67 ± 18.86	186.67 ± 37.71	n.d.	328.89 ± 55.51
Ethyl dodecanoate	n.d.	n.d.	n.d.	n.d.	n.d.

Table 4 (continued)

	Y1M2	Y2M2	Y3M2	Y4M2	Y5M2
Ethyl acetate	255.56 ± 56.70	466.67 ± 18.86	358.33 ± 21.21	1,273.33 ± 122.57	516.67 ± 14.14
Isobutyl acetate	n.d.	n.d.	n.d.	n.d.	n.d.
Isoamyl acetate	7,730.00 ± 183.85	3,084.44 ± 111.02	2,826.67 ± 270.64	7,533.33 ± 546.83	2,222.22 ± 114.96
Butyl acetate	n.d.	n.d.	n.d.	n.d.	n.d.
Hexyl acetate	n.d.	n.d.	n.d.	n.d.	26.67 ± 0.00
Ethyl butanoate	166.67 ± 24.04	266.67 ± 37.41	228.89 ± 19.25	226.67 ± 56.57	186.67 ± 37.71
Ethyl hexanoate	66.67 ± 18.86	1,048.89 ± 181.52	1,813.33 ± 226.27	4,160.00 ± 37.71	3,040.00 ± 263.99
Ethyl octanoate	n.d.	4,231.11 ± 858.46	2,106.67 ± 462.65	19,866.67 ± 1,395.36	7,680.00 ± 1,244.51
Ethyl decanoate	n.d.	106.67 ± 0.00	95.00 ± 16.50	623.33 ± 61.28	266.67 ± 57.61
Ethyl dodecanoate	n.d.	n.d.	n.d.	n.d.	n.d.

According to the ANOVA, statistically significant differences ($p < 0.05$) were obtained for most of the sensory attributes assessed with the exception of overall odour intensity ($p = 0.61$), ‘apple-like’ in odour ($p = 0.08$), ‘apple-like’ in taste ($p = 0.10$), sourness in odour ($p = 0.19$), and astringency ($p = 0.98$). The results of sensory analysis with the exception of statistically insignificant parameters were then subjected to principal component analysis (PCA). The obtained PCA biplot is presented in Fig. 4. The Principal Component 1 accounted for 54.54% of the differences between the samples; the Principal Component 2 – for 17.18%. Based on the biplot, ciders produced with the apple must M2 possessed strong correlation with fruitiness, sweetness, and ‘cooked apple’ characteristic. However, the samples made with the apple must M2 contained more residual sugar at the end of fermentation than the samples made with M1 (Table 3). This might have partially contributed to an enhanced perception of sweetness and fruitiness. The ciders made with the must M1 strongly correlated with sourness, which corresponds well with its higher titratable acidity and higher malic acid content in finished ferments. Correlation with other parameters in these samples is negative, which means the intensities were considerably lower in comparison with the samples made with M2.

In the course of sensory analysis, the ciders also received additional commentary by the panel members. According to this, all samples made with the must M1 had an off-flavour described as ‘animalic’ and ‘sulfur’. The occurrence of the off-flavour of significant intensity in the ciders made with M1 could also mask the fruitiness of these ciders. Based on the description, the most likely source of this off-flavour was proposed to be hydrogen sulphide. Indeed, the overproduction of hydrogen sulphide is regarded as one of the main challenges in cider production (Boudreau et al., 2017). The accumulation of hydrogen sulphide during fermentation can be related to multiple different factors such as susceptibility of yeast strain to produce it as well as nutritional composition of the environment (e.g., YAN and vitamins content) (Boudreau et al., 2017). The difference in initial YAN content was not the case in this study as it was

brought to the same level with Fermaid nutritional supplement prior to the start of fermentation. However, the difference in intrinsic amino acid and/or vitamin composition in the apple must could still be a key factor in off-flavour production. For example, Bohlscheid et al. (2011) have noted that biotin and pantothenic acid deficiency in the fermentation environment could result in excessive production of hydrogen sulphide by yeasts.

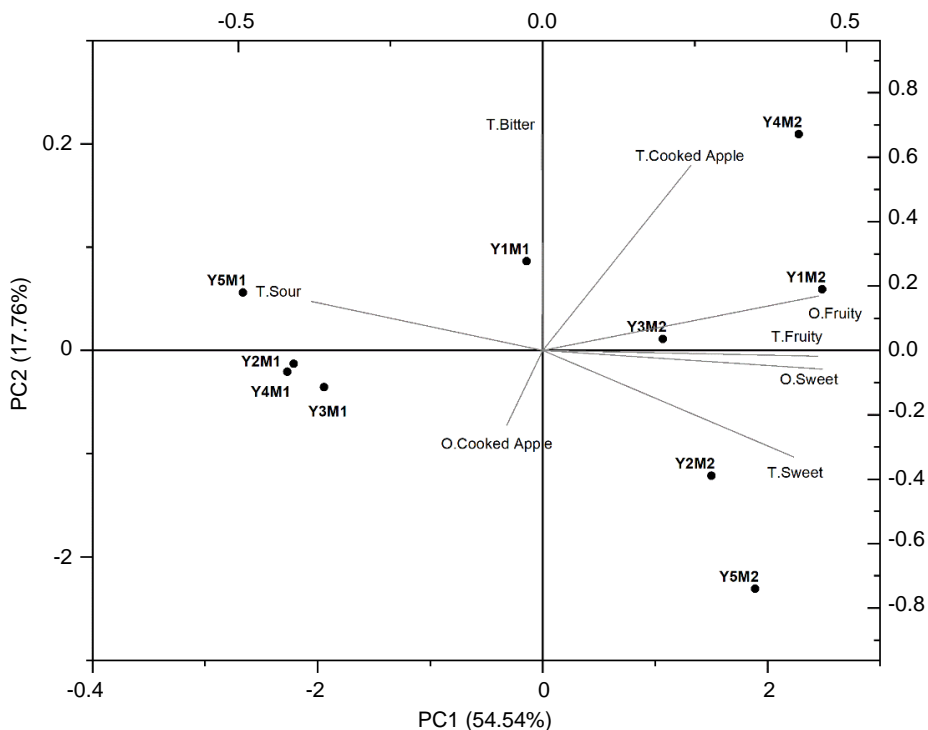


Figure 4. Grouping of the samples on the PCA biplot according to statistically significant ($p < 0.05$) sensory properties perceived at the end of fermentation with each combination of yeast (Y1-5) and fermentation matrix (M1 and M2).

CONCLUSIONS

Yeast performance in the fermentation of cider from the apple musts with similar nitrogen content was studied in this work. The differences in yeast fermentation activity, consumption of nutrients (sugars, malic acid, nitrogen), production of selected volatile esters and development of sensory properties were characterised. Based on the results the fermentative activity of yeasts and consumption of certain nutrients like fructose and nitrogen did not depend on the must. Malic acid consumption was found to depend on the initial malic acid content in the environment. The main differences between the two apple musts used for the fermentations were related to the content of volatile esters and sensory properties of cider. Despite the similar level of initial YAN content in the musts, the yeast performance in terms of the development of sensory properties was not the same. Lower volatile ester formation and synthesis the off-flavour was noted with one of the musts used for the experiments. Thus, initial nitrogen content adjustment did not

guarantee a good quality of the finished product. Since the sensory properties are the driving force behind consumer behaviour, a proper approach to off-flavour management should be implemented. Further research is required to establish the factors/combination of factors that could allow for simultaneous reduction of off-flavour production risks and an increase in the production of volatile esters in cider.

ACKNOWLEDGEMENTS. This research was supported by the Enterprise Estonia project EU48667. This work has been partially supported by ASTRA TUT 'Institutional Development Programme for 2016–2022' Graduate School of Functional Materials and Technologies (2014–2020.4.01.16-0032).

REFERENCES

- Alberti, A., Vieira, R.G., Drilleau, J.F., Wosiacki, G. & Nogueira, A. 2011. Apple wine processing with different nitrogen contents. *Brazilian Archives of Biology and Technology* **54**, 551–558.
- Barbosa, C., Falco, V., Mendes-Faia, A. & Mendes-Ferreira, A. 2009. Nitrogen addition influences formation of aroma compounds, volatile acidity and ethanol in nitrogen deficient media fermented by *Saccharomyces cerevisiae* wine strains. *Journal of Bioscience and Bioengineering* **108**, 99–104.
- Barbosa, C., Mendes-Faia, A. & Mendes-Ferreira, A. 2012. The nitrogen source impacts major volatile compounds release by *Saccharomyces cerevisiae* during alcoholic fermentation. *International Journal of Food Microbiology* **160**, 87–93.
- Barnett, J.A. & Kornberg, H.L. 1960. The utilisation by yeast of acids of the tricarboxylic acid cycle. *Journal of General Microbiology* **23**, 65–82.
- Belda, I., Ruiz, J., Esteban-Fernandez, A., Navascues, E., Marquina, D., Santos, A. & Moreno-Arribas, M.V. 2017. Microbial contribution to wine aroma and its intended use for wine quality improvement. *Molecules* **22**, 189.
- Bohlscheid, J.C., Osborne, J.P., Ross, C.F. & Edwards, C.G. 2011. Interactive effects of selected nutrients and fermentation temperature on H₂S production by wine strains of *Saccharomyces*. *Journal of Food Quality* **34**, 51–55.
- Boles, E., Jong-Gubbels, P. & Pronk, J.T. 1998. Identification and characterization of MAE1, the *Saccharomyces cerevisiae* structural gene encoding mitochondrial malic enzyme. *Journal of Bacteriology* **180**, 2875–2882.
- Boudreau, T.F., Peck, G.M., O'Keefe, S.F. & Stewart, A.C. 2017. The interactive effect of fungicide residues and yeast assimilable nitrogen on fermentation kinetics and hydrogen sulfide production during cider fermentation. *Journal of the Science of Food and Agriculture* **97**, 693–704.
- Boudreau, T.F., Peck, G.M., O'Keefe, S.F. & Stewart, A.C. 2018. Free amino nitrogen concentration correlates to total yeast assimilable nitrogen concentration in apple juice. *Food Science and Nutrition* **6**, 119–123.
- Carrau, F.M., Medina, K., Farina, L., Boido, E., Henschke, P.A. & Dellacassa, E. 2008. Production of fermentation aroma compounds by *Saccharomyces cerevisiae* wine yeasts: effects of yeast assimilable nitrogen on two model strains. *FEMS Yeast Research* **8**, 1196–1207.
- Cruz, S. H., Cilli, E. M. & Ernandes, J. R. 2002. Structural complexity of the nitrogen source and influence on the yeast growth and fermentation. *Journal of the Institute of Brewing* **108**, 54–61.
- Delfini, C. & Formica, J. 2001. *Wine Microbiology: Science and Technology*. Boca Raton, CRC Press, 496 pp.

- Dennis, E.G., Keyzers, R.A., Kalua, C.M., Maffei, S.M., Nicholson, E.L. & Boss, P.K. 2012. Grape contribution to wine aroma: production of hexyl acetate, octyl acetate, and benzyl acetate during yeast fermentation is dependent upon precursors in the must. *Journal of Agricultural and Food Chemistry* **60**, 2638–2646.
- Downing, D.L. 1995. Apple Cider. In Downing, D.L. (Eds.). *Processed Apple Products*. New York, Springer, 169–188.
- Drilleau, J.F. 1990. Fermentation of cider. *Rev. Pomme à cidre* **21**, 20–22.
- Eden, A., Simchen, G. & Benvenisty, N. 1996. Two yeast homologs of ECA39, a target for c-Myc regulation, code for cytosolic and mitochondrial branched chain amino acid aminotransferases. *Journal of Biological Chemistry* **271**, 20242–20245.
- Fairbairn, S., McKinnon, A., Musarurwa, H.T., Ferreira, A.C. & Bauer, F.F. 2017. The impact of single amino acids on growth and volatile aroma production by *Saccharomyces cerevisiae* strains. *Frontiers in Microbiology* **8**, 2554.
- Gobert, A., Tourdot-Marechal, R., Morge, C., Sparrow, C., Liu, Y., Quintanilla-Casas, B., Vichi, S. & Alexandre, H. 2017. Non-*Saccharomyces* yeasts nitrogen source preferences: impact on sequential fermentation and wine volatile compounds profile. *Frontiers in Microbiology* **8**, 2175.
- Herraiz, G., Reglero, M., Herraiz, P., Alvarez, M. & Cabezudo, M. 1990. The influence of the yeast and type of culture on the volatile composition of wine fermented without sulphur dioxide. *American Journal of Enology and Viticulture* **41**, 313–318.
- Laaksonen, O., Kuldj arv, R., Paalme, T., Virkki, M. & Yang, B. 2017. Impact of apple cultivar, ripening stage, fermentation type and yeast strain on phenolic composition of apple ciders. *Food Chemistry* **233**, 29–37.
- Lambrechts, M.G. & Pretorius, I.S. 2000. Yeast and its importance to wine aroma. *South African Journal of Enology and Viticulture* **21**, 97–129.
- Lea, A.G.H. & Piggott, J.R. 2003. Cidermaking. In Lea, A.G.H. & Drilleau, J.F. (Eds.). *Fermented beverage production (2nd Ed.)*. New York, Springer, pp. 59–87.
- Lemos Junior, W.J.F., Viel, A., Bovo, A., Carlot, M., Giacomini, A. & Corich, V. 2017. *Saccharomyces cerevisiae* vineyard strains have different nitrogen requirements that affect their fermentation performances. *Letters in Applied Microbiology* **65**, 381–387.
- Nordstr om, K. 1962. Formation of ethyl acetate in fermentation with brewer's yeast III: participation of coenzyme A. *Journal of the Institute of Brewing* **68**, 398–407.
- Plata C., Millan C., Mauricio, J.C. & Ortega, J.M. 2003. Formation of ethyl acetate and isoamyl acetate by various species of wine yeasts. *Food Microbiology* **20**, 217–224.
- Saerens, S.M.G., Delvaux, F.R., Verstrepen, K.J. & Thevelein, J.M. 2010. Production and biological function of volatile esters in *Saccharomyces cerevisiae*. *Microbial Biotechnology* **2**, 165–177.
- Santos, C.M.E., Pietrowski, G.A.M., Braga, C.M., Rossi, M.J., Ninow, J., Santos, T.P.M., Wosiacki, G., Jorge, R.M.M. & Nogueira, A. 2015. Apple amino acid profile and yeast strains in the formation of fusel alcohols and esters in cider production. *Journal of Food Science* **80**, 1170–1177.
- Santos, C.M.E., Alberti, A., Pietrowski, G.A.M., Zielinski, A.A.F., Wosiacki, G., Nogueira, A. & Jorge, R.M.M. 2016. Supplementation of amino acids in apple must for the standardization of volatile compounds in ciders. *Journal of the Institute of Brewing* **122**, 334–341.
- Seguinot, P., Rollero, S., Sanchez, I., Sablayrolles, J.M., Ortiz-Julien, A., Camarasa, C. & Mouret, J.R. 2018. Impact of the timing and the nature of nitrogen additions on the production kinetics of fermentative aromas by *Saccharomyces cerevisiae* during winemaking fermentation in synthetic media. *Food Microbiology* **76**, 29–39.

- Swiegers, J.H., Bartowsky, E.J., Henschke, P.A. & Pretorius, I.S. 2005. Yeast and bacterial modulation of wine aroma and flavour. *Australian Journal of Grape and Wine Research* **11**, 139–173.
- The European Cider and Fruit Wine Association. 2018. *European Cider Trends*. Global Data, 24 pp.
- Ugliano, M., Henschke, P.A., Herderich, M.J. & Pretorius, I.S. 2007. Nitrogen management is critical for wine flavour and style. *Australian and New Zealand Wine Industry Journal* **22**, 24–30.
- Ugliano, M., Travis, B., Francis, I.L. & Henschke, P.A. 2010. Volatile composition and sensory properties of shiraz wines as affected by nitrogen supplementation and yeast species: Rationalizing nitrogen modulation of wine aroma. *Journal of Agricultural and Food Chemistry* **58**, 12417–12425.
- Ugliano, M., Kolouchova, R. & Henschke, P.A. 2011. Occurrence of hydrogen sulfide in wine and in fermentation: Influence of yeast strain and supplementation of yeast available nitrogen. *Journal of Industrial Microbiology & Biotechnology* **38**, 423–429.
- Volschenk, H., van Vuuren, H.J.J. & Viljoen-Bloom, M. 2003. Malo-ethanolic fermentation in *Saccharomyces* and *Schizosaccharomyces*. *Current Genetics* **43**, 379–391.
- Zhang, B.Q., Luan, Y., Duan, C.Q. & Yan, G.L. 2018. Use of *Torulaspora delbrueckii* co-fermentation with two *Saccharomyces cerevisiae* strains with different aromatic characteristic to improve the diversity of red wine aroma profile. *Frontiers in Microbiology* **9**, 606.

Analysis of flight parameters and georeferencing of images with different control points obtained by RPA

L.M.D. Santos^{1,*}, G.A.S. Ferraz¹, M.T. Andrade¹, L.S. Santana¹,
B.D.S. Barbosa¹, D.T. Maciel² and Giuseppe Rossi³

¹Federal University of Lavras, Department of Agricultural Engineering, University Campus, BR37.200-000 Lavras-MG, Brazil

²Federal University of Lavras, Department of Engineering, University Campus, BR37.200-000 Lavras, Brazil

³University of Florence, Department of Agriculture, Food, Environment and Forestry (DAGRI), Via San Bonaventura, 13, IT50145 Florence, Italy

*Correspondence: luanna_mendess@yahoo.com.br

Abstract. New techniques for analysing the earth's surface have been explored, such as the use of remotely piloted aircraft (RPA) to obtain aerial images. However, one of the obstacles of photogrammetry is the reliability of the scenes, because in some cases, considerable geometric errors are generated, thus necessitating adjustments. Some parameters used in these adjustments are image overlaps and control points, which generate uncertainties about the amount and arrangement of these points in an area. The aim of this study was to test the potential of a commercial RPA for monitoring and its applicability in the management of and decision-making about coffee crops with two different overlaps and to evaluate geometric errors by applying four grids of georeferenced points. The study area is located in an experimental Arabica coffee plantation measuring 0.65 ha. To capture the images, the flight altitude was standardized to a 30 m altitude from the ground, and a constant travel speed of 3 m s⁻¹ was used. The treatments studied were two combinations of image overlap, namely, 80/80% and 70/60%. Six points were tracked through Global Navigation Satellite System (GNSS) receivers and identified with signs, followed by an RPA flight for image collection. The obtained results indicated distinct residual error rates pointing to larger errors along Cartesian axis Y, demonstrating that the point distribution directly affects the residual errors. The use of control points is necessary for image adjustments, but to optimize their application, it is necessary to consider the shape of the area to be studied and to distribute the points in a non-biased way relative to the coordinate axes. It is concluded that the lower overlap can be recommended for use in the flight plan due to the high resolution of the orthomosaic and the shorter processing time.

Key words: orthorectification of images, geometric error, photogrammetry, UAS (Unmanned Aircraft System), overlap.

INTRODUCTION

Photogrammetry consists of the analysis of a terrestrial surface strip using a set of aerial photographs, providing the observer with information about the objects on the land surface and a safe way to analyse the environment. According to Moriya (2015), remote

sensing and photogrammetry products have great potential for use in precision agriculture, encouraging the development of new methodological approaches and applications that produce good spatial information to support rural farmers in crop planning and decision-making.

To facilitate classical photogrammetry, new technologies have been tested, such as the use of remotely piloted aircraft (RPA). The use of RPA in precision agriculture can help rural farmers identify management strategies, supporting measures to increase efficiency in the management of the production process, maximizing crop yields, and reducing input costs, thus making this activity more competitive (Oliveira et al., 2007; Silva et al., 2008; Carvalho et al., 2009). These platforms are being studied and used to obtain images with a high temporal resolution (for example, acquired several times a day), high spatial resolution (in centimetres and even millimetres), and low operating costs (Lelong et al., 1998; Hunt et al., 2005; Nebiker et al., 2008; Rango et al., 2009; Hardin & Hardin, 2010; Laliberte & Rango, 2011; Xiang & Tian, 2011; Honkavaara et al., 2013; Torres-Sánchez et al., 2014). They can be applied in smaller areas and in specific locations for obtaining data in less time, accompanying the growth of several crops, for example.

In addition, photogrammetry and remote sensing stand out due to the speed and quality of the data obtained, as indicated by Volterrani (2003), enabling the use of remote images to identify plant species; to calculate leaf areas, biomass and soil cover; and even to quantify levels of nitrogen, chlorophyll, water or nutritional deficiencies. The use of aerial images has emerged as a promising alternative since they are already used in agriculture for mapping crops, evaluating cultivated areas, and detecting different types of deficiencies (Molin, 2015).

Although RPA has built-in GPS, its accuracy is not high enough for direct georeferencing, requiring soil control points (GCPs) (Chang et al., 2017). Thus it is necessary to use referenced points for in order to obtain a correct georeferencing in projects that require good geometric precision, such as the generation of a digital terrain model (DTM), planting rows monitoring, monitoring crop growth and obtaining information for field interventions. According to Zanetti et al. (2017), GCPs are necessary to ensure accuracy in the generation of orthophotos and can directly influence the positional quality of the products generated. GCPs can greatly increase the accuracy of maps, and these control points can either be marked on the ground or be landmarks such as the intersections of roads or the corners of buildings that can be identified in the image (Wang et al., 2012). According to Agüera-Vega et al. (2017) at least three GCPs are needed for this process, but it is recommended to use significantly more to reach better accuracies.

The flight parameters used when obtaining images such as the overlap, height, and speed may affect the quality and accuracy of the orthomosaic. Studies carried out by Mesas-Carrascosa et al. (2016) show that the overlap is a factor that can affect the accuracy and quality of the final product. The authors tested two configurations of longitudinal and transverse overlaps (80%–50% and 70%–40%) and found that the highest overlap (longitudinal 80% and transverse 50%) was the most recommended for creating the orthomosaic. However, depending on the purpose and final product, larger overlaps will increase the capture time of the images, which will result in a larger number of point clouds and, consequently, a longer processing time. Therefore, whether there is a need for a high amount of overlap for an intended purpose should be studied and

evaluated. Siebert & Teizer (2014) recommend using longitudinal and transverse coverage areas of at least 70 and 40%, respectively.

In this context, overlap for coffee crop analysis and the number of GCPs to be used in a given area is still unknown, requiring accurate and precise data from aerial images processed with different GCPs.

The aim of the present work was to test the potential of a commercial RPA for monitoring and applicability in the management of and decision-making about coffee crops with two different overlaps and to evaluate geometric errors by applying four grids of georeferenced points.

MATERIALS AND METHODS

The study was carried out at the Federal University of Lavras (UFLA) (Fig. 1), in the city of Lavras, Minas Gerais, Brazil. The study site comprises 0.65 hectares of an experimental area at 21°13'33.23" South latitude, 44°58'17.63" West longitude. A área de estudo é considerada um terreno plano

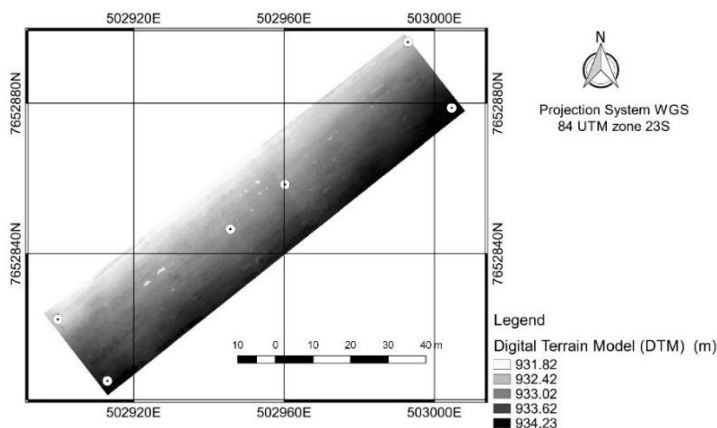


Figure 1. Digital model of elevation of the study area and distribution of control points.

The study site is the remnant area of an experiment described by Caldas et al. (2018) and was established in February 2009 with *Coffea arabica* L., cultivar Travessia, with 2.60×0.60 m spacing, totalling 36 blocks with 3 planting rows and 14 plants per row. The coffee plants were pruned (‘esqueletamento’) in the third week of July 2016. According to Queiroz-Voltan et al. (2006), ‘esqueletamento’ is considered a drastic pruning that consists of removing a large part of the plagiotropic branches, approximately 20 cm at the top, and ending with 40 cm in the low plagiotropic branches, with the recovery of production in around one year. In 2017, the irrigation and fertigation treatments were not applied, although there was likely a residual effect from the previous fertilization.

In this area, 6 GCPs were pre-defined and were fixed and tracked in the field using a pair of Global Navigation Satellite System (GNSS) devices with Real Time Kinematics (RTK), composed of a base and rover, and the Spectra Precision SP60 model with the following characteristics: 240-channel receptors operating at frequencies C/A, L1, L2 and L3 and in kinematic mode (RTK). Data were processed to improve data quality.

Four points were collected at the extremes of the area and two points in the middle of the area. The rover rod was 2.0 m high, the height of the coffee trees ranged from 1.80 to 2.10 m, with no multi-streaming effect. The collections were made on the floor, on the control plates fixed to the floor. The points were fixed to the field in the RTK mode with accuracy of 0.03 m, if there were the distance between the base and the rover, it would be corrected with the longest follow-up time. Thus, the distance between the points and the base was small to consider the effect of the distance on the errors.

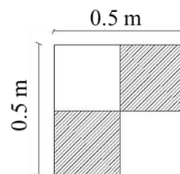


Figure 2. Control point model for characterization of the georeferenced points.

An identification sign was placed on each tracking site (Fig. 2 and Table 1) for identification in the images obtained by RPA.

Table 1. Description of the control points and their distance from the base of the GPS RTK

GCP	North (m)	East (m)	Altitude (m)	Point Distance With RTK Base (m)
1	7652806.21	502913.00	931.45	67.81
2	7652822.58	502899.8	929.78	79.00
3	7652846.57	502945.72	930.46	40.98
4	7652858.42	502960.23	930.42	40.52
5	7652896.29	502992.93	929.83	75.19
6	7652878.80	503004.58	931.61	61.97

An RPA DJI Phantom 3 Professional was used, which is a four-bladed rotary-wing aircraft with four battery-powered motors, vertical landing and take-off, 23 minute flight autonomy, a gimbal for camera stabilization, and damping of vibrations and correction of camera orientation when taking photos. It is oriented perpendicular to the ground, has an integrated Global Positioning System (GPS), and is operated by remote control. It has a coupled Sony digital camera, model EXMOR 1/ 2.3”, with 12 megapixel resolution, obtaining images in true colour (red R, green G, blue-B) and 8-bit radiometric resolution; the camera has a 20 mm lens with an f/2.8 aperture and a maximum image resolution of 4,000×3,000 pixels, and its photos are stored on an SD card.

To capture the images, the flight height was standardized to an altitude of 30 m from the ground with a constant travel speed of 3 m/s, with two combinations of forward and side overlaps, namely, 80/80% and 70/60%.

For processing the images and creating the orthomosaics, PhotoScan software from Agisoft Pro version 1.4.4 (Agisoft LLC, St. Petersburg, Russia) was used. This software identifies homologous points in the images, forming a dense point cloud, thus enabling the reconstruction of the model and the creation of the orthomosaic as a final product. The orthomosaic was exported in GEOTIFF format and later processed on GIS software. The GCPs were analysed with the highest overlap, 80/80%, to ensure the accuracy and quality of the final product.

The GCPs obtained from the GNSS tracking were divided into three sets of 4, 5, and 6 points, as shown in Fig. 3. The georeferencing was performed as follows: linear transformation and re-sampling method, coordinate reference system SRC, SIRGARS 2000 UTM and zone 23 south. Then, the points were adjusted manually, informing the

software of the locations of the points and generating an accuracy report that contained the residual errors of each adjusted point. Fig. 3 shows the conformation of how the tracking was performed and the final product of the georeferencing of the images.

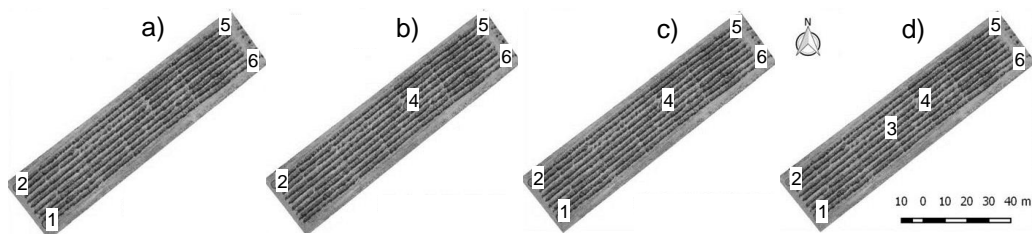


Figure 3. Locations of georeferenced GCPs: a) 4 points; b) 4 points with a centre point; c) 5 points; d) 6 points.

RESULTS AND DISCUSSION

From the image processing, and with the orthomosaics observed in Fig. 4 as the end result, it was possible to analyse the generated images. The evaluation of the two overlaps reveals the presence of invasive plants in the canopies of some of the coffee plants. In addition, with the analysis of the images, it is possible to characterize the crop uniformity, with the northeast region of the area displaying a block of uneven coffee plants, in addition to detecting the planting and alignment gaps.

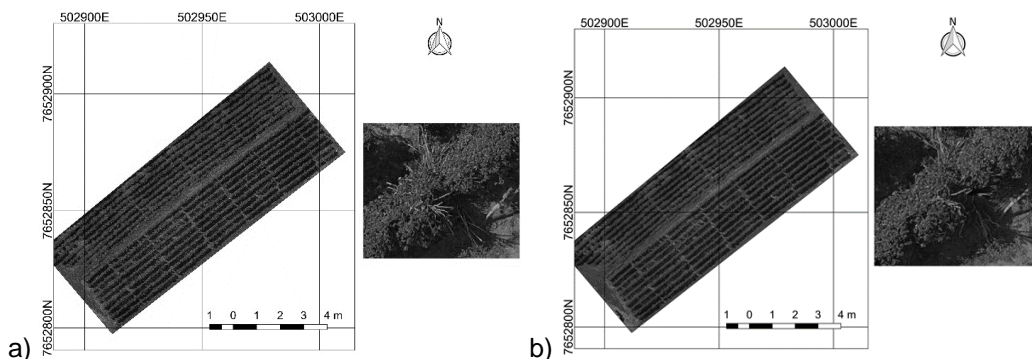


Figure 4. Ortomosaics obtained through field image processing with vertical / horizontal overlap of (A) 80/80% and (A) 60/70% respectively.

From the results, it is justifiable to use RPA as a tool for guiding crop management practices with greater assertiveness in the field, citing as an example the uses of agricultural inputs at variable rates. Castaldi et al. (2016), who carried out the mapping of invasive species for the targeted application of herbicides in a corn crop, concluded that the use of post-emergence image data obtained by RPA led to a decrease in herbicide use, increasing the untreated areas from 14% to 39.2% for uniform spraying and from 16 to 45 € ha. This fact justifies the adoption of such technologies in the coffee crop.

Analysing the data described in Table 2, as well as the results of the image processing, it is possible to conclude that the resolution of the images is lower than 1.5 cm pixel⁻¹.

From the parameters observed in Table 2, it is possible to infer that the spatial resolutions observed in the field images are very close, with a difference of only 0.02 cm/pixel, which is a negligible value for the purpose of the present evaluation. Another relevant point is the flight time for each of the observed overlaps, in which the 70/60% overlap leads to a 26.9% shorter flight time of the RPA for collecting the images for the same area.

Table 2. Result of the image processing, demonstrating the evaluated flight parameters for the two image overlaps

Overlap (%)	Image evaluation parameters			
	Flight time (min)	Number of Images	Processing time (h)	Space Resolution (cm pixel ⁻¹)
80 × 80	7.88	93	4.79	1.31
70 × 60	5.76	90	4.88	1.33
Fixed flight parameters				
Velocity (m s ⁻¹)	3.0			
Flight height (m)	30			

Regarding the processing time, it is known that images collected with a high overlap generate more points and that the cloud is one of the processing procedures that requires the most time; such processes are differentiated by the quantity of the images and the quality of the product. However, a higher-quality procedure results in a higher quality of the model generated. For both overlaps evaluated, high-quality parameters were used, both of which resulted in high-quality products. Therefore, there was no significant difference in the processing time, which was 0.09 hours or slightly more than 5 minutes.

Obtaining images with a low overlap, less than that recommended by photogrammetry (60/30%), may affect the accuracy and quality of the final product and the estimates (Mesas-Carrascosa et al., 2016). The overlap is a factor that must be taken into account, as it may compromise the analyses of the biophysical parameters of crops, as observed in studies by Haas et al. (2016), where the authors used a 60/60% overlap and obtained a non-homogeneous point density and data holes, due to the low overlap and consequently few points in the dense cloud, which hinders model construction, causing gaps in the images. Dandois et al. (2015) used an 80% overlap with good accuracy, and Guerra-Hernández et al. (2017) used an 80% longitudinal overlap and 75% lateral overlap and obtained good results. The greater the overlap was, the greater the number of points in the point cloud the consequently longer the processing time and the hardware and software demand to support such processing.

Chang et al. (2017) used overlays with 90% frontal and lateral overlap, the authors state that source error may include uncertainties in DTM generation, inaccurate geo-spatial data product geo-referencing and unstable data acquisition conditions. These uncertainties in the generation of DTMs include flight planning and its features such as overlap, flight height, flight speed, as well as the quality of processing of these images.

Another parameter that can be discussed is the flight height of the aircraft, which in this case for both overlaps evaluated was 30 m. The flight height of the RPA is directly

related to the spatial resolution of the images. In this situation, due to the height of the aircraft being very close to the target, it allowed greater detail of the crop, which had a positive effect on the final products generated in the processing. In studies carried out by Romero et al. (2015), the authors obtained a spatial resolution of 10 cm using an RPA model Phantom 2, with a flight height of 120 m, that is, the spatial resolution and the coverage of the area are directly affected by the flight height.

The visual displacement of the tacked point relative to the georeferenced point is observed in Fig. 5. This shows the need for adjustments in the obtained images, as the square should have been overlapped with the circle.

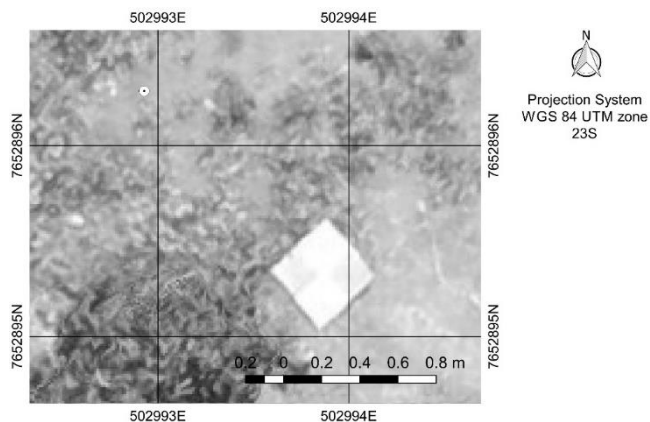


Figure 5. Error found before the georeferencing of images. The circle represents the point tracked through GNSS, and the square is a point that was visualized by the RPA.

As observed in Table 3, the field-tracking data in RTK mode indicates the high reliability of the tie points, showing an accuracy between 0.014 and 0.024 m. These standard deviation rates are indicative of a high accuracy. According to the standard NBR 13133 (1994), GNSSs are considered to be highly accurate electronic distance metres (EDM), as they reach minimum errors of 3 mm.

Tahar & Ahmad (2013) studied the GCPs on a area of 150 ha and observed that any number and distributions of GCPs studied, as in this work, the horizontal accuracy was better than the vertical one.

Table 3. Results of the reports resulting from post-processing adjustments of the field data collected through GNSS in RTK mode

Vector ID	Type of solution	Precision H (m)	Precision V (m)
1	Fixo	0.017	0.024
2	Fixo	0.021	0.029
3	Fixo	0.014	0.022
4	Fixo	0.021	0.027
5	Fixo	0.017	0.027
6	Fixo	0.019	0.027

From the analysis in Table 4, it is possible to observe the residual errors in metres, indicating the differences between the points tracked by the GNSS and the points visualized by the RPA, that is, the displacement of the coordinates in metres obtained in both systems. When analysing the average error, the arrangement with 4 points located at the vertex of the area was the most advantageous of the conformations, which may have been due to the small size of the area studied, responding better to the points in the vertices only.

Table 4. Residual errors in metres of the UTM coordinates "X and Y"

ID	4 points		4 points A		5 points		6 points	
	Res X	Res Y	Res X	Res Y	Res X	Res Y	Res X	Res Y
1	-	-	3.83	-6.16	4.33	-8.94	4.58	-10.77
2	1.77	0.42	-3.03	4.27	-1.74	9.03	-0.96	10.52
3	-	-	-	-	-	-	0.45	4.09
4	-4.11	-8	-	-	-4.46	-2.92	-7.72	-6.88
5	-0.36	-9	-2.85	-12.14	-1.44	-11.82	-0.36	-11.8
6	2.69	17	2.06	14.03	3.32	14.64	4	14.84
Mean error	2.23	8.60	2.94	9.15	3.05	9.47	3.011	9.81

The results indicate that the latitude (Y) coordinates are the ones with the highest errors, generating high residual error rates. Fig. 3, b (3 points in the vertex and one central point) and Fig. 3, d (6 points), 17 and 14.84 m, respectively, showed that the residual values of (Y) are better in the conformation represented in Fig. 3, a (4 points located at the vertices of the area), with better results when the points are positioned at the vertices. This indicates the influence of the position of the points in the area and may complement the recommendations of Pix4d, which stipulate only a minimum of 5 control points for small surface areas and recommends 5 to 10 control points for large projects.

At the longitude points (X), the values are relatively low relative to the (Y) axis, making it clear that the shape of the area influences the residual errors of the GCPs, since the smaller distances are on the (X) axis, indicating that the clustering of the points improves the residual errors. However, this work reaches results different from those found by Tahar & Ahmad (2013) and Perin et al. (2016), who concluded that the higher the number of points, the greater the accuracy. Although the number of points is important, the results show the high level of significance of the clustering and distribution of points and the size of the area studied.

Studies by Wallace et al. (2016) used 24 targets as GCPs collected with dual-frequency RTK GPS in a 30×50 m area, obtaining a position error within ± 0.05 m horizontally and ± 0.20 m vertically. Turner et al. (2015) collected 23 GCPs with a dual-frequency GPS RTK in an area of 125×60 m and obtained position errors of approximately 0.04–0.05 m horizontally and 0.03–0.04 m vertically. Both authors used a small area with a considerable amount of points, however the present study had good results using a minimum number of points when they were scattered in the study area.

CONCLUSIONS

It was possible to test the use of a commercial RPA using two different flight plans in a coffee crop area. The presence of weeds both in between the planting rows and in the coffee canopy, gaps in the planting, and the alignment and uniformity of the crop in both overlaps studied were identified.

It was also concluded that the number of GCPs for the area evaluated did not alter the accuracy but did alter the distribution of the points. The evaluation of the geometric errors for the study area showed the importance of the distribution of the GCPs and that their clustering or distance can have an isolated effect on each coordinate axis evaluated. The study showed that for the better development of this application, it is important to

consider the shape of the study area and to distribute the points in a scattered and non-biased way relative to the coordinate axis.

ACKNOWLEDGEMENTS. The authors thank, the Foundation for Research of the State of Minas Gerais (FAPEMIG), the National Council for Scientific and Technological Development (CNPq), the Coordination for the Improvement of Higher Education Personnel (CAPES), the Federal University of Lavras (UFLA) and University of Firenze (UniFI).

REFERENCES

- Agüera-Vega, F., Carvajal-Ramírez, F. & Martínez-Carricondo, P. 2017. Assessment of photogrammetric mapping accuracy based on variation ground control points number using unmanned aerial vehicle. *Measurement* **98**, 221–227.
- Caldas, A.L.D., Lima, E.M.C., Rezende, F.C., Faria, M.A.D., Diotto, A.V. & Júnior, M.C.R.L. 2018. Yield and quality of coffee cv. Travessia under different irrigation and phosphate fertilization. *Revista Brasileira de Agricultura Irrigada* **12**, 2357–2365 (in Portuguese).
- Carvalho, G.R., Botelho, C.E., Bartholo, G.F., Pereira, A.A., Nogueira, Â.M. & Carvalho, A.M. 2009. Behavior of F4 progenies obtained by 'Icatu' crosses with 'Catimor'. *Ciência e Agrotecnologia* **33**, 47–52 (in Portuguese).
- Castaldi, F., Pelosi, F., Pascucci, S. & Casa, R. 2016. Assessing the potential of images from unmanned aerial vehicles (UAV) to support herbicide patch spraying in maize. *Precision Agriculture* **18**, 76–94.
- Chang, A., Jung, J., Maeda, M.M. & Landivar, J. 2017. Crop height monitoring with digital imagery from Unmanned Aerial System (UAS). *Computers and Electronics in Agriculture* **141**, 232–237.
- Dandois, J.P., Olano, M. & Ellis, E.C. 2015. Optimal altitude, overlap, and weather conditions for computer vision UAV estimates of forest structure. *Remote Sensing* **7**, 13895–13920.
- Guerra-Hernández, J., González-Ferreiro, E., Monleón, V.J., Faias, S.P., Tomé, M. & Díaz-Varela, R.A. 2017. Use of Multi-Temporal UAV-Derived Imagery for Estimating Individual Tree Growth in Pinus pinea Stands. *Forests* **8**, 300–319.
- Haas, F., Hilger, L., Neugirg, F., Umstaedter, K., Breitung, C., Fischer, P. & Schmidt, J. 2016. Quantification and analysis of geomorphic processes on a recultivated iron ore mine on the Italian island of Elba using long-term ground-based lidar and photogrammetric SfM data by a UAV. *Natural Hazards and Earth System Sciences* **16**, 1269–1288.
- Hardin, P.J. & Hardin, T.J. 2010. Small-scale remotely piloted vehicles in environmental research. *Geography Compass* **4**, 1297–1311.
- Honkavaara, E., Saari, H., Kaivosoja, J., Pölonen, I., Hakala, T., Litkey, P. & Pesonen, L. 2013. Processing and assessment of spectrometric, stereoscopic imagery collected using a lightweight UAV spectral camera for precision agriculture. *Remote Sensing* **5**, 5006–5039.
- Hunt, E.R., Cavigelli, M., Daughtry, C.S.T., McMurtrey, J.E. & Walthall, C.L. 2005. Evaluation of digital photography from model aircraft for remote sensing of crop biomass and nitrogen status. *Precision Agriculture* **6**, 359–378.
- Laliberte, A.S. & Rango, A. 2011. Image processing and classification procedures for analysis of sub-decimeter imagery acquired with an unmanned aircraft over arid rangelands. *GIScience e Remote Sensing* **48**, 4–23.
- Lelong, C.C.D., Pinet, P.C. & Poilve, H. 1998. Hyperspectral imaging and stress mapping in agriculture: A case study on wheat in Beauce (France). *Remote Sensing of Environment* **66**, 179–191.
- Mesas-Carrascosa, F.J., Notario García, M.D., Meroño De Larriva, J.E. & García-Ferrer, A. 2016. An Analysis of the Influence of Flight Parameters in the Generation of Unmanned Aerial Vehicle (UAV) Orthomosaics to Survey Archaeological Areas. *Sensors* **16**, 1838–1852.

- Molin, J.P., do Amaral, L.R. & Colaço, A. 2015. *Precision Agriculture (Agricultura de precisão)*. São Paulo, Brazil, 224 pp. (in Portuguese).
- Moriya, E.A.S. 2015. *Identification of spectral bands to detect healthy and diseased sugarcane using hyperspectral camera on board UAV*. Doctoral Thesis. UNESP. (in Portuguese)
- NBR, ABNT. 13133-1994. *Execution of topographic survey: procedure*. Rio de Janeiro.
- Nebiker, S., Annen, A., Scherrer, M. & Oesch, D. 2008. A light-weight multispectral sensor for micro UAV: Opportunities for very high resolution airborne remote sensing. *The International Archives of the Photogrammetry, Remote Sensing and Spatial Information Sciences* **37**, 1193–1200.
- Oliveira, E.D., Silva, F.M.D., Guimarães, R.J. & Souza, Z.M.D. 2007. Elimination of lines in coffee beans with semi-mechanized. *Ciência e Agrotecnologia* **31**, 1826–1830 (in Portuguese).
- Perin, G., Gerke, T., Lacerda, V.S., da Rosa, J.Z., Caires, E.F. & Guimarães, A.M. 2016. Accuracy Analysis of Georeferencing of Mosaics of Images Obtained by RPA. *Anais do EATI-Encontro Anual de Tecnologia da Informação e STIN-Simpósio de Tecnologia da Informação da Região Noroeste do RS, Rio Grande do Sul*, pp. 193–199 (in Portuguese).
- Queiroz-Voltan, R.B., Perosin Cabral, L., Paradela Filho, O. & Fazuoli, L.C. 2006. Efficiency of pruning in coffee trees in the control of *Xylella fastidiosa*. *Bragantia, Campinas*, **65**, pp. 433–440 (in Portuguese).
- Rango, A., Laliberte, A., Steele, C., Herrick, J.E., Bestelmeyer, B., Schmutz, T. & Jenkins, V. 2006. Using unmanned aerial vehicles for rangelands: current applications and future potentials. *Environmental Practice* **8**, 159–168.
- Romero, V.R., Villareal, A.M., León, J.L.T. & Hernández, A.H. 2015. Perspectives of UAV technology in oil palm cultivation: crop monitoring using high resolution aerial images. *Revista Palmas* **36**, 25–41 (in Spanish).
- Siebert, S. & Teizer, J. 2014. Mobile 3D mapping for surveying earthwork projects using an Unmanned Aerial Vehicle (UAV) system. *Automation in Construction* **41**, 1–14.
- Silva, F.M.D., Souza, J.C.S.D. & Alves, M.C. 2008. Influence of manual harvest in the spatial variability of coffee yield and defoliation along two agricultural harvests. In: *International Conference of Agricultural Engineering*, Foz do Iguaçu (in Portuguese).
- Tahar, K. & Ahmad, A. 2013. An evaluation on fixed wing and multi-rotor UAV images using photogrammetric image processing. *International Journal of Computer, Electrical, Automation, Control and Information Engineering* **7**, 48–52.
- Torres-Sánchez, J., Peña, J.M., Castro, A.I.D. & López-Granados, F. 2014. Multi-temporal mapping of the vegetation fraction in early-season wheat fields using images from UAV. *Computers and Electronics in Agriculture* **103**, 104–113.
- Turner, D., Lucieer, A. & de Jong, S. 2015. Time series analysis of landslide dynamics using an unmanned aerial vehicle (UAV). *Remote Sensing* **7**, 1736–1757.
- Volterrani, M. 2003. Effects of nitrogen nutrition bermudagrass spectral reflectance. *International Turfgrass Society* **10**, 1005–1014.
- Wallace, L., Lucieer, A., Malenovský, Z., Turner, D. & Vopěnka, P. 2016. Assessment of forest structure using two UAV techniques: A comparison of airborne laser scanning and structure from motion (SfM) point clouds. *Forests* **7**, 1–16.
- Wang, J., Ge, Y., Heuvelink, G.B., Zhou, C. & Brus, D. 2012. Effect of the sampling design of ground control points on the geometric correction of remotely sensed imagery. *International Journal of Applied Earth Observation and Geoinformation* **18**, 91–100.
- Xiang, H. & Tian, L. 2011. Method for automatic georeferencing aerial remote sensing (RS) images from an unmanned aerial vehicle (UAV) platform. *Biosystems Engineering* **108**, 104–113.
- Zanetti, J., Junior, J.G. & Santos, A.D.P.D. 2017. Influence of number and distribution of control points on orthophotos generated from a survey by vane. *Revista Brasileira de Cartografia* **69**, 263–277 (in Portuguese).

Some morphological and chemical characteristics of oregano (*Origanum vulgare* L.) in Latvia

I. Sivicka^{1,*}, A. Adamovics¹, S. Ivanovs¹ and E. Osinska²

¹Latvia University of Life Sciences and Technologies, Liela iela 2, LV-3001 Jelgava, Latvia

²Warsaw University of Life Sciences, Nowoursynowska 159, PL02-776 Warsaw, Poland

*Correspondence: Irina.Sivicka@llu.lv

Abstract. By European Cooperative Programme for Plant Genetic Resources (ECPGR), oregano (*Origanum vulgare* L.) is included on the list of priority species of medicinal and aromatic plants. In Latvia, it is important to cultivate oregano for keeping biodiversity and for meeting the needs of medicinal plant's production. 44 accessions of oregano from the *ex situ* collection of genetic resources of medicinal and aromatic plants, attached to the Latvia University of Life Sciences and Technologies, were analysed during 2012–2014. Plants' morphological characteristics were described by the Draft Descriptor List of oregano, using the methodology of ECPGR. The essential oil was isolated using solvent-free microwave extraction method and analysed by gas chromatograph Hewlett Packard 6890 equipped with flame ionization detector FID and polar capillary column HP 20M. The results showed, that oregano accessions differ morphologically. Accessions are characterized with dense branching and the possibility to create big biomass. Local oregano is poor in content of essential oil, but 17 compounds were identified as the principal. As well as the correlation between the content of essential oil and colour of flowers in full flowering stage was observed – it is higher for accessions with dark flowers. Also, the influence of meteorological conditions per vegetation period (year) on chemical characteristics was significant ($p < 0.05$).

Key words: essential oil, Draft Descriptor List, accessions.

INTRODUCTION

Oregano (*Origanum* spp.) is one of the most used medicinal, spice- and ornamental plants in the world (Hammer & Spahillari, 2000). Oregano can be used in the development of a sustainable agrosystem and for the reconstruction of over-cropped land (Asdal et al., 2006). By European Cooperative Programme for Plant Genetic Resources (ECPGR), oregano (*Origanum vulgare* L.) is included on the list of priority species of medicinal and aromatic plants. In Europe, also in Latvia, wild populations of oregano are limited. For meeting the needs of oregano production as well as for preservation of local biodiversity, oregano should be grown in conventional and organic cultivation systems (Asdal et al., 2006).

Oregano cultivation needs to get as rich and qualitative biomass as possible. It is better to cultivate the genetic resources of medicinal plants collected from natural habitats as they are adapted to the local agroecological conditions and possible stress situations in a specific environment. That is why oregano genetic resources must be explored carefully with the aim to select the most productive plants. It is important to evaluate the quantitative and qualitative indices of cultivated accessions, their productivity, organoleptic and biochemical properties, winter hardiness, resistance to diseases and pests, biotic stress susceptibility and other parameters (Sivicka et al., 2015).

Oregano plants bloom from June to the end of vegetation, but during August produce seeds. Because of heterogeneity, it creates various, morphologically and chemically different forms, which are related to the place of their occurrence (Asdal et al., 2006; Nurzyńska-Wierdak, 2009). Oregano differs by colour of flowers and leaves, in a density of inflorescence as well as in plant height and other indices (Droushiotis & Dell, 2002).

The essential oil is a complex mixture of volatile compounds that are present in aromatic plants (Leyva-López et al., 2017). Oregano essential oil is characterized by changeable chemical composition, depending on the population or variation, cultivation conditions and developmental stage of plants in herb harvesting period (Osińska et al., 2000; Nurzyńska-Wierdak, 2009).

An International Standard, which specifies the quality requirement for dried oregano, claims that whole oregano must contain 1.8% of essential oil and ground oregano – about 1.5% of essential oil (Tucker & Rollins, 1989). Oregano essential oil has antimicrobial and antioxidant agents as well as antioxidant properties, effective in retarding lipid peroxidation and scavenging free radicals (Ortega-Ramirez et al., 2016). The main components are terpenes, but aldehydes, alcohols and esters are also presented as minor components (Leyva-López et al., 2017).

The essential oil composition is variable with obvious appearances of different chemotypes (Asdal et al., 2006; Lukas et al., 2011). The research of European oregano genetic resources showed, that by main compounds it is possible to define carvacrol/thymol, linalool and sesquiterpene oregano chemotypes (Lukas et al., 2011). The chemical composition of oregano essential oil is genetically controlled (D'Antuono et al., 2000; De Mastro et al., 2004; Węglarz et al., 2006; Lukas et al., 2011).

Oregano is covered with glandular trichomes (hairs) which serve as a reserve of essential oil. The trichomes are easily exposed with the help of a microscope. Thus, it is possible to prognose the content of essential oil. De Mastro et al. (2004) report that 1 cm³ of oregano leaf blade contain from 207 to 734 oil hairs and the amount of essential oil in dry herb varies from 0.50 to 5.1%, depending on the population.

By Nurzyńska-Wierdak (2009), the content of oil systematically increased with the progressive development of the plant, reaching its maximum in the flowering period. The lack of significant differences between mean essential oil contents in oregano herb harvested in the initial phase of flowering and in full bloom was founded in this research. It means, that harvesting plants in full blooming stage make it possible to obtain high quality yield.

Previous researches with Latvian oregano showed the differences in biochemical compounds between accessions inside one natural population. It is important to understand the influence of the colour of petals on the content and composition of essential oil of oregano accession.

The aim of this research was to explore some morphological and chemical characteristics of oregano (*Origanum vulgare* L.) in Latvia.

MATERIALS AND METHODS

Plant Material and Growing Conditions. The samples for the experiment were selected from an *ex situ* collection of spice- and medicinal plants (latitude: N 56°39'47''; longitude: E 23°45'13''), attached to the Latvia University of Life Science and Technologies. There are 44 accessions of oregano genetic resources in this collection. The plants had been collected from nature in 2001–2006, using the modified method of Professor E. Muižarāja (Žukauska, 2008). The main point of this method is the initial visual division of an area into squares and zigzag passing through these squares as well as the random gathering of samples.

In spring 2012, 44 accessions were propagated by cloning and grown in the field conditions. After methodology of Draft Descriptor List *Origanum vulgare* L., plants' morphological characteristics were described in 2012–2014 (Žukauska & Sivicka, 2011). For research in essential oil, samples had been dried at +26 °C temperature in a special drying cabinet with ventilation.

The soil at the trial site was strongly altered by cultivation loam with organic matter content of 2.7 g kg⁻¹, soil reaction pH_{KCl} 6.3, the phosphorus (P) content was 102 g kg⁻¹ and potassium (K) level content was 207 g kg⁻¹. Plant care was provided for this collection.

Meteorological Conditions. According to data of the Latvian Environment, Geology and Meteorology Centre, the average air temperature in 2012 was +6.1 °C (0.2 °C above long-term average observations), +7.0 °C (1.1 °C above long-term average observations) in 2013 and +7.4 °C (1.5 °C above long-term average observations) in 2014. The quantity of rainfall was 832 mm (125% of normal) in 2012, 622 mm or 94% of normal in 2013 and in 2014–725 mm (107% of normal). In vegetation period (from May to the end of September), the average temperature was 14.3 °C and the total quantity of rainfall was about 373 mm in 2012, 11.4 °C and 330 mm in 2013 and 12.3 °C and 441.6 mm in 2014.

Isolation of essential oil. The research in oregano essential oil was made in the Department of Vegetable and Medicinal Plants of the Warsaw University of Life Sciences.

Isolation process description. Glass vessel (2 L) was filled with dry material (50 g). This method suggests adding as much water how much air-dried raw materials are. The risk of possible ignition of raw material is eliminated by this method. Prepared glass vessel with the moistened sample was placed in a microwave oven with a power 300 W for 30 minutes. The essential oil was extracted and collected in 2 mL glass vials for storage without light at 0–4 °C.

Chromatographic separation conditions. The analysis of distilled essential oils was performed using a gas chromatograph Hewlett Packard 6890 equipped with flame ionization detector FID and polar capillary column HP 20M. The separation conditions were: initial oven temperature 60 °C for 2 min, then the temperature increases of 4 °C per min. Injector chamber temperature was 220 °C for 5 min. As a carrier gas helium was used (1.1 mL per min). Injector chamber temperature was 210 °C, detector – 260 °C. Split 1:70. The essential oil was injected (0.1 µL) manually into the chromatography

column. Reference mixtures components were identified based on the retention times of the patterns (RT) and by comparing their retention indices (RI) to a series of n-alkanes (C7-C30), analysed in the above described separation conditions, using the following formula:

$$RI = 100 \frac{tR'(x) - tR'(n)}{tR'(m) - tR'(n)} + 100n \quad (1)$$

where n – the number of carbon atoms in the smaller n-alkane, eluting before target compound; $tR'(x)$ – retention time of target compound; $tR'(n)$ – retention time of the reference n-alkane eluting immediately before targeting chemical compound; $tR'(m)$ – retention time of the reference n-alkane eluting immediately after targeting chemical compound.

To obtain the percentage of the individual compounds in the essential oil normalization method was used without using the correction factor.

Data are presented as the mean, and differences among means were determined by analysis of variance (ANOVA), using Microsoft Office Excel 16.0 version software, and comparisons were made with Fisher test ($p < 0.05$).

RESULTS AND DISCUSSION

Describing oregano accessions, the differences were found in characters as 'plant height' and 'width of inflorescence'. The plant height varied from 50.1 to 85.0 cm in 2012, from 45.0 to 75.2 cm in 2013, from 30 to 85.9 cm in 2014. In average, it was 68.14 cm in 2012, 59.7 cm in 2013, 74.12 cm in 2014 – more than the results in other research (Nurzyńska-Wierdak). It is recommended to cultivate oregano with a plant height up to 50 cm as productive accessions (Sivicka & Žukauska, 2011). The width of inflorescence varied from 8.4 to 15.8 cm in 2012, from 7.3 to 20.0 cm in 2013, from 9.5 to 20.4 cm in 2014. In average, it was 12.6 cm in 2012, 17.2 cm in 2013, 11.15 cm in 2014. It is recommended to cultivate oregano with width of inflorescence up to 10 cm in agroecology as productive accessions (Sivicka & Žukauska, 2011). Considering these two parameters, the data statistical analysis showed that the variability between accessions was significant ($p < 0.05$), but between samples of each accession - non-significant ($p > 0.05$). The variability between years was significant ($p < 0.05$).

Plant growth habit was prostrate for 4 accessions (9%), semi-erect for 10 (23%) and erect for 30 (68%) of the accessions. It is recommended to grow plants with erect habitus in agroecology for mechanical harvest (Sivicka & Žukauska, 2011). Branching density was dense for 35 accessions (79%) of accession, for 9 (21%) it was sparse. It means, that Latvian oregano can produce high fresh biomass. The previous research showed, that plants created the average fresh biomass 12.72 g per plant in 2012, 127.50 g per plant in 2013 and 195.08 g per plant in 2014, but the average air-dry biomass per plant was 5.11 g in 2012, 55.90 g in 2013, 77.96 g in 2014 (Sivicka et al., 2015).

The density of the flowers was very sparse for 2 accessions (5%), sparse – for 5 accessions (11%), medium – for 10 accessions (23%), dense – for 15 accessions (34%) and very dense – for 12 accessions (27%). Colour of petals was pink for 34 accessions (77%), for others it varied from white to lilac. For understanding the influence of petals' colour on the content and composition of oregano essential oil, accessions were grouped as dark-, semi-dark- and light-coloured petals for analysis (Table 1).

Results showed, that local oregano is poor in the essential oil. But the higher content of essential oil was observed for oregano with dark flowers. Also, the influence of meteorological conditions per vegetation period (year) on chemical characteristics was significant ($p < 0.05$). In scientific literature it was proved that during the vegetation period the influence of air temperature from +20 to +30 °C and of the quantity of rainfall of about 600 mm on oregano biomass is positive (Rzekanowski et al., 2008; Caliskan et al., 2010). The results suggest that in 2012–2014 the meteorological conditions were not optimal for oregano cultivation and plant biomass creation. For local oregano, 17 compounds were identified as the principal (Table 2).

Table 1. The influence of year and petals` colour on the average content of oregano essential oil, mL 100 g 10⁻¹ dry matter

Year	Dark petals	Semi-dark petals	Light petals
2012	0.11 ± 0.01	0.10 ± 0.01	0.13 ± 0.02
2013	0.10 ± 0.02	0.10 ± 0.02	0.11 ± 0.01
2014	0.27 ± 0.01	0.15 ± 0.01	0.17 ± 0.01

Table 2. The influence of year and petals` colour on principal compounds of oregano essential oil, %

	Dark petals			Semi-dark petals			Light petals		
	2012	2013	2014	2012	2013	2014	2012	2013	2014
Limonene	0.37	0.44	0.49	0.24	-	-	1.10	1.20	1.22
β-phellandrene	2.35	3.31	3.33	2.13	-	1.18	5.78	7.12	6.11
1.8-cineole	-	-	-	0.61	-	-	3.35	1.98	3.61
γ-terpinene	0.29	-	-	0.32	-	-	2.66	2.23	0.85
ρ-cymene	3.52	3.08	3.96	2.33	-	1.41	5.39	8.70	4.93
Linalool	4.47	3.28	3.26	6.47	0.93	1.16	8.87	5.38	5.65
α-terpineol	2.09	2.44	3.09	2.26	1.30	1.62	2.16	2.35	2.42
Borneol	0.40	0.37	0.28	0.96	0.26	0.24	1.78	0.96	0.37
γ-cadinene	0.54	0.54	0.91	0.80	0.97	0.77	1.22	1.07	1.42
β-caryophyllene	5.22	5.52	13.08	4.85	12.28	1.59	7.76	6.94	8.41
Germacrene D	4.98	4.51	0.87	6.85	9.92	-	5.63	6.00	5.96
Caryophyllene oxide	23.58	25.69	15.53	16.73	27.19	30.30	11.23	12.30	9.92
Spathulenol	5.22	5.55	7.49	5.32	5.47	6.97	3.09	3.59	3.13
Farnesyl acetate	1.85	1.97	0.87	1.80	2.22	1.54	1.23	1.56	1.20

For accessions, the most important compounds were caryophyllene oxide, β-caryophyllene, spathulenol, germacrene D and linalool. Oregano samples were not rich in thymol and carvacrol. From our results, sesquiterpene chemotype can be defined for oregano accessions.

By Nurzyńska-Wierdak (2009), oregano from Poland had the greatest content of sabinene and germacrene D, but the content of sabinene and β-pinene as well as germacrene-D-4-ol, thymol, and carvacrol depended on the climatic conditions and were the most changeable in the study years. Particularly it is concluded also in this research (Sivicka et al., 2017).

By De Mastro et al. (2004), about 44 components with the predominance of carvacrol, thymol, γ-terpinene, linalyl acetate, germacrene D and cis-ocymene were detected in oregano from Italy. Carvacrol ranged between 0.18 and 66.74%, thymol from

0.20 to 43.68% as well as linalyl acetate between 51.27 and 60.93%, thus outlining a new oregano chemotype.

By Lukas et al. (2011), *Origanum vulgare* L. wild populations from Italy, Israel, Turkey, Greece and Croatia can be regarded as rich in thymol or carvacrol. Also, oregano mainly comes from wild populations in Turkey and Greece (Asdal et al., 2006). Some populations can be classified into thymol-‘pure’, carvacrol-‘pure’ and thymol/carvacrol mixed. Some populations showed the content of thymol or carvacrol till 20%. In Ukraine it was found, that for oregano propagation by cuttings increases the content of essential oil significantly in comparison with plants propagated by division (Boiko & Konik, 2010). As oregano accessions from Latvia also were propagated by division, this factor could be negative for essential oil synthesis.

By Falco et al. (2013), oregano growth conditions influence the composition of essential oil significantly. In particular, the oil from plants grown in single rows was rich in sabinene, but plants grown in double rows – in ocimenes.

CONCLUSIONS

Despite of non-optimal meteorological conditions, oregano accessions can produce high biomass in Latvia.

Oregano accessions from Latvia are poor in essential oil, but its` content is higher for plants with dark coloured flowers. Seventeen (17) compounds were identified as the principal, the caryophyllene oxide had the greatest content. Sesquiterpene chemotype can be defined for local oregano.

In the future, it is important to research the influence of propagation methods and agrotechnics on content and composition of oregano essential oil more carefully.

REFERENCES

- Asdal, A., Galambosi, B., Bjorn, G., Olsson, K., Pihlik, U., Radušiene, J., Porvaldsdottir, E., Wedelsback Bladh, K. & Žukauska, I. 2006. *Spice- and medicinal plants in the Nordic and Baltic countries. Conservation of genetic resources. Report from a project group at the Nordic Gene Bank*, NGB, Alnarp, Norway, 157 pp.
- Boiko, J. & Konik, R.J. 2012. The productivity of *Origanum vulgare* L. and *O. tyttanthum* Gontsch, dependently from the methods of planting material producing. *Modern Phytomorphology* **2**, 79–81.
- Caliskan, O., Odabas, M., Cirak, C., Radušiene, J. & Odabas, F. 2010. The quantity effect of temperature and light intensity at growth in *Origanum onites* L. *Journal of Medicinal Plants Research* **4**(7), 551–558.
- D’Antuono, L.F., Galetti, G.C. & Bocchini, P. 2000. Variability of essentials oil contents and composition of *Origanum vulgare* L. populations from North Mediterranean Area (Liguria Region, Northern Italy). *Annals of Botany* **86**, 471–478.
- De Falco, E., Mancini, E., Roscigno, G., Mignola, E., Tagliatalata-Scafati, O. & Senatore, F. 2013. Chemical composition and biological activity of essential oils of *Origanum vulgare* L. subsp. *vulgare* L. under different growth condition. *Molecules* **18**, 14948–14960.
- De Mastro, G., Ruta, C. & Marzi, V. 2004. Agronomic and technological assessment of oregano (*Origanum vulgare* ssp.) biotypes. *Acta Horticulturae* **629**, 355–362.

- Droushiotis, D., Della, A. 2002. Genetic resources of medicinal and aromatic plants in Cyprus with emphasis on the selection, evaluation and management of *Origanum dubium*. *Report of a Working Group on Medicinal and Aromatic Plants. First Meeting, 12-14 September 2002, Gozd Martuljek, Slovenia*, pp. 39–41.
- Hammer, K. & Spahillari, M. 2000. Crops of European origin. In: *Report of a Network Coordinating Group on Minor Crops. First Meeting 16 June 1999, Turku, Finland*, International Plant Genetic Resources Institute, Rome, pp. 35–43.
- Leyva-López, N., Gutiérrez-Grijalva, E.P., Vazquez-Olivo, G. & Basilio Heredia, J. 2017. Essential Oils of Oregano: Biological Activity beyond Their Antimicrobial Properties. *Molecules* **22**(6), 989. <https://doi.org/10.3390/molecules22060989>
- Lukas, B., Schmiderer, C. & Novak, J. 2011. *Conservation and characterization of oregano (Origanum vulgare L.) wild populations in Europe. Genetic Structure and Variability of Essential Oil*. University of Veterinary Medicine, Institute for Applied Botany, Wien, Austria, 19 pp.
- Nyrzyńska-Wierdak, R. 2009. Herb yield and chemical composition of common oregano (*Origanum vulgare* L.) essential oil according to the plant's development stage. *Herba Polonica* **55**(3), 55–62.
- Ortega-Ramirez, L.A., Rodriguez-Garcia, I., Silva-Espinoza, B.A. & Avala-Zavala, J.F. 2016. Oregano (*Origanum* spp.) Oils. In book: *Essential Oils in Food Preservation, Flavor and Safety, Academic Press*, pp. 625–631.
- Osińska, E. 2000. Developmental and chemical variability of several forms of wild marjoram (*Origanum vulgare* L.). *Roczniki Akademii Rolniczej w Poznaniu CCCxxIII*, 391–395 (in Polish).
- Rzekanowski, C., Marynowska, K., Rolbiecki, S. & Rolbiecki, R. 2008. The influence of selected meteorological factors on some elements of the yield of four herb species cultivated under irrigation conditions. *Acta Agrophysica* **12**(1), 163–171 (in Polish).
- Sivicka, I., Osinska, E., Kruma, Z. & Adamovics, A. 2017. Content and composition of essential oil of oregano genetic resources in Latvia. In: *FoodBalt 2017: 11th Baltic conference on food science and technology "Food science and technology in a changing world": abstract book, Jelgava, April 27–28*, Latvia University of Agriculture, pp. 99.
- Sivicka, I., Žukauska, I., Balode, A. & Adamovičs, A. 2015. Fresh and air-dry biomass of oregano (*Origanum vulgare* L.) accessions. In: *Nordic view to sustainable rural development: proceedings of the 25th NJF Congress, Riga, Latvia, 16th-18th of June, 2015*, Nordic Association of Agricultural Scientists, Riga, pp. 46–51.
- Tucker, A.O. & Rollins, E.D. 1989. The species hybrids and cultivars of *Origanum* (*Lamiaceae*) cultivated in the United States. *Baileya* **23**(1), 14–27.
- Węglarz, Z., Osińska, E., Geszprych, A. & Przybył, J. 2006. Intraspecific variability of wild marjoram (*Origanum vulgare* L.) naturally occurring in Poland. *Revista Brasileira de Plantas Medicinai* **8**, 23–26.
- Žukauska, I. 2008. Genetic resources of culinary plants. *Agronomijas Vēstis* **10**, 241–247 (in Latvian).
- Žukauska, I. & Sivicka, I. 2011. *Draft Descriptor List Origanum vulgare L.* European Cooperative Programme for Plant Genetic Resources, Rome, 8 pp.

Effect of multi-component fertilizers on seeds yield, yield components and physiological parameters of winter oilseed rape (*Brassica napus* L.)

S. Stankowski¹, M. Bury¹, A. Jaroszewska¹, B. Michalska² and
M. Gibczyńska^{3,*}

¹West Pomeranian University of Technology in Szczecin, Department of Agronomy, Papieża Pawła street VI 3, PL71-459 Szczecin, Poland

²West Pomeranian University of Technology in Szczecin, Department of Meteorology, Botany and Green Areas Management, Papieża Pawła street VI 3, PL71-459 Szczecin, Poland

³West Pomeranian University of Technology in Szczecin, Department of Chemistry, Microbiology and Environmental Biotechnology, Słowackiego street 17, PL71-434 Szczecin, Poland

*Correspondence: marzena.gibczynska@zut.edu.pl

Abstract. Subject of the discussed studies was an analysis of the impact of mineral multi-component fertilizers, from Polish and foreign producers, on the yield and yield components of winter oilseed rape (*Brassica napus* var. oleifera). Two field experiments were carried out in 2015–2017 in Lipnik. The experimental crop was winter oilseed rape, hybrid cultivar DK EXPLICIT. Two factors were studied in the experiment A: 4 multi-component mineral fertilizers - two Belarusian (1 i 2), one Russian and one Polish (Polifoska 6) and 4 doses of fertilization (250, 500 and 750 kg ha⁻¹). In the experiment (B) were compared two factors: 3 multi-component mineral fertilizers - Belarusian, Russian and Polish production - Polifoska 8 and 4 doses of fertilization (200, 400 and 600 kg ha⁻¹). The fertilizers applied in the experiments, manufactured in Belarus, Russia and Poland, did not show variations in the amount of yield of winter rape. The number of winter rapeseed plants on the area unit (in autumn and spring) was independent of the type of fertilizers. In the experiment B, higher number of rapeseed siliques was obtained after application of Polifoska 8, than other fertilizers. Rapeseed grown on soil with the fertilizers manufactured in Belarus showed a lower value of greenness index (SPAD) and leaf area index (LAI). As a result of the application of multi-component fertilizers, manufactured in Belarus, Russia and Poland, the recorded differences in the winter rapeseed yield, yield components and physiological parameters did not exceed 10%.

Key words: doses of fertilization, fertilizers NPK(S): Belarusian, Russian, Polish, winter rape yield structure.

INTRODUCTION

Winter oilseed rape (*Brassica napus* L.), in Poland and in other countries of the cold temperate climate zone, is one of the most important oil crop. In European

conditions, it is the basic raw material for the production of oil for consumption and industrial purposes. In Poland in 2017, the total yield of rape seeds amounted to 2697.3 thousand tons and was higher by 478.0 thousand tons compared to the previous year (CSO 2017; CSO 2018). Increased oil seed rape yield results from the increase in cultivation area and technological progress expressed, among others, by obtaining more efficient population and hybrid cultivars. The quality of seed yield determines the value of agriculture and use of winter rape cultivars. On the area of Poland, after joining the European Union, cultivars appearing in the list of the Common Catalogue of Varieties of Agricultural Plant Species, may be grown. In 2010, an intensive hybrid cultivar DK EXPLICIT was registered and recommended in all regions of Poland.

Winter rape is classified as crop species with very high nutritional needs (Kowalska & Remlein-Starosta, 2011). The most important element affecting the dynamics of growth and yield of rapeseed is nitrogen used in spring in two parts (Friedt et al., 2003; Szczepaniak et al., 2015). Among fertilizer components, nitrogen has the greatest impact on seed quality (Bartkowiak-Broda, 2005). Winter rape belongs to plants with very high requirements in relation to potassium and strongly responsive to fertilizing this component, (Damon et al., 2007) Oilseed rape as a cruciferous plant, also requires good potassium and phosphorus nutrition. Winter oilseed rape, well supplied with phosphorus and potassium, creates strong leaf rosettes and strongly roots before winter, which promotes good wintering. In the spring, phosphorus and potassium facilitate rapid formation of new leaves and stems, while in the summer they accelerate the maturation of seeds in siliques, increase the yield of seeds and content of fat (Orlovius, 2003; Piekarczyk et al., 1014).

Cruciferous plants, to which oilseed rape belongs, are characterized by the highest demand for sulfur. Sulfur fertilization, especially at appropriately high nitrogen doses, may also favorably affect the maintenance or increase of fat content in rape seeds as a result of yield increase (Podleśna, 2002; Lośák & Richter, 2003). Orlovius (2003) emphasizes that the high probability of sulphur deficit is mainly present on lighter mineral soils.

Commonly, multi-component fertilizers are currently used for oilseed rape, both complex NPK and mixed NP and PK, generally having better physical properties than single components, which should be done in a rational way (Nogalska et al., 2012). Fertilizers used in rapeseed cultivations are, for example, Polifoska 6 or Polifoska 8. Due to granulation and thus uniform composition, they have good physical properties and are comfortable to use. They differ in the fixed proportion of nutrients established by the manufacturer. In the following years, an increase in the production and consumption of multi-component fertilizers is noted. In Poland, in the 2016/2017 marketing year, the use of these fertilizers amounted to 2.0 million tons and increased by 0.2 million tons compared to the previous year (Domańska, 2018). The multi-component fertilizers present on the Polish market are diversified in terms of chemical composition as well as national and foreign producers. So far, there have been no comparative studies effects operations of fertilizers of Polish, Russian and Belarusian production. There are indications that fertilizers of eastern production, despite similar composition, give a much worse effect.

The subject of the discussed studies was an analysis of the impact of mineral multi-component fertilizers, from Polish and foreign producers (Belarusian and Russian), on the yield and yield components of winter rape (*Brassica napus* var. *oleifera*). The

conducted research also analyzed the impact of different doses of multi-component fertilizers.

MATERIALS AND METHODS

Field experiment

Two field experiments were carried out in 2015–2017 in Lipnik (53°41'N, 14°97'E) at the Agricultural Experimental Station belonging to the West Pomeranian University of Technology in Szczecin. The experimental plant was winter oilseed rape, hybrid cultivar DK EXPLICIT. The plot area was 15 m². The experiments were laid out as randomized blocks in 4 replications. The soil was loamy sand (Polish Soil Classification 2011). The scope of the research included two experiments.

Experiment A

Two factors were studied the experiment: I. factor: 4 multic-omponent mineral fertilizers (NPK 6-20-30). i.e. two Belarusian (1 i 2), Russian and Polish (Polifoska 6), II. factor: 4 doses of fertilization: 0 - control variant, minimum, optimum, maximum. The dose of multi-component fertilizer was determined for phosphorus, which is the most expensive ingredient. The doses were calculated based on the demand of rape in relation to phosphorus. The minimum dose was 50% lower than the optimal dose of 100 kg P₂O₅ per hectare, and the maximum dose was 50% higher than that. Doses of multi-component fertilizers were 250, 500 and 750 kg per hectare, respectively. Polifoska 6 is a complex granular NPK(S) 6-20-30(7). The producer of the fertilizer is 'POLICE' S.A. This fertilizer is recommended for use on potassium-poor soils, in conditions of low organic fertilization and for potassophilic plants such as: sugar beet, potato, maize and rapeseed (<https://nawozy.eu>).

Experiment B

The study compared two factors: I. factor: 3 multi-component mineral fertilizers of Belarusian, Russian and Polish production – Polifoska 8. Applied fertilizers were characterized by the following composition of NPK(S): Belarusian 8-24-24, Russian 9-25-25(4) and Polish 8-24-24(9). II. factor: 4 doses of fertilization: 0 - control variant, minimum, optimum, maximum, amounting respectively 200, 400 and 600 kg per hectare. Fertilization levels were calculated based on the soil phosphorus supply. The minimum dose was 50% less than the optimal dose of 100 kg P₂O₅ per hectare, and the maximum dose was 50% higher. Polifoska 8 is a fertilizer NPK(S) 8-24-24-(9). It is the fertilizer with uniform light gray to dark gray granules or light pink, sized 2–5 mm, not less than 92%. Polifoska 8 contains 8% nitrogen (N) in ammonium form, 24% phosphorus (P₂O₅) soluble in neutral ammonium citrate and water, i.e. available in the form of mono- and di-ammonium phosphate, including 21% soluble in water. The fertilizer contains 24% potassium (K₂O) soluble in water, in the form of potassium chloride and 9% sulfur dioxide (SO₃) soluble in water, in the form of sulfate. Chemical composition of Polifoska 8 is to promote good root formation and proper development. The producer of the fertilizer is 'POLICE' S.A. (<https://nawozy.eu>).

In the successive years of the experiment the cultural practices were applied to oilseed rape. After harvesting the preceding oat crop, the stubble was turned down using a stubble cultivator. Then, after about two weeks, plowing was carried out using medium

rotary plow. Just before sowing, after manual application of multi-component fertilizers, the soil was tilled to a depth of about 8 cm with cultivator with a string roller. The sowing was carried out using the ØYORD seed drill on August 26. About a week after sowing, insecticide protection was applied (Alstar Pro 100 EW 0.1 dm³ ha⁻¹), and after the next 7 days, a supplement herbicidal treatment was carried out to volunteer cereal plants and other monocot weeds (Supero 05 EC). Then, after 14 days from the sowing of rape, when the seedlings developed at least one pair of true leaves, herbicidal spraying was performed (Metazanex 500 SC 2 dm³ ha⁻¹). The last treatment performed after subsequent 7 days was a fungicide treatment with double action: fungicidal and regulating the crop stand the plants conformation (Toprex 375 EC at dose of 0.4 dm³ ha⁻¹). In early spring with the start of vegetation (about 3–4 March), the first nitrogen fertilization was carried out in the amount of 80 kg N ha⁻¹ as ammonium nitrate. The second dose of nitrogen fertilization was applied in the phase of the third internode elongation (5–7 April) at 80 kg N ha⁻¹ as ammonium nitrate. Then, the first fungicide treatment was performed within a few days' interval (Alstar Pro 100 EW 0.1 dm³ ha⁻¹). In the final stage of flowering, an insecticide-fungicide treatment was performed (Trion 250 EW 0.6 dm³ ha⁻¹ plus Proteus 110 OD 0.6 dm³ ha⁻¹). The harvest was carried out using a combine harvester after reaching the full maturity of rape seeds.

Methodology of analysis

When carrying out the research, the following traits were determined: seeds yield, number of plants per m² (autumn and spring), number of siliques per plant, number of seeds per silique, plant height, SPAD (greenness index) and LAI (leaf area index). During the vegetation in the autumn, after emergence in the phase of 4–6 leaves (BBCH 16) and in spring, the plantation density was determined by counting plants in four places on each plot (4×0.125 m²) and recalculating the obtained results into 1 m². Plant height was determined by measuring 20 plants on each plot at full maturity (BBCH 89). Before harvest, the samples of plants were collected from the same places where plants were counted after emergence in order to assess the yield components – number of siliques on the plant, number of seeds in silique and weight of 1,000 seeds. The harvest was made with a field combine-harvester (Wintersteiger nursery master elite). The weight of 1,000 seeds was determined in accordance with the PN-68/R-74017: 1968 standard. The LAI parameter was measured using a Decagon AccuPar ceptometer with an external PAR LI 190 S.A. sensor by Licor (USA). Five measurements were taken on each plot, making readings from 20 sensors within one measurement. The chlorophyll content was determined by the photo-optical method using the Minolta SPAD-502 analyzer (USA) on randomly selected 10 plants from each variant.

Statistical analysis

The results were statistically processed using the analysis of variance in a 2-factor random blocks design. Confidence sub-intervals (LSD) were calculated using Tukey's multiple test, assuming a significance level of $P \leq 0.05$. In addition, the analysis of variance with regression for the main effect of quantitative factor - the dose of fertilizer - was performed for selected soil features. The significance of regression equations was determined using the ANOVA with regression with F-Fisher-Snedecor test. Regression lines are shown on figures. Statistical analysis of results was carried out using the Statistica 10.0 software.

Soil and weather conditions

Soil from the experiment A was characterized by the following parameters: $\text{pH}_{\text{KCl}} 5.2 \pm 0.3$ available phosphorus ($\text{P}_{\text{avail}} = 56.5 \pm 6.2$), available potassium ($\text{K}_{\text{avail}} = 110.9 \pm 9.3$), exchangeable magnesium ($\text{Mg}_{\text{exchan}} = 64.4 \pm 4.5 \text{ mg kg}^{-1}$). It was the soil with an average content of analysed macronutrients (Egner et al., 1960, ISO 13536:2002P).

Soil from the experiment B was characterized by the following parameters: $\text{pH}_{\text{KCl}} 5.3 \pm 0.4$, $\text{P}_{\text{avail}} = 47.5 \pm 5.7$, $\text{K}_{\text{avail}} = 97.9 \pm 8.5$, $\text{Mg}_{\text{exchang}} = 54.4 \pm 5.3 \text{ mg kg}^{-1}$. It was the soil with moderate content of available phosphorus and exchangeable magnesium and low of available potassium (Egner et al., 1960; ISO 13536:2002P).

In the years of research, meteorological conditions in Lipnik were very diverse. In autumn 2015, it initially did not deviate from the norm in terms of temperature and rainfall, while the end of the year was very warm: in December, the air temperature exceeded the norm by even $5.1 \text{ }^\circ\text{C}$. From October to April, very low rainfall was recorded, hence these months were classified as dry and very dry. During those 7 months, only 143 mm of rain fell, which was only 56% of the average value. In the first quarter of 2016, the temperature fluctuated within the normal range, while May and June were very warm, exceeding the long-term value by respectively $2.9 \text{ }^\circ\text{C}$ and $2.0 \text{ }^\circ\text{C}$. High rainfall in June was somewhat complemented by shortages from the earlier period. The second half of 2016 was in thermal terms within the norm, except from September, which turned out to be anomalously warm – $16.6 \text{ }^\circ\text{C}$ and very dry – only 13 mm of rainfall. The rainfall shortages lasted until March 2017. Large precipitation appeared in the summer, in June–August there was 310 mm of rain, which constituted 174% of the long-term sum (183 mm). These months were slightly warmer than average. The average air temperature in the season from September 2015 to August 2016 was $10.3 \text{ }^\circ\text{C}$ and exceeded the norm by $2.1 \text{ }^\circ\text{C}$, and the total rainfall was 423 mm, which accounted for only 79% of the average, in the 2016/2017 season; these values were respectively: $9.1 \text{ }^\circ\text{C}$ – exceeding the standard by $1.1 \text{ }^\circ\text{C}$ and 604 mm – constituting 113% of the long-term value.

RESULTS AND DISCUSSION

Effect of different multi-component fertilizers on winter rape productivity

In experiments A and B, the average yield of winter rape seeds from two years was respectively in the range from 2.30 to 2.58 and from 2.55 to 2.64 Mg ha^{-1} . Relatively low yield of 2.50 Mg ha^{-1} obtained in the experiment was the result of unfavourable humidity conditions and high temperatures in most of the growing season in 2015 and 2016, which significantly hindered the preparation of the soil for the sowing of winter rape and its subsequent growth. Results of many studies confirm particularly high sensitivity of rape to the weather course during the growing season (Diepenbrock, 2000; Dunker & Tiedemann, 2004; Bartkowiak-Broda, 2005; Szczepaniak, 2014; Weymann et al., 2015; Oleksy, 2018). Polish and imported fertilizers used in the experiments, having the same percentage composition, did not differentiate the yield. The results indicate that macronutrients present in tested fertilizers are characterized by the same availability for cultivated rape (Table 1, 2).

The rapeseed plant density is a trait that significantly affects the size and quality of the crop. In the literature, there are presentations showing justified use of lower sowing density of winter rape seeds, because the yield of seeds and fat did not significantly differ

from those obtained in conditions of higher sowing density (Kwiatkowski, 2012). In autumn, before the inhibition of vegetation in both experiments, the number of plants was obtained at a similar level, ranging from 50.3 to 55.7 plants per square meter. After starting the spring vegetation, a plant losses of 38% was found. In research by Czarnik et al. (2015), similar results were obtained for plant density for the hybrid cultivar Primus, i.e. 53.6 plants. Regarding the number of plants per area unit determined in autumn and spring, no statistically significant differences were found under the influence of Polish and imported fertilizers applied (Table 1, 2).

Table 1. Effect of multi component fertilizers on seeds yield, yield components and physiological parameters seeds of winter rape, experiment A, average from 2016–2017

Trait	Fertilizer				LSD _{0.05}
	Belarusian 1 NPK 6-20- 30	Belarusian 2 NPK 6-20- 30	Russian NPK 6-20- 30	Polifoska 6 NPK 6-20- 30(7)	
Seeds yield [Mg ha ⁻¹]	2.30	2.58	2.37	2.38	n.s.
Number of plants per m ² (autumn)	51.0	55.7	52.0	51.3	n.s.
Number of plants per m ² (spring)	32.7	32.0	32.7	33.0	n.s.
Number of siliques per plant	114	120	109	106	n.s.
Number of seeds per silique	12.3	13.7	13.4	14.0	n.s.
Plant height [cm]	132	138	138	141	n.s.
Weight of 1,000 seeds [g]	4.66	4.62	4.54	4.74	n.s.
Greenness index (SPAD)	55.0	62.9	63.3	64.1	7.59
Leaf area index (LAI)	1.86	2.22	2.12	2.32	0.206

n.s. – not significant difference.

Table 2. Effect of multi component fertilizers on seeds yield, yield components and physiological parameters of winter rape, experiment B, average from 2016–2017

Trait	Fertilizer			LSD _{0.05}
	Belarusian NPK 8-24-24	Russian NPK 9-25-25(4)	Polifoska 8 NPK 8-24-24(9)	
Seeds yield [Mg ha ⁻¹]	2.55	2.47	2.64	n.s.
Number of plants per m ² (autumn)	50.3	52.5	52.3	n.s.
Number of plants per m ² (spring)	32.7	32.8	32.7	n.s.
Number of siliques per plant	114	124	130	14.2
Number of seeds per silique	14.2	12.1	12.4	n.s.
Plant height [cm]	140	138	142	n.s.
Weight of 1,000 seeds [g]	4.44	4.62	4.69	n.s.
Greenness index (SPAD)	57.0	59.2	55.2	n.s.
Leaf area index (LAI)	2.03	2.10	2.06	n.s.

n.s. – not significant difference.

Plants cultivated in the experiment A established a number of siliques on the plant of 110 pieces. This amount is comparable to that obtained by Jarecki et al. (2013) for Primus F1 and Visby F1 and smaller compared to data provided by Malarz et al. (2006) for Kaszub cv. rape – 162 pieces. Fertilizers used in the experiment A did not differentiate the amount of siliques per plants. Using Polifoska 8 in experiment B, more siliques were produced on rapeseed plants than after using the two other fertilizers and this was confirmed by statistical calculations (Table 2). Fertilizers used in both experiments did

not differentiate values of the number of seeds in the rapeseed rape within the range from 12.3 to 14.2.

In experiments carried out in 2015 by the Central Research Center for Cultivated Plants (COBORU 2016), in the West Pomeranian province, the average height of plants of cultivar DK EXPLICIT was 166 cm, the weight of a thousand seeds – 4.6 g. Winter rape plants cultivated in experiment A and B were about 16% lower. The weight of one thousand seeds of winter oilseed rape cultivated in both experiments was analogous to that obtained in the COBORU experiments (Table 1, 2). In relation to the number of seeds in silique and the weight of one thousand seeds, no statistically significant differences were found under the influence of the applied Polish and imported fertilizers (Table 1 and 2). Wielebski & Wójtowicz (1998), on the basis of results obtained in the experiment with five cultivars of winter oilseed rape, concluded that the number of siliques per plant was significantly different in reference to the nitrogen dose, and the remaining elements of the yield structure, such as: number of seeds in silique and weight of 1,000 seeds did not significantly differ.

In the experiment A, significantly higher level of SPAD (greenness index) was obtained by plants growing on soils fertilized with Belarusian 2, Russian and Polifoska 6 fertilizers, taking 62.9, 63.3 and 64.1 values. The physiological index LAI (leaf area to soil surface) was significantly differentiated as a result of the fertilizers used. The use of Belarusian 1 fertilizer was a factor causing the rapeseed plants growing on these objects to have a lower greenness index of 55.0 and LAI index of 1.86. Fertilizers used in experiment B, Belarusian, Russian and Polifoska 8 did not differentiate the SPAD and the LAI index (Table 2).

Effect of different multi-component fertilizers doses on winter rape productivity

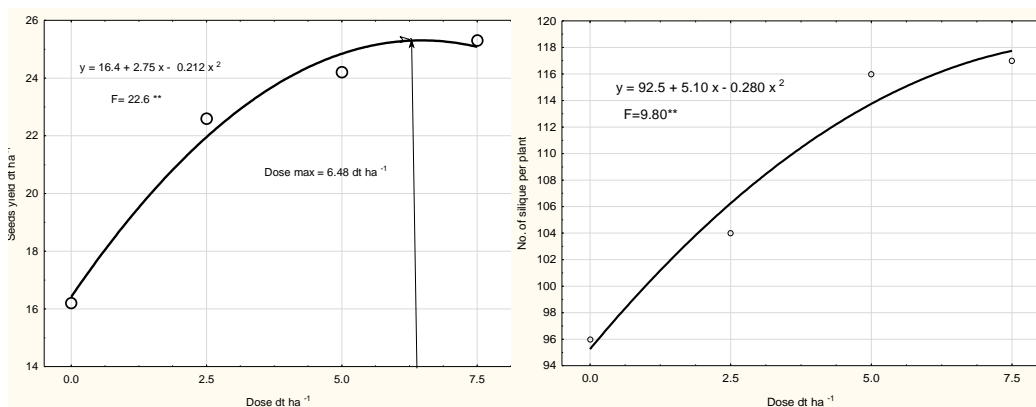


Figure 1. Regression line between dose of fertilizer and seeds yield and number of siliques per plant, experiment A.

The analysis of the effect of varied doses conducted in experiment A showed statistically confirmed differences in the yield of winter rapeseed. The calculations showed that it was possible to obtain the highest yield using fertilizer in the dose of 6.58 Mg ha⁻¹. Further increase of the dose had no rationale (Fig. 1). The results of the experiment B showed an analogous relationship, the highest yield (2.80 Mg ha⁻¹) was

obtained using the dose of 4.15 Mg ha⁻¹. Further increase of the applied fertilizer dose resulted in a decrease in yield (Fig. 2). It needs to be highlighted that the application of the minimum dose of the analysed fertilizers resulted in a very high increase in rapeseed yield as compared with variant without fertilization (Table 3 and 4). According to the analysis of the effect of fertilization on the yield of winter rapeseed by Gaj (2010), the object variation was mainly due to the contrast's significance: the absolute control (without NPK fertilization) and other fertilization variants.

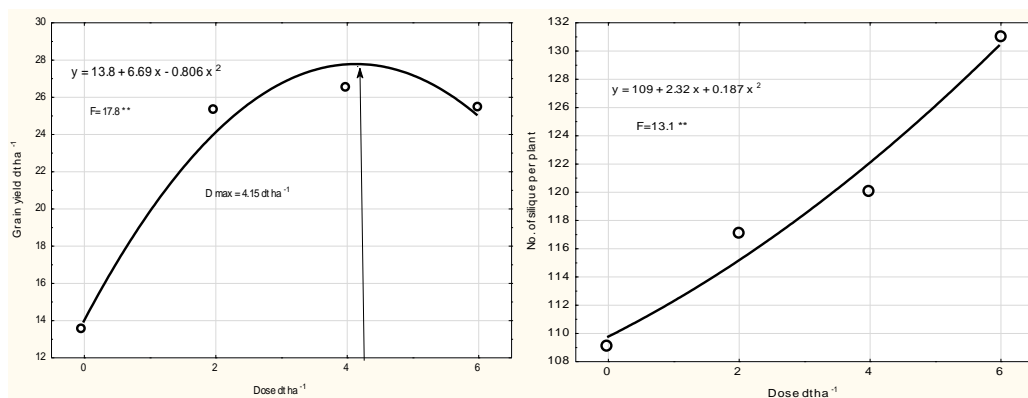


Figure 2. Regression line between dose of fertilizer and seeds yield and number of siliques per plant, experiment B.

In both experiments, the number plants per m² of winter rapeseed which was measured in autumn and spring was independent of the applied fertilizers and doses (Table 3, 4).

Table 3. Comparison of the effect of fertilizers on seeds yield, yield components and physiological parameters of winter rape experiment A, average from 2016–2017

Trait	Fertilizer dose [kg ha ⁻¹]				LSD _{0.05}
	0	250	500	750	
Seeds yield [Mg ha ⁻¹]	1.62	2.26	2.42	2.53	0.231
Number of plants per m ² [autumn]	50.5	52.3	55.9	49.5	n.s.
Number of plants per m ² [spring]	30.0	32.2	32.6	32.9	n.s.
Number of siliques per plant	96	104	116	117	10.2
Number of seeds per silique	11.1	13.9	13.0	13.2	1.57
Plant height [cm]	125.0	136.9	137.3	137.7	9.92
Weight of 1,000 seeds [g]	4.61	4.60	4.66	4.66	n.s.
Greenness index (SPAD)	43.3	59.6	63.9	65.5	4.86
Leaf area index (LAI)	1.60	2.09	2.20	2.32	0.236

n.s. – not significant difference.

The three parameters determining the yield of winter rapeseed (the number of siliques per a plant, the number of seeds in the siliques and the plant height) showed higher values with an increase of the applied dose. However, the significant difference was found only regarding data for fertilized and unfertilized objects (Table 3, 4, Figs 1, 2).

In A and B experiment, the application of multi-compound fertilizers to the soil had no effect on the weighty of 1,000 seeds values (relatively high, 4.6 g) (Tables 3, 4). Ranjbar et al. (2014) report that the weight of 1,000 seeds was not dependent on different tillage system, which suggesting the stability of this trait.

Table 4. Comparison of the effect of fertilizers on seeds yield, yield components and physiological parameters of winter rape experiment B, average from 2016–2017

Trait	Fertilizer dose [kg ha ⁻¹]				LSD _{0.05}
	0	200	400	600	
Seeds yield [Mg ha ⁻¹]	1.34	2.53	2.60	2.54	0.254
Number of plants per m ² (autumn)	51.5	52.8	50.6	51.7	n.s.
Number of plants per m ² (spring)	30.5	32.3	33.5	32.3	n.s.
Number of siliques per plant	109	117	120	131	13.3
Number of seeds per silique	9.0	13.5	13.6	11.9	1.73
Plant height [cm]	126	138	140	142	14.1
Weight of 1,000 seeds [g]	4.45	4.62	4.53	4.60	n.s.
Greenness index (SPAD)	47.3	56.7	55.9	58.9	4.57
Leaf area index (LAI)	1.60	2.09	2.07	2.03	0.215

n.s. – not significant difference.

The physiological SPAD and LAI indices were higher for winter rapeseed plants grown on all objects with fertilization. The three applied doses of fertilizers did not show differences in the analysed indices, values of which were in the same homogenous group (Table 3, 4).

CONCLUSIONS

The fertilizers applied in the experiments, manufactured in Belarus, Russia and Poland, did not show variations in the amount of yield of winter oilseed rape, cultivar DK EXPLICIT. The number of winter rapeseed plants on the area unit (in autumn and spring) was independent of the type of fertilizers. In the experiment B, higher number of rapeseed siliques was obtained after application of Polifoska 8, than other fertilizers. Rapeseed grown on soil with the fertilizers manufactured in Belarus showed a lower value of greenness index (SPAD) and leaf area index (LAI).

The seeds yield obtained at increasing fertilizer dose was differentiated. The three parameters determining the yield of winter rapeseed (the number of silique per plant, the number of seeds in the siliques and the plant height) showed higher values with an increase of the applied dose. The applied doses of fertilizers did not show differences in greenness index (SPAD) and leaf area index (LAI), values of which were in the same homogenous group. As a result of the application of multi-component fertilizers, manufactured in Belarus, Russia and Poland, the recorded differences in the winter rapeseed yield, yield components and physiological parameters did not exceed 10%.

REFERENCES

- Bartkowiak-Broda, I. Włakowski, T. & Ogródowczyk, M. 2005. Biological and agrotechnical possibilities of creating rapeseed seed quality. *Pam. Pul.* **139**, 7–25 (in Polish, English abstr.).
- COBORU 2016. *Results of Post-registration Variety Experiments, Oleiste (winter oilseed rape, spring rape)* Dev. Broniarz, J. Paczocha, J. Słupia Wielka, **121**, 1–50 (in Polish, English abstr.).
- CSO 2017. *Statistical Yearbook of Agriculture 2017*, Warsaw, Poland, 495 pp.
- CSO 2018. *Statistical Yearbook of Agriculture 2018*, Warsaw, Poland, 460 pp.
- Czarnik, M., Jarecki, W., Bobrecka-Jamro, D. & Jarecka, A. 2015. The effects of sowing density and foliar feeding on yielding of winter oilseed rape cultivars. *Rośl. Oleiste – Oilseed Crops*, **36**, 60–68 (in Polish, English abstr.).
- Damon, P.M., Osborne, L.D. & Rengel, Z. 2007. Canola genotypes differ in potassium efficiency during vegetative growth. *Euphytica* **156**, 387–397.
- Diepenbrock, W. 2000. Yield analysis of winter oilseed rape (*Brassica napus* L.): a review. *Field Crops Res.* **67**, 35–49.
- Domańska, W. 2018. *Environment 2018. Statistics Poland Spatial and Environmental Surveys* Department Warsaw, Poland, 219 pp.
- Dunker, S. & Tiedemann, A. 2004. Disease/yield loss analysis for Sclerotinia stem rot in winter oilseed rape. Integrated protection in oilseed crops. *IOBC/WPRS Bulletin* **27**(10), 59–65.
- Egner, H., Riehm, H. & Domingo, W. 1960. Untersuchungen über die chemische Bodenanalyse als Grundlage für die Beurteilung des Nährstoffzustandes der Böden. II. Chemische Extraktions- methoden zur Phosphor- und Kalium Bestimmung. *Kunigliga Lantbrukshögskolans Annaler* **26**, 199–215.
- Friedt, W., Lühs, W., Müller, M. & Ordon, F. 2003. Utility of Winter Oilseed Rape (*Brassica napus* L.). Cultivars and New Breeding Lines for Low-input Cropping System. *Pflanzenbauwissenschaften* **7**(2), 49–55.
- Gaj, R. 2010. Effect of different level of potassium fertilization on winter oilseed rape nutritional status at the initiation of the main stem growth and on the seed yield. *Rośl. Oleiste – Oilseed Crops* **31**, 115–124 (in Polish, English abstr.).
- ISO 13536:2002P Soil quality - Determination of the potential cation exchange capacity and exchangeable cations using barium chloride solution buffered at pH = 8,1.
- Jarecki, W., Bobrecka-Jamro, D. & Noworól, M. 2013. Reaction of winter rapeseed to varied number of sown seeds in Podkarpaciearea. *Rośl. Oleiste – Oilseed Crops* **34**(1), 65–74 (in Polish, English abstr.).
- Kowalska, J. & Remlein-Starosta, D. 2011. Research of nonchemical methods of winter oilseed rape protection in Poland. *J. Res. Appl. Agri. Eng.* **56**(3), 220–223.
- Kwiatkowski, C.A. 2012. Response of winter rape (*Brassica napus* L. ssp. oleifera Metzg., Sinsk) to foliar fertilization and different seeding rates. *Acta Agrobot.* **65**(2), 161–170.
- Lošák, T. & Richter, R. 2003. The influence of nitrogen and sulphur on the yield and oils content of winter rape. *Nawozy i Nawoż.* **4**(17), 160–168.
- Malarz, W., Kozak, M. & Kotecki, A. 2006. The effect of plant density in the field on yield quantity and quality of three winter rape cultivars. *Rośl. Oleiste – Oilseed Crops* **27**, 299–310 (in Polish, English abstr.).
- Nogalska, A., Czaplą, J. Sienkiewicz, S. & Skwierawska, M. 2012. The effect of multi-component fertilizers on the yield and mineral composition of winter wheat and macronutrient uptake. *J. Element.* **17**(4), 629–638.

- Oleksy, A. 2018. Production and development reaction of winter rape cultivars for various nitrogen and sulphur doses. *Fragmen. Agron.* **35**(2), 79–97.
- Orlovius, K. 2003. Fertilising for high yield and quality: oilseed rape. *Bulletin No.16, ed. Kirkby, E.A. International Potash Institute (IPI)*, Horgen, Switzerland, **16**, 1–130.
- Piekarczyk, M., Jaskulska, I., Gałęzewski, L., Kotwica, K., Jaskulski, D., 2014. Productivity of winter oilseed rape and changes in soil under the influence of fertilization with the use of ash from straw. *Acta Sci. Pol. Agric.* **13**(3), 45–56.
- PN-68/R-74017:1968. Grains of cereals and edible leguminous seeds. Determination of the weight of 1,000 grains. (in Polish).
- Podleśna, A. 2002. Reaction of winter oilseed rape to different sulfur fertilization. *Zesz. Probl. Postępów Nauk Rol.* **481**, 335–339 (in Polish, English abstr.).
- Polish Soil Classification 2011. Ed. D. Czepińska-Kamińska. *Soil Science Annual* **62**(3), 1–195.
- Ranjbar, H., Mansouri, M., Salar, M.R. & Ala, A. 2014. Effects of different tillage system, seeding method and rates on yield and seed oil percentage of rapeseed. *Int. J Adv. Biol. Biomed. Res.* **2**(1), 192–201.
- Szczepaniak, W. 2014. A mineral profile of winter oilseed rape in critical stages of growth – nitrogen. *J. Elemen.* **19**(3).
- Szczepaniak, W., Grzebisz, W., Potarzycki, R., Łukowiak, R. & Przygocka-Cyna, K. 2015. Nutritional status of winter oilseed rape in cardinal stages of growth as the yield indicator. *Plant, Soil Environ.* **61**(7), 291–296.
- Weymann, W., Bottcher, U., Sieling, K. & Kage, H. 2015. Effects of weather conditions during different growth phases on yield formation of winter oilseed rape. *Field Crops Res.* **173**, 41–48.
- Wielebski, F. & Wójtowicz, M. 1998. Response of winter rape varieties to high nitrogen fertilization in rye soils in Experimental Station Zielęcín. *Rośl Oleiste – Oilseed Crops* **29**, 507–514. (in Polish, English abstr.).
- <https://nawozy.eu/nawozy/wieloskladnikowe/>. 15.02.2019. (in Polish).

Possibility and prospects of preservation of minor components in technology of fruit raw materials conservation

V. Strizhevskaya, M. Pavlenkova, S. Nemkova, N. Nosachyova, I. Simakova*
and E. Wolf

Federal State Budgetary Educational Institution of Higher Education Saratov State Agrarian University named after N.I. Vavilov, Department of Veterinary Medicine, Biotechnology and Food Technology, Sokolovaya street, 335, RU410000 Saratov, Russian

Correspondence: simakovaiv@yandex.ru

Abstract. According to modern research, traditional methods of preserving fruits and vegetables do not allow obtaining products identical to natural products for biological value. At the same time, there is a need to provide the population with minor components of food, including concentrated form. The aim of the study was to preserve the minor components in canned fruit raw materials for a long time. The study was carried out comparing the data of bioflavonoids and vitamin C in fresh oranges and dehydrated oranges (immediately after dehydration and storage for 12 months). The analysis was performed by reversed-phase HPLC on Dionex Ultimate 3,000 chromatograph ('Thermo Scientific', USA) using Luna 5U C18(2) 100A, 5 μ m 4.6 mm \times 150 mm column ('Phenomenex', USA), system number 125617-12. The identification of components was performed by comparison of retention times of standard flavonoid samples. Dehydration was done by means of resonant IR drying, gradually lowering the temperature from intense (67–75 °C) to soft (32–35 °C) temperature regimes. Analysis of chromatograms of fresh and dehydrated oranges shows that they all have a similar profile, but differ significantly in the content of certain components. The presence of vitamin C 1,926.9 mg per 1 g of dehydrated oranges was noted, which is identical to the content of 10 g of fresh orange. The following flavonoids have been found: prunus and a component related to the polymer form of naringin, the content in 1 g of dehydrated oranges is approximately seven times more than that for 1 g of fresh orange. The loss of vitamin C by 8% during storage of dehydrated orange for 12 months was noted, the amount of flavonoids varies insignificantly by 2–3%. Studies have shown that the technology of dehydration with the help of resonance IR drying allows to keep the minor components in the native state for a long time.

Key words: dehydration, flavonoids, preservation of minor components, vitamin C.

INTRODUCTION

The increase in the consumption of industrially produced food, changes in daily physical activity, and factors that increase oxidative stress lead to the necessity of strengthening of the today people diet by minor components of food.

Flavonoids are one of the important groups related to minor components. These substances are not synthesized in the body and can only be replenished by the

introduction of plant foods (vegetables, fruits and berries) into the diet (Mennen et al., 2008; Tarahovsky et al., 2013).

The question of the effect of flavonoids on the human body remains open to the present time, and what is more, it is known that flavonoids play a vital role in protecting against infections, prevent oxidative stress, contribute to the prevention of neurodegenerative diseases. According to WHO, a person needs to consume at least 400 g of fruits and vegetables per day to prevent cardiovascular diseases, cancer, obesity, and diabetes (Gu et al., 2010; Kontou et al., 2011; Davidson et al., 2016; Mayne et al., 2016).

Often in the modern diet lacks a sufficient number of minor components of food. The main reasons are: irrational living conditions, including inadequate nutrition; irregular working hours and, as a result, eating fast food; lack of quality fruits and vegetables associated with intensive farming and breeding. Taking BADS containing dietary fiber and minor components do not have a significant impact on disease prevention. It should be noted that the complex of native dietary fibers and flavonoids of vegetables and fruits is most effective in the prevention of diseases (Egert, et al., 2011).

According to recent research, the consumption of canned vegetables by salting and marinating, increase the risk of developing cancer (Zakrevsky & Lifyandsky, 2017). The solution to this problem can contribute to the use of new technological methods of preservation of bioactive substances in the production of food. The focus of these studies is aimed at improving accessibility by selecting gentle methods of treatment, one of which is IR treatment (dehydration). A feature of the use of long-wave resonance IR radiation in the food industry is the possibility of penetration of electromagnetic waves into products to a depth of several millimeters to 3 cm, which is 60 times higher than the degree of penetration of conventional heat. The predominant part of radiant energy is resonantly absorbed by water molecules, accelerating the process of dehydration without excessive heating of the product. The study of pulse modes of IR processing showed that the duration of the process and the cost of electricity are reduced by 2–3 times compared, for example, with convective drying.

High density of infrared radiation actively destroys harmful microflora in the product, so that it remains for a long time without deterioration of consumer qualities (Krishnamurthy et al., 2008; Demidov et al., 2015). This technology of dehydration allows preserving vitamins and other biologically active substances contained in the products. Thus, the complex problem of insufficiency of consumption of native fruits and vegetables, and also preservation of nutrients for a long time without creation of special conditions is solved.

The aim of the study was to develop a technology of preservation of fruit raw materials by dehydration to preserve minor components.

MATERIALS AND METHODS

The work was carried out at Saratov State Vavilov Agrarian University and the center for collective use (CCP) of scientific equipment in the field of physicochemical biology and nanobiotechnology ‘Symbiosis’ of the Federal state budgetary institution of science of the Institute of biochemistry and physiology of plants and microorganisms of the Russian Academy of Sciences (IBFM RAS).

The study examined fresh and dehydrated oranges. Dehydration was performed by the method of resonant IR drying on the wavelength of the near- and mid-infrared range of 1.8–3 microns by stepwise lowering of temperature from intense (67–75 °C) to mild (32–35 °C) temperature regimes. For resonant infrared drying, the equipment was used by Sator LLC, equipped with ceramic shell emitters, the design and composition of which are the know-how of this company.

The study was carried out by comparing the data of bioflavonoids and vitamin C in fresh oranges and dehydrated (immediately after dehydration and after storage for 12 months).

The analysis was performed by reversed-phase HPLC on Dionex Ultimate 3,000 chromatograph ('Thermo Scientific', the USA) using Luna 5U C18(2) 100A, 5 µm 4.6 mm × 150 mm column ('Phenomenex', the USA), serial number 125617-12. Identification of the components was performed by comparing the retention times of standard flavonoid samples (rutin in the form of hydrate (≥ 94%, 'Sigma-Aldrich', the USA), quercetin in the form of dihydrate (97%, 'Alfa Aesar', the UK), naringin (≥ 95%, 'Sigma-Aldrich', the USA), apigenin (≥ 97%, 'Sigma-Aldrich', the USA), naringenin (≥ 95%, 'Sigma-Aldrich', the USA).

The resulting material was processed on a personal computer using Stat Plus and Microsoft Excel (Egert & Rimbach, 2015).

RESULTS AND DISCUSSION

Traditional methods of dehydration lead to certain changes and cannot ensure the safety of biological substances. Thus, the proteins contained in the raw material, pectin substances undergo biochemical and colloidal chemical changes that affect the hydrophilic properties of dried products. Thermal drying does not allow obtaining a product with high recovery capacity due to chemical and physical processes with the formation of colloids occurring during drying. Freeze-drying allows preserving the quality of raw materials. Such food concentrates are characterized by high consumer properties. The only drawback is the high cost of processing.

The use of IR-dehydration of fruits in modes that preserve the native component by 80–90% solves several problems at once: the concentration of minor components per kilogram of food substance increases, and food fibers – cellulose, hemicellulose, pectose – remain in the native state, thus providing a substrate for microorganisms.

Technology of production of snack preserved with minor components is standard hydromechanical processing: washing, cleaning and cutting slices with a thickness of 3–4 mm on the disk knife. Dehydration by IR resonance drying, without forced convection. Radiation at the wavelength at the boundaries between the near and middle infrared ranges of 1.8–3 microns, which corresponds to the absorption of electromagnetic radiation by water. It should be noted that the introduction of forced convection will lead to overheating of the product and loss of valuable minor components due to thermal shock. Resonance occurring by the wave exposure prevents the interaction of molecules osmotically and physico-mechanically bound moisture, prevailing in fruit raw materials, with substances in the intact cell structure (Demidov et al., 2015). Thus, the most intense impact of temperature (65–70 °C) occurs in the first hour and due to intense evaporation allows you to remove surface moisture from the orange cantles. In this case, the main moisture remains in excess. Further, the

temperature is reduced to 45–50 °C and most of the moisture removal occurs in this range for 2–3 hours. The last stage of drying occurs at a temperature of 35–38 °C, the residue of osmotically-retained water is removed. The final moisture content of the product is 8–9% with an initial average humidity of $80 \pm 2\%$. The dehydrated product is air cooled to 20 °C and packed in a sealed package. The packaged product was stored without moisture, at the temperature of 20 ± 2 °C and normal atmospheric pressure.

Noted that during dehydration, the mass of the product changes in 7–7.5 times.

A comparative analysis of the content of ascorbic acid (vitamin C) in freshly squeezed orange juice, residue, after extraction and dehydrated orange showed that this method of dehydration allows preserving vitamins as much as possible (Fig. 1). The presence of vitamin C 1,926.9 mg per 1 g of dehydrated oranges was noted, which is identical to the content of 10 g of fresh orange. Losses of vitamin C during storage of dehydrated orange for 12 months amounted to 8%.

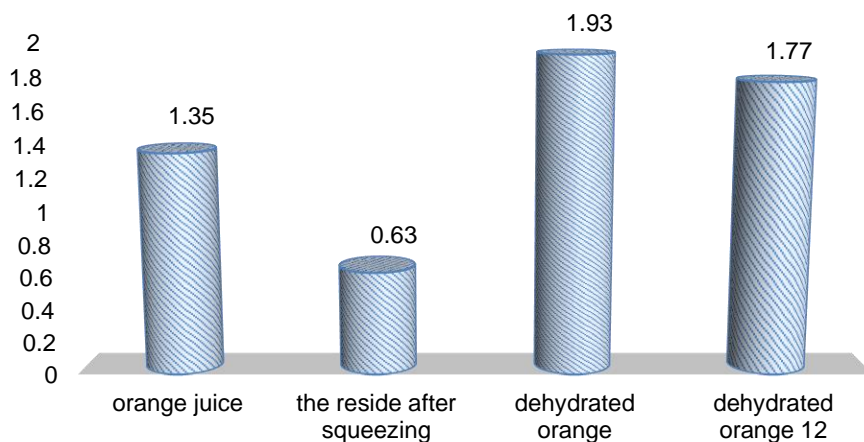


Figure 1. Content of vitamin C, mg per g (for juice and residue after pressing mg per 10 g) 1–3% deviation.

Analysis of chromatograms of orange juice (Figs 2–3), chips (Figs 4–5), the residue of fresh orange after separation of juice (Figs 6–7) shows that they all have a similar profile, but differ significantly in the content of certain components.

In the chromatograms of all the studied samples a group of peaks corresponding to polyphenolic compounds, in particular flavonoids, is observed. Thus, the most representative flavonoid found in the extracts is prunin, which is a monoglycoside of naringenin - Naringenin-7-O-Glucoside (component 18 in Fig. 1, component 17 in Figs 3–5). The retention time (15.00 min) and UV-visible spectrum coincide with those of the component obtained as a result of partial acid hydrolysis of the naringin sample. Component 17 (Fig. 1), component 16 (Fig. 3), component 15 (Fig. 4) has an almost identical absorption spectrum with prunin, however, it is characterized by a slightly shorter retention time (14.60 min) than the standard naringin sample (14.80 min), which allows us to assume that this component is a polymer form of naringin with a low degree of polymerization (dimer, trimer, etc). Component 23 (Figs 2–4), the component 21 (Fig. 6) has similar chromatographic and spectral characteristics with one of the

components detected after acid hydrolysis of naringin, which suggests the presence of aglycone naringenin.

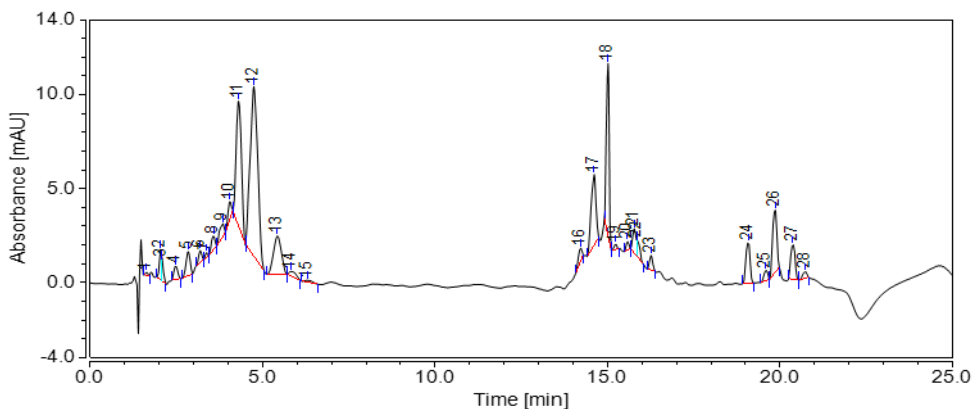


Figure 2. A chromatogram sample of orange juice, integration at a wavelength of 342 nm.

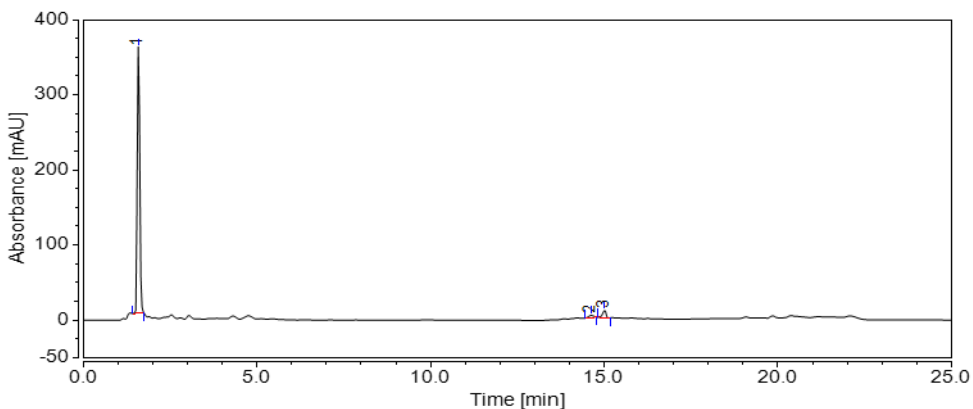


Figure 3. A chromatogram sample of orange juice, integration at a wavelength of 252 nm.

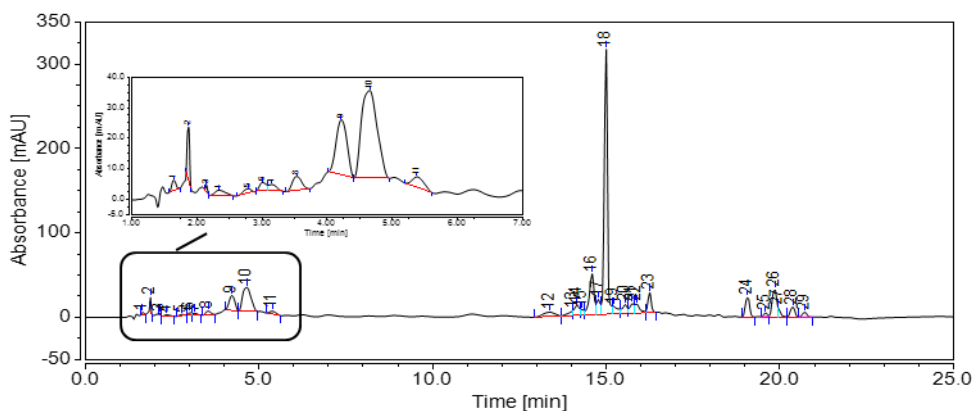


Figure 4. A chromatogram sample of dehydrated orange, integration at a wavelength of 342 nm.

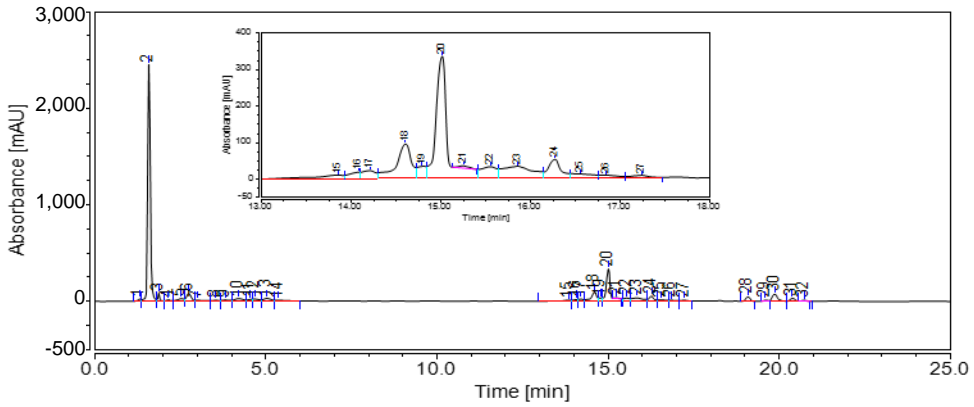


Figure 5. A chromatogram sample of dehydrated orange, the integration at the wavelength of 252 nm.

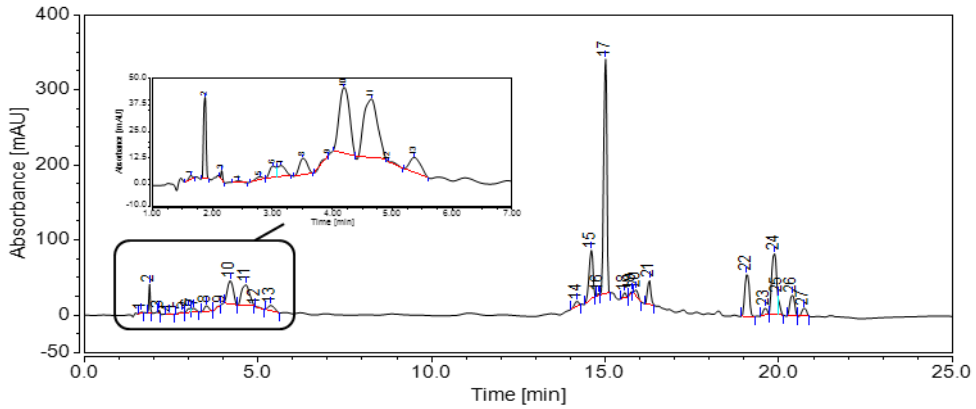


Figure 6. A chromatogram sample of the alcoholic extract of the fresh orange residue after separation of the juice, the integration on the wavelength of 342 nm.

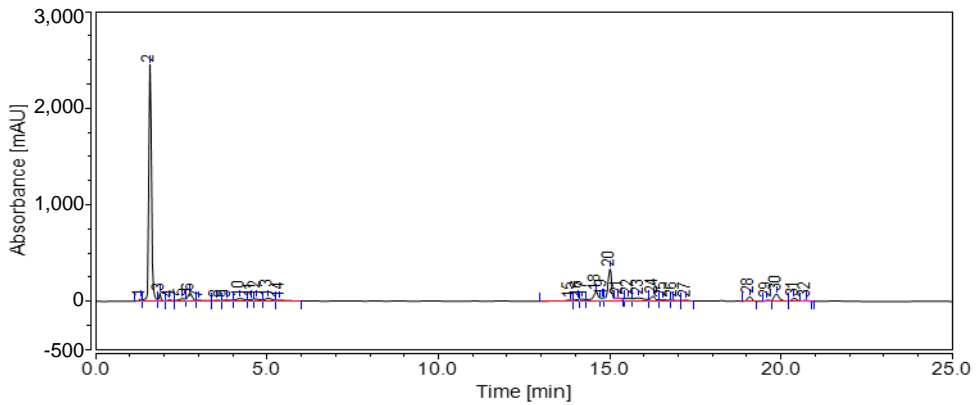


Figure 7. A chromatogram sample of the alcoholic extract of the fresh orange residue after separation of the juice, the integration at the wavelength of 252 nm.

The amount of detected prunin and the component related to the polymer form of naringin in the dehydrated orange is about seven times more than that for fresh orange. When storing dehydrated orange for 12 months. The amount of flavonoids varies insignificantly – 2–3%.

CONCLUSIONS

The result of the research was the developed technology of dehydration with the use of resonant IR drying and step-down temperature from intense (67–75 °C) to mild (32–35 °C) temperature conditions, which allows you to save the minor components. Analysis of the data of the experiments showed that the content of vitamin C in dehydrated oranges is 10 times higher than in fresh ones. Decoding of chromatograms of objects of research: orange juice, orange chips, the rest of fresh orange after juice separation - shows that all of them have a similar profile and contain a significant amount of polyphenolic compounds – flavonoids. In particular, prunin, which is a monoglycoside of naringenin – Naringenin-7-O-Glucoside. It should be noted that the content of the detected prunin and the component related to the polymer form of naringin in the dehydrated orange is approximately 7 times greater than that for fresh orange. When storing dehydrated orange for 12 months. The amount of flavonoids varies insignificantly – 2–3%, and the 8% loss of vitamin C was detected.

REFERENCES

- Davidson, K.T., Zhu, Z. & Fang, Y. 2016. Phytochemicals in the fight against cancer. *Pathol. Oncol. Res.* **22**(4), 655–660.
- Demidov, S.F., Voronenko, B.A. & Bazhanova, I.A. 2015. Kinetics of infrared drying of chopped beet. *J. The scientific journal of NRU ITMO. Series: processes and apparatus of food production* **3**, 158–163 (in Russian).
- Egert, S. & Rimbach, G. 2011. Which sources of flavonoids: complex diet or dietary supplements?, *Adv.Nutr.* **2**, 8–14.
- Gu, Y., Luchsinger, J.A., Stern, Y. & Scarmeas, N., 2010. Mediterranean diet, inflammatory and metabolic biomarkers, and risk of Alzheimer's disease. *J. Alzheimers. Dis.* **2**, 483–492.
- Kontou, N., Psaltopoulou, T., Panagiotakos, D., Dimopoulos, M.A. & Linos, A. 2011. The Mediterranean diet in cancer prevention: a review. *J. Med. Food* **14**, 1065–1078.
- Krishnamurthy, K., Khurana, H.K., Soojin, J., Irudayaraj, J. & Demirci, A. 2008. Infrared heating in food processing: An overview. *Comprehensive Reviews in Food Science and Food Safety* **7**(1), 2–13.
- Mayne, S.T., Playdon, M.C. & Rock, C.L. 2016. Diet, nutrition, and cancer: past, present and future. *Nat. Rev. Clin. Oncol.* **13**(8), 504–515.
- Mennen, L.I., Sapinho, D., Ito, H., Galan, P., Hercberg, S. & Scalbert, A., 2008. Urinary excretion of 13 dietary flavonoids and phenolic acids in freelifing healthy subjects – variability and possible use as biomarkers of polyphenol intake. *Eur.J.Clin.Nutr.* **62**, 519–525.
- Tarahovsky, Yu.S., Kim, Yu.A., Abdrasilov, B.S. & Musafarov, Ye.N. 2013. Flavonoids: Biochemistry, Biophysics, ex. ed. Mayevsky Ye.I., Synchronbook. 310 pp. (in Russian).
- Zakrevsky, V.V. & Lifyandsky, V.G. 2017. Vegetables and fruits in the prevention and treatment of cancer in the light of evidence-based medicine (part 1), *J. Vestnik of Saint Petersburg University. Medicine* **12**(4), 407–418 (in Russian).

Occurrence of archaeophytes in agrophytocoenoses – field survey in the Czech Republic

L. Tyšer, M. Kolářová* and T.T. Hoová

Czech University of Life Sciences Prague, Faculty of Agrobiolgy, Food and Natural Resources, Department of Agroecology and Crop Production, Kamýcká 129, CZ-165 00 Prague-Suchdol, Czech Republic

*Correspondence: mkolarova@af.czu.cz

Abstract. Archaeophytes are alien plants introduced to the Czech Republic before the year 1500. Their occurrence is strongly connected with agricultural production. The aim of this study was to assess the occurrence of archaeophytes in arable fields in the Czech Republic in terms of applied management systems (conventional and organic farming), crops (winter cereals, spring cereals, wide-row crops) and environmental site conditions at different altitudes. In 2006–2018, a phytocoenological survey was conducted in selected farms across the Czech Republic. Totally, 180 weed species were found, of which 48.89% were considered as archaeophytes (88 species). In view of the invasive status, 5 archaeophytes were considered as invasive, the other 83 species were regarded as naturalized. The net effects of all variables studied on the occurrence of archaeophytes were statistically significant. The majority of the variation was explained by altitude, followed by crop and type of farming. Incidence of archaeophytes increases with an increasing altitude and is also related to their affinity with environmental factors. The highest occurrence of archaeophytes was found in cereals, some species, however, occur more frequently in wide row crops. The higher occurrence of archaeophytes was observed in organically managed fields.

Key words: altitude, cereals, conventional farming, organic farming, weed communities, wide-row crops.

INTRODUCTION

The archaeophytes are a particularly group of species as they constitute ‘cultural relics’, which testify to the fundamental shift from the nomadic phase in human development, related to hunter-gathering lifestyles, to the sedentary agricultural phase (Comin & Poldini, 2009). These more significant changes came at the beginning of the Neolithic era (around 5700 BC), which was characterized by the beginning and expansion of the planting of cultivated crops accompanied by the first alien weeds (Medvecká et al., 2012). The diaspore pressure, a crucial condition for a successful invasion, must have been intense and continuous, and facilitated the early invasion of archaeophytes into local communities (Pyšek et al., 2005).

Archaeophytes belong to a group of alien plants, which were introduced by humans either intentionally or unintentionally in different ways. According to the introduction

period, alien species can be distinguished into archaeophytes, introduced during ancient times and neophytes, introduced more recently (Preston et al., 2004). As a milestone, the year of the European arrival on the American continent has been considered, i.e. 1492, as since this event voyages of discovery started and therefore possibilities of plants dispersal greatly increased (roughly then this limit is determined by the year of 1500). The definition of archaeophytes, however, is more complicated. Holub & Jirásek (1967) for example define archaeophytes solely as accidentally introduced species. For simplicity and compatibility with the recent usage of the term, we apply it without any relation to whether the given species arrived accidentally or were brought in by humans. We only consider its residence time (species introduced before the year 1500) regardless of the mean of introduction (Pyšek et al., 2002).

Richardson et al. (2000) distinguish between different types of alien plants: casual, naturalized and invasive taxa. Casual alien plants may flourish and even reproduce occasionally in an area, but do not form self-replacing populations, and rely on repeated introductions for their persistence. Naturalized plants reproduce consistently and sustain populations over many life cycles without direct intervention by humans (or in spite of human intervention); they often recruit offspring freely, usually close to adult plants, and do not necessarily invade natural, seminatural or human-made ecosystems. Invasive plants are naturalized plants that produce reproductive offsprings, often in very large numbers, at considerable distances from parent plants, and thus have the potential to spread over a considerable area. This division, however, does not usually address the specific meaning and potential harmfulness of alien taxons. Therefore, environmental and socio-economic impacts of alien species and their appropriate management strategy in the Czech Republic are presented in the so-called Black, Gray and Watch List of Alien Species (Pergl et al., 2016).

The alien flora of the Czech Republic consists of 1,454 taxa, made up by 350 archaeophytes (24.1%) and 1,104 neophytes (75.9%), which represent addition to ca 2,945 native taxa known from the country and form 33.1% of the total plant diversity ever recorded there (Pyšek et al., 2012b). Danihelka et al. (2012) mention that the flora of the Czech Republic includes 3,557 species. Of these, 2,256 species are native, 464 naturalized (228 archaeophytes and 236 neophytes) and 837 casual aliens (62 archaeophytes and 775 neophytes).

The habitats with the greatest proportion of aliens belong to two groups, anthropogenic habitats (arable land, ruderal vegetation, trampled areas) and coastal, littoral and riverine habitats. Neophytes were found commonly in habitats also occupied by archaeophytes. Thus, the number of archaeophytes can be considered as a good predictor of the neophyte invasion risk. However, neophytes had a stronger affinity to wet habitats and disturbed woody vegetation while archaeophytes tended to be more common in dry to mesic open habitats (Chytrý et al., 2008). Archaeophytes occupy more habitats and plots due to longer residence time because they had more time to disperse and adapt (Küzmič & Šilc, 2017). In terms of field conditions, aliens are most common in lowland agricultural and urban areas, whereas they are sparsely represented in mountainous areas. At intermediate elevations, agricultural areas are more invaded than forested areas. General similarity of the invasion maps for archaeophytes and neophytes reflects the high correlation between the occurrence of these two groups of aliens. However, there are some fine-scale differences between them, contrary to the similarity revealed at a coarse scale. For example, neophytes more strongly respond to altitude, being

more concentrated in the lowlands than archaeophytes. Also, neophytes more heavily invade river corridors than archaeophytes (Chytrý et al., 2009; Pyšek et al., 2012a).

Representation of aliens in agrophytocoenoses is related to the farming intensity and a crop structure. Medvecká et al. (2014) support that two of the main factors affecting the invasibility of plant communities are disturbance and an excess of nutrients. Intensification of agriculture (e.g. large amounts of fertilizer) may promote invasion of neophytes (Soukup et al., 2004; Kovács-Hostyánszki et al., 2011). Lososová & Cimalová (2009) stated that cereal fields and root crop fields were richer in archaeophytes and neophytes, respectively. Archaeophytes are common in old crops introduced with the beginning of agriculture (cereals), but are poorly represented in rather recently introduced crops (rape, maize), where neophytes are most numerous (Pyšek et al., 2005).

Neophytes have been progressively more numerous in arable fields and their proportion significantly increased during the second half of the 20th century (Pyšek et al., 2003, 2005; Šilc & Čarni, 2005). Archaeophytes have been shifting from anthropogenous to more natural habitats in recent time (Medvecká et al., 2014; Kůzmič & Šilc, 2017). Lososová et al. (2004) indicate a decline in archaeophytic annuals (e.g. *Papaver argemone*, *Neslia paniculata*, *Raphanus raphanistrum*) and an increase in neophytes. Comin & Poldini (2009) present that those archaeophytes that are declining or extinct have specialised pollination and dispersal, brevity of phenophases, S- and/or R-type functional strategies, and the ability to colonise predominantly segetal habitats. Some of them have either virtually disappeared from the European scene or have become very rare, including *Agrostemma githago*, *Silene linicola* and *Turgenia latifolia*.

So far, the question of the representation of archaeophytes in agrophytocoenoses has been only sparsely addressed in the Czech Republic; therefore, the objective of this study is to assess the current occurrence of archaeophytes in arable fields in representative areas of the Czech Republic based on the following criteria (i) applied management systems (farming type - conventional and organic), (ii) crop type (winter cereals, spring cereals, wide-row crops), and (iii) environmental site conditions (temperature, precipitation, soil type) integrated with altitude.

MATERIALS AND METHODS

Study area

In 2006–2018, a phytocoenological survey was carried out on selected farms across the Czech Republic at various climate and soil conditions. The farms were selected based on three criteria: (1) applied management systems: conventional farms (common chemical weed control) and organic farms (using methods according to an appropriate valid legislation without applying herbicides and with at least 2 years of organic management practices) were chosen; (2) crop type: winter cereals (winter wheat, winter barley, rye, spelt, triticale), spring cereals (spring barley, oat, naked oat, spring wheat, spring rye, spring triticale) and wide-row spring crops (sugar beet, potatoes, maize, oil pumpkin, feeding carrots, fodder beet, beet-root, sunflower, onion) were observed; (3) elevation gradient: we selected areas of which the altitude varied between 170 and 681 m above sea level. In total, 320 phytocoenological relevés were recorded (Fig. 1), 163 thereof represented conventionally farmed fields and 157 organic fields. Concerning crops, 107 relevés were recorded in winter cereals, 108 in spring cereals and 105 in wide-row crops. Weediness was assessed in June and July in cereals and in late July, August,

September and at the beginning of October in wide row crops. With respect to the altitude, 116 relevés were recorded at altitudes lower than 250 m, 92 relevés at 250–350 m, and 112 relevés at levels higher than 350 m.

Evaluation

The cover was visually estimated by means of the nine-degree Braun-Blanquet scale (Braun-Blanquet, 1964; modified by Barkman et al., 1964). The size of one phytocoenological relevé was 100 m², and each relevé was performed in the central part of an individual field. Fungi, non-vascular plants and self-seeded seedlings of trees were not included into the evaluation. The native/alien status was classified for each taxon (Pyšek et al., 2012b). The nomenclature followed that of Kubát et al. (2002).

Data analysis

The frequencies of individual species were calculated, while the presence of the species in a relevé only was taken into account for these calculations. The total frequency (%) is calculated as the proportion of the sum of presences of archeophytes in relevés taken in the frame of individual factors to the sum of presences of archeophytes in all relevés.

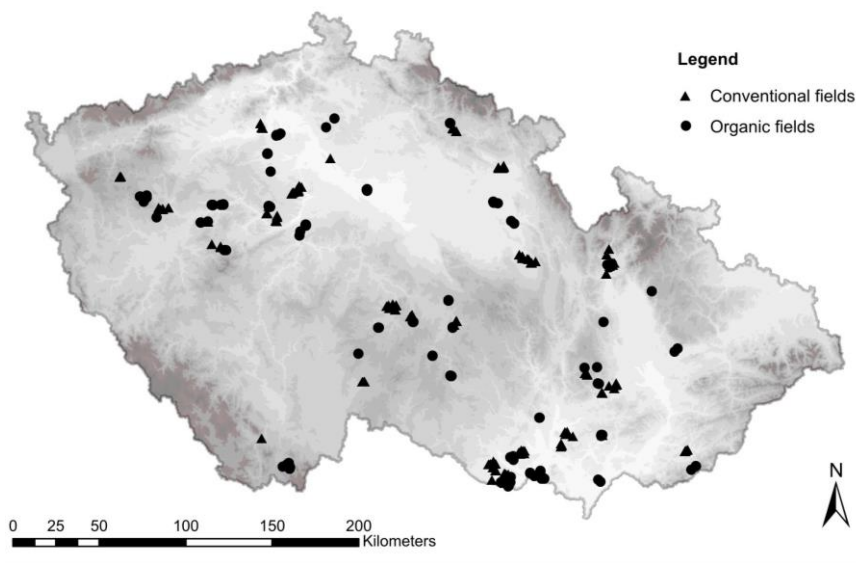


Figure 1. Map of the Czech Republic showing recorded relevés.

The archaeophyte occurrence in different farming types, crops and altitudes was analysed by multivariate analyses in the CANOCO 4.5 software (ter Braak & Šmilauer, 2002). Values of the Braun-Blanquet scale were transformed to an ordinal scale 1–9 (van der Maarel, 1979). As the gradients on the first canonical axis (4.906 SD units) in the compositional turnover in a detrended correspondence analysis (DCA) were long, the canonical correspondence analysis (CCA) was chosen as a direct analysis. In the CCA, net effects of all explanatory variables on archaeophytes occurrence were determined. As explanatory variables, the type of farming (conventional, organic), crop (winter

cereals, spring cereals and wide-row crops) and altitude were used. After an exclusion of the effects shared with other variables, the net effects of individual variables were obtained and tested using partial CCAs, when only one explanatory variable was used and the other variables were used as covariables (Lososová et al., 2004). The ratio of a certain canonical eigenvalue to the sum of all eigenvalues (total inertia) was used to estimate the proportion of the explained variation (Borcard et al., 1992). The effects were evaluated using Monte Carlo permutation tests (ter Braak & Šmilauer, 2002) for the first or all canonical axes (999 permutations were used).

RESULTS AND DISCUSSION

In total, 180 weed species were found (volunteer crops were not included). Among the observed species, 48.89% were considered as archaeophytes (88 species), 43.33% as apophytes (78 species) and 7.78% as neophytes (14 species). Pyšek et al. (2012b) state that the alien flora of the Czech Republic forms 33.10% of the total plant diversity. Danihelka et al. (2012) add a similar percentage of alien flora representation (36.6%). The high proportion of alien flora in our research (56.67%) is related to the character of studied areas as they have been under permanent disturbance and human (farmer) influence each year (Chytrý et al., 2008). The highest proportion of alien species occurs on arable land (Kůzmič & Šilc, 2017). This finding correlates with the data reported by Holec et al. (2008), who mentioned approximately 30% of apophytes, 60% of archaeophytes, and 10% of neophytes among arable weeds occurring in the Czech Republic. According to Lososová & Simonová (2008), the representation of archeophytes, natives and neophytes in weed vegetation in Moravia is 45%, 49% and 6%, respectively.

Compared to neophytes, archaeophytes occurred in agrophytocoenoses more frequently. This fact could be explained mainly by the character of plants accompanying agricultural crops already spreading since the Neolithic due to move of agricultural production from Middle East and Mediterranean areas to northern countries. The occurrence of this big group of plants stays restricted primarily to arable land and gardens (Arlt et al., 1991). Moreover, neophytes had much less time for their spread into agrophytocoenoses.

Species frequencies in relation to individual factors are shown in Table 1.

Table 1. Species frequencies (%) related to studied factors

Species	All	Type of farming Crop					Altitude (m.a.s.l.)		
		conv	org	WC	SC	WR	< 250	250–350	> 350
<i>Fallopia convolvulus</i>	67.50	55.21	80.25	73.83	82.41	45.71	55.17	64.13	83.04
<i>Cirsium arvense</i>	55.00	40.49	70.06	52.34	56.48	56.19	53.45	55.43	56.25
<i>Tripleurospermum inodorum</i>	49.69	28.83	71.34	52.34	54.63	41.90	37.93	48.91	62.50
<i>Capsella bursa-pastoris</i>	44.38	28.83	60.51	36.45	50.93	45.71	25.86	35.87	70.54
<i>Thlaspi arvense</i>	39.38	17.18	62.42	28.97	50.00	39.05	25.86	41.30	51.79
<i>Convolvulus arvensis</i>	28.75	23.31	34.39	24.30	23.15	39.05	50.00	18.48	15.18
<i>Anagallis arvensis</i>	26.56	17.18	36.31	20.56	45.37	13.33	23.28	32.61	25.00
<i>Euphorbia helioscopia</i>	25.63	17.79	33.76	19.63	36.11	20.95	14.66	35.87	28.57
<i>Myosotis arvensis</i>	25.31	9.82	41.40	30.84	30.56	14.29	0.86	26.09	50.00

Table 1 (continued)

<i>Lamium purpureum</i>	25.31	18.40	32.48	19.63	36.11	20.00	9.48	28.26	39.29
<i>Echinochloa crus-</i> <i>galli</i>	24.69	23.93	25.48	11.21	16.67	46.67	42.24	27.17	4.46
<i>Apera spica-venti</i>	22.81	18.40	27.39	42.99	21.30	3.81	19.83	21.74	26.79
<i>Geranium pusillum</i>	21.25	17.18	25.48	16.82	21.30	25.71	6.03	16.30	41.07
<i>Silene noctiflora</i>	18.13	9.82	26.75	14.02	33.33	6.67	21.55	27.17	7.14
<i>Veronica arvensis</i>	17.81	7.36	28.66	28.04	16.67	8.57	4.31	16.30	33.04
<i>Avena fatua</i>	17.81	18.40	17.20	14.95	25.00	13.33	11.21	23.91	19.64
<i>Fumaria officinalis</i>	14.69	11.04	18.47	6.54	24.07	13.33	4.31	11.96	27.68
<i>Sonchus arvensis</i>	14.38	3.68	25.48	11.21	15.74	16.19	5.17	9.78	27.68
<i>Lamium</i> <i>amplexicaule</i>	14.38	10.43	18.47	13.08	19.44	10.48	12.93	13.04	16.96
<i>Papaver rhoeas</i>	14.06	5.52	22.93	20.56	15.74	5.71	11.21	17.39	14.29
<i>Veronica polita</i>	13.44	10.43	16.56	11.21	18.52	10.48	12.93	19.57	8.93
<i>Sonchus asper</i>	11.56	7.98	15.29	5.61	18.52	10.48	12.93	8.70	12.50
<i>Erodium cicutarium</i>	10.63	2.45	19.11	7.48	10.19	14.29	2.59	4.35	24.11
<i>Lactuca serriola</i>	10.31	3.68	17.20	15.89	12.04	2.86	12.93	10.87	7.14
<i>Setaria pumila</i>	10.00	3.68	16.56	4.67	9.26	16.19	20.69	7.61	0.89
<i>Atriplex patula</i>	9.69	8.59	10.83	7.48	9.26	12.38	6.03	7.61	15.18
<i>Lycopsis arvensis</i>	9.06	2.45	15.92	2.80	12.04	12.38	2.59	5.43	18.75
<i>Lapsana communis</i>	9.06	4.29	14.01	10.28	12.04	4.76	0.00	5.43	21.43
<i>Descurainia sophia</i>	8.75	2.45	15.29	13.08	5.56	7.62	13.79	11.96	0.89
<i>Centaurea cyanus</i>	8.75	2.45	15.29	11.21	12.04	2.86	0.00	3.26	22.32
<i>Solanum nigrum</i>	8.75	9.20	8.28	1.87	7.41	17.14	14.66	8.70	2.68
<i>Spergula arvensis</i>	8.44	1.84	15.29	0.93	13.89	10.48	0.00	4.35	20.54
<i>Consolida regalis</i>	7.81	4.91	10.83	15.89	4.63	2.86	7.76	11.96	4.46
<i>Sinapis arvensis</i>	7.81	2.45	13.38	5.61	11.11	6.67	9.48	8.70	5.36
<i>Matricaria recutita</i>	7.50	0.61	14.65	5.61	12.04	4.76	0.86	6.52	15.18
<i>Galium spurium</i>	7.19	2.45	12.10	14.02	5.56	1.90	5.17	13.04	4.46
<i>Geranium dissectum</i>	6.88	4.91	8.92	10.28	9.26	0.95	1.72	6.52	12.50
<i>Vicia angustifolia</i>	6.56	0.61	12.74	8.41	4.63	6.67	1.72	4.35	13.39
<i>Mercurialis annua</i>	5.00	4.91	5.10	1.87	4.63	8.57	6.03	9.78	0.00
<i>Raphanus</i> <i>raphanistrum</i>	4.69	0.61	8.92	3.74	5.56	4.76	2.59	5.43	6.25
<i>Arctium tomentosum</i>	4.38	2.45	6.37	5.61	4.63	2.86	4.31	8.70	0.89
<i>Euphorbia exigua</i>	4.38	2.45	6.37	6.54	5.56	0.95	4.31	7.61	1.79
<i>Setaria viridis</i>	3.75	0.61	7.01	0.93	1.85	8.57	6.90	4.35	0.00
<i>Lathyrus tuberosus</i>	3.13	2.45	3.82	6.54	2.78	0.00	2.59	6.52	0.89
<i>Papaver dubium</i>	2.81	0.61	5.10	7.48	0.00	0.95	0.86	4.35	3.57
<i>Anthemis arvensis</i>	2.81	0.00	5.73	1.87	1.85	4.76	0.00	3.26	5.36
<i>Veronica agrestis</i>	2.81	0.61	5.10	1.87	2.78	3.81	0.00	1.09	7.14
<i>Malva neglecta</i>	2.81	2.45	3.18	1.87	0.00	6.67	4.31	3.26	0.89
<i>Conium maculatum</i>	2.81	3.68	1.91	3.74	2.78	1.90	6.03	2.17	0.00
<i>Sonchus oleraceus</i>	2.81	3.68	1.91	1.87	2.78	3.81	3.45	3.26	1.79
<i>Veronica hederifolia</i>	2.81	1.84	3.82	1.87	5.56	0.95	2.59	2.17	3.57
<i>Atriplex sagittata</i>	2.50	1.23	3.82	1.87	4.63	0.95	3.45	2.17	1.79
<i>Microrrhinum minus</i>	2.50	0.00	5.10	1.87	3.70	1.90	0.00	4.35	3.57
<i>Neslia paniculata</i>	2.50	0.00	5.10	0.00	2.78	4.76	0.86	3.26	3.57
<i>Erysimum</i> <i>cheiranthoides</i>	2.50	0.61	4.46	0.93	2.78	3.81	4.31	1.09	1.79

Table 1 (continued)

<i>Silene latifolia</i> subsp. <i>alba</i>	2.19	1.23	3.18	0.93	3.70	1.90	0.00	5.43	1.79
<i>Sisymbrium officinale</i>	2.19	0.00	4.46	0.93	0.00	5.71	1.72	2.17	2.68
<i>Viola tricolor</i>	2.19	0.61	3.82	1.87	4.63	0.00	0.86	0.00	5.36
<i>Digitaria sanguinalis</i>	1.88	0.00	3.82	0.00	0.00	5.71	5.17	0.00	0.00
<i>Linaria vulgaris</i>	1.88	0.00	3.82	2.80	1.85	0.95	0.00	1.09	4.46
<i>Stachys annua</i>	1.88	0.61	3.18	0.93	2.78	1.90	1.72	3.26	0.89
<i>Hyoscyamus niger</i>	1.88	1.84	1.91	0.93	4.63	0.00	3.45	2.17	0.00
<i>Carduus acanthoides</i>	1.56	0.61	2.55	0.00	3.70	0.95	2.59	1.09	0.89
<i>Fumaria vaillantii</i>	1.56	0.61	2.55	1.87	1.85	0.95	1.72	2.17	0.89
<i>Senecio vulgaris</i>	1.56	0.61	2.55	0.00	0.93	3.81	2.59	1.09	0.89
<i>Portulaca oleracea</i>	1.56	0.61	2.55	0.00	0.93	3.81	3.45	1.09	0.00
<i>Chenopodium pedunculare</i>	1.25	0.00	2.55	0.00	0.00	3.81	1.72	0.00	1.79
<i>Bromus sterilis</i>	1.25	2.45	0.00	1.87	0.93	0.95	0.00	2.17	1.79
<i>Fumaria rostellata</i>	0.94	0.61	1.27	0.00	2.78	0.00	0.00	0.00	2.68
<i>Sherardia arvensis</i>	0.94	0.00	1.91	0.93	1.85	0.00	0.00	1.09	1.79
<i>Valerianella dentata</i>	0.94	0.00	1.91	1.87	0.93	0.00	0.00	1.09	1.79
<i>Adonis aestivalis</i>	0.94	1.84	0.00	2.80	0.00	0.00	0.86	2.17	0.00
<i>Anthemis austriaca</i>	0.63	0.00	1.27	0.93	0.93	0.00	0.86	1.09	0.00
<i>Ranunculus arvensis</i>	0.63	0.00	1.27	1.87	0.00	0.00	0.00	0.00	1.79
<i>Setaria verticillata</i>	0.63	0.00	1.27	0.00	0.00	1.90	1.72	0.00	0.00
<i>Anagallis foemina</i>	0.63	0.61	0.64	0.93	0.93	0.00	0.00	2.17	0.00
<i>Papaver argemone</i>	0.63	1.23	0.00	0.93	0.00	0.95	0.00	0.00	1.79
<i>Armoracia rusticana</i>	0.31	0.00	0.64	0.93	0.00	0.00	0.00	1.09	0.00
<i>Camelina microcarpa</i>	0.31	0.00	0.64	0.93	0.00	0.00	0.00	1.09	0.00
<i>Cardaria draba</i>	0.31	0.00	0.64	0.00	0.93	0.00	0.00	1.09	0.00
<i>Coronopus squamatus</i>	0.31	0.00	0.64	0.00	0.00	0.95	0.00	1.09	0.00
<i>Diploaxis muralis</i>	0.31	0.00	0.64	0.93	0.00	0.00	0.00	1.09	0.00
<i>Euphorbia falcata</i>	0.31	0.00	0.64	0.00	0.93	0.00	0.00	1.09	0.00
<i>Lithospermum arvense</i>	0.31	0.00	0.64	0.93	0.00	0.00	0.00	0.00	0.89
<i>Onopordum acanthium</i>	0.31	0.00	0.64	0.93	0.00	0.00	0.86	0.00	0.00
<i>Crepis tectorum</i>	0.31	0.00	0.64	0.00	0.00	0.95	0.00	0.00	0.89
<i>Bromus hordeaceus</i>	0.31	0.61	0.00	0.93	0.00	0.00	0.00	0.00	0.89
<i>Urtica urens</i>	0.31	0.61	0.00	0.00	0.93	0.00	0.86	0.00	0.00
The total frequency (%)	100.00	31.22	68.78	31.45	39.36	29.19	28.54	29.16	42.30

conv – conventional farming; org – organic farming; WC – winter cereals; SC – spring cereals; WR – wide-row crops.

The average number of archaeophytes species per 1 relevé in different types of farming, crops and altitudes are shown in Fig. 2.

According to Kropáč (1988), the highest frequencies can be found for eurycoenotic species, i. e. they occur in most weed communities of cereals and wide-row crops as constant dominants and can also be found outside of arable land as ruderal species, e. g. *Fallopia convolvulus* (67.50%), *Tripleurospermum inodorum* (49.69%), *Cirsium arvense* (55.00%), *Convolvulus arvensis* (28.75%) and others. Their high appearance in agrophytocoenoses is relatively stable (Lososová & Simonová, 2008).

With respect to invasion status proposed by Pyšek et al. (2012b), 5 archaeophytes were considered invasive (*Cirsium arvense*, *Echinochloa crus-galli*, *Conium maculatum*, *Atriplex sagittata*, *Portulaca oleracea*).

The other 83 species were regarded as naturalized. An absolutely large proportion of naturalized species is related to the long term occurrence in our region. Archaeophytes, which would not have become naturalized could hardly be recorded in our times (Pyšek et al., 2002). The absence of casual archaeophytes could be explained by the fact that volunteer crops were not included into this analysis. *Cirsium arvense* is classified as one of the most troublesome and invasive plants worldwide (Tiley, 2010; Guggisberg et al., 2012). In Europe it was considered the third most harmful agricultural weed in the past (Schroeder et al., 1993). Also, *Echinochloa crus-galli* belongs to the most serious weeds in the world (Holm et al., 1991). Under conditions of the Czech Republic, it has been spreading together with an enhanced growing of silage corn and an increasing temperature at higher altitudes (Jursík et al., 2011). Another important invasive weed species is *Conium maculatum* (Vetter, 2004) which currently expands in ruderal areas and enters also field crops (Brant et al., 2008; Jursík et al., 2011). The most remarkable increase of *Atriplex sagittata* starts after the Second World War. The species is closely confined to ruderal sites and habitats facilitating transport (Mandák & Pyšek, 1998). On fields, it occurs only to a limited extent,

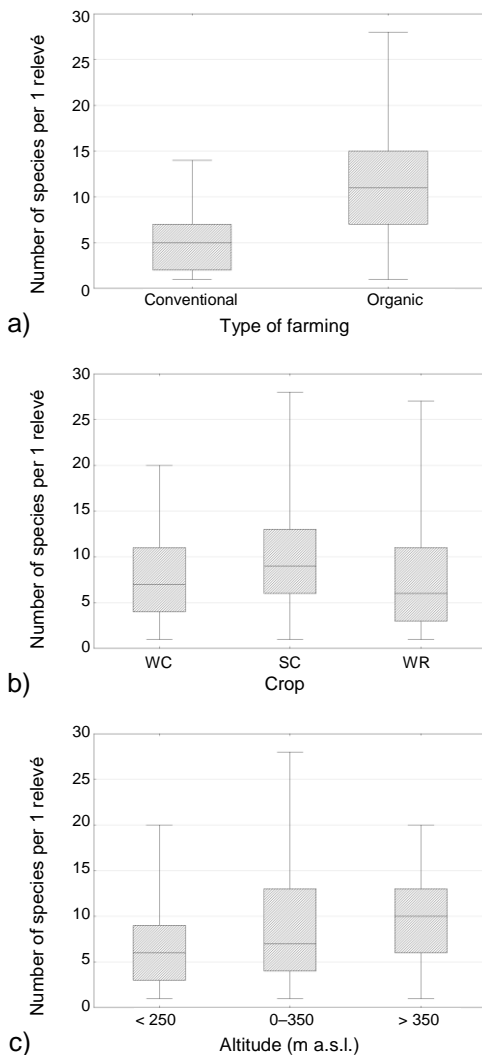


Figure 2. Number of species per 1 relevé in different types of farming (a), crops (b) and altitudes (c). Box and whisker plot: median, 25th to 75th percentile, minimum and maximum value.

it spreads from adjacent ruderal areas, roads and dunghills to other sites. *Portulaca oleracea* belongs to the most harmful world weeds (Holm et al., 1991). In our region, it has started spreading into warm areas and causing increasing problems in vegetables.

Pergl et al. (2016) mention invasive archaeophytes described above also. They classify the species *Cirsium arvense*, *Echinochloa crus-galli*, *Conium maculatum*, *Portulaca oleracea* and also *Setaria verticillata* as the Species group BL 3 with predominantly moderate environmental and socio-economic impacts. The recommended strategy for these species is a stratified approach balancing between the local needs and the available resources for eradication. Considering large spread and agricultural harmfulness of *Cirsium arvense* and *Echinochloa crus-galli* (Table 1), there is a need of their regular eradication using all available methods (Jursík et al., 2011). *Conium maculatum*, *Portulaca oleracea*, *Setaria verticillata* usually occur only locally and at suitable environmental and farming conditions, therefore, methods of their regulation will depend on a specific situation.

Besides archaeophytes mentioned, there is a big number of neophytes which can be found in the Species group BL 3 (for example *Amaranthus powellii*, *Amaranthus retroflexus*, *Conyza canadensis*, *Galinsoga quadriradiata* and others). Considering their relatively recent introduction to our country, their spread is of a contemporary issue. Also these species are already significantly represented on arable land of the Czech Republic (Kolářová et al., 2017) and their eradication is needed.

Only *Atriplex sagittata* belongs to the Grey List (Pergl et al., 2016) with limited environmental and socio-economic impacts and with a management strategy tolerance. As *Atriplex sagittata* occur only rarely on arable land, normally it is not necessary to take it into account during weed control strategies.

No any archaeophytes found are listed in the the official list of alien expansive weeds (sensu Jehlík, 1998). This absence arises from the fact that especially neophytes newly spreading in our country occur on this list.

The occurrence of archaeophytes in agrophytocoenoses may vary over years. Farm management practices and climatic changes have an influence on the composition of weed spectra. With the advent of intensive agriculture, the richness of weed flora and the weed vegetation consisting of specialized annual archaeophytes declined (Holzner, 1982; Lososová, 2003; Comin & Poldini, 2009). Also Pyšek et al. (2005) mention that on a half-century time scale (1955–2000), numbers of archaeophytes have significantly decreased in sample plots on arable land in the Czech Republic. Many archaeophytes were strongly connected to the traditional way of farm management and did not survive modern growing technologies (crop rotation, effective seed cleaning, fertilization, herbicide application, etc.). Examples are species like *Agrostemma githago*, *Camelina alyssum*, *Lolium remotum* and *temulentum* or *Scandix pecten-veneris* (Korneck et al., 1998; Schumacher & Schick, 1998). They are listed on the Red Lists of endangered species of the Czech Republic and of neighbour countries (Grulich, 2012; Eliáš et al., 2015). For some archaeophytes, however, even the conditions of intensive farming were suitable and they remained important weeds on arable land, e. g. species from the *Poaceae* family such as *Apera spica-venti*, *Avena fatua* and *Echinochloa crus-galli*. Grass weeds are more difficult to control due their relation with cereals and due to the long period in which mainly herbicides against dicotyledonous were used (Kühn, 1987). In most field crops the occurrence of some grass weeds increased even after the introduction of specific post-emergence grass herbicides (ACCase inhibitors). The main

reasons for this increase are crops favourable for grass weeds, reduced tillage, early sowing time, high nitrogen levels, and in some regions the development of herbicide resistant populations (Hurle, 1993; Soukup et al., 2006).

Many archaeophytes, which were decreasing in the last decades, have reacted sensitively to changes in farming systems related to society transformation in the Czech Republic after 1989 (disintegration of the socialist large-scale farming, creation of new economic entities, low financial inputs into agriculture like limited use of fertilizers and pesticides). Nowadays they increase their abundance again, even causing economic harm. Some factors causing this change are different soil cultivation (*Bromus sterilis*), increasing cropping areas of winter crops and delayed time of weed control to autumn (*Centaurea cyanus*, *Papaver rhoeas*, *Fallopia convolvulus*, *Adonis aestivalis*), low intensity of management in field surrounding areas (*Conium maculatum*) (Soukup et al., 2004). An interesting history can be seen for example at the species *Centaurea cyanus*. This archaeophyte was one of the most abundant cereal weeds in the Czech Republic still in the mid-20th century. In following decades, however, it considerably decreased due to an agriculture intensification and in the 1970s and 1980s it belonged to endangered species. In recent years, especially in connection with the expanding growing of winter oilseed rape, it has been experiencing its renaissance and, especially in middle altitudes, it is again becoming an economically important weed (Jursík et al., 2009). In a recent version of the Red List of Endangered Plants (Grulich, 2012) it is no longer recorded among endangered species.

Besides the farm management practices, the climatic changes affect the composition of weed spectra as well. Over the past decades, climate change has induced transformation in the weed flora of arable ecosystems. For instance, thermophile weeds, late-emerging weeds, and some opportunistic weeds have become more abundant in cropping systems. Also some late emergers archaeophytes such as *Echinochloa crus-galli* and *Setaria* spp. have expanded their distribution range (Peters et al., 2014).

The net effects of all studied variables (type of farming, crop, altitude) on the occurrence of archaeophytes were found as statistically significant (Table 2). All together, these variables explained 6.81% of the total variation in the studied species data. The majority of the variability was explained by altitude (3.01%), followed by crop (2.66%) and type of farming (1.06%). Lososová et al. (2004) found the primary role of altitude and associated climatic factors in weed species composition. They stressed that human-made habitats consisting of a large proportion of alien species and strongly depending on farm management, seems to be more affected by primary environmental factors than by human activities.

Table 2. Net effects of explanatory variables on the occurrence of archaeophytes

	Eigenvalue	%	F-ratio	p-value
All	0.522	6.81	5.617	0.001
Type of farming	0.081	1.06	3.464	0.001
Crop	0.204	2.66	4.382	0.001
Altitude	0.230	3.01	9.885	0.001

Eigenvalue – sum of all canonical eigenvalues (total inertia = 7.656); % – percentage of explained variance; *F-ratio* for the test of significance of all (first) canonical axes; *p-value* – corresponding probability value obtained using the Monte Carlo permutation test (999 permutations).

In Table 1, Fig. 2 and in the ordination diagram representing the occurrence of archaeophytes in different types of farming (Fig. 3) the higher occurrence of archaeophytes in organic areas is clearly visible. Organic farming may be less intensive and aggressive to the adjacent weed flora than a massive pressure of herbicides in conventional systems. In addition, diverse crop rotations in organic farming support biodiversity more than narrow crop rotations in conventional systems (Bengtsson et al., 2005). Due to this fact, in organic areas many sensitive, descending and rare species may occur. Organic fields serve then as reservoirs of today rare archaeophytes and can play a certain role in the frame of saving programs for endangered species (Albrecht & Mattheis, 1998).

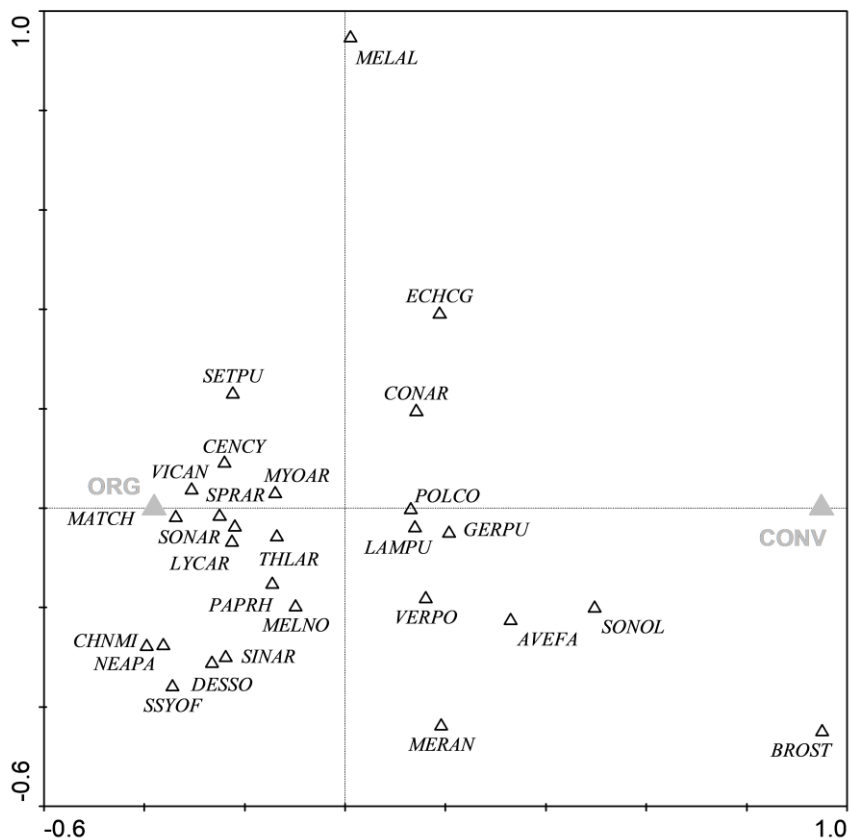


Figure 3. Ordination diagram, *pCCA*. Occurrence of archaeophytes in different types of farming. Minimum species fit 2% – 27 species from 88.

Abbreviations: CONV – conventional farming; ORG – organic farming; AVEFA – *Avena fatua*; BROST – *Bromus sterilis*; CENCY – *Centaurea cyanus*; CHNMI – *Microrrhinum minus*; CONAR – *Convolvulus arvensis*; DESSO – *Descurainia sophia*; ECHCG – *Echinochloa crus-galli*; GERPU – *Geranium pusillum*; LAMPU – *Lamium purpureum*; LYCAR – *Lycopsis arvensis*; MATCH – *Matricaria recutita*; MELAL – *Silene latifolia* subsp. *alba*; MELNO – *Silene noctiflora*; MERAN – *Mercurialis annua*; MYOAR – *Myosotis arvensis*; NEAPA – *Neslia paniculata*; PAPRH – *Papaver rhoeas*; POLCO – *Fallopia convolvulus*; SETPU – *Setaria pumila*; SINAR – *Sinapis arvensis*; SONAR – *Sonchus arvensis*; SONOL – *Sonchus oleraceus*; SPRAR – *Spergula arvensis*; SSSYOF – *Sisymbrium officinale*; THLAR – *Thlaspi arvense*; VERPO – *Veronica polita*; VICAN – *Vicia angustifolia*.

Just a few species occur with a higher frequency and affinity to the conventional type of farming. They are often tough and harmful weed taxons, often with an important economic significance. One of them is *Bromus sterilis*, which has been recently strongly spreading on agricultural farms applying shallow or no tillage soil management systems. As it is an overwintering weed species, a high proportion of cash winter crops (winter wheat, winter oil seed rape) in reduced crop rotations and also its tolerance to herbicides may be responsible (Valičková et al., 2017).

As seen in Table 1 and Fig. 2, the highest share of archaeophytes can be found in cereals, namely in spring ones. This is confirmed by data of Lososová & Cimalová (2009), that cereal fields were richer in archaeophytes and root crop fields were richer in neophytes. Archaeophytes are common in old crops introduced with the beginning of agriculture (cereals), but are poorly represented in rather recently introduced crops (oilseed rape, maize) (Pyšek et al., 2005). Our ordination diagram showing the occurrence of archaeophytes in different crops (Fig. 4) present species with the highest affinity to crops studied. From the diagram, it is apparent that archaeophytes do not have a relation only to cereals, but many of them occur more in wide-row crops, namely summer annual species (e. g. millet grasses – *Echinochloa crus-galli*, *Setaria spp.*, *Digitaria sanguinalis*; *Solanum nigrum*; *Portulaca oleracea*; *Chenopodium pedunculare*), which have a character of root crops, vegetables and other wide-row crops (Jursík et al., 2011).

From the table of species frequencies (Table 1) and number of archaeophytes species per 1 relevé (Fig. 2) we can see an increasing occurrence of archaeophytes with an increasing altitude (as a factor representing different climatic and soil conditions like precipitation, temperature, soil type, etc.). Also, the ordination diagram displaying the occurrence of archaeophytes at different altitudes (Fig. 5), proves an increase in the occurrence of archaeophytes along the altitude axis. From our results, we can conclude then, that most archaeophytes unlike neophytes (Jehlík, 1998; Chytrý et al., 2009; Pyšek et al., 2012a; Kolářová et al., 2017) frequently occur in higher altitudes and in many places they reach even the upper border of arable land in the Czech Republic. Archaeophytes occupy more habitats and plots due to a longer residence time because they had more time to disperse and adapt (Küzmič & Šilc, 2017). Pyšek et al. (2011) has shown that higher altitudes were increasingly invaded by alien species in the last 250 years as a consequence of increasing anthropogenic disturbances, higher propagule pressure and climate change manifested in elevated temperatures. Therefore, we may presume that as long as human influence in higher altitudes does not decrease, the spread of alien species to higher altitudes will continue. On the contrary, Medvecká et al. (2014) describe a general decrease in the relative richness and total cover of archaeophytes and neophytes with increasing altitude in the invaded habitats. This is especially the case for archaeophytes that are predominantly of Mediterranean and Sub-Mediterranean origin. Distribution of archaeophytes is associated also with their ecological demands for environmental conditions - in lowlands we can find termophilous species preferring conditions of fertile and basic soils (e. g. *Sinapis arvensis*, *Hyoscyamus niger*, *Portulaca oleracea*), on the contrary species tolerating cold, acid and poor soils occur in higher altitudes (e. g. *Spergula arvensis*).

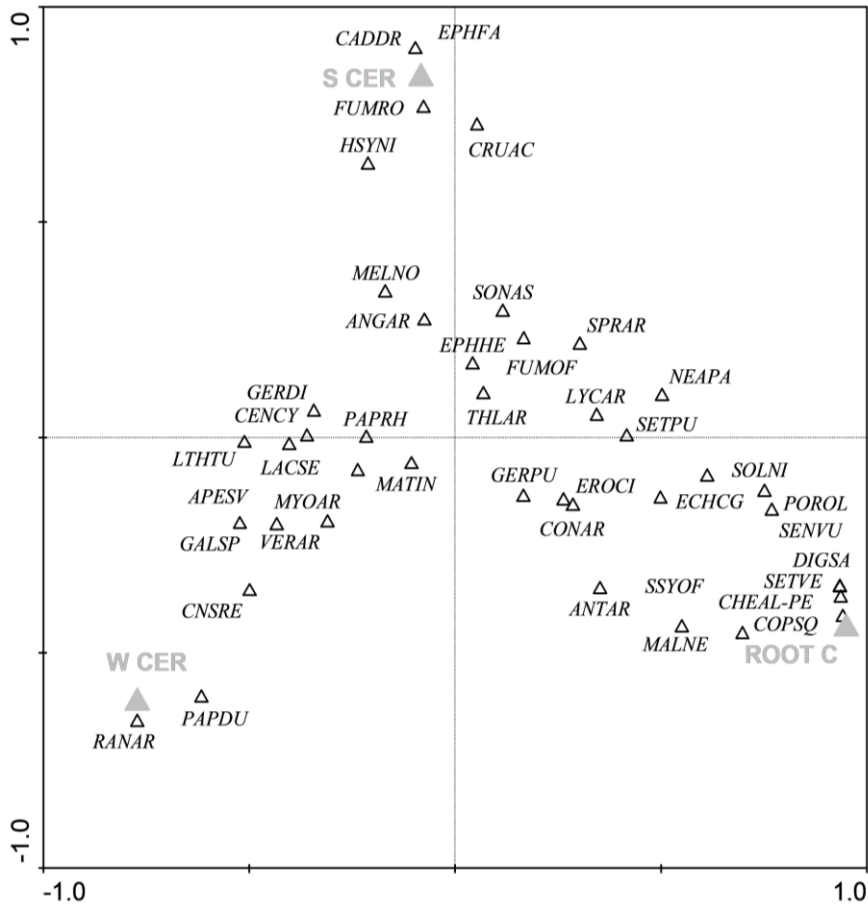


Figure 4. Ordination diagram, *pCCA*. Occurrence of archaeophytes in different crops. Minimum species fit 2% – 42 species from 88.

Abbreviations: W CER – winter cereals; S CER – spring cereals; ROOT C – wide-row crops; ANGAR – *Anagallis arvensis*; ANRAR – *Anthemis arvensis*; APESV – *Apera spica-venti*; CADDR – *Cardaria draba*; CENCY – *Centaurea cyanus*; CHEAL-PE – *Chenopodium pedunculare*; CNSRE – *Consolida regalis*; CONAR – *Convolvulus arvensis*; COPSQ – *Coronopus squamatus*; CRUAC – *Carduus acanthoides*; DIGSA – *Digitaria sanguinalis*; ECHCG – *Echinochloa crus-galli*; EPHFA – *Euphorbia falcata*; EPHHE – *Euphorbia helioscopia*; EROCI – *Erodium cicutarium*; FUMOF – *Fumaria officinalis*; FUMRO – *Fumaria rostellata*; GALSP – *Galium spurium*; GERDI – *Geranium dissectum*; GERPU – *Geranium pusillum*; HSYNI – *Hyoscyamus niger*; LACSE – *Lactuca serriola*; LTHTU – *Lathyrus tuberosus*; LYCAR – *Lycopsis arvensis*; MALNE – *Malva neglecta*; MATIN – *Tripleurospermum inodorum*; MELNO – *Silene noctiflora*; MYOAR – *Myosotis arvensis*; NEAPA – *Neslia paniculata*; PAPDU – *Papaver dubium*; PAPRH – *Papaver rhoeas*; POROL – *Portulaca oleracea*; RANAR – *Ranunculus arvensis*; SENVU – *Senecio vulgaris*; SETPU – *Setaria pumila*; SETVE – *Setaria verticillata*; SOLNI – *Solanum nigrum*; SONAS – *Sonchus asper*; SPRAR – *Spergula arvensis*; SSYOF – *Sisymbrium officinale*; THLAR – *Thlaspi arvense*; VERAR – *Veronica arvensis*.

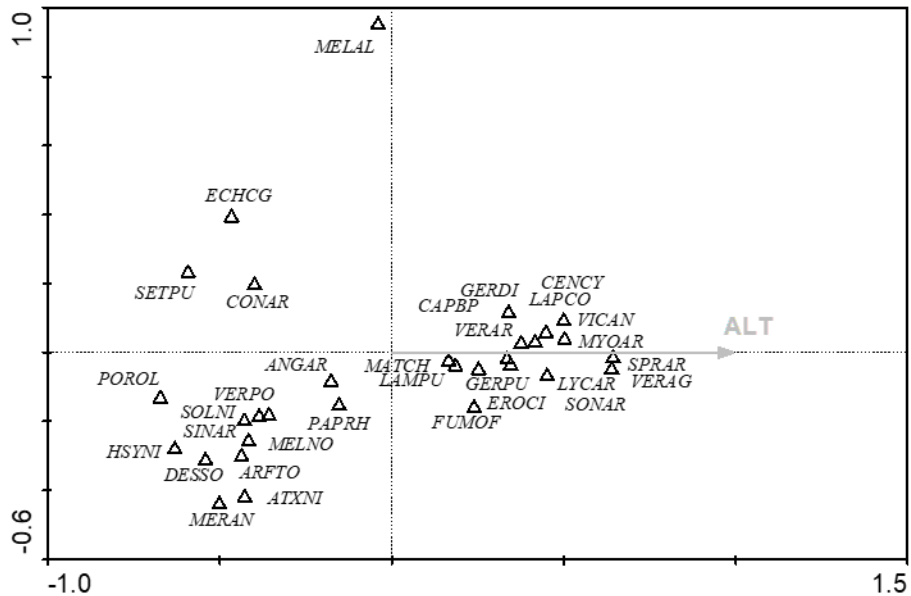


Figure 5. Ordination diagram, *pCCA*. Occurrence of archaeophytes at different altitudes. Minimum species fit 3% – 32 species from 88.

Abbreviations: ALT – altitude; ANGAR – *Anagallis arvensis*; ARFTO – *Arctium tomentosum*; ATXNI – *Atriplex sagittata*; CAPBP – *Capsella bursa-pastoris*; CENCY – *Centaurea cyanus*; CONAR – *Convolvulus arvensis*; DESSO – *Descurainia sophia*; ECHCG – *Echinochloa crus-galli*; EROCI – *Erodium cicutarium*; FUMOF – *Fumaria officinalis*; GERDI – *Geranium dissectum*; GERPU – *Geranium pusillum*; HSYNI – *Hyoscyamus niger*; LAMPU – *Lamium purpureum*; LAPCO – *Lapsana communis*; LYCAR – *Lycopsis arvensis*; MATCH – *Matricaria recutita*; MELAL – *Silene latifolia* subsp. *alba*; MELNO – *Silene noctiflora*; MERAN – *Mercurialis annua*; MYOAR – *Myosotis arvensis*; PAPRH – *Papaver rhoeas*; POROL – *Portulaca oleracea*; SETPU – *Setaria pumila*; SINAR – *Sinapis arvensis*; SOLNI – *Solanum nigrum*; SONAR – *Sonchus arvensis*; SPRAR – *Spergula arvensis*; VERAG – *Veronica agrestis*; VERAR – *Veronica arvensis*; VERPO – *Veronica polita*; VICAN – *Vicia angustifolia*.

CONCLUSION

On arable land, almost half of all weed species are archaeophytes. The most abundant species include *Fallopia convolvulus*, *Cirsium arvense*, *Tripleurospermum inodorum*, *Capsella bursa-pastoris*, *Thlaspi arvense* and *Convolvulus arvensis*. At the same time, these are harmful, economically important weeds that need to be suppressed regularly in crops.

Although the vast majority of archaeophytes (about 94%) are naturalized taxa, some species have an invasive status and spread to other habitats. In this respect, *Cirsium arvense* and *Echinochloa crus-galli* deserve particular attention. Attention should also be paid to the spread of other species such as *Conium maculatum* and *Portulaca oleracea*. The recommended strategy for these species is a stratified approach balancing between the local needs and the available resources for eradication

From the point of view of the monitored factors, the majority of the variation was explained by altitude. Unlike the neophytes, archaeophytes also appear in the higher arable land of the Czech Republic. The highest occurrence of archaeophytes was found in cereals, especially in spring ones. Many archaeophytes, however, occur more in wide row crops. A higher presence of archaeophytes was proved in organically managed areas. Nevertheless, *Bromus sterilis* is associated with conventionally cultivated areas.

ACKNOWLEDGEMENTS. This work was supported by the Institutional Support Program for Long Term Conceptual Development of Research Institution provided by Ministry of Education, Youth and Sports of the Czech Republic. We thank Dr. Hansjoerg Kraehmer for his assistance with a final revision and for comments that greatly improved the manuscript.

REFERENCES

- Albrecht, H. & Mattheis, A. 1998. The effects of organic and integrated farming on rare arable weeds on the Forschungsverbund Agrarökosysteme München (FAM) research station in southern Bavaria. *Biol. Conserv.* **86**, 347–356.
- Arlt, K., Hilbig, W. & Illig, H. 1991. *Field weeds*. Ziemsen Verlag, Wittenberg Lutherstadt, 160 pp. (in German).
- Barkman, J.J., Doing, H. & Segal, S. 1964. Critical remarks and proposals for quantitative vegetation analysis. *Acta Bot. Neerl.* **13**, 394–419 (in German).
- Bengtsson, J., Ahnström, J. & Weibull, A.-C. 2005. The effects of organic agriculture on biodiversity and abundance: a meta-analysis. *J. Appl. Ecol.* **42**, 261–269.
- Borcard, D.P., Legendre, P. & Drapeau, P. 1992. Partialling out the spatial component of ecological variation. *Ecology* **73**, 1045–1055.
- Brant, V., Neckář, K., Venclová, V. & Krump, M. 2008. The influence of field border plant societies on the weedage of agrophytocoenoses by *Conium maculatum* L. (Poison hemlock) in the Czech Republic. *J. Plant Dis. Protect., Spec. Iss.* **21**, 385–388 (in German).
- Braun-Blanquet, J. 1964. *Phytosociology*. Springer, Wien, New York, 865 pp. (in German).
- Chytrý, M., Maskell, L.C., Pino, J., Pyšek, P., Vilà, M., Font, X. & Smart, S.M. 2008. Habitat invasions by alien plants: a quantitative comparison among Mediterranean, subcontinental and oceanic regions of Europe. *J. Appl. Ecol.* **45**, 448–458.
- Chytrý, M., Wild, J., Pyšek, P., Tichý, L., Danihelka, J. & Knollová, I. 2009. Maps of the level of invasion of the Czech Republic by alien plants. *Preslia* **81**, 187–207.
- Comin, S. & Poldini, L. 2009. Archaeophytes: Decline and dispersal – A behavioural analysis of a fascinating group of species. *Plant Biosystems* **143**(suppl. 1), S46–S55.
- Danihelka, J., Chrtek, J.Jr. & Kaplan, Z. 2012. Checklist of vascular plants of the Czech Republic. *Preslia* **84**, 647–811.
- Eliáš, P.Jr., Dítě, D., Kliment, J., Hrivnák, R. & Feráková, V. 2015. Red list of ferns and flowering plants of Slovakia. 5th edition (October 2014). *Biologia* **70**(2), 218–228.
- Grulich, V. 2012. Red List of vascular plants of the Czech Republic: 3rd edition. *Preslia* **84**, 631–645.
- Guggisberg, A., Welk, E., Sforza, R., Horvath, D.P., Anderson, J.V., Foley, M.E. & Rieseberg, L.H. 2012. Invasion history of North American Canada thistle. *Cirsium arvense*. *J. Biogeogr.* **39**, 1919–1931.
- Holec, J., Nečasová, M. & Tyšer, L. 2008. Biodiversity of agrophytocoenosis. In *Biodiversity of weed communities, its importance and sustainable use*. VURV Praha, Praha, pp. 10–25 (in Czech).
- Holm, L.G., Plucknett, D.L., Pancho, J.V. & Herberger, J.P. 1991. *The world's worst weeds*. Krieger publishing company, Malabar, Florida, 609 pp.

- Holub, J. & Jirásek, V. 1967. Remarks to the unification of terminology in phytogeography. *Folia geobot. phytotax.* **2**, 69–113 (in German).
- Holzner, W. 1982. Concepts, categories and characteristics of weeds. In Holzner, W. & Numata, M. (eds): *Biology and ecology of weeds*. W. Junk Publishers, The Hague, pp. 3–20.
- Hurle, K. 1993. Integrated management of grass weeds in arable crops. In: *Brighton crop protection conference – weeds*, pp. 81–88.
- Jehlík, V. 1998. *Alien expansive weeds of the Czech Republic and the Slovak Republic*. Academia, Praha, 506 pp. (in Czech).
- Jursík, M., Holec, J., Hamouz, P. & Soukup, J. 2011. *Weeds. Biology and control*. Kurent, České Budějovice, 232 pp. (in Czech).
- Jursík, M., Holec, J. & Andr, J. 2009. Biology and control of another important weeds of the Czech Republic: Cornflower (*Centaurea cyanus* L.). *Listy Cukrov. Repar.* **125**, 90–93 (in Czech).
- Kolářová, M., Tyšer, L. & Krähmer, H. 2017. Occurrence of neophytes in agrophytocoenoses – field survey in the Czech Republic. *Acta Univ. Agric. Silv. Mendelianae Brun.* **65**(2), 661–668.
- Korneck, D., Schnittler, M., Klingenstein, F., Ludwig, G., Takla, M., Bohn, U. & May, R. 1998. Why our flora is getting impoverished? Evaluation of the Red List of Fern and Flowering Plants in Germany. *Schr.-R. f. Vegetationskunde* H. **29**, 299–444 (in German).
- Kovács-Hostyánszki, A., Batáry, P., Báldi, A. & Harnos, A. 2011. Interaction of local and landscape features in the conservation of Hungarian arable weed diversity. *Appl. Veg. Sci.* **14**, 40–48.
- Kropáč, Z. 1988. Changes in weed communities in Czechoslovakia and the consequences for agricultural practice. *Wiss. Z. Univ. Halle* **37**, 100–126 (in German).
- Kubát, K., Hrouda, L., Chrtěk, J., Kaplan, Z., Kirschner, J. & Štěpánek, J. 2002. *Key to the flora of the Czech Republic*. Academia, Praha, 927 pp. (in Czech).
- Kühn, F. 1987. Frequency changes of weed species in Moravia 1950 – 1985. *Wiss. Z. Univ. Halle* **36**, 69–73 (in German).
- Küzmič, F. & Šilc, U. 2017. Alien species in different habitat types of Slovenia: analysis of vegetation database. *Period. Biol.* **119**(3), 199–208.
- Lososová, Z. 2003. Estimating past distribution of vanishing weed vegetation in South Moravia. *Preslia* **75**, 71–79.
- Lososová, Z., Chytrý, M., Cimalová, Š., Kropáč, Z., Otýpková, Z., Pyšek, P. & Tichý, L. 2004. Weed vegetation of arable land in Central Europe: Gradients of diversity and species composition. *J. Veg. Sci.* **15**, 415–422.
- Lososová, Z. & Cimalová, Š. 2009. Effects of different cultivation types on native and alien weed species richness and diversity in Moravia (Czech Republic). *Basic Appl. Ecol.* **10**, 456–465.
- Lososová, Z. & Simonová, D. 2008. Changes during the 20th century in species composition of synanthropic vegetation in Moravia (Czech Republic). *Preslia* **80**, 291–305.
- Mandák, B. & Pyšek, P. 1998. History of the spread and habitat preferences of *Atriplex sagittata* (*Chenopodiaceae*) in the Czech Republic. In Starfinger, U., Edwards, K., Kowarik, I. & Williamson, M. (eds): *Plant invasions: ecological mechanisms and human responses*. Backhuys Publishers, Leiden, The Netherlands, pp. 209–224.
- Medvecká, J., Jarolímek, I., Senko, D. & Svitok, M. 2014. Fifty years of plant invasion dynamics in Slovakia along a 2,500 m altitudinal gradient. *Biol. Invasions* **16**(8), 1627–1638.
- Medvecká, J., Kliment, J., Májeková, J., Halada, Ľ., Zaliberová, M., Gojdičová, E., Feráková, V. & Jarolímek, I. 2012. Inventory of the alien flora of Slovakia. *Preslia* **84**, 257–309.
- Pergl, J., Sádlo, J., Petrušek, A., Laštůvka, Z., Musil, J., Perglová, I., Šanda, R., Šefrová, H., Šíma, J., Vohralík, V. & Pyšek, P. 2016. Black, Grey and Watch Lists of alien species in the Czech Republic based on environmental impacts and management strategy. *NeoBiota* **28**, 1–37.

- Peters, K., Breitsameter, L. & Gerowitt, B. 2014. Impact of climate change on weeds in agriculture: a review. *Agron. Sustain. Dev.* **34**, 707–721.
- Preston, C.D., Pearman, D.A. & Hall, A.R. 2004. Archaeophytes in Britain. *Bot. J. Linn. Soc.* **145**, 257–294.
- Pyšek, P., Chytrý, M., Pergl, J., Sádlo, J. & Wild, J. 2012a. Plant invasions in the Czech Republic: current state, introduction dynamics, invasive species and invaded habitats. *Preslia* **84**, 575–629.
- Pyšek, P., Danihelka, J., Sádlo, J., Chrtěk, J.Jr., Chytrý, M., Jarošík, V., Kaplan, Z., Krahulec, F., Moravcová, L., Pergl, J., Štajerová, K. & Tichý, L. 2012b. Catalogue of alien plants of the Czech Republic (2nd edition): checklist update, taxonomic diversity and invasion patterns. *Preslia* **84**, 155–255.
- Pyšek, P., Jarošík, V., Chytrý, M., Kropáč, Z., Tichý, L. & Wild, J. 2005. Alien plants in temperate weed communities: prehistoric and recent invaders occupy different habitats. *Ecology* **86**, 772–785.
- Pyšek, P., Jarošík, V., Pergl, J. & Wild, J. 2011. Colonization of high altitudes by alien plants over the last two centuries. *Proc. Natl. Acad. Sci. U. S. A.* **108**(2), 439–440.
- Pyšek, P., Sádlo, J. & Mandák, B. 2002. Catalogue of alien plants of the Czech Republic. *Preslia* **74**, 97–186.
- Pyšek, P., Sádlo, J., Mandák, B. & Jarošík, V. 2003. Czech alien flora and a historical pattern of its formation: what came first to Central Europe? *Oecologia* **135**, 122–130.
- Richardson, D.M., Pyšek, P., Rejmánek, M., Barbour, M.G., Panetta, F.D. & West, C.J. 2000. Naturalization and invasion of alien plants: concepts and definitions. *Divers. Distrib.* **6**, 93–107.
- Schroeder, D., Mueller-Schaerer, H. & Stinson, C.S.A. 1993. A European weed survey in 10 major crop systems to identify targets for biological control. *Weed Res.* **33**, 449–458.
- Schumacher, W. & Schick, H.-P. 1998. Decline of plants of fields and vineyards – causes and need for action. *Schr.-R. f. Vegetationskunde H.* **29**, 49–57 (in German).
- Soukup, J., Holec, J., Hamouz, P. & Tyšer, L. 2004. Aliens on arable land. In *Scientific Colloquium – Weed Science on the Go*. University of Hohenheim, pp. 11–22.
- Soukup, J., Nováková, K., Hamouz, P. & Náměstek, J. 2006. Ecology of silky bent grass (*Apera spica-venti* (L.) Beauv.), its importance and control in the Czech Republic. *J. Plant Dis. Protect. Spec. Iss.* **20**, 73–80.
- Šilc, U. & Čarni, A. 2005. Changes in weed vegetation on extensively managed fields of central Slovenia between 1939 and 2002. *Biologia* **60**, 409–416.
- Ter Braak, C.J.F. & Šmilauer, P. 2002. *CANOCO 4.5*. Biometris, Wageningen, České Budějovice, 500 pp.
- Tiley, G.E.D. 2010. Biological flora of the British Isles: *Cirsium arvense* (L.) Scop. *J. Ecol.* **98**, 938–983.
- Valičková, V., Hamouzová, K., Kolářová, M. & Soukup, J. 2017. Germination responses to water potential in *Bromus sterilis* L. under different temperatures and light regimes. *Plant Soil Environ.* **63**, 368–374.
- Van der Maarel, E. 1979. Transformation of cover-abundance values in phytosociology and its effect on community similarity. *Vegetatio* **39**, 97–114.
- Vetter, J. 2004. Poison hemlock (*Conium maculatum* L.). *Food Chem. Toxicol.* **42**, 1373–1382.

Determining external friction angle of barley malt and malt crush

A. Vagová¹, M. Hromasová^{2,*}, M. Linda² and P. Vaculík¹

¹Czech University of Life Sciences Prague, Faculty of Engineering, Department of Technological Equipment of Buildings, Kamýcká 129, CZ165 21 Prague 6-Suchdol, Czech Republic

²Czech University of Life Sciences Prague, Faculty of Engineering, Department of Electrical Engineering and Automation, Kamýcká 129, CZ165 21 Prague 6-Suchdol, Czech Republic

*Correspondence: hromasova@tf.czu.cz

Abstract. This paper deals with determining the amount of external friction angle of barley malt and malt crush depending on the load size. Barley malt is a basic raw material for production of the traditional Czech Pilsner type of beer. The angle of internal and external friction is one of the basic parameters of bulk materials. Friction among individual grains of material, i.e. a connection with the forces, applied between individual material particles, includes the internal friction angle. Conversely, the external friction angle is the angle in which the bulk material begins to move on the other material (steel). A two-roll mill (or disc mill and hammer mill) was used for the malt crush manufacture, which is used in the traditional malt processing in beer production. During crushing on this machine, we used the passage of the milled material through a gap between two counter-rotating cylinders. The results of barley malt and malt crush external friction angle, depending on the load size of the barley malt and the malt crush on mobile prototype device, are from 8 to 22°. The mobile prototype device is based on the following principle: a square chamber filled with a loaded material moves on the pad (steel).

Key words: barley malt, external friction angle, food industry, particulate matter.

INTRODUCTION

The light malt is a product made from barley, after four- to five- week ripening in containers. The germinating process is interrupted by drying the malt and kilning to prevent further transformation and losses. To do this, one aims for the following: The water content is lowered from over 40.0% to less than 5.0% to make the malt more storable and to increase its preservability. With the lowering of the water content, all life processes in the malt such as germination and modification as well as further enzymic activity are stopped. In contrast, the enzymatic potential formed should be completely retained. Great attention must be paid to the formation or avoidance of colour and flavour compounds corresponding to the type of beer to be produced from the malt during this process. The rootlets are cut off and removed. Based on the targets set, the following

occur: The water content is lowered. Germination and modification are stopped. Colour and flavour compounds are formed.

To make the malt storable, the water content must be decreased from over 40.0% to 4.0 to 5.0%. Water removal is effected by passing a large amount of hot air through the green malt. When heating the moist green malt during kilning, care must be taken not to destroy the enzymes by wet heat - they withstand dry heat much better. Because the enzymes are needed to break down substrates in the brewhouse it is important to protect the enzymes to a large extent. To protect the enzymes the malt must first be predried before it is subjected to high temperatures. The moist starch in the green malt gelatinises at high temperatures and after cooling the malt is no longer suitable for use. Its inside has a steely appearance (vitreous malt).

On heating whilst the starch is wet, unusable vitreous steely malt is formed. The temperature must only be raised above 50.0 °C when the water content has been decreased to 10.0 to 12.0%. The slow lowering of the water content at temperatures of 40.0 to 50.0 °C is known as stewing. Long stewing times at low temperatures have a favourable effect on the flavour stability of the beer (Basařová, 2010; Kunze, 2010).

The storage and the transport require knowledge of the basic parameters of the processed materials, i.e. bulk materials (Smejtková et al., 2016). Among basic properties of the bulk materials, which are undoubtedly malt barley and malt crush, are: density, bulk density, internal friction angle, external friction angle (Arias Barreto et al., 2013; Chotěborský & Linda, 2014; Bogdan & Kordialik-Bogacka, 2017).

The aim of this paper is a determination of selected physical parameters of colored and light malt, i.e. angle of external friction angle and determination of tension limits (Afzalnia & Roberge, 2007; Boac et al., 2010; Gil et al., 2013; Khachatourian & Binelo, 2008; Silva, L.C. et al., 2012).

MATERIAL AND METHODS

Before the actual determination of tension limits of the barley malt and the malt crush, depending on the material of storage area, the moisture content of the processed materials was defined.

The water content slowly increases during storage to 4.0 to 5.0%. This results in physical and chemical changes in the endosperm which make further processing easier. Freshly kilned malt if used immediately can cause lautering and fermentation difficulties. Malt is therefore stored at least 4 weeks in silos or stores. Since most of the seedlings are no longer alive and respiration in the corn would only cause undesirable losses, the malt silo is not ventilated. A precondition for proper storage is that the malt does not become moist because it is hygroscopic. Moist air therefore has to be kept away. The malt which is to be stored has to be well cleaned, cold and dry. In silo storage, because of the smaller surface area, the risk of water uptake is lower than when storing in malt stores. In malt stores the malt layer is about 3 m high. Previously this was often covered by a layer of germs which absorbed the moisture and consequently prevented water uptake by the malt (Kosař & Procházka, 2000; Dendy & Dobraszczyk, 2001; Kunze, 2010).

Knowledge of the moisture content is necessary to ensure optimal conditions for further experiments (Fourar-Belaifa et al., 2011; Hammami et al., 2017). Determining the moisture content of the assessed barley malt was implemented using a moisture

analyzer OHAUS MB25 (Table 1 and Fig. 1). The OHAUS MB25 provides precise moisture content determination at value. With a large backlit LCD display, standard RS232 port, 110.0 g capacity with a readability of 0.005 g/0.05% and halogen heating, the OHAUS MB25 offers moisture analysis.

Sieve analysis of grist. For the determination of crushed malt dispersity, a test sieve shaker (sieve analyzer) HAVER EML 200 digital plus T (Table 2 and Fig. 2).



Figure 1. Moisture analyzer OHAUS MB 25 (Source: <https://asiapacific.ohaus.com/en-AP/Products/Balances-Scales/Moisture-Analyzers/MB25/MB25>).

Table 1. Technical parameters of Moisture analyzer OHAUS MB 25

Maximum capacity	(g)	110.0
Readability moisture content	(mg / %)	5.0 / 0.05
Pan size	(mm)	90.0
Heater type	(-)	Halogen lamp
Communication	(-)	RS232 (Included)
Dimensions (h x l x w)	(mm)	127.0 x 280.0 x 165.0
Display	(-)	LCD, backlight
In-use cover	(-)	Included
Net weight	(kg)	2.1
Power	(-)	AC power (included)
Shut-off criteria	(-)	Automatic - preset weight loss/time; timed; manual
Temperature range	(°C)	50.0–160.0
Units of measurement	(g)	Gram
Working environment	(°C)	10.0–40.0

Table 2. Technical parameters of test sieve shaker HAVER EML 200 digital plus T

Sieve diameters	(mm)	76.0, 100.0, 150.0, 200.0, 203.0
Sample weight	(kg)	approx. 3.0
Weight of sieve set	(kg)	max. 8.7
Amplitude	(mm)	max. 3.0
Sound emission	(dBA)	≤ 70.0 dBA
Weight (without test sieves)	(kg)	approx. 34.0
Dimensions (h x l x w)	(mm)	345.0×285.0×950.0



Figure 2. Test sieve shaker HAVER EML 200 digital plus T (Source: <https://www.haverparticleanalysis.com/en/sieve-analysis/haver-test-sieve-shakers/haver-eml-200-pure/>)

The results of the moisture content establishing of the individual samples of processed raw materials are shown in Table 3. Selected mechanical and physical parameters (density, volume weight, friction angle) of the colored and light barley malt and the malt crush are in (Vaculík et al., 2013; Hromasova et al., 2018; Chladek et al., 2018). Grain size was determined by network analysis (Table 3).

Table 3. The results of the moisture content establishing (Hromasova et al., 2018).

Light barley malt		Humidity (%)	Colored barley malt	
Whole grain	Crushed grain		Whole grain	Crushed grain
1.904 ± 0.014	1.997 ± 0.127		1.877 ± 0.073	1.983 ± 0.097
		Size (mm)		
3.6 ± 0.11	0.91 ± 0.155		3.48 ± 0.131	1.05 ± 0.133

The following methods is aimed at determining external friction angle of barley malt and malt crush. Angle of external friction - the angle between the abscissa and the tangent of the curve representing the relationship of shearing resistance to normal stress acting between material and the surface of material of storage area (also known as angle of wall friction) (Fig. 3).

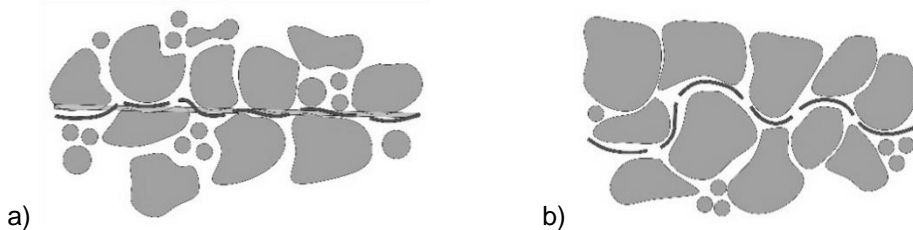


Figure 3. The shear area in material: a) the shear area in material – idealized; b) the shear area in material – realistic.

For the incoherent bulk materials, the maximum tangential stress is dependent. τ_{max} in areas of normal tension σ described by (Feynman et al., 2011, Hromasova et al., 2018).

For the cohesive bulk materials, the ratios are more complex and the characteristic is described by (Maloun, 2001; ČSN ISO TS 17892-10; Feynman et al., 2011; Hromasova et al., 2018).

Particle substance parameter measurements were performed on the device (Fig. 4).

When determining of limit tensions in relation to a load size of the barley malt and the malt crush on the prototype device, which was adapted to measure the properties of bulk materials. The measurement procedure is as follows (Fig. 4):

- using a electric motor 1, the upper square chamber 2 (area of the chamber is 8,100 mm²) slides down the steel plate 3;
- in between chamber 2 and steel plate 3 is the particular material stressed by tangential force T (N);
- normal force N (N), exerted by the weight 5 acting on the malt through the loading plate 6 (weight of the load plate was 219.68 g);
- load weights were used for loading 1,000; 2,000; 3,000; 4,000 and 5,000 g;

- depending on the size of the deformation, the force can be determined T (N) (Hromasova et al., 2018).

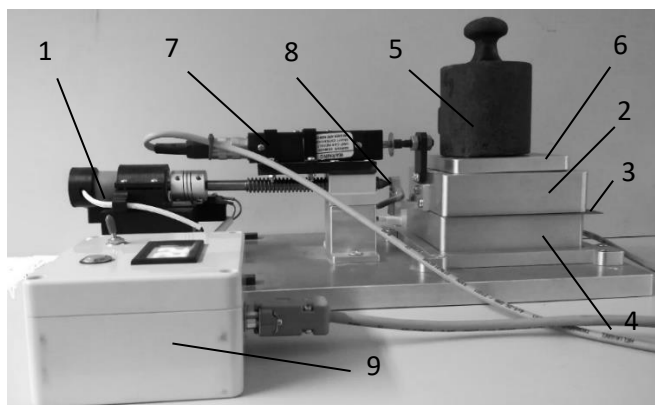


Figure 4. Device for measuring shear cohesion and friction properties of bulk materials (Evolution 2). Annotations: 1 – electric motor; 2 – the upper square chamber - movable; 3 – steel plate; 4 – the dividing gap between the chambers; 5 – weight; 6 – loading plate; 7 – shift sensor; 8 – deformational component with strain gauges for measurement of the force; 9 – control device. The device is complemented with measuring electronics and evaluation software.

The strain gauges were silicon resistance type AP130-3-12/SP/Au. The data are given in Table 4 for used strain gauges.

Table 4. Parameters on strain gauges

Parameters	Type
Type A (-)	layout without pad
Type P (-)	positive deformation sensitivity
Value of multiplier of deformation sensitivity (-)	130.0
Lenght (mm)	3.0
End shape of silicon part of strain gauges (-)	SP
Material for outlets (-)	gold

In Eq. 1 is calculated dependence of strain gauge resistance on deformation. The constants C_1 , C_2 are calculated from the resistance changes of the strain gauges stick to with cyanoacrylate adhesive glue. The coefficients are given in Table 5.

$$R_{\varepsilon,25} = R_{0,25}(1 + C_1\varepsilon + C_2\varepsilon^2) \quad (1)$$

where $R_{0,25}$ – electrical resistance of the free strain gauge (Ω); $R_{\varepsilon,25}$ – electrical resistance of the strain gauge deformed at a constant temperature of 25 °C (Ω); C_1 – linear coefficient of deformation equation (-); C_2 – quadratic coefficient of deformation equation (-); ε – ratio of deformation (m).

Table 5. The coefficients for strain gauges

Coefficients	Value
$R_{0,25}$ ($\Omega \pm\%$)	119.4 $\Omega \pm 0.24$
C_1 ($\pm\%$)	127.3 $\pm 2.00\%$
C_2 ($\pm\%$)	5,101 $\pm 8.00\%$
A ($\% \cdot ^\circ\text{C}^{-1}$)	0.0932 $\pm 0.38\%$
B ($\% \cdot ^\circ\text{C}^{-1}$)	-0.18

RESULTS AND DISCUSSION

In the following figures (Fig. 5 to 8) are shown the courses of the limit tensions (Table 6) for the barley malt and malt crush in relation to the load size 1,000 and 5,000 g. The point charts were chosen because it is measured for each sample at least 2,000 values.

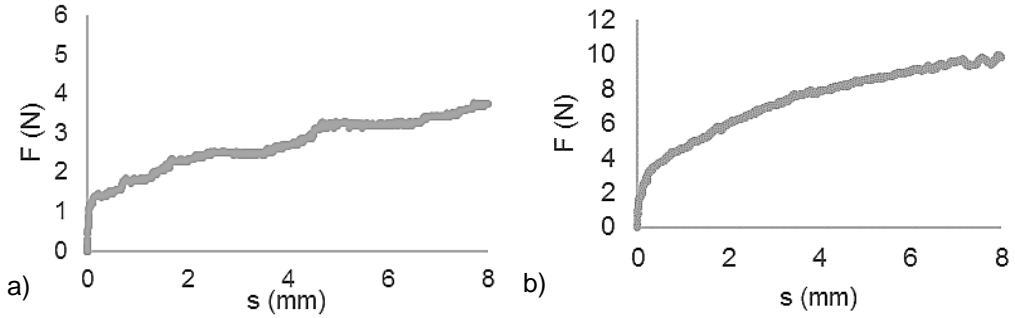


Figure 5. The graph of force dependence on the displacement for light barley malt – crushed grain – a) load 1,000 g, b) load 5,000 g.

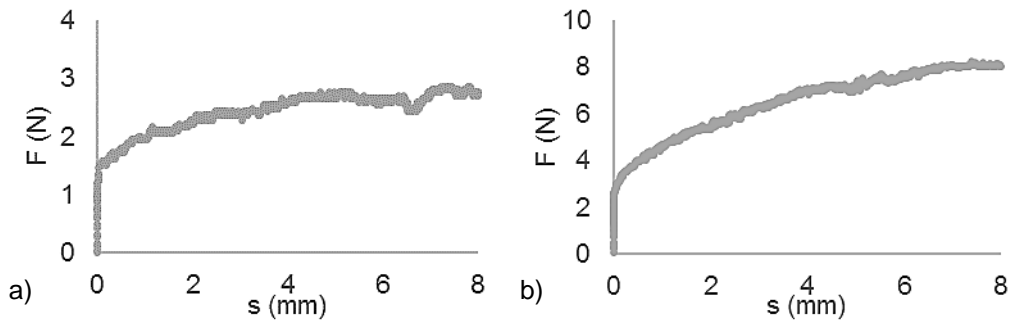


Figure 6. The graph of force dependence on the displacement for light barley malt – whole grain – a) load 1,000 g, b) load 5,000 g.

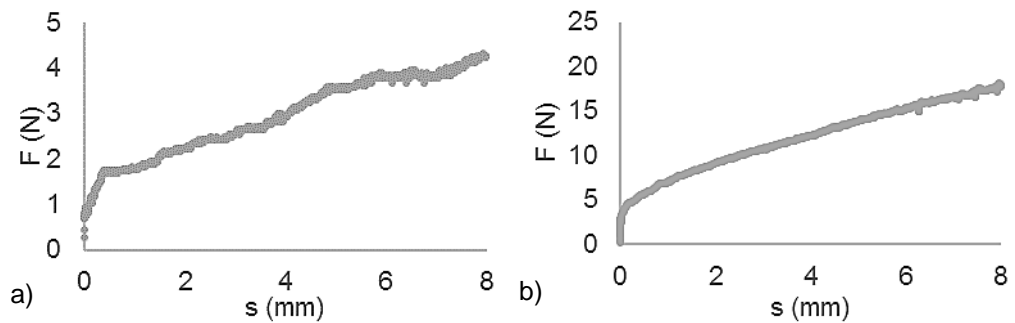


Figure 7. The graph of force dependence on the displacement for colored barley malt – crushed grain – a) load 1,000 g, b) load 5,000 g.

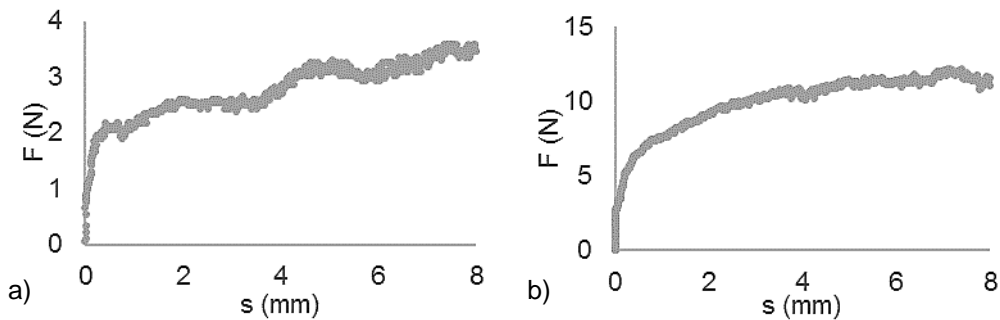


Figure 8. The graph of force dependence on the displacement for colored barley malt – whole grain – a) load 1,000 g, b) load 5,000 g.

The Table 6 shows limit tension, which is maximal force of tension at 8 mm displacement. For the crushed malt it is necessary to provide greater force of at least 22% compared with the whole grain (light barley malt). For the crushed malt it is necessary to provide greater force of at least 19% compared with the whole grain (colored barley malt).

The external friction angle (Table 7) of the whole grain light barley malt is less by 4.71° than the colored malt; the crushed colored barley malt is lower by 13.26° than the colored malt. The external friction angle by steel is from 6% to 17% (Kovalyshyn et al., 2014) for different particular material.

The external friction angle of the barley is from 13.77° to 33.50° (Kaliniewicz, 2013) when humidity at 12.6%. The external friction angle of the barley is from 15.66° to 38.05° (Kaliniewicz et al., 2018) when humidity at 10.2%.

Table 6. The results of the limit tension

Loading mass (g)	Limit tension (N)			
	Light barley malt		Colored barley malt	
	Whole grain	Crushed grain	Whole grain	Crushed grain
1,000	2.87	5.03	3.57	4.38
2,000	4.44	6.14	5.25	6.71
3,000	6.28	7.85	6.82	10.66
4,000	7.20	8.93	10.23	14.04
5,000	8.61	11.31	12.18	19.81

Table 7. The external friction angle

External friction angle ($^\circ$)			
Light barley malt		Colored barley malt	
Whole grain	Crushed grain	Whole grain	Crushed grain
8.19	8.31	12.90	21.57

CONCLUSION

By optimizing the angle of inclination of the hopper and the outer friction angle parameter at the inner wall can be achieved that the material flows through the entire cross section. To ensure mass flow in the magazine, the following applies: The smaller external friction angle and the smaller inclination angle of the hopper mean better flow properties of the material in the container.

Based on knowledge of the parameters of individual substances (eg limiting force, angles of internal and external friction) we can calculate storage and manipulation devices. All results can be used for DEM modeling in warehouse management.

Measured values correspond with the results published in article ‘Mathematical-model of filtration process in beer production’ (Chládek, 1977), ‘Impact of malt granulometry on lauter proces’ (Chládek et al., 2013), ‘Pivovarnictví (Brewing)’ (Chládek, 2007) and ‘Pivovarství: teorie a praxe výroby piva’ (Basařová, 2010) and others.

ACKNOWLEDGEMENTS. The measurements were made on the device ‘Mobile device for shear soil testing’ utility model number 29836, authors CHOTĚBORSKÝ, R., LINDA, M., NÝČ, M.

Thank doc. Ing. Rostislav Chotěborský, Ph.D. and Department of Material Science and Manufacturing Technology for borrowing the device.

REFERENCES

- Afzalnia, S. & Roberge, M. 2007. Physical and mechanical properties of selected forage materials. *Can. Biosys. Eng.* **49**, ISSN 223–227.
- Arias Barreto, A., Abalone, R., Gastón, A. & Bartosik, R. 2013. Analysis of storage conditions of a wheat silo-bag for different weather conditions by computer simulation. *Biosystems Engineering* **116**(4), 497–508. ISSN 15375110.
- Basařová, G. 2010. *Pivovarství: teorie a praxe výroby piva (Brewing: the theory and practice of beer production)*. 1st edition. Publisher: Vydavatelství VŠCHT. Prague, 863 pp. (in Czech).
- Boac, J.M, Casada, M.E., Maghirang, R.G. & Harner III, J.P. 2010. Material and Interaction Properties of Selected Grains and Oilseeds for Modeling Discrete Particles. *Trans. ASABE* **53**(4), 1201–1216. ISSN 2151-0032
- Bogdan, P. & Kordialik-Bogacka, E. 2017. Alternatives to malt in brewing. *Trends in Food Science and Technology* **65**, 1–9.
- Czech standard for examination ČSN ISO TS 17892-10.
- Dendy, D.A.V. & Dobraszczyk, B.J. 2001. *Cereals and Cereal Products: Chemistry and Technology*. 2nd edition. Publisher: Aspen Publishers, Inc., 429 pp. ISBN: 0-8342-1767-8
- Feynman, R.P., Leighton, B.R. & Sands, M. 2011. *The Feynman Lectures on Physics, boxed set: The New Millennium Edition*. 1st edition. Publisher: Basic Books, 1552 pp. ISBN-10: 0465023827
- Fourar-Belaifa, R., Fleurat-Lessard, F. & Bouznad, Z. 2011. A systemic approach to qualitative changes in the stored-wheat ecosystem: Prediction of deterioration risks in unsafe storage conditions in relation to relative humidity level, infestation by *Sitophilus oryzae* (L.), and wheat variety. *Journal of Stored Products Research* **47**(1), 48–61. ISSN: 0022474X
- Gil, M., Schott, D., Arauzo, I. & Teruel, E. 2013. Handling behavior of two milled biomass: SRF poplar and corn stover. *Fuel Processing Technology* **112**, 76–85.
- Hammami, F., Ben Mabrouk, S. & Mami, A., 2017. Numerical investigation of low relative humidity aeration impact on the moisture content of stored wheat. *International Journal of Modeling, Simulation, and Scientific Computing* **8**(2), 1740002. ISSN 17939623
- Hromasova, H., Vagova, A., Linda, M. & Vaculik, P. 2018. Determination of the tension limit forces of a barley malt and a malt crush in correlation with a load size. *Agronomy Research* **16**(5), 2037–2048.
- Chládek, L. 1977. Mathematical- model of filtration process in beer production. *Lebensmittel industrie* **24**(9), 416–420.
- Chládek, L. 2007. *Pivovarnictví (Brewing)*. 1st edition. Publisher: Grada. Prague. 207 pp. (in Czech).

- Chládek, L., Vaculík, P., Příkryl, M., Vaculík, M. & Holomková, M. 2013. Impact of malt granulometry on lauter proces. In *5th International Conference on Trends in Agricultural Engineering 2013, TAE 2013 03.09.2013*, Prague. Prague: Czech University of Life Sciences Prague, pp. 244–248.
- Chladek, L., Vaculik, P. & Vagova, A. 2018. The measurement of energy consumption during milling different cereals using the sieve analyses. *Agronomy Research* **16** (Special Issue 2), 1341–1350.
- Chotěborský, R. & Linda, M. 2014. Evaluation of friction force using a rubber wheel instrument. *Agronomy research* **12**(1), 247–254. ISSN 1406894X.
- Kaliniewicz, Z. 2013. Analysis of frictional properties of cereal seeds. *African Journal of Agricultural Research* **8**(45), 5611–5621.
- Kaliniewicz, Z., Žuk, Z. & Krzysiak, Z. 2018. Influence of steel plate roughness on the frictional properties of cereal kernels. *Sustainability* **10**, 1–11.
- Khatchatourian, O.A. & Binelo, M.O. 2008. Simulation of three-dimensional airflow in grain storage bins. *Biosystems Engineering* **101**(2), 225–238. ISSN 15375110
- Kovalyshyn, S., Dadak, V., Sokolyk, V., Grundas, S., Stasiak, M. & Tys, J. 2014. Geometrical and friction properties of perennial grasses and their weeds in view of an electro-separation method. *International Agrophysics* **29**, 185–191.
- Kosař, K. & Procházka, S. 2000. Technologie výroby sladu a piva (Technology of malt and beer production). 1st edition. Publisher: Výzkumný ústav pivovarský a sladařský (Research Institute of Brewing and Malting), Prague, 398 pp. (in Czech).
- Kunze, W. 2010. *Technology Brewing and Malting*. 4th updated English Edition. Berlin: Versuchs- und Lehranstalt für Brauerei in Berlin (VLB), 1047 pp. ISBN 978-3-921690-64-2 (in German).
- Maloun, J. 2001. *Technological equipment and main processes in feed production*. 1st edition. Publisher: Czech University of Life Sciences Prague, Faculty of Engineering, 201 pp. ISBN 80-213-0783-8 (in Czech).
- Silva, L.C., Queiroz, D.M., Flores, R.A. & Melo, E.C. 2012. A simulation toolset for modeling grain storage facilities. *Journal of Stored Products Research* **48**, 30–36. ISSN 0022474X
- Smejtková, A., Vaculík, P., Příkryl, M. & Pastorek, Z. 2016. Rating of malt grist fineness with respect to the used grinding equipment. *Research in Agricultural Engineering (Zemědělská technika)* **62** (3), pp. 141–146. ISSN 1212-9151
- Vaculík, P., Maloun, J., Chládek, L. & Příkryl, M. 2013. Disintegration process in disc crushers. *Research in Agricultural Engineering (Zemědělská technika)* **59**(3), 98–104.

A holistic vision of bioeconomy: the concept of transdisciplinarity nexus towards sustainable development

L. Zihare*, I. Muizniece and D. Blumberga

Institute of Energy Systems and Environment, Riga Technical University, Āzenes iela 12/1, LV-1048 Riga, Latvia

*Correspondence: lauma.zihare@rtu.lv

Abstract. Current issue of bioeconomy development has been largely addressed on a linear or interdisciplinary level, however holistic view of bioeconomy requires a transdisciplinary system analysis. Developed methodology clarifies vision on bioeconomy definition, bioeconomy disciplines and disciplinary definition in context of nexus interlinkage, in the result concept of transdisciplinary approach connection to bioeconomy is determined as processes for sustainable bioeconomy, that not only replace fossil resources with biobased resources, but strengthens different disciplines, taken into account interlinkages, knowledge, and stakeholders and limitations set by planetary boundaries, different dimensions should be included in transition towards sustainable bioeconomy. Methodology bases on critical literature analysis. Different bioeconomy disciplines are defined and the obtained results are represented graphically. The obtained results can be used for further research as a transdisciplinarity basis of the bioeconomy, studying specific systems, factors influencing them and evaluating potential scenarios and their impacting tools. Results from implementing holistic vision would provide practical benefit to policy makers and industry actors by providing an analysis how to improve industrial practice, policy and how more effectively transfer to sustainable bioeconomy.

Key words: bio-economy, disciplines, transdisciplinary approach, nexus, sustainability.

INTRODUCTION

In 2013–2015 there were addressed a pathway for need to look on bioeconomy from interdisciplinary point of view, mostly because of novel technologies and need to use side streams, therefore engineering, environmental and socioeconomic challenges affect products and processes (Golembiewski et al., 2015). Also integration of knowledge from different disciplines is necessary (Golembiewski et al., 2015). In 2018 the vision of bioeconomy pathway is determined more complex and one-dimensional approaches are not suited, therefore more holistic and systemic perspective and solutions are needed (Schütte, 2018). According to (Bugge et al., 2016) categories that has been researched in bioeconomy are: biotechnology & applied microbiology, energy & fuels, environmental science, chemistry, multidisciplinary, environmental engineering, food science & technology, chemical engineering, forestry, applied chemistry, agronomy, agricultural engineering, plant sciences, social sciences, biomedical, multidisciplinary sciences (Bugge et al., 2016). Three bioeconomy visions are set in this article – biotechnology vision (research, application and commercialisation), bio-resource vision

(RD&D, biological materials in agriculture, marine, forestry and bioenergy) and bio-ecology vision (potential for regionally circular and integrated processes and systems) (Bugge et al., 2016). In 2009 OECD (Organisation for Economic Co-operation and Development) has created an analysis of future developments of bioeconomy on three sectors – agriculture, health and industry. It has been stated as interdisciplinary research. Implementation pathways determined technology –based approach and socio-ecological approach, where the second includes inter- and transdisciplinary approach in research (Priefer et al., 2017). In other article multi-, inter- and transdisciplinary environment is stated as ‘social process of knowledge production’ (Klein, 2008).

Current issue of bioeconomy development has been largely addressed on a linear or interdisciplinary level. But the future development of the bioeconomy should be viewed more widely, not as limited system. It involves many, sometimes very radically different, disciplines, both tangible and intangible, which are interrelated and can have an impact on the development of the bioeconomy, both directly and indirectly. For example, natural science –chemistry and social science – economics are related, thus increasing added value by creating new biochemical potential increases economic development. Other example applied science – agriculture and humanities – history and natural science – biology, were history about cultures and field research can improve agriculture practices. Knowledge in physics can improve agriculture technology thus improving efficiency. Including mutual interaction. The increasing demand of food and feed, population growth and climate changes require new holistic vision on bioeconomy, bringing together various stakeholders. It has been acknowledged that holistic view of bioeconomy requires a transdisciplinary system analysis (Schütte 2018). There are some evident need for interdisciplinary approach for bioeconomy (Golembiewski et al., 2015), so it is important to understand if there is really a need for transdisciplinary approach or interdisciplinary approach.

Systemic approach will be achieved by nexus thinking and the concept of transdisciplinary approach in bioeconomy. Transdisciplinary research encompasses broad, deep and equal opportunities with different interests, which usually do not evolve in the study of policy. There is a need to align the principles of circular economy and bioeconomy involving system approaches across sectors and macro regional nexus thinking. This research gives a comprehensive view about holistic vision in bioeconomy and clear concept with a graphical representation of transdisciplinarity nexus. It should be noted that the development of the bioeconomy cannot be promoted in all regions at the same structure, but it is essential to understand the discipline and which factors should be considered in the assessment.

The aim of this study is to clarify the difference between interdisciplinary, multidisciplinary and transdisciplinary approach in bioeconomy and to develop the concept of bioeconomy transdisciplinarity approach. Therefore, understanding is the bioeconomy transdisciplinarity and what are the essential components of this system. Therefore, critical literature analysis was carried out and holistic approach used to analyse and aggregate the information. Different bioeconomy disciplines are defined and the obtained results are represented graphically. The obtained results can be used for further research as a transdisciplinary basis of the bioeconomy, studying specific systems, factors influencing them and evaluating potential scenarios and their impacting tools.

Hypothesis is that to achieve holistic approach in bioeconomy, transdisciplinarity should be evaluated.

MATERIALS AND METHODS

First to have a clear vision on bioeconomy disciplines and transdisciplinary nature, it is important to clarify bioeconomy definition, discipline definition and disciplinary definition in context of nexus interlinkage, then it should be clear how the disciplinary approach connects to bioeconomy. Therefore, a methodology algorithm was developed for this study (Fig. 1).

Methodology is based on concept development for transdisciplinary bioeconomy nexus, where the result is graphical representation, that can be easy understood and be basis and framework for further studies. Methodology bases on critical literature analysis (step 1), to understand interlinkage from planetary boundaries (step 2) to bioeconomy (step 4) and definition of bioeconomy (step 3), to understanding the disciplines overall (step 5) and in context of bioeconomy (step 6), as well as nexus approach (step 7) and its linkage to transdisciplinarity approach (step 8) and taking it all to account come with concept of transdisciplinary bioeconomy nexus (step 9) with graphical representation (step 10).

In first step clarifying that everything should be based on critical literature analysis, it means not quantity, but quality assessment of literature, in the second step, one of the most important factor, that impacts the overall use of resources and limits is planetary boundaries (step 2), that should not be exceeded and suppressed if already is beyond limits. Step three clarifies that bioeconomy has not one clear definition and can be understood with variations, here the several definitions from different perspectives is analysed. Step four elevates bioeconomy concept based on different bioeconomy definitions is created, to understand the complexity and include all the main factors from definitions. Next to build and understand the disciplines in bioeconomy, the overall definition of disciplines is gathered (step 5). In step six clarifying the different disciplines in term of bioeconomy is determined. As the last year development shows (Muizniece et al., 2018) that nexus approach should be considered and has strong interlinks with transdisciplinary approach (step 7).

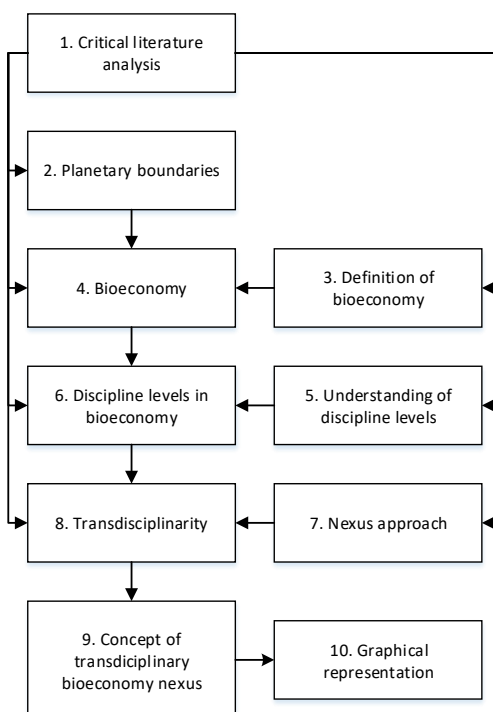


Figure 1. Methodology algorithm.

Therefore, in step 8 transdisciplinarity definition in terms of bioeconomy is determined, to create concept of transdisciplinary bioeconomy nexus (step 9). In final step, the concept is represented graphically that can be stated as future framework for analysing bioeconomy transdisciplinarity (step 10).

The methodology algorithm is designed to take into account and critically analyse the diversity of opinions. Common to capture links between views from different industries is recorded and compiled. Thus justifying transdisciplinary researched issue.

RESULTS AND DISCUSSION

In order to understand the meaning of bioeconomy on global scale (not only in terms of international but also of ecosystems), it is necessary to identify the bioeconomy area. According to the literature, there are nine planetary boundaries (Mace et al., 2014; Heo et al., 2016; Stockholm Resilience Centre n.d.), which are close related to three bioeconomy main pillars – resource scarcity, climate change and food security (Fig. 2), (Lewandowski 2017). Planetary boundaries are not system that could show development of society, but it can clearly show the boundaries of safe development area and risk zone.

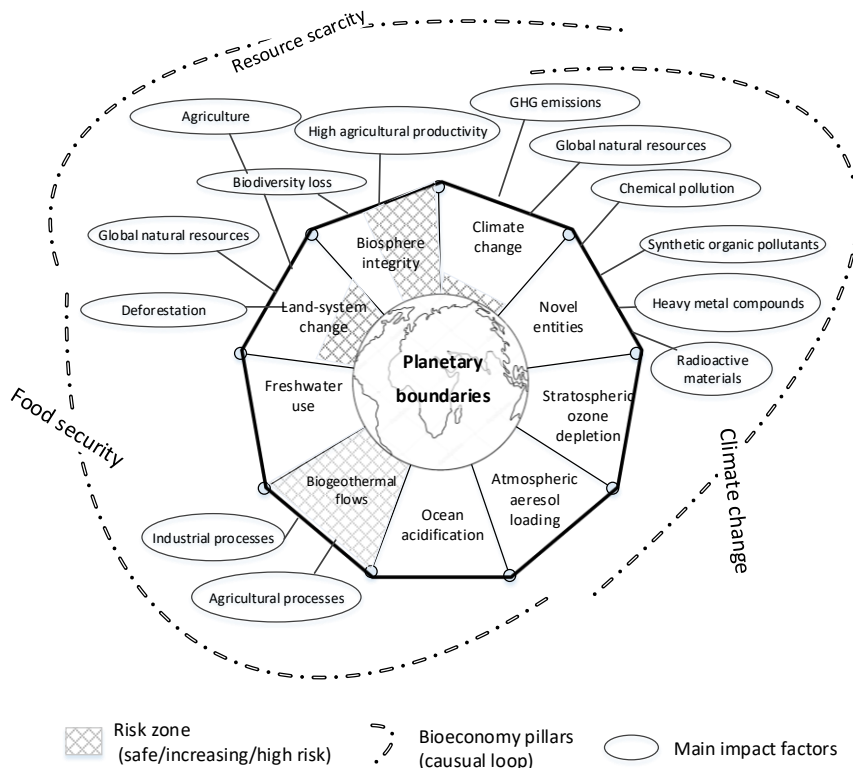


Figure 2. Planetary boundaries and bioeconomy pillars (Lewandowski 2017).

The nine planetary boundaries, that has to be taken into account in bioeconomy development, are:

- 1) stratospheric ozone depletion;

- 2) loss of biosphere integrity (functional and genetic diversity), that includes biodiversity loss and extinctions;
- 3) chemical pollution and the release of novel entities;
- 4) climate change;
- 5) ocean acidification,
- 6) freshwater consumption and the global hydrological cycle;
- 7) land system change;
- 8) biogeochemical flows - nitrogen and phosphorus flows to the biosphere and oceans;
- 9) atmospheric aerosol loading.

Planetary boundaries interlink with bioeconomy pillars, that show the global necessity for sustainable system development, taking into account safe development zone, therefore it shows complexity of the system required and bioeconomy transdisciplinary nature is suspected, but there should be clear division between disciplines and vision on development.

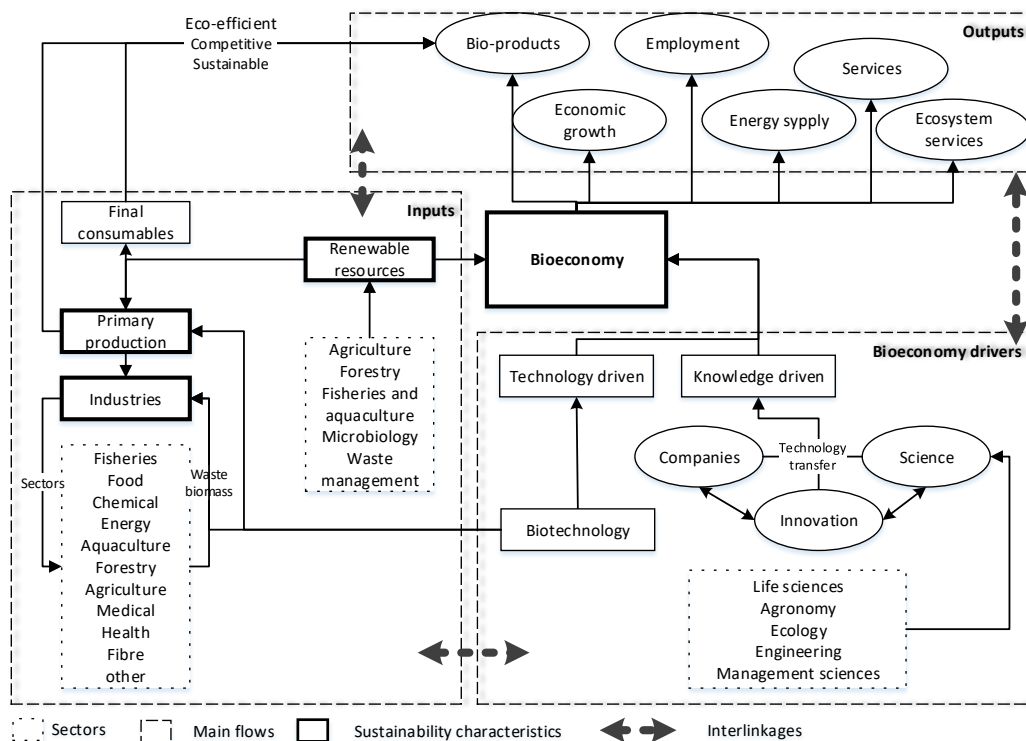


Figure 3. Bioeconomy schematic representation.

From the definition of bioeconomy and the analysis of different understandings, bioeconomy concept is summarized and graphically illustrated in Fig. 3. Bioeconomy is stated as knowledge and technology driven (Golembiewski et al., 2015) and biotechnology is set as first priority (Ahn, 2012). Bioeconomy covers different science fields, that is, but not limited to – life sciences, agronomy, ecology, engineering and management sciences (Golembiewski et al., 2015). According to OECD, bioeconomy is an innovative approach of transforming knowledge into new sustainable and eco-

efficient product that is also competitive (OECD, 2009). Bioeconomy knowledge drivers is not only science, but also innovative companies with large knowledge on bioproducts and services offer (Woźniak & Twardowski 2018).

Bioeconomy interconnect with different topics such as primary resources – forestry, agriculture, fisheries and aquaculture, and sectors- industrial, such as food, chemical, energy, ecosystem services of nature like recreation and wellbeing (VTT, 2018). The main outputs from bioeconomy is sustainable bioproducts, economic growth, energy supply, employment, services (such as health services) and ecosystem services (Woźniak & Twardowski 2018). Bioeconomy also implies the sustainable exploitation of biological resources to produce new bio-based products (Lainez et al., 2018), providing conditions for increased standard of living (Aguilar et al., 2013).

The main bioeconomy system is driven by three main flows – bioeconomy drivers, inputs and outputs, which all are interconnected. It means that changes in one part of the system would have an impact not only on each other, but also directly on the development of the bioeconomy. This demonstrates the crucial role of bioeconomy extensive coverage, which has long exceeded the level of one industry or country. Therefore, it is essential to understand how transdisciplinarity of the bioeconomy is manifested. First of all, it is necessary to understand the essence of transdisciplinarity, which, like the concept of bioeconomy, is interpreted very differently.

Discipline relations in nexus context

Nexus approach is generic-conceptual approach with the aim to find interactions among different processes, that depends on the impact of various factors (Muizniece et al., 2018). There are many illustration options on discipline levels, the one that is closest in order to understand nexus, is chosen.

Crossdisciplinary (Fig. 4, a) concept is viewing one discipline from the perspective of another, crossdisciplinary involves associative relations between different methods that are primarily comparative (Stirling, 2015). Here one discipline, for example agriculture farming interacts with other discipline, for example agriculture economics, to find solution on one issue. Results are solution – oriented.

Multidisciplinary (Fig. 4, b) is where people from different disciplines working together, each use their disciplinary knowledge. In multidisciplinary, relationship is usually

centralised and hierarchical – it uses the power to define ‘discipline’ in research, in the language of this word. Thus, a particular discipline (in the academic terms, along with related methods) investigation is a privileged development of other methods of ordering and the final results of the general interpretation (Stirling, 2015).

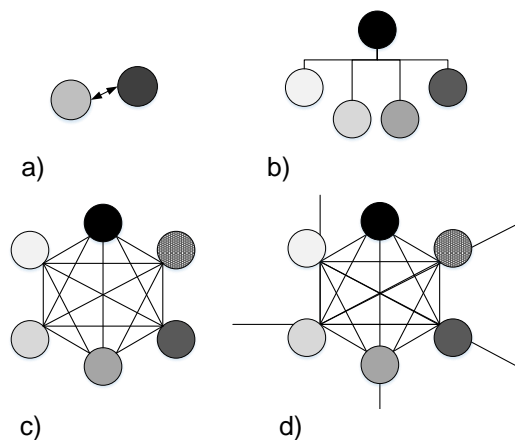


Figure 4. Illustration of discipline levels (Stirling, 2015).

As for bioeconomy point of view, would be different discipline experts, that are working on the same bioeconomy issue, for example, on issue of using agriculture waste, microbiologist can give his knowledge and expertise on how to add value to agriculture waste, engineer can find solutions for most effective equipment on various solutions and economist can give his expertise on solutions that he believes is the most cost effective. In this stage, they do not interact with each other. Or interaction is stated as weak link. Results is more subjective.

Interdisciplinary (Fig. 4, c) integrates knowledge and methods from different disciplines, using real-world approach of synthesis. In contrast, interdisciplinary has more symmetrical relationship between disciplines, and different methods can be used to address the contrasting aspects of the existing problem. However, even if participatory practice is used in subsequent parts of the process, non-academic interests are often excluded in the most important research, development and interpretation processes (Stirling, 2015). Here the disciplines that interacts are from different basis, they interaction are solution- oriented and with strong links, for example, issue on how to add value on agriculture waste, is a policy question, will it give social benefits and improve national economic situation and on what scale, microbiologist, that can help to find solution, that would give highest added value, economics, that help to find the most cost effective solution and computer science, that can perform modelling on different solution scenarios and their impact to various economic, socioeconomic, health and environmental processes.

Transdisciplinary (Fig. 4, d) creates the integrity of intellectual systems beyond a disciplinary perspective. Only in the field of transdisciplinarity, research or evaluation engages in broad, deep and equal ways with different interests, which are usually left outside the formal processes of policy research. Transdisciplinary engagement not only takes place in disciplines, nor is it the case that certain methods are implemented in a way that is subject to wider involvement (Stirling, 2015). According to J.A. Bergendahl et al., nexus projects are going to be more successful if transdisciplinary approach is applied (Bergendahl et al., 2018). If previous disciplines focused only on academic disciplines, this approach interacts with non-academic disciplines (society) as equals, broadening the view of issue and solution. If we look at previous mentioned example, in this case it would be supplemented with non-academic disciplines – different non-governmental organizations, local communities, local people, industries and also government agencies, etc. It means, we take into account opinions not only on previous mentioned disciplines on agricultural waste management with high added value, but also e.g. farmer's opinion, local communities' opinion, municipalities opinion and industries opinion on different solutions and possibilities to create a new path for bioeconomy development, in this case adding value to agriculture waste by new product production, that is feasible not only in theoretical level, but also realistic on implementation stage, economic and environmental aspect and with market potential.

Transdisciplinary bioeconomy

In order to research, demonstrate and define transdisciplinary approach of the bioeconomy, it is necessary to understand not only the bioeconomy on a largest scale, but also understand what is transdisciplinary nature. Therefore, a broad analysis of the scientific literature was carried out and various opinions on transdisciplinary definition were compiled. Some of them are summarized in Table 1.

Table 1. Evolution of transdisciplinary definition

Definition of transdisciplinary	Reference
‘Transdisciplinarity is the incorporation of a broad set of scientific and policy disciplines, including industries and actors, for addressing broad and complex problems, e.g., sustainability. Transdisciplinarity is meant to address concerns of traditional scientific methods relying on reductionist, reasoned, studies that investigate a phenomenon or research question typically from a single disciplinary perspective.’	(Bergendahl et al., 2018)
‘Transdisciplinary is the ontological specification of knowledge constructs on a higher, boundary-transcending, level of abstraction.’	(Colpaert, 2018)
‘The science of team science: assessing the value of transdisciplinary research problems; meaningful collaborations, particularly between academic researchers and non-academics.’	(Scholz, 2017)
‘Transdisciplinarity is seen as a specific methodology of efficient utilization and a way to relay knowledge from practice and science to the management of complex sustainable transitions.’	(Scholz et al., 2014)
‘Transdisciplinarity is a reflexive research approach that addresses societal problems by means of interdisciplinary collaboration as well as the collaboration between researchers and extra-scientific actors; its aim is to enable mutual learning processes between science and society; integration is the main cognitive challenge of the research process.’	(Jahn et al., 2012)
‘Transdisciplinary studies incorporate interdisciplinary integration and add additional research dimensions by (a) addressing problems that are user inspired and context driven, (b) embracing complexity; and (c) acknowledging and incorporating multi-stakeholder perspectives and values...’	(Roux et al., 2010)
‘TR deals with problem fields in such a way that it can: (a) grasp the complexity of problems, (b) take into account the diversity of life-world and scientific perceptions of problems, (c) link abstract and case-specific knowledge, and (d) develop knowledge and practices that promote what is perceived to be the common good [...] We define TR by these four requirements for knowledge production.’	(Pohl & Hadorn, 2008)
‘Transdisciplinarity is a new form of learning and problem solving involving cooperation among different parts of society and academia in order to meet complex challenges of society. Transdisciplinary research starts from tangible, real-world problems. ... Ideally, everyone who has something to say about a particular problem and is willing to participate can play a role. Through mutual learning, the knowledge of all participants is enhanced ... The sum of this knowledge will be greater than the knowledge of any single partner. In the process, the bias of each perspective will also be minimized.’	(Zierhofer & Burger, 2007)
‘Transdisciplinarity represents a move from science on/about society towards science for/with society.’	(Scholz & Marks, 2001)

All definitions show that transdisciplinary approach is the transition from science to practice, seen as complex and sustainable way to meet complex challenges of society. Transdisciplinary approach itself is complex and consists of four dimensions (Fig. 5).

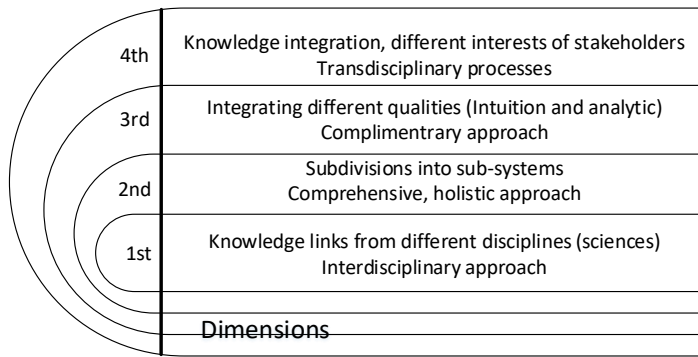


Figure 5. Transdisciplinary approach dimensions (Scholz & Marks, 2001).

Transdisciplinarity processes is way from unsustainable management moving towards sustainable management, covering four dimensions with the aim to connect science (disciplinarity) with practice (stakeholders) (Scholz et al., 2014). According to (Scholz & Tietje, 2002), knowledge that has to be implemented to preceptors go through four dimensions:

1st dimension – helix approach – this dimension brings together different fields from natural – life sciences (biology, medicine, chemistry), economics, applied sciences. It should ensure interdisciplinarity (Scholz & Tietje, 2002).

Different types of helix approach could be implemented: triple helix, quadruple helix or quintuple Helix (Carayannis & Campbell, 2014), see Fig. 6.

2nd dimension – Systems: dividing in subsystems, for example in environmental study can separate regions water, air, soil systems and their interlinkages. For stakeholders it is management, financial and equipment as individual systems or complex systems. Needs to be integrated and related to the soft factors – gives circumstances (Scholz & Tietje, 2002).

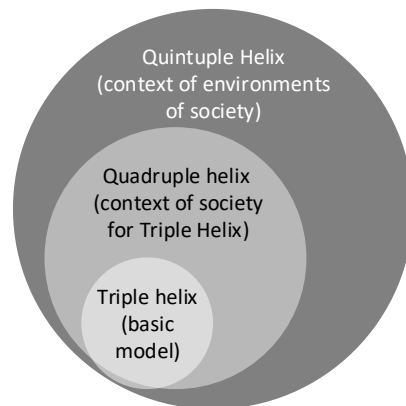


Figure 6. Helix approaches (Carayannis & Campbell, 2014).

3rd dimension Interests: Interests of research or practical perspective. For example different interests of farmers, residents, policy, different interests of stakeholders. Methods are socially integrating and mediating (Scholz & Tietje, 2002).

4th dimension Modes of thought; cognitive or epistemological perspective analysis or understanding. Methods that integrate different cognitive representations, for example experience of a farmer and the expertise of a scientist (Scholz & Tietje, 2002).

Transdisciplinary processes connects science with society, adapted Brunswikian Lens model (Scholz & Tietje, 2002) in Fig. 7 (Scholz et al., 2014), to adapt this processes for sustainable bioeconomy, that not only replace fossil resources with biobased

resources, but strengthens different disciplines, taken into account interlinkages, knowledge, and stakeholders and limitations set by planetary boundaries, different dimensions should be included in transition towards sustainable bioeconomy. Syntheses is application of methods of knowledge integration (Scholz & O.Tietje, 2002; Scholz et al., 2006).

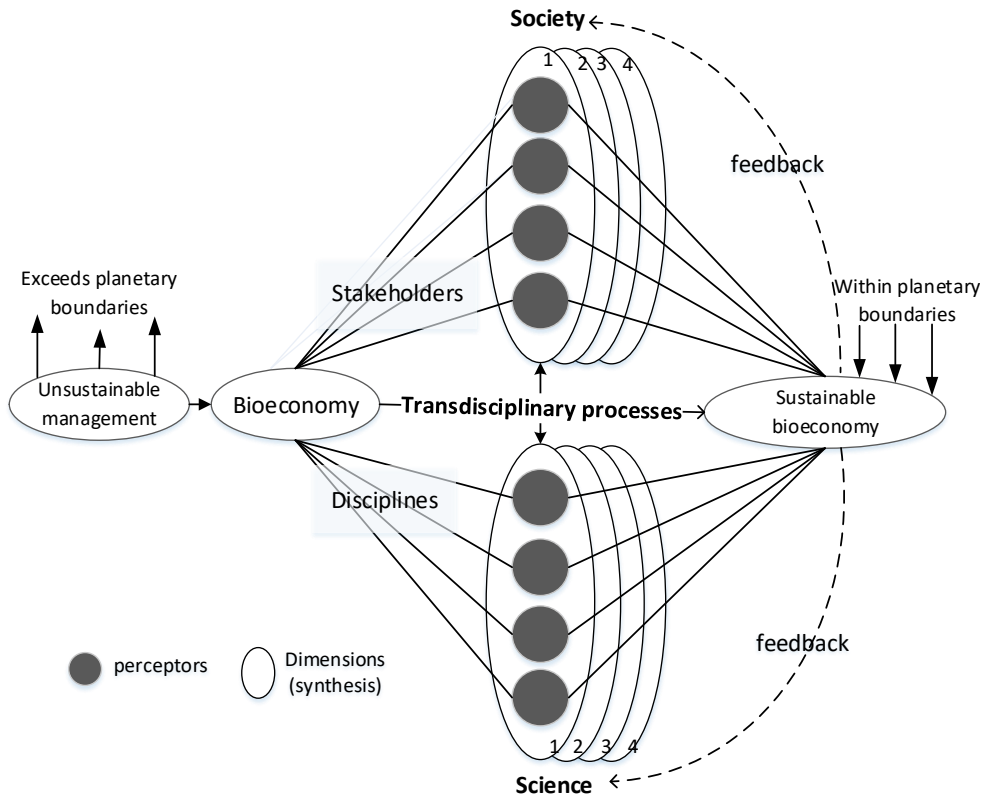


Figure 7. Transdisciplinary process towards sustainable bioeconomy (modified (Scholz et al., 2014)).

The concept of how to view and should act in order to achieve a transdisciplinary approach and outcome for sustainable bioeconomy development (Fig. 7). This type of approach can be used as a basis for developing the research issue into quantitative results, which would allow comparing the situation in different regions of the world and evaluating different development of scenarios, taking into account the views and actions of the various stakeholders. For example, this graphical representation can be used as a basis for creating a system dynamics model.

CONCLUSIONS

By carrying out critical analysis of literature on various bioeconomy perceptions, it was found that bioeconomy is essentially of transdisciplinary nature. An analysis of the understanding of transdisciplinary bioeconomy was also carried out to prove this. By interconnecting these two ideas that are not directly related to each other, an appropriate

approach to expressing the bioeconomics through transdisciplinarity using the Brunswikian Lens model was found.

Developed graphical representation is applicable to further case studies. Methods that is applicable to use in order to achieve best possible result, still need to evaluate and verify.

Further research in the context of bioeconomy should be carried out directly through the prism of transdisciplinary and a solution should be found to quantify this view.

It is clear that bioeconomy should be looked as complex system through transdisciplinary approach, but obstacles have to be determined.

Results from implementing holistic vision would provide practical benefit to policy makers and industry actors by providing an analysis how to improve industrial practice, policy and how more effectively transfer to sustainable bioeconomy by taking into account society opinion, easing practical implementation and transformation to sustainable bioeconomy.

ACKNOWLEDGEMENTS. This research is funded by the Latvian Council of science, Project 'Bioresources Value Model (BVM)', Project No. Izp-2018/1-426.

REFERENCES

- Aguilar, A., Bochereau, L. & Matthiessen, L. 2013. Biotechnology as the engine for the Knowledge- Based Bio-Economy. *Biotechnology and Genetic Engineering Reviews* **26**(1), 371–388. doi:10.5661/bger-26-371
- Ahn, M.J. 2012. High technology in emerging markets Building biotechnology clusters, capabilities and competitiveness in India. *Asia-Pacific Journal of Business* **4**(1), 23–41. doi:10.1108/17574321211207953
- Bergendahl, J.A., Sarkis, J. & Timko, M.T. 2018. Transdisciplinarity and the food energy and water nexus: Ecological modernization and supply chain sustainability perspectives. *Resources, Conservation and Recycling* **133**, 309–319. doi:10.1016/j.resconrec.2018.01.001
- Bugge, M.M., Hansen, T. & Klitkou, A., 2016. What is the bioeconomy? A review of the literature. *Sustainability* **8**(7), 691. doi.org/10.3390/su8070691
- Carayannis, E.G. & Campbell, D.F.J. 2014. Developed democracies versus emerging autocracies: arts, democracy, and innovation in Quadruple Helix innovation systems. *Journal of Innovation and Entrepreneurship* **3**(12). doi:10.1186/s13731-014-0012-2
- Colpaert, J. 2018. Transdisciplinarity revisited. *Computer Assisted Language Learning* **8221**, 1–7. doi:10.1080/09588221.2018.1437111
- Golembiewski, B., Sick, N. & Bröring, S. 2015. The emerging research landscape on bioeconomy: What has been done so far and what is essential from a technology and innovation management perspective? *Innovative Food Science and Emerging Technologies* **29**, 308–317. doi:10.1016/j.ifset.2015.03.00
- Heo, J., Kang, H., Sang, B., Kim, Y., Min, J., Mitchell, R.J. & Hyung, J. 2016. Bioresource Technology Feasibility of a facile butanol bioproduction using planetary mill pretreatment. *Bioresource Technology* **199**, 283–287. doi:10.1016/j.biortech.2015.08.074
- Jahn, T., Bergmann, M. & Keil, F. 2012. Transdisciplinarity: Between mainstreaming and marginalization. *Ecological Economics* **79**, 1–10. doi:10.1016/j.ecolecon.2012.04.017
- Klein, J.T. 2008. Evaluation of Interdisciplinary and Transdisciplinary Research. A Literature Review. *American Journal of Preventive Medicine* **35**(2 SUPPL), pp. 116–123.

- Lainez, M., González, J.M., Aguilar, A. & Vela, C. 2018. Spanish strategy on bioeconomy: Towards a knowledge based sustainable innovation. *New Biotechnology* **40**, 87–95. doi:10.1016/j.nbt.2017.05.006
- Lewandowski, I. 2017. *Bioeconomy: Shaping the transition to a sustainable, biobased economy*. eBook, Springer International Publishing AG. doi:10.1007/978-3-319-68152-8
- Mace, G.M., Reyers, B., Alkemade, R., Biggs, R., Jennings, S., Leadley, P., Chapin, F.S., Cornell, S.E., Di, S., Mumby, P.J., Purvis, A., Scholes, R.J., Seddon, A.W.R., Solan, M., Steffen, W. & Woodward, G. 2014. Approaches to defining a planetary boundary for biodiversity. *Global Environmental Change* **28**, 289–297. doi:10.1016/j.gloenvcha.2014.07.009
- Muizniece, I., Kubule, A. & Blumberga, D. 2018. Towards understanding the transdisciplinary approach of bioeconomy nexus. *Energy Procedia* **147**, 175–180. doi:10.1016/j.egypro.2018.07.052
- OECD, 2009. The Bioeconomy to 2030 Main Findings and Policy Conclusions.
- Pohl, C. & Hadorn, G.H. 2008. Methodological challenges of transdisciplinary research. *Natures sciences societies* **16**, 111–121. doi:10.1051/nss
- Roux, D.J., Stirzaker, R.J., Breen, C.M., Lefroy, E.C. & Cresswell, H.P. 2010. Framework for participative reflection on the accomplishment of transdisciplinary research programs. *Environmental Science and Policy* **13**(8), 733–741. doi:10.1016/j.envsci.2010.08.002
- Scholz, R.W. & Tietje, O. 2002. Embedded case study methods Integrating quantitative and qualitative knowledge. *International Journal of Sustainability in Higher Education* **7**(3), 352–356. doi.org/10.1108/14676370610677892
- Scholz, R.W., Lang, D.J., Wiek, A., Walter, A.I., Stauffacher, M., Scholz, R.W., Lang, D.J., Wiek, A., Walter, A.I., Stauffacher, M., Scholz, R.W., Lang, D.J., Wiek, A., Walter, A.I. & Stauffacher, M. 2006. Framework and theory Transdisciplinary case studies as a means of sustainability learning Historical framework and theory. *International Journal of Sustainability in Higher Education* **7**(3), 226–251. doi:10.1108/14676370610677829
- Scholz, R.W., Roy, A.H., Hellums, D.T., Ulrich, A.E. & Brand, F.S. 2014. Sustainable phosphorus management: A global transdisciplinary roadmap. *Sustainable Phosphorus Management: A Global Transdisciplinary Roadmap*. eBook, Springer Dordrecht Heidelberg, New York London. doi:10.1007/978-94-007-7250-2
- Scholz, R.W. 2017. The normative dimension in Transdisciplinarity, Transition Management, and Transformation Sciences: New roles of science and universities in sustainable transitioning. *Sustainability* **9**(6), 991. doi.org/10.3390/su9060991
- Scholz, R.W. & Marks, D. 2001. Learning about transdisciplinarity : Where are we? Where have we been? Where should we go? *Transdisciplinarity: Joint Problem Solving among Science, Technology, and Society*. eBook, pp. 236–237. https://doi.org/10.1007/978-3-0348-8419-8_17
- Schütte, G. 2018. What kind of innovation policy does the bioeconomy need? *New Biotechnology* **40**, 82–86. Available at: https://doi.org/10.1016/j.nbt.2017.04.003
- Stirling, A. 2015. Developing ‘Nexus Capabilities’: towards transdisciplinary methodologies. *Transdisciplinary Methods for Developing Nexus Capabilities*. Report of a workshop held at the University of Sussex June 29 and 30.
- Stockholm Resilience Centre, The nine planetary boundaries - Stockholm Resilience Centre. Available at: https://www.stockholmresilience.org/research/planetary-boundaries/planetary-boundaries/about-the-research/the-nine-planetary-boundaries.html [Accessed February 15, 2019].
- Woźniak, E. & Twardowski, T. 2018. The bioeconomy in Poland within the context of the European Union. *New Biotechnology* **40**(1), 96–102.
- Zierhofer, W. & Burger, P. 2007. Disentangling Transdisciplinarity: An Analysis of Knowledge Integration in Problem-Oriented Research. *Science Studies* **20**(1), 51–74.

Optimization of cattle by-products amino acid composition formula

O. Zinina^{1,*}, S. Merenkova¹, M. Rebezov², D. Tazeddinova¹,
Z. Yessimbekov³ and V. Victoris⁴

¹South Ural State University (National Research University), Lenin Avenue 76, RU454080 Chelyabinsk, Russia

²Ural State Agrarian University, Karl Liebknecht 42, RU620075 Ekaterinburg, Russia

³Shakarim State University of Semey, Glinki street 20a, KZ071400 Semey, Kazakhstan

⁴Slovak University of Agriculture in Nitra, Hlinku 2, SK94901 Nitra, Slovakia

*Correspondence: zininaov@susu.ru

Abstract. The aim of this research was to develop optimal formulations of by-product mixtures in terms of biological value using MS Excel Solver standard software application. The objects of study were underutilized cattle by-products as tripe, ears, lips, lungs, and heart. Physical and chemical studies were carried out to compile a database of the by-products used. As a result, the protein content was 14.3% in tripe, 24.6% in lips, 24.9% in ears, 15.2% in lungs, and 16.8% in heart ($P < 0.05$). The content of essential amino acids in various by-products, determined by high-performance liquid chromatography, did not have significant differences compared with the results obtained by other researchers. While conducting optimization of the by-product formulation, focused on the physiologically-based content of the essential amino acids in the 'ideal' protein according to the Food and Agriculture Organization of the United Nations and the World Health Organization (FAO/WHO). Essential amino acids index (EAAI) was chosen as the goal function. In the process of optimization, indicators such as chemical score, EAAI, biological value, and coefficient of amino acid score differences (CAASD) were calculated. Several variants of the formulations with high biological value were obtained as a result of the optimization. According to the results of the research it was found that more balanced ratio of the essential amino acids was in the following formulations: 1 – tripe (4.9%), ears (28.4%) and heart (66.7%) or 2 – ears (25.4%), lips (8.9%) and heart (65.7%). According to the results, the highest *in vitro* protein digestibility was in compositions number 1 and 2 (78.2% and 76.8%), which correlated with the calculated biological value. Thus, the use of computer modeling allowed obtaining the formulations of the by-products composition with the highest possible biological value by varying the content of the various by-products.

Key words: biological value, amino acid, optimization, by-product.

INTRODUCTION

During the slaughter of farm animals, large quantities of by-products such as bone, blood, skin, offal, etc., are produced. According to various scientific data, on average, the output of by-products is about 40% of cattle live weight, 50% of sheep and goats, 30% of pigs and poultry live weight, and 35% of lambs live weight (Smith, 1993;

Vernooij, 2012). According to Ockerman & Basu (2004) the yield of offal ranges from 10 to 30% of the live weight of pigs and cattle, respectively. Processing and recycling of by-products possess a problem from an economic and environmental point of view (Jayathilakan et al., 2012; Toldrá et al., 2016). However, these can be an additional source of food and make up for the deficit of animal protein. One of the main problems in feeding the world's growing population is a lack of protein foods, which is seen as especially urgent in developing countries (Subba, 2002). Due to the high cost of meat, meat organs, referred to as 'offal' or the 'fifth quarter', are an alternative source of animal origin nutrients (Bester et al., 2018). Therefore, more attention should be paid to the possibility of using animal proteins, including those which are contained in by-products (Van Heerden & Morey, 2014; Bester et al., 2018).

By-products are of high value as a source of cheap protein. They are important for the majority of developing countries which are very poor. Here, offal is a staple food in the diets of many people (Jayathilakan et al., 2012). For instance, the consumption of offal in Turkey and India is higher than in most other countries (Jayathilakan et al., 2012; Coskuntuna et al., 2015). Offal is widely used in food in South Africa (Van Heerden & Morey, 2014). Offal is quite varied in regards to composition and functionality, most of it contains a good amount of nutrients such as essential amino acids, minerals and vitamins (Aristoy, 2011; Honikel, 2011). Most by-products are characterized by good digestibility of proteins. Spleen, kidney, lungs and tripe proteins have the highest rate of digestibility (in vitro); hearts, udders and tongue proteins have a medium rate; meat heads and lips proteins have the lowest rate (Anonymous, 1985). Despite high nutritional value, usage of by-products in the composition of meat products is often limited due to variations in composition or functionality and unattractive organoleptic qualities (Smith, 1993). Offal consumption and utilization in meat processing sausage-type products or traditional dishes may be increased (Florek et al., 2012).

Offal with a high content of connective tissue proteins are promising for producing hydrolysates of these proteins and compositions for the production of the antioxidant peptides (Aristoy, 2011; Lasekan et al., 2013; Mora et al., 2014). For example, a collagen composition, protein-collagen emulsion, protein concentrate is widely used as a protein component in production of sausages and ready-to-eat products (Kurt & Zorba, 2007; Kalenik et al., 2017). Protein hydrolysates from meat by-products are an interesting alternative to soy products due to the lack of allergenic proteins and the presence of large amounts of all essential amino acids (Martínez-Alvarez et al., 2015).

The need for improving the use of food by-products to reduce food waste is noted (Government Office for Science, 2011). One of the ways to solve the problem of protein deficiency mentioned by Sun-Waterhouse et al. (2014) is to increase the economic efficiency of using proteins from raw materials, including by-products, and to improve the functionality of protein ingredients through modification. The application of appropriate processing, such as enzymatic hydrolysis, thermal treatment, dehydration, emulsification, and ultrafiltration contributes to obtaining modified substances and proteins, which are considered value-added food ingredients (Mora et al., 2014; Sun-Waterhouse et al., 2014).

The search for alternative protein sources has advanced in recent years and provides a relevant approach to meeting global protein requirements. Given the above, it can be concluded that by-products, including offal, are a source of animal protein and can be used directly in food or modified into certain protein substances.

It has been proved that offal is a good source of essential and limiting amino acids. However, some by-products such as ears, feet, or lips are rich in connective tissue, which is mainly composed by glycine, proline and alanine. This lack of essential amino acids can be overcome by blending ingredients to achieve a balanced amino acid profile in the final product (Mullen & Álvarez, 2016).

Many researchers recommend using methods of linear and experimental-statistical programming to obtain a multi-component products with a balanced composition (Musina & Lisin, 2012; Nadtochii, 2013; Musina & Lisin, 2015; Lisitsyn et al., 2016).

The problem of designing recipes with a large number of components while achieving the required quality indicators is quite difficult without using the software. Manual solution the system of linear equations and inequalities with a considerable number of variables is a significant difficulty, at which the probability of calculation errors is high (Musina & Lisin, 2012; Musina & Lisin, 2015). One of the most commonly used criteria for optimality in the development of product formulations is the biological value. Zhackslykova et al. (2014) proposed to use various indicators of the biological value of protein (amino acid score, index Osera, essential amino acid index, PDCAAS) as optimality criteria in the development of meat products formulations with the addition of by-products. Satina & Yudina (2010) developed a methodology for the designing meat products formulations based on the modeling of amino acid and fatty acid compositions. Nadtochii (2013) proposed to simulate the biological value of the protein component of a multi-component product using standard add-in Solver processor spreadsheet Microsoft Excel.

The aim of the research was to develop optimal formulations of by-product mixtures in terms of biological value using MS Excel Solver standard software application.

MATERIALS AND METHODS

Optimization of the formulation of by-product composition

Cattle by-products such as lungs, tripe, ears, lips and heart were selected as starting components of the formulation composition. These by-products were obtained after slaughtering 6 cows of Holstein-Friesian at the age of three years.

Construction of a multi-component by-product composition was produced using SOLVER standard software of Microsoft Excel 2013. The calculation of the formulation consisted of several steps: compiling a data bank and balance equations for the amino acid composition, defining the objective function to optimize formulations, solving the problem by using the tool SOLVER, and analyzing and selecting a recipe appropriate for the goal. To compile a data bank on by-product amino acid composition, the content of essential amino acids was experimentally found in the studied by-products by High Performance Liquid Chromatography (HPLC).

Essential amino acid index (EAAI), which is defined as the average geometric ratio of each amino acid in test protein to its quantity in the whole egg protein according to Oser method (1951), was selected as the goal function:

$$EAAI = \sqrt[n]{a_1 \times a_2 \times \dots \times a_n} \quad (1)$$

where a_n is the ratio of the amount of each essential amino acid in the investigated protein to its amount in the whole egg protein and n is the amount of EAA ($n = 8$).

The basic indicators and criteria such as coefficient of amino acid score differences (CAASD) and biological value (BV) were used to evaluate the food adequacy and the most important protein components (Lipatov, 1995).

The indicators of biological value were calculated in the following sequence:

4. Chemical score (amino acid score (AAS) was calculated using the following formula [FAO/WHO, 1990]

$$AAS = \frac{EAA\text{ in test protein}}{total\ EAA\text{ in test protein}} \times \frac{total\ EAA\text{ in egg}}{EAA\text{ in egg}} \times 100 \quad (2)$$

5. The CAASD (%) shows that the average value of EAA amino acid score is excessive as compared to the lowest level of any essential amino acid.

CAASD was calculated, %, applying the formula:

$$CAASD = \sum \frac{\Delta AASD}{n} \quad (3)$$

where n is the amount of the essential amino acid ($n = 8$).

Amino acid score difference (AASD), %, was calculated according to the formula:

$$\Delta AASD = C_i - C_{\min} \quad (4)$$

where C_i – amino acid excess and C_{\min} is the minimal amino acid score of the test protein against the ideal protein, %.

6. Biological value (BV), %, was calculated according to the formula:

$$BV = 100 - CAASD, \quad (5)$$

7. Nutritional index (NI) NI was calculated using the formula:

$$NI = \frac{EAAI \times \% \text{ protein}}{100} \quad (6)$$

8. Computed protein efficiency ratio (C-PER) was calculated according to the formula:

$$C - PER = -2.107 + 7.1312 \times SPC - 2.5188 \times SPC^2 \quad (7)$$

where SPC is the EAA score ratio of sample to casein.

Preparation of samples for hydrolysis

The by-products were removed through 30 min after slaughtering. The by-products were washed under running tap water to remove blood clots and trimmed of the visible fatty and connective tissue. The treated by-products were packed individually in polyethylene bags, transported to the laboratory and stored at 4 °C during 48 h and then were chopped in a meat grinder (Fimar 32/RS Unger, Italy) with a plate having 3 mm diameter holes. After that, an average sample for each by-product was formed. To carry out hydrolysis, 100 mg of the by-product was taken from the sample and placed in glass ampoules with a tapered end. Then, 10 mL of a 6 M solution of hydrochloric acid was added. Subsequently, the mixture was thoroughly stirred and blown with a stream of nitrogen for 2 min. The glass ampoules were sealed and placed into a thermostat. Hydrolysis was carried out at 110 °C for 24 h. After cooling, the hydrolysates were filtered through membrane filters with 0.45 μm pore diameter, and 0.5 mL aliquots were taken. The aliquots were dried at 65 °C in a stream of air. Afterwards, 0.10 mL of 0.15 M NaOH solution was added to the dried aliquots and thoroughly mixed. Then, 0.35 mL of

phenyl isothiocyanate solution in isopropanol was added to the resulting mixture and stirred. The solution obtained after filtration was subjected to chromatographic analysis. The concentration of amino acids in the samples was calculated depending on the protein content in gram per 100 g of the product. The protein content of the by-products was determined using the Kjeldahl method (AOAC 2000, Method No. 988.05).

Determination of by-product amino acid composition

Determination of amino acids was carried out on a HPLC SHIMADZU LC-20 Prominence (Japan) with fluorimetric and spectrophotometric detectors. We used the chromatographic column 25 cm × 4.6 mm SUPELCO C18, 5 μm (USA) with the precolumn to protect the main column from impurities. The chromatographic analysis was carried out in eluent gradient mode at a flow rate of 1.2 mL min⁻¹ and the column thermostat temperature of 40 °C. The measurement was performed by HPLC on a reversed phase column with fluorimetric and spectrophotometric detectors at wavelengths of 246 and 260 nm using acid hydrolysis and amino acid modification by phenylisothiocyanate solution in isopropanol to obtain phenylthiohydantoin. A mixture of 6.0 mM CH₃COONa solution at pH 5.5 (component A), 1% isopropanol in an acetonitrile solution (component B), and a 6.0 mM CH₃COONa solution at pH 4.05 (component C) was used as a mobile phase. We used standard samples of amino acids produced by Sigma Aldrich (Germany).

Preparation of samples for *in vitro* digestibility

Compositions were prepared from the ground by-products according to the data obtained during the optimization. By-products were thoroughly mixed and formed into meatballs weighing 11 ± 1 g each. The meatballs were cooked in the air-o-steam (Rational AQ, mod. SCC 61, Germany) at 80 ± 2 °C until the core temperature reached 70 °C (Wen et al., 2015).

***In vitro* digestibility**

Cooked meatballs were ground, then 500 mg samples were taken and homogenized with 2 mL of distilled water to determine digestibility, as described by Wen et al. (2015) with slight modification. The homogenate was suspended in 15 mL 0.1 N HCl containing 8 mg pepsin and incubated for 2 h at pH 2.0, temperature 37 ± 1 °C with continuous shaking.

The resultant suspension was neutralized with 0.2 N NaOH and treated with 15 mg trypsin in 15 mL of phosphate buffer (0.2 M, pH 8.0). The mixture was shaken for 24 h at 37 ± 1 °C. After that, the enzyme was inactivated by the addition of 10 mL 10% trichloroacetic acid.

The mixture was then filtered using ashless filter paper (MN 640 m), and the precipitate was washed with distilled water (1:10, w/v), air-dried, and used for protein determination by Kjeldahl method.

In vitro protein digestibility (IVPD) was calculated using the following formula:

$$IVPD(\%) = \frac{P_b - P_a}{P_b} \times 100, \quad (8)$$

where P_b – protein content of sample before digestion, %; P_a – protein content of sample after digestion, %.

Statistical Analysis

The values are presented as the mean \pm SEM. Probability values ≤ 0.05 were taken to indicate statistical significance. The data were analyzed by One-Way ANOVA using free web-based software offered by Assaad et al. (2014).

RESULTS AND DISCUSSION

Modelling and optimization of multi-component composition of food products require considerable time, so it is appropriate to use modern computer technologies. Microsoft Excel provides great opportunities for calculating recipes of multicomponent food compositions. One tool for solving optimization problems is the standard add-on SOLVER of Microsoft Excel program spreadsheets included in Microsoft Office. In terms of functionality, the added SOLVER Excel application is not inferior to analogous special mathematical programs, for example MathCAD. Other things being equal, Excel is characterized by interface simplicity (Nadtochii, 2013).

One of the most important factors in designing new food formulations is protein biological value which was determined by balanced amino acid composition. The human body is able to produce 10 out of 20 amino acids. Shortage of even one essential amino acid results in an inability to synthesize proteins and other biological substances (Feiner, 2006).

In this regard, we carried out the formulation optimization in what concerns the biological value of the feedstock, in particular the content of the essential amino acids.

Optimization of the formulation was carried out in relation to the recommended values of the essential amino acids content in the 'ideal' (standard) protein according to the Food and Agriculture Organization FAO/WHO (1990).

We entered the data on amino acid composition expressed in gram of EAA per 100 g of protein into Excel calculation sheet to get balance equations (Fig. 1). Table 1 presents the protein and amino acids contents (mg amino acid per 100 g product) obtained by chromatographic determination.

=ПРОИЗВЕД(D9/D10,E9/E10,F9/F10,G9/G10,H9/H10,I9/I10,J9/J10,K9/K10)/Y1/8)**100												
	A	B	C	D	E	F	G	H	I	J	K	L
1												
2				The content of amino acids (g amino acid/ 100 g protein)								
3	Ingredients	Designation	Mass of raw materials, ppm	Valine	Isoleucine	Leucine	Lysine	Methionine + Cystine	Threonine	Tryptophan	Phenylalanine+Tyrosine	
4	tripe	x1	0.049	3.92	3.43	6.12	5.82	1.58	3.62	0.91	5.86	
5	lungs	x2	0.000	5.56	3.65	8.46	6.24	2.08	3.54	0.78	9.17	
6	ears	x3	0.284	3.48	2.08	4.16	4.18	1.67	2.18	0.52	3.86	
7	lips	x4	0.000	3.52	3.12	5.74	6.38	1.92	3.08	0.74	5.68	
8	heart	x5	0.667	6.12	4.86	8.82	7.94	4.42	4.92	1.36	8.24	
9			1	5.26	4.00	7.36	6.77	3.50	4.08	1.10	6.88	
10	FAO/WHO			5.00	4.00	7.00	5.50	3.50	4.00	1.00	6.00	
11	Chemical score, %			105.2	100.0	105.2	123.1	100.0	101.9	109.9	114.6	
12	Coefficient of amino acid score differences (CAASD), %											7.5
13	calculated Biological value (BV)											92.5
14	Essential amino acid index (EAAI), %											107.2

Figure 1. Example of the calculation sheet in Excel.

Table 1. By-product indicators*

Indicators	ears	heart	lips	lungs	tripe
EAA, (mg per 100 g product)					
Valine	864 ± 5.44 ^{bc}	1030 ± 4.35 ^a	852 ± 5.40 ^c	878 ± 7.07 ^b	558 ± 6.58 ^d
Isoleucine	516 ± 3.07 ^d	819 ± 4.41 ^a	755 ± 6.88 ^b	554 ± 3.02 ^c	487 ± 3.77 ^e
Leucine	1030 ± 6.94 ^d	1490 ± 15.10 ^a	1390 ± 19.10 ^b	1290 ± 8.86 ^c	872 ± 5.26 ^e
Lysine	1040 ± 5.39 ^c	1340 ± 8.26 ^b	1540 ± 11.00 ^a	947 ± 6.59 ^d	829 ± 5.23 ^e
Methionine + Cystine	415 ± 4.53 ^c	745 ± 5.41 ^a	464 ± 5.55 ^b	316 ± 4.60 ^d	224 ± 3.70 ^e
Threonine	541 ± 7.09 ^c	830 ± 3.03 ^a	746 ± 5.37 ^b	537 ± 6.95 ^{cd}	516 ± 2.52 ^d
Tryptophan	129 ± 3.05 ^c	229 ± 3.04 ^a	179 ± 5.49 ^b	118 ± 2.81 ^c	129 ± 3.27 ^c
Phenylalanine+Tyrosine	958 ± 5.57 ^b	1390 ± 8.22 ^a	1380 ± 10.10 ^a	1390 ± 5.51 ^a	836 ± 3.01 ^c
Protein, %	24.9 ± 0.314 ^a	16.8 ± 0.074 ^b	24.6 ± 0.146 ^a	15.2 ± 0.138 ^c	14.3 ± 0.200 ^d

*Values are means ± SEM, n = 5 per treatment group. Means in a row without a common superscript letter differ statistically ($P < 0.05$) as analyzed by One-Way ANOVA and the TUKEY test.

We introduced the following designations of the ingredients used: X_1 – mass fraction of tripe, X_2 – mass fraction of lungs, X_3 – mass fraction of ears, X_4 – mass fraction of lips, X_5 – mass fraction of heart.

The balance equation prepared in accordance with the established requirements:

- 1) $5.0 \leq (3.92 \times X_1 + 5.56 \times X_2 + 3.48 \times X_3 + 3.52 \times X_4 + 6.12 \times X_5)$ – content of Valine;
- 2) $4.0 \leq (3.43 \times X_1 + 3.65 \times X_2 + 2.08 \times X_3 + 3.12 \times X_4 + 4.86 \times X_5)$ – content of Isoleucine;
- 3) $7.0 \leq (6.12 \times X_1 + 8.46 \times X_2 + 4.16 \times X_3 + 5.74 \times X_4 + 8.82 \times X_5)$ – content of Leucine;
- 4) $5.5 \leq (5.82 \times X_1 + 6.24 \times X_2 + 4.18 \times X_3 + 6.38 \times X_4 + 7.94 \times X_5)$ – content of Lysine;
- 5) $3.5 \leq (1.58 \times X_1 + 2.08 \times X_2 + 1.67 \times X_3 + 1.92 \times X_4 + 4.42 \times X_5)$ – content of Methionine and Cystine;
- 6) $4.0 \leq (3.62 \times X_1 + 3.54 \times X_2 + 2.18 \times X_3 + 3.08 \times X_4 + 4.92 \times X_5)$ – content of Threonine;
- 7) $1.0 \leq (0.91 \times X_1 + 0.78 \times X_2 + 0.52 \times X_3 + 0.74 \times X_4 + 1.36 \times X_5)$ – content of Tryptophan;
- 8) $6.0 \leq (5.86 \times X_1 + 9.17 \times X_2 + 3.86 \times X_3 + 5.68 \times X_4 + 8.24 \times X_5)$ – content of

Phenylalanine and Tyrosine;

- 9) $(X_1 + X_2 + X_3 + X_4 + X_5) = 1$ – the sum of the mass fractions of the components.

- 10) We introduced the following requirement for the goal function: $EAAI \geq 100$.

While running the tool SOLVER in a window, we entered the set of parameters. The objective of the program is to determine the optimum ratio of the components for which EAAI reaches 100% under these limitations.

The program offers multiple combinations of the ingredients (Fig. 1) which satisfy the expected requirements for the biological value of the composition and at the same time present the results of the calculated CAASD and BV.

The proposed program of formulation compositions and their biological value indices is presented in Table 2.

The content of protein in our samples of beef lungs was 15.2% ($P < 0.05$), which is similar to the content determined by Skurikhin & Volgarev (1987), but differs from the data obtained by Seong et al. (2014) in the study of Hanwoo cattle offal ($17.64 \pm 0.72\%$). The amount of protein in 100 g raw beef heart have been reported as 16.0 g (Skurikhin & Volgarev, 1987) or 14.9–28.5 g (Ockerman & Basu, 2004) and also $18.62 \pm 0.53\%$ (Seong et al., 2014). We found that beef heart contained 16.8 g of protein ($P < 0.05$). Florek et al. (2012) determined the protein content in veal calves heart is 18.74 ± 0.30 (g (100 g)⁻¹) ($P \leq 0.05$).

The amino acid composition of the different offal varies widely. For example, the content of valine in tripe (558 mg per 100 g product) is approximately 2 times less than in heart (1,030 mg per 100 g product). The content of lysine in lips (1,540 mg per 100 g product) is more than in other by-products, the content of leucine and isoleucine in lips is close to the parameters for heart (Table 1).

According to Skurikhin & Volgarev (1987), the content of valine, leucine, and threonine in the beef heart is slightly lower than that determined by us: 911 mg in 100 g product against 1,030 mg, 1,408 mg in 100 g against 1,490 mg, and 740 mg in 100 g against 830 mg. Data on the content of isoleucine and tryptophan in 100 g product are similar: 838 mg per 100 g product against 819 mg and 222 mg 100 g⁻¹ product against 229 mg. The content of methionine in the Hanwoo cattle heart was 3.8 g 100 g⁻¹ of protein (Seong et al., 2014), while we have determined the content of sulfur-containing amino acids methionine and cystine 4.42 g 100 g⁻¹ of protein (Fig. 1). The content of methionine in the lungs determined by Cardoso-Santiago & Areas (2001) was 2.38 g 100 g⁻¹ of protein.

The results of chromatographic analysis showed the highest content of essential amino acids – lysine, methionine and tryptophan in the heart and lips, slightly lower content of these amino acids noted in the ears and lungs. While Venegas Fornias (1996) identified that in the heart of cattle, these three amino acids were found in an amount of 8.2 g, 2.6 and 1.1 g 100 g⁻¹ of protein, and in the lungs – 7.1, 2.0 and 0.9g 100 g⁻¹ of protein, respectively. The amount of lysine and methionine in present study were slightly lower (6.24 and 2.08 g 100 g⁻¹ of protein) than the values reported by Cardoso-Santiago & Areas (2001) – 7.07 and 2.38 g 100 g⁻¹ of protein for bovine lungs.

In determining the indicators of biological value, it is important to identify the limiting amino acid, the amino acid score of which is less than 100%. However, in compliance with the limitations in all the compositions offered by the program, there is no limiting amino acid, which indicates that they have high biological value. There is a small difference in amino acid score in relation to the ideal protein in various variants of the compositions. For variants 1, 2 and 4 – the content of isoleucine, methionine and cysteine is equal to the value of the ideal protein, threonine content slightly exceeds the value of the ideal protein. For variant 3 – methionine and cysteine content is close to the values of the ideal protein and the content of other essential amino acids exceeds the ideal protein range by 9% to 35% value. According to the results of biological value calculation, a more balanced ratio of the essential amino acids variants of the compositions 1 and 2 was achieved. The third variant of the composition is characterized by the excessive content of lysine, phenylalanine and tyrosine (Table 2).

Offal is a good source of essential amino acids, in particular such limiting amino acids as lysine, methionine and tryptophan, noted by Mullen et al. (2017). The amino acid composition of offal differs from that of muscle tissue due to the great quantity of connective tissue (Unsal & Aktas, 2003). Seong et al. (2014) noted that the differences in levels and quality of amino acid contents may be attributed due to the differences in protein types between the by-products. According to report, such by-products as ears, legs, lungs, and stomach contain large amounts of proline, hydroxyproline, and glycine as well as lower levels of tryptophan and tyrosine (Jayathilakan et al., 2012). However, when the by-products are combined it is possible to obtain more biologically valuable protein compositions. Aristoy (2011) reported that levels of the essential amino acids in

meat by-products is slightly reduced after cooking or heating treatment due to the low-reducing sugar content of these by-products.

Table 2. Biological value indicators of by-products compositions

Indicators	Value			
	Variant 1	Variant 2	Variant 3	Variant 4
Recipe ingredients content, %				
tripe	4.9	-	-	-
lungs	-	-	22.5	1.9
ears	28.4	25.4	0.3	26.3
lips	-	8.9	13.7	6.1
heart	66.7	65.7	63.5	65.7
Content of EAA, g per 100 g protein				
Valine	5.26	5.22	5.63	5.26
Isoleucine	4.00	4.00	4.34	4.00
Leucine	7.36	7.36	8.31	7.40
Lysine	6.77	6.85	7.33	7.82
Methionine + Cystine	3.50	3.50	3.54	3.50
Threonine	4.08	4.06	4.35	4.06
Tryptophan	1.10	1.09	1.14	1.09
Phenylalanine + Tyrosine	6.88	6.90	8.09	6.95
EAAI, %	107.5	107.5	116.5	107.7
CAASD, %	7.5	7.5	14.4	7.7
Calculated BV, %	92.5	92.5	85.6	92.3
Nutritional index	20.4	20.9	20.4	20.9
C-PER	1.986	1.986	2.095	1.667
IVPD, %	78.2	76.8	68.6	76.3

According to the results, the highest *in vitro* protein digestibility was in compositions number 1 and 2 (78.2% and 76.8%), which correlated with the calculated biological value (Table 2). The third composition was characterized by the lowest *in vitro* protein digestibility – 68.6% ($P < 0.05$), due to the higher content of collagen in this composition compared to other compositions. Wen et al. (2015) detected that the digestibility of pork by pepsin is significantly higher than of beef – 47.22% against 42.75% ($P < 0.05$). The authors explain this by the fact that raw meat contain different levels of collagen. However, digestibility of pork and beef by pepsin and trypsin was not significantly different ($P > 0.05$). However, connective tissue proteins can be hydrolyzed using an acid, alkali, or enzymes to produce hydrolysates, peptides, and amino acids containing a short chain, which are digested well by the human body (Sun-Waterhouse et al., 2014).

CONCLUSIONS

A technique of developing and optimization of by-product composition on indicators of biological value was described in the work. It is obvious that amino acid composition depends on the type of the by-products and the animal species from which they are derived. Computer modeling allowed obtaining the formulation of by-product

composition with the highest possible biological value by varying the content of the by-products in a short time.

Optimization of by-products composition using MS Excel Solver standard software applications allowed obtaining a more balanced ratio of the essential amino acids in the following formulations: 1 – tripe (4.9%), ears (28.4%) and heart (66.7%) or 2 – ears (25.4%), lips (8.9%) and heart (65.7%). According to the results, the highest biological value and *in vitro* protein digestibility were established in these compositions. The obtained by-product compositions may be used as a meat product component or as a separate product after pre-treatment (thermal, enzymatic, mechanical, and other processing).

ACKNOWLEDGEMENTS. New scientific cooperation and research was performed by project VEGA 1/0280/17: Validation of Functional Food Development by Sensory Analysis and Artificial Perception Devices.

The work was also supported by Act 211 Government of the Russian Federation, contract No. 02.A03.21.0011.

The authors thank the staff of the accredited regional engineering laboratory, Scientific Center of Radioecological Research of Shakarim State University of Semey, for their help with analysis, as well as the reviewers for valuable comments in preparing this article.

REFERENCES

- Anonymous. 1985. Animal by-products. Their use in animal nutrition. *Feed Compounder* **5**(10), 15–16.
- Aristoy, M.C. 2011. Essential amino acids. In: Nollet, L.M.L., Toldrá, F. (ed.): Handbook of analysis of edible animal by-products. CRC Press, Boca Raton FL, USA, pp. 123–135.
- Assaad, H., Zhou, L., Carroll, R.J. & Wu, G. 2014. Rapid publication-ready MS-Word tables for one-way ANOVA. *Springer Plus* **3**, 474, 8 p. <https://doi.org/10.1186/2193-1801-3-474>
- Bester, M., Schönfeldt, H.C., Pretorius, B. & Hall, N. 2018. The nutrient content of selected South African lamb and mutton organ meats (offal). *Food Chem* **238**, 3–8.
- Cardoso-Santiago, R.A. & Areas, J.A.G. 2001. Nutritional evaluation of snacks obtained from chickpea and bovine lung blends. *Food Chem.* **74**, 35–40.
- Coskuntuna, L., Gecgel, U., Yilmaz, I., Gecgel, U. & Dulger, G.C. 2015. Investigating Fatty Acid Composition of Samples were Homogenized Various Meat and Offal Products from Turkey. *J. Am Oil Chem. Soc.* **3**, 659–665.
- FAO/WHO. 1990. Energy and protein requirements Report of joint FAO/ WHO/UNU Expert Consultation Technical Report. FAO/WHO and United Nations University, Geneva, Series 724, pp.116–129.
- Feiner, G. 2006. *Meat products handbook*. Cambridge: Wood Head Publishing Limited, 671 pp.
- Florek, M., Litwińczuk, Z., Skąlecki, P., Kędzierska-Matysek, M. & Grodzicki, T. 2012. Chemical composition and inherent properties of offal from calves maintained under two production systems. *Meat. Sci.* **90**, 402–409.
- Government Office for Science. 2011. The future of food and farming: Challenges and choices for global sustainability. London: The Government Office for Science.
- Honikel, K.O. 2011. *Composition and calories*. In: Nollet, L.M.L., Toldrá, F. (ed.): Handbook of analysis of edible animal by-products. CRC Press, Boca Raton FL, USA, pp. 105–121.
- Jayathilakan, K., Sultana, K., Radhakrishna, K. & Bawa, A.S. 2012. Utilization of byproducts and waste materials from meat, poultry and fish processing industries: a review. *J. Food Sci. Technol.* **49**(3), 278–293.

- Kalenik, T.K., Costa, R., Motkina, E.V., Kosenko, T.A., Skripko, O.V. & Kadnikova, I.A. 2017. Technological development of protein-rich concentrates using soybean and meat by-products for nutrition in extreme conditions. *Acta Sci. Pol. Technol. Aliment.* **16**(3), 255–268.
- Kurt, S. & Zorba, O. 2007. Emulsion characteristics of beef and sheep offal. *J. Muscle Foods* **18**, 129–142.
- Lasekan, A., Abu Bakar, F. & Hashim, D. 2013. Potential of chicken by-products as sources of useful biological resources. *Waste Manage* **33**(3), 552–565.
- Lipatov, N.N. 1995. The background of the computer design of products and diets with the specifiable nutritional value. *Storage and Processing of Farm Products* **3**, 4–9 (in Russian).
- Lisitsyn, A.B., Nikitina, M.A., Zakharov, A.N., Sus, E.B., Nasonova, V.V. & Lebedeva, L.I. 2016. Prediction of meat product quality by the mathematical programming methods. *Theory and Practice of Meat Processing* **1**, 75–90.
- Martínez-Alvarez, O., Chamorro, S. & Brenes, A. 2015. Protein hydrolysates from animal processing by-products as a source of bioactive molecules with interest in animal feeding: A review. *Food Res. Intern.* **73**, 204–212.
- Mora, L., Reig, M. & Toldrá, F. 2014. Bioactive peptides generated from meat industry by-products. *Food Res. Intern.* **65**, 344–349.
- Mullen, A.M. & Álvarez, C. 2016. Offal: Types and composition. The encyclopedia of food and health, pp. 152–157.
- Mullen, A.M., Álvarez, C., Zeugolis, D.I., Henchion, M., O'Neill, E. & Drummond, L. 2017. Alternative uses for co-products: Harnessing the potential of valuable compounds from meat processing chains. *Meat. Sci.* **132**, 90–98.
- Musina, O.N. & Lisin, P.A. 2012. The system modeling of the multicomponent food products. *Food Processing: Techniques and Technology* **4**, 32–38 (In Russian).
- Musina, O.N. & Lisin, P.A. 2015. An approach to the choice of alternatives of the optimized formulations. *Foods and Raw Materials* **3**(2), 65–73.
- Nadtochii, L.A. 2013. Designing a protein component of food in the Microsoft Excel spreadsheet editor. *Scientific journal NRU ITMO. Processes and Food Production Equipment* **4**. <http://processes.ihbt.ifmo.ru/file/article/10755.pdf> (in Russian).
- Ockerman, H.W. & Basu, L. 2004. By-products. In: Jensen, WK, Devine C, Dikeman M, editors. *Encyclopedia of meat sciences*. Amsterdam, London: Elsevier Academic Press, pp. 104–112.
- Oser, B.L. 1951. Methods for the integrating essential amino acid content in the nutritional evaluation of protein. *J Am Dietet Assoc* **27**, 399–404.
- Satina, O.V. & Yudina, S.B. 2010. Information technologies of designing gerontological food products. *Meat Industry* **6**, 56–58. (in Russian).
- Seong, P.N., Kang, G.H., Park, K.M., Cho, S.H., Kang, S.M. & Park, B.Y. 2014. Characterization of Hanwoo Bovine By-products by Means of Yield, Physicochemical and Nutritional Compositions. *Korean J. Food Sci. An.* **34**(4), 434–447.
- Skurikhin, I.M. & Volgarev, M.N. 1987. Chemical Composition of Food Products *Agropromizdat*, pp. 166–167 (in Russian).
- Smith, J. 1993. *Technology of Reduced-Additive Foods*. London: Blackie Academic and Professional, Chapman and Hall, 239 pp.
- Subba, D. 2002. Acceptability and nutritive value of keropok-like snack containing meat offal. *J. Food Sci. Tech.* **37**(6), 681–685.
- Sun-Waterhouse, D., Zhao, M. & Waterhouse, G. 2014. Protein Modification During Ingredient Preparation and Food Processing: Approaches to Improve Food Processability and Nutrition. *Food Bioprocess Technol.* **7**, 1853–1893.

- Toldrá, F., Mora, L. & Reig, M. 2016. New insights into meat by-product utilization. *Meat. Sci.* **120**, 54–59.
- Unsal, M. & Aktas, N. 2003. Fractionation and characterization of edible sheep tail fat. *Meat. Sci.* **63**(4), 235–239.
- Van Heerden, S.M. & Morey, L. 2014. Nutrient content of South African C2 beef offal. *Food Measure* **8**, 249–258.
- Venegas Fornias, O. 1996. Edible by-products of slaughter animals. FAO animal production and health paper (FAO).
- Vernooij, A. 2012. The return of animal by-products. Rabobank industry note #335.–Dec.2012. <http://ausrenderers.com.au/index.php/downloads/category/1-general-documents>. Accessed 28.04.2019.
- Wen, S., Zhou, G., Song, S., Xu, X., Voglmeir, J. & Liu, L. 2015. Discrimination of *in vitro* and *in vivo* digestion products of meat proteins from pork, beef, chicken, and fish. *Proteomics* **15**, 3688–3698.
- Zhackslykova, S.A., Khabibullin, R.E. & Reshetnik, O.A. 2014. Approaches to optimization of the composition of balanced meat products. *Bulletin of Kazan Technological University* **17**(21), 242–247.

INSTRUCTIONS TO AUTHORS

Papers must be in English (British spelling). English will be revised by a proofreader, but authors are strongly urged to have their manuscripts reviewed linguistically prior to submission. Contributions should be sent electronically. Papers are considered by referees before acceptance. The manuscript should follow the instructions below.

Structure: Title, Authors (initials & surname; an asterisk indicates the corresponding author), Authors' affiliation with postal address (each on a separate line) and e-mail of the corresponding author, Abstract (up to 250 words), Key words (not repeating words in the title), Introduction, Materials and methods, Results and discussion, Conclusions, Acknowledgements (optional), References.

Layout, page size and font

- Use preferably the latest version of **Microsoft Word**, doc., docx. format.
- Set page size to **ISO B5 (17.6 x 25 cm)**, all **margins at 2 cm**. All text, tables, and figures must fit within the text margins.
- Use single line spacing and **justify the text**. Do not use page numbering. Use **indent 0.8 cm** (do not use tab or spaces instead).
- Use font Times New Roman, point size for the title of article **14 (Bold)**, author's names 12, core text 11; Abstract, Key words, Acknowledgements, References, tables, and figure captions 10.
- Use *italics* for Latin biological names, mathematical variables and statistical terms.
- Use single ('...') instead of double quotation marks ("...").

Tables

- All tables must be referred to in the text (Table 1; Tables 1, 3; Tables 2–3).
- Use font Times New Roman, regular, 10 pt. Insert tables by Word's 'Insert' menu.
- Do not use vertical lines as dividers; only horizontal lines (1/2 pt) are allowed. Primary column and row headings should start with an initial capital.

Figures

- All figures must be referred to in the text (Fig. 1; Fig. 1 A; Figs 1, 3; Figs 1–3). Use only black and white or greyscale for figures. Avoid 3D charts, background shading, gridlines and excessive symbols. Use font **Arial, 10 pt** within the figures. Make sure that thickness of the lines is greater than 0.3 pt.
- Do not put caption in the frame of the figure.
- The preferred graphic format is Excel object; for diagrams and charts EPS; for half-tones please use TIFF. MS Office files are also acceptable. Please include these files in your submission.
- Check and double-check spelling in figures and graphs. Proof-readers may not be able to change mistakes in a different program.

References

- **Within the text**

In case of two authors, use '&', if more than two authors, provide first author 'et al.':
Smith & Jones (1996); (Smith & Jones, 1996);

Brown et al. (1997); (Brown et al., 1997)

When referring to more than one publication, arrange them by following keys: 1. year of publication (ascending), 2. alphabetical order for the same year of publication:

(Smith & Jones, 1996; Brown et al., 1997; Adams, 1998; Smith, 1998)

- **For whole books**

Name(s) and initials of the author(s). Year of publication. *Title of the book (in italics)*. Publisher, place of publication, number of pages.

Shiyatov, S.G. 1986. *Dendrochronology of the upper timberline in the Urals*. Nauka, Moscow, 350 pp. (in Russian).

- **For articles in a journal**

Name(s) and initials of the author(s). Year of publication. Title of the article. *Abbreviated journal title (in italic)* volume (in bold), page numbers.

Titles of papers published in languages other than English, should be replaced by an English translation, with an explanatory note at the end, e.g., (in Russian, English abstr.).

Karube, I. & Tamiya, M.Y. 1987. Biosensors for environmental control. *Pure Appl. Chem.* **59**, 545–554.

Frey, R. 1958. Zur Kenntnis der Diptera brachycera p.p. der Kapverdischen Inseln. *Commentat.Biol.* **18**(4), 1–61.

Danielyan, S.G. & Nabaldiyan, K.M. 1971. The causal agents of meloids in bees. *Veterinariya* **8**, 64–65 (in Russian).

- **For articles in collections:**

Name(s) and initials of the author(s). Year of publication. Title of the article. Name(s) and initials of the editor(s) (preceded by In:) *Title of the collection (in italics)*, publisher, place of publication, page numbers.

Yurtsev, B.A., Tolmachev, A.I. & Rebristaya, O.V. 1978. The floristic delimitation and subdivisions of the Arctic. In: Yurtsev, B.A. (ed.) *The Arctic Floristic Region*. Nauka, Leningrad, pp. 9–104 (in Russian).

- **For conference proceedings:**

Name(s) and initials of the author(s). Year of publication. Name(s) and initials of the editor(s) (preceded by In:) *Proceedings name (in italics)*, publisher, place of publishing, page numbers.

Ritchie, M.E. & Olf, H. 1999. Herbivore diversity and plant dynamics: compensatory and additive effects. In: Olf, H., Brown, V.K. & Drent R.H. (eds) *Herbivores between plants and predators. Proc. Int. Conf. The 38th Symposium of the British Ecological Society*, Blackwell Science, Oxford, UK, pp. 175–204.

.....
Please note

- Use ‘.’ (not ‘,’) for decimal point: 0.6 ± 0.2; Use ‘,’ for thousands – 1,230.4;
- Use ‘-’ (not ‘-’) and without space: pp. 27–36, 1998–2000, 4–6 min, 3–5 kg
- With spaces: 5 h, 5 kg, 5 m, 5 °C, C : D = 0.6 ± 0.2; *p* < 0.001
- Without space: 55°, 5% (not 55 °, 5 %)
- Use ‘kg ha⁻¹’ (not ‘kg/ha’);
- Use degree sign ‘°’ : 5 °C (not 5 °C).